

Perspectives on the relationship between local interactions and global outcomes in spatially explicit models of systems of interacting individuals

Thomas P. Oléron Evans

June 17, 2015

A dissertation submitted in partial fulfilment of the requirements for the degree of Doctor of Philosophy.

Department of Mathematics
University College London

I, Thomas P. Oléron Evans, confirm that the work presented in this thesis is my own. Where information has been derived from other sources, I confirm that this has been indicated in the thesis.

Abstract

Understanding the behaviour of systems of interacting individuals is a key aim of much research in the social sciences and beyond, and a wide variety of modelling paradigms have been employed in pursuit of this goal. Often, systems of interest are intrinsically spatial, involving interactions that occur on a local scale or according to some specific spatial structure. However, while it is recognised that spatial factors can have a significant impact on the global behaviours exhibited by such systems, in practice, models often neglect spatial structure or consider it only in a limited way, in order to simplify interpretation and analysis.

In the particular case of individual-based models used in the social sciences, a lack of consistent mathematical foundations inevitably casts doubt on the validity of research conclusions. Similarly, in game theory, the lack of a unifying framework to encompass the full variety of spatial games presented in the literature restricts the development of general results and can prevent researchers from identifying important similarities between models.

In this thesis, we address these issues by examining the relationship between local interactions and global outcomes in spatially explicit models of interacting individuals from two different conceptual perspectives.

First, we define and analyse a family of spatially explicit, individual-based models, identifying and explaining fundamental connections between their local and global behaviours. Our approach represents a proof of concept, suggesting that similar methods could be effective in identifying such connections in a wider range of models.

Secondly, we define a general model for spatial games of search and concealment, which unites many existing games into a single framework, and we present theoretical results on its optimal strategies. Our model represents an opportunity for the development of a more broadly applicable theory of spatial games, which could facilitate progress and highlight connections within the field.

Contents

Title	1
Declaration	2
Abstract	3
Contents	4
List of Figures	7
List of Tables	9
Supervisors	10
I Introduction and background	11
1 Introduction	12
1.1 Overall aim	12
1.2 Complexity and spatial structure	12
1.3 Explanation of thesis title	13
1.4 Motivations	14
1.5 Research objectives	16
1.6 Thesis structure	17
1.7 Advances to knowledge	20
1.8 Notes on notation	21
1.9 Research context	21
2 Background	23
2.1 Complex systems	23
2.2 Agent-based and individual-based models	30
2.3 Cellular automata	50
2.4 Stochastic processes	59

II Understanding the connection between micro and macro-scale behaviour in individual-based models	64
3 Key Concepts	65
3.1 Introduction to Part II	65
3.2 Mean field theory	66
3.3 Models from mathematical ecology	74
4 Definition and initial discussion of a general family of simple IBMs	79
4.1 Introduction	79
4.2 The NANIA predator-prey model: An ODD description	79
4.3 Behaviour of the NANIA model	85
4.4 Generalising the NANIA model	103
4.5 Summary and conclusions	119
5 Categorisation and initial analysis of the different behavioural regimes of the one-dimensional, single species \mathfrak{B}-model	120
5.1 Introduction	120
5.2 Single species \mathfrak{B} -models	121
5.3 Simulation experiments	126
5.4 Autocorrelation analysis	156
5.5 Summary and conclusions	165
6 Understanding the relationship between local transitions and global dynamics in the one-dimensional, single species \mathfrak{B}-model	166
6.1 Introduction	166
6.2 Reversible and irreversible local transitions	168
6.3 Transforming the microstates of a \mathfrak{B} -model into a new space	171
6.4 The dynamics of the transformed model	182
6.5 Taking account of the spatial distribution of individuals	199
6.6 Using clumping to understand global behaviour	209
6.7 Summary and conclusions	219

III A general framework for static, spatially explicit games of search and concealment

223

7 Background and motivation	224
7.1 Introduction to Part III	224
7.2 Game theoretic concepts	226
7.3 Games of search and security: A review	230
7.4 Motivation for the Static Spatial Search Game	234
8 Defining and analysing spatial games	235
8.1 Introduction	235
8.2 The Static Spatial Search Game (SSSG)	235
8.3 The Graph Search Game (GSG)	247
8.4 Summary and conclusions	258
9 Methods for solving GSGs	259
9.1 Introduction	259
9.2 Simplifying GSGs algorithmically	259
9.3 Further methods for analysing GSGs	273
9.4 Games on poly-level graphs	287
9.5 Summary and conclusions	295
10 Extensions and adaptations of the SSSG	296
10.1 Introduction	296
10.2 Games over spaces of non-uniform value	297
10.3 Optimal mixed strategies of games over spaces of non-uniform value .	299
10.4 The Graph Patrol Game (GPG)	310
10.5 Summary and conclusions	328
IV Conclusions	330
11 Conclusions, synthesis and further work	331
11.1 Research outcomes	331
11.2 Discussion	334
11.3 Directions for further research	341
11.4 Concluding remarks	348
Acknowledgements	350
Bibliography	351

List of Figures

1	Introduction	12
1.1	Flow diagram of thesis concepts, methods and outcomes	22
4	Definition and initial discussion of a general family of simple IBMs	79
4.1	Comparison of Von Neumann and Moore adjacency schemes	81
4.2	Flow diagram illustrating possible evolution of the NANIA model . .	86
4.3	“Check Pattern” microstates of the NANIA model	89
4.4	Example of a Markov chain exhibiting quasi-stable oscillations	90
4.5	Sample dynamics of the NANIA model	91
4.6	Transitions of the “factory” in the NANIA model	96
4.7	Invalid locations for the “factory” in the proof of Proposition 4.3.1 .	97
4.8	Visual presentation of the proof of Proposition 4.3.1: Steps 1-5 . . .	98
4.9	Visual presentation of the proof of Proposition 4.3.1: Steps 6-9 . . .	99
4.10	A valid location for a “factory” in a “Check Pattern” microstate . .	102
4.11	Transformations to the “factory” with Moore adjacency	102
4.12	Equivalence classes of a one-dimensional single species \mathfrak{A} -model . . .	114
5	Categorisation and initial analysis of the different behavioural regimes of the one-dimensional, single species \mathfrak{B}-model	120
5.1	Bifurcation diagram for equation (5.1)	123
5.2	Parameter space diagram for equation (5.1).	124
5.3	Simulated evolution of a one-dimensional, one species \mathfrak{B} -model	130
5.4	Simulated evolution of a one-dimensional, one species \mathfrak{B} -model	130
5.5	Simulated evolution of a one-dimensional, one species \mathfrak{B} -model	131
5.6	Simulated evolution of a one-dimensional, one species \mathfrak{B} -model	131
5.7	Simulated evolution of a one-dimensional, one species \mathfrak{B} -model	132
5.8	Simulated evolution of a one-dimensional, one species \mathfrak{B} -model	132
5.9	Simulated evolution of a one-dimensional, one species \mathfrak{B} -model	134
5.10	Simulated evolution of a one-dimensional, one species \mathfrak{B} -model	134
5.11	Simulated evolution of a one-dimensional, one species \mathfrak{B} -model	135
5.12	Simulated evolution of a one-dimensional, one species \mathfrak{B} -model	135
5.13	Simulated evolution of a one-dimensional, one species \mathfrak{B} -model	136
5.14	Simulated evolution of a one-dimensional, one species \mathfrak{B} -model	136
5.15	Simulated evolution of a one-dimensional, one species \mathfrak{B} -model	137
5.16	Simulated evolution of a one-dimensional, one species \mathfrak{B} -model	137
5.17	Density dynamics of a one-dimensional single species \mathfrak{B} -model	140

5.18	Density dynamics of a one-dimensional single species \mathfrak{B} -model	141
5.19	Density dynamics of a one-dimensional single species \mathfrak{B} -model	142
5.20	Density dynamics of a one-dimensional single species \mathfrak{B} -model	143
5.21	Density dynamics of a one-dimensional single species \mathfrak{B} -model	144
5.22	Density dynamics of a one-dimensional single species \mathfrak{B} -model	145
5.23	Parameter space plots for the one-dimensional single species \mathfrak{B} -model	150
5.24	Autocorrelation plots of a one-dimensional single species \mathfrak{B} -model . .	161
5.25	Autocorrelation plots of a one-dimensional single species \mathfrak{B} -model . .	162
5.26	Autocorrelation plots of a one-dimensional single species \mathfrak{B} -model . .	163
5.27	Autocorrelation plots of a one-dimensional single species \mathfrak{B} -model . .	164
6	Understanding the relationship between local transitions and global dynamics in the one-dimensional, single species \mathfrak{B}-model	166
6.1	Reversibility of transitions in a single species \mathfrak{B} -model	169
6.2	Diagram of the transformation between Ω_n , Ψ_n and Δ^{n-1}	170
6.3	Alternative representations of a microstate in Ω_n , Ψ_n and Δ^{n-1}	178
6.4	The effect of each of the \mathfrak{B} -model transitions on the vector δ	183
6.5	Complete summary of Ω_n , Ψ_n and Δ^{n-1} , for the case $n = 3$	193
6.6	Visualisation of the effect of β , γ and η -transitions over Δ^2 , for $n = 3$	194
6.7	Visualisation of the effect of α -transitions over Δ^2 , for $n = 3$	195
6.8	Visualisation of the effect of β , γ and η -transitions over Δ^5 , for $n = 6$	197
6.9	Visualisation of the effect of α -transitions over Δ^5 , for $n = 6$	198
6.10	The function $y = (\text{Re} - \text{Im})[\sqrt{x}]$ for $x \in [-1, 1]$	201
6.11	A geometric interpretation of the natural clumping measure	206
8	Defining and analysing spatial games	235
8.1	Visualisation of the Static Spatial Search Game (SSSG)	236
8.2	Visualisation of the Graph Search Game (GSG)	248
8.3	Four simple graphs (see Table 8.1)	257
9	Methods for solving GSGs	259
9.1	An example of the GSG	268
9.2	The orbits of the rectangular grid graph $G_{5,5}$	276
9.3	Visualisation of the OMSs of the GSG played over $G_{5,5}$	279
9.4	Visualisation of the OMSs of the GSG played over $G_{6,6}$	279
9.5	Visual representation of a poly-level graph	287
9.6	Poly-level graph with $h = 4$, $j = 2$, $k = 1$, $l = 1$, $c_1 = 4$	288
9.7	Poly-level graph with $h = 3$, $j = 2$, $k = 2$, $l = 1$, $c_1 = 3$	288
9.8	Poly-level graph with $h = 2$, $j = 3$, $k = 1$, $l = 2$, $c_1 = 16$	289
9.9	Topologically different poly-level graphs with identical parameters . .	289
9.10	A poly-level graph that admits two different sets of parameters . . .	289

List of Tables

4 Definition and initial discussion of a general family of simple IBMs	79
4.1 Summary of possible events in the NANIA model	93
4.2 A \mathfrak{B} -model transition rule producing NANIA model behaviour	116
4.3 Valid local transitions in a \mathfrak{B} -model	118
5 Categorisation and initial analysis of the different behavioural regimes of the one-dimensional, single species \mathfrak{B}-model	120
5.1 Local transitions for a single species \mathfrak{B} -model	121
6 Understanding the relationship between local transitions and global dynamics in the one-dimensional, single species \mathfrak{B}-model	166
6.1 The equivalence classes of \sim , \smile and \frown , for $n = 6$	181
6.2 Maxima and minima of terms (and combinations of terms) of δ	188
6.3 Expectations of terms (and combinations of terms) of δ	192
8 Defining and analysing spatial games	235
8.1 Bounds, values and OMSs for the graphs of Figure 8.3	257
9 Methods for solving GSGs	259
9.1 Equal oddments solutions for the graphs shown in Figures 9.6-9.8 . .	295

Supervisors

Primary: Prof. Steven R. Bishop (Dept. of Mathematics, UCL)

Second: Prof. Frank T. Smith (Dept. of Mathematics, UCL)

I would like to thank my supervisors for their advice and assistance throughout the course of the research presented in this thesis.

Part I

Introduction and background

Chapter 1

Introduction

1.1 Overall aim

The principal aim of this thesis is to investigate the three-way relationship between local interactions, global outcomes and spatial structure in systems of interacting individuals. This overarching goal is addressed from two different perspectives, a ‘wide-angle’ perspective, focusing on the collective dynamics of very simple individuals, and a ‘close-up’ perspective, focusing on the strategic decisions of more sophisticated individuals. Each of these perspectives involves a different modelling paradigm that is employed in the field of complexity science: individual-based modelling and game theoretic modelling.

1.2 Complexity and spatial structure

If a system of interacting entities exhibits behaviours on a global scale that could not be predicted or understood by studying the entities in isolation, then it is described as complex. For example, the shape and motion of a large flock of birds could not easily be predicted by studying the behaviour of a single bird, but these collective features are nonetheless determined by the aggregated effect of the interactions between individuals. In this example, the importance of spatial structure is also evident; distances between individual birds, lines of sight and the direction in which gravity acts might all be supposed to have a significant effect on the global behaviour of the flock. A detailed discussion of complex systems and the property of complexity is provided in Chapter 2, while the importance of spatial structure in such systems is a key thread that runs throughout this thesis.

1.3 Explanation of thesis title

The precise nature of the “individuals” referred to in the thesis title is different under each of the two perspectives to be considered, and will therefore be described in detail in the relevant sections. At this stage, it suffices to state that the term will refer to the entities of certain simple individual-based models in Part II and to the players in a family of game theoretic models in Part III. Conceptually, however, thinking in terms of real world systems rather than mathematical models, the term should be understood in its broadest possible sense. An individual may be any entity – whether a human being, an animal, a computer, a company, an elementary particle or a coordinated group of such entities – which interacts with others that may be of the same type or of different types. Individuals may have an associated “state”, meaning some description of their properties, which may or may not vary in time, and may perform “actions” of some kind, which together constitute their “behaviour”.

The term “system” is used to refer to the object formed by all individuals of interest and the rules or principles governing their behaviour, along with the space that they inhabit and any other features that are considered to affect them. The word may be used to refer either to something observed in the real world, whether specific or generic, or to the abstract construct represented by a mathematical model, which need not necessarily have a particular real world interpretation. Systems may vary in time, and may be described by their current “state”, a complete or partial description of their properties. Particular states observed within a system at a certain time may be referred to as “events”.

By the phrase “spatially explicit model” we mean a mathematical representation of a system in which the space that the individuals inhabit (sometimes referred to as the “model geography”) is represented in a detailed manner, rather than in a strictly implicit sense through its influence on the actions or states of the individuals only. In all the work presented in this thesis, space is represented either as a graph (or network) or as a metric space. The phrase “local interactions” is then taken to mean any effect which involves more than one individual and whose occurrence or effect is dependent on the positions of the individuals in the space. Specifically, the local interactions that we will consider will involve two individuals that are located in close proximity to each other.

The broad phrase “global outcome” is intended to refer to any event or state that relates to the entirety of a system, rather than to a particular individual or group

of individuals, but which is nevertheless determined, at least in part, by the states of the individuals (rather than simply on the structure of the space, for example). The global outcomes that we will be interested in will involve long-term population density dynamics in simple individual-based models (in Part II) and the payoffs and optimal strategies in certain game theoretic models (in Part III).

1.4 Motivations

1.4.1 Perspective one: Individuals as automata

The first of our two perspectives makes use of the theory of individual-based modelling. One of the most important and challenging research questions in this field, and indeed in the field of complexity science more generally, is to understand the connections between local and global features. More specifically, we might desire to understand how the local interactions between individuals in a model or in a real system give rise to observed emergent global behaviours.

General results relating to such questions are scarce and, indeed, no consolidated theory of individual-based models yet exists. The absence of these theoretical foundations represents a serious problem, since the *use* of such models is now widespread, particularly in the social sciences. Because the theoretical basis of much of this work is patchy or non-existent, conclusions drawn from these models may not be reliable or the circumstances in which they are valid may not be known. Furthermore, a lack of understanding of the mechanisms driving observed outcomes may make the planning of appropriate interventions to modelled systems difficult or impossible.

What is acknowledged is that spatial structure can be crucially important in determining the characteristics of the global behaviour of a system of interacting individuals. However, spatial systems (such as ecological systems of different species interacting within a habitat) are often represented with non-spatial models, in which the behaviours of individuals are represented implicitly, through the dynamics of aggregated quantities such as population densities. One method for producing such simplified models is provided by mean field theory (see Section 3.2), in which spatial correlations are neglected and individuals are assumed to be, in some sense, ‘evenly distributed’ throughout the system.

While, in many cases, such simplifications may be appropriate, the lack of general theory in the area means that it is often not possible to determine whether or not this will be the case without explicit comparison of model outputs with empirical

observations. Even then, it can be impossible to determine the extent to which a model captures the full spectrum of system dynamics, since rare or extreme behaviours may not be represented in the data.

Traditional reductive models, utilising ordinary differential equations (ODEs) or partial differential equations (PDEs) to describe temporal and spatial variation, which have long been successfully deployed to analyse physical systems such as fluid motion, diffusion and heat transfer, may fail to capture all the emergent phenomena of crowds of interacting individuals. However, it is not at all obvious how to formulate an alternative description of these complex systems that would preserve their fundamental character as collections of separate elements, or indeed whether such a description would be possible or valuable.

The relationship between ‘simplified’ representations of complex systems (such as those based on ODEs or PDEs) and ‘comprehensive’ representations (based on detailed ABMs) and the extent to which they exhibit similar behaviour, both to each other and to the original system, is therefore a key question in the field.

In Part II of this thesis, we address these issues through analysing the links between local events and global dynamics in a particular family of individual-based models, focusing on the key role played by the spatial distribution of individuals. In these models, individuals are not treated as decision-making entities, but rather as basic automata, whose behaviour is governed by very simple stochastic rules. Although the results obtained relate to the particular models under consideration, the simplicity of the approach and of the system concerned are such that we believe the methods may serve as foundations for the development of more general approaches.

1.4.2 Perspective two: Individuals as decision-making agents

The approach outlined above could be described as a ‘wide-angle’ perspective on spatial systems of interacting entities, since it seeks to develop understanding through consideration of the combined effect of the simultaneous local actions of large groups of very simple individuals. In contrast, our second approach is a ‘close-up’ perspective in which we consider the relationship between spatial structure and the strategies employed by more sophisticated, decision-making individuals in certain game theoretic models.

Spatial game theoretic models have been studied in relation to various situations of search and concealment, attack and defence, patrol and rendez-vous. However, as in the case of individual-based modelling, such analyses lack a common theoretical

framework at an appropriate level of generality. Furthermore, the role of spatial structure in such models is often limited to determining how players may move through a space. Only rarely is consideration given to the impact of local spatial structure on the way in which players interact with nearby opponents or collaborators. However, proximity-based interactions are of key importance in many of the situations that spatial games seek to model. For example, in a game theoretic model of the policing of urban riots, a police unit deployed at a particular location would be able to respond to incidents in some neighbourhood of that point, the precise form of which would depend on the local structure of the street network.

The formulation of a general framework of spatial game theory would allow for a strategic analysis of spatial interactions from the perspective of a particular individual, in parallel with the analysis of the connections between local interactions and global dynamics afforded by our work on simple individual-based models.

In Part III, we address these issues through the development and analysis of a general search game that takes explicit account of the local structure of the space over which it is played. We consider both a static version of the game, in which the searching player deploys at a particular location, and a dynamic version, in which the searching player chooses a randomised patrol strategy. While some of the results relate to games played over specific spaces, the model is formulated in a highly general way so as to unite many existing models in the literature.

These twin approaches, based on individual-based modelling and game theory, provide complementary perspectives on the complex connections between spatial structure, individual behaviours, local interactions and global outcomes, allowing us to move towards a greater understanding of the general principles underlying these features in a wide variety of spatial models.

1.5 Research objectives

Having established our overall aims and our motivations for each modelling perspective, we now crystallise these into a more specific set of research objectives. In relation to the first perspective, discussed above in Section 1.4.1 and covered in Part II, our objectives are:

- To improve understanding of the relationship between the long term population dynamics of spatially explicit individual-based models and the dynamics predicted by corresponding non-spatial models, derived using mean field theory.

- To develop methods to understand and explain the causal link between local spatial interactions and global population dynamics in such models.

In relation to the second perspective, covered in Part III, our objectives are:

- To create a general, explicitly spatial, search and concealment game, in order to unite many similar games presented in the literature under a single theoretical framework.
- To develop general results on the optimal mixed strategies of this game and on how these strategies may be determined.

1.6 Thesis structure

In this section, we present a detailed breakdown of the content of the thesis. A visualisation illustrating the connections between the aims, concepts, methods and outcomes, is provided in Figure 1.1, at the end of the chapter.

Part I : Introduction and background

Chapters 1-2

In **Chapter 1**, we explain our broad aims and motivations, define the scope and objectives of the thesis and discuss the ideas that link the various sections. We then provide a detailed breakdown of the structure of the thesis and the content of each part, along with a list of the key contributions to knowledge, with references to where in the text they may be found. Following this, in **Chapter 2**, we discuss some of the main concepts used throughout the thesis in more depth, with reference to key literature. Further background is introduced at the start of each of the remaining parts of the thesis, as and when it is necessary.

Part II : Understanding the connection between micro and macro-scale behaviour in individual-based models

Chapters 3-6

In Part II, our main goal is to find ways to understand the connection between local interactions and global behaviour in a family of simple individual-based models through observation of the collective dynamics of the individuals. After presenting some necessary background information in **Chapter 3**, **Chapter 4** introduces the model that forms the basis of this part of the thesis: a spatially and temporally discrete stochastic model created by Professor Graeme Ackland¹ as part of the NANIA

¹ Professor Ackland was identified as the creator of the model through personal correspondence with researchers from the NANIA project.

project (Novel Approaches to Networks of Interacting Autonomes, 2009), related to the widely studied ecological patch model (see McKane and Newman, 2004), designed to represent predator-prey relationships, much like those described by the well-known Lotka-Volterra equations (see Section 3.3.2).

The basic NANIA predator-prey model has two species with a specific set of possible interactions and is run over a rectangular or toroidal lattice of cells. However, we recognise that it is just one representative of a much broader family of possible models, which could be run over any graph, and which admit a much wider variety of possible interactions between any number of different species. We therefore proceed to define the entire family of possible models, which we label \mathfrak{A} . However, \mathfrak{A} includes cases which no longer have a reasonable interpretation as individual-based models, so we also define a subfamily, \mathfrak{B} , containing the models that preserve those features of the NANIA model that are conducive to an individual-based perspective.

Having clearly defined \mathfrak{B} , in **Chapter 5**, we go on to perform a thorough investigation of all the possible model behaviours in the simplest of all possible cases, that of a single species on a one-dimensional ring of cells. The investigation is carried out through performing a large number of computer simulations to extensively explore the parameter space of the rules that govern the behaviour of individuals in the model, resulting in the creation of a taxonomy of possible behavioural regimes. Through a quantitative analysis of the results of these simulations, we observe that, of all those local transitions that may occur at a given iteration, there exists one in particular that seems to cause the model to diverge from the behaviour predicted by mean field theory.

Finally, in **Chapter 6**, we focus on these local transitions in an attempt to understand the discrepancy between the majority that respect the mean field analysis and the one that does not. To do this, we transform the state space of the model, taking a perspective on its dynamics that more directly represents the spatial distribution of the individuals. This new perspective, alongside the introduction of a measure of the degree of clumping of individuals in the system, allows us to identify key differences in the effect of the particular transition of interest, thus explaining its disruptive effect on the behaviour predicted by mean field analysis.

Part III : A general framework for static, spatially explicit games of search and concealment

Chapters 7-10

In Part III, our perspective shifts to consider models of search and concealment scenarios, involving more sophisticated individuals, capable of making reasoned strategic decisions. The overarching goal is to define and analyse a general, explicitly spatial game to model such scenarios, which could unite other games from the literature, potentially allowing for the formulation of results with relevance to a wide range of different spatial games.

After setting out some necessary game theoretic concepts in **Chapter 7** and presenting a review of the literature of search and security games, in **Chapter 8**, we define a two-player game that will form the basis for all our subsequent work: the Static Spatial Search Game (SSSG). This game is formulated both over a general metric space and in the special case in which this space is a graph (the “Graph Search Game” or GSG), and the connections between the SSSG and certain other games from the literature are highlighted. Initial results related to the concepts of strategic dominance and equivalence in the SSSG are presented, and bounds on the value of the game to each player are identified.

In **Chapter 9**, we discuss various methods for simplifying and solving the GSG (finding optimal mixed strategies (OMSs) for each player and their respective game values). These include a version of the established IEDS algorithm (iterated elimination of dominated strategies) for the SSSG on a graph, along with a proof that, in the special case of games played on trees, this procedure is always successful in identifying trivially simple solutions. Other methods presented include a means of exploiting symmetries of the underlying graph and a technique for determining exact solutions of a particular family of games over a particular family of graphs, which we describe as “poly-level graphs”.

Chapter 10 is built around two significant extensions to the SSSG. Firstly, we allow the value of the space over which the game is played to be non-uniform and examine how this affects the OMSs. Secondly, we consider a scenario in which one player is able to patrol around the space while the other attempts to avoid detection, demonstrating a fundamental relationship between the optimal strategies of the static game and those of this new dynamic version. We conclude by formulating the situation of the patrolling player as an optimisation problem, to allow this individual to choose between alternative strategies in a more sophisticated way.

Part IV : Conclusions

Finally, in **Chapter 11**, we reflect on the main results of the thesis. We consider the relationships between the different perspectives examined in Parts II and III, including a way in which they may be brought together to form a more holistic view of systems of interacting individuals, involving both a broad perspective on the collective dynamics of the individuals and a strategic perspective, focusing on individual decision making. We propose directions for further research, to build on the results that we have presented, and we discuss potential applications, both of the work in its current form and of its possible extensions.

1.7 Advances to knowledge

For ease of reference, we present a list of some of the key original contributions contained in this thesis:

- Comprehensive analysis of the microstates (possible configurations) of the NANIA predator-prey model (over a rectangular lattice) and the transitions between them (**4.3.1-4.3.2**).
- Generalisation of the NANIA model to define the two more fundamental classes of discrete space-time models: \mathfrak{A} and \mathfrak{B} (**4.4**).
- Use of computer simulation to produce a complete taxonomy of behavioural types for a family of individual-based models derived from the NANIA model (**5.3**).
- Presentation of a method for the transformation of model states into a new space in which the dynamics may be more naturally observed, for the above family of models (**6.3-6.4**).
- Identification of a causal link between local individual behaviours and the spatial distribution of individuals on a global scale, in the above family of models, through consideration of a measure of the clumping of individuals (**6.6.3**).
- Use of this clumping measure to explain the relationship between the equilibrium population density and the predicted “mean field” equilibrium, in the above family of models (**6.6.4**).

- Definition of the Static Spatial Search Game (SSSG), a generalisation of many games considered separately in the literature (over a general metric space: **8.2.1-8.2.2**; over a graph: **8.3.1**; over spaces of non-uniform value: **10.2.1-10.2.2**).
- Various results on strategic dominance and equivalence in different versions of the SSSG, including an algorithm to simplify games over graphs and a proof of the effectiveness of this procedure for the special case of games played on trees (**8.2.4**, **8.3.3**, **9.2.1-9.2.5**).
- Various results on OMSs and game values for different versions of the SSSG (**8.2.3**, **8.3.4**, **9.3.1-9.3.4**, **9.4.2-9.4.3**, **10.3.3-10.3.4**).
- Reformulation of the SSSG as a patrol game (**10.4.1-10.4.3**).
- Identification of a relationship between OMSs of the SSSG and optimal strategies of the patrol game (**10.4.4**).

1.8 Notes on notation

It should be noted that, throughout this thesis, the symbol \mathbb{N} is taken to represent the set of strictly positive integers; it does not contain 0. Where necessary, the set of *non-negative* integers will be referred to as $\mathbb{N} \cup \{0\}$.

Note also that, beyond standard mathematical symbols, there is no crossover of notation between Parts II and III, which comprise the main body of the thesis.

1.9 Research context

This thesis was completed as part of ENFOLD-ing - Explaining, Modelling, and Forecasting Global Dynamics (see ENFOLD-ing, 2010, Wilson, 2010), a research project funded by the UK Engineering and Physical Sciences Research Council (EPSRC, 2015), grant reference EP/H02185X/1.

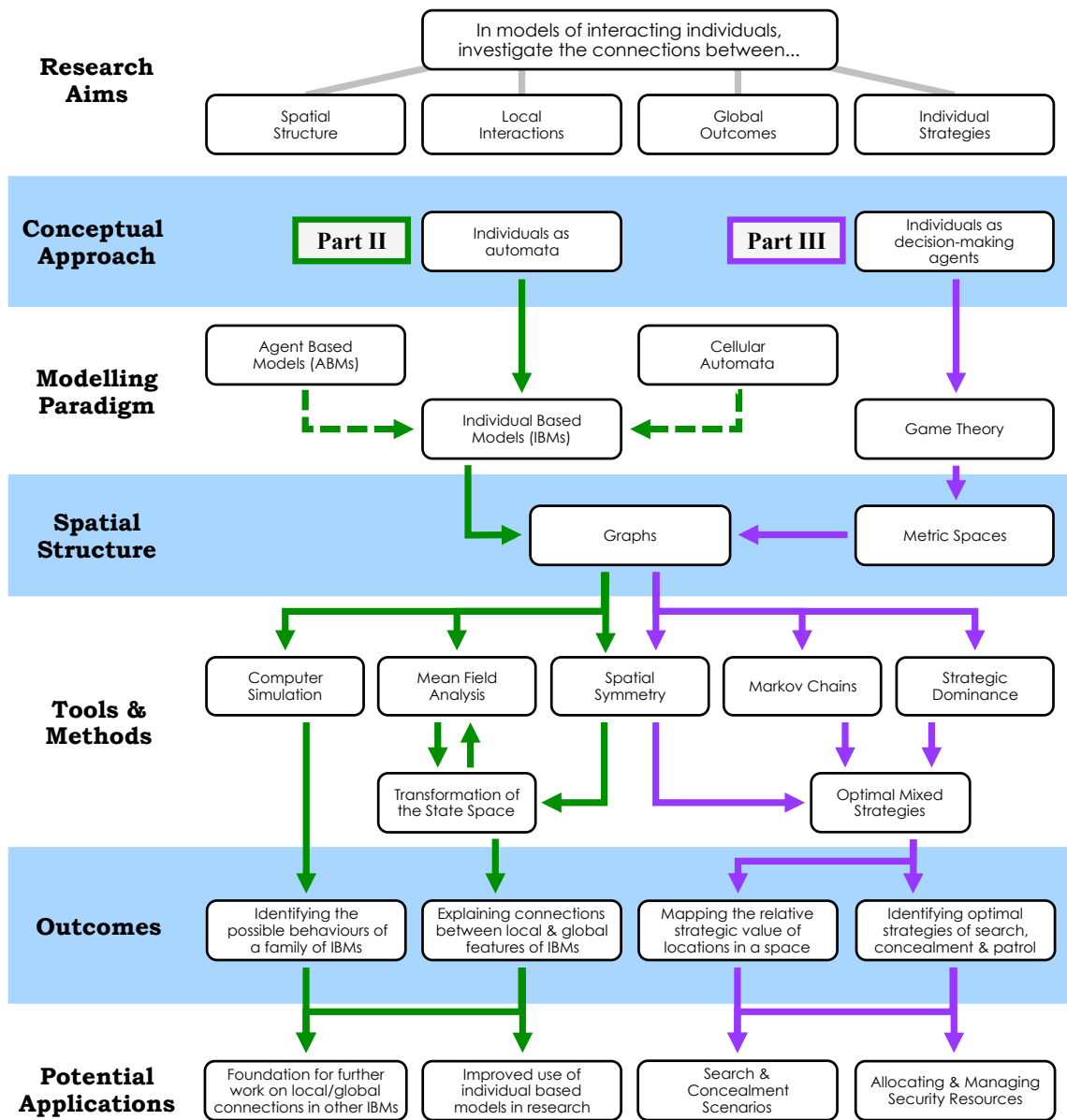


Figure 1.1: Diagram illustrating the connections between the aims, concepts, modelling paradigms, representations of spatial structure, mathematical tools and methods, research outcomes and potential applications of the work presented in this thesis.

The relationship between the different approaches presented in Part II, which focuses on an investigation of the behaviours of certain individual-based models, and Part III, which presents a strategic analysis of a variety of search and concealment games, may be observed through a comparison of the green and purple paths through the chart.

Chapter 2

Background

2.1 Complex systems

2.1.1 Definitions

In broad terms, the foundation of this thesis is the field of **complex systems** or **complexity science**. Although the concept of complexity is now fairly well established in the academic scientific consciousness, having inspired a large amount of attention in recent years, there is still no universally agreed mathematical definition of a complex system. However, the following qualitative description, drawn from a wide-ranging review of the field by Newman (2011), is fairly typical:

“... a system composed of many interacting parts, such that the collective behavior of those parts together is more than the sum of their individual behaviors.”

San Miguel et al. (2012), in the introduction to their broad review of contemporary challenges in complexity science, prefer to define complex systems in the negative, through contrasting them with more well behaved physical systems, which consist of:

“... objects that could be described in terms of a few variables, [and that] could be well separated from their environment...”

The implication is that complex systems cannot be adequately represented using a small number of variables and their component parts cannot be meaningfully studied (at least in terms of their role in the dynamics of the complete system) without considering their interactions with their environment, particularly with other parts of the system itself.

The collective behaviours mentioned by Newman are referred to as **emergent** features and understanding the way in which the particular details of a given complex

system give rise to its emergent behaviours is a key question behind much research in the field.

Many works on complex systems make a point of highlighting the difference between *complexity* and mere *complication*, the former being a property of systems whose parts interact in ways that give rise to unpredictable or unforeseeable behaviours on a global scale, while the latter is a property of systems whose parts may be connected in an intricate fashion, but which nonetheless have specific roles and which contribute in an identifiable way to the overall “purpose” of the system. San Miguel et al. explain this distinction through drawing a comparison between the human brain, a complex system of interacting neurones exhibiting a wide range of unforeseeable behaviours, and an aeroplane, a complicated system of mechanical parts designed to fly through the air.

While loose qualitative descriptions of complexity, such as those discussed above, may be broadly accepted, one of the obstacles to a more specific or rigorous definition of the term is the fact that the field of complex systems research is a highly transdisciplinary one. As noted by San Miguel et al., systems that might be described as complex can be found in practically all branches of science (and indeed beyond the sciences), each of which brings its own preconceptions, interests and concerns to the subject. It can therefore be difficult to determine the extent to which two articles from different disciplines are truly referring to the same thing when they use the term “complex systems”; compare, for example the work of Lewis (2007), which examines complex systems from a medical perspective, with that of Buhr (1996), which comes at the subject from the perspective of computer science.

This ubiquity, coupled with the fact that the word “complex” may also be used in its colloquial sense, means that any attempt to pin down the concept to a greater degree would likely struggle to gain universal acceptance or even to be widely understood. Attempts at broader definitions of “complexity” can consequently occasionally verge on the philosophical rather than the formal (see, for example, Hübler, 2007).

2.1.2 Features

Owing to the difficulty of defining complex systems in a consistent and specific way, it can be helpful to consider the field of complexity science in terms of a set of key concepts and features around which research is focused, rather than in terms of any overarching and clearly defined framework. San Miguel et al. provide a useful starting point for such an approach, presenting the following list of “reasons why

systems might be considered to be complex”:

- many heterogeneous interacting parts
- complicated transition laws
- unexpected or unpredictable emergence
- sensitive dependence on initial conditions
- path-dependent dynamics
- networked hierarchical connectivities
- interactions of autonomous agents
- self-organisation or collective shifts
- non-equilibrium dynamics
- combinatorial explosion
- adaptivity to changing environments
- co-evolving subsystems
- ill-defined boundaries
- multilevel dynamics

To the ideas of emergence and self-organisation, we may add the related and more specific concept of self-organised criticality (see Bak et al., 1987; Drossel and Schwabl, 1992), in which systems may tune themselves to a critical point at which aspects of their behaviour follow a power-law distribution. Indeed, power-law behaviour, which has the property of being invariant under rescaling of a variable of interest, is a key concept of complexity science in its own right, with power-laws governing behaviours across a wide range of different systems (Clauset et al., 2009; Newman, 2011).

Other focuses of complexity research include the ability (whether observed or desired) of complex systems to learn from their interactions and experiences, either at the global level or at the level of their component parts (a stronger concept than the “adaptivity” mentioned by San Miguel et al.), and the concept of resilience, “the ability of a system to spontaneously recover after strong perturbations” (Deffuant and Gilbert, 2011). Complex systems may also display features familiar from the field of nonlinear dynamical systems, such as multiple equilibria, phase transitions and chaos (related to, but not the same as, the “sensitive dependence on initial conditions” mentioned above). An introduction to the concepts and techniques of dynamical systems is provided by Strogatz (1994).

2.1.3 Applications

Naturally, the problems to which complexity theory has been applied are as diverse as the range of disciplines that have embraced it. Newman identifies five extensive areas of application: physical systems (such as condensed matter systems); ecosystems and evolution; human societies; economics and markets; and pattern formation and collective motion (such as flocking behaviour in animals). Structures described and analysed as complex systems run the full spectrum from the practical and political, such as the US health care system (Lipsitz, 2012), to the highly abstract, such as the structure of mathematics itself (Foote, 2007).

2.1.4 Modelling

The way in which a given complex system is ultimately analysed will depend to a large extent on how it is modelled, since different theory and tools are available for different types of model. However, general principles for the study of complex systems have been set down, with San Miguel et al. outlining a five step programme:

1. Exploration, observation and basic data acquisition
2. Identification of correlations, patterns and mechanisms
3. Modelling
4. Model validation, implementation and prediction
5. Construction of a theory

Although stated with reference to complex systems specifically, while the identification of “patterns and mechanisms” may admittedly be particularly relevant in the context of complexity, it is not immediately obvious how this approach is considered different from that which would be applied to the scientific modelling of any other phenomena. In practice, it is more the way in which complex systems are modelled and the sorts of research question that are posed about them that may differ from other forms of study.

Given a particular complex system, it would of course be possible to take a purely empirical approach to its study, gathering and analysing data on the system without the creation of any ‘structural’ mathematical model. In this case, the model created at Step 3 of the above process would be purely statistical. However, as Newman observes, such empirical studies are “usually not considered a part of the field of complex systems itself”.

If the decision is made to represent a particular complex system by means of a structural model, one of the key questions is which modelling paradigm to use to represent its behaviour. Newman and San Miguel et al. highlight two main approaches.

The first can be described as the *reductionist* approach, in which a system is represented through simple abstract descriptions of a small number of relevant features; for example, the relationship between different species in an ecosystem may be represented by a set of differential equations describing the changes in their populations, with no explicit consideration of their spatial distribution or environment.

The second approach could be labelled the *comprehensive* approach, in which the researcher seeks to create as faithful as possible a representation of a system and its functioning, down to the modelling of each specific part and the interactions between such parts, potentially with an explicit representation of the space over which the system operates. Such models are generally analysed through computer simulation.

Before the advent of powerful computing technology, the majority of scientific research was necessarily based around reductionist models, so the use and analysis of comprehensive models is consequently more weakly supported by fundamental theory. While reductionist models may offer the advantage of simplicity and tractability, the question of which details to include and which to ignore in order to produce useful results is not always straightforward. Comprehensive models, on the other hand, allow for a far greater amount of detail to be included, but it can be extremely difficult to determine whether the way in which their component parts and their interactions are modelled is truly a good representation of the system of interest. For these reasons, among others, San Miguel et al. identify both the relationship between simple and comprehensive models and the question of how to identify a sufficiently informative set of descriptive variables to represent complex behaviour in a given system as fundamental open challenges for complexity theory.

Going a little deeper into the subject of complex modelling, Newman divides the field into eight strands, each of which involves different modelling paradigms and underlying theory: lattices and networks; dynamical systems; discrete dynamics and cellular automata; scaling and criticality; adaptation and game theory; information theory; computational complexity; and agent-based modelling. Of these, cellular automata, game theory and agent-based modelling are directly relevant to the work presented in this thesis and will be examined in more detail in future sections. Lattices and networks are also relevant, in that they underpin all the models that will be defined and investigated, though only a relatively basic level of theoretical knowledge and

methodology from this area is actually applied and required in this thesis.

The potential of statistical mechanics for the representation and analysis of complex systems has been recognised by many authors (e.g. Wang, 2011). One approach of this nature that is worthy of note is the “kinetic theory of active particles” (KTAP), which extends the tools of statistical mechanics to allow for the modelling of entities that interact in a manner that goes beyond the strictly physical and which may indeed affect their physical properties (De Angelis and Delitala, 2006; Bellomo et al., 2009). This is achieved through the introduction of “activity” variables alongside the physical variables of position and velocity to describe the complete state of each particle in a system. The method has also been extended to model complex nonlinear interactions (Bellomo et al., 2010).

A final issue of complex systems modelling that should not be overlooked is the question of model comprehensibility. If a comprehensive modelling approach has been chosen, the resulting model may be extremely complicated, potentially involving many different types of entity, hierarchical structures or the combination of different modelling paradigms (in the case of an agent-based model run over a complex network, for example). Even understanding how a model functions and the structure of its interactions can be a significant challenge and communicating this understanding to someone else may be an even greater one. Buhr (1996) proposes a solution to this issue through the use of “use case maps” to visualise the structure of complex systems. Although use case maps were conceived in the context of understanding software systems, Buhr claims that “they are useful for systems of all kinds”.

2.1.5 Prediction and control

The twin issues of prediction and control in the context of complex systems also represent a significant research topic, for obvious reasons. San Miguel et al. set out some of the main difficulties of prediction, including divergence of true behaviour from model behaviour due to sensitivity to initial conditions; the accumulation of small inexactitudes in the representations of particular processes over many thousands of interactions; the possibility that systems (particularly human systems) may change their behaviour in response to a particular prediction; and the dangers of overfitting and underfitting of predictive functions when working with a high number of dimensions.

To add to this, with reference to a model of plant growth, Hübler (2005) notes the tendency of complex systems to form structures both in a “top-down” sense, in which large scale effects are reproduced on smaller and smaller scales, and a “bottom-up”

sense, in which local patterns grow to influence the entire system. Hübler claims that the interference of these two processes, coupled with issues of path dependence, can lead to behaviour whose character may be difficult to determine without a “holistic perspective” on the system, thus rendering prediction difficult.

Given these difficulties, one approach to prediction in certain complex systems is to use symbolic dynamics, reducing the ‘resolution’ at which the system is analysed and only attempting to make predictions that are meaningful at this level of detail. Using this method, the state space of a complex system or of a model of a complex system, which may have a very high dimension, is partitioned into discrete regions, with the dynamics of the system tracked only to the extent of recording which of these regions the system occupies at particular times. This transforms the dynamics of the system into a time series of symbols (representing the regions), which may be analysed as a stochastic process, allowing for the estimation of probabilities that the system will occupy a particular region at a particular future time, given its current state and possibly its previous states. This approach also allows for the identification of anomalous system behaviour where an observed series of symbols does not match expectations with regard to its statistical properties (Ray, 2004).

Regarding the control of complex systems, San Miguel et al. set out a number of issues. In particular, attempts at precision control of such systems can be subject to significant unintended consequences due to the difficulty of understanding the true relationship between local interactions and global emergent behaviours that is characteristic of complexity. This necessitates the use of “weak” control, in which the objective is to ensure that the *probability distribution* of future states of the system displays an observed behaviour, rather than the future system state itself.

Another approach to the control of complex systems, particularly in the case of human systems, involves setting up the conditions for the system to lead itself towards a desired outcome. For example, this concept has been discussed in the context of improving health care, in which increasing the quality and quantity of interactions between the entities of the system (doctors, patients, etc.) and ensuring that they share the correct goals and incentives could allow the system to move towards a desired state without the need for a single guiding hand (Lipsitz, 2012).

Control may also be considered from the point of view of an individual entity, through its attempts to use its interactions to optimise some property or properties. In this case the problem is in determining a successful strategy for each entity in its interactions with others, which may be achieved through game theoretic

analysis or through allowing for the evolution of the entities by means of genetic algorithms (Holland, 1992), artificial neural networks (see, for example, Gilbert, 2008) or similar.

2.2 Agent-based and individual-based models

2.2.1 Definitions

Agent-based modelling is a means of representing certain kinds of complex system, through which the local interactions that are characteristic of such systems may be explicitly described and observed. While agent-based models (ABMs) may be analysed from a theoretical perspective, in practice their behaviour is generally investigated through computer simulation, an approach to which these models are particularly well suited.

Much as in the case of complex systems themselves, there is no universally agreed formal mathematical definition of an ABM. In his introductory book on the subject, Gilbert (2008) describes agent-based modelling as:

“... a *computational* method that enables a researcher to create, analyze, and *experiment* with *models* composed of *agents* that interact within an *environment*.” [author’s emphasis]

Gilbert subsequently provides qualitative definitions for each of the italicised terms. While most of these are in line with what one might intuitively expect, the explanations of the terms “agent” and “environment” merit further examination.

Having described agent-based modelling as a “computational method”, Gilbert proceeds to define agents in principally computational terms, describing them as “separate computer programs” or “distinct parts of a program” that represent “social actors” (humans or human organisations), which are programmed to react to their computational environment and which interact by passing informational messages (whether voluntarily or involuntarily) and acting on what they learn.

This definition is later developed through the enumeration of four features that agents should possess:

1. Perception (particularly within some local neighbourhood)
2. Performance (incorporating all behaviours that an agent is capable of performing, including “motion” and “communication”)

3. Memory (of previous states and actions)

4. Policy (rules governing how behaviour is determined)

Gilbert explains that these features were chosen with a particular view to the programming of ABMs, making reference to a similar list of features (autonomy, social ability, reactivity, proactivity) proposed by Wooldridge and Jennings (1995), which he judged to be too broad or too vague for this purpose.

In describing the environment of an ABM, Gilbert highlights the distinction between *spatially explicit* models, in which the environment represents a geographical space inhabited by the agents, and spatially non-explicit models, in which agents are linked by means of some abstract network.

In their own practical introduction to agent-based modelling, Railsback and Grimm (2012) provide a similar, if slightly broader, perspective, defining ABMs as:

“... models where individuals or agents are described as unique and autonomous entities that usually interact with each other or their environment locally.”

The authors go on to specify that agents generally possess heterogeneous features, pursue their own objectives, aim to “survive and reproduce” and display “adaptive behaviour”, changing their approach in response to other agents and to the environment. Besides Gilbert’s “social actors”, Railsback and Grimm’s definition encompasses “organisms” and “any other entity that possesses a certain goal.” Again, both spatially explicit and non-explicit environments are mentioned.

Although most authors provide definitions of ABMs that are broadly in line with these, there is a degree of variation over which particular features are emphasised or considered necessary. For example, Macal (2010) specifically underlines the importance of agent learning:

“Agents interact with and influence each other, learn from their experiences, and adapt their behaviors so they are better suited to their environment.”

The general lack of consensus over which features are necessary for the definition of an ABM can occasionally lead to subtle inconsistencies between different authors, such as in this definition by Cartwright (2010), which would appear to contradict Gilbert’s requirement that agents have “memory”:

“Agents are automata that take actions that depend on their current state and that of their neighbourhood.”

Adding to the confusion, inconsistency of terminology extends to the name of the modelling paradigm itself, with Hare and Deadman (2004) identifying at least seven alternative terms that have been used to describe agent-based modelling. To take a single example, while the term multi-agent systems (MAS) is generally used to refer to a specific computational implementation of an ABM or to a software system built on the principles of an ABM (see, for example, Cartwright, 2010), the terms MAS and ABM are occasionally used interchangeably. Shoham and Leyton-Brown (2009) explain that a precise definition of an MAS cannot be provided, owing to the fact that “many competing, mutually inconsistent answers have been offered in the past.” The loose definition of an MAS that they subsequently provide does not differ significantly from the definitions of ABMs given above, this time focusing on the importance of heterogeneity over interaction or adaptation:

“... systems that include multiple autonomous entities with either diverging information or diverging interests or both.”

To attempt a synthesis of these definitions, then, we might state that ABMs involve a large number of entities, distributed throughout some environment, which may represent a geographical or a more abstract space. The entities interact with this environment and with one another, their behaviour being governed by rules that exhibit *some degree of sophistication*, be it in terms of communication of information, adaptation and learning from past experience, goal-oriented decision making, or similar.

Unfortunately, this definition is not entirely satisfactory, since some of the most well known agent-based models *do not* display the sophisticated behavioural features that are explicitly referred to in the definitions quoted above. For example, the Schelling model of segregation (Schelling, 1971) is often held up as one of the first agent-based models, but its ‘agents’ are very basic automata, able to perform only one action (moving) dependent on a single extremely simple calculation of the colour of their neighbours on a grid. They have no memory, they do not communicate or learn and they adapt only in the sense of changing their position until they share their colour with a sufficient proportion of their neighbours.

The phrase “individual-based models” (IBMs) is also frequently encountered in the literature, and may offer a degree of flexibility in the way that models are described. Although Railsback and Grimm explicitly state that the terms IBM and ABM are absolutely synonymous, McKane and Newman (2004) assert that there is in fact a distinction based on the amount of variation between model entities, contrasting homogeneous “individuals” with heterogeneous “agents”. Considering the field as

a whole, there does appear to be a loose distinction made between the two terms, though not necessarily over the question of agent heterogeneity. In general, agent-based models tend to involve more sophisticated entities, displaying more of the special features mentioned in the definitions above (possibly including heterogeneity), while individual-based models may involve simpler entities which display more automatic and “unconsidered” behaviours. However, there is admittedly a high degree of inconsistency in this usage and there is certainly no agreement over where the threshold of sophistication should be traced, beyond which “individuals” become “agents”.

Since the models presented in Part II of this thesis all involve extremely simple entities, which interact in limited and deterministic ways, with no real intention to model true decision making processes or communication, we follow the above distinction, using the phrase “individual-based models” throughout the relevant chapters (Part III involves game theoretic models, for which this distinction is essentially not relevant). However, owing to the wider use of the phrase “agent-based models” in the literature, we will continue to use this more common phrase for the remainder of this review chapter to avoid confusion.

It is worth highlighting the distinction between agent-based modelling and the related field of microsimulation (see Gilbert, 2008). Microsimulation is a technique used principally in demographic modelling, in which a database of records is generated from real data relating to a particular population (either recorded at the individual level or summarised in terms of population statistics), with each record representing an individual. The database is then updated according to assumptions, hypotheses or knowledge of how the population is expected to change over time, with the results being used to make predictions about the profile of the population in the future.

Note that this approach differs from agent-based or individual-based modelling through the lack of a model environment for the individuals to inhabit and through the lack of any kind of interaction between the individuals represented. The use of real data also represents a difference in the common usage of microsimulation models as compared with ABMs, although ABMs are often initialised from real data to some extent when used in experimental research (see, for example, Dunstan and Johnson, 2005).

2.2.2 Types of model and corresponding research questions

Since the definition of an ABM is fairly loose, the term accommodates a very wide variety of different kinds of model.

The overall characteristics of an ABM are determined to a large extent by its intended purpose. The question of how to identify different types of ABM cannot, therefore, be disentangled from the question of the sorts of research questions that ABMs are capable of addressing. On this basis, Gilbert outlines three broad classes of ABM, each of which is associated with different types of research question:

- **Abstract Models** are generally fairly simple and aim to represent real systems only in terms of a few basic or fundamental properties. Such models may provide a proof of concept for some theoretical effect (such as the Schelling model, which demonstrates that high levels of racial segregation can potentially emerge from low levels of racial bias) or they may provide a means for investigating the kinds of local interactions that might give rise to particular global behaviours.
- **Middle Range Models** aim to provide a general representation of a particular class of system, such as a city or a forest ecosystem, without representing any specific real world system. Such models can be used to understand the cause and effect relationships of certain processes in that class of systems (for example, importance of biodiversity for the resilience of an ecosystem) or to examine possible behaviours that the class may exhibit.
- **Facsimile Models** aim to provide as accurate and comprehensive a representation as possible of a specific real world system. Such models are used to predict future behaviour within the system and to determine the effect of potential interventions (such as the effect that a new road may have on traffic patterns within a particular city) A facsimile model may be developed in isolation or through enhancement of a middle range model.

In terms of this thesis, the NANIA model that is defined and analysed in Chapter 4 (and all the models derived from it) falls into the first of these categories. It is an extremely simple and abstract model, whose objective is to investigate the links between local and global behaviour in a theoretical sense. Meanwhile, the SSSG of Chapter 8, while not an ABM, could nevertheless be described as a middle range model of search and concealment situations with the potential to be developed into a facsimile model if developed further, though it remains quite abstract in its current formulation.

Going beyond the broad categories that Gilbert has identified, Hare and Deadman (2004) have attempted to create a complete taxonomy of ABMs. Although their work is now ten years old and although it nominally relates specifically to ABMs used in the field of environmental management, it nonetheless remains a useful tool for understanding the range of different characteristics that such models may display.

Much like the distinction that we established between agent-based and individual-based modelling in the previous section, Hare and Deadman identify the spectrum from simple mechanical entities at one extreme to complex cognitive agents at the other as the most important axis of variation in the field. They then proceed to outline a series of “requirements” that a prospective agent-based modeller may have and use these to create a taxonomic tree by which agent-based models may be categorised, providing examples of models lying at the end of each branch, each drawn from the environmental modelling literature.

The potential “modelling requirements” by which a model may be characterised fall into the following six categories. Note that the names of these areas have been altered from those provided by Hare and Deadman for reasons of clarity:

1. **Modelling space.** This essentially amounts to the distinction between spatially explicit and spatially non-explicit models that we have already established. However, it is interesting to note that Hare and Deadman include models in their framework of “Agent Based Simulation” that essentially have no representation of space at all (for example, the “Rangeland” model of Janssen et al., 2000), and which would therefore not strictly be covered by the majority of the definitions of agent-based modelling discussed in the previous section.
2. **Modelling decision making.** This places a model on a continuum from those whose agents exhibit fixed behaviour to those whose agents use sophisticated rules and algorithms to choose their course of action.
3. **Modelling interaction.** Here, Hare and Deadman identify three distinct categories: completely asocial models, in which agents do not interact; models with “group based interaction”, in which agents interact to perform tasks collectively; and “social adaptation”, in which agents interact through imitation of the behaviour of others (or through some similar process that does not directly affect the state of other agents) either locally, through observation of their neighbours, or globally, through access to summary statistics on the population as a whole.

4. **Modelling intrinsic behavioural adaptation.** While the previous category refers to the character of the interactions within a model, this refers to the freedom that agents have to alter their behaviour in an absolute sense. Hare and Deadman consider three possibilities: models in which agents have no capability to change their decision making strategy; those in which agents may choose between a number of predetermined strategies; and those in which agents may “fine tune” their strategy in a detailed fashion in response to their current state, their observations and their experiences.
5. **Modelling population-level adaptation.** This refers to the existence or otherwise of evolutionary dynamics within the model. Some models have a constant population of agents, while others allow new agents to be created and existing agents to be removed. Removals may occur as a direct or an indirect result of agent performance, often with the goal of determining an optimal strategy or set of characteristics.
6. **Modelling on multiple scales.** This consideration separates mono-scale models, in which all agents operate on an equal footing and in the same environment, from multi-scale models, in which hierarchies of agents may exist, with some able to operate on different time scales, with greater power or with access to higher level information. Alternatively, a model may involve multi-scale agent behaviours, where decision rules involve both individual actions, which operate locally, and collective actions, which operate globally.

Through consideration of each of these six categories, a specific profile may be built up for a particular ABM, with Hare and Deadman using this method to characterise the models used in eleven representative case studies.

2.2.3 Communicating and representing ABMs

A particular problem in the field of agent-based modelling is the lack of consistency in the way that modelling methodologies are reported, leading to problems with the verification and reproducibility of research. Grimm et al. (2006) comment that there exists “no standard protocol” for the description of ABMs and that published descriptions of ABM methodology have often been “hard to read, incomplete, ambiguous, and therefore less accessible [than descriptions of analytical models]”, meaning that they are “not easily reproduced.” Itakura et al. (2010) add that, since ABM research is generally based on computational simulation, there may be discrepancies between the results obtained when models are implemented using different softwares, owing to the effect of bugs or to differences in the accuracy to which floating point values are handled, which may accumulate over a large number of

iterations.

In an attempt to address these issues of inconsistency, a large group of authors working in the field of agent-based modelling combined to propose a standard framework for the presentation of ABMs in the scientific literature: the ODD protocol (Overview, design concepts, details) (Grimm et al., 2006). The protocol was subsequently revised following an extensive review of its use and a consultation with researchers working with ABMs (Grimm et al., 2010). Both the original ODD article and the more recent revised version have been highly influential, particularly in the field of ecological modelling in which the protocol was first proposed. At time of writing, in total the two articles have received over 700 citations (Thomson Reuters, 2014) and the ODD protocol has been employed many times.

The ODD protocol specifies the precise areas that should be discussed when presenting an ABM and the order in which they should be presented. The revised version of the framework is as follows:

1. **Purpose.** The model description begins with a thorough statement of the purpose of the model and the research question that it is designed to address.
2. **Entities, state variables and scales.** The entities that make up the model are described, including specification of any variables associated with them and the way in which these variables relate to real world quantities (if appropriate). Here, the word “entities” is intended to be taken in a very broad sense, including any relevant groupings of agents as well as the environment itself or its component parts.
3. **Process overview and scheduling.** This section sets out the events that occur within the model and the order in which they occur. At this stage, events are described in general terms only. Detailed descriptions are reserved for the section on “submodels” below.
4. **Design concepts** In this section, after an initial discussion of the fundamental theory or methodology that informs the model design (“basic principles”), any key concepts relevant to the model are discussed in more detail. Several of the concepts listed by Grimm et al. are among the features of complexity that we discussed in Section 2.1.2 or were mentioned in the many definitions of agent-based modelling discussed in Section 2.2.1. The complete list is: Emergence; Adaptation; Objectives; Learning; Prediction; Sensing; Interaction; Stochasticity; Collectives; Observation. Some of these concepts are discussed in Section 2.2.4.

5. **Initialisation** The initial conditions used in implementations of the model, or the procedures used to generate these initial conditions, are stated here.
6. **Input data** This section is used to explain which data, if any, are used as inputs to the model while it is running (as opposed to data that is used to initialise the model, which should be discussed in the previous section).
7. **Submodels** This section is reserved for a detailed description of all processes that occur within the model, including equation based submodels, agent decision rules and so on.

As well as making ABM descriptions more readable and making agent-based research easier to reproduce, it has been suggested that the ODD protocol “promotes rigorous model formation”, “facilitates reviews and comparisons of ABMs” and promotes “holistic approaches to modelling and theory”. However, it has also been criticised as being inefficient, particularly for simple models, and as relating poorly to the structures of object-oriented programming (Grimm et al., 2010). It has also been suggested that the ODD protocol provides only a partial solution to the issue of model representation, with ABMs still lacking a standard *mathematical* language (Hinkelmann et al., 2011).

In this thesis, the ODD protocol is used to provide a framework for the description of the NANIA predator-prey model in Section 4.2, a model that provides the foundation for all the material in Part II. Although the NANIA model is fairly simple and could therefore probably be described efficiently without recourse to ODD, the decision to use the protocol was made both for the sake of consistency with the literature and to support this valuable effort to bring uniformity to the field of agent-based modelling research.

In terms of the actual implementation of ABMs, the modelling paradigm is particularly well suited to the techniques of object-oriented programming, in which the environment and agents of all types may be programmed as distinct objects, possessing all the code relevant to their own behaviours and decision making functions (see Gilbert, 2008). Gilbert also compares a number of specific languages and software packages for the programming of ABMs, including the widely used NetLogo (Wilensky, 2015) and Repast (Argonne National Laboratory, 2013), and discusses good practice for presenting agent-based research, without reference to the ODD protocol.

2.2.4 Key concepts and considerations

As we have discussed, one of the most important concepts associated with ABMs, and with complex systems more generally, is that of emergence. Attempting to “figure out what underlying processes give rise to the emergent outcomes” is one of the main goals of much agent-based modelling research (Railsback and Grimm, 2012, chap. 8).

Perhaps unsurprisingly given the general lack of consensus over terminology in the field, there is no universally agreed formal definition of this property. Indeed, attempting to produce a definition of emergence that would be valid and meaningful across the entire domain of complexity science and agent-based modelling research would probably be impossible owing to the wide variety of approaches, perspectives and requirements encompassed by these disciplines.

Luck et al. (1998) root the idea of emergence in economics, tracing it back to Adam Smith’s description of the “natural regulation” of market prices (Smith, 1776, chap. 7). In the modern context, the following criteria, outlined by Railsback and Grimm (2012, chap. 8), provide a useful basis for the understanding of emergent phenomena.

Emergent phenomena or behaviours...

- “... [are] not simply the sum of the properties of the model’s individuals...”
- “... [are] a different type of result than individual-level properties...”
- “... cannot easily be predicted from the properties of the individuals.”

Railsback and Grimm go on to comment that the distinction between emergent and “imposed” behaviours is generally not straightforward and that emergent properties can be hard to quantify.

The authors also remark that “stable” emergent properties may not always manifest themselves immediately in the behaviour of a particular model. Instead, there may be a “warm up” period that must elapse before the effects of interest become apparent, a consideration that should be taken into account when designing ABMs.

Strongly related to the concept of emergence, is that of agent “collectivities”. This phrase is used by Gilbert (2008, chap. 3) to refer to any cluster, organisation or grouping of agents, whether spatially defined or otherwise, that may be observed in an ABM. While a collectivity can be built into the design of a model, they often arise within models as emergent phenomena, and it is these spontaneously generated

collectivities that are generally of most interest to complexity researchers.

As described by Gilbert, collectivities will generally be difficult to define precisely, with ambiguities of membership or shifting membership criteria. Not all members of a collectivity need be of equal status; some may be more “central” than others or exhibit different abilities.

Collectivities are principally identified by some form of shared characteristics or knowledge among their members. Indeed, the sharing of knowledge may significantly increase the reasoning power of a collectivity, beyond that of the individual agents, since it has been shown that, under certain assumptions, the collective knowledge of a group can be considered to be strictly greater than the sum of the knowledge of its members (Nguyen, 2008).

While the *concept* of a collectivity is widely recognised as being central to much agent-based modelling research (consider the many models that seek to understand the formation of animal flocks or shoals, for example Gómez-Mourelo, 2005; Mirabet et al., 2007; Sun, 2013) the specific terminology is not. For example, Railsback and Grimm (2012, chap. 16) prefer the term “collectives”, which they define as “groups that strongly affect both the agents and the overall system”. Nonetheless, “collectivity” remains the most attractive term to describe this phenomenon, because, since the word itself is otherwise rarely used, it carries fewer unhelpful prior associations than other alternatives.

Adaptation is also a key concept of agent-based modelling research. Agent behavioural adaptation is often based around the optimisation of a particular objective function that the agent wishes to maximise through its decisions and interactions. Alternatively, agents may have binary goals that they wish to achieve; for example, they may wish to arrive at a particular destination. In this case, the aim of behavioural adaptation would be to improve their chance of achieving this goal or to reduce the time required to achieve it.

A common approach to the programming of adaptive behaviour is the use of “satisficing optimisation” (see Railsback and Grimm, 2012, chap.11). This technique is necessitated by the fact that individual agents seeking to achieve a particular objective often cannot determine the optimal behaviour to achieve their goal, since they do not have access to sufficient information. They therefore choose behaviours for which their objective function or some measurable projected outcome exceeds a certain “satisficing threshold”. In this way, agents attempt to attain states that are

in some sense ‘good enough’, rather than searching for strictly optimal states.

The concept of learning is related to that of adaptation, but while adaptation may be motivated exclusively by an agent’s current state, the term “learning” implies a more sophisticated process, in which individual agents or groups of agents may use past experience and inference to build up some form of model of their environment or of other agents, using this model to determine appropriate behaviours. Gilbert (2008, chap. 1) lists three forms of learning in ABMs:

- Individual learning, in which agents learn from their personal experience;
- Evolutionary learning, in which an entire system ‘learns’ by means of the ‘survival of the fittest’;
- Social learning, in which agents learn through imitating or adapting the behaviour of others.

One of the most important considerations in the design of ABMs is the question of how events should be scheduled and how time should be modelled. In most ABMs, time proceeds at a constant rate by means of a series of iterations, at which some or all agents ‘take turns’ to take some form of action. This process may involve “sequential asynchronous execution”, in which the sequence in which agents take their turns at each iteration is predetermined, with the effects of an agent’s actions being resolved immediately; “random asynchronous execution”, in which the sequence of agents is randomly generated after each iteration, again with actions being resolved immediately; or “simulated synchronous execution”, in which agents take turns according to any sequence, but with all actions being resolved simultaneously (Gilbert, 2008, chap. 2).

The importance of scheduling decisions on the results obtained from ABMs has been demonstrated by Caron-Lormier et al. (2008), who broadly argue for asynchronous over synchronous execution, asserting that it offers a “good approximation of real continuous time” and that models based on synchronous approaches may offer “a poor representation of reality”. This conclusion is based on a comparison of the different scheduling methods in a simple ABM of an ecosystem, in which the authors noted that the synchronous approach produced oscillations in the energy of trophic levels that did not correspond to the behaviour observed in real ecosystems. The conclusion directly contradicts that of Gilbert, who claims (without explanation) that synchronous execution is the best option.

An alternative option for the modelling of time is “event-driven simulation”, in which time is represented indirectly through the sequence of events that occur in a model,

with the durations between these events left unspecified (Gilbert, 2008).

When designing an ABM, it is also necessary to decide which features will be modelled by means of stochastic processes and which will be modelled by deterministic processes. Provided that care is taken over the choice of statistical distributions, stochastic processes can provide a useful representation of effects that would be too complex to include in a strictly deterministic model. They can also be matched to observed variations in a real system even if the true underlying processes governing these variations are not understood. However, for any given scenario, models involving stochastic elements must generally be run many times to determine the full spread of possible outcomes and their relative probabilities (see Railsback and Grimm, 2012, chap. 15).

Stochasticity can also be employed in “middle range models” to ensure that artificial scenarios are truly representative of the diversity of systems observed in the class that the model is intended to represent. For example, a model of an industrial network may generate random links between firms according to some appropriate algorithm in order to represent a variety of different possible networks that share some desired property, such as a particular degree distribution for their nodes (see Gilbert, 2008, chap. 2).

2.2.5 Motivations for agent-based modelling

Many criticisms have been levelled against agent-based modelling as a scientific approach. Difficulties have been highlighted in the design, calibration and manipulation of ABMs and in the verification of the results derived from them. It has also been suggested that ABMs are not able to simultaneously “cope with multiple levels of abstraction” and as a result of these criticisms, the very nature of these models as valid research tools has been called into question (Drogoul, 2008). It is therefore important to consider what advantage ABMs may have over alternative types of model.

It is worth mentioning that, while there is naturally a universal recognition that agent-based modelling, in common with all other modelling paradigms, has its weaknesses, there is not necessarily a universal agreement over what these weaknesses are. For example, Railsback and Grimm (2012, chap. 1) dispute the assertion that ABMs are unsuitable for the modelling of “multiple levels of abstraction”, instead seeing them as fundamentally “across level” models, in which a system, its inhabitants, and the relationships between these two representational scales may be modelled simultaneously.

The most obvious potential benefit of ABMs over reductive equation based models is that the former represent processes in greater detail and may therefore provide more information on the functioning of a system (Macal, 2010). This reasoning is supported by a number of pieces of work, including an investigation by Itakura et al. (2010), which found that an ABM was able to provide a better match to the dynamics of a chronic viral infection than a model based on differential equations (in common with the work of Caron-Lormier et al. (2008), the difference was largely related to the presence of dynamic oscillations that did not correspond to the behaviour of the real system).

ABMs may also prove advantageous for the modelling of systems in which little data is available on the global characteristics of a population, but where the behaviour of individuals is much better understood. For example, Mock et al. (2007) offered this reason for their decision to use an ABM to model the interaction between killer whales and their prey.

Cartwright (2010) similarly presents the case for the use of ABMs to represent systems that resist traditional equation based approaches. Cartwright's particular concern is the topic of "excitable media", materials that require a period of inactivity (the "refractory period") between periods of stimulation, thus limiting the possible behaviours of waves that propagate through them. The author goes on to argue that media for which global behavioural laws cannot be easily derived but for which local behavioural rules *can* be simply described (such as crowds participating in a "Mexican Wave") may be most naturally and effectively modelled by means of agent-based approaches.

Oakes (2008) argues for the importance of agent-based modelling (particularly in the field of epidemiology), citing the ability of ABMs to successfully model complex dynamics, to explicitly examine the effect of policy interventions on multiple agents simultaneously, to represent the two-way interactions between people and their environment, to model "purposeful" individual activity and to explicitly represent the mechanisms behind observed changes in a system, rather than only the effects of such changes. Patlolla et al. (2006) also advocate the power of agent-based modelling (again focusing on its epidemiological applications), with particular reference to the representation of agents whose behaviour is governed by their desires to achieve personal goals (such as finding something to drink when they are thirsty) rather than by abstract rules derived from global theory. This explicit linking of intention and behaviour is not possible in other forms of modelling.

Several authors also outline the specific benefits of explicitly spatial ABMs over non-spatial models. Itakura et al. (2010) comment on the importance of spatial factors in drawing meaningful biological conclusions from their virus infection model, while Dunstan and Johnson (2005) state that the explicit modelling of space is essential to provide good representations of certain real ecologies, which may display multi-scale spatial patterns, high levels of variability between individuals at different spatial locations, and in which species may interact on a highly localised basis (referring in particular to communities of marine organisms living on a jetty wall). The authors argue that these factors mean that only spatially explicit agent-based models are capable of exhibiting the emergent features of interest in such systems.

Meanwhile, Railsback and Grimm (2012, chap. 1) highlight the example of an ABM that was designed to model the spread of rabies in fox populations and later extended to include the modelling of vaccination programmes. This model was shown to provide more accurate results than traditional population ecology models (based on differential equations) owing to its explicit modelling of space and to the fact that it was able to accurately represent the rare long range migrations of individuals that drove the characteristic spatial patterns of rabies outbreaks that were observed in the field (Jeltsch et al., 1997; Eisinger et al., 2005; Eisinger and Thulke, 2008; Thulke and Eisinger, 2008).

It should however be noted that, in the absence of other factors, the importance of the explicit modelling of space does not constitute an argument in favour of agent-based modelling. Other forms of modelling – for example, deterministic models based on systems of partial differential equations – are also capable of representing space explicitly and of generating spatial patterns.

2.2.6 Application and analysis

Gilbert (2008, chap. 1) provides a list of different areas in which agent-based modelling has been applied, with examples of published models in each area. The list includes models of urban systems, opinion dynamics, consumer behaviour, industrial networks, supply chains and electricity markets.

ABMs have also been used for such diverse purposes as designing evacuation schemes for large buildings (Rahman et al., 2008), investigating the supply of Halal food (Lam and Alhashmi, 2008), understanding the spread of the H5N1 virus (Amouroux et al., 2008) and helping tourists to plan holidays (Valdés and Cubillos, 2008).

However, despite the wide use of ABMs, tools for their analysis remain underdevel-

oped and lack a standard framework; Hinkelmann et al. (2011) comment that “it is difficult to bring mathematical analysis tools to bear [on ABMs]”. For this reason, as discussed by Railsback and Grimm (2012, chap. 5), it may often be necessary to develop improvised and *ad hoc* metrics for the measurement of the effects that we may wish to observe in any specific ABM.

Because there are no standard tools, discussion of the analysis of ABMs is restricted to the description of loose heuristics, which must be interpreted to suit the particular model that is being studied. Railsback and Grimm (2012, chap. 22) present the following list of ten such heuristics:

1. Examine the behaviour of the system for extreme parameter values;
2. Find “tipping points” in the emergent behaviour of the model;
3. Visualise the model in different ways;
4. Step through a simulation iteration by iteration to understand the causal mechanisms driving observed behaviour;
5. Identify interesting or unusual patterns in the observed behaviour;
6. Fix certain parameters at “interesting” values and allow others to vary;
7. Use different “currencies” (see below) to evaluate model outcomes;
8. Analyse simplified versions of a model;
9. Understand a model from the ‘bottom up’, first examining individual entities, then the relationships between them, building up a picture of the complete system;
10. Consider unrealistic scenarios or parameter values to determine which realistic features are necessary to produce the observed behaviour and which could be neglected.

The word “currencies” is used here to describe different ways of measuring model behaviour. The examples of such “currencies” proposed by Railsback and Grimm (2012) include global statistical quantities, parameters of best-fit statistical distributions, statistics derived from time series, spatial statistics, measures of heterogeneity between agents and properties related to model stability (such as the time required to return to equilibrium after a perturbation or the size of the basin of attraction of a particular fixed point).

As evidenced by these heuristics, the analysis of ABMs remains largely reliant on the gathering of data from repeated computer simulation rather than on any form of theoretical analysis of the rules that govern the behaviour of individual agents.

2.2.7 The practice of agent-based modelling

Owing to the fundamental differences between agent-based modelling and more established reductive mathematical modelling techniques, the design and implementation of an ABM requires a specific procedure and set of considerations. Gilbert (2008, chap. 3) sets out the process in detail.

After defining a research question suitable for investigation by means of agent-based modelling, Gilbert suggests that the first step should be to specify all the agents that will feature in the model and to identify the ways in which they may affect or be affected by their environment (including other agents). The form of this environment should be carefully considered, with decisions made over which features to include and which to omit. The next step is to design and program the model in an appropriate programming language so that it can be implemented computationally. When an initial version of the model program has been created, it must be subjected to verification (testing to ensure that the program does what it is intended to do) and validation (testing to determine whether the behaviour of the model provides a good representation of the real system or systems of interest). Finally, the model is ready for use as an analytical tool, and sensitivity analyses and robustness analyses may be performed. If possible, model outputs may also be compared against empirical data from the real system.

An alternative perspective on the design of ABMs is provided by Railsback and Grimm (2012, chaps. 17-19), who discuss the question in terms of “pattern-oriented modelling”. With this approach, the starting point of the design process is the identification of a number of large-scale qualitative patterns observed in a real system or systems, the aim being to create a simple ABM that replicates these patterns. In this way, it may be possible to determine the nature of the local processes and interactions that are driving the emergence of these patterns in the real system.

Gilbert’s procedure for verification is focused on the use of good programming practices, including the use of an object-oriented rather than a linear programming language, the insertion of debugging switches, the addition of checks that variables take valid values and so on. In comparison, his proposed procedure for validation involves the investigation a series of questions about the model’s behaviour, the particular focus of which varies according to the type of model to be validated. For abstract models, validation involves determining whether the model produces any expected large scale patterns (as in Railsback and Grimm’s interpretation of “verification”); for middle range models, it involves checking that model behaviour is statistically similar to the behaviour of relevant systems in the real world; and for facsimile mod-

els, it involves the attempted ‘prediction’ of past system behaviours given historical data.

Unfortunately, the distinction drawn by Gilbert between the terms “verification” and “validation” is not universally recognised. Gómez-Mourelo (2005), for instance, outlines a five step “verification” procedure, which involves the derivation of a set of partial differential equations (PDEs) from a given ABM. The behaviour described by the PDEs is then statistically compared with the behaviour of the ABM, which “builds up our confidence in the [model] and results in a verification of the [model]”. This procedure is clearly more in line with Gilbert’s description of “validation” than “verification”, although it is not altogether clear that matching the behaviour of an ABM to that of a set of equations that were derived from it would reveal anything of value about the quality of the model itself. However, such a procedure could potentially provide grounds for confidence that analytical results calculated from the derived PDEs were also relevant to the original ABM.

Railsback and Grimm (2012, chap. 18) have another interpretation of the terms “verification” and “validation”, considering the former to refer to the practice of ensuring that a model reproduces those large scale emergent patterns of the real system that it was *designed* to reproduce, and the latter to refer to the practice of checking that the model also reproduces secondary patterns or features of the real system that were *not considered* during the design process. This approach does have similarities to that of Gilbert, in that it distinguishes between checking that a model does what it was intended to do and checking that it is a good match to the real system of interest, though the interpretation is somewhat different.

Sensitivity analyses and robustness analyses, as described by Gilbert, are both means of determining the effect of changes on model behaviour, but the two terms refer to changes of different natures. Sensitivity analyses involve changing parameters to see how model behaviour is affected and to see which changes have the largest impact on this behaviour across the parameter space. Robustness analyses involve making fundamental changes to the structure of the model, perhaps removing certain features, altering assumptions or changing the form of submodels, assessing whether these changes have a significant impact on model behaviour and thus determining whether the features, assumptions or submodels that were changed are genuinely necessary to produce the observed dynamics. For an example of a thorough robustness analysis, see the work of Dunstan and Johnson (2005), who systematically remove processes from their marine epibenthic community ABM to determine how each one contributes to the overall system behaviour.

Railsback and Grimm (2012, chap. 23) provide detailed explanations of how to conduct sensitivity and robustness analyses, also adding a third analytical approach: uncertainty analysis. Uncertainty analysis is used to determine the extent to which the uncertainty associated with calibrated parameter values could affect model behaviour (the issue of choosing and calibrating model parameters in the first place poses problems of its own; see Railsback and Grimm, 2012, chap. 20). The method of uncertainty analysis described by Railsback and Grimm involves the creation of prior distributions on the values of parameters, with normal or uniform distributions, and determining the resulting distribution of possible model outcomes by means of Monte Carlo simulation. This provides a means of establishing the level of confidence that should be afforded to the conclusions drawn from a model.

2.2.8 Mathematical foundations

Perhaps the most significant issue associated with ABMs is the lack of rigorous mathematical theory to support and inform their use. Cartwright (2010) comments on this issue in the context of the discipline of sociology:

“At present, progress [...] is hampered by the fact that there is not the same depth of knowledge about how to deal theoretically with discrete systems such as cellular automata and agent-based models as there is of the continuum systems studied in the past...”

Nguyen et al. (2008) make a similar point:

“There are no general theories linking the knowledge of the individuals’ rules to the emergence of a global property.”

McBurney and Omicini (2008) further emphasise the importance of this issue, describing the situation as:

“... a point of crisis for agent-based models and technologies, where foundations have to be reconsidered...”

These quotations demonstrate the broad agreement that exists over the necessity for a significant improvement in the theoretical foundations and mathematical understanding of agent-based modelling. As long as the discipline is not built on a solid foundation of theory, our confidence in the conclusions drawn from ABMs must always be called into question. Furthermore, the lack of a unified theoretical framework means that tools for the analysis of ABMs are frequently invented and reinvented on a case-by-case basis, leading to a considerable amount of wasted intellectual effort and meaning that, when reviewing agent-based modelling research,

methodology must frequently be evaluated from scratch.

Naturally, attempts have been made to create a theoretical framework for agent-based modelling, but none has yet gained universal acceptance. In any case, certain of these attempts, such as KTAP (De Angelis and Delitala, 2006, see Section 2.1.4), do not address the issue directly, preferring to represent the behaviour of an ABM in a form that is already well understood (such as a system of PDEs) rather than attempting to create a true mathematical theory of agent-based modelling itself.

Since the concept of emergence is such an important one in the field of agent-based modelling, general theoretical results on the links between local processes and global emergent behaviours would be extremely valuable to the discipline. However, although many researchers have attempted to address this issue, few definite formal conclusions have been drawn.

Global features are commonly stated to emerge from local interactions, without further explanation of how this might occur and without attempts to draw parallels or to identify general rules that apply to similar emergent processes across other models (see, for example, Dunstan and Johnson, 2005). Other authors identify causal links between the nature of local interactions and the character of global behaviour (such as the link between the way in which individuals observe their neighbours and the structure of resulting flocks, Mirabet et al., 2007; Chen et al., 2008), but this is not equivalent to the development of a genuine theory that links local and global behaviours. Those more theoretical approaches that do exist tend to focus on specific types of model or specific types of behaviour rather than on general theories of agent-based modelling (see, for example, the more formal examination of flocking models presented by Sun, 2013).

The lack of consensus over the definitions of ABMs and of the key terms associated with them and the consequent diversity of models to be found in the literature represent formidable barriers to the formalisation of the discipline. These factors also mean that there is no agreement on what the starting point of such a local-to-global theory might be.

Although novel approaches to the problem have been investigated in recent years, such as the use of “equation free” methods (see, for example, Siettos, 2011), the question of how to create a theory of agent-based modelling, which roots the concept of emergent behaviour in a formal mathematical foundation, remains largely open.

These issues, relating to the lack of formal foundations for agent-based modelling and, more specifically, to the lack of a general framework for understanding the connections between local interactions and global emergent behaviours in ABMs, are key motivators for the work presented in Chapter 6 of this thesis, in which we investigate the divergent influences of different types of local transition on the long term equilibrium behaviour of a particular family of IBMs.

2.3 Cellular automata

2.3.1 Context and definitions

A cellular automaton¹ (CA) is a form of spatially and temporally discrete dynamical system. The most well-known example is Conway’s “Game of Life”, which generated considerable interest after being featured in Gardner’s *Mathematical Games* feature in *Scientific American* in the early 1970s (Gardner, 1970, 1971). However, the origins of these models are often traced back to work on self-reproducing systems by Von Neumann and Ulam in the 1950s (Gardner, 1971; Wolfram, 1983) or to work on “finite automata” by Tsetlin in the 1960s (Vanag, 1999).

One of the most thorough and influential works on the subject of CAs is Wolfram’s, *A New Kind of Science* (2002), in which the author puts forward the case for these models (and other similar discrete systems, described collectively as “simple programs”) as representing a new class of mathematical objects, with the potential to model the behaviour of the universe on a deep and fundamental level.

In contrast with ABMs, there is broad consensus over the definition of a CA, although, owing to the wide range of fields in which CAs are used, definitions are often formulated loosely rather than in formal mathematical terms. For example, Gardner (1971) defines CAs (referred to as “uniform cellular spaces”) as:

“... equivalent to an infinite checkerboard. Each cell can have any finite number of “states,” including a “quiescent” (or empty) state, and a finite set of “neighbor” cells that can influence its state. The pattern of states changes in discrete time steps according to a set of “transition rules” that apply simultaneously to every cell.”

¹ Although some authors use the term “cellular automata” to refer to a single model (considering the separate cells to constitute the “automata”), in this thesis, the terms “cellular automaton” and “cellular automata” are used as the respective singular and plural forms when referring to such models. In any case, for the most part, the terms will be substituted by the abbreviations CA and CAs, thus avoiding any potential source of confusion.

While the description of an “infinite checkerboard” suggests a square lattice, Gardner later states that other tessellations may be used, but qualifies this with the comment that any such regular tessellation can, in any case, be simulated on a square lattice through an appropriate definition of the neighbourhood of a cell, which need not necessarily be contiguous (indeed, Wolfram (2002, pp. 327-336) observes that, in many cases, the structure of the underlying lattice does not affect large scale behavioural patterns in CAs and CA-like systems).

Gardner’s description was streamlined by Wolfram (1983), who shifted the focus slightly to the role of CAs as models of physical phenomena:

“Cellular automata are mathematical idealizations of physical systems in which space and time are discrete and physical quantities take on a finite set of discrete values. A cellular automaton consists of a regular uniform lattice... usually infinite in extent... A cellular automaton evolves in discrete time steps... [and the state of a cell is] affected by the values of variables at sites in its “neighborhood” on the previous time step... [Cell states are] updated simultaneously... according to a definite set of “local rules.”

Wolfram went on to limit the scope of these “local rules”, suggesting that configurations in which all cells occupy the “null” state should remain so for all future times and that rules should have a degree of spatial symmetry in terms of how they consider the neighbours of a cell. However, these restrictions were described as “inessential”, apparently intended to limit the number of possible rules and to focus on rules with the most physically relevant behaviour, rather than to narrow the definition of CAs as mathematical objects.

A more formal description is provided by Hogeweg (1988), who defines CAs as “large tessellations of identical finite-state” cells, each of which is defined by a triplet $\langle I, S, W \rangle$, where I is a finite set of inputs (an ordered or unordered n -tuple of states of some locally defined neighbourhood of cells), S is a finite set of states that a cell may take on (and which also establishes the possible values of the inputs I) and W is a function that maps from a particular state and set of input states to a new state in S .

While other authors may place more or less emphasis on particular features to suit the requirements of their discipline, the majority of definitions are in line with these (see, for example, Itami, 1994; Vanag, 1999; García-Morales, 2013). Drawing on all these sources, we formulate the following (non-rigorous) definition, which should be

broad enough to be applicable in the large majority of cases found in the literature.

Definition 2.3.1. A *cellular automaton* (CA) consists of the following:

- A simple graph², G , whose vertices are referred to as **cells**;
- A countable set, \mathcal{C} , containing the states that individual cells can exhibit;
- A deterministic local transition rule, $\mathfrak{T}_{\text{local}}$, which establishes a new state for each cell, given its current state and the current states of its neighbours.
- A global transition rule, \mathfrak{T} , which applies the local transition rule to all cells simultaneously.

The CA may be run by specifying initial states for all cells and iteratively applying \mathfrak{T} to create a sequence of new generations of cell states.

Note that this definition permits CAs to be defined over any finite simple graph G rather than restricting them to two-dimensional lattices based on tessellations of regular polygons. This more general type of CA is discussed by Wolfram (2002, p. 930), who observes that such a generalisation is reasonable provided either that G has the same structure around each vertex, thus making it clear how vertices in a neighbourhood should be ordered (thus allowing $\mathfrak{T}_{\text{local}}$ to differentiate between the “northern”, “eastern”, “southern” and “western” neighbours of a cell in a rectangular lattice, for example), or that the local transition rule does not depend on the order of cells in a neighbourhood (with the exception of the central cell).

2.3.2 Special cases and extensions

Within the framework of those CAs that are consistent with Definition 2.3.1, there are a number of special cases of interest. For example, **totalistic** CAs, such as Conway’s “Game of Life”, have numerical cell states and local transition rules that depend only on the sum (or the mean) of the states of cells in a neighbourhood (and possibly on the state of the central cell) (Wolfram, 2002, p. 60), **additive** CAs have local transition rules that can be written in terms of sums of states in the neighbourhood (typically using modular arithmetic) (Wolfram, 2002, pp. 952-953) and **reversible** CAs have bijective global transition rules, such that the behaviour may be evolved backwards as well as forwards in time (Wolfram, 2002, pp. 435-457).

² A “simple graph” is an unweighted, undirected graph, in which every edge joins two distinct vertices, and every pair of vertices is joined by at most one edge (see Bondy and Murty, 1976, p. 3).

Going beyond the most basic CAs, many authors have considered extensions to the concept through the relaxation of certain of the rules. While many such extensions amount to alterations to the graph structure, the number of states in \mathcal{C} or the way that neighbourhoods are defined (see Wolfram, 1983), all of which are covered by Definition 2.3.1, more fundamental changes to the concept have also been made. For example, CAs may be defined with probabilistic transition rules (Vanag, 1999) or with behaviour that is subject to noise (Wolfram, 1983), they may be influenced by external inputs or the structure of their underlying graph may change over time (Hogeweg, 1988). CAs have also been adapted for use in conjunction with geographic information systems (GIS), such that they may be more easily applied in real world contexts.

Continuous CAs, in which the discrete cell state space \mathcal{C} is substituted by a continuous subset of the real numbers, have been considered by several authors (see, for example, Wolfram, 2002, p.155) and are of particular importance, owing to their ability to represent the behaviour of systems of partial differential equations (Rausch, 2001) in a manner akin to the finite difference method (see Strauss, 2008, pp. 199-222). Some models also involve continuous times, such as CA-ODE models, described by Vanag (1999) as being “intermediate between... simple CA and DE in partial derivatives”.

2.3.3 Behaviours and key concepts

The concept of emergence (referred to as “unexpected behaviour” by Vanag, 1999) is key to the study of CAs. Since CAs are generally described with fairly simple rules and often display patterns on larger scales, emergent behaviour is an intrinsically important feature of many such models.

The most widely acknowledged system for classifying CAs in terms of their behaviour was provided by Wolfram (2002, from work first published in 1983), who undertook a comprehensive investigation of one-dimensional CAs alongside a broader examination of more general CAs and related discrete systems. As a result of this research, Wolfram concluded that almost all CAs (barring rare borderline cases) could be assigned to one of four categories, based (initially) on a qualitative observation of their behaviour when run from randomly generated initial conditions (implicitly assuming a random uniform selection of initial conditions across a model’s complete state space) (Wolfram, 2002, pp. 231-249):

- **Class 1.** In these CAs, all cells evolve to the same state; the system tends to a uniform equilibrium. In such systems, almost all the information contained

initial conditions is destroyed, although the initial conditions may determine which of several uniform equilibria the system ultimately attains.

- **Class 2.** These CAs evolve to either an invariant (though spatially non-uniform) state or to a periodic sequence of states. In these systems, information contained in the initial conditions may be preserved, but is not transmitted spatially throughout the system.
- **Class 3.** These CAs exhibit apparently random, non-periodic behaviour which persists for all time (discounting the enforced long term periodicity of systems of finite size, with a finite set of cell states). In these systems, information contained in the initial conditions is transmitted throughout the system.
- **Class 4.** These CAs exhibit complex non-periodic behaviour, with self-organisation into persistent localised structures, which displace themselves through space and interact with one another. In these systems, information contained in the initial conditions is transmitted, but in a limited way, through the behaviour of the localised structures.

It should be noted that these classes are based on the behaviour exhibited by a CA for the majority of possible initial conditions. There may exist specific initial conditions for which a given CA exhibits behaviour of a different class from that to which it properly belongs. For example, Conway’s “Game of Life” is a class 4 CA (Wolfram, 2002), but any initial condition over any graph involving only cells in the “quiescent” state (Gardner, 1970) is invariant (class 1 behaviour).

A discussion of the specific relevance of Wolfram’s four classes for the IBMs considered in Part II of this thesis may be found in Section 5.3.6.

One of the most important results in CA theory is Wolfram’s proof (2002, pp. 675-691) that even very simple class 4 CAs can be capable of universal computation, which utilises the ability of certain CAs to simulate the behaviour of other discrete systems, and ultimately to simulate the behaviour of a Turing machine.

The concept of randomness is also important in the field of CAs. In particular, Wolfram (2002, p. 299-301) suggests that the simple rules behind certain CAs (and related discrete systems) may represent the only fundamental mathematical processes capable of generating ‘randomness’ from order, dismissing two other candidates in stochastic systems (in which randomness is an external input) and chaotic systems (in which randomness is reproduced from the initial conditions on larger scales). Wolfram (2002, pp. 596-597) even suggests that CAs may be used to test

patterns for ‘randomness’, since, given a set of initial conditions that appear to be random, through their evolution, CAs may highlight subtle regularities that would not otherwise be readily apparent.

Many of the concepts and methods familiar from the field of nonlinear dynamical systems, such as the existence of multiple equilibria, phase transitions and conserved quantities, have also been studied in the context of cellular automata (Hogeweg, 1988; Wolfram, 2002, pp. 337-342, 981-983, 1022-1023), as have concepts drawn from statistical mechanics, such as entropy and the convergence of systems to dynamic equilibria, defined by global quantities analogous to temperature or pressure (Wolfram, 1983, 2002, pp. 441-457).

One concept that is specific to CAs (although linked to the notion of irreversibility more generally) is the idea of a “Garden of Eden”, a particular configuration of states for the cells of a given CA that can never occur as the result of the ongoing dynamics of the system (including as an invariant state) and which can therefore only be observed in the initial conditions. While it is often easy to prove the existence of “Garden of Eden” configurations, finding particular examples can be challenging (Gardner, 1971); the search for “Gardens of Eden” of minimal size in Conway’s “Game of Life” has been ongoing since the 1970s (Hartman et al., 2013).

2.3.4 Applications and relevance

Vanag (1999) describes CAs as a “universal tool with which the highly complex behaviour of nonlinear dynamical systems can be analyzed and modelled” and CAs have indeed been used as models for a wide variety of real world systems. In terms of Gilbert’s (2008) classification scheme for ABMs (see Section 2.2.2), the nature of CAs as extremely simple models dictates that, in the majority of applications, they fall into the category of “Abstract Models”, used to explore possible mechanisms driving observed global behaviours or to understand processes in very general terms.

For example, through comparing various candidate transition rules, Xiang and Bishop (2010) use a CA model of sand dune dynamics to determine the nature of local processes that generate large scale dune patterns in the real world. Itami (1994) similarly uses a CA to model vole population dynamics, in an attempt to understand the mechanisms that may be responsible for the significant fluctuations observed in such populations in the wild. Other applications of CA modelling include understanding the growth of cancerous tumours (Hatzikirou et al., 2010), traffic flow (Tian, 2009), the proliferation of invasive tree species (Cannas et al., 2003) and the collisions of microscopic particles, using the well-known “Lattice-Gas Cellular Automata”

model (Vanag, 1999). Additional applications are summarised by Gardner (1971), Wolfram (1983) and Vanag (1999).

Beyond their role as abstract models of real world systems (and, in the case of continuous CAs, as discretisations of continuous systems, as discussed in Section 2.3.2), other uses for CAs have been suggested. Hogeweg (1988) discusses the use of CAs as “paradigm systems”, which may be used to investigate important concepts, such as symmetries, causality or emergence, without reference to a specific real world context, while Vanag (1999) suggests that CAs may be used to test the validity of the results of aggregated models in statistical physics. More speculative applications include the use of CAs as an encryption tool (Wolfram, 2002, pp. 598-606).

As mentioned in Section 2.3.1, some of the boldest claims for the relevance of CAs are to be found in the work of Wolfram, who describes the discovery of complex behaviour in CAs and other related systems, referred to collectively as “simple programs”, as “one of the more important single discoveries in the whole history of theoretical science” (Wolfram, 2002, p. 2). He proposes CA-like processes as the fundamental mechanisms behind the patterns and behaviour observed in a wide of physical and biological phenomena (see pp. 363-432), going on to suggest that, on the most basic level, the universe itself may be a simple program and that “the vast majority of physical laws discovered so far are not truly fundamental, but are instead merely emergent features of the large-scale behavior of some ultimate underlying rule” (p. 470), thus echoing the hypothesis of “the universe... [as] a cellular automaton run by an enormous computer”, which had been proposed as far back as the early 1970s (Gardner, 1971).

2.3.5 Advantages and disadvantages

Although stated with specific reference to a model of forest succession, the comments of Hogeweg (1988) on the advantages of CAs over other modelling paradigms are of general relevance. The first stated advantage (described by Hogeweg as “extendability”) is that, since CAs are based on local rules that are frequently intuitively straightforward to understand, CAs are often easy to alter to take account of alternative or additional assumptions and features. The second advantage (“observability”) is that making observations of a CA model is generally simple, since “the output of the model is “similar” to the real system”. Both these advantages, then, are related to the clarity and comprehensibility of CAs as modelling tools.

On the other hand, Hogeweg cites the synchronous updating of cell states as a disadvantage of CAs, since it can lead to “artefacts” and behaviours not present in a

corresponding physical system. She also cautions against the use of CAs, a space-oriented modelling approach, in situations where an agent-oriented approach would be more natural.

The clarity of “the correspondence between physical and computational processes” in CA models is also noted as an advantage by Itami (1994), before going on to list several further advantages, some of which are not in line with general opinion. The claimed advantages include the ability of CAs to produce more “comprehensive” behaviour than mathematical equations, the fact that they can be simulated precisely without approximation and their capacity to “mimic the action of any possible physical system”. While the second of these claims is clearly true and the first is open to interpretation, the last claim (which is not justified by the author) would appear to be rather strong, since there exist many real world systems that are not generally modelled using CAs. The irreducibility of certain CAs (in the sense that their behaviour cannot be simulated by any more efficient system) is also cited as an advantage by Itami, since systems whose behaviour is governed by any such CA can only be precisely simulated with the CA itself. However, it could be argued that this property could only truly be considered an advantage if it had previously been established that the behaviour of a given system of interest was genuinely determined by a CA process and that no other model could provide a sufficiently accurate representation of its behaviour.

Vanag (1999) asserts that CAs are particularly well-suited to modelling noisy systems (owing to the fundamental characteristics of their discrete dynamics), systems involving cooperative local behaviour and those exhibiting a high degree of heterogeneity, such that quantities averaged across the system provide a poor representation of its state. It should be noted, however, that many of these stated advantages could equally be applied to ABMs. It would perhaps be most accurate to say that it is the combination of these features with the unique simplicity of the CA approach that sets the modelling paradigm apart from its alternatives.

2.3.6 Understanding and analysing

One approach for understanding and analysing CAs is to attempt to define algebraic formulae that precisely represent their behaviour, such that, given a particular model, for any future time, the state of every cell could be calculated without the need for explicit simulation. It might be expected, however, that the value of such a strategy would be limited, since the fact that CAs are driven by simple discrete rules rather than by equations is one of their defining features.

Indeed, Wolfram (2002, pp. 606-616) argues that, in the vast majority of cases of CAs that exhibit complex behaviour, no formula could be found that would offer any computational advantage over explicit simulation of the system for the purpose determining future states. For example, while Boolean expressions for the configuration of any two-state CA can be stated, in all but the most trivial cases, separate expressions must be written for each future time step and the length of these expressions may grow extremely rapidly for more distant prediction horizons, such that the expressions have little practical value (Wolfram, 2002, pp. 616-618).

On the other hand, useful formulae can sometimes be stated for particular families of CAs, such as those whose transition rules are equivalent to simple arithmetic operations (generally defined in modular arithmetic, to ensure that the cell state space is finite), such as addition or multiplication Wolfram (2002, pp. 613-615). Even where CAs do exhibit complex behaviour and precise and explicit formulae cannot be found, partial solutions may exist. García-Morales (2013) has demonstrated that, in some cases, it is possible to create formulae to determine future states that are “mostly valid” save for rare “defects” in the model dynamics, whose nature and effects may be predicted, even if their occurrence may not.

So far, we have discussed attempts to create formulae that represent CA behaviour exactly. An alternative approach is to represent the behaviour approximately, through equations that describe changes in key summary variables, such as the global density of cells exhibiting a particular state. Such approaches may be data-focused, attempting to create equations that match observations made from the CA (see Hogeweg, 1988, pp. 92-94), they may draw on the techniques of statistical mechanics (see Wolfram, 1983) or they may be based on mean field methods, which are discussed in more detail in Section 3.2.

Alternatively, the statistical properties of CAs may be used to analyse model behaviour without attempting to produce equations or formulae to represent their dynamics. Since CAs are explicitly spatial models, alongside the quantities used in statistical mechanics, we may also consider quantities intended to identify spatial patterns and regularities, such as correlation coefficients calculated on the cell states or the relative frequencies of occurrence of particular small configurations of cell states (Wolfram, 1983, 2002, pp. 588-597).

Other authors have attempted to analyse CAs through consideration of the equilibria and their basins of attraction, taking a more traditional dynamical systems approach to the issue (see, for example, Tian, 2009). However, owing to the inherent

complexity of the behaviour that CAs are capable of displaying, a phenomenon that is, by definition, difficult to analyse reductively in terms of simple expressions and processes, one of the most important analytical approaches for the study of CAs has been repeated simulation and visualisation of the dynamics, allowing researchers either to exhaustively explore the spaces of possible rules and initial conditions (where these are sufficiently small) or to sample these spaces, thus gaining a qualitative understanding of the range of behaviours that a given family of CAs may exhibit and the types of transition rules that are associated with each of these behaviours. This is the approach taken by Wolfram, when he examined the complete set of one-dimensional, two-state CAs (Wolfram, 2002), and it is the approach that we take in this thesis when examining a different family of models (related to CAs) in Chapter 5.

2.4 Stochastic processes

The work presented in Parts II and III requires the use of a limited amount of terminology and theory drawn from the field of stochastic processes. Some key aspects of this topic are presented here. However, it should be noted that this section is not intended to serve as a comprehensive introduction to the field, but merely to collect together those definitions and results that are necessary to support later work.

The material on stochastic processes presented in this section is derived from a variety of sources, including Ross (1996), Grimmett and Stirzaker (2001), Stirzaker (2005), Cotar (2012) and Stroock (2014).

A **stochastic process** is a collection of random variables $\{X(t) : t \in T\}$ taking values in a particular set \mathcal{X} (the **state space**), each corresponding to a particular time $t \in T$, where T is generally a subset of \mathbb{Z} or \mathbb{R} , depending on whether the process is discrete or continuous. A particular set of realisations of these random variables, $\{x_t \in \mathcal{X} : t \in T\}$ is called a **sample path** of the process, with x_t referred to as the **state** of the process at time t .

The variables of a stochastic process may be dependent or independent. For example, consider an infinite sequence of coin flips, indexed by \mathbb{N} . If we let $X(t)$ represent the outcome of flip t , then $\{X(t) : t \in T\}$ is a stochastic process consisting of mutually independent, identically distributed random variables, with $\mathcal{X} = \{\text{"Heads"}, \text{"Tails"}\}$ and $T = \mathbb{N}$. However, if we instead let $X(t)$ represent the number of heads that appear in the first t flips, then $\mathcal{X} = \mathbb{N} \cup \{0\}$ and the random variables of $\{X(t) : t \in T\}$ are clearly not independent.

In this thesis, we will largely be concerned with discrete time stochastic processes, with $T = \mathbb{N} \cup \{0\}$. We will also restrict our focus to consideration of stochastic processes for which \mathcal{X} is a countable set.

The following definition specifies a particular family of stochastic processes:

Definition 2.4.1. *Given a stochastic process $\{X(t) : t \in T\}$ with state space \mathcal{X} and $T = \mathbb{N} \cup \{0\}$, we say that the process fulfils the **Markov property** if and only if, for all $t \in T$, $y \in \mathcal{X}$ and $x_0, \dots, x_t \in \mathcal{X}$:*

$$\mathrm{P}[X(t+1) = y | X(0) = x_0, \dots, X(t) = x_t] = \mathrm{P}[X(t+1) = y | X(t) = x_t]$$

A stochastic process that fulfils the Markov property is called a **Markov process**. A discrete time Markov process is called a **Markov chain**. In this thesis, we will exclusively consider Markov chains that also fulfil the following property:

Definition 2.4.2. *A stochastic process $\{X(t) : t \in T\}$ with state space \mathcal{X} and $T = \mathbb{N} \cup \{0\}$, is described as **time homogeneous** if and only if, for all $t \in T$ and $y_0, y_1 \in \mathcal{X}$:*

$$\mathrm{P}[X(t+1) = y_1 | X(t) = y_0] = \mathrm{P}[X(1) = y_1 | X(0) = y_0]$$

Combining these two definitions, we see that a time homogeneous Markov chain is a discrete time stochastic process in which, at all times, future states depend exclusively on the current state. Past states essentially have no influence on future behaviour in such processes, beyond their role in having determined the current state.

The property of time homogeneity implies that the probability of moving from a particular current state x to a particular state y remains constant over time. We may denote these **transition probabilities** as p_{xy} . If the state space \mathcal{X} of a time homogeneous Markov chain is finite, with cardinality n , then the states may be identified with the integers $1, \dots, n$, and the transition probabilities may be collected in a **transition matrix** M , defined by³:

$$M^\top = (p_{ij})_{i,j \in \{1, \dots, n\}}$$

For a time homogeneous Markov chain, the following concepts may also be defined:

³ The decision to define M^\top rather than M is made for convenience, providing a better match to the notation used in Section 10.4. If $M = (m_{ij})$, this choice implies that $m_{ij} = p_{ji}$, so m_{ij} represents the probability of a transition to i from j .

Definition 2.4.3. Consider a time homogeneous Markov chain $\{X(t) : t \in T\}$ with state space \mathcal{X} and $T = \mathbb{N} \cup \{0\}$. Consider two possible states $x, y \in \mathcal{X}$ and a time interval $\Delta t \in \mathbb{N}$:

- The **Δt -step transition probability** $p_{xy}^{(\Delta t)}$ is the probability that the process will move from state x to state y in precisely Δt steps:

$$p_{xy}^{(\Delta t)} = P[X(t + \Delta t) = y | X(t) = x], \quad \forall t \in T$$

- x **communicates with** y (denoted $x \rightarrow y$) if and only if there exists $k \in \mathbb{N}$ such that $p_{xy}^{(k)} > 0$.
- x and y **intercommunicate** (denoted $x \leftrightarrow y$) if and only if $x \rightarrow y$ and $y \rightarrow x$.
- The Markov chain is described as **irreducible** if and only if $x \rightarrow y, \forall x, y \in \mathcal{X}$.

In other words, one state communicates with another if the second may possibly be reached from the first after a certain number of steps in the process, while an irreducible Markov chain is a chain in which every state may be reached from every other state. Knowing which states communicate with one another is a first step in understanding how the sample path produced by a Markov chain might evolve.

For the purposes of all that follows, let Π_n be the set of valid probability distributions for a random variable that takes values in the finite state space $\mathcal{X} = \{1, \dots, n\}$. In other words:

$$\Pi_n = \left\{ \boldsymbol{\rho} = (\rho_1, \dots, \rho_n)^\top \in [0, 1]^n : \sum_{i=1}^n \rho_i = 1 \right\}$$

The following definition relates to the long term behaviour of a Markov chain:

Definition 2.4.4. Consider a time homogeneous Markov chain $\{X(t) : t \in T\}$ over the finite state space $\mathcal{X} = \{1, \dots, n\}$, with $T = \mathbb{N} \cup \{0\}$, defined by the transition matrix M . If there exists $\boldsymbol{\pi} \in \Pi_n$ such that:

$$M\boldsymbol{\pi} = \boldsymbol{\pi}$$

then $\boldsymbol{\pi}$ is described as a **stationary distribution**. If, in addition:

$$\lim_{N \rightarrow \infty} [M^N \boldsymbol{\rho}] = \boldsymbol{\pi}, \quad \forall \boldsymbol{\rho} \in \Pi_n$$

then $\boldsymbol{\pi}$ is described as a **limiting distribution**.

This definition may be interpreted as follows. Suppose that ρ_t represents the distribution of the random variable $X(t)$:

$$\rho_t = (\Pr[X(t) = 1], \dots, \Pr[X(t) = n])^\top$$

By the definition of the transition matrix, we may observe that, for all $N \in \mathbb{N} \cup \{0\}$:

$$\begin{aligned} M^N \rho_t &= (\Pr[X(t + N) = 1], \dots, \Pr[X(t + N) = n])^\top \\ &= \rho_{t+N} \end{aligned}$$

So we see that a stationary distribution represents an initial distribution of probabilities across the states of the Markov chain that remains constant for all future times. If it is also a limiting distribution, then the probabilities that the process will be found in each state at any future time will converge to the limiting distribution, for any initial conditions.

Given a time homogeneous Markov chain $\{X(t) : t \in T\}$ with state space \mathcal{X} and $T = \mathbb{N} \cup \{0\}$, it is valuable to define the following family of random variables, called **times of first return**⁴, each of which corresponds to a particular state $x \in \mathcal{X}$:

$$\Lambda(x) = \inf \{\Delta t \in \mathbb{N} : X(t + \Delta t) = x \mid X(t) = x\} \quad (2.1)$$

$\Lambda(x)$ represents the time that it takes for the process to return to the current state x for the first time, after leaving it. If the process never returns to x , then $\Lambda(x) = \infty$. Since $\Lambda(x)$ is a random variable, whose distribution is determined by the joint distribution of the $X(t)$, we can make the following further definitions:

Definition 2.4.5. Consider a particular state $x \in \mathcal{X}$ of a time homogeneous Markov chain $\{X(t) : t \in T\}$, with $T = \mathbb{N} \cup \{0\}$.

- x is described as **recurrent** if and only if $\Pr[\Lambda(x) < \infty] = 1$. Otherwise, x is described as **transient**.
- If x is recurrent, then x is described as **positive recurrent** if and only if $E[\Lambda(x)] < \infty$. Otherwise, x is described as **null recurrent**.
- A Markov chain is described as **positive recurrent** if and only if all states are positive recurrent.

⁴ Note that, strictly speaking, (2.1), which defines the random variable $\Lambda(x)$, requires that we choose a particular $t \in T$. However, since we are concerned only with time homogeneous Markov chains, the value of t is arbitrary.

Broadly speaking, a positive recurrent Markov chain is one in which all states are visited and revisited infinitely often.

We end this section with the following propositions, which are presented without proof. Proofs of Proposition 2.4.6 may be found in Stirzaker (2005, pp. 132-134) and Grimmet and Stirzaker (2001, pp. 223-225), while proofs of Proposition 2.4.7 may be found in Grimmet and Stirzaker (2001, pp. 227-230) and Ross (1996, pp. 175-177).

Proposition 2.4.6. *Given a time homogeneous Markov chain $\{X(t) : t \in T\}$ with a finite state space \mathcal{X} and $T = \mathbb{N} \cup \{0\}$, if the chain is irreducible, then it is positive recurrent.*

Proposition 2.4.7. *Consider a time homogeneous Markov chain $\{X(t) : t \in T\}$ with a finite state space \mathcal{X} , of cardinality n , where $T = \mathbb{N} \cup \{0\}$. If the chain is positive recurrent then it has a unique stationary distribution $\boldsymbol{\pi} \in \Pi_n$.*

Finally, we observe that while the unique stationary distribution guaranteed by Proposition 2.4.7 is not necessarily a limiting distribution in the sense of Definition 2.4.4, it may nonetheless be demonstrated that its terms provide the “long-run proportion of time that the Markov chain is in [each state]” (Ross, 1996, p. 177; Stroock, 2014, pp. 33-35, also deals with this issue). This fact will prove crucially important for our work on the optimal strategies of patrol games, presented in Section 10.4.

Part II

**Understanding the connection
between micro and macro-scale
behaviour in individual-based
models**

Chapter 3

Key Concepts

3.1 Introduction to Part II

In Part II, we concentrate on the first two research objectives stated in Section 1.5. These objectives require that we investigate the relationship between the dynamics of systems of interacting individuals and those of corresponding models derived using mean field theory (see Section 3.2), and the causal mechanisms that link local and global scale dynamics in IBMs. In addressing these issues, we employ the first of our two modelling perspectives (see Section 1.4.1), with individuals modelled as basic automata, whose behaviour is governed by simple stochastic rules, rather than sophisticated decision making.

Our starting point for these investigations will be a particular IBM, which we call the NANIA model. This model was mentioned in Section 2.2.2 and is defined in detail in Section 4.2. The NANIA model is of interest because it has been used as something of an exemplar for the purposes of the teaching and visualisation of agent-based and individual-based models, as discussed briefly in Section 4.2.1. After a short investigation of the possible behaviours of the NANIA model, we shift our focus to a particular generalisation: a family of discrete space-time IBMs, which we label as \mathfrak{B} -models.

In Chapter 5, concentrating specifically on \mathfrak{B} -models over one-dimensional spaces, in which all individuals are identical, we perform simulation experiments to compare the behaviour of these models with the predictions of mean field theory, in terms of their observed population densities at equilibrium. The findings from these experiments are then used as the foundation for a more theoretical approach in Chapter 6, where the model dynamics are translated into a new space to facilitate the identification of a causal link between particular individual behaviours at a local scale and population dynamics on the global scale, built upon a close investigation of the

spatial distribution of individuals.

Throughout Part II, borrowing terminology from the field of statistical mechanics, we use the term “microstate” to refer to a precise and complete description of the instantaneous configuration of a system, in which every possible degree of freedom is specified. In terms of individual-based modelling, the microstate of a system would specify the precise location of every individual, along with the values of any other individual-specific and global variables. Anything that remain unchanged while a model is operating, such as the values of any model parameters and the underlying geography of a spatially explicit model (where this geography is fixed), is not considered part of a model microstate, but rather part of the model structure.

The term “state” is used in a more general sense, referring either to the status of a particular part of a system (a single cell, for example) or to a reductive description of the complete system in terms of a limited number of global properties, such as the population densities of various species in a particular environment.

3.2 Mean field theory

3.2.1 System dynamics

Mean field theory is a method for representing the behaviour of a system by means of one or more differential equations or difference equations. The method itself will be discussed in Sections 3.2.2 (the non-spatial case) and 3.2.4 (the spatial case), but we first take the time to consider such representations in more general terms.

System dynamics is a means of representing the dynamics of complex systems through consideration of a set of dynamical summary variables and their relationships. This modelling approach is often applied to systems of interacting entities, which may be divided into a number of distinct types or which may exhibit a number of distinct states or both. The summary variables represent the number or proportion of entities of each possible type or occupying each possible state at each time, as well as any important system-wide quantities that may also vary with time (such as the amount of available food in an ecological model). The relationships between these quantities are described in terms of differential equations or difference equations establishing the rate of change of each one as a function of the current values (and, occasionally, of certain past values) of all variables. In this way, system dynamics are able to describe the flows of individuals between a number of different states or the simultaneous and interrelated changes in the sizes of a number of dif-

ferent populations, based on considerations of known or supposed cause and effect relationships within a system.

A general discussion of system dynamics is presented by Gilbert (see 2008, chap. 1), with a more formal description being provided by Macal (2010). Wolfram (2002, p. 984) also discusses a system dynamics type approach to the study of CAs (described simply as “rate equations”). It should be noted that system dynamics is a more specific and narrow concept than the field of general system theory, as discussed by Von Bertalanffy (1969) and others.

Gilbert suggests that system dynamics offers a useful approach for “topics where there are large populations of behaviourally similar agents...” but argues that it is not appropriate for systems in which agent heterogeneity, agent memory or agent learning are important, since these features cannot be efficiently represented in such a model. It should also be noted that since system dynamics models of systems of interacting entities only monitor the sizes of different groups within a system, in general, any information about the spatial distribution of these entities is lost, whether or not such information is of relevance to the model dynamics.

A relationship exists between the system dynamics approach and the concept of a master equation, used in the analysis of certain stochastic systems. Given a system that moves between different states (such as a Markov process), a master equation is a system of differential or difference equations that describes the rates of change of the probabilities that the system occupies each state as functions of the current values of these probabilities (see Macal, 2010).

If the summary variables of a system dynamics model represent the proportions of a population occupying different states or belonging to different types, then these summary variables clearly represent the probabilities of a master equation that describes the process of selecting a single entity randomly uniformly from the population and recording its state or type. The entity states or types of the system dynamics are therefore identified with the system states of the master equation and the same dynamical equations apply in each case.

For a particular example of this, consider the many variations of the widely used SIR epidemiological model¹, used to study disease transmission in a population (see, for

¹ SIR stands for “Susceptible, Infected, Removed”, referring to three possible infection states of an individual. Although the “R” is sometimes taken to stand for “recovered”, “removed” is a more general term, encompassing all those individuals who can no longer infect others, whether owing to recovery, quarantine or death.

example, Funk et al., 2010; Macal, 2010; Fenichel et al., 2011; Meloni et al., 2011). In its most basic form, SIR is a system dynamics model, in which a population is divided into three groups based on their infection status for a particular disease, with the dynamics of movement between these groups modelled by differential equations. In this model, the master equation for the stochastic procedure defined by selecting an individual at random at any time and noting its disease status is equivalent to the differential equations that define the system dynamics.

The non-spatial mean field techniques that we discuss in the next section may be thought of as a particular approach for constructing a system dynamics model from a given ABM or CA by means of some key simplifying assumptions.

3.2.2 Non-spatial mean field techniques for models of interacting entities

In this thesis, we are primarily interested in the role of mean field theory as a technique for the derivation of differential or difference equations to describe the behaviour of models of interacting entities. This technique of producing one model to represent the behaviour of another is described by Huet and Deffuant (2008) as “double-modelling”. The authors cite this approach as a means to “provide explanations of the collective effects observed in IBM simulations”, as well as being a tool for the prediction of the long term behaviour of an IBM without recourse to simulation. They also suggest that “double-modelling” represents a useful exploratory approach for the study of IBMs, allowing for the easier formulation and verification of hypotheses. Our interest in mean field theory will be motivated mainly by the first of these features, the potential of the technique to aid in understanding the connection between local interactions and global behaviour in IBMs.

In the non-spatial case, the mean field approach is based on a single key assumption, which may be described in a number of different ways, depending on the precise features of the model to which it is being applied. Note that the qualifier “non-spatial” relates to the equations derived using mean field techniques and not to the original model or system. Indeed, mean field theory is most commonly applied to spatial systems to simplify the description of their behaviour.

In loose terms, the mean field assumption states that, given some population of entities, when each of these entities is considered individually, it may be supposed to interact with the others as if they formed a “mean field”, a uniform medium whose properties correspond to the averages of those of the individual entities.

In some circumstances, it may be appropriate to state the mean field assumption as relating to the “homogeneous mixing” of agents within the system (McKane and Newman, 2004; Wessel et al., 2011), in the sense that all pairs of agents are equally likely to interact or that the location of an agent at any time may be considered to be random, following a uniform distribution across the space of the system.

In systems with discrete spatial entities, such as CAs or IBMs over cellular lattices or general networks, the mean field assumption may instead be taken to imply that the state of each spatial entity can be treated as an independent random variable, constrained by global averages (such as the proportions of the entities known to occupy each state or the population densities of different types of agent) but with all spatial correlations neglected (see Wolfram, 1983, p. 615; Wolfram, 2002, p. 952; Fibich and Gibori, 2010, p. 1460).

For example, consider a CA over some finite graph G with n cells, in which each cell may occupy one of two states, labelled 0 or 1, with neighbourhoods defined according to adjacency in G and with some local transition rule $\mathfrak{T}_{\text{local}}$ to govern its dynamics (see Section 2.3.1). Suppose that the proportion of cells in state 1 at time t is given by the dynamic variable p_t , where $t \in \mathbb{N} \cup \{0\}$. A mean field analysis of this CA would assume that the states of all cells at time t could be treated as independent random Bernoulli variables with parameter p_t . The dynamics of the system could then be modelled by considering the expected change in p_t given this assumption (see Seck-Tuoh-Mora et al., 2014, pp. 946-7).

Note that, in the example given above, provided that $n \gg 1$, $np_t \gg 1$ and $n(1 - p_t) \gg 1$, the independence assumption may often be considered to be effectively equivalent to the assumption that all possible configurations of cell states with global density p_t are equally likely, since the stated inequalities ensure that those dependencies between the states of adjacent cells that arise from counting arguments are negligible. Similarly, in cases in which the graph G is regular, the mean field technique may sometimes be considered to refer to the dynamics in the limit as $n \rightarrow \infty$. For example, McKane and Newman (2004, pp. 3-5) provides a thorough demonstration of the mean field technique as applied to a certain family of IBMs over a regular lattice, in the large n limit.

A key question in mean field theory is to understand the conditions under which the dynamics of a particular system or family of systems are well represented by the corresponding mean field equations. For example, McKane and Newman (2004)

examine the conditions under which mean field equations provide a good representation of the dynamics of a certain family of ecological models, while Huet and Deffuant (2008) addresses the same question for an IBM of the dynamics of changing attitudes. This question is also the principal focus of Chapter 6 of this thesis, in the context of a particular family of IBMs, which will be defined in Chapter 4.

3.2.3 Benefits and limitations of mean field analysis

Mean field analysis can be advantageous, since it offers a simplified representation of the dynamics of a complex system. As noted by Nguyen et al. (2008), a model defined by systems of equations, such as a mean field representation, admits a huge number of analytical techniques and approaches which are notably lacking in the field of IBMs (see Section 2.2.6). Nguyen et al. also observe that an equation-based representation of a dynamical system may be easier to calibrate than a corresponding IBM, since the behaviour of the equations may depend on a much smaller number of parameters.

Huet and Deffuant (2008) suggest that an equation-based representation of a system facilitates a richer analysis, since it “provides a more compact view of the processes, which eases their understanding.” The authors also note the capacity of mean field type models to exhibit “asymptotic results, corresponding to an infinite population.”

However, since mean field analysis necessarily involves aggregation and simplification, the resulting equations cannot precisely capture the complete behaviour of a complex system of interacting entities. There are therefore some inevitable limitations of mean field analysis that must be understood.

The most obvious of these limitations (and indeed one of the key drivers behind several others that we will go on to describe) is the fact that mean field analysis, in the non-spatial form in which it is most frequently applied, takes no account of the spatial distribution of the entities that make up a system of interest. In the specific example of a model of viral infection, Itakura et al. (2010) note that the lack of space in aggregated models, and specifically the lack of consideration of non-uniform agent densities across a system, can result in unrealistic behavioural features that are not present in a corresponding ABM. In a similar vein, Wolfram (1983) notes that the discrepancies between equilibrium densities exhibited by CAs and those predicted by corresponding mean field equations are due to the inability of mean field analysis to take account of spatial correlations between cell states produced as a result of the characteristics of the local transition rule.

Another key limitation of mean field equations is that they are deterministic, while the systems that they are intended to represent may involve significant stochastic elements. Such a deterministic model may demonstrate only a reduced range of the possible system behaviours (Macal, 2010). McKane and Newman (2004) observe that mean field models are generally not able to represent rare stochastic events that may occur within a system, such as rare stochastic extinctions in a model of an ecosystem, and this problem persists even when the equations are adapted to include the dynamics of the variances of summary variables.

Nguyen et al. (2008) identify the inability of equation-based models to efficiently represent the heterogeneity of agents as a further limitation, concluding that, owing to their increased degree of abstraction and lower level of detail as compared with ABMs, such models “cannot be very realistic”. Meanwhile, Huet and Deffuant (2008) remark that aggregated models, such as those generated by mean field analysis, can be impractically complicated for highly detailed systems. The authors claim further that, in certain cases, it may be impossible to find a single aggregated model that provides a good representation of the behaviour of a given system, since this behaviour may differ very significantly depending on the initial conditions and the particular choices of parameter values.

Finally, Seck-Tuoh-Mora et al. (2014, pp.946-948) observe that mean field techniques often do not provide a satisfactory representation of the behaviour of CAs, since the equations are intrinsically incapable of reproducing the inherent complexity that is so often of fundamental importance in the study of these models.

3.2.4 Spatial mean field techniques

Although mean field analysis is usually taken to mean the generation of ODEs or difference equations to represent the dynamics of a system, with quantities of interest being globally aggregated and spatial structure ignored (as described in Section 3.2.2), it is also possible to perform a form of mean field analysis that retains a significant amount of spatial information. Under this technique, system behaviour is represented by partial rather than ordinary differential equations, or by difference equations with a spatial dependency, such that the values of summary variables may be non-uniform across space.

The apparent contradiction between the term “mean field”, which we have described as involving an assumption of spatial uniformity and homogeneous mixing, and a spatially explicit interpretation is clarified by McKane and Newman (2004), who write:

“By “mean field” we mean the neglect of correlations between degrees of freedom, allowing one to write the mean of the product of two stochastic variables as the product of their means. Thus, a spatial model in which statistical correlations are neglected is still a “mean-field model” within this usage.”

In a spatial mean field model, we can imagine that, rather than each entity of a system interacting with a single global “mean field”, each distinct location or patch has its own such field. An entity is supposed to interact with those that share its patch as if they formed a “mean field”, as in the non-spatial case, but is also supposed to interact with the “mean fields” of neighbouring patches, according to certain spatial relationships derived from the dynamics of the original system. In this way, each patch, which may be a single point or a larger area, has its own values for the summary variables, representing the means or expectations of these quantities over the corresponding spatial region.

This approach results in system dynamics type equations to represent the behaviour of the system within each patch, with interdependencies between the equations of neighbouring patches. If the underlying geography of the model is suitable (as in the case of square lattices, for example), PDEs may be formulated from these equations through consideration of the limiting dynamics (if it exists) as spatial and temporal increments tend to zero.

An example of a spatial mean field procedure is provided by McKane and Newman (2004) for two variations of an ecological patch model.

Spatial mean field techniques distinguish between those processes of a system that occur at a particular point or whose effects are sufficiently locally to be modelled as occurring at a particular point (such as the death of an individual organism in a model of an ecosystem) and those processes that occur across space (such as the movement of organisms between locations). When expressed as systems of PDEs, the former involve temporal derivatives only, while the latter involve temporal and spatial derivatives. Which processes may be considered to be local and which should be considered to be spatial will vary depending on the precise nature of the system to be modelled and the way that it is divided into patches.

Spatial mean field equations will often resemble the corresponding non-spatial equations, with the introduction of additional diffusion terms to model spatial dynamics. However, care must be taken, since while spatial interactions are often modelled as simple diffusion processes, in many cases the true spatial dynamics

of a system would be more accurately represented by more complex expressions (McKane and Newman, 2004).

Spatial mean field models are strongly related to the “CA-ODE models” described by Vanag (1999, p. 418), in which a continuous-valued CA is derived from a spatial system through the discretisation of space into a cellular lattice. Vanag describes CA-ODE models as being an intermediate class of models lying between CAs and PDE models.

3.2.5 Alternative methods for translating between different representations of complex systems

While mean field approaches allow for the translation from CA or ABM representations of systems to models based on ordinary or partial differential equations, many other techniques have been proposed for translating between different modelling paradigms.

For instance, the “kinetic theory of active particles” (De Angelis and Delitala, 2006; Bellomo et al., 2009), discussed in Section 2.1.4, offers an alternative approach to the representation of systems of interacting entities by systems of differential equations, as does the method for representing IBMs with systems of PDEs set out by Gómez-Mourela (2005), which makes use of an intermediate representation of the system in terms of stochastic ODEs.

A different approach is taken by Hinkelmann et al. (2011), who outline a method for the exact representation of certain spatially discrete ABMs using systems of polynomials over finite fields. The authors argue that, although the resulting algebraic representations appear to be extremely complicated, the number of variables required in these expressions increases much more slowly than the number of microstates of the ABM, suggesting that they may offer a more efficient route for precise dynamical analysis than prohibitively time consuming simulation-based explorations of the state space.

Certain continuous CAs can be represented concisely by systems of differential equations without recourse to the assumptions of mean field theory (see Rausch, 2001). Meanwhile, the well-known method of finite differences, which provides numerical solutions to PDEs (see, for example, Strauss, 2008, pp. 199-222), is effectively a means of translating a differential equation model into a discrete time, continuous-valued CA, as noted by Wolfram (2002, p.924). Wolfram also observes that both

these types of model can exhibit complex behaviour of a very similar character (pp. 155-168).

Transforming an ODE or PDE model of a system into an ABM (the reverse translation of that achieved by the mean field approach) is not straightforward owing to the additional detail inherent in the latter modelling paradigm and to the many different ways in which ABMs may be described. Methods to achieve this translation generally involve loose algorithmic procedures in which features of the original equations are progressively “distributed” to a population of agents, with the resulting ABM and its subprocesses being repeatedly validated against the equation-based model by means of simulation (see Nguyen et al., 2008; Macal, 2010).

3.3 Models from mathematical ecology

3.3.1 The place of ecology models in this thesis

As discussed in Chapter 1, the main aims of this thesis are largely theoretical in nature, relating to the way in which certain mathematical models operate rather than to any particular practical applications. However, since close links exist between the models studied in Part II and some particular models from the field of mathematical ecology, a brief overview of these models is necessary. Note that, as with the discussion of stochastic processes provided in Section 2.4, the purpose of this section is neither to provide a detailed analysis of ecological models, nor an in-depth review of the literature surrounding them, but merely to provide sufficient information to support the work presented in later sections.

3.3.2 The Lotka-Volterra equations

In their most basic form, the Lotka-Volterra equations are a system of ODEs representing the rates of change of the sizes of two interacting populations, a prey species and a predator species. Letting the population density per unit area of the prey species be represented by u and that of the predator species be represented by v , and letting u and v be functions of the time $t \in \mathbb{R}$, the equations may be written:

$$\begin{aligned}\dot{u} &= u(a - bv) \\ \dot{v} &= -v(c - du)\end{aligned}\tag{3.1}$$

where \dot{u}, \dot{v} represent the time derivatives of u and v and where a, b, c and d are positive constants (see, for example, Murray, 1993, p. 63).

In the context of interacting species, the equations were originally proposed by Volterra (1926)². However, they had also previously been derived by Lotka (1920) to model certain types of chemical reaction.

It may be observed that, when $u = 0$, the dynamics of the predator species is given by the equation $\dot{v} = -cv$, which indicates that, in the absence of prey, the predator population decays exponentially. Similarly, when $v = 0$, the dynamics of the prey species is given by the equation $\dot{u} = au$, indicating that, in the absence of predators, the prey population grows exponentially. We also observe that the presence of prey stimulates growth of the predator population (through the term duv), while the presence of predators inhibits growth of the prey population (through the term $-bu v$), thus representing the nature of the predatory interaction between the two species. Furthermore, the equations clearly guarantee that $\dot{u} = 0$ when $u = 0$ and $\dot{v} = 0$ when $v = 0$, thus ensuring that the system remains in the region $u, v \geq 0$, where the values of u and v are physically meaningful.

Setting $\dot{u} = \dot{v} = 0$, we see that the Lotka-Volterra equations have two physically meaningful equilibria. The first is the trivial equilibrium $(u_0^*, v_0^*) = (0, 0)$ representing the extinction of both species. The second is $(u_1^*, v_1^*) = (c/d, a/b)$, which represents a state of persistent coexistence.

The Lotka-Volterra equations are of particular interest because, despite their simplicity, they exhibit undamped oscillations (periodic coupled population cycles) in u and v about the non-trivial equilibrium (u_1^*, v_1^*) , a form of behaviour that, prior to analysing the equations, Lotka had considered to be “improbable” in such systems (1920, p. 1595). Population cycles of this kind have been observed in a wide range of interacting species, and while the Lotka-Volterra equations tend to be too simplistic to provide a realistic model of any particular real world system, they have nonetheless formed a foundation upon which more detailed models of ecosystems have been constructed (see Murray, 1993, pp. 66-68).

One limitation of the basic Lotka-Volterra equations given in (3.1) is that the exponential growth assumption for the prey species is clearly unrealistic. However, this issue may be addressed by altering the equations such that, in the absence of predators, the prey population instead exhibits logistic growth, limited by a pre-determined carrying capacity, the maximum density of the prey species that the environment can support (see, for example, Wilson, 2011, pp. 46-47).

² The source is in Italian. See also the English translation: Volterra, 1931

As discussed by Volterra (1926), the basic Lotka-Volterra equations shown in (3.1) can also be generalised to model ecosystems with multiple species, which may exhibit a wider range of types of interaction, going beyond predation to mutual competition, symbiosis and parasitism. For a system with n species, Murray (1993, p. 85) provides the following highly generalised form of the equations:

$$\dot{u}_i = u_i f_i(u_0, \dots, u_{n-1}), \quad \text{for } i \in \{0, \dots, n-1\} \quad (3.2)$$

where u_i represents the population density of species i , with the general function $f_i(u_0, \dots, u_{n-1})$ describing the nature of the influence of each species on the rate of change of u_i . Note that (3.2) preserves the key property of (3.1), that general extinction is an equilibrium, while the extinction of any individual species is irreversible.

Spatial versions of the Lotka-Volterra equations, based on PDEs, often incorporating diffusion-like processes to represent the movement of individuals, have been widely studied (see, for example, Cosner and Lazer, 1984; McLaughlin and Roughgarden, 1991; Wilson, 2011, p. 238). A large number of predator-prey CAs and ABMs have also been proposed (see, for example, He et al., 2003; Mock et al., 2007; Pineda-Krueger et al., 2007). In this thesis, we are particularly interested in two of these models: the ecological patch model, discussed in Section 3.3.3, and the NANIA model (Ackland, 2009), which will be introduced in Section 4.2.

3.3.3 Ecological patch models

The ecological patch model is a temporally and spatially discrete, stochastic IBM, which represents the interactions between species within an ecosystem. The “patches” in question correspond to discrete geographical areas, within and between which individuals move and interact. Ecological patch models may be spatial, with many connected patches, or non-spatial, with all events occurring within a single patch, which represents the complete system of interest. In each case, it is assumed that within each patch there is perfect mixing of individuals, such that all possible pairwise interactions between them may be considered to be equally likely.

McKane and Newman (2004) present a detailed description of the ecological patch model alongside a review of its use, both in ecological contexts and beyond (see, for example, Svirezhev, 1999; Alonso and McKane, 2002). A related patch model is considered by Nguyen et al. (2008). In the context of this thesis, the ecological patch model is of importance owing to its close relationship to the NANIA predator-prey model (Ackland, 2009), which forms the basis of the work presented in Part II.

In the version of the patch model described by McKane and Newman (2004), each patch is subdivided into a number of “plots” (possibly only one), which may be either empty or occupied by a single individual. The maximum capacity of a patch is therefore equal to the number of plots that it contains. In a spatial model, patches form the vertices of a graph, whose structure reflects the geography of the modelled region.

The model dynamics proceed in discrete time steps, with one of three possible types of transition occurring at each step. The choice of which of the three forms of transition occurs is governed by a predetermined set of probabilities. The different types of transition are outlined below:

- **Mortality:** This type of transition involves the selection of a single plot, according to a discrete uniform distribution across all plots, across all patches. If the plot is empty, there is no change. Otherwise, if the selected plot contains an individual then that individual is removed with a predetermined probability, specific to its species.
- **Interaction (non-spatial):** This type of transition involves the selection of a single patch, according to a discrete uniform distribution across all patches, followed by the selection of two plots from this patch, by means of a simple random sample. If the two plots are empty, there is no effect. Otherwise, there may be a change in the number or species of the individuals occupying the plots, as determined by a specified stochastic transition function. Note that this transition is only possible in models whose patches each contain more than one plot.
- **Interaction (spatial):** This type of transition involves the selection of a single patch, according to a discrete uniform distribution across all patches, followed by a neighbouring patch (in the sense of adjacency in the underlying graph), according to a discrete uniform distribution across all such neighbours. One plot is then selected from each of these two patches, according to the appropriate discrete uniform distributions. If the two plots are empty, there is no effect. Otherwise, there may be a change in the number or species of the individuals occupying the plots or individuals may move from one plot to the other, as determined by a specified stochastic transition function (which may or may not be the same as the function that is applied in the non-spatial case). Note that this transition is only possible in the spatial (multi-patch) version of the model.

Through careful selection of the transition functions mentioned in the above descriptions, the ecological patch model is sufficiently flexible to represent a wide variety of different processes and interactions, both those that can be considered to occur at a particular point (such as reproduction or predation) and those whose effect takes place across space (such as migration).

McKane and Newman (2004) use mean field theory (see Section 3.2) to identify a close relationship between a particular version of the ecological patch model and the Lotka-Volterra equations, in both spatial and non-spatial contexts. In Section 4.3.4, we use a similar method to demonstrate a connection between the NANIA model (defined in Section 4.2) and the Lotka-Volterra equations.

Chapter 4

Definition and initial discussion of a general family of simple IBMs

4.1 Introduction

In this chapter, we introduce the NANIA predator-prey model, which forms the basis for all of the work presented in Part II. After defining this model, we present an initial discussion of its behaviour and look at the connection between it and the Lotka-Volterra equations (see Section 3.3.2). We observe that the NANIA model is a particular example of a broader family of simple IBMs and we describe this family in detail. We discuss the models that belong to this family and the importance of spatial symmetries in limiting the variety of their possible dynamics.

Our ultimate intention is to determine ways to analyse the connections between local and global behaviours in IBMs, a problem whose importance was discussed in Section 2.2.8. The family of simple IBMs that we derive from the NANIA model here provides an ideal subject for the investigation of this goal in later chapters.

4.2 The NANIA predator-prey model: An ODD description

4.2.1 Background

Novel Approaches to Networks of Interacting Autonomes (NANIA) was a complexity science project funded by the Engineering and Physical Sciences Research Council (EPSRC), which ran from 2004 to 2009 (Marion, 2004; NANIA, 2009). One page of the NANIA website was dedicated to an interactive simulation of a predator-prey

model (created by Ackland, 2009), described as “[an] autonome model¹ which simulates the behaviour of [a Lotka-Volterra] system and introduces space, with either periodic or fixed boundaries”. The page has since been removed, but can still be accessed at the Internet Archive (1996).

We refer to this model simply as the “NANIA model” (although many other models were also created as part of the NANIA project). As discussed in Section 2.2.1, owing to the simplicity of its entities and interactions, we classify the NANIA model as an individual-based model (IBM) rather than an agent-based model (ABM), and we accordingly refer to “individuals” rather than “agents” throughout.

Although we focus specifically on the NANIA model, many predator-prey models have been proposed based on similar or identical mechanisms. Since these models are often presented in informal contexts, such as in lecture notes (Ackland, 2008; He, 2013; Forrest, 2014) or as interactive web simulations (Tyl, 2009; Idkowiak and Komosinski, 2014; Sayama, 2015), it is not possible to definitively identify any particular example as the original version. However, despite its simplicity, the fact that versions of the NANIA model may be found in such a diverse range of sources, and that it is often employed as an exemplar for the teaching and visualisation of IBMs, underlines its importance and relevance as an object of study.

The NANIA model is presented here using the ODD protocol (see Section 2.2.3).

4.2.2 Purpose

No specific aim was stated for the NANIA model beyond demonstrating that an ‘autonome’ model was capable of simulating the dynamics of the Lotka-Volterra equations. However, it may be assumed that the model was intended to feed into the overall objectives of the NANIA project. On the project website (NANIA, 2009), the overall aim of the project is stated as:

“... the search for overarching principles which apply in complex natural systems such as geophysical and ecological systems, and how such principles might be exploited for novel computation.”

This general statement is then broken down into six “overarching scientific questions”. However, it is unclear which of these, if any, the predator-prey model was

¹ The NANIA website (NANIA, 2009) defines an “autonome” as “any interacting multi-state system which can encompass cellular automata, agent, organisms or species”. Although this definition is a little ambiguous, in context, the word appears to be intended to serve as a generic term to cover all forms of interacting entity in complex models (rather than the models themselves).

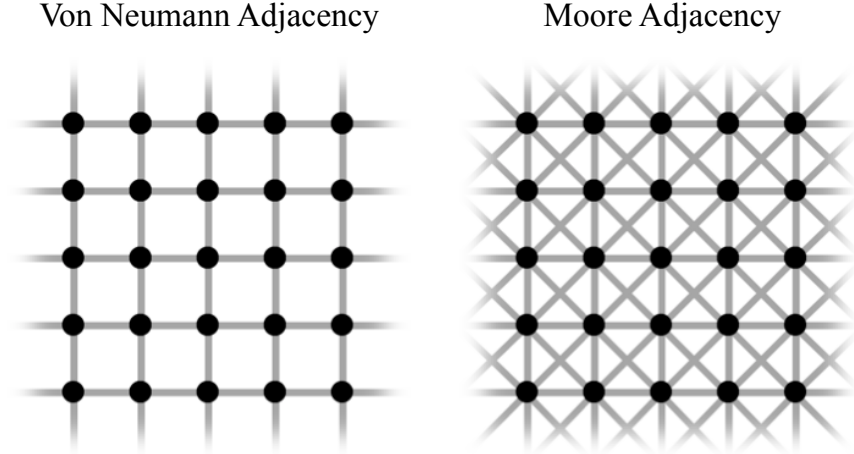


Figure 4.1: Comparison of the Von Neumann and Moore adjacency schemes in graphs over rectangular lattices (see, for example, Hogeweg, 1988).

intended to address.

In the context of this thesis, the purpose of the NANIA model is to act as a particular example of a broader family of simple IBMs, forming the basis for a series of investigations relating to the links between local and global behaviours in such models.

4.2.3 Entities, state variables and scales

The model involves two different types of entity: ‘biological’ entities (the individuals) and ‘geographical’ entities, comprising particular cells and the network that links them.

The individuals of the model are divided into two species, described as rabbits (the prey) and foxes (the predators), represented by the letters ‘R’ and ‘F’ respectively. The space inhabited by the individuals is a rectangular lattice of cells $L = \{C_{xy} : x, y \in \{0, \dots, n - 1\}\}$ of size $n \times n$. This lattice forms the vertex set of a graph whose edges are defined as linking either orthogonally adjacent cells (Von Neumann adjacency) or orthogonally and diagonally adjacent cells (Moore adjacency, see Figure 4.1). The boundaries of the lattice graph may be fixed, forming a square region or periodic, forming a toroidal region.

At time t , a particular cell $C_{xy} \in L$ may be empty $C_{xy}[t] = ‘E’$, inhabited by a rabbit $C_{xy}[t] = ‘R’$ or inhabited by a fox $C_{xy}[t] = ‘F’$. A cell may never be occupied

by more than one individual. The only variables associated with a particular cell are therefore its fixed x and y coordinates in the lattice and its current occupancy status. For a particular cell C_{xy} , the expression $N(C_{xy})$ refers to its neighbourhood², the set of all cells adjacent to C_{xy} in L .

The only state variable associated with an individual of a particular species is the current cell that it occupies. Individuals of a particular species are therefore indistinguishable and effectively interchangeable. Since cells may not contain more than one individual, the state of the model (and its behaviour) may be described entirely in terms of the cells and their occupancies. In this formulation of the model, the individuals are therefore disregarded as independent entities, considered to exist only implicitly through the occupancy states of the cells.

Note that, in common with many cellular automata (CAs), this model is based on a rectangular lattice of cells each of which can take on one of a finite set of distinct states at each discrete time step. However, the model differs from typical CAs in the respect that cells are not updated simultaneously, but in randomly chosen pairs at each time step. Thus, it is more sensible to consider it as a temporally and spatially discrete IBM (even if individuals are only modelled indirectly), rather than as a CA.

Since the model is highly abstract, the spatial and temporal increments are not intended to correspond to any particular units in the real world.

4.2.4 Process overview and scheduling

Beginning at $t = 0$, time advances in discrete increments of size δt . For convenience, we suppose that $\delta t = 1$. At each time step:

1. A cell C_{xy} is randomly selected by means of a discrete uniform distribution over L ;
2. One of its neighbours $C_{x'y'}$ is randomly selected according to a discrete uniform distribution over $N(C_{xy})$;
3. The occupancy states of these cells are updated according to a particular local transition rule $\mathfrak{T}_{\text{local}} : (C_{xy}[t], C_{x'y'}[t]) \rightarrow (C_{xy}[t + 1], C_{x'y'}[t + 1])$.

The details of the local transition rule $\mathfrak{T}_{\text{local}}$ are described in Section 4.2.8.

² More specifically, $N(C_{xy})$ is the **open neighbourhood** of C_{xy} . The **closed neighbourhood** of C_{xy} , denoted by $N[C_{xy}]$, includes the cell C_{xy} itself: $N[C_{xy}] = N(C_{xy}) \cup \{C_{xy}\}$.

4.2.5 Design concepts

Basic principles: The model is intended to represent the interaction of the populations of a prey species (called “rabbits”) and a predator species (called “foxes”) in a shared habitat, albeit in a highly abstract form. The fundamental implicit hypothesis underlying the model is that its behaviour in some sense matches that described by the Lotka-Volterra equations (see Section 3.3.2).

Emergence: If the behaviour of the model *does* match that of the Lotka-Volterra equations, then we would expect to observe the emergence of cycles in the predator and prey populations similar to those of the equations. However, since the model also involves a spatial element, we may also expect to observe some form of emergent spatial waves in the densities of the two populations.

Interaction: The only direct interactions between individuals in the model involve the predation of a rabbit by a fox, possibly resulting in the creation of a new fox individual. However, since cells cannot be occupied by more than one individual, there is also *indirect* interaction, through individuals blocking space and preventing movement and reproduction.

Reproduction in the NANIA model is essentially asexual, since it does not require any interaction between individuals of the same species. The processes governing the model are discussed in detail in Section 4.2.8.

Stochasticity: The model is governed almost entirely by stochastic processes. As described in Section 4.2.4, individuals may only ‘act’ at a particular time step if they are randomly selected. Reproduction and mortality are also modelled stochastically, as described in Section 4.2.8.

As discussed in Section 2.2.4, it has been argued that asynchronous stochastic updating, such as is employed in this model, may provide a good representation of the behaviour of systems of individuals in the real world (Caron-Lormier et al., 2008).

Observation: Since the model is extremely simple, provided that the size of the lattice L is not too great, it is not unreasonable to store a complete description of the system at a given iteration. However, owing to the fact that only two cells are updated at each time step, for all but fairly small lattices, the model dynamics tend to evolve extremely slowly, such that meaningful temporal patterns can only be observed over many thousands or tens of thousands of iterations.

In all simulations of the model performed in this thesis (and of any models derived from this model), complete descriptions of the system state are recorded at fixed intervals, starting with the state at $t = 0$. However, while complete descriptions of the system are recorded, summary measures of the system state will sometimes be used, particularly the global population density of each species.

The interval between observations ranges from 3200 iterations, in the one-dimensional models examined in Chapter 5, to 16 000 iterations, for the two-dimensional model from which Figure 4.5 was generated.

4.2.6 Initialisation

The model is initialised through assigning occupancy statuses to all cells. This may be achieved by means of any stochastic or deterministic process. The particular means of initialisation employed will be described separately each time the model is used.

4.2.7 Input data

The model does not use any external data inputs during the course of a simulation.

4.2.8 Submodels

The local transition rule $\mathfrak{T}_{\text{local}} : (C_{xy}[t], C_{x'y'}[t]) \rightarrow (C_{xy}[t+1], C_{x'y'}[t+1])$ for the model is defined as follows:

1. If the first cell contains a rabbit and its neighbour is empty, $C_{xy}[t] = 'R'$, $C_{x'y'}[t] = 'E'$, then the rabbit reproduces with probability κ , $C_{xy}[t+1] = 'R'$, $C_{x'y'}[t+1] = 'R'$. Otherwise there is no change, $C_{xy}[t+1] = 'R'$, $C_{x'y'}[t+1] = 'E'$.
2. If the first cell contains a fox and its neighbour is a rabbit, $C_{xy}[t] = 'F'$, $C_{x'y'}[t] = 'R'$, then the fox eats the rabbit and reproduces with probability ς , $C_{xy}[t+1] = 'F'$, $C_{x'y'}[t+1] = 'F'$. Otherwise the fox eats the rabbit but does not reproduce, $C_{xy}[t+1] = 'F'$, $C_{x'y'}[t+1] = 'E'$.
3. If the first cell contains a fox and its neighbour is not a rabbit, $C_{xy}[t] = 'F'$, $C_{x'y'}[t] = 'F'$ or $'E'$, then the fox dies with probability τ , $C_{xy}[t+1] = 'E'$, $C_{x'y'}[t+1] = C_{x'y'}[t]$. Otherwise there is no change, $C_{xy}[t+1] = 'F'$, $C_{x'y'}[t+1] = C_{x'y'}[t]$.
4. If the first cell is empty, $C_{xy}[t] = 'E'$, then any adjacent individual moves into the cell $C_{xy}[t+1] = C_{x'y'}[t]$, $C_{x'y'}[t+1] = C_{xy}[t]$.

5. In any other case, there is no change, $C_{xy}[t+1] = C_{xy}[t]$, $C_{x'y'}[t+1] = C_{x'y'}[t]$.

Transitions that result in no change will be referred to as “null transitions”.

4.3 Behaviour of the NANIA model

4.3.1 The NANIA model as a stochastic process

Before attempting to analyse or generalise the NANIA model, it will be useful to understand its behaviour in the most simple and fundamental terms possible. We wish to know, in a very broad sense, which microstates the model may occupy and how it is able to move between these states.

To achieve this aim, we formulate the model as a stochastic process, as described in Section 2.4. This approach is in line with McKane and Newman’s discussion of the closely related ecological patch models as stochastic processes (2004, Section I).

Consider the NANIA model on an $n \times n$ square or toroidal grid, with either Von Neumann or Moore adjacency. Relabel the cells C_{xy} , $x, y \in \{0, \dots, n-1\}$ with a single index C_i , $i \in \{0, \dots, n^2 - 1\}$ by means of the transformation $i = nx + y$ and relabel the states taken by particular cells with a pair of binary variables $(r_i, f_i) \in \{0, 1\}^2$, constrained by the inequality $r_i + f_i \leq 1$, such that the states ‘R’, ‘F’ and ‘E’ correspond respectively to the pairs $(1, 0)$, $(0, 1)$ and $(0, 0)$.

The model may now be described as a stochastic process $\{\mathbf{X}(t) : t \in T\}$, where $T = \mathbb{N} \cup \{0\}$ and where the $\mathbf{X}(t)$ are discrete vector random variables taking values in the state space:

$$\Omega = \left\{ (r_0, \dots, r_{n^2-1}, f_0, \dots, f_{n^2-1}) \in \{0, 1\}^{2n^2} : r_i + f_i \leq 1, \forall i \in \{0, \dots, n^2 - 1\} \right\} \quad (4.1)$$

Ω consists of the 3^{n^2} microstates representing all possible arrangements of foxes and rabbits across the lattice and is a subset of the $2n^2$ -dimensional space \mathbb{R}^{2n^2} . If we specify a probability distribution for $\mathbf{X}(0)$, then the family of joint probability density functions:

$$p_t(\mathbf{x}_0, \dots, \mathbf{x}_t) = P[\mathbf{X}(0) = \mathbf{x}_0, \dots, \mathbf{X}(t) = \mathbf{x}_t], \quad t \in T, \quad \mathbf{x}_0, \dots, \mathbf{x}_t \in \Omega$$

is unambiguously defined by the local transition rule $\mathfrak{T}_{\text{local}}$ described in Section 4.2.8 (assuming that the values of the parameters κ , ς and τ have been specified). Moreover, since $\mathfrak{T}_{\text{local}}$ determines the microstate at time $t + 1$ with reference only to

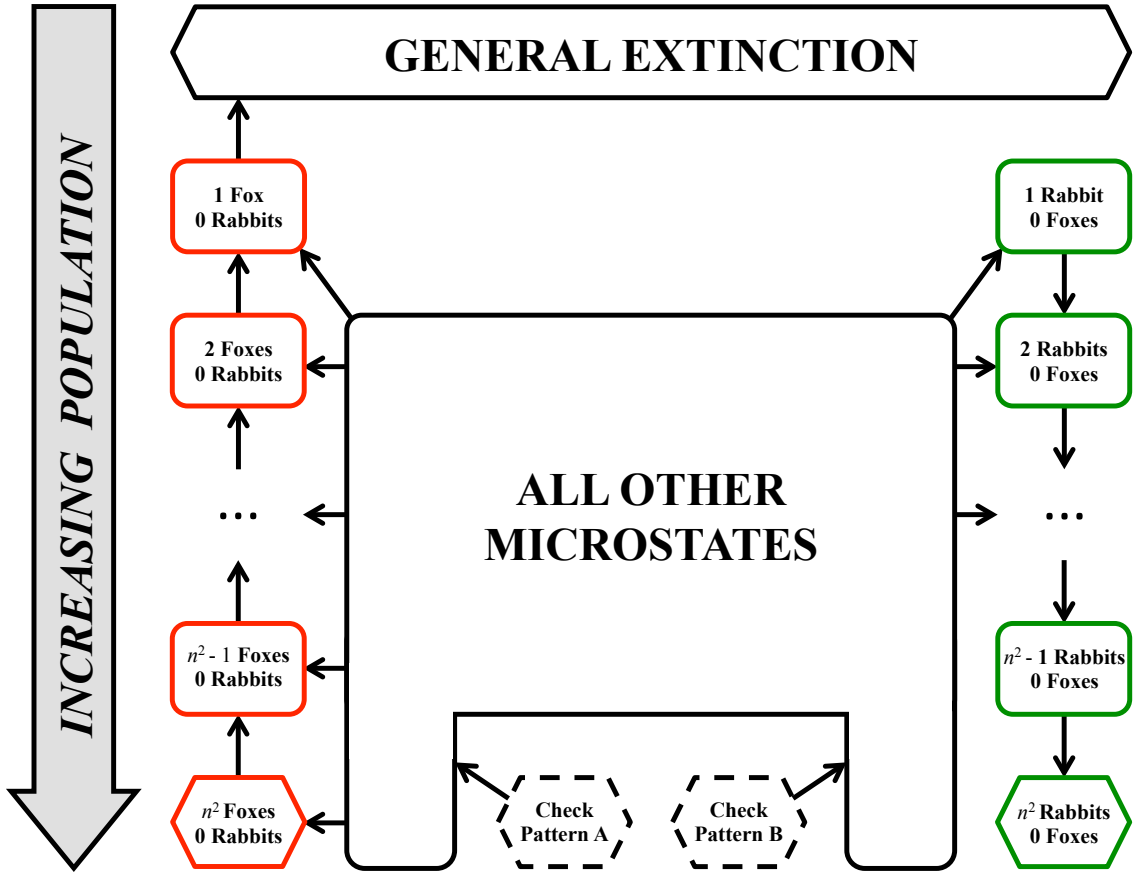


Figure 4.2: Figure illustrating the communication between different microstates of the NANIA model (in the sense of Definition 2.4.3), valid for models on grids of side length $n \geq 2$ with $\kappa, \varsigma, \tau \in (0, 1)$. Rounded boxes represent collections of microstates, all of which intercommunicate with one another. Hexagonal boxes represent particular microstates. Arrows indicate that all microstates in the box at the tail of the arrow communicate with all microstates in the box at the head of the arrow. The dashed boxes are only separate from the box labelled “ALL OTHER MICROSTATES” under certain circumstances, as discussed in the main text.

the microstate at time t and not to any previous microstates or to the value of t itself, considering Definitions 2.4.1 and 2.4.2, we see that the NANIA model is a time homogeneous Markov chain. Hence, consideration of communication between microstates (in line with Definition 2.4.3) is meaningful, and this will be the focus of the following section.

4.3.2 Communication between microstates in the NANIA model

In light of the previous section, we now examine which microstates of the NANIA model communicate with one another and thus determine the broad sweep of possible model behaviours. The complete network of communications is summarised in Figure 4.2 and the remainder of this section is dedicated to explaining and justifying

this structure.

The figure relates only to models for which the underlying lattice L has side-length of $n \geq 2$ and for which the three parameters κ , ς and τ lie in the open interval $(0, 1)$ (meaning that, when cells of the appropriate states have been selected, the processes of rabbit reproduction, fox reproduction and fox mortality are each possible, but not automatic). The model lattice may have Von Neumann or Moore adjacency and fixed or periodic boundaries. These choices do affect microstate communication to a certain degree, as discussed later.

In the figure, rounded boxes represent collections of microstates, all of which inter-communicate with one another. Hexagonal boxes represent particular microstates (for example, there is only one microstate corresponding to the extinction of both species and only one for which all n^2 cells are occupied by rabbits). Arrows indicate that all microstates in the box at the tail of the arrow communicate with all microstates in the box at the head of the arrow (more strictly, they indicate that there exists a microstate in the head box that may be reached from a microstate in the tail box by means of a *single* transition). Therefore, given any particular initial microstate, the behaviour of the NANIA model traces a path through the diagram, moving between microstates within its current box or moving between boxes in the direction of the arrows.

We consider each part of the figure in turn. Firstly, the right hand column of green boxes relate to microstates in which the fox population is extinct. Since a population of rabbits of a given size may clearly move to take on any particular arrangement over L (recall that individuals of the same species are indistinguishable), all microstates for which the rabbit population has a particular size must intercommunicate. Similarly, since rabbits may reproduce (even when alone), such microstates also communicate with microstates of a higher rabbit population, but since there is no mechanism for the removal of rabbits in the absence of foxes, communication does not operate in the opposite direction.

The left hand column of red boxes relates to microstates in which the rabbit population is extinct. The logic here is almost identical to that of the right hand column, except that fox populations may decrease, owing to mortality, but cannot increase, since fox reproduction is dependent on the presence of rabbits. This explains why the direction of communication in the left column is opposite to that of the right column. We also observe that microstates involving a single fox and no rabbits are the only microstates from which general extinction can be reached in a single tran-

sition.

All other microstates (with two possible exceptions, represented by the dashed hexagons) lie in the large central box and they all intercommunicate. Also, almost all single species microstates may be reached from a microstate with a mixture of species by means of a single transition, since, in a mixed population, a single fox may die or a single rabbit may be predated (replaced either by a fox or by an empty cell). The exceptions are due to the fact that, in order to die, a single fox requires an adjacent empty cell or an adjacent cell containing another fox, meaning that populations of $n^2 - 1$ or n^2 rabbits cannot be accessed from the central box by means of a single transition, which accounts for the omitted arrows in the bottom right hand corner of the diagram.

The diagram shows that there are two absorbing microstates of the model dynamics. These are, as expected, the microstate representing general extinction and that in which every cell is occupied by a rabbit.

The assertion that all (or all but two) microstates involving mixed populations of foxes and rabbits intercommunicate requires further justification. For very dense populations of rabbits and foxes, particularly those with no empty cells, in which movement is impossible, it is not immediately obvious that a possible series of transitions exists from any such microstate to any other. It also remains to explain the role of the two “Check Pattern” microstates, which occupy the dashed boxes at the bottom of Figure 4.2. Both of these issues are addressed in the proof of the following proposition, which summarises the results of this section:

Proposition 4.3.1. *Consider a NANIA model over an $n \times n$ lattice L , with $n \geq 2$ and parameters $\kappa, \varsigma, \tau \in (0, 1)$.*

- *If using Von Neumann adjacency with **either** fixed boundaries **or** periodic boundaries and an even value of n , then all microstates for which neither species is extinct intercommunicate **except** the two microstates for which no cell is empty and in which no two adjacent cells are occupied by the same species (denoted “Check Pattern A” and “Check Pattern B”).*
- *Otherwise, all microstates for which neither species is extinct intercommunicate.*

In the former case, the microstates denoted “Check Pattern A” and “Check Pattern B” communicate with all other microstates that involve mixed populations of rabbits and foxes. However, no microstate communicates with either of these microstates and they do not communicate with each other.

Owing to its length, the proof of Proposition 4.3.1 is presented separately, in Section 4.3.5. Examples of the two “Check Pattern” microstates are presented in Figure 4.3.

From Proposition 4.3.1, we see that, for NANIA models with Von Neumann adjacency with fixed boundaries or with periodic boundaries and even side-length, the two “Check Pattern” microstates play a similar role to “Gardens of Eden” in CAs (see Gardner, 1971), arrangements of cells that can never occur spontaneously as a result of model dynamics. However, the “Check Patterns” are not strictly the same as “Gardens of Eden”, since there do exist null transitions from a “Check Pattern” to itself, which occur automatically when the initial cell selected at a particular iteration is a rabbit.

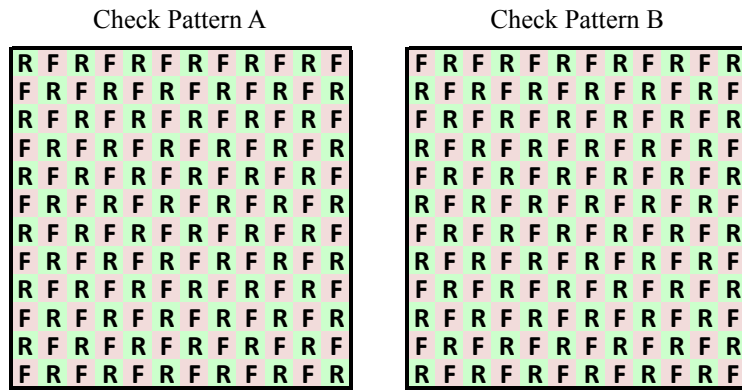


Figure 4.3: An example of the two “Check Pattern” microstates on a 12×12 lattice. The designations “A” and “B” are arbitrary and may be applied to the two microstates in either order.

4.3.3 From the NANIA model to the Lotka-Volterra equations

From Figure 4.3.1, we can draw some important conclusions about the model behaviour. Since we clearly see that every microstate in the model communicates with one or other of the two absorbing microstates (the “General Extinction” microstate, in which every cell is empty, and the microstate in which every cell is occupied by a rabbit), we conclude that all but these two microstates are transient: when occupying such a microstate, the probability of returning to it at some point in the future is strictly less than 1 (see Definition 2.4.5). Since the total number of possible microstates is finite, one consequence is that any initial condition will eventually necessarily evolve to one of the two absorbing states. Therefore, in any such model,

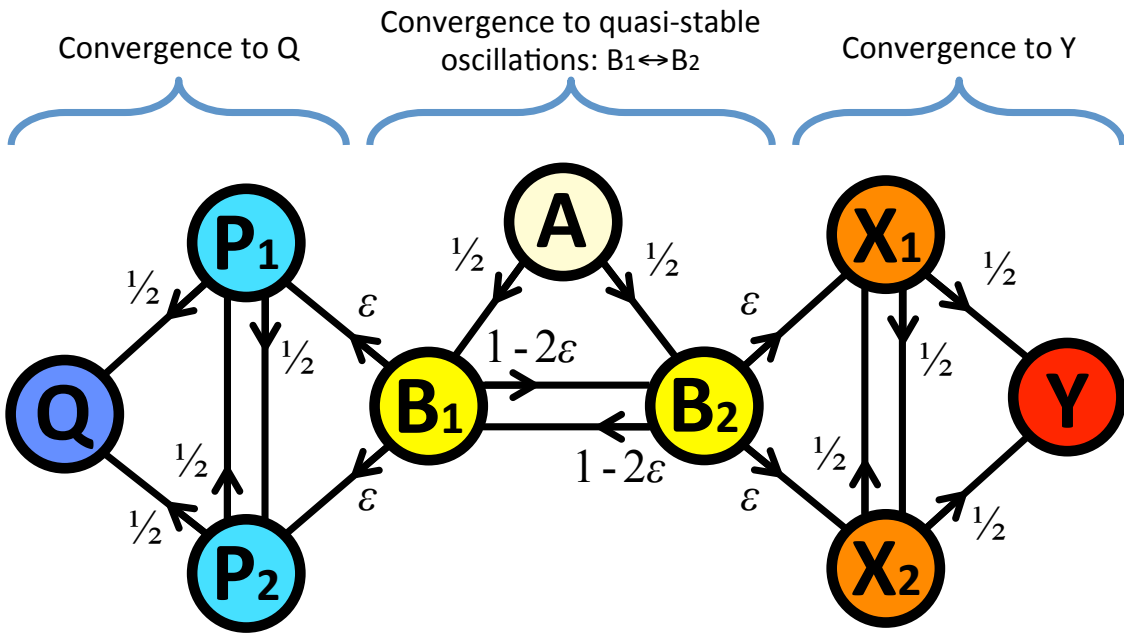


Figure 4.4: An example of a Markov chain that exhibits quasi-stable oscillations, despite the fact that the system is certain to evolve to an absorbing state in the long term. Vertices represent states of the system and edge weights represent the probabilities of moving between states.

For $\epsilon > 0$, any initial condition will eventually evolve to one of the two absorbing states Q or Y . However, if $0 < \epsilon \ll 1$, the state space can be divided into three distinct regions: a region of rapid convergence to Q , $\{P_1, P_2, Q\}$, a region of rapid convergence to Y , $\{X_1, X_2, Y\}$, and a region of convergence to quasi-stable oscillations $\{A, B_1, B_2\}$. Though the system will not remain in the third region indefinitely, through a suitable choice of ϵ , the expected time spent in this region can be made arbitrarily large. Note that A is in the third region, though A itself does not form part of the oscillations.

extinction of the fox population is certain in the long term, leading either to extinction of both species, or to the expansion of the rabbit population to fill the lattice.

However, while these observations are true, they are not necessarily very helpful in practice, since it may be the case that, for certain models and from certain initial microstates, the expected time required to evolve to one of the two absorbing states is so large that we can, in fact, meaningfully talk about situations of quasi-stable coexistence between the two species. This would be the case if, for example, evolving from a particular microstate to either of the absorbing microstates would require sequences of transitions that only occur with very low probability. Figure 4.4 illustrates a simple Markov chain which exhibits similar behaviour to this.

Ackland (2009) asserts that the evolution of the populations of rabbits and foxes in the NANIA model has dynamics similar to those of the widely studied Lotka-Volterra

equations (see Section 3.3.2):

$$\begin{aligned}\dot{u} &= u(a - bv) \\ \dot{v} &= -v(c - du)\end{aligned}\tag{4.2}$$

As discussed in Section 3.3.2, these equations display regular oscillations of the predator and prey population densities (u and v) about the fixed point $(u^*, v^*) = (c/d, a/b)$, but we have shown that the NANIA model necessarily evolves to one of its two absorbing states. It is therefore through this concept of quasi-stable coexistence in the NANIA model that the claims of Ackland should be understood. While it cannot truly replicate the permanent oscillatory behaviour of the Lotka-Volterra equations, over long time periods, the NANIA model could exhibit quasi-stable behaviour that does display similar oscillatory dynamics.

An implementation of the NANIA model was created in Python (Python Software Foundation, 2012) using the NumPy (Numpy Developers, 2012) package. Figure 4.5 shows an example of the population dynamics of the NANIA model, demonstrating that, for suitably chosen values of the parameters, it does indeed display distinct cycles in the densities of the two species.

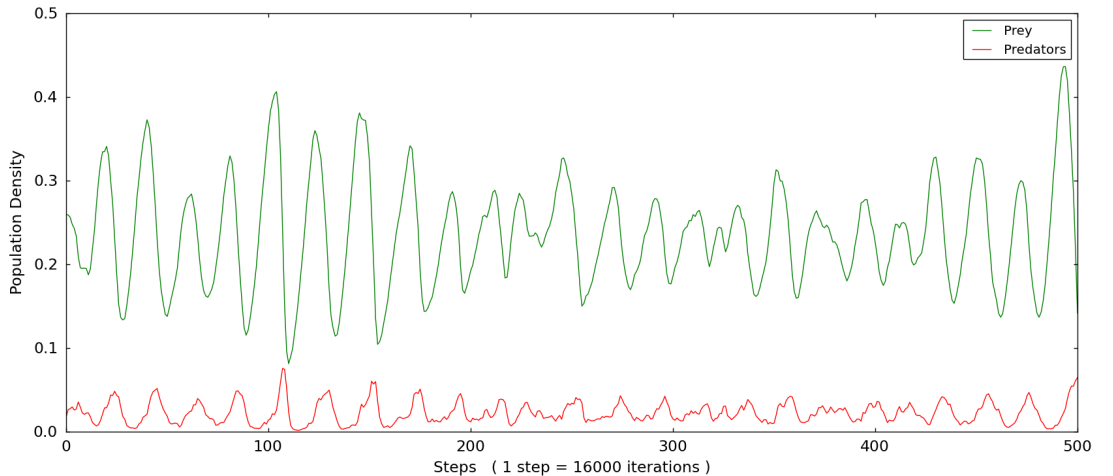


Figure 4.5: Sample dynamics of the NANIA model over a 120×120 toroidal lattice, with Moore adjacency and parameter values $\kappa = 0.02$, $\varsigma = 1.00$, $\tau = 0.15$. The plot shows 8 million iterations of the model, with observations made at intervals of 16 000 iterations. This is an extract from the dynamics of a longer simulation (for which the initial conditions were randomised) and is displayed since it provides a clear illustration of the population cycles of the system.

In the next section, we discuss one way in which an analytical connection may be made between the NANIA model and the Lotka-Volterra equations.

4.3.4 Connecting the NANIA model and the Lotka-Volterra equations using mean field theory

As discussed in Section 3.2.1, mean field theory is a method for representing the dynamics of systems of interacting entities as sets of differential equations that describe the evolution of globally aggregated quantities, such as population densities. In this section, we apply non-spatial mean field techniques to the NANIA model, in order to determine whether and to what extent the resulting ODEs match the Lotka-Volterra equations (4.2), with which the NANIA model is claimed to share certain dynamical features. Mean field theory will also form a key part of the analysis of a more general family of NANIA-like models, presented in Chapter 5.

Here, we consider a NANIA model over a toroidal lattice of size $n \times n$, with Moore adjacency. It should however be noted that the nature of the model geography is not actually relevant for the non-spatial mean field approach deployed in this section.

The dynamic variables of the Lotka-Volterra equations are the global population densities of the prey (“rabbits” in the NANIA model) and predator species (“foxes”), denoted respectively by u and v in equation (4.2). These will therefore be the summary variables used in the mean field analysis of the NANIA model.

We write $u(t)$ and $v(t)$ to represent the global densities of rabbits and foxes in the NANIA model at a particular time t . The continuous-time variables u and v will later be generated through consideration of a limiting case where δt (the time between iterations) is allowed to go to zero.

Based on the discussion of Section 3.2.2, and employing the notation introduced in Section 4.2, the mean field assumptions for the NANIA model will be stated as follows:

1. The states of all cells at a particular time t may be treated as independent identically distributed random variables, with the probability that a cell C_{xy} exhibits a particular state being proportional to the total number of cells in that state at that time.
2. The changes in $u(t)$ and $v(t)$ at any iteration will be assumed to be precisely equal to the expected values of these changes, as calculated under the previous assumption.

Note that, under assumption 1, two different forms of dependence between cell states are neglected. The first of these is the dependence induced by spatial correlations

Event	$C_{xy}[t]$	$C_{x'y'}[t]$	Probability of Event	δu	δv
Rabbit born	'R'	'E'	$\kappa u(1 - u - v)$	n^{-2}	0
Fox eats rabbit, fox born	'F'	'R'	ςvu	$-n^{-2}$	n^{-2}
Fox eats rabbit, no fox born	'F'	'R'	$(1 - \varsigma)vu$	$-n^{-2}$	0
Fox dies	'F'	'F' or 'E'	$\tau v(1 - u)$	0	$-n^{-2}$

Table 4.1: Summary of those events of a NANIA model that result in a change δu or δv in $u(t)$ or $v(t)$ respectively. Also presented are the probabilities of these changes under the mean field assumptions and their magnitudes (assuming an $n \times n$ lattice). The t dependence of u and v has been omitted for the sake of clarity.

generated by the transition rule of the NANIA model, the neglect of which is the basis of the mean field approach. The second form of dependence is that which follows from the knowledge of the global densities of different cell states, $u(t)$, $v(t)$ and $1 - u(t) - v(t)$ (the density of empty cells).

For the neglect of the second form of dependence to be reasonable, we require that n^2 , $n^2u(t)$, $n^2v(t)$ and $n^2(1 - u(t) - v(t))$ are all sufficiently large that the effect of conditioning the probability distribution for the state of $C_{x'y'}[t]$ (the second cell to be chosen at a particular iteration) on the state of $C_{xy}[t]$ (the first cell chosen) would be negligible. The following mean field analysis can therefore only be considered to be valid if the lattice of the NANIA model is sufficiently large and in situations in which none of the three cell states is too scarce.

Assumption 2 fulfils a similar role to a consideration of the limiting behaviour of the model as $n \rightarrow \infty$, a procedure that would not otherwise be possible in this case, since the rates of change of $u(t)$ and $v(t)$ are clearly proportional to n^{-2} and would therefore go to zero in this limit.

Given assumption 1, we may state that, $\forall X \in \{'R', 'F', 'E'\}$:

$$\begin{aligned} P(C_{xy}[t] = 'R') &= P(C_{x'y'}[t] = 'R' | C_{xy}[t] = X) = u(t) \\ P(C_{xy}[t] = 'F') &= P(C_{x'y'}[t] = 'F' | C_{xy}[t] = X) = v(t) \\ P(C_{xy}[t] = 'E') &= P(C_{x'y'}[t] = 'E' | C_{xy}[t] = X) = 1 - u(t) - v(t) \end{aligned} \quad (4.3)$$

Using (4.3), the expected changes in $u(t)$ and $v(t)$ over a single time interval can be derived from the transition rule given in Section 4.2.8. Those events that result in a change δu or δv in $u(t)$ or $v(t)$ are summarised in Table 4.1, along with the magnitudes of these changes and their probabilities.

From Table 4.1, with reference to assumption 2, mean field difference equations can

be constructed through considering the expected change in $u(t)$ and $v(t)$:

$$\begin{aligned} u(t + \delta t) &= u(t) + \frac{1}{n^2} u(t)[\kappa - \kappa u(t) - (1 + \kappa)v(t)] \\ v(t + \delta t) &= v(t) - \frac{1}{n^2} v(t)[\tau - (\varsigma + \tau)u(t)] \end{aligned} \quad (4.4)$$

In order to transform these difference equations into ODEs, to allow for comparison with the Lotka-Volterra equations, we must take the limit as $\delta t \rightarrow 0$. Unfortunately, such a limit is not meaningful in the context of the original model, since there is one fixed discrete time increment over which the transition rule operates and the behaviour of the model is not defined over shorter intervals. Observe that, for such a limit to exist, we certainly require that the magnitude of the changes in $u(t)$ and $v(t)$ should be dependent on δt .

We resolve this issue by supposing that the basic time increment of the original NANIA model is equal to 1. This allows us to rewrite (4.4) as follows:

$$\begin{aligned} u(t + \delta t) - u(t) &= \frac{\delta t}{n^2} u(t)[\kappa - \kappa u(t) - (1 + \kappa)v(t)] \\ v(t + \delta t) - v(t) &= -\frac{\delta t}{n^2} v(t)[\tau - (\varsigma + \tau)u(t)] \end{aligned} \quad (4.5)$$

These equations do have a meaningful limiting form as $\delta t \rightarrow 0$.

So, letting $a = \kappa/n^2$, $b = [1 + \kappa]/n^2$, $c = \tau/n^2$ and $d = [\varsigma + \tau]/n^2$ and taking the limit as $\delta t \rightarrow 0$, these equations become:

$$\begin{aligned} \dot{u} &= u(a - bv) - au^2 \\ \dot{v} &= -v(c - du) \end{aligned} \quad (4.6)$$

These equations are identical to the standard Lotka-Volterra equations, save for the $-au^2$ term. From the derivation of the equations, it can be seen that this term represents the limitation on rabbit population growth due to overcrowding, since rabbits cannot reproduce into cells that are already occupied by other rabbits.

In the standard Lotka-Volterra equations, the prey population grows exponentially in the absence of predators. By contrast, the mean field equations for the IBM suggest that the rabbit population grows logistically in the absence of foxes, with a carrying capacity of n^2 , indicating that the population can no longer increase when every cell is occupied by a rabbit.

At this stage, it should be reiterated that, while the non-spatial continuous mean

field model (4.6) has been derived from the NANIA model, the behaviours of the two models are not equivalent, even in terms of the expected dynamics of the individual densities u and v . Firstly, we know that the mean field assumptions are not true in the case of the NANIA model, since there are clearly dependencies between the states of nearby cells due to the local nature of the transition rule. Secondly, the NANIA model is discrete and has no true limiting behaviour as $\delta t \rightarrow 0$. Creating a continuous time system from the difference equations of (4.4) required that further assumptions be made about how the dynamics would scale as δt varied.

Therefore, as with all mean field models, (4.6) should be seen as a proposed representation of the dynamics of the NANIA model, which may or may not provide a good match to the true dynamics of the system in any given scenario. However, the fact that the mean field equations are equivalent to a logistic growth version of the Lotka-Volterra equations does provide a possible route to understanding why both models exhibit similar predator-prey population cycles, as observed in Figure 4.5.

4.3.5 Proof of Proposition 4.3.1

For convenience, the proposition is reproduced below:

Proposition 4.3.1. *Consider a NANIA model over an $n \times n$ lattice L , with $n \geq 2$ and parameters $\kappa, \varsigma, \tau \in (0, 1)$.*

- *If using Von Neumann adjacency with **either** fixed boundaries **or** periodic boundaries and an even value of n , then all microstates for which neither species is extinct intercommunicate **except** the two microstates for which no cell is empty and in which no two adjacent cells are occupied by the same species (denoted “Check Pattern A” and “Check Pattern B”).*
- *Otherwise, all microstates in which neither species is extinct intercommunicate.*

In the former case, the microstates denoted “Check Pattern A” and “Check Pattern B” communicate with all other microstates that involve mixed populations of rabbits and foxes. However, no microstate communicates with either of these microstates and they do not communicate with each other.

For two microstates to communicate, all that is required is that a series of valid transitions exists to transform the first microstate to the second, and that this series of transitions would occur with non-zero probability. Beyond this requirement, no consideration is necessary of how likely such a series might be. To prove communication between two microstates, it therefore suffices to identify a suitable series of transitions.

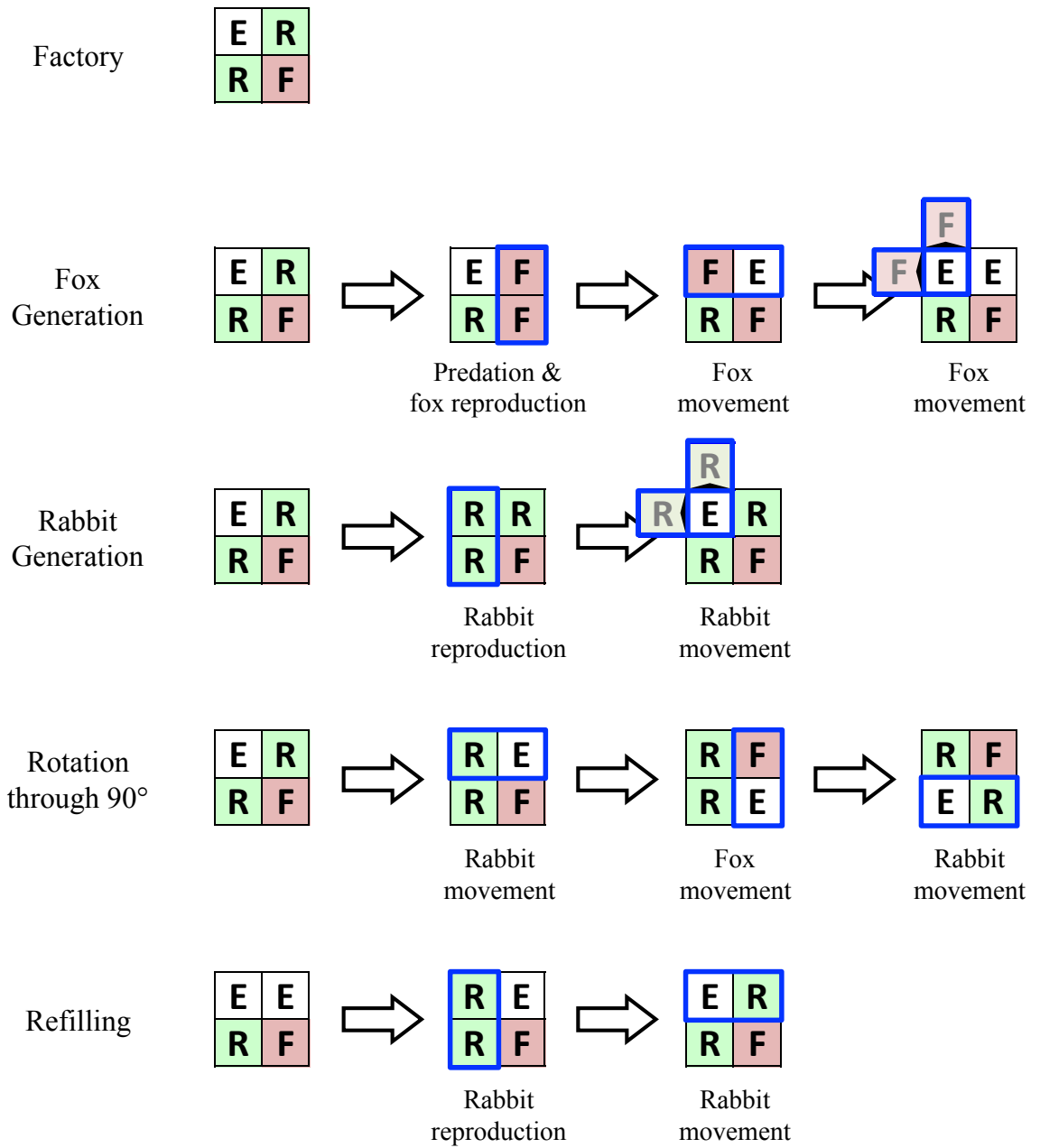


Figure 4.6: The “factory” arrangement of cells and some associated sequences of transitions. At each step, the cells in which a transition has occurred are outlined in blue. Note that, in the two “Generation” sequences, rabbits and foxes may leave the factory in two possible directions and that the “Fox Generation” sequence must be followed by the “Refilling” sequence to restore the factory.

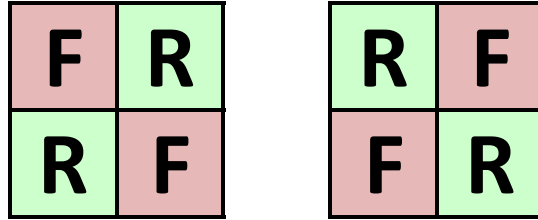


Figure 4.7: Disallowed arrangements for the location of the factory.

On this basis we present an algorithmic proof of Proposition 4.3.1. The concept behind the proof has similarities to Wolfram’s proof of universal computation in the “Rule 110” CA (2002, pp. 675-689), in that we explicitly construct configurations and dynamics within the model to demonstrate that a desired behaviour is possible.

Proof. To prove the proposition, we present an algorithm that constructs a series of transitions to transform any microstate that involves a mixed population of foxes and rabbits into any other such microstate (except in two special cases, which we consider separately at the end). The algorithm relies on the properties of a particular 2×2 arrangement of cells, which, in the interests of economy, we will call a “factory”. The factory is illustrated in Figure 4.6, along with several important sequences of transitions associated with it.

As seen in the figure, a factory is capable of generating fox and rabbit individuals and restoring itself to its original state (provided that one of the two external cells into which new individuals will move is empty). It can operate in any of its four possible orientations and is capable of rotating itself repeatedly through 90° .

We now set out the algorithm for transforming between microstates with mixed populations. Note that, whether using Von Neumann or Moore adjacency, all transitions should be considered to occur exclusively in pairs of *orthogonally* adjacent cells. Also, whether using fixed or periodic boundaries, we proceed *as if* they were fixed, with no transitions permitted for pairs of adjacent cells straddling the boundary.

Each step of the algorithm is illustrated by a corresponding image in Figures 4.8-4.9.

Consider two microstates $\mathbf{x}_1, \mathbf{x}_2 \in \Omega$ (using the definition of (4.1)) of a NANIA model over an $n \times n$ lattice L , with $n \geq 2$ and parameters $\kappa, \varsigma, \tau \in (0, 1)$, for which the fox and rabbit populations are both positive. We construct a series of possible model transitions to transform \mathbf{x}_1 into \mathbf{x}_2 as follows:

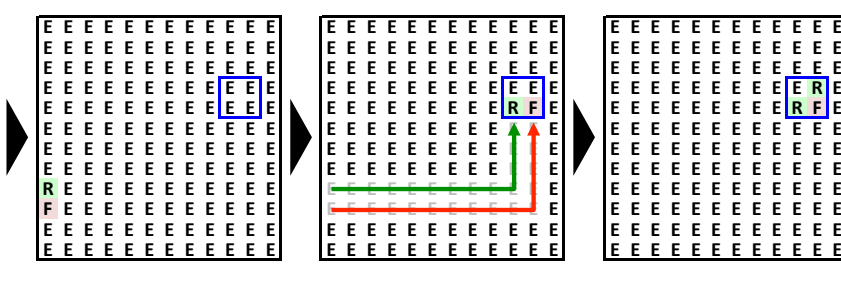
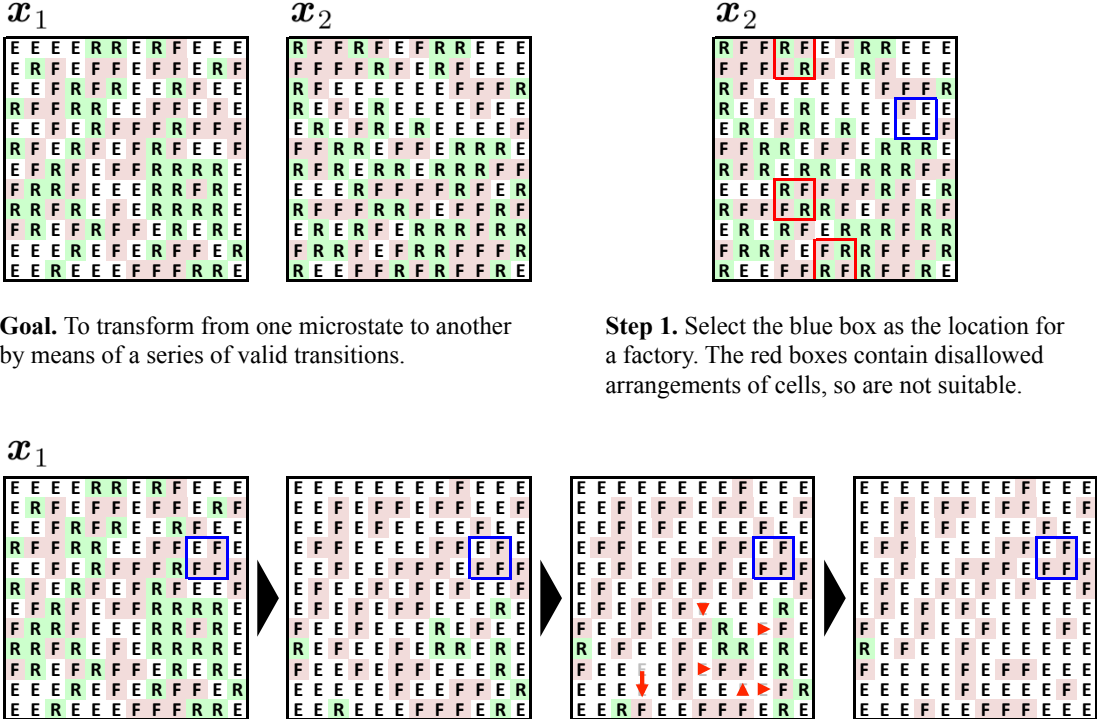


Figure 4.8: Visual presentation of the algorithm from the proof of Proposition 4.3.1. Steps 1-5.

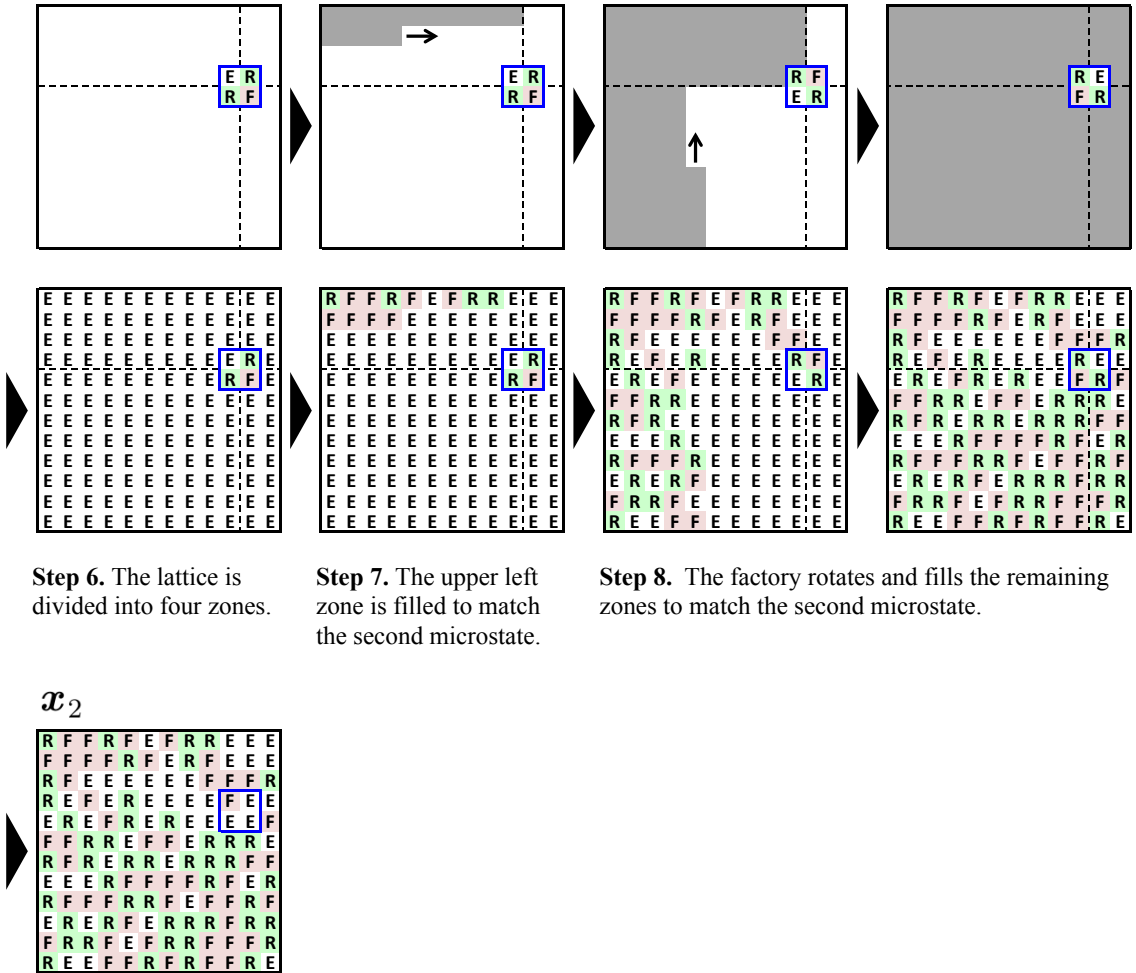


Figure 4.9: Visual presentation of the algorithm from the proof of Proposition 4.3.1. Steps 6-9.

1. Identify a 2×2 region of L for which the occupancies of the cells in \mathbf{x}_2 do not form either of the two patterns shown in Figure 4.7. For the time being, we assume both that such a region exists and, in the case that L has periodic boundaries, that it does not ‘cross’ the boundary of the lattice. This region will be used as the location of a factory.
2. Consider a series of transitions of \mathbf{x}_1 in which the foxes eat every rabbit (without reproducing) except the one occupying the cell C_i with the lowest index i (based on the transformation given in Section 4.3.1, roughly speaking, this is the rabbit that is closest to the bottom left corner of the grid, where the x coordinate is considered to increase from left to right and the y coordinate is considered to increase from bottom to top). The only processes that should be used are predation of rabbits by foxes and fox movement. Given the simple graph structures employed in the model (and the requirement that $n \geq 2$), this is clearly possible, since it is impossible for the single surviving rabbit to block access to others.
3. Following these transitions, suppose that the series continues with the death of every fox except the one occupying the cell C_i with the lowest index i . Since there is only one rabbit remaining, and since all cells have at least two neighbours, every fox must be adjacent to an empty cell or to a cell occupied by another fox, ensuring that this sequence of deaths is possible.
4. At this stage, the only remaining individuals are a single rabbit and a single fox. Suppose that the series of transitions continues with the rabbit moving to the lower left corner of the region identified at Step 1, followed by the fox moving to the lower right corner of this region.
5. Now suppose that the series continues with the construction of a factory in the region by means of the “Refilling” procedure illustrated in Figure 4.6.
6. Consider the horizontal and vertical lines that intersect at the centre of the factory. If the effect of any periodic boundaries is ignored, these lines divide L into four rectangular zones, which may be of unequal size, each of which includes a single cell of the factory.
7. The factory is able to generate fox and rabbit individuals which may move out into the upper left zone (see Figure 4.6). Consider, therefore, a series of transitions in which the appropriate individuals are generated in the factory to fill this zone such that its occupancy matches that of the corresponding area in \mathbf{x}_2 . The zone should be filled row by row, from left to right and from

top to bottom. In this zone, only the single cell lying in the factory will not necessarily match the occupancy of \mathbf{x}_2 .

8. Since the factory is able to rotate (see Figure 4.6), we may consider the series of transitions in which the factory successively rotates through 90° and fills each of the remaining three zones in the same fashion as described in Step 7.
9. At this stage, only the four cells of the factory may not have the same occupancy as that of \mathbf{x}_2 . However, it is simple to verify that a factory may be transformed into any 2×2 arrangement of foxes, rabbits and empty cells by means of a series of transitions applied only to orthogonally adjacent pairs of these cells, *except* the two arrangements illustrated in Figure 4.7³. Since the location of the factory was chosen specifically such that the occupancies of the cells in \mathbf{x}_2 did not match either of these two patterns, the series of transitions may therefore be continued such that the occupancy of the four cells comprising the factory matches that of the corresponding cells in \mathbf{x}_2 . The state of every cell in \mathbf{x}_1 has now therefore been transformed to the state of the corresponding cell in \mathbf{x}_2 by means of a series of transitions applied only to orthogonally adjacent pairs of cells.

At this point, we pause to consider exactly what has been proved. The above algorithm demonstrates that there exists a sequence of transitions to transform any microstate with a mixed population of foxes and rabbits to any other such microstate (and therefore that any two such microstates intercommunicate), *provided that* the assumption made at Step 1, relating to the second of these microstates, is true. Since we have only considered transitions on pairs of orthogonally adjacent cells, this result holds for both Von Neumann and Moore adjacency. Also, since we have proceeded as if the boundaries were fixed, the result must hold for fixed or periodic boundaries, since any transitions that can occur in the former case can also occur in the latter case.

Recall that the assumption made at Step 1 states that it is possible to find a 2×2 block of the lattice L for which the occupancies of the cells in \mathbf{x}_2 do not match either of the patterns depicted in Figure 4.7. Furthermore, this block was not permitted to cross the boundary of L , whether or not periodic boundary conditions were in operation (if this were permitted, it would interfere with Step 6). We have not yet given any consideration to the conditions under which this assumption is valid or to the implications of the assumption being false.

³ The proof of this assertion is omitted, since it simply requires a lengthy series of mechanical manipulations. Given that the factory may be rotated and that individuals may move through empty cells, 15 separate target arrangements must be considered.

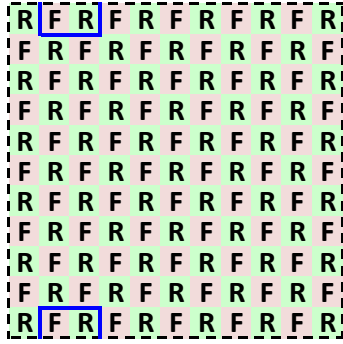


Figure 4.10: Given a “Check Pattern” microstate for a lattice with odd side length and periodic boundary conditions, a suitable 2×2 block for the location of a factory can be found lying across the boundary, as seen here.

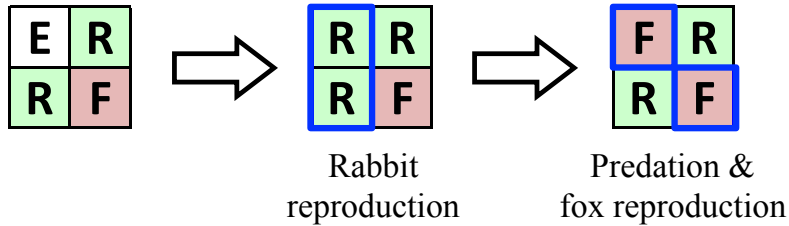


Figure 4.11: Factories can be transformed into either of the arrangements depicted in Figure 4.7 by means of valid transitions if using Moore adjacency. One example is given here; the other arrangement may be reached by rotating the factory through 90° before performing the above sequence of transitions.

Consider the first of these issues. It is clear that the only arrangements of foxes and rabbits across a lattice, such that it is impossible to find a 2×2 block that *does not* look like one of the two images given in Figure 4.7 are those that look like chessboards, where there are no empty cells, and no orthogonally adjacent cells containing individuals of the same species. These are “Check Pattern A” and “Check Pattern B”, as described in the Proposition (see Figure 4.3). Note that the designations “A” and “B” are arbitrary and may be applied to the two microstates in either order.

With fixed boundaries, these two microstates do not contain a suitable 2×2 block for the placement of a factory. The same is true for periodic boundaries in lattices with an even side length n , even allowing for blocks lying across the boundaries. However, observe that with periodic boundaries in lattices with an odd side length n , observe that suitable 2×2 blocks can nonetheless be found lying across the boundary of the lattice (see Figure 4.10). In such circumstances, a relabelling of the cells to represent an appropriate shift in the x or y coordinate axes reduces the situation to which the algorithm may be applied, and all mixed population microstates intercommunicate.

Now consider the cases in which the algorithm fails: lattices with fixed boundary conditions and lattices with periodic boundary conditions and even side-length. In these cases, it is easy to see that, with Von Neumann adjacency, no microstates communicate with either of the two “Check Patterns”. In the NANIA model, no non-null transition exists whose output (in terms of the states of the two selected cells) includes one fox and one rabbit. However, every pair of orthogonally adjacent cells in the “Check Patterns” is of this form.

It only remains to consider these same cases, lattices with fixed boundary conditions and lattices with periodic boundary conditions and even side-length, with Moore adjacency. We observe that, in this case, a factory *can* be transformed into either of the disallowed arrangements shown in Figure 4.7, by means of the process depicted in Figure 4.11. In this case, the algorithm can therefore successfully be applied with *any* location chosen for the factory.

This proves the proposition and thus justifies the dynamical structure of the NANIA model presented in Figure 4.2. \square

4.4 Generalising the NANIA model

4.4.1 Motivation and aims

Clearly, the NANIA model is just one particular example of a wider family of possible autonome models that might be defined using similar mechanisms. In specifying the model, a number of decisions were taken regarding the structure of the space over which individuals move, the number of species of individual and the ways in which individuals can and cannot interact, each of which could be generalised to define a broader family of models.

The NANIA model has some similarities with CAs (see Section 2.3), in that it operates in discrete time over a regular lattice of cells, with each cell able to exhibit a discrete range of states at each time step. However, it differs from a CA in other key ways, in that updates are performed asynchronously and stochastically, both in terms of which pairs of cells are updated at a given time step and in terms of what the outcome of an update will be.

These features make the NANIA model similar to other kinds of Wolfram’s “simple programs”, such as randomised versions of “mobile automata” (2002, pp. 71-77),

“sequential cellular automata” with random updating (p. 1032) or the Eden model (pp. 331-332). It also has similarities to the predator-prey CA of He et al. (2003) and could be formulated as a special case of the ecological patch models described by McKane and Newman (2004) (see Section 3.3.3 for further details of these models).

While CAs have received a large amount of theoretical attention since their creation, asynchronous stochastic cellular models similar to the NANIA model have received far less. However, given the links between these models and others – particularly to ecological patch models, which have been widely applied in the field of population biology, and to the Eden model, for which there is “no known way to make a rigorous mathematical analysis” (Wolfram, 2002, p. 332) – we would argue that a thorough examination of models of this kind would be equally valuable. Indeed, the asynchronous scheduling of updates in the NANIA model could make it a better basis for the representation of real systems than CAs, as argued by Caron-Lormier et al. (2008, see Section 2.2.4).

Like CAs, a generalised version of the NANIA model could also provide an ideal “paradigm system” (in the sense outlined by Hogeweg (1988), as discussed in Section 2.3.4) for the investigation of important concepts in complexity theory, since, according to San Miguel et al. (2012, p. 250):

“Simple models are essential to uncover the basic mechanisms [of complex systems] and provide insight into fundamental questions.”

In the spirit of this argument, in this section, we isolate those features of the NANIA model that could be considered to be fundamental from those that we judge to be arbitrary and we examine the full family of models that result from relaxing the assumptions that relate to these arbitrary features. In this way, we aim to create a general model that may provide insights, not just into the NANIA model itself, but into a far broader range of systems.

4.4.2 \mathfrak{A} -models: A fundamental generalisation of the NANIA model

The following features of the NANIA model will be taken as fundamental characteristics, to be used as the basis for a broader family of models. Where appropriate, to emphasise the points of connection between these models and CAs, we employ similar notation to that used in the definition of a CA that was presented in Section 2.3.1.

- The model is spatially explicit, with a specific, fixed, discrete, finite geography. In the most general case, this geography may be any specified finite graph G ,

which may be directed or undirected. The vertices of G will be referred to as “cells”.

- Time is discrete and proceeds in steps of size δt .
- There are m species of individual: ‘S’₁, …, ‘S’ _{m} (in the NANIA model, $m = 2$). At any time t a particular cell C may be empty ($C[t] = ‘E’$) or occupied by an individual of a particular species ($C[t] = ‘S’ _{$i$}$). A cell may not be occupied by more than one individual. The set $\mathcal{C} = \{‘E’, ‘S’_1, \dots, ‘S’_m\}$ is called the **cell state space** of the model.
- At each time step, a cell $C^{(I)}$ is selected at random by means of a discrete uniform distribution over all the cells. A neighbour $C^{(II)}$ of $C^{(I)}$ is then selected by means of a discrete uniform distribution over the set of neighbours of $C^{(I)}$.
- Cells $C^{(I)}$ and $C^{(II)}$ are then updated according to some deterministic or stochastic local transition rule $\mathfrak{T}_{\text{local}}$, which depends only on the current states of these two cells:

$$\begin{array}{ccc} \mathfrak{T}_{\text{local}} : & \mathcal{C}^2 & \rightarrow & \mathcal{C}^2 \\ & (C^{(I)}[t], C^{(II)}[t]) & \mapsto & (C^{(I)}[t + \delta t], C^{(II)}[t + \delta t]) \end{array}$$

Note that $\mathfrak{T}_{\text{local}}$ is defined as a transition operating on the states of adjacent pairs of cells. However, in practice, it will be more convenient to consider a global transition rule \mathfrak{T} , which operates on the microstates, mapping from Ω to Ω (recall that Ω is the state space of the model – the set of all possible microstates – as described in (4.1)). \mathfrak{T} encompasses the entire updating process, including the selection of the cells $C^{(I)}$ and $C^{(II)}$ and the subsequent application of the rule $\mathfrak{T}_{\text{local}}$. In this way, $\mathfrak{T}_{\text{local}}$ and \mathfrak{T} are equivalent to the corresponding local and global transition rules for CAs described in Definition 2.3.1.

The framework described above represents a generalisation of the NANIA model, in which the lattice over which the individuals move has been replaced with a general graph G , the number of species of individual has been generalised from 2 to m and the transition rule for the chosen cells may take any form. We label this family of models \mathfrak{A} (“Fraktur A”).

4.4.3 The range of possible transition rules for \mathfrak{A} -models

We now examine the range of valid local rules $\mathfrak{T}_{\text{local}}$. For a model in \mathfrak{A} , any particular local transition rule $\mathfrak{T}_{\text{local}}$ may be specified by means of a four-dimensional array of

parameters, A , representing the probabilities of each possible outcome given any possible pair of initial states:

$$A = \left\{ \alpha_{XYZW} \in B : X, Y, Z, W \in \mathcal{C} \text{ and } \sum_{Z,W \in \mathcal{C}} \alpha_{XYZW} = 1, \forall X, Y \in \mathcal{C} \right\}$$

$B = [0, 1]$ (the closed unit interval) for stochastic models and $B = \{0, 1\}$ for deterministic models. α_{XYZW} represents the probability that $\mathfrak{T}_{\text{local}}$ transforms a given pair of cell states $(X, Y) \in \mathcal{C}^2$ to the pair $(Z, W) \in \mathcal{C}^2$.

Since a given local transition rule $\mathfrak{T}_{\text{local}}$ may transform any of the $(m + 1)^2$ possible ordered pairs of cell states in \mathcal{C}^2 to any other such pair, then, given a set G , there are clearly $(m + 1)^2(m + 1)^2$ distinct deterministic transition rules that correspond to models in \mathfrak{A} .

We may also consider the dimension of the parameter space of the stochastic transition rules for models in \mathfrak{A} . In this case, each of the $(m + 1)^2$ ordered pairs (X, Y) of cell states in \mathcal{C}^2 has associated with it $(m + 1)^2$ parameters α_{XYZW} , representing the probabilities that such a pair will be transformed to each of the elements of \mathcal{C}^2 . However, since these probabilities must sum to one, the number of free parameters associated with the pair (X, Y) is actually $(m + 1)^2 - 1$ and these parameters lie on an $[(m + 1)^2 - 1]$ -simplex embedded in $\mathbb{R}^{(m+1)^2}$.

The complete parameter space is a Cartesian product of $(m + 1)^2$ such $[(m + 1)^2 - 1]$ -simplexes, and therefore has $(m + 1)^2 [(m + 1)^2 - 1] = m(m + 2)(m + 1)^2$ free dimensions.

4.4.4 Equivalence of microstates in \mathfrak{A} -models

In analysing the dynamics of a \mathfrak{A} -model, it should be noted that certain choices for the underlying geography (the graph G) may introduce a degree of redundancy into the way in which microstates of the model are described due to any symmetries of the graph. Since the existence of such equivalences between microstates may significantly reduce the scope of possible model behaviours and will therefore have consequences for any investigation of the model dynamics, we take the time to examine such equivalences in detail here.

In this section, unless otherwise stated, we consider \mathfrak{A} -models with m species and transition rule \mathfrak{T} over a finite undirected graph $G = (V(G), E(G))$, where $V(G)$ and

$E(G)$ are respectively the vertex set and the edge set of G , defined as:

$$V(G) = \{C_0, \dots, C_{n-1}\}$$

$$E(G) = \{\{C, D\} \subseteq V(G) : C \text{ is adjacent to } D\}$$

Also, C and D will be used to represent general cells, and the notation $N(C)$ will be used to denote the open neighbourhood of the cell C (the set of cells adjacent to C , excluding C itself), as in Section 4.2.3. The state space of the model will be represented as $\Omega = \{0, \dots, m\}^n$, with a specific microstate $\mathbf{x} = (x_0, \dots, x_{n-1}) \in \Omega$ defined such that $x_i = 0$ indicates that cell C_i takes state ‘E’, while $x_i = k > 0$ indicates that vertex C_i takes state ‘S’ _{k} .

Recall that an automorphism of a graph G is a mapping of the vertex set of G to itself such that vertex adjacencies are preserved. The following definition, adapted from Bondy and Murty (1976, pp. 5-7), is a formalised version of this:

Definition 4.4.1. Consider a simple graph G .

- An **automorphism** ϕ of G is a permutation of the vertices:

$$\begin{aligned} \phi &: V(G) \rightarrow V(G) \\ v &\mapsto \phi(v) \end{aligned}$$

such that:

$$\{v, w\} \in E(G) \Leftrightarrow \{\phi(v), \phi(w)\} \in E(G)$$

- The **automorphism group** $\Gamma(G)$ is the permutation group formed by the set of all automorphisms of G , with the operation of composition.

Note that, since an automorphism ϕ is a permutation, it has a well defined inverse ϕ^{-1} . Also, for the sake of simplicity, for the remainder of this chapter, an automorphism ϕ of the underlying graph G of a particular \mathfrak{A} -model is considered to act both as a permutation of the cells $\{C_0, \dots, C_{n-1}\}$ and as the corresponding permutation of the integers $\{0, \dots, n-1\}$, such that:

$$\phi(C_i) = C_j \Leftrightarrow \phi(i) = j, \forall i, j \in \{0, \dots, n-1\}$$

Once we have identified the automorphisms of G , it will be useful to talk about the effect of automorphisms on the microstates of the system. The following definition allows us to do this:

Definition 4.4.2. Consider a \mathfrak{A} -model with m species and transition rule \mathfrak{T} over a finite graph G with n cells.

Given that ϕ is a specific automorphism of G , the function $\hat{\phi}$ is defined in the following way:

$$\begin{aligned}\hat{\phi} &: \Omega \rightarrow \Omega \\ \mathbf{x} &\mapsto \hat{\phi}(\mathbf{x})\end{aligned}$$

where $\hat{\phi}(\mathbf{x}) = (\hat{x}_0, \dots, \hat{x}_{n-1})$ with $\hat{x}_i = x_{\phi^{-1}(i)}$ for all $i \in \{0, \dots, n-1\}$.

Since ϕ^{-1} is well defined, the function $\hat{\phi}^{-1}$ is also well defined with:

$$\mathbf{y} = \hat{\phi}(\mathbf{x}) \Leftrightarrow \mathbf{x} = \hat{\phi}^{-1}(\mathbf{y})$$

Using the above terminology, we now define a binary relation on the state space Ω of the model:

Definition 4.4.3. Consider a \mathfrak{A} -model with m species and transition rule \mathfrak{T} over a finite graph G with n cells. Consider specific microstates of the system $\mathbf{x}, \mathbf{y} \in \Omega$. The binary relation \sim on Ω is defined such that $\mathbf{x} \sim \mathbf{y}$ if and only if there exists an automorphism ϕ of G such that $\mathbf{y} = \hat{\phi}(\mathbf{x})$.

Observe that \sim is clearly an **equivalence relation**. This follows automatically from the fact that the automorphisms of G form a group. The existence of an identity automorphism ensures that \sim is reflexive, the fact that every automorphism has an inverse ensures that \sim is symmetric and the fact that $\Gamma(G)$ is closed under composition ensures that \sim is transitive.

The state space Ω of the model may therefore be partitioned into **equivalence classes**, each containing microstates that may be transformed from one to another by means of graph automorphisms. The equivalence class of a particular microstate \mathbf{x} is denoted $[\mathbf{x}]$ and the set of all equivalence classes of \sim is denoted Ω/\sim .

The following proposition will have important implications for any analysis of the dynamics of a \mathfrak{A} -model:

Proposition 4.4.4. Consider a \mathfrak{A} -model with m species and transition rule \mathfrak{T} (considered here as a stochastic mapping from Ω to Ω) over a finite graph G with n cells. Suppose that $\mathbf{x} \in \Omega$ is the microstate occupied by the system at any given iteration and let $p(\mathbf{x}, [\mathbf{y}])$ represent the probability that $\mathfrak{T}(\mathbf{x}) \in [\mathbf{y}]$, where $\mathfrak{T}(\mathbf{x})$ is a discrete random variable taking values in Ω , which represents the microstate of the system

after the application of the transition rule \mathfrak{T} , and $\mathbf{y} \in \Omega$ is any microstate of the system. Then, for any $\mathbf{x}_1, \mathbf{x}_2 \in \Omega$:

$$[\mathbf{x}_1] = [\mathbf{x}_2] \Rightarrow p(\mathbf{x}_1, [\mathbf{y}]) = p(\mathbf{x}_2, [\mathbf{y}])$$

Proof. For the purposes of this proof only, we extend the notation for an open neighbourhood $N(\cdot)$ to act as a function on the set of integers $\{0, \dots, n-1\}$ in the following way. Letting $V(G) = \{C_0, \dots, C_{n-1}\}$, as usual, we define:

$$\begin{aligned} N : \{0, \dots, n-1\} &\rightarrow 2^{\{0, \dots, n-1\}} \\ i &\mapsto \{j \in \{0, \dots, n-1\} : C_j \in N(C_i)\} \end{aligned}$$

where $2^{\{0, \dots, n-1\}}$ is the power set of $\{0, \dots, n-1\}$ (the set of all subsets of the integers from 0 to $n-1$). Observe that $N(\cdot)$ maps the index of a given cell to the set of the indices of that cell's neighbours.

Now, recall that, for a \mathfrak{A} -model, the transition rule \mathfrak{T} selects an initial cell $C^{(I)}$ according to a uniform random distribution over $V(G)$ and selects a neighbour $C^{(II)}$ of $C^{(I)}$ according to a uniform random distribution over $N(C^{(I)})$. Here, $C^{(I)}$ and $C^{(II)}$ are treated as random variables taking values in $V(G)$.

The probability $p(\mathbf{x}, [\mathbf{y}])$ may therefore be written as follows:

$$\begin{aligned} &p(\mathbf{x}, [\mathbf{y}]) \\ &= \sum_{\mathbf{z} \in [\mathbf{y}]} \sum_{i=0}^{n-1} \sum_{j \in N(i)} P(C^{(I)} = C_i) P(C^{(II)} = C_j | C^{(I)} = C_i) P(\mathfrak{T}(\mathbf{x}) = \mathbf{z} | C^{(I)} = C_i, C^{(II)} = C_j) \\ &= \frac{1}{n} \sum_{\mathbf{z} \in [\mathbf{y}]} \sum_{i=0}^{n-1} \sum_{j \in N(i)} \frac{1}{|N(C_i)|} P(\mathfrak{T}(\mathbf{x}) = \mathbf{z} | C^{(I)} = C_i, C^{(II)} = C_j) \end{aligned}$$

where $P(\mathfrak{T}(\mathbf{x}) = \mathbf{z} | C^{(I)} = C_i, C^{(II)} = C_j)$ denotes the probability of a transition from \mathbf{x} to \mathbf{z} , at any iteration at which the system occupies the microstate \mathbf{x} , given particular realisations of the random variables $C^{(I)} = C_i$ and $C^{(II)} = C_j \in N(C_i)$.

Observe that, owing to the way in which the transition rule is defined and given that $C^{(I)}$ and $C^{(II)}$ must be adjacent, we have that:

$$\begin{aligned} & \text{P}(\mathfrak{T}(\mathbf{x}) = \mathbf{z} \mid C^{(\text{I})} = C_i, C^{(\text{II})} = C_j) \\ &= \begin{cases} 0, & \text{if } \exists k \in \{0, \dots, n-1\} \setminus \{i, j\} \text{ such that } x_k \neq z_k \\ f(x_i, x_j, z_i, z_j), & \text{otherwise.} \end{cases} \end{aligned}$$

The key point here is not the form of the function f but the fact that it depends only on the four cell states that comprise its arguments. From this expression, given an automorphism ϕ of G , we derive the following:

$$\begin{aligned} & \text{P}(\mathfrak{T}(\hat{\phi}(\mathbf{x})) = \hat{\phi}(\mathbf{z}) \mid C^{(\text{I})} = \phi(C_i), C^{(\text{II})} = \phi(C_j)) \\ &= \begin{cases} 0, & \text{if } \exists k' \in \{0, \dots, n-1\} \setminus \{\phi(i), \phi(j)\} \text{ such that } \hat{x}_{k'} \neq \hat{z}_{k'} \\ f(\hat{x}_{\phi(i)}, \hat{x}_{\phi(j)}, \hat{z}_{\phi(i)}, \hat{z}_{\phi(j)}), & \text{otherwise.} \end{cases} \\ &= \begin{cases} 0, & \text{if } \exists k' \in \{0, \dots, n-1\} \setminus \{\phi(i), \phi(j)\} \text{ such that } x_{\phi^{-1}(k')} \neq z_{\phi^{-1}(k')} \\ f(x_i, x_j, z_i, z_j), & \text{otherwise.} \end{cases} \\ &= \begin{cases} 0, & \text{if } \exists k \in \{0, \dots, n-1\} \setminus \{i, j\} \text{ such that } x_k \neq z_k \text{ [with } k = \phi^{-1}(k') \text{]} \\ f(x_i, x_j, z_i, z_j), & \text{otherwise.} \end{cases} \\ &= \text{P}(\mathfrak{T}(\mathbf{x}) = \mathbf{z} \mid C^{(\text{I})} = C_i, C^{(\text{II})} = C_j) \end{aligned}$$

Now, if $[\mathbf{x}_1] = [\mathbf{x}_2]$, then $\exists \phi \in \Gamma(G)$ such that $\mathbf{x}_2 = \hat{\phi}(\mathbf{x}_1)$. We therefore observe that:

$$\begin{aligned} & \text{P}(\mathfrak{T}(\mathbf{x}_1) = \mathbf{z} \mid C^{(\text{I})} = C_i, C^{(\text{II})} = C_j) \\ &= \text{P}(\mathfrak{T}(\mathbf{x}_2) = \hat{\phi}(\mathbf{z}) \mid C^{(\text{I})} = \phi(C_i), C^{(\text{II})} = \phi(C_j)) \end{aligned}$$

Also, since ϕ preserves adjacencies, $|N(C_i)| = |N(\phi(C_i))|$ for all $i \in \{0, \dots, n-1\}$. Therefore:

$$\begin{aligned} & p(\mathbf{x}_1, [\mathbf{y}]) \\ &= \frac{1}{n} \sum_{\mathbf{z}' \in [\mathbf{y}]} \sum_{i'=0}^{n-1} \sum_{j' \in N(i')} \frac{1}{|N(\phi(C_{i'}))|} \text{P}(\mathfrak{T}(\mathbf{x}_2) = \hat{\phi}(\mathbf{z}') \mid C^{(\text{I})} = \phi(C_{i'}), C^{(\text{II})} = \phi(C_{j'})) \end{aligned}$$

Furthermore, letting $i = \phi(i')$, $j = \phi(j')$ and $\mathbf{z} = \hat{\phi}(\mathbf{z}')$ and observing that $\hat{\phi}$ operates as a bijection from $[\mathbf{y}]$ to itself, while ϕ is both a permutation of $V(G)$ and, since it preserves adjacencies, may also operate as an bijection from $N(\phi^{-1}(C_i))$ to

$N(C_i)$, we may write:

$$\begin{aligned} p(\mathbf{x}_1, [\mathbf{y}]) &= \frac{1}{n} \sum_{\mathbf{z} \in [\mathbf{y}]} \sum_{i=0}^{n-1} \sum_{j \in N(i)} \frac{1}{|N(C_i)|} P(\mathfrak{T}(\mathbf{x}_2) = \mathbf{z} \mid C^{(I)} = C_i, C^{(II)} = C_j) \\ &= p(\mathbf{x}_2, [\mathbf{y}]) \end{aligned}$$

This proves the proposition. \square

An important implication of this proposition is that if the cells of a \mathfrak{A} -model differ only in their adjacencies and their numbering in such a way that the graph G is indistinguishable from $\phi(G)$ (the graph whose vertices have been relabelled according to the action of the automorphism ϕ), then the dynamics of the model do not depend on the precise microstate occupied by the system at a particular iteration, but rather on the equivalence class of that microstate with respect to the automorphisms of G . This is because the probability that a single transition will send the system to any microstate in a particular equivalence class is the same for all microstates in the current class. In other words, to understand the dynamics of a \mathfrak{A} -model it suffices to monitor these equivalence classes, *not* the precise microstates occupied by the system. To all intents and purposes, at all times, the system may be considered to occupy *any* convenient microstate in its current class.

This result will be of fundamental importance in Chapter 6, in which we take advantage of the equivalences between microstates to transform the model dynamics into a new space, in order to better examine the relationship between local transitions and global behaviour.

4.4.5 Example: Equivalent microstates of a one-dimensional \mathfrak{A} -model

As an example of the ideas outlined in the previous section, consider the possible microstates of a single species (i.e. $m = 1$) \mathfrak{A} -model, where the underlying graph G is a one-dimensional ring of n cells C_0, \dots, C_{n-1} , where cells whose indices differ by 1 (mod n) are adjacent, such that each cell has precisely two neighbours. For reasons of convenience, rather than representing the microstates of the model as vectors, they will be represented as periodic binary sequences $\mathbf{c} = (c_i)_{i \in \mathbb{Z}} \in \{0, 1\}^{\mathbb{Z}}$, with $c_i = c_{n+i}$, $\forall i \in \mathbb{Z}$, where $c_i = 0 \Leftrightarrow C_{i \bmod n} = \text{'E}'$ and $c_i = 1 \Leftrightarrow C_{i \bmod n} = \text{'S}'$. Models over rings of cells will be investigated in detail in Chapter 5.

Note that these sequences are indexed by the complete set of integers, rather than only the non-negative integers as would be usual, and are thus infinite in both the

positive and negative directions. When discussing periodic sequences of this kind, the following notation will be used:

Definition 4.4.5. Consider $X^{\mathbb{Z}}$, the set of sequences of elements of a set X indexed by the set of all integers \mathbb{Z} . Given an element $\mathbf{v} = (v_i)_{i \in \mathbb{Z}} \in X^{\mathbb{Z}}$, the notation:

$$\mathbf{v} = (\dots, x_0, x_1, x_2, \dots, x_{u-1}, \dots)$$

where $x_0, \dots, x_{u-1} \in X$ and $u \in \mathbb{N}$, indicates that \mathbf{v} is a periodic sequence in $X^{\mathbb{Z}}$ of period u (or of period equal to a factor of u if the terms x_1, \dots, x_u themselves consist of a repeating subset of elements), with:

$$v_i = x_{i \bmod u}, \quad \forall i \in \mathbb{Z}$$

In this particular model, the set of all microstates will be denoted by Ω_n . We also let $U(\mathbf{c})$ represent the **population** of \mathbf{c} , the number of occupied cells in the model or (equivalently) the sum over any n consecutive terms of \mathbf{c} .

In the scenario considered here, the automorphisms of G are reflections and translations of the cells (and combinations of these transformations). Formally then, letting $\mathbf{c}_1 = (c_{1,i})_{i \in \mathbb{Z}}$ and $\mathbf{c}_2 = (c_{2,i})_{i \in \mathbb{Z}}$, the equivalence relation \sim for $\mathbf{c}_1, \mathbf{c}_2 \in \Omega_n$ may be written:

$$\mathbf{c}_1 \sim \mathbf{c}_2 \Leftrightarrow \exists a \in \{-1, 1\}, b \in \mathbb{Z}, \text{ such that } c_{2,i} = c_{1,ai+b}, \forall i \in \mathbb{Z} \quad (4.7)$$

The equivalence classes that partition Ω_n are sets containing all those microstates that may be transformed into one another by means of translations and reflections and which are therefore effectively identical from the point of view of the dynamics of the system, as demonstrated by Proposition 4.4.4.

However, these equivalence classes will not generally be of the same size. Rather, given a particular microstate $\mathbf{c} = (c_i)_{i \in \mathbb{Z}} \in \Omega_n$, the number of microstates in its class may be determined through consideration of its **period** $P(\mathbf{c})$, which must be a factor of n , and its **chirality** $R(\mathbf{c}) \in \{0, 1\}$, which is equal to zero if and only if there exists a translation that maps \mathbf{c} on to its own reflection⁴:

⁴ Note that the binary property described as “chirality” is used here purely to distinguish between those microstates that are chiral ($R(\mathbf{c}) = 1$) and those that are achiral ($R(\mathbf{c}) = 0$), not between different versions of a particular chiral microstate, as might otherwise be expected.

$$R(\mathbf{c}) = \begin{cases} 0 & , \text{ if } \exists b \in \mathbb{Z}, \text{ such that } c_{-i} = c_{i+b}, \forall i \in \mathbb{Z} \\ 1 & , \text{ otherwise.} \end{cases} \quad (4.8)$$

Having defined these quantities, observe that the number of distinct microstates in the equivalence class of \mathbf{c} is equal to $P(\mathbf{c})[1 + R(\mathbf{c})]$.

To see this, note that, including \mathbf{c} itself, the number of distinct microstates that may be obtained from \mathbf{c} by translation is equal to its period $P(\mathbf{c})$, since any translation of size $b \in \mathbb{Z}$ is identical in effect to a translation of size $b \bmod P(\mathbf{c})$. Furthermore, if $R(\mathbf{c}) = 0$ then a reflection of \mathbf{c} is identical in effect to one of these translations, so the total number of microstates in the relevant equivalence class is equal to $P(\mathbf{c}) = P(\mathbf{c})[1 + R(\mathbf{c})]$. Alternatively, if $R = 1$ then each of the microstates obtained by translation may be reflected to create a distinct microstate in the equivalence class, so the total number of microstates in the class is $2P(\mathbf{c})$, which is again equal to $P(\mathbf{c})[1 + R(\mathbf{c})]$.

Figure 4.12 depicts the complete set of 13 equivalence classes for this model with $n = 6$, depicted as lines of shaded and unshaded cells. Note that in this case, only one class (Class VI) contains chiral microstates.

Understanding which microstates of the model are essentially equivalent from the point of view of the transition rule may allow for the creation of simplified representations of the model dynamics. This will be discussed further in Chapter 5.

4.4.6 \mathfrak{B} -models: An individual-focused subfamily of \mathfrak{A}

Although the family of models \mathfrak{A} described in Section 4.4.2 does represent the most general form of a NANIA-like model, it may be argued that certain key properties of the model have been lost. The NANIA model was described as an individual-based model, but \mathfrak{A} includes models that are not consistent with an individual-based interpretation. For example, a model in the family may involve transitions such as $(\text{'E}', \text{'E'}) \rightarrow (\text{'S'}_1, \text{'S'}_2)$, in which individuals are spontaneously generated from empty cells. The family has been generalised to such an extent that it has become disconnected from its original status as a framework for individual-based modelling.

We therefore propose some alterations to the family to make it more consistent with an individual-based interpretation. This approach is in line with that of Conway (see



Figure 4.12: The 13 equivalence classes of the 64 possible microstates of a one-dimensional single species \mathfrak{A} -model on a ring of 6 cells. For any two microstates lying in the same class, there exists a translation, reflection or combination of these transformations (mod 6) mapping from one to the other. The microstates making up a given equivalence class are therefore effectively indistinguishable from the point of view of the dynamics of the model.

Gardner, 1970, p. 120) and Wolfram (1983, p. 603), who each (initially, at least) reduced the scope of the CAs that they studied through the introduction of various restrictions on their behaviour, in order to focus on those models whose behaviour was of most interest.

Suppose that each species ‘ S_i ’ has an associated subset \mathcal{C}_i of the cell state space \mathcal{C} and consider the following constraints to the local transition rule $\mathfrak{T}_{\text{local}}$:

1. If the first cell chosen is empty, then no changes are made.

$$\mathfrak{T}_{\text{local}} : ('E', X) \rightarrow ('E', X), \quad \forall X \in \mathcal{C}$$

2. Otherwise, if the first cell chosen has state ‘ S_i ’ and the second has any state $X \in \mathcal{C}$, then four types of transition are possible.

- No change. $\mathfrak{T}_{\text{local}} : ('S_i, X) \rightarrow ('S_i, X)$
- The first cell chosen may change to a state in \mathcal{C}_i , while the second cell remains unchanged. $\mathfrak{T}_{\text{local}} : ('S_i, X) \rightarrow (Y, X), \quad \text{for some } Y \in \mathcal{C}_i$
- The second cell chosen may change to a state in \mathcal{C}_i , while the first cell remains unchanged. $\mathfrak{T}_{\text{local}} : ('S_i, X) \rightarrow ('S_i, Y), \quad \text{for some } Y \in \mathcal{C}_i$
- The two chosen cells may exchange states. $\mathfrak{T}_{\text{local}} : ('S_i, X) \rightarrow (X, 'S_i)$

The family of models that fulfil these constraints will be labelled \mathfrak{B} (“Fraktur B”), a subfamily of \mathfrak{A} . Note that the first condition prohibits spontaneous generation of individuals (this is similar to the first of Wolfram’s restrictions), while the second states that the only transition in which both the chosen cells may change their state simultaneously is that in which the cells exchange their states. Among other things, this latter restriction prohibits situations of mutual annihilation, where $\mathfrak{T}_{\text{local}} : ('S_i, 'S_j) \rightarrow ('E, 'E)$.

One reason for imposing these particular constraints is that they enhance the individual-based interpretation of the model. The permitted transitions may all be interpreted as actions taken by the individual occupying the first cell to be chosen (with empty cells unable to take actions). An individual may: take no action, transform its own state, transform the state of a neighbour, or switch places with a neighbour.

For many model interpretations, including the predator-prey interpretation of the NANIA model, it may also be sensible to include the following additional constraint:

- *No Metamorphosis Condition:*

$$\mathcal{C}_i \subseteq \{\text{'E}', \text{'S'}_i\}, \quad \forall i \in \{1, \dots, m\}$$

The *No Metamorphosis Condition* ensures that transitions do not create individuals of a species that is not already represented in the two chosen cells.

At first glance, it might appear that the NANIA model is not a true \mathfrak{B} -model, because individual movement (as defined in the NANIA model) is not a valid transition in this family, since it occurs only when the first cell selected is empty (see Section 4.2). However, it can be shown that the NANIA model is equivalent to a model in \mathfrak{B} in a certain sense (the nature of this equivalence will be qualified in a moment), provided that it is run on a toroidal lattice (or indeed on any regular graph G) rather than a square one.

Consider the stochastic local transition rule $\mathfrak{U}_{\text{local}}$ for a two species model (where species 1 and 2 represent rabbits and foxes respectively) defined by the transition probabilities given in Table 4.2 (where $\kappa, \varsigma, \tau \in [0, 1]$ are the parameters of the NANIA model, as defined in Section 4.2).

Possible transitions			
Initial pair	Final pair	Probability	Interpretation
	(‘S’ ₁ , ‘S’ ₁)	$\kappa/2$	rabbit reproduces
(‘S’ ₁ , ‘E’)	(‘E’, ‘S’ ₁)	1/2	rabbit moves
	unchanged	otherwise	no action
	(‘E’, ‘E’)	$\tau/2$	fox dies
(‘S’ ₂ , ‘E’)	(‘E’, ‘S’ ₂)	1/2	fox moves
	unchanged	otherwise	no action
	(‘S’ ₂ , ‘E’)	$(1 - \varsigma)/2$	fox eats rabbit
(‘S’ ₂ , ‘S’ ₁)	(‘S’ ₂ , ‘S’ ₂)	$\varsigma/2$	fox eats rabbit and reproduces
	unchanged	otherwise	no action
(‘S’ ₂ , ‘S’ ₂)	(‘E’, ‘S’ ₂)	$\tau/2$	fox dies
	unchanged	otherwise	no action
other	unchanged	1	no action

Table 4.2: Description of the local transition rule $\mathfrak{U}_{\text{local}}$, which produces a \mathfrak{B} -model whose behaviour is effectively equivalent to that of the NANIA model.

Firstly, we observe that $\mathfrak{U}_{\text{local}}$ satisfies both the conditions required to define a \mathfrak{B} -model and the *No Metamorphosis Condition*. Secondly, for such a model run over a toroidal lattice, it may be shown (as discussed below) that given this rule, the probability of any particular transition occurring at a given iteration (for example that a *particular* pair of neighbouring cells undergoes the transition $(\text{'S'}_1, \text{'E'}) \rightarrow (\text{'S'}_1, \text{'S'}_1)$: rabbit reproduction) is precisely half the probability of the same transition occurring in the NANIA model. The ‘spare probability’ that results from this model transformation is all allocated to the outcome that the system remains unchanged.

This means that the \mathfrak{B} -model over a toroidal lattice defined by the local transition rule $\mathfrak{U}_{\text{local}}$ has the same dynamics as the NANIA model, but these dynamics progress at half the speed. This model will be referred to as the \mathfrak{B} -NANIA model.

To justify the claim about the relationship between the two models, first observe that the rules of the \mathfrak{B} -NANIA model are identical to those of the original NANIA model, but with the relevant probabilities halved, for all transitions except those relating to individual movement. In the original NANIA model, individual movement occurred automatically if the first cell selected was empty and the second contained an individual. In the \mathfrak{B} -NANIA model, movement occurs with probability $1/2$ when the first cell selected is an individual and the second is empty.

Observe that, provided that the graph over which the model is run is regular (such as a toroidal rectangular lattice), in both the NANIA model and the \mathfrak{B} -NANIA model the probability of selecting a particular cell followed by a particular one of its neighbours, is the same as the probability of picking the same two cells but in the opposite order. Call this probability p .

In the NANIA model, given a particular microstate, the probability that a particular individual will move into a particular empty neighbouring cell is equal to p ; the probability of picking the empty cell followed by the cell occupied by the individual in question. In the \mathfrak{B} -NANIA model, given the same microstate, the probability of the same event happening is equal to $p/2$; the probability of picking the cell occupied by the individual followed by the empty cell multiplied by $1/2$ (the probability of movement in $\mathfrak{U}_{\text{local}}$). This demonstrates the claim.

4.4.7 The range of possible transition rules for \mathfrak{B} -models

We now examine the range of valid local rules $\mathfrak{T}_{\text{local}}$ for \mathfrak{B} -models. Counting the number of distinct deterministic transition rules and determining the dimension of the parameter space of the possible stochastic transition rules for an m -species

\mathfrak{B} -model is less straightforward than counting the valid transition rules in \mathfrak{A} . Table 4.3 provides a breakdown of the possible transitions.

Initial pair:		Number of possible transitions:		Number of such pairs
First cell	Second cell	General case	<i>No Metamorphosis</i>	
'E'	any	1	1	$m + 1$
'S'_i	'E'	$2m + 2$	4	m
'S'_i	'S'_i	$2m + 1$	3	m
'S'_i	'S'_j (for $j \neq i$)	$2m + 2$	5	$m(m - 1)$

Table 4.3: Summary of the valid local transitions in a \mathfrak{B} -model, with and without the *No Metamorphosis Condition*.

Consider the second line of the table. It states that, given a \mathfrak{B} -model with m species, for each of the m possible initial pairs of the form ('S'_i, 'E'), there are $2m + 2$ possible transitions consistent with the constraints of \mathfrak{B} , of which 4 also fulfil the *No Metamorphosis* condition.

From the table we deduce that there are:

$$(2m + 2)^m (2m + 1)^m (2m + 2)^{m(m-1)} = [2^m (m + 1)^m (2m + 1)]^m$$

possible deterministic transition rules that satisfy the conditions of \mathfrak{B} , of which:

$$4^m 3^m 5^{m(m-1)} = [12 \times 5^{(m-1)}]^m$$

also satisfy the *No Metamorphosis* condition.

We may also deduce that the dimension of the parameter space of stochastic transition rules for \mathfrak{B} -models is:

$$m(2m + 1) + m(2m) + m(m - 1)(2m + 1) = m^2[2m + 3],$$

while the dimension of the parameter space of those rules that also satisfy the *No Metamorphosis* condition is:

$$3m + 2m + 4m(m - 1) = m[4m + 1].$$

As in the case of \mathfrak{A} -models, the parameter space is a Cartesian product of simplexes, although in this case, these simplexes do not all have the same dimension.

Combining these observations with those of Section 4.4.3, we observe that the dimension of the parameter space of stochastic transition rules increases like m^4 for \mathfrak{A} -models, like m^3 for \mathfrak{B} -models and like m^2 for \mathfrak{B} -models that satisfy the *No Metamorphosis* condition. This reduction in the order of magnitude of the rule space will facilitate a thorough investigation of possible model behaviours in Chapter 5.

4.5 Summary and conclusions

In this chapter, we have introduced the NANIA model, a predator-prey IBM that is closely related to the ecological patch models discussed in Section 3.3.3. Through consideration of the NANIA model as a stochastic process, we have examined its long term dynamics, identifying two absorbing microstates to which the model is ultimately guaranteed to evolve. However, we have also observed that, for certain values of the model parameters, the expected time required to reach these absorbing states may be so large that, over all practical time scales, the system could instead be considered to display a form of quasi-stable coexistence between its two species.

Mean field theory suggests that this quasi-stable behaviour may be similar to that predicted by a form of the Lotka-Volterra equations (see Section 3.3.2), in which the prey species exhibits logistic (rather than exponential) growth in the absence of predators. However, while simulations do appear to exhibit behaviour similar to the coupled population cycles characteristic of the Lotka-Volterra equations (see Figure 4.5) further work would be required to determine the extent to which the true model dynamics actually correspond to the mean field equations.

It has been observed that the NANIA model is merely one example of a much broader range of possible discrete space-time stochastic models that could be specified. We have defined the most general family of such models, labelled as class \mathfrak{A} , before refining this definition to focus on a subclass containing only those models that are consistent with an individual-based interpretation, labelled as class \mathfrak{B} . We have also considered equivalences between the microstates of these models, and identified the range of possible transition rules that could be applied in such settings.

In Chapter 5, we will build on these concepts, investigating the relationship between the predictions of mean field theory and the dynamics of a certain family of \mathfrak{B} -models, through the performance and analysis of a large number of simulation experiments. This empirical work will then pave the way for a more theoretical analysis of the connections between local interactions and global behaviours in such models in Chapter 6, in line with the research objectives set out in Section 1.5.

Chapter 5

Categorisation and initial analysis of the different behavioural regimes of the one-dimensional, single species \mathfrak{B} -model

5.1 Introduction

Having defined \mathfrak{B} -models in Chapter 4, we now attempt to understand their behaviour. In this chapter, as an initial investigation, we take the same approach as Wolfram (2002) in his investigation of elementary CAs. Specifically, we undertake a thorough exploration of the parameter space of the valid transition rules in \mathfrak{B} , perform simulations for different parameter sets, visualise the results and attempt to classify the different behavioural types that we observe.

Unfortunately, for models with even a relatively small number of species, the high dimension of the parameter space (see Section 4.4.7) makes a systematic examination of the behaviour of the entire family of models impossible. Also, the dynamics of models over geographies of dimension greater than one (such as two-dimensional square lattices) is difficult to visualise in two-dimensions in a comprehensive way.

For these reasons, once again in line with the approach of Wolfram, we focus our analysis on the simplest case, that of models with only one species over a one-dimensional ring of cells (though the results presented in Sections 5.2.1-5.2.2 are valid for single species \mathfrak{B} -models over any geography). A description of models over rings of cells, together with an explanation of some key notation, can be found in Section 4.4.5.

The main focus of our analysis is a comparison between the population dynamics observed in the simulations and that which is predicted by mean field theory. The results of this analysis will then lead into a more in-depth investigation of the links between local transitions and global dynamics in Chapter 6.

5.2 Single species \mathfrak{B} -models

5.2.1 Summary of possible model transitions

Table 5.1 summarises all possible transitions of a \mathfrak{B} -model with only one species ‘S’ (recall that the state ‘E’ represents an empty cell).

Initial pair	Final pair	Probability	Interpretation	Population change
$(\text{'S}', \text{'E'})$	(‘E’, ‘E’)	α	individual dies	−1
	(‘E’, ‘S’)	β	individual moves	0
	(‘S’, ‘S’)	γ	individual reproduces	+1
	unchanged	otherwise	no action	0
$(\text{'S}', \text{'S'})$	(‘E’, ‘S’)	ϵ	individual dies	−1
	(‘S’, ‘E’)	ζ	individual eats neighbour	−1
	unchanged	otherwise	no action	0
other	unchanged	1	no action	0

Table 5.1: All possible local transitions for a single species \mathfrak{B} -model and their effects on total population.

From the table, we see that the general \mathfrak{B} -model over a given graph G is fully defined by the five-dimensional parameter vector $(\alpha, \beta, \gamma, \epsilon, \zeta) \in [0, 1]^5$, with the constraints $\alpha + \beta + \gamma \leq 1$ and $\epsilon + \zeta \leq 1$. Observe that this is consistent with the results of Section 4.4.7 on the number of free parameters in a \mathfrak{B} -model.

Recall that if the geography of a particular model is an undirected regular graph, then the probability of selecting any particular cell followed by a particular neighbour of that cell is identical to the probability of selecting the same two cells in the opposite order. Therefore, in such models, the transitions $(\text{'S}', \text{'S'}) \rightarrow (\text{'E}', \text{'S'})$ and $(\text{'S}', \text{'S'}) \rightarrow (\text{'S}', \text{'E'})$ are equivalent and the behaviour of the model depends on the parameters ϵ and ζ only through their sum $\epsilon + \zeta$. In such cases, the dimension of the parameter set is therefore reduced to four.

Since, in this chapter, we will only consider models over regular graphs, without loss of generality we may replace the parameters ϵ and ζ with the single parameter $\eta = \epsilon + \zeta$. Also, for the sake of simplicity, the different types of transition will henceforth be referred to by their corresponding Greek letter (α -transitions, η -transitions, etc.).

5.2.2 Mean field analysis

Applying the mean field analysis of Section 3.2 to the general one species \mathfrak{B} -model (in the same fashion as was demonstrated in Section 4.3.4) yields the following differential equation for the population density $u \in [0, 1]$ of the individuals:

$$\dot{u} = (\gamma - \alpha)u - (\gamma - \alpha + \eta)u^2 \quad (5.1)$$

This is an equation of logistic growth (see, for example, Strogatz, 1994, pp. 22-24).

Recall from Section 4.3.4 that the independence assumption necessary for the derivation of (5.1) requires that the numbers of cells in each state, un and $(1 - u)n$ (and also, by implication, the number of cells itself, n), are sufficiently large. Therefore, whether or not it is valid to neglect spatial correlations, as is implicit in the mean field approach, we would not expect the equation to provide a good representation of the behaviour of the model for situations where the population is close to extinction or where the underlying graph is too small.

The first thing to notice about equation (5.1) is that the parameter β , which governs the rate of movement of the individuals, does not appear. This is because the mean field approach only takes account of processes that affect the total population density. The consequence of this is that the mean field equation supposes that individual movement has no impact on the way in which the population density changes over time.

Secondly, note that the equation depends on the parameters α and γ only through the difference $\gamma - \alpha$. However, unlike the observation regarding dependence on ϵ and ζ through the sum $\epsilon + \zeta$, which is an intrinsic property of any \mathfrak{B} -model over a regular graph (see Section 5.2.1), this observation on the influence of α and γ is only a property of the mean field equation and not of the underlying model.

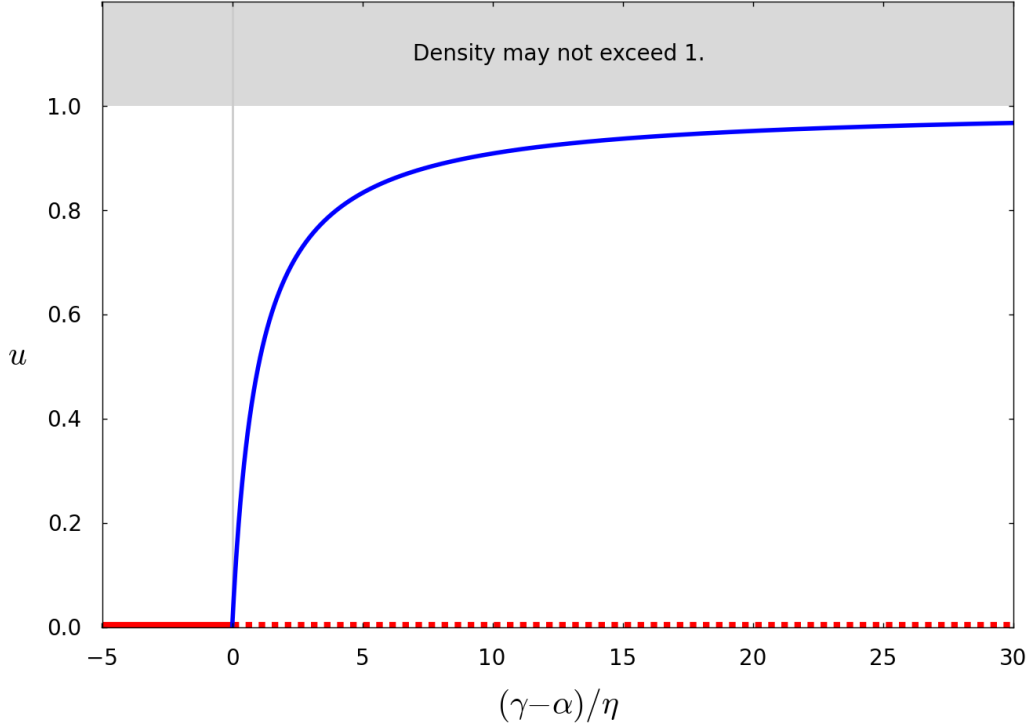


Figure 5.1: Bifurcation diagram showing the stable equilibria (continuous line) and unstable equilibria (dotted line) of equation (5.1) as the parameter expression $(\gamma - \alpha)/\eta$ varies, for $\eta \neq 0$. The equilibria are $u_0^* = 0$ (red) and $u_1^* = (\gamma - \alpha)/(\gamma - \alpha + \eta)$ (blue). Note that the density u lies in $[0, 1]$, while $(\gamma - \alpha)/\eta$ may take any real value. There is a constrained transcritical bifurcation at $u = 0$ when $\gamma = \alpha$.

Assuming for the moment that $\gamma - \alpha + \eta \neq 0$, the dynamical system defined by equation (5.1) has two potential equilibria:

$$u_0^* = 0 \quad (5.2)$$

$$u_1^* = \frac{\gamma - \alpha}{\gamma - \alpha + \eta} \quad (5.3)$$

The stability of these equilibria may be analysed by means of a simple local linearisation of the system (see Strogatz, 1994, pp. 24-26), considering the derivative of \dot{u} with respect to u and evaluating it at each of the fixed points, as follows:

$$\begin{aligned} \left. \frac{\partial \dot{u}}{\partial u} \right|_{u=0} &= \gamma - \alpha \\ \left. \frac{\partial \dot{u}}{\partial u} \right|_{u=u_1^*} &= \alpha - \gamma \end{aligned}$$

A negative value of $\partial \dot{u} / \partial u$ indicates a stable equilibrium, while a positive value indicates an unstable equilibrium. Therefore, when $\gamma > \alpha$, 0 is a repellor and u_1^* is an attractor. When $\gamma < \alpha$, 0 is an attractor, but u_1^* does not exist since it does not lie in the range $[0, 1]$ in this case.

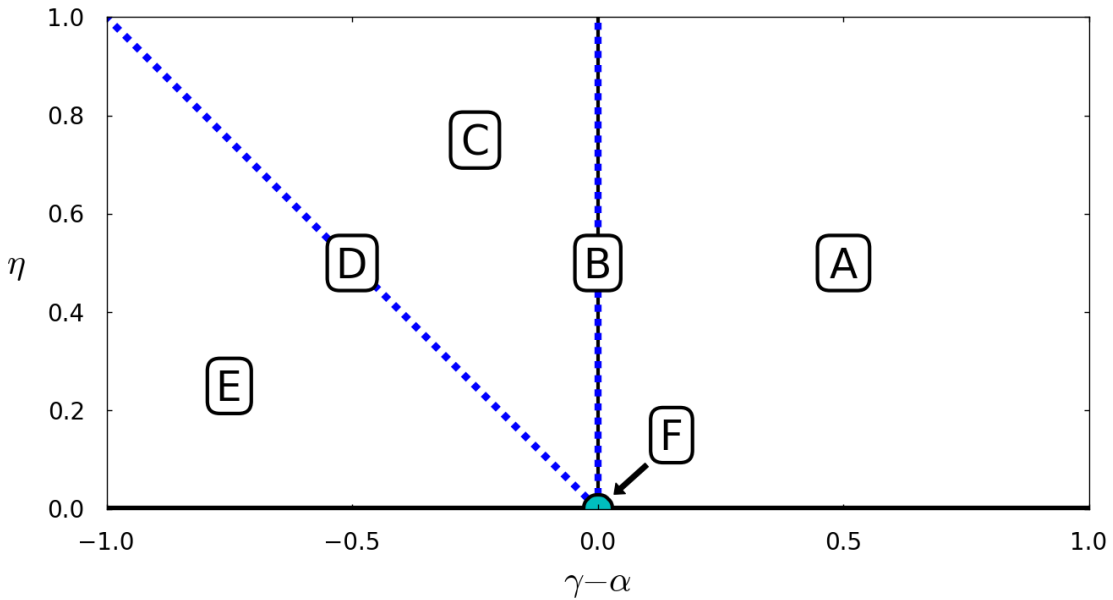


Figure 5.2: Parameter space diagram for equation (5.1). Any point $(\gamma - \alpha, \eta)$ in $[-1, 1] \times [0, 1]$ represents a valid choice of parameters. The space is divided into six regions:

- Region A. $\gamma - \alpha \in (0, 1]$: 0 a repellor ; $u_1^* \in (0, 1]$ an attractor.
- Region B. $\gamma - \alpha = 0$, $\eta \in (0, 1]$: 0 = u_1^* an attractor.
- Region C. $\gamma - \alpha < 0$, $\gamma - \alpha + \eta > 0$: 0 an attractor ; $u_1^* \notin [0, 1]$.
- Region D. $\gamma - \alpha < 0$, $\gamma - \alpha + \eta = 0$: 0 a linear attractor ; u_1^* undefined.
- Region E. $\gamma - \alpha < 0$, $\gamma - \alpha + \eta < 0$: 0 an attractor ; $u_1^* \notin [0, 1]$.
- Region F. $\gamma - \alpha = \eta = 0$: $\dot{u} = 0$ in all cases.

There is therefore a constrained transcritical bifurcation at $\gamma = \alpha$, where the two equilibria exchange their stability. The term “constrained” here is used to indicate that one of the equilibria (u_1^*) only defines a valid population density on one side of the bifurcation point, so effectively does not exist in its unstable form.

Substituting $\gamma - \alpha = 0$ into (5.1) gives the equation $\dot{u} = -\eta u^2$ and we can see that, in this case, the single equilibrium at $u = 0$ is stable from above and therefore is an attractor, since negative densities are impossible.

A bifurcation diagram for the case when $\eta \neq 0$ is presented in Figure 5.1.

If $\gamma \neq \alpha$ and $\gamma - \alpha + \eta = 0$, then equation (5.1) degenerates to the linear form $\dot{u} = (\gamma - \alpha)u$ and the only equilibrium is a linear attractor at $u = 0$. Finally, if $\gamma = \alpha$ and $\eta = 0$, then equation (5.1) degenerates to form $\dot{u} = 0$ and the density is constant.

These results are summarised in Figure 5.2.

5.2.3 Discussion of the mean field equation

At this stage, it should be noted that in the cases in which mean field theory predicts the existence of an attracting fixed point $u_1^* \in (0, 1)$ (i.e. $\gamma > \alpha$ and $\eta > 0$), if $\alpha > 0$ then the population dynamics of a single species \mathfrak{B} -model over any finite graph cannot possibly be well-represented by equation (5.1) over very long periods, even allowing for stochastic noise. The reasons for this are the same as those discussed in Section 4.3.3 in relation to the basic NANIA model and its relationship to the Lotka-Volterra equations.

Like the NANIA model, a single species \mathfrak{B} -model can be considered a time homogeneous Markov chain (see Sections 2.4 and 4.3), where extinction is an absorbing microstate owing to the constraint of \mathfrak{B} -models that prohibits the spontaneous generation of individuals. When $\alpha > 0$ and $\eta > 0$, it is clear that all microstates communicate with the extinction microstate, since a series of consecutive α and η -transitions can destroy any continuous block of occupied cells. All microstates except extinction are therefore transient, since for any such microstate, the probability of reaching extinction before returning to the current microstate is strictly positive. Since, for a \mathfrak{B} -model over a finite graph, there are a finite number of possible microstates, any such model will eventually reach the extinction microstate with probability 1, and u_1^* therefore cannot be considered a stable equilibrium.

However, as with our discussion of the NANIA model in Section 4.3.3, for certain models and initial conditions, sequences of transitions that would lead the system to extinction may occur with such low probability that the expected time to extinction is so large as to be irrelevant for all practical purposes. In such situations, it may therefore be meaningful to talk about situations of convergence to a quasi-stable positive equilibrium density (up to stochastic noise), which may or may not match that predicted by the mean field equation.¹ In discussing the results of the simulation experiments of Section 5.3, when we talk about the long term persistence of populations, it this quasi-stability that is meant. Further discussion of the concept of quasi-stable equilibrium, in the context of ecological patch models, may be found in McKane and Newman (2004).

As noted in the previous section, the mean field equation (5.1) predicts that individual movement, as represented by the parameter β , has no effect on the dynamics of the population density. However, this is clearly not a realistic expectation.

¹ See Figure 5.16 for an example of a \mathfrak{B} -model in which, strictly speaking, extinction is inevitable in the long term, (since $\alpha, \eta > 0$), but which nonetheless maintains a population density far from zero over all practically relevant time intervals.

The derivation of the mean field equation supposes that, at any given iteration, individuals are “uniformly” distributed throughout the system (in the sense that they appear to be distributed according to a simple random sample of the cells). In reality, since all the processes in the model only effect local changes, there will exist considerable dependencies between the states of adjacent cells. We may hypothesise however that higher amounts of individual movement (higher values of β) will lead to increased dispersal of individuals and therefore a better correspondence between the results of simulations and the behaviour predicted by the mean field equation. The results of the simulation experiments described in Section 5.3 will be used to examine this hypothesis.

5.3 Simulation experiments

5.3.1 Aims

We now describe a set of simulation experiments, whose aims are to understand the full range of possible dynamical behaviours of the single species \mathfrak{B} -model and to determine to what extent and under what conditions the mean field equation derived in Section 5.2.2 provides a good representation of the model dynamics. To achieve this we must observe the results of simulations of the model for a wide variety of parameters.

As discussed in Section 5.1, we consider the simplest possible geography G for the model, a one-dimensional line of n cells, C_0, \dots, C_{n-1} , whose opposite ends are connected to form a ring (see Section 4.4.5 for further details of models defined on rings of cells and related notation). Note that this is a regular graph of degree 2, so the observation that ϵ and ζ -transitions may be considered equivalent and combined as η -transitions (taking $\eta = \epsilon + \zeta$) will be applied (see Section 5.2.1).

5.3.2 Choosing the model parameters

In order to fully understand the behaviour of the model, it is necessary to perform simulations with sets of parameters $(\alpha, \beta, \gamma, \eta)$ that explore the full extent of the parameter space. However, the number of parameter sets that must be considered may be substantially reduced by means of the following observation.

Given a regular graph G of degree k with n cells, consider the probability that a particular cell in state ‘S’ and a particular adjacent cell in state ‘E’ undergo the transition ‘(S, E) \rightarrow (E, E)’ in a single iteration. This probability is equal to $\alpha/(nk)$

(the probability that the first cell is chosen $1/n$, multiplied by the probability that the neighbour is chosen $1/k$, multiplied by the probability of the given transition α).

Assuming that $\eta \neq 0$, this probability may be written as $[\eta/(nk)][\alpha/\eta]$. In a similar way, the probabilities of particular β , γ and η -transitions may respectively be written as $[\eta/(nk)][\beta/\eta]$, $[\eta/(nk)][\gamma/\eta]$ and $[\eta/(nk)]$.

In this way, we see that, if $\eta > 0$, the behaviour of the model is fully determined by the three-dimensional parameter vector $(\alpha^*, \beta^*, \gamma^*) = \eta^{-1}(\alpha, \beta, \gamma) \in [0, \infty)^3$ and a rate parameter $\theta = \eta/(nk)$. Note particularly that θ does not affect the character of the dynamics (since, for any particular microstate, changing θ while holding α^* , β^* and γ^* constant does not affect the relative probabilities of α , β , γ and η -transitions), but only the rate at which these dynamics progress.

To understand the character of the dynamics of a single species \mathfrak{B} -model on a particular regular graph, it therefore suffices to explore the three-dimensional parameter space of $(\alpha^*, \beta^*, \gamma^*) \in [0, \infty)^3$ and the three-dimensional parameter space of $(\alpha, \beta, \gamma) \in [0, 1]^3$ for the special case when $\eta = 0$.

5.3.3 Method

Setting the number of cells $n = 1000$, simulations were performed of a single species \mathfrak{B} -model on a ring of cells for all parameter vectors in the following two sets:

$$\begin{aligned} P_1 &= \{(\alpha, \beta, \gamma, \epsilon, \zeta) \in [0, 1]^5 : \alpha, \beta, \gamma \in P_1^\dagger, \epsilon, \zeta = 0\} \\ P_2 &= \{(\alpha, \beta, \gamma, \epsilon, \zeta) \in [0, 1]^5 : \alpha, \beta, \gamma \in P_2^\dagger, \epsilon = 0.08, \zeta = 0\} \end{aligned}$$

where:

$$\begin{aligned} P_1^\dagger &= \{0, 0.05, 0.1, 0.15, 0.2, 0.25\} \\ P_2^\dagger &= \{0, 0.02, 0.04, 0.06, 0.08, 0.16, 0.24, 0.32\} \end{aligned}$$

Using the notation of Section 5.3.2, P_1 represents the case $\eta = 0$, while P_2 represents the case $\eta \neq 0$ and corresponds to the set:

$$\{(\alpha^*, \beta^*, \gamma^*) : \alpha^*, \beta^*, \gamma^* \in \{0, 0.25, 0.5, 0.75, 1, 2, 3, 4\}\}$$

These values of the parameters were chosen to ensure the consideration of scenarios in which α , β and γ may be several times greater than η , several times smaller than η or equal to η .

Ten simulations of 1.6 million iterations were performed for each set of parameters. The initial conditions for each simulation were randomly generated, with each cell independently allocated the state ‘E’ or ‘S’, with equal probability. The complete state of the model was recorded every 3200 iterations, such that ten sets of 501 states (including the initial conditions), $\omega_{i,0}, \dots, \omega_{i,500}$, for $i \in \{1, \dots, 10\}$, were recorded for each set of parameter values.

For each state ω_{ij} , the corresponding population density is denoted u_{ij} , while \bar{u}_j and \bar{s}_j^2 respectively represent the observed mean and variance of the population density, calculated over the ten independent simulations performed for each set of parameter values:

$$\bar{u}_j = \frac{1}{10} \sum_{i=1}^{10} u_{ij} \quad (5.4)$$

$$\bar{s}_j^2 = \frac{1}{10} \sum_{i=1}^{10} (u_{ij} - \bar{u}_j)^2 \quad (5.5)$$

To examine the behaviour of the 7280 simulations, each was plotted with space on the horizontal axis and time on the vertical axis, with occupied cells at each iteration coloured black and unoccupied cells left blank, such that all 501 recorded states of each simulation were displayed in a vertical stack. This method allows for the complete evolution of the system’s behaviour over a particular simulation to be visualised in a single plot.²

Some examples of the behaviour plots can be seen in Figures 5.3-5.16. The examples presented in the figures have been specifically chosen to represent and explain the various distinct types of observed model behaviour, as will be discussed in Sections 5.3.4-5.3.5.

For each of the 728 sets of parameters under consideration, the dynamics of the mean population density \bar{u}_j , calculated over the ten independent simulations, were also plotted against time. Where the mean field analysis of Section 5.2.2 predicts the existence of a unique stable equilibrium population density, this was included on the plots in order to compare the observed dynamics with these theoretical equilibria.

Examples of these plots can be seen in Figures 5.17-5.22. Here, the examples presented in the Figures have been chosen both to represent a broad range of different

² This approach is the same as that used by Wolfram (2002) for the visualisation of elementary CAs. However, in Wolfram’s figures, time proceeds in a downward rather than an upward direction.

model behaviours and to demonstrate the effect of varying a particular parameter (or pair of parameters), while others are held constant. These plots are discussed in more detail in Section 5.3.7.

5.3.4 Results for $\eta = 0$

Initially, consider the simulations where $\eta = 0$. Note that in these cases, all dynamical activity must occur on the boundaries between regions of occupied and empty cells (since η -transitions are the only transitions that can occur when both the selected cells are occupied). Continuous blocks of occupied cells remain occupied until affected by behaviour on their boundary, in the same way that blocks of empty cells behave for all values of the parameters (owing to the condition of \mathfrak{B} family models that prohibits the spontaneous generation of individuals).

Simulations for which $\alpha = \gamma = \eta = 0$ display special behaviour, since the global population density is conserved in these cases. If β is also equal to 0, there are no dynamics at all and every iteration reproduces the initial conditions exactly. For the random uniform initial conditions used here, this results in ‘barcode’ style simulations (See Figure 5.3). For higher values of β , individual movement results in an increasing degree of scrambling of the initial conditions, though areas of higher and lower density in the initial conditions may persist for long periods (See Figure 5.4).

If at least one of α and γ is non-zero, only three possible behaviours may occur and a very simple rule relates these behaviours to the parameters.

If $\alpha > \gamma$, then the death rate is greater than the rate of reproduction on the boundaries between blocks of occupied and empty cells, leading to the shrinking of the blocks of occupied cells, and the system reaches an equilibrium in which all cells are empty (Figure 5.5).

If $\alpha < \gamma$, the opposite behaviour occurs and the system reaches an equilibrium in which all cells are occupied (Figure 5.6).

If $\alpha = \gamma$, then the death rate and the birth rate are perfectly balanced and blocks of occupied and unoccupied cells tend to be preserved, though their boundaries meander randomly (if $\beta = 0$ and if iterations in which no movement occurs are neglected, this movement is an unbiased random walk), leading to the occasional merging of blocks, producing a pattern resembling zebra-stripes (Figure 5.7).

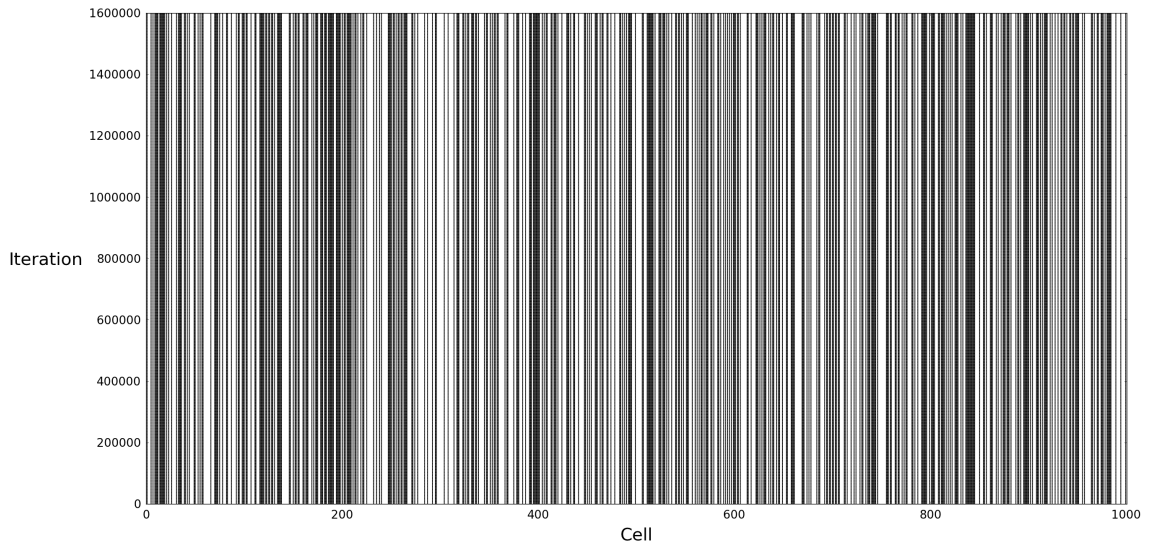


Figure 5.3: 1.6 million iterations of a one-dimensional, one species \mathfrak{B} -model on a ring of 1000 cells, with the following parameters: $\alpha = 0$, $\beta = 0$, $\gamma = 0$, $\epsilon = 0$, $\zeta = 0$. The initial conditions were generated by setting each cell to be occupied with a probability of 0.5.

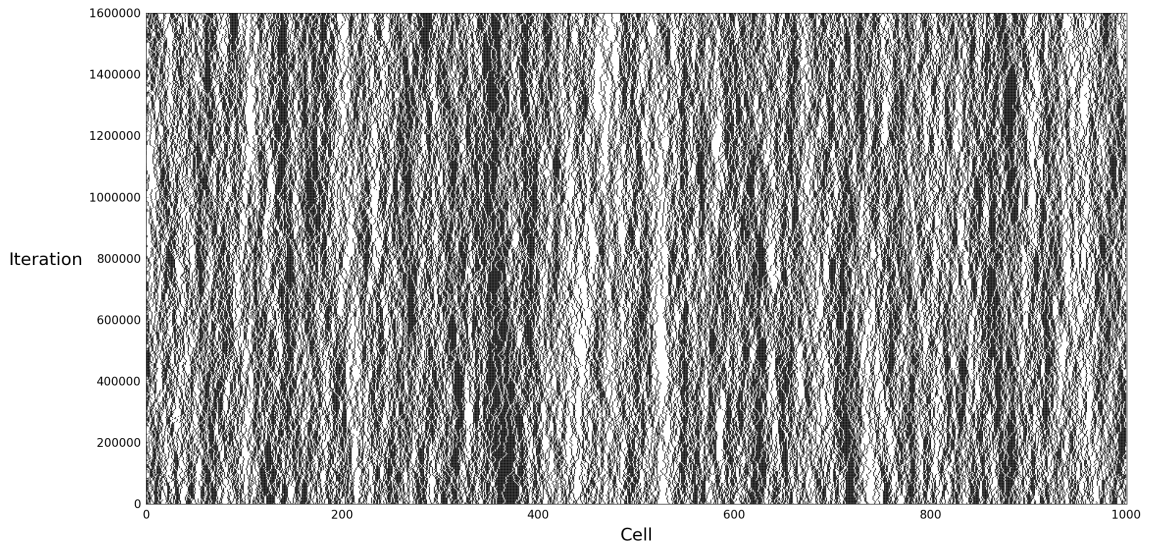


Figure 5.4: 1.6 million iterations of a one-dimensional, one species \mathfrak{B} -model on a ring of 1000 cells, with the following parameters: $\alpha = 0$, $\beta = 0.25$, $\gamma = 0$, $\epsilon = 0$, $\zeta = 0$. The initial conditions were generated by setting each cell to be occupied with a probability of 0.5.

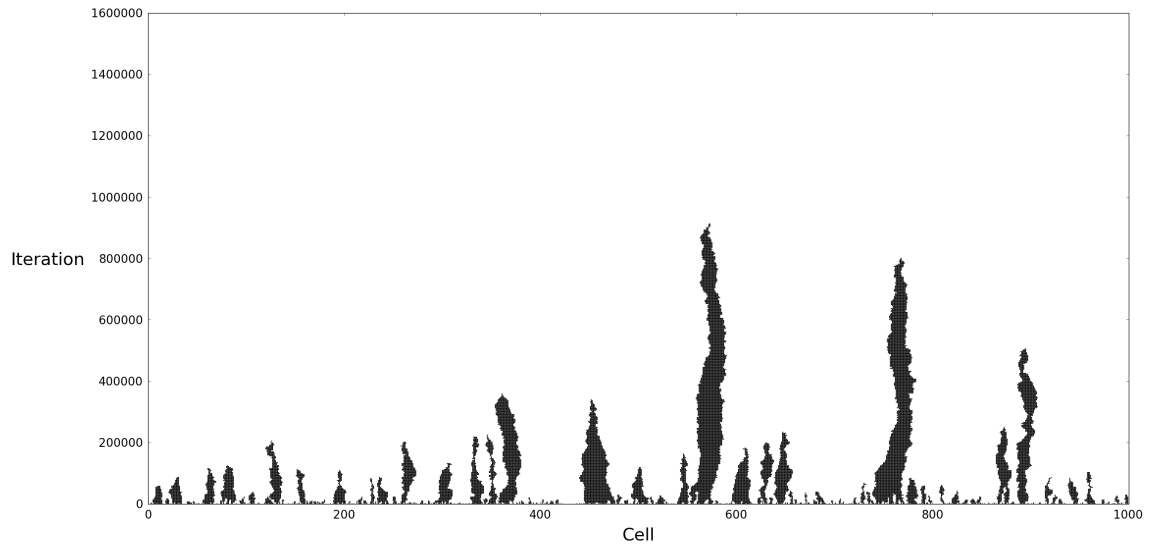


Figure 5.5: 1.6 million iterations of a one-dimensional, one species \mathfrak{B} -model on a ring of 1000 cells, with the following parameters: $\alpha = 0.25$, $\beta = 0$, $\gamma = 0.2$, $\epsilon = 0$, $\zeta = 0$. The initial conditions were generated by setting each cell to be occupied with a probability of 0.5.

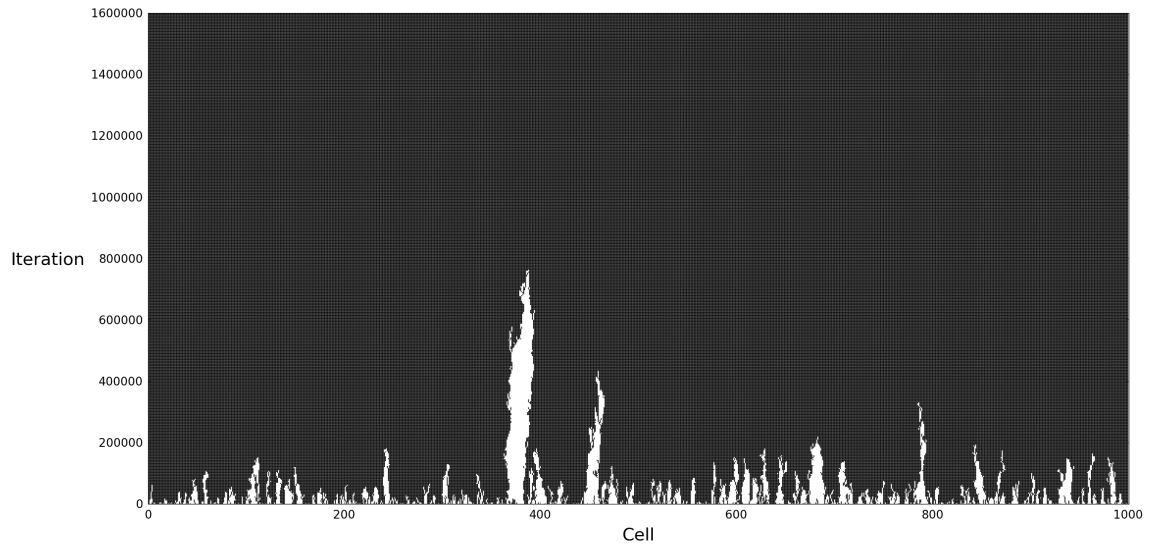


Figure 5.6: 1.6 million iterations of a one-dimensional, one species \mathfrak{B} -model on a ring of 1000 cells, with the following parameters: $\alpha = 0.05$, $\beta = 0.05$, $\gamma = 0.1$, $\epsilon = 0$, $\zeta = 0$. The initial conditions were generated by setting each cell to be occupied with a probability of 0.5.

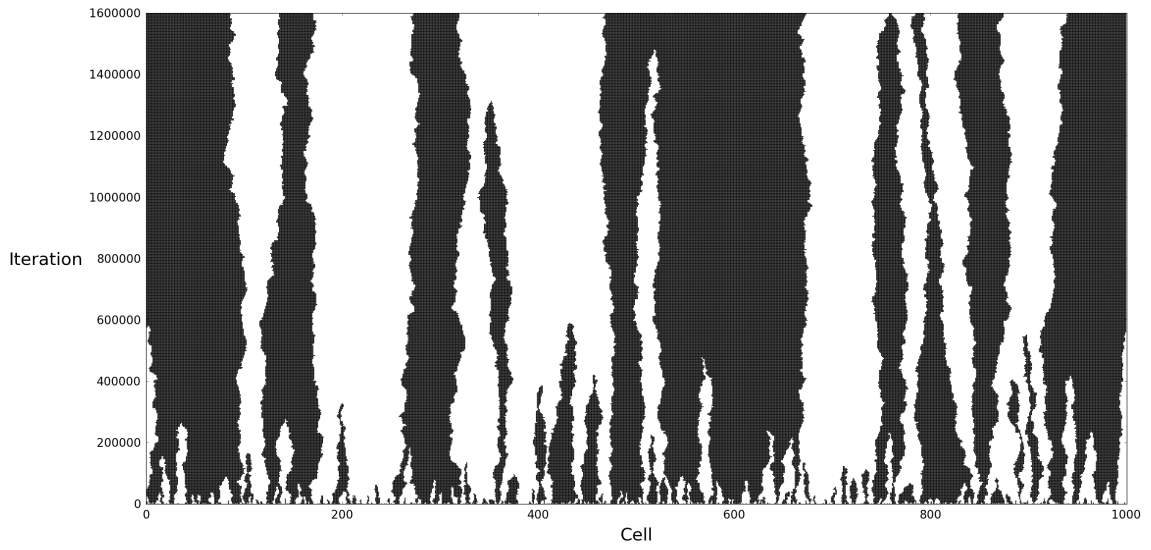


Figure 5.7: 1.6 million iterations of a one-dimensional, one species \mathfrak{B} -model on a ring of 1000 cells, with the following parameters: $\alpha = 0.2$, $\beta = 0$, $\gamma = 0.2$, $\epsilon = 0$, $\zeta = 0$. The initial conditions were generated by setting each cell to be occupied with a probability of 0.5.

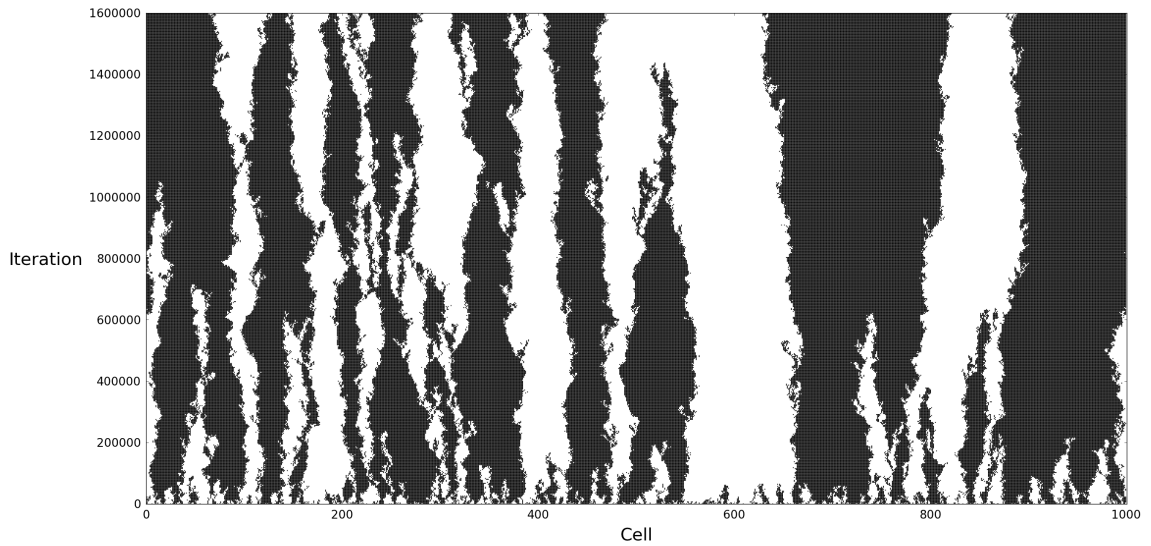


Figure 5.8: 1.6 million iterations of a one-dimensional, one species \mathfrak{B} -model on a ring of 1000 cells, with the following parameters: $\alpha = 0.2$, $\beta = 0.25$, $\gamma = 0.2$, $\epsilon = 0$, $\zeta = 0$. The initial conditions were generated by setting each cell to be occupied with a probability of 0.5.

Higher values of β result in a ‘feathering’ effect of the boundaries between occupied and unoccupied cells, but do not have any significant effect on the long-term dynamics of the system (Figure 5.8). If scenarios with $\beta \gg \alpha, \gamma$ were considered, we would expect more thorough mixing, but we would not expect any fundamental changes to the behaviour of the system, owing to the simplicity of the processes involved.

5.3.5 Results for $\eta \neq 0$

The behaviour of the model in scenarios where $\eta \neq 0$ is considerably more complex to categorise and understand than the behaviour of the model when $\eta = 0$. Note that a summary of the results presented in this section is provided in Figure 5.23, in the form of four parameter space diagrams (see Section 5.3.8).

Setting aside the special cases where $\gamma = \alpha = 0$, in which the system rapidly degenerates to a collection of persistent isolated cells, which may be immobile and invariant if $\beta = 0$ (Figure 5.9)³ or mobile and decreasing in number owing to collisions and η -transitions if $\beta > 0$ (Figure 5.10), a continuum of behavioural types can be identified.

First, there are sets of parameters for which the individuals go extinct fairly rapidly, where α and η -transitions cause clusters of individuals to decay to nothing before any complex persistent structures can be formed. An example of this behaviour can be seen in Figure 5.11.

When the chosen parameters are slightly more favourable for individual survival, simulations may be observed in which small clusters of individuals persist for longer periods, perhaps enjoying brief periods of growth, before ultimately dying out (see Figure 5.12).

For still more favourable parameter sets, such clusters become larger and more numerous, some surviving the full 1.6 million iterations of a simulation, although the isolated nature of the clusters and the observed extinction of similar clusters at earlier iterations suggests that they will not persist in the long term (see Figure 5.13).

As the parameters become ever more conducive to survival, the gaps between such clusters become smaller and frequent incidences of cluster merging are observed, such that it is no longer clear whether the population will persist or become extinct in the long term (see Figure 5.14).

³ Note that the behaviour depicted in Figure 5.9 is not the same as that seen in Figure 5.3. In Figure 5.9, the system converges rapidly to a state in which no pair of adjacent cells are occupied, then remains unchanged, whereas in Figure 5.9 there is no change at any iteration.

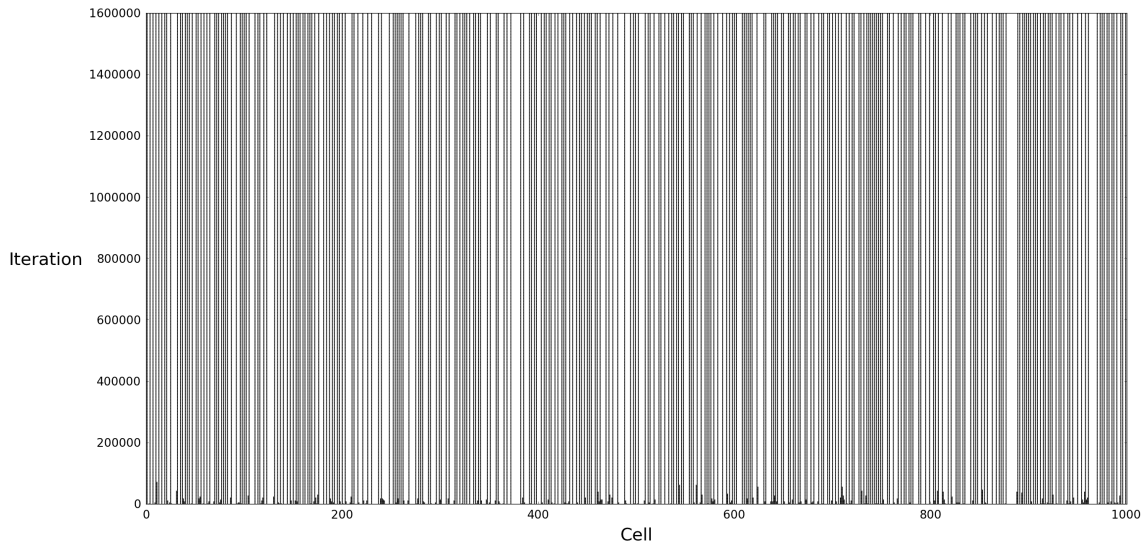


Figure 5.9: 1.6 million iterations of a one-dimensional, one species \mathfrak{B} -model on a ring of 1000 cells, with the following parameters: $\alpha = 0$, $\beta = 0$, $\gamma = 0$, $\epsilon = 0.08$, $\zeta = 0$. The initial conditions were generated by setting each cell to be occupied with a probability of 0.5.

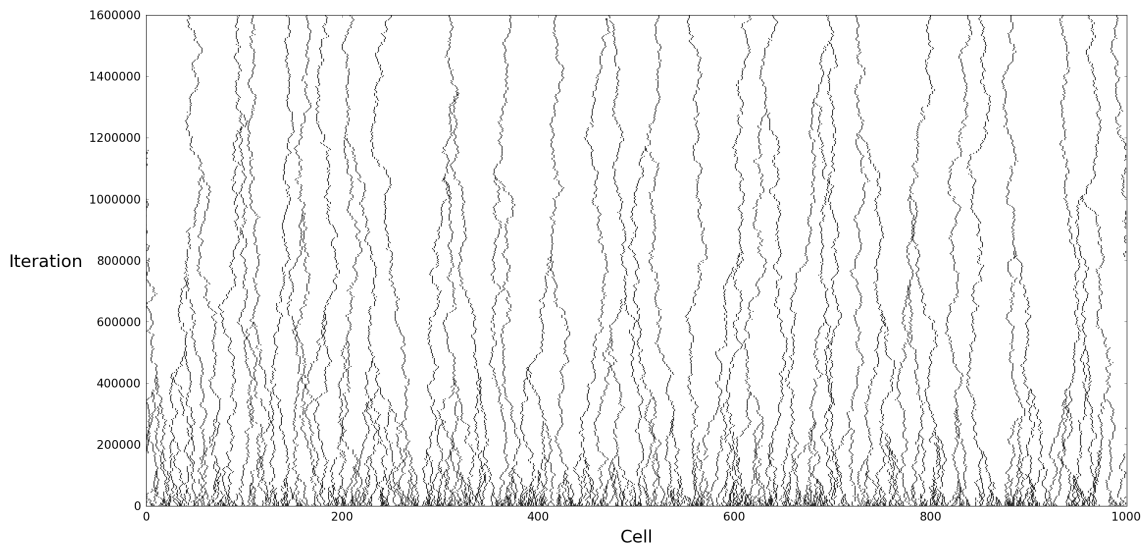


Figure 5.10: 1.6 million iterations of a one-dimensional, one species \mathfrak{B} -model on a ring of 1000 cells, with the following parameters: $\alpha = 0$, $\beta = 0.32$, $\gamma = 0$, $\epsilon = 0.08$, $\zeta = 0$. The initial conditions were generated by setting each cell to be occupied with a probability of 0.5.

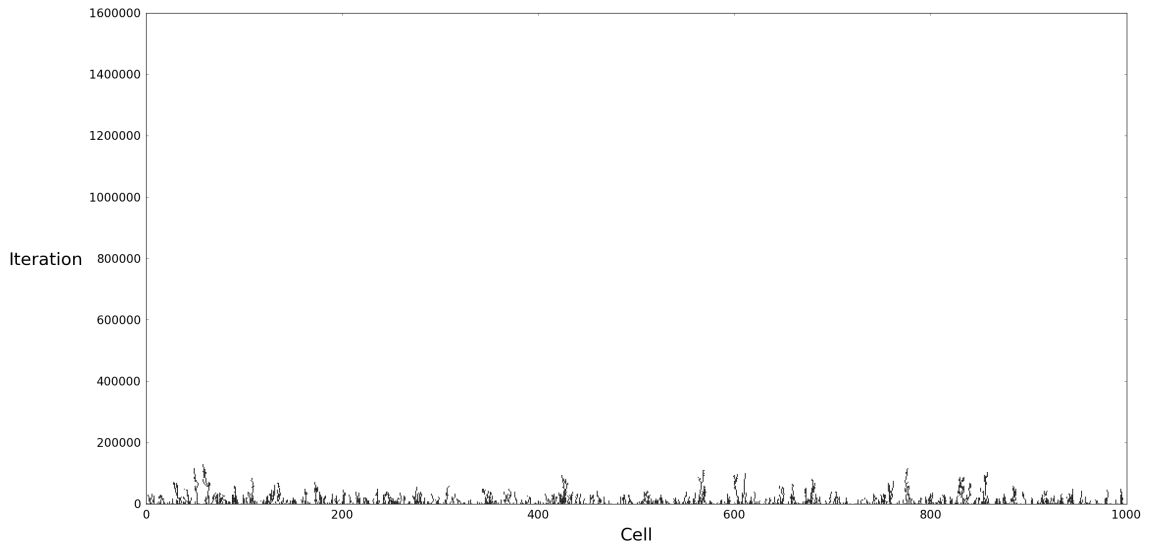


Figure 5.11: 1.6 million iterations of a one-dimensional, one species \mathfrak{B} -model on a ring of 1000 cells, with the following parameters: $\alpha = 0.08$, $\beta = 0.06$, $\gamma = 0.06$, $\epsilon = 0.08$, $\zeta = 0$. The initial conditions were generated by setting each cell to be occupied with a probability of 0.5.

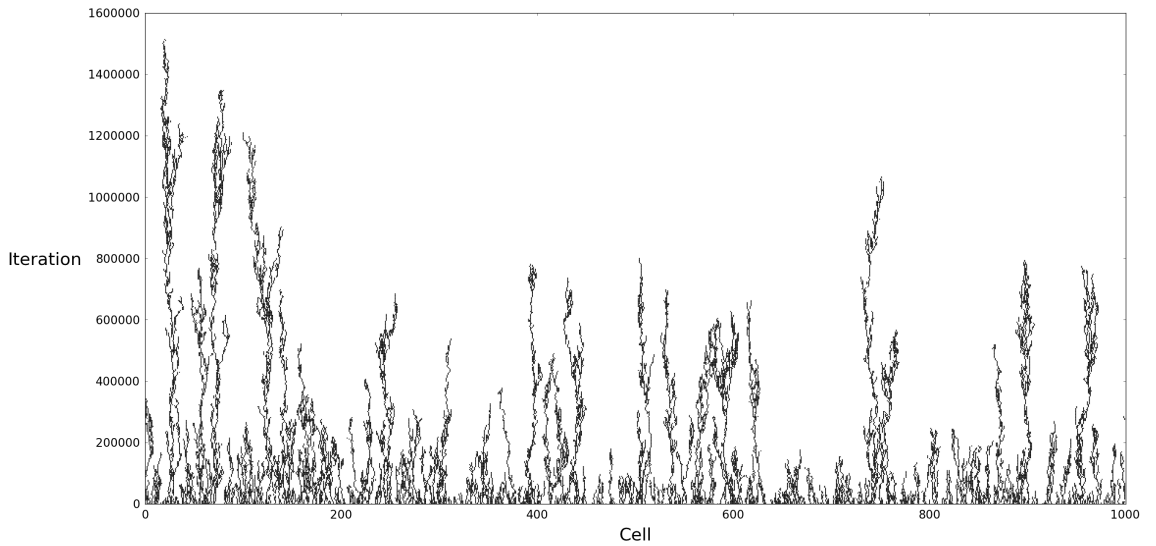


Figure 5.12: 1.6 million iterations of a one-dimensional, one species \mathfrak{B} -model on a ring of 1000 cells, with the following parameters: $\alpha = 0.02$, $\beta = 0.08$, $\gamma = 0.06$, $\epsilon = 0.08$, $\zeta = 0$. The initial conditions were generated by setting each cell to be occupied with a probability of 0.5.

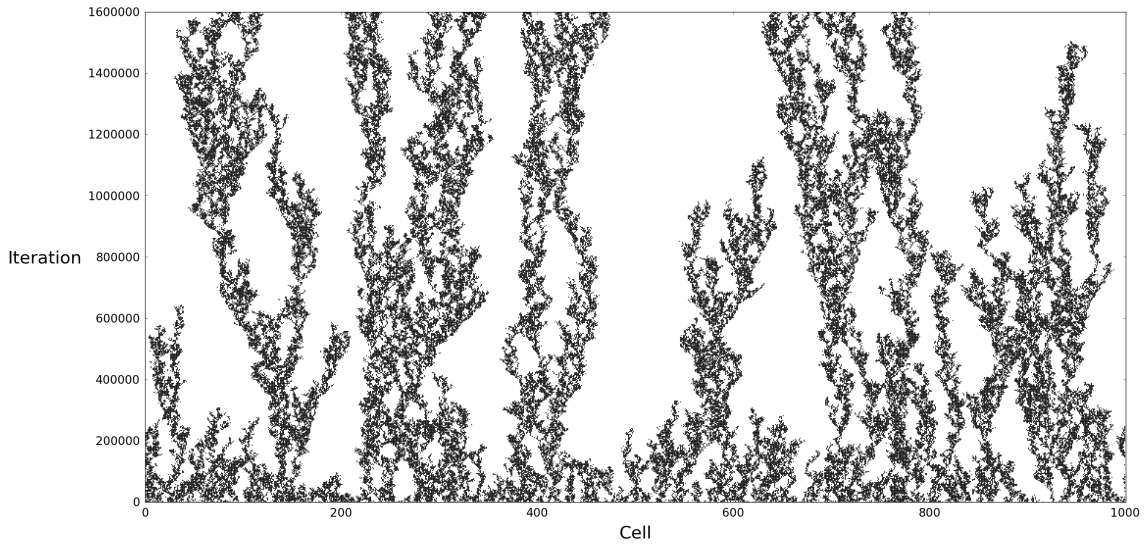


Figure 5.13: 1.6 million iterations of a one-dimensional, one species \mathfrak{B} -model on a ring of 1000 cells, with the following parameters: $\alpha = 0.16$, $\beta = 0.32$, $\gamma = 0.32$, $\epsilon = 0.08$, $\zeta = 0$. The initial conditions were generated by setting each cell to be occupied with a probability of 0.5.

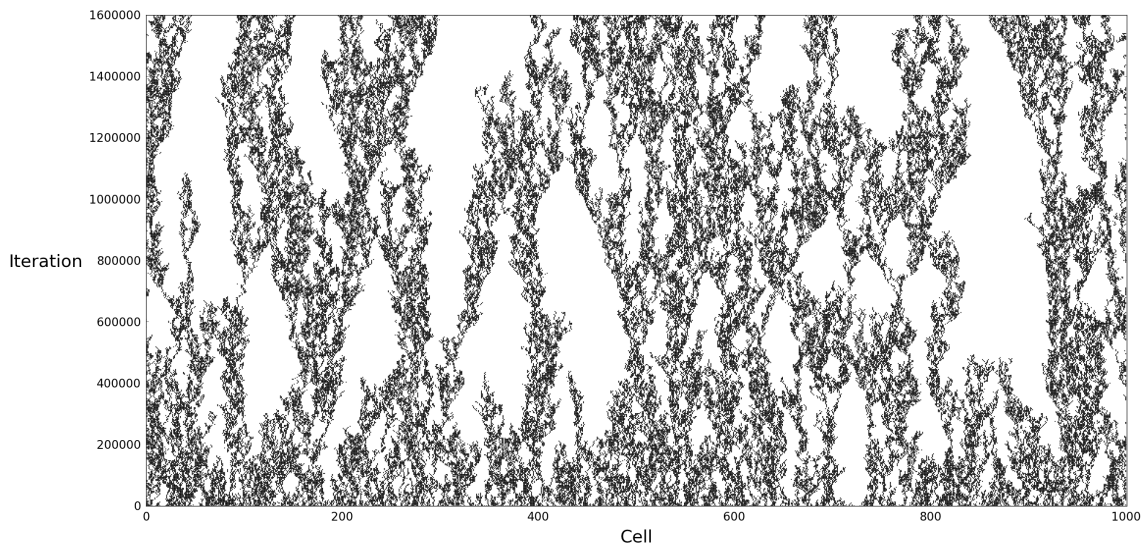


Figure 5.14: 1.6 million iterations of a one-dimensional, one species \mathfrak{B} -model on a ring of 1000 cells, with the following parameters: $\alpha = 0.06$, $\beta = 0.32$, $\gamma = 0.16$, $\epsilon = 0.08$, $\zeta = 0$. The initial conditions were generated by setting each cell to be occupied with a probability of 0.5.

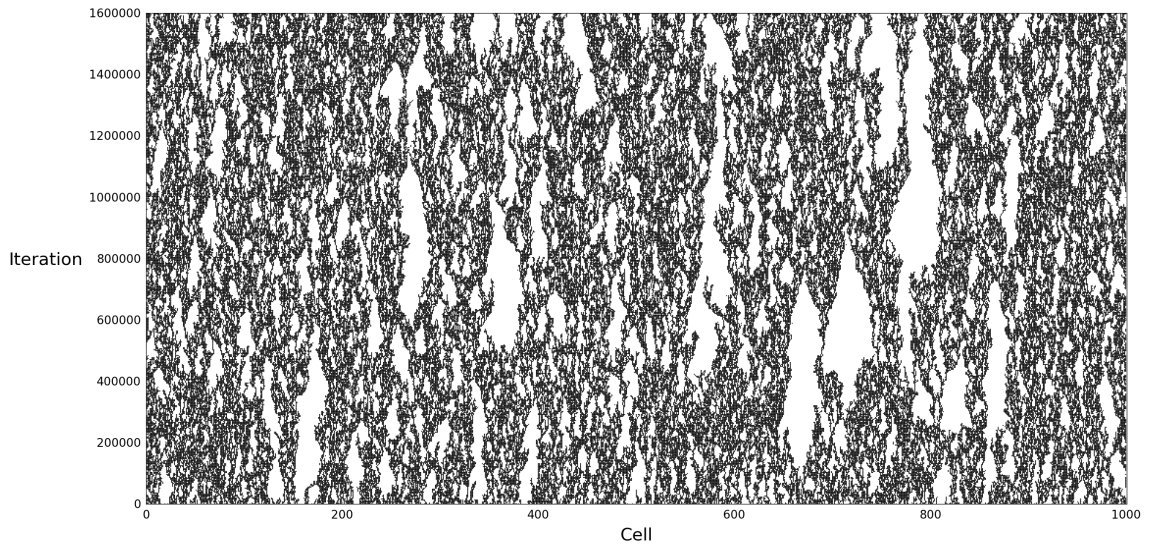


Figure 5.15: 1.6 million iterations of a one-dimensional, one species \mathfrak{B} -model on a ring of 1000 cells, with the following parameters: $\alpha = 0.06$, $\beta = 0.02$, $\gamma = 0.24$, $\epsilon = 0.08$, $\zeta = 0$. The initial conditions were generated by setting each cell to be occupied with a probability of 0.5.

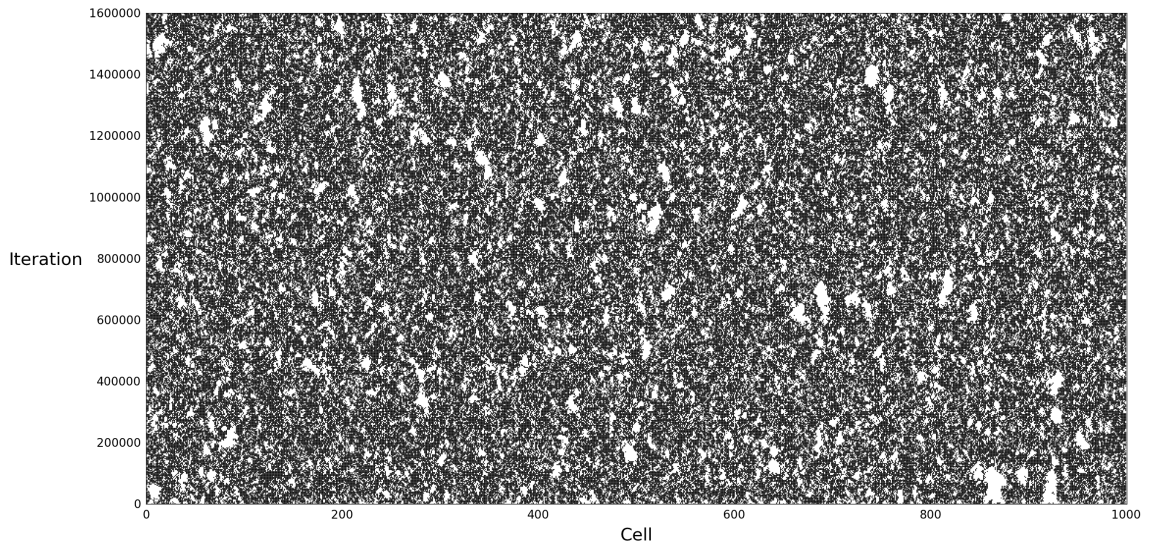


Figure 5.16: 1.6 million iterations of a one-dimensional, one species \mathfrak{B} -model on a ring of 1000 cells, with the following parameters: $\alpha = 0.08$, $\beta = 0.32$, $\gamma = 0.32$, $\epsilon = 0.08$, $\zeta = 0$. The initial conditions were generated by setting each cell to be occupied with a probability of 0.5.

Ultimately, for parameter sets weighted heavily in favour of individual survival, rather than systems of separate clusters, simulations begin to resemble a continuous mass of individuals punctuated by characteristic vertical holes, which may display a loose ‘tear drop’ shape, wider at the base (earlier iterations) and tapering towards the top (later iterations) (see Figure 5.15).

In cases where individuals are most prolific, holes are filled rapidly and these vertical ‘tear drop’ shapes are not observed. In these cases, the visualisations resemble a dense ‘sponge’ of individuals (see Figure 5.16).

The link between these behaviours and the values of the model parameters will be explored in the remainder of this chapter.

5.3.6 Comparisons with Wolfram’s work on CAs

Before presenting a synthesis of the results of Section 5.3.5, we briefly consider the similarities between the model visualisations of Figures 5.3-5.16 and the many visualisations of CAs presented by Wolfram in *A New Kind of Science* (2002), particularly those in Chapter 6 (pp. 223-296), in which he investigates the behaviour of CAs with random initial conditions, which represents the closest analogue of the work presented here.

In Figures 5.3-5.16, we can observe behaviour that is visually similar to that which characterises each of Wolfram’s four classes of CA (see Section 2.3.3):

- Figures 5.5, 5.6 and 5.11 display class 1 behaviour (convergence to a uniform equilibrium);
- Figures 5.3, 5.7, 5.8, 5.9 and 5.10 display behaviour resembling that of class 2 CAs (persistent, simple discrete structures);
- Figures 5.4, 5.15 and 5.16 appear to display class 3 behaviour (apparently random spatial patterns), with the ‘tear drop’ shaped holes of 5.15 being analogous to the triangular structures seen in many class 3 CAs (see, for example, Wolfram, 2002, p. 262);
- Figures 5.13 and 5.14 display behaviour resembling that of certain class 4 CAs (complex interacting structures) (see, particularly, Wolfram, 2002, p. 236, p. 282).

The remaining model, visualised in Figure 5.12, strictly exhibits class 1 behaviour, although the dynamics are visually similar to those of certain class 4 systems (see,

for example, the continuous CA labelled “{0.5, 1.13}”, Wolfram, 2002, p. 244).

While Wolfram’s four classes are largely intended to apply to simple deterministic systems, rather than stochastic models like those in family \mathfrak{B} , the above observations are of interest for the following reasons.

Wolfram describes class 4 systems as lying at the boundary between the trivial ordered behaviour of classes 1 and 2 and the random behaviour of class 3 (pp. 240-242). In the same way, the simulations visualised in Figures 5.13 and 5.14 , which display behaviour resembling that of certain class 4 CAs, lie on the boundary between simulations that rapidly reach extinction, such as that of Figure 5.11, and those exhibiting dense, apparently random behaviour, such as that of Figure 5.16. In both the case of Wolfram’s deterministic models and in that of these stochastic models, the key feature at this boundary appears to be the ability of the underlying local rules to produce some form of global structure, be it through the complex interacting forms of Wolfram’s deterministic systems or the simpler spatial clusters of our stochastic models.

Attempting to understand the mechanisms that connect local transitions and global spatial structure will be the principal aim of Chapter 6.

5.3.7 Population density dynamics

In addition to examining the ‘complete’ visualisations of the model behaviour provided in Figures 5.3-5.16, we can also plot the dynamics of the observed population density and visually compare these against the predicted mean field equilibria (similar approaches are taken by Wolfram (1983, pp. 614-615), McKane and Newman (2004) and Huet and Deffuant (2008)). Recall that \bar{u}_j denotes the observed population density at the $3200j$ th iteration, averaged over ten independent simulations (see (5.4)).

For the simulations with $\eta = 0$, the simple behavioural types identified in Section 5.3.4 may also be observed in these density dynamics plots. For example, Figure 5.17 displays the change in the dynamics as the value of $\gamma - \alpha$ decreases from a positive value (0.2) through 0 to a negative value (-0.2), when $\eta = 0$, for a particular value of β . The plots in this figure clearly illustrate the exchange of stability of the stationary points $u_0^* = 0$ and $u_1^* = 1$ at the bifurcation value $\gamma - \alpha = 0$, leading to the three possible behaviours previously identified: convergence to 1 when $\gamma - \alpha > 0$, convergence to 0 when $\gamma - \alpha < 0$ and no convergence when $\alpha = \gamma$, with the density subject only to random drift in this last case.

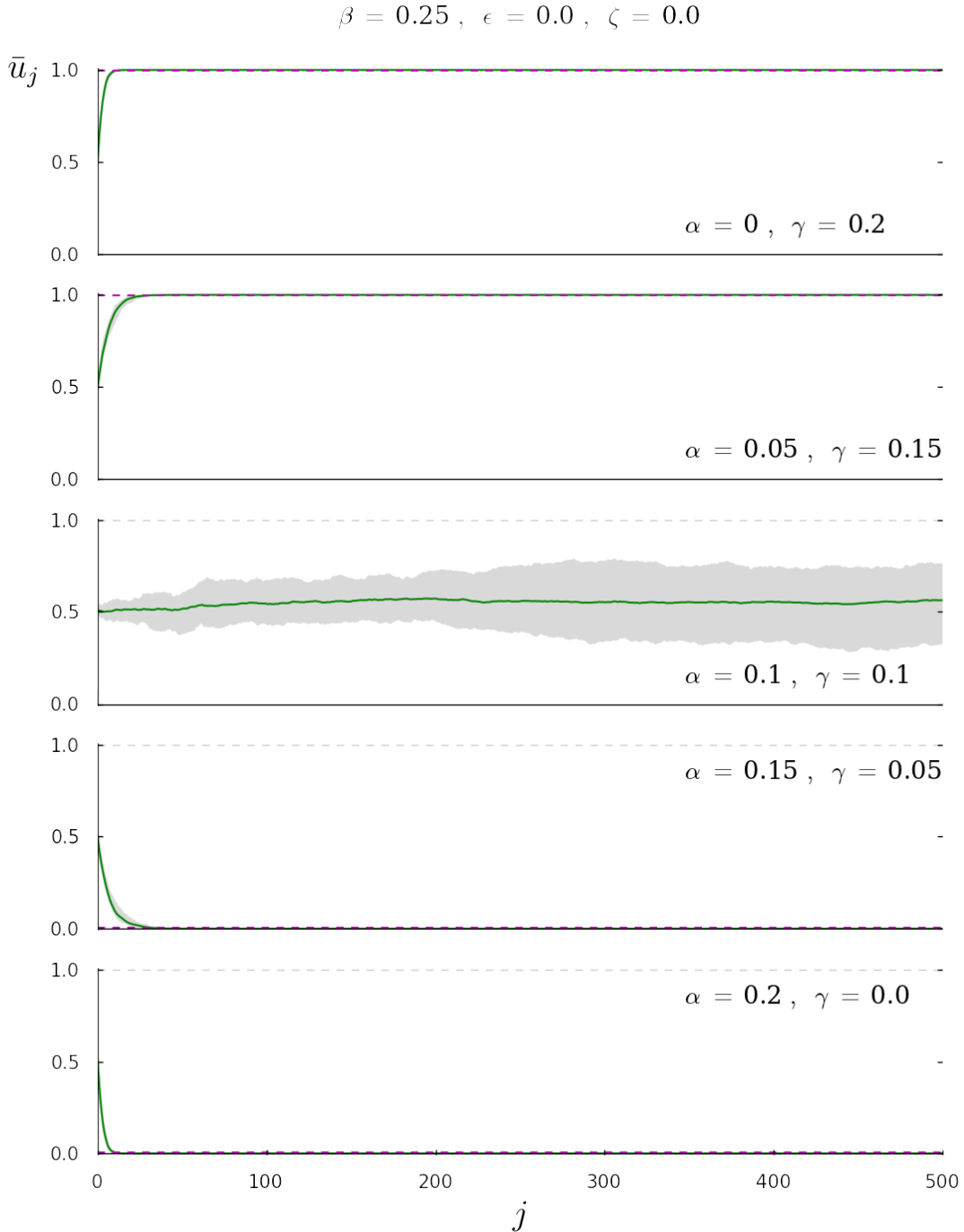


Figure 5.17: The dynamics of the population density over 1.6 million iterations of a one-dimensional single species \mathfrak{B} -model on a ring of 1000 cells. The plotted value \bar{u}_j is the mean density calculated over ten independent runs, using data from the simulation experiments described in Section 5.3.3, for various values of the parameters α and γ , with $\beta = 0.25$, $\epsilon = 0$, $\zeta = 0$. Mean densities are plotted at intervals of 3200 iterations, with the grey region covering the range from the minimum to the maximum density observed across the ten runs. The dashed pink line denotes the unique stable equilibrium of the dynamics predicted by the mean field analysis of Section 5.2.2, where it exists. In the third plot, mean field theory predicts that any initial density should be invariant, hence no unique stable equilibrium is displayed in this case.

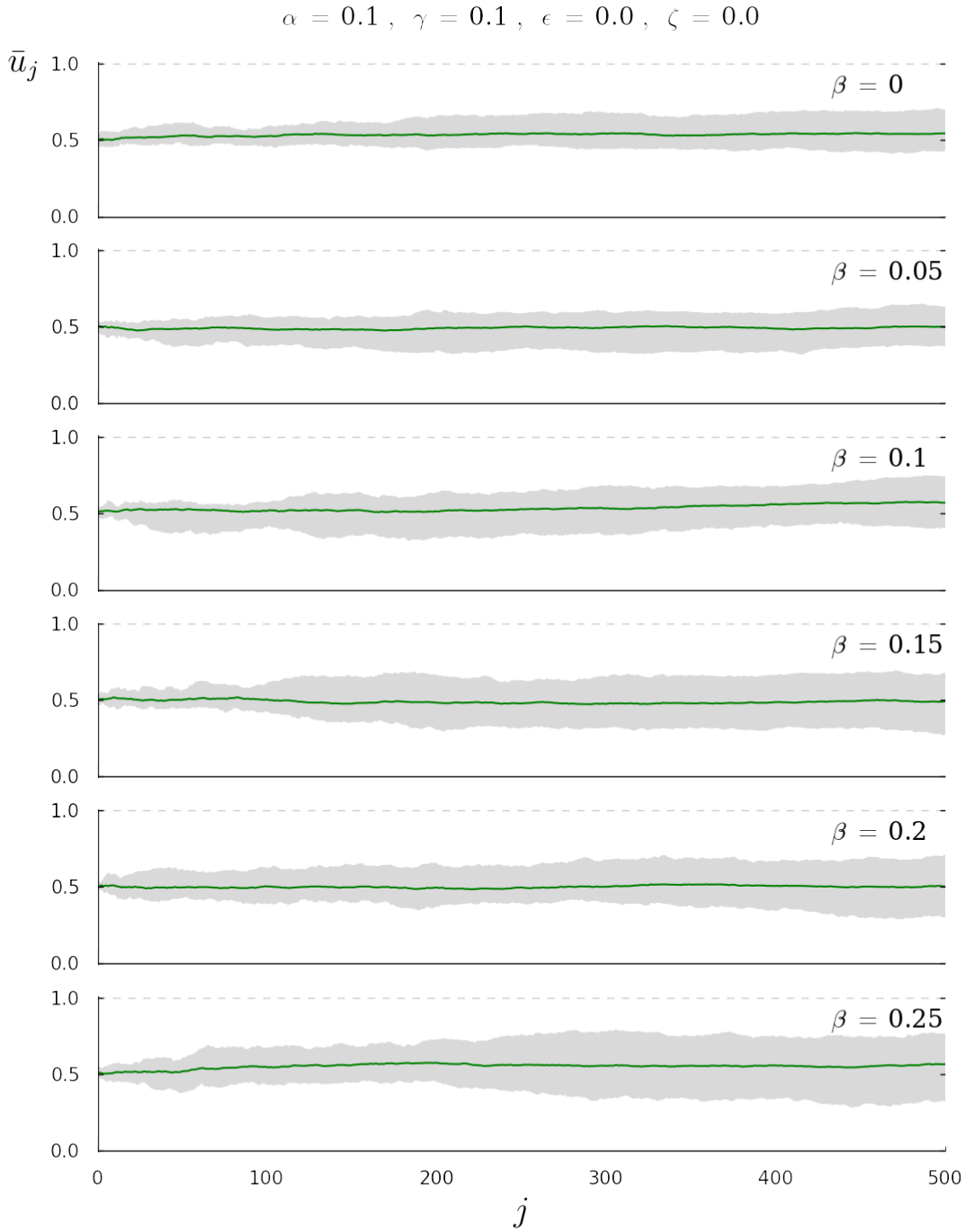


Figure 5.18: The dynamics of the population density over 1.6 million iterations of a one-dimensional single species \mathfrak{B} -model on a ring of 1000 cells. The plotted value \bar{u}_j is the mean density calculated over ten independent runs, using data from the simulation experiments described in Section 5.3.3, for various values of the parameter β , with $\alpha = 0.1, \gamma = 0.1, \epsilon = 0, \zeta = 0$. Mean densities are plotted at intervals of 3200 iterations, with the grey region covering the range from the minimum to the maximum density observed across the ten runs. In all these plots, mean field theory predicts that any initial density should be invariant, hence no unique stable equilibria are displayed.

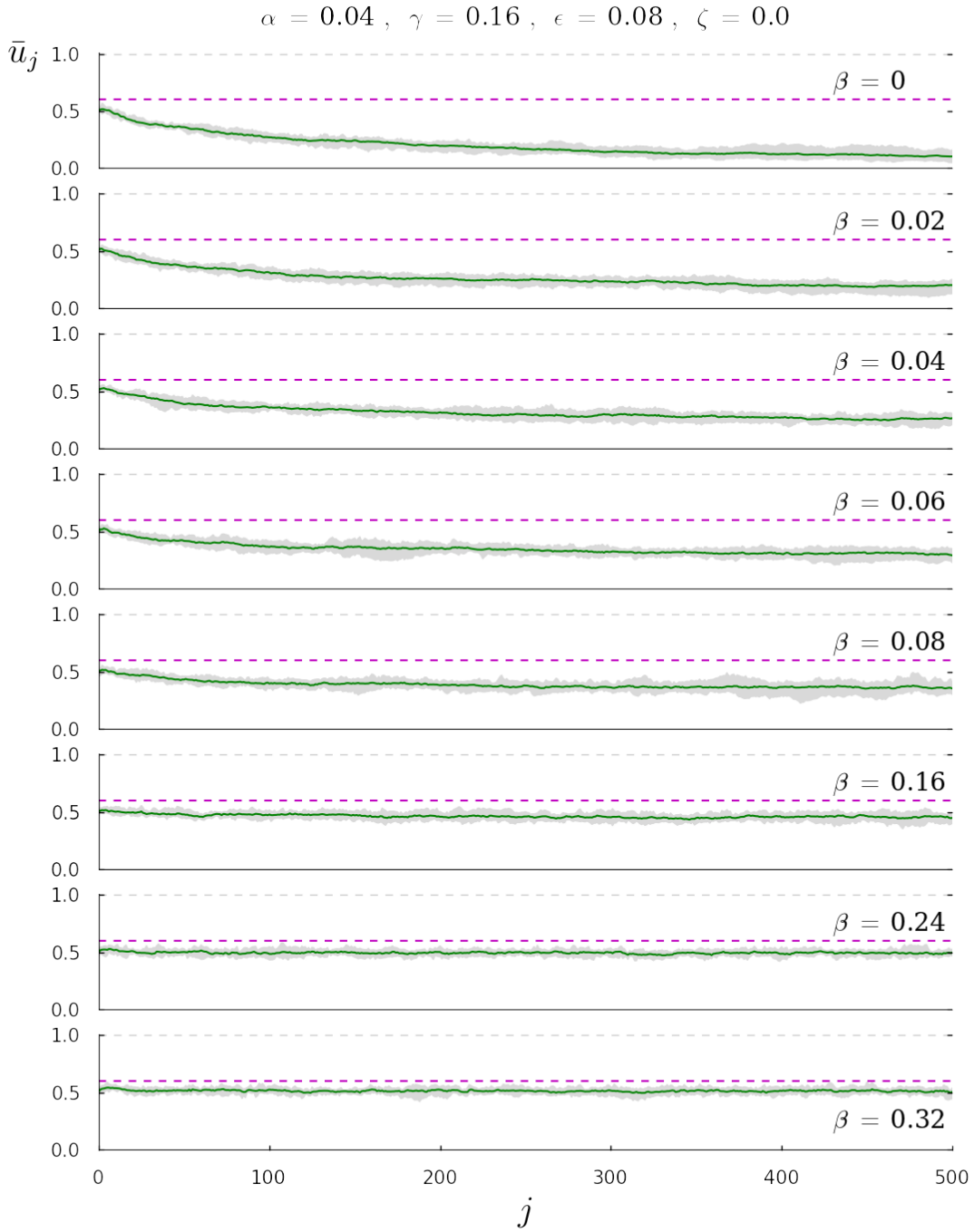


Figure 5.19: The dynamics of the population density over 1.6 million iterations of a one-dimensional single species \mathfrak{B} -model on a ring of 1000 cells. The plotted value \bar{u}_j is the mean density calculated over ten independent runs, using data from the simulation experiments described in Section 5.3.3, for various values of the parameter β , with $\alpha = 0.04$, $\gamma = 0.16$, $\epsilon = 0.08$, $\zeta = 0$. Mean densities are plotted at intervals of 3200 iterations, with the grey region covering the range from the minimum to the maximum density observed across the ten runs. The dashed pink line denotes the unique stable equilibrium ($u_1^* = 0.6$) predicted by the mean field analysis of Section 5.2.2.

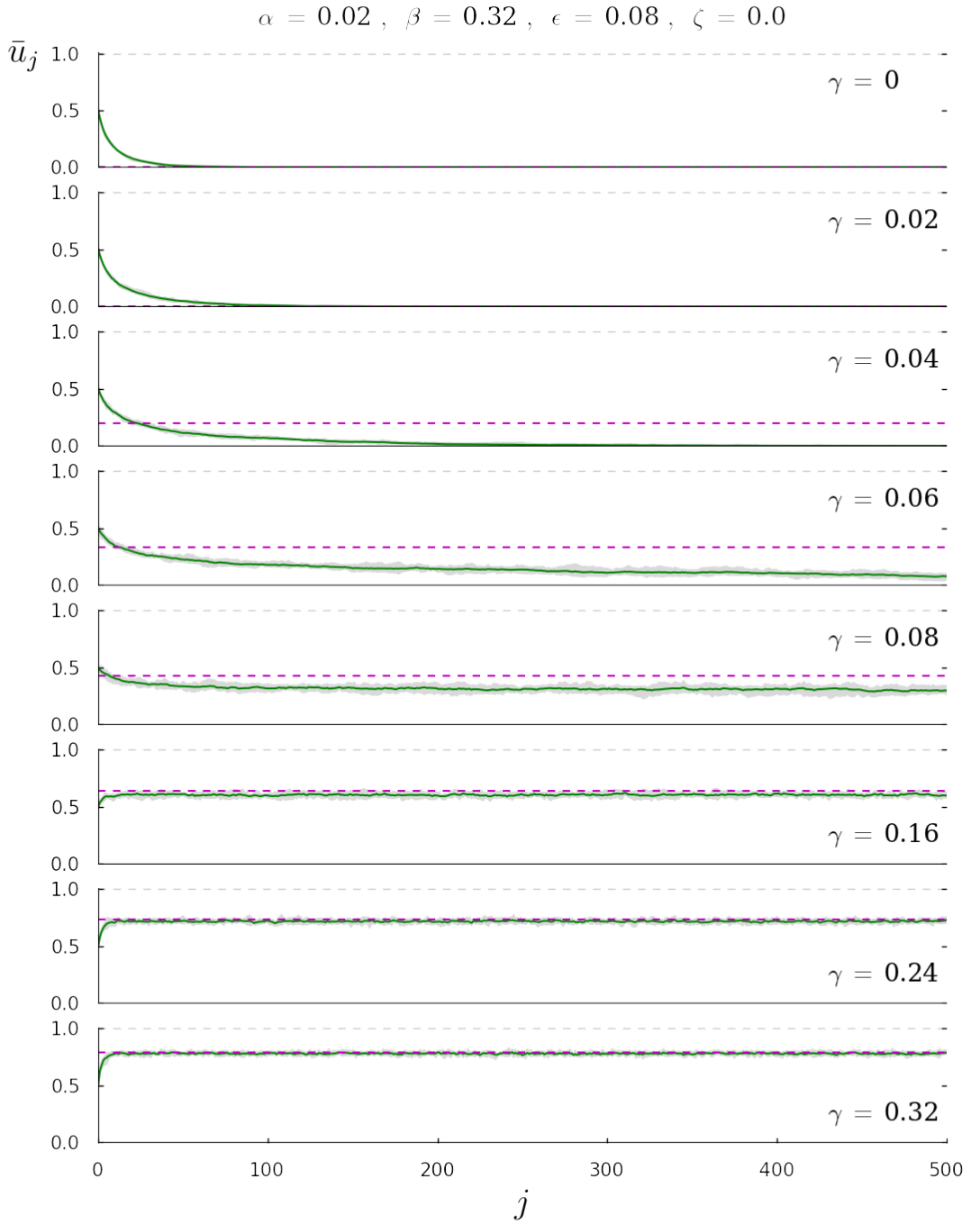


Figure 5.20: The dynamics of the population density over 1.6 million iterations of a one-dimensional single species \mathfrak{B} -model on a ring of 1000 cells. The plotted value \bar{u}_j is the mean density calculated over ten independent runs, using data from the simulation experiments described in Section 5.3.3, for various values of the parameter γ , with $\alpha = 0.02$, $\beta = 0.32$, $\epsilon = 0.08$, $\zeta = 0$. Mean densities are plotted at intervals of 3200 iterations, with the grey region covering the range from the minimum to the maximum density observed across the ten runs. The dashed pink line denotes the unique stable equilibrium of the dynamics predicted by the mean field analysis of Section 5.2.2.

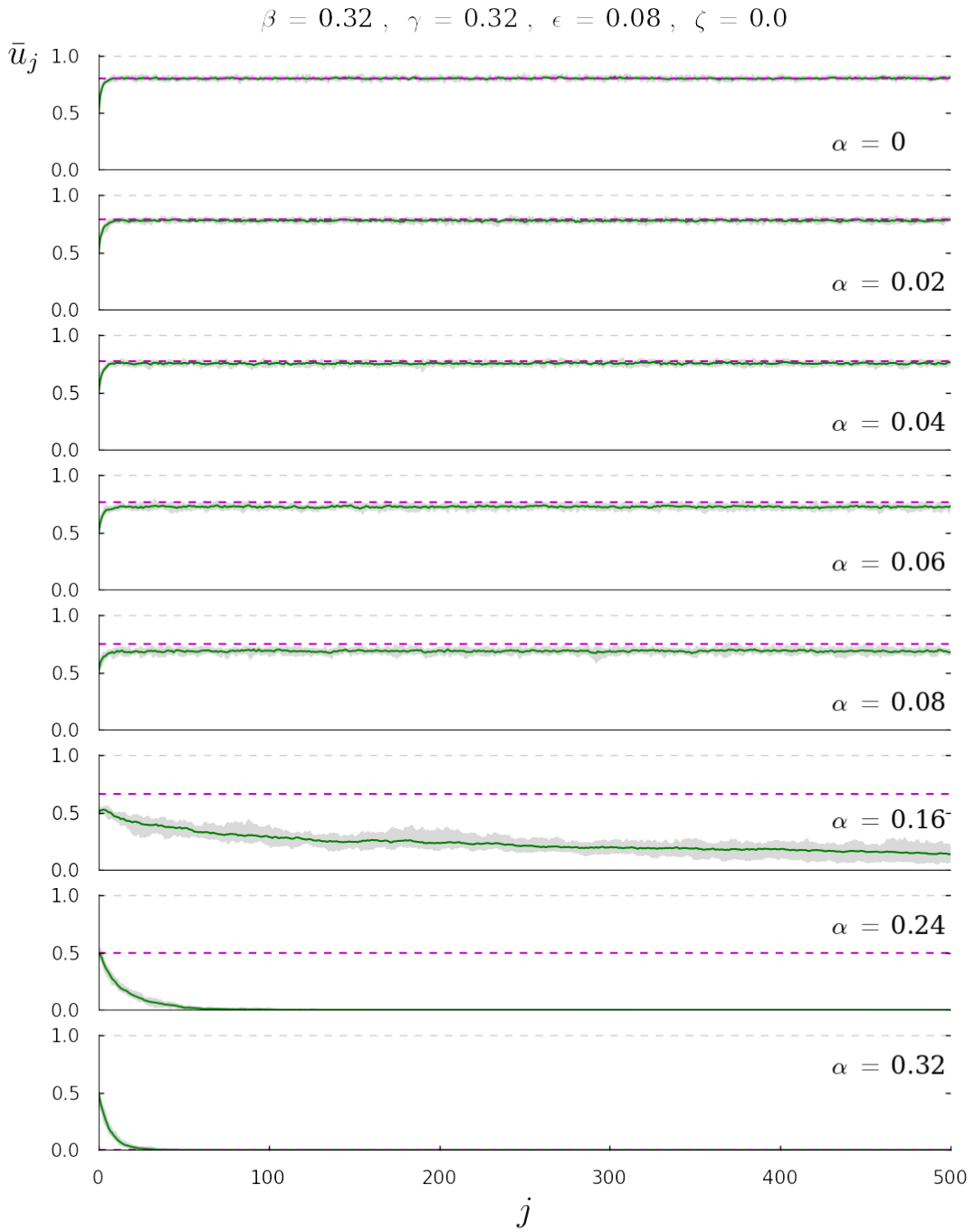


Figure 5.21: The dynamics of the population density over 1.6 million iterations of a one-dimensional single species \mathfrak{B} -model on a ring of 1000 cells. The plotted value \bar{u}_j is the mean density calculated over ten independent runs, using data from the simulation experiments described in Section 5.3.3, for various values of the parameter α , with $\beta = 0.32$, $\gamma = 0.32$, $\epsilon = 0.08$, $\zeta = 0$. Mean densities are plotted at intervals of 3200 iterations, with the grey region covering the range from the minimum to the maximum density observed across the ten runs. The dashed pink line denotes the unique stable equilibrium of the dynamics predicted by the mean field analysis of Section 5.2.2.

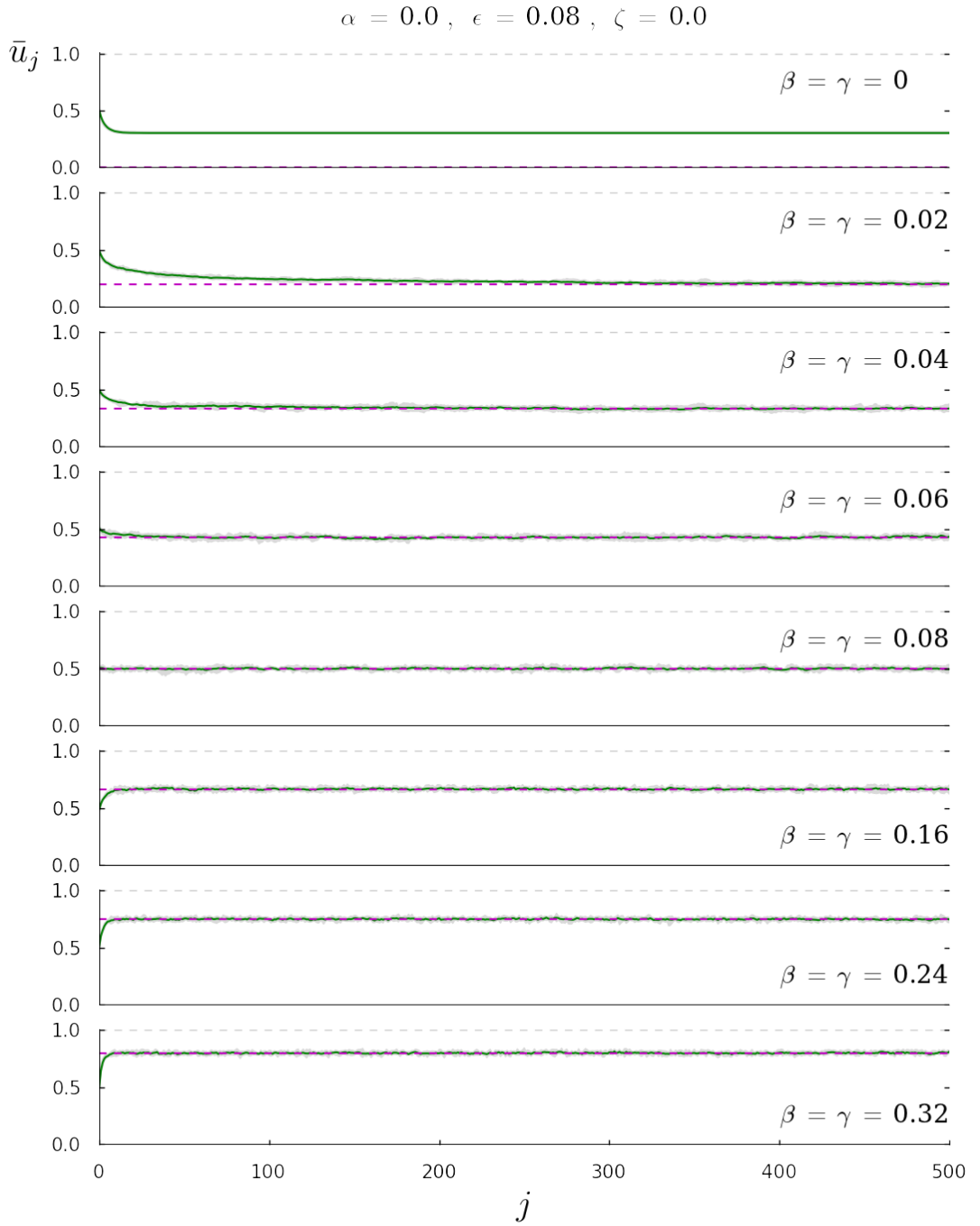


Figure 5.22: The dynamics of the population density over 1.6 million iterations of a one-dimensional single species \mathfrak{B} -model on a ring of 1000 cells. The plotted value \bar{u}_j is the mean density calculated over ten independent runs, using data from the simulation experiments described in Section 5.3.3, for various values of the parameters β and γ , with $\alpha = 0$, $\epsilon = 0.08$, $\zeta = 0$. Mean densities are plotted at intervals of 3200 iterations, with the grey region covering the range from the minimum to the maximum density observed across the ten runs. The dashed pink line denotes the unique stable equilibrium of the dynamics predicted by the mean field analysis of Section 5.2.2.

The simulations exhibiting this random drift are further explored in Figure 5.18, which displays the dynamics for simulations with $\alpha = \gamma$ and $\eta = 0$, as β increases from 0 to 0.25. In all plots, the mean density across the ten runs remains fairly constant, in line with the mean field analysis of Section 5.2.2, which suggests that the dynamics are governed by the equation $\dot{u} = 0$ in such cases. However, the plots show a large amount of variation between runs, as evidenced by the extent of the grey regions, which indicate the range between the maximum and minimum observed densities.

For the sets of parameter values considered in the figure, increasing β seems to have little impact on the density dynamics, though higher values of β do appear to be associated with an increase in the spread of the observed densities. This is to be expected, since the ‘feathering’ discussed in Section 5.3.4, which is associated with higher values of β , increases the number of potential locations at which α and γ -transitions may occur, thus accelerating the dynamics and the expected rate of stochastic divergence of the densities across the ten simulation runs.

Naturally, the behavioural types relating to simulations with $\eta \neq 0$, discussed in Section 5.3.5, cannot be so easily identified from the density dynamics plots, since they were defined in terms of explicitly spatial features, such as visible clusters, which are not represented by the density alone. While correspondences can still be drawn between these behavioural types and the density dynamics plots in these cases, Figures 5.19-5.22 are perhaps more useful for observing the relationships between parameters, model dynamics and the mean field equilibria.

For example, Figure 5.19 displays the density dynamics for models with fixed positive values of α , γ and η , for increasing values of β . The quantity $\gamma - \alpha$ is positive, and mean field theory therefore predicts the existence of a positive stable equilibrium u_1^* ($u_1^* = 0.6$, in these examples). The density dynamics depicted in the figure are broadly representative of the dynamics observed in all simulations whose parameters exhibit these properties.

Firstly, observe that in every plot, the range of the observed dynamics across the ten runs conducted for each parameter set, represented by the grey region, is concentrated relatively closely around the mean density. This implies that the mean density \bar{u} provides a fairly good representation of the true model dynamics in these cases.

Secondly, in each plot, the density seems either to settle to a quasi-stable equilib-

rium that is significantly below the value predicted by the mean field approach, or to decay slowly towards $u = 0$, such that it is impossible to judge by eye whether the long-term behaviour will be a low-density quasi-stable equilibrium or extinction. It is clear, however, that as β increases, the long term density approaches the mean field equilibrium more and more closely.

This last observation suggests that higher values of β may be conducive to dynamics that correspond more closely with those predicted by mean field analysis. An explanation for this result is provided in Section 5.3.10.

Figure 5.20 illustrates the effect on the density dynamics of varying the value of γ for fixed positive values of α , β and η . The specific examples chosen are, once again, broadly representative of the dynamics observed in all simulations with positive values for these three parameters.

The plots seen in Figure 5.20 are similar to those of Figure 5.19, in that higher values of the parameter being varied, γ in this case, appear to be associated with a better correspondence between the observed density dynamics and the predicted mean field equilibria. However, in this case, the effect is stronger, with the density tending fairly rapidly to extinction for smaller values of γ , both where such behaviour is predicted by the mean field equations ($\gamma = 0$, $\gamma = 0.02$) and where it is not ($\gamma = 0.04$), and settling to a quasi-stable equilibrium very close to or indistinguishable from the mean field equilibrium for larger values of γ .

This suggests that, as with β , higher values of γ may be conducive to dynamics that correspond more closely with those predicted by mean field analysis.

Observe also that, while the range of densities is once again fairly concentrated around the mean, there is noticeably more variation for the intermediate values of γ ($\gamma = 0.06$ and $\gamma = 0.08$) that lie between those for which the density clearly tends to extinction and those for which it tends to a quasi-stable equilibrium close to the mean field equilibrium. We return to this observation in a moment.

Figure 5.21 displays the changes in the density dynamics as α increases, for fixed positive values of β , γ and η . Note that the plots for $\alpha = 0.08$ and $\alpha = 0.16$ correspond to the behaviour visualised in Figures 5.16 and 5.13 respectively.

In this figure, we observe an opposite effect to that seen in Figure 5.20, with higher values of α corresponding to poorer correspondence with the dynamics predicted by

the mean field equations. Rapid convergence to quasi-stable equilibria close to or indistinguishable from the mean field equilibria is observed when α is small, while the system tends to extinction when α exceeds a certain threshold. Note that this threshold is below the bifurcation value of the mean field equations, $\alpha = \gamma$, with convergence to extinction occurring in some simulations for which the existence of a positive stable equilibrium is predicted (e.g. in the plot with $\alpha = 0.24$).

These observations would suggest that higher values of α are somehow not conducive to dynamics that correspond to those predicted by mean field analysis.

Observe also that, once again, while densities are generally concentrated very closely around the mean, the simulations depicted in the plot with $\alpha = 0.16$ exhibit a significantly greater range of densities across the ten sample runs under consideration. As before, this parameter value lies between those values for which simulations exhibit clear convergence to non-zero quasi-stable equilibria and those for which simulations tend to extinction.

This observation, combined with the similar observation made in relation to Figure 5.20, suggests that uncertainty about the future evolution of a model of this kind is greatest when parameters lie near the boundaries of regions of parameter space where simulations exhibit qualitatively different dynamical behaviours (i.e. near bifurcations of the true model dynamics). Note that these boundary zones are precisely where the clustering behaviour identified in Section 5.3.5 occurs (see Figures 5.13-5.14). We may hypothesise that the increased range in the densities observed could relate to variations in the number of clusters that happen to form and to survive in the course of a particular simulation.

Finally, consider Figure 5.22, which depicts the change in density dynamics as β and γ are varied, while fixing $\eta > 0$ and $\alpha = 0$. For the sake of simplicity, $\beta = \gamma$ in all plots, though the dynamics presented are representative of the model behaviour for all simulations with positive β , γ and η and with $\alpha = 0$.

The plot for which $\beta = \gamma = 0$, in which the density converges to a genuine stable equilibrium well above the predicted mean field equilibrium at $u = 0$, corresponds to the special case where the system rapidly degenerates into a collection of persistent isolated immobile cells, as seen in Figure 5.9. Aside from this exceptional case, all other plots in Figure 5.22 display similar behaviour, with convergence to the mean field equilibrium in all cases. Furthermore, the range of densities around the mean is highly concentrated, with very little stochastic divergence from the average

behaviour, indicating that the density dynamics are highly predictable in these cases.

The fact that these plots, for which $\alpha = 0$ and β, γ and η are positive, all display tight convergence to the mean field equilibria, coupled with the observations on the effects of increasing α that were made in relation to Figure 5.21, suggests that there is a fundamental relationship between α -transitions and the validity of mean field analysis in the single species, one-dimensional \mathfrak{B} -model. This issue will be revisited in Section 5.4.1 and examined in detail in Chapter 6.

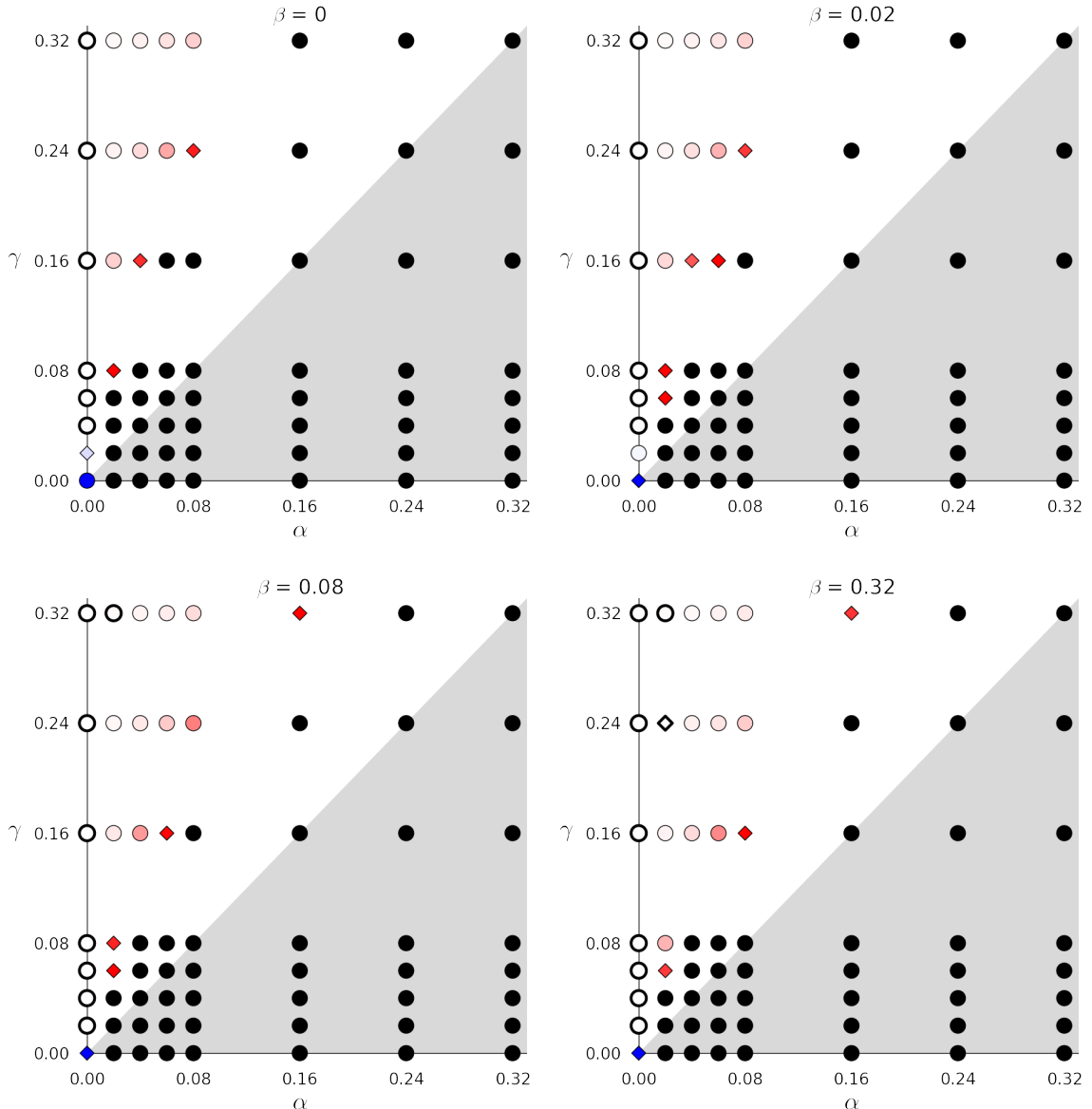
5.3.8 Mapping the parameter space for $\eta \neq 0$

We now seek to understand the link between the values of the model parameters and the type of behaviour displayed by the system in a more systematic and quantitative way than was attempted in Section 5.3.7, for the case $\eta \neq 0$. To achieve this, parameter space diagrams have been created and are presented in Figure 5.23. The plots were constructed empirically from the results of the simulations for which $\eta = 0.08$, with each plot representing experimental outcomes for a different value of β ; specifically for $\beta \in \{ 0, \eta/4, \eta, 4\eta \}$.

The grey shaded area of each plot represents the region where $\alpha \geq \gamma$ in which the mean field equation (5.1) predicts that $u = 0$ is the unique stable equilibrium of the system. In the unshaded region, where $\alpha < \gamma$, the mean field equation predicts that $u = 0$ is unstable and that there exists a unique stable equilibrium $u = u_1^* > 0$, defined in equation (5.3).

Each triplet α, β, γ of parameter values considered is represented by a point on the relevant plot. The shape of the point corresponds to whether or not, for that particular set of parameters, simulation results were consistent with convergence to a stable or quasi-stable equilibrium density after the full 1.6 million iterations (up to a certain amount of stochastic noise). Circular points represent parameter sets for which convergence was detected in the corresponding simulations, while square points represent those for which convergence was not detected. The test used to determine convergence is detailed in Section 5.3.9.

The colour of the points is related to the final mean density of the corresponding simulations in the following way. Black points indicate that all corresponding simulations had converged to zero density after 1.6 million iterations (necessarily a stable equilibrium). Points for which the final mean density of the corresponding simulations was between zero and the predicted mean field equilibrium for the relevant parameters (defined by (5.3)) were coloured on a scale from red for the lowest densi-

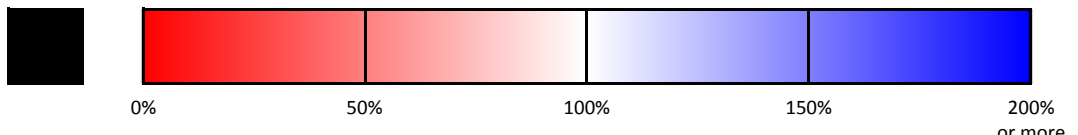


Key to point colours :

Observed equilibrium density (or final mean density) is...

... exactly zero.

... greater than zero.



Observed equilibrium density (or final mean density) as a percentage of stable mean field equilibrium

Figure 5.23: Parameter space diagrams for the population dynamics of the one-dimensional single species \mathfrak{B} -model on a ring of 1000 cells, derived from the simulation experiments described in Section 5.3.3. Each point represents ten simulations conducted using the corresponding values of α , β and γ , with $\epsilon = 0.08$ and $\zeta = 0$ in all cases. A detailed explanation of the plots is provided in Section 5.3.8.

ties, to white for densities closest to the mean field equilibrium. Points for which the final mean density of the corresponding simulations was above the predicted mean field equilibrium were similarly coloured on a scale from white to blue. A colour bar for these scales is provided in the figure.

The method of calculating the final mean density differs between those simulations that had converged and those that had not. For those parameter sets for which simulations were found to converge to a non-zero equilibrium density, the value determining the colour of the corresponding point is the mean density taken over the set $\{u_{ij} : i \in \{1, \dots, 10\}, j \in \{380, 385, 390, \dots, 500\}\}$. Note that observations are taken at intervals of 5 steps (16000 iterations) in order that stochastic noise around an equilibrium value is uncorrelated. For those parameter sets where convergence was not detected, the value used to determine the colour was simply the mean density over all ten corresponding simulations at the final iteration.

Whether or not convergence was detected, parameter sets for which the final mean density or equilibrium density was calculated to lie within two percent of the mean field equilibrium density (i.e. points coloured white or very nearly white) are depicted with bold borders.

A discussion of the parameter space plots is presented in Section 5.3.10.

5.3.9 Convergence test

To determine whether or not the experimental observations associated with a particular set of parameters $(\alpha, \beta, \gamma, \epsilon, \zeta)$ exhibit convergence to a stable or quasi-stable equilibrium within the 1.6 million iterations of the corresponding simulations, we employ a test that assumes a particular model of the data. Specifically, we suppose that observations made at intervals of 16 000 iterations (every fifth observation for a given run) may be modelled by the expression:

$$u_{i,5k} = \mu_{5k} + \mathfrak{N}_{i,5k} , \quad \text{for } i \in \{1, \dots, 10\}, k \in \{0, \dots, 100\} \quad (5.6)$$

where μ_{5k} is the current mean, which is assumed to vary deterministically over the course of a simulation, but to be identical across the ten repetitions $i \in \{1, \dots, 10\}$, and where $\mathfrak{N}_{i,5k}$ is a random noise term. For a given set of model parameters, the noise terms $\mathfrak{N}_{i,5k}$ are supposed to be independent and identically distributed, with $\mathfrak{N}_{i,5k} \sim N(0, \sigma^2)$, for some fixed variance σ^2 .

An informal observation of the density-time plots provided in Figures 5.17-5.22 sug-

gests that the assumption of constant variance about a dynamic mean may be reasonable for models with $\eta \neq 0$, but not for models with $\eta = 0$, in which variation between the ten runs conducted with each set of parameters (as represented by the grey region in the plots), appears to grow over time. The convergence test described here will therefore be applied only to simulations with $\eta \neq 0$.

Given this model, to draw a conclusion on whether or not convergence has occurred in the ten runs associated with a particular set of parameter values, we must determine whether the relevant observations are consistent with the theoretical mean μ_{5k} being constant for all $k \geq K$, where $K \in \{0, \dots, 99\}$ is a positive integer of our choice, with lower values of K indicating a requirement of more rapid convergence. This is equivalent to the statement that, from observation $5K$ onwards, all variation both between and within runs can be explained as random noise about some fixed equilibrium value. In what follows, we take $K = 50$, thus requiring that a quasi-stable equilibrium is attained by iteration 800 000, the half-way point of the simulations.

The test that we choose to employ actually verifies a weaker result and therefore does not strictly guarantee convergence under these conditions. However, it is sufficiently accurate for our purposes and provides a good match to intuition, when convergence is assessed from density-time plots (such as Figures 5.17–5.22) by eye.

In essence, the test supposes that the mean μ_{5k} remains constant (at a supposed equilibrium value) across the third quarter of the data $k \in \{50, \dots, 74\}$ and asks whether the final observations $u_{1,500}, \dots, u_{10,500}$ are consistent with the hypothesis that the final mean μ_{500} is also equal to this same value.

The variance σ^2 is estimated by s^2 , the pooled variance of the twenty-five samples $\{u_{1,5k}, \dots, u_{10,5k}\}$, for $k \in \{50, \dots, 74\}$, about their respective observed means \bar{u}_{5k} :

$$s^2 = \frac{1}{250} \sum_{i=1}^{10} \sum_{k=50}^{74} (u_{i,5k} - \bar{u}_{5k})^2 = \frac{1}{25} \sum_{k=50}^{74} s_{5k}^2$$

In other words, s^2 is simply equal to the mean of the observed variances s_{5k}^2 , for $k \in \{50, \dots, 74\}$.

The potential equilibrium value is estimated by \bar{u} , calculated by:

$$\bar{u} = \frac{1}{250} \sum_{i=1}^{10} \sum_{k=50}^{74} u_{i,5k} = \frac{1}{25} \sum_{k=50}^{74} \bar{u}_{5k}$$

Now, if each of the final observations $u_{1,500}, \dots, u_{10,500}$ were truly drawn from the distribution $N(\bar{u}, s^2)$, then their observed mean \bar{u}_{500} should be drawn from the distribution $N(\bar{u}, s^2/10)$. Identification of convergence is therefore identified with the result of the following two-tailed normal hypothesis test, conducted at the 1% significance level, with the null hypothesis corresponding to the conclusion that the simulations had converged:

Hypothesis Test Given \bar{u} , s^2 and \bar{u}_{500} , consider the random variable $\mathcal{U} \sim N(\mu_{500}, \sigma^2)$, where $\sigma^2 = s^2/10$ and μ_{500} is unknown. Suppose that \bar{u}_{500} is a particular realisation of \mathcal{U} . Our null and alternative hypotheses are as follows:

- $H_0 : \mu_{500} = \bar{u}$
- $H_1 : \mu_{500} \neq \bar{u}$

At the 1% significance level, H_0 is rejected if and only if:

$$P[\mathcal{U} \in (\bar{u} - \lambda, \bar{u} + \lambda) | \mu_{500} = \bar{u}] > 0.99$$

where $\lambda = |\bar{u}_{500} - \bar{u}|$.

Note that the condition of the hypothesis test may be written more simply as:

$$\Phi\left(\left|\sqrt{10} \left(\frac{\bar{u}_{500} - \bar{u}}{s}\right)\right|\right) > 0.995$$

where Φ is the cumulative distribution function of the standard normal distribution $N(0, 1)$.

As remarked earlier, this test would clearly not be suitable to determine convergent behaviour in all sequences of the form given in (5.6). In particular, the result of the test can only be meaningfully identified with convergence if the underlying trend, represented by the sequence $(\mu_{5k})_{k \in \{0, \dots, 100\}}$, can be considered to be monotonic from observation $5K$ onward (a condition which may be observed to be satisfied for all simulations under consideration). We therefore reiterate that the test is intended only to identify convergence in these particular experiments (and then, only those for which $\eta \neq 0$), essentially in order to automate and render quantifiable a process that could otherwise have been performed qualitatively by eye.

5.3.10 Discussion of experimental results

In this section, we provide a discussion and synthesis of the results of the simulation experiments, with a particular focus on the parameter space diagrams of Figure 5.23,

which were introduced in Section 5.3.8.

The first thing to observe from Figure 5.23 is that, for all values of β under consideration, the black points indicating convergence to zero density extend beyond the grey region $\alpha \geq \gamma$ where such behaviour is predicted by (5.1). This confirms that the mean field equation does not generally provide a good representation of the behaviour of the system, as was noted in Section 5.3.7.

To understand why this is, recall the assumptions made in the derivation of mean field equations outlined in Section 4.3.4. The mean field method assumes that, for every cell in the system, the probability that a neighbouring cell is occupied is equal to the current global density u , and that these probabilities may be considered to be independent for all neighbours and for all cells. In other words, the mean field equation is associated with perfect mixing of individuals (see Section 3.2.2 for further discussion of the interpretations of the mean field assumptions). In the actual model, for situations where the system is well mixed, the probability that any given cell contains an individual will be equal to u and may be considered to be broadly independent of the states of other cells. However, if the system is not well mixed, there may be considerable clumping of individuals and increased levels of correlation between the occupancy status of nearby cells.

Intuitively, we might expect the parameter β , which governs the rate of individual movement, to be associated with good mixing and therefore that simulations with higher values of β would exhibit behaviour that corresponds more closely to that predicted by the mean field equation. Figure 5.23 confirms this expectation (as do the density dynamics plots in Figure 5.19), since increasing the value of β leads both to more points in the white region converging to values close to the predicted non-zero mean field equilibrium and to fewer points in this region converging to zero. However, comparing the plots for $\beta = 0.02$ and $\beta = 0.32$, we see that the effect of β is quite weak in comparison with that of the parameters α and γ , with this sixteen-fold increase in β resulting in only minor changes to simulation behaviours across the parameter space.

Note the bright blue points at $\alpha = \gamma = 0$ in each of the four plots, indicating final mean densities (or in the case where $\beta = 0$, an equilibrium density) above the predicted mean field equilibrium of $u = 0$. These points correspond to special cases, like those seen in Figures 5.9 and 5.10, in which the system is reduced to a set of isolated occupied cells.

In each of these special cases, whether or not the plots indicate convergence, the behaviour of the system is highly predictable. For $\beta = 0$, since there is no movement (and consequently no mixing), after η -transitions have reduced the system to a set of non-adjacent cells the density remains unchanged, converging to a value between 0 and the density of the initial condition (Figure 5.9), which is approximately equal to 0.5 in all experimental simulations. For higher values of β , isolated cells meander randomly through the system with all but one ultimately being destroyed as the result of increasingly infrequent collisions and subsequent η -transitions, leading to (potentially very slow) convergence of the density to $u = 1/n$ (Figure 5.10).

Putting these special cases aside, consider those points representing simulations that converged to non-zero equilibrium densities. Of these points, a clear distinction can be made between those where $\alpha = 0$, for which the corresponding simulations converged almost universally to the mean field equilibrium density, and those where $\alpha > 0$, for which the corresponding simulations almost all converged to densities *below* the mean field equilibrium.

Since mean field type behaviour is associated with good mixing of occupied and unoccupied cells, this observation suggests that there is a significant difference between β , γ and η -transitions on the one hand and α -transitions on the other in terms of their effect on the mixing of the system. Since the former three transition types are observed to interact to produce behaviour that corresponds closely to that predicted by the mean field equation (at least in terms of their equilibrium behaviour), they seem in some sense to have a positive or neutral effect on individual mixing, while α -transitions seem to have a negative effect. This concept will be explored further in Chapter 6.

The final point to note from the figures is the loose collection of points representing non-convergent simulations, which lie between points indicating convergence to non-zero equilibria and points indicating convergence to zero. In most cases, the final mean densities for these points are rather low and direct observation of the corresponding simulations indicates that they are associated with the formation of isolated clusters of various densities, like those seen in Figure 5.13. Although there is insufficient information to draw firm conclusions about the long term behaviour of such simulations from these results, as discussed in Section 5.3.5, we might hypothesise that such systems would also converge to zero density, as isolated clusters undergo stochastic extinctions.

In Section 5.3.6, we noted that Wolfram (2002) describes class 4 systems,

which exhibit complex interacting structures, as lying on the boundary between class 1 and 2 systems, which display trivial ordered behaviour, and class 3 systems, which display random behaviour. It is interesting to note, therefore, that the two figures that we identified as displaying behaviour that resembled that of Wolfram's class 4 systems, Figure 5.13 and Figure 5.14, correspond to parameter sets ($(\alpha, \beta, \gamma, \epsilon, \zeta) = (0.16, 0.32, 0.32, 0.08, 0)$ and $(\alpha, \beta, \gamma, \epsilon, \zeta) = (0.06, 0.32, 0.16, 0.08, 0)$, respectively) that lie in or near the boundary zone of parameter space identified in the previous paragraph, between a region associated with simulations that converge to 0 (class 1 behaviour) and simulations that converge to a non-zero density (which produce figures resembling class 3 behaviour).

In this section, we have conducted a set of simulation experiments to attempt to understand the full range of possible behaviours of the single species, one-dimensional \mathfrak{B} -model on a ring of cells. Having assessed the results of these experiments, we have hypothesised that there is a difference between α -transitions on the one hand and β , γ and η -transitions on the other, in terms of their effect on individual mixing and the emergence of spatial clumping at the global scale. This idea will be investigated further in Section 5.4 and will form the principal focus of Chapter 6.

5.4 Autocorrelation analysis

5.4.1 Concept and methods

In Section 5.3.10, it was observed that β , γ and η -transitions seem to be associated with good mixing of individuals, while α -transitions seem to be associated with poor mixing. In this section, we examine what exactly we mean by good mixing and attempt to understand why these transitions might have these effects.

For the purposes of the mean field equation (5.1), the system is well mixed if the states of the cells can be considered to be independent. In other words, a system with individual density u should look like the state of each cell has been generated as the result of an independent Bernoulli trial with parameter u . If the system is not well mixed - if the individuals display a degree of clumping which would not be expected from such a process, for example - correlations between the states of nearby cells may be observed.

The degree of mixing of a particular iteration of a simulation may therefore be observed through consideration of the autocorrelation structure of the binary sequence $\mathbf{c} = (c_i)_{i \in \mathbb{Z}} \in \{0, 1\}^{\mathbb{Z}}$, derived from the system using the approach described in

Section 4.4.5 :

$$c_i = \begin{cases} 1, & \text{if } i \in \{0, \dots, n-1\} \text{ and cell } i \text{ is occupied;} \\ 0, & \text{if } i \in \{0, \dots, n-1\} \text{ and cell } i \text{ is empty;} \\ c_{i \bmod n}, & \text{if } i \notin \{0, \dots, n-1\}. \end{cases}$$

The Pearson product-moment correlation coefficient $\rho_{X,Y}$ of two random variables X and Y is defined as:

$$\rho_{X,Y} = \frac{\mathbb{E}[(X - \mu_X)(Y - \mu_Y)]}{\sigma_X \sigma_Y} \in [-1, 1]$$

where μ_X , μ_Y and σ_X , σ_Y are the expectations and standard deviations of X and Y .

This correlation coefficient measures the level of linear statistical dependence of X and Y . If $(X_i)_{i \in \mathbb{Z}}$ is a sequence of random variables, the correlation between X_i and X_{i+k} is known as the autocorrelation of lag k for the sequence. Note that this quantity is only well-defined if the joint distribution of X_i and X_{i+k} is independent of i , a property known as second order stationarity (see Upton and Cook, 2011, pp. 21, 90-93, 371).

For a given set of parameters, $\alpha, \beta, \gamma, \epsilon, \zeta$, with the initialisation used in the simulation experiments (see Section 5.3.3), the terms of the sequence \mathbf{c} corresponding to the final iteration performed (iteration 1.6 million) are random variables with a clearly defined joint distribution determined by the rules of a single species \mathfrak{B} -model. What is more, second order stationarity is guaranteed by the symmetry of the model geography with respect to translations of any integer k . It is therefore meaningful to consider the autocorrelations of \mathbf{c} .

It should be noted that, while we are using these autocorrelations to assess the degree of mixing of individuals in the model at a particular iteration, they do not provide complete information about the ‘randomness’ of a periodic binary sequence. A thorough test for randomness should verify that a given sequence or collection of sequences appears to be consistent with having been generated by a process that has the property that, for all $k \in \{1, \dots, n\}$, all possible blocks of black and white cells of length k are equally likely to be observed at any location (see Wolfram, 2002, pp. 593-595). However, as a proxy indicator of good mixing, the autocorrelations of \mathbf{c} are sufficient for the current purposes.

Observe that the mean of the terms representing a single period of a particular realisation of \mathbf{c} is equal to the individual density u , while the corresponding standard deviation is equal to $\sqrt{u(1-u)}$. An empirical measure of the autocorrelation of lag k for the sequence $\{c_i\}_{i \in \mathbb{Z}}$ is hence given by the following formula:

$$\rho(\mathbf{c}, k) = \frac{1}{nu(1-u)} \sum_{i=0}^{n-1} (c_i - u)(c_{i+k} - u) = \frac{1}{u(1-u)} \left[\frac{1}{n} \left(\sum_{i=0}^{n-1} c_i c_{i+k} \right) - u^2 \right] \quad (5.7)$$

However, given N independent realisations, with \mathbf{c} considered to be a random periodic sequence as described above, an unbiased estimate $r(\mathbf{c}, k)$ of the true theoretical autocorrelation $\rho(\mathbf{c}, k)$ of the terms of \mathbf{c} may be generated by employing the Bessel correction (see Upton and Cook, 2011, pp. 401-402), as follows:

$$r(\mathbf{c}, k) = \frac{Nn - 1}{Nn} \left[\frac{1}{\bar{u}(1-\bar{u})} \right] \left[\frac{1}{Nn} \left(\sum_{j=0}^{N-1} \sum_{i=0}^{n-1} c_i^{(j)} c_{i+k}^{(j)} \right) - \bar{u}^2 \right] \quad (5.8)$$

where \bar{u} is the mean global density over the N realisations, as in Section 5.3.7, and where the superscript (j) refers to the particular realisation from which a value is drawn.

5.4.2 Results and discussion

For a given set of parameters $\alpha, \beta, \gamma, \epsilon, \zeta$, plotting $r(\mathbf{c}, k)$ for $k \in \{0, \dots, n\}$ with $N = 10$ (i.e. calculated over the 10 realisations of the simulation experiments), allows us to visualise the complete autocorrelation structure of the system. See Figures 5.24-5.27 (which correspond respectively to the population density dynamics figures, 5.19-5.22) for examples of such plots. Note that for sets of parameters for which the individuals became extinct in every run, the autocorrelations are undefined and cannot be plotted.

The figures are plotted for $k \in \{-n/2, \dots, n/2\}$ rather than $\{0, \dots, n\}$, since this draws attention to the most interesting features, which appear around $k = 0$. This shift in the range is valid because the imposed periodicity of \mathbf{c} ensures that $r(\mathbf{c}, k) = r(\mathbf{c}, k+n)$, $\forall k \in \mathbb{Z}$. Also note that $r(\mathbf{c}, k)$ is an even function of k owing to the symmetry of the autocorrelation formula, so the plots are symmetric about $k = 0$.

Clearly, the true autocorrelation of lag 0 is equal to 1 for all values of the parameters, since $\rho(\mathbf{c}, 0)$ represents the correlation of every cell with itself. In this case therefore, Bessel's correction clearly leads to an underestimate of the autocorrelation: $r(\mathbf{c}, 0) = (Nn - 1)/Nn$. However, since the experimental value of $Nn = 10000$

is large, for the purposes of plotting, this discrepancy is negligible.

The plots broadly confirm the observations of Section 5.3.10, regarding the effect of different transitions on individual mixing. Roughly speaking, the size of the ‘peak’ in the centre of each plot (taken to mean some measure of the area lying between the central points of the plot and the horizontal axis, rather than the maximum value of $r(\mathbf{c}, k)$, which is constant across all plots) provides information about the degree of mixing of the individuals after 1.6 million iterations of a simulation with the corresponding parameter values, in the sense that these peaks represent correlations in the occupancy of nearby cells. Flatter plots indicate greater independence of nearby cells and therefore better mixing of individuals.

For example, the large peak in the centre of the first plot of Figure 5.24 indicates that, for the specified values of the parameters, the probability that two nearby cells share the same state after 1.6 million iterations is greater than would be expected if the states of the cells were generated independently, given the global density of the system.

However, this effect can be seen to weaken rapidly as the distance between the two cells increases, with no visible correlation between cells separated by more than 50 units (beyond statistical variation) in any of the plots, indicating that (after 1.6 million iterations) the states of cells separated by greater distances than this may be considered to be independent, at least for the range of parameters visualised here. A result of this nature was to be expected, since all transitions in the model are the result of strictly local interactions.

A rapid comparison of the plots presented in Figures 5.24-5.27 with their counterparts in Figures 5.19-5.22 very clearly supports the assertion (first made in Section 5.3.10) that greater levels of individual mixing, interpreted here to mean lower local autocorrelations of cell states, are associated with better correspondences between the observed population density dynamics in a simulation and those predicted by the mean field equations.

Switching our perspective to a closer analysis of the separate autocorrelation plots, we see that, for particular values of the other parameters, Figure 5.24 shows that greater values of β result in better mixing of individuals (lower local autocorrelations). Figure 5.25 shows the same effect for increasing values of γ . However, Figure 5.26 shows that greater values of α result in poorer mixing of individuals, again for specific values of the other parameters. Note that the plots for $\alpha = 0.08$

and $\alpha = 0.16$ in this figure correspond to the behaviour visualised in Figures 5.16 and 5.13 respectively.

Although plots are only presented for certain sets of parameters, these observations of the effect of α , β and γ on individual mixing are representative of all sets of parameters used in the simulation experiments.

Figure 5.27 presents autocorrelation plots with $\alpha = 0$ and $\beta = \gamma$. Setting aside the case where $\alpha = \beta = \gamma = 0$, the remaining plots all appear to show practically perfect individual mixing, with all autocorrelations close to zero. This further confirms the hypothesis of Section 5.3.10, that provided that β and γ are not too small (relative to η), when $\alpha = 0$, β , γ and η -transitions interact to produce near perfect mixing of individuals, while positive values of α lead to imperfect mixing.

As noted in Section 5.3.7 in relation to Figure 5.22, the first plot of Figure 5.27, in which $\alpha = \beta = \gamma = 0$, is a special case, corresponding to the behaviour seen in Figure 5.9. For these parameter values, empty cells never change their state, acting as barriers through which information cannot pass, thus prohibiting correlations of any significant length. Furthermore, as seen in Figure 5.27, owing to η -transitions, a system with these parameter values converges to an equilibrium in which no two adjacent cells are both occupied, resulting in strong negative autocorrelations of lag ± 1 , which are clearly visible in the plot. Aside from further weak positive autocorrelations of lag ± 2 , there are no other visible correlations in this case.

Figures 5.25 and 5.26 also support the observation made in Section 5.3.10 that for parameter sets close to the boundary between the region of parameter space in which simulations converge to states with non-zero individual density and the region in which simulations converge to extinction, the corresponding model simulations exhibit high individual clumping. In both figures, the autocorrelation plot with the largest peak (greatest evidence of clumping) occurs at the transition point between parameter values for which all simulations resulted in extinction and those for which this was not the case.

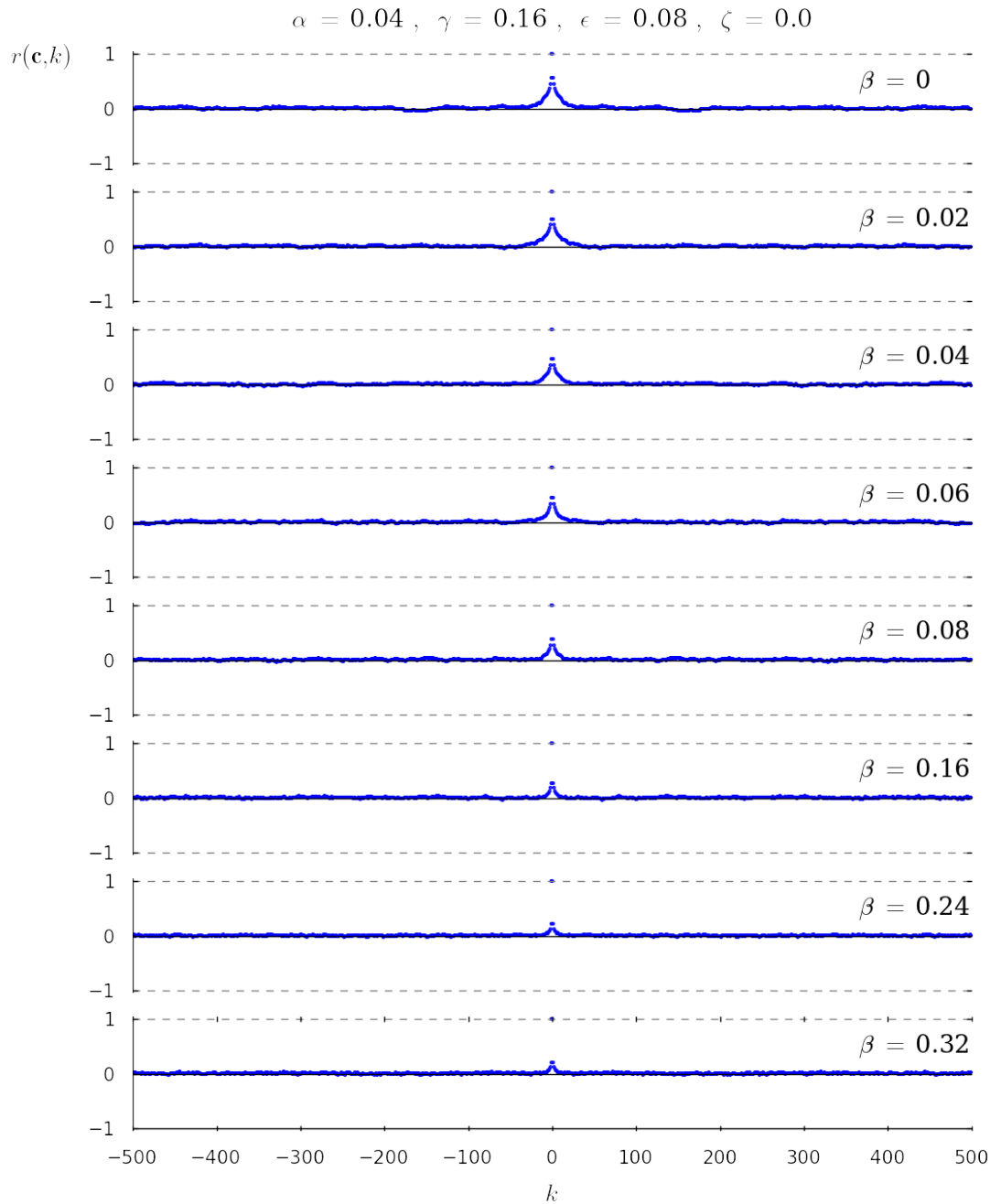


Figure 5.24: Plots of spatial autocorrelation estimates $r(\mathbf{c}, k)$ for the 1.6 millionth iteration of a one-dimensional single species \mathfrak{B} -model with 1000 cells, for various values of the parameter β , with $\alpha = 0.04, \gamma = 0.16, \epsilon = 0.08, \zeta = 0.0$. Autocorrelations were calculated from ten independent runs following the method of Section 5.4.1, using data from the simulation experiments described in Section 5.3.3.

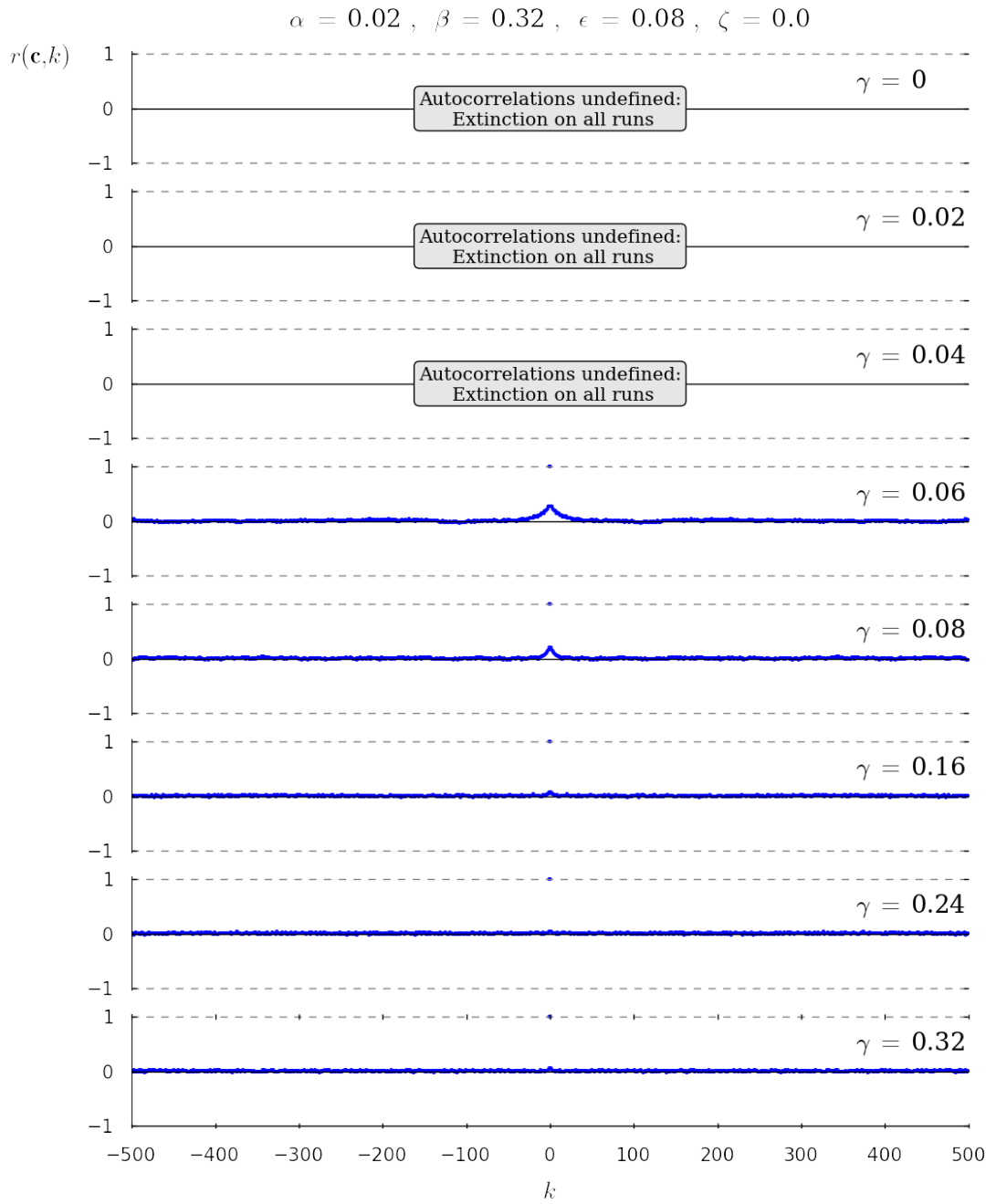


Figure 5.25: Plots of spatial autocorrelation estimates $r(\mathbf{c}, k)$ for the 1.6 millionth iteration of a one-dimensional single species \mathfrak{B} -model with 1000 cells, for various values of the parameter γ , with $\alpha = 0.02, \beta = 0.32, \epsilon = 0.08, \zeta = 0.0$. Autocorrelations were calculated from ten independent runs following the method of Section 5.4.1, using data from the simulation experiments described in Section 5.3.3.

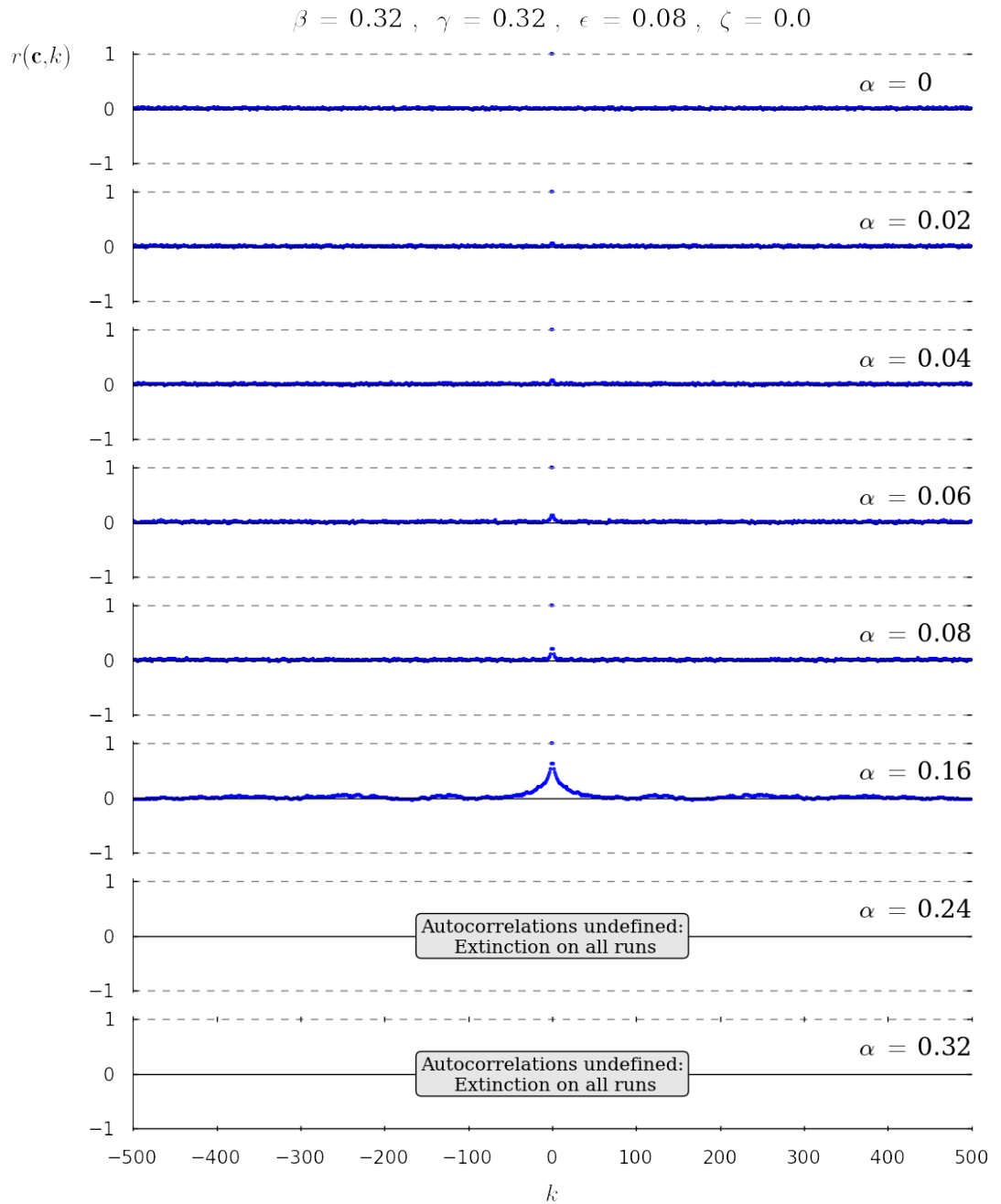


Figure 5.26: Plots of spatial autocorrelation estimates $r(\mathbf{c}, k)$ for the 1.6 millionth iteration of a one-dimensional single species \mathfrak{B} -model with 1000 cells, for various values of the parameter α , with $\beta = 0.32, \gamma = 0.32, \epsilon = 0.08, \zeta = 0.0$. Autocorrelations were calculated from ten independent runs following the method of Section 5.4.1, using data from the simulation experiments described in Section 5.3.3.

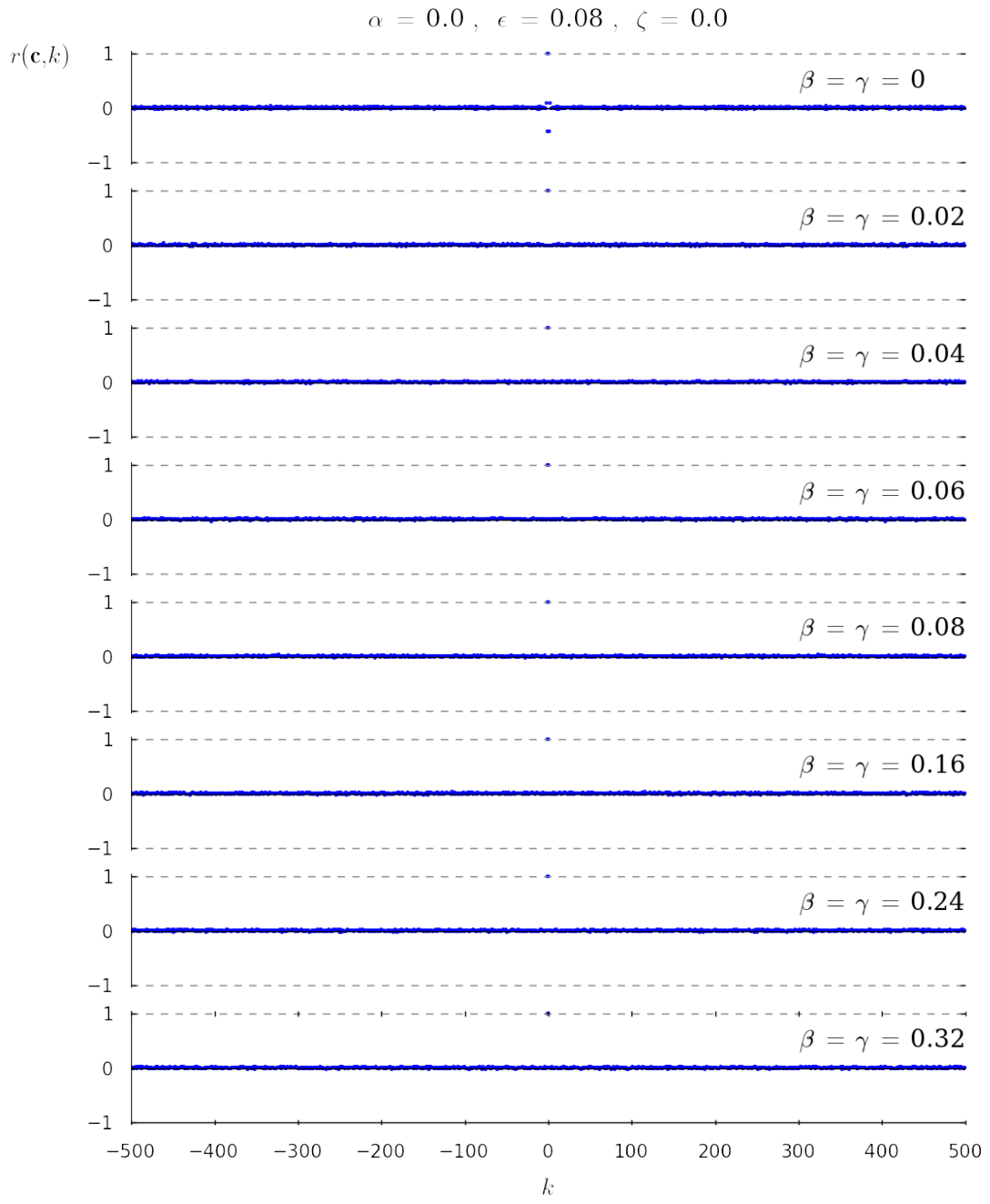


Figure 5.27: Plots of spatial autocorrelation estimates $r(\mathbf{c}, k)$ for the 1.6 millionth iteration of a one-dimensional single species \mathfrak{B} -model with 1000 cells, for various values of the parameters β and γ , with $\alpha = 0.00$, $\epsilon = 0.08$, $\zeta = 0.0$. Autocorrelations were calculated from ten independent runs following the method of Section 5.4.1, using data from the simulation experiments described in Section 5.3.3.

5.5 Summary and conclusions

In this chapter, we have undertaken an investigation into the possible behaviours of the one-dimensional single species \mathfrak{B} -model.

In Section 5.2, we identified all possible local transitions that can occur in a single species \mathfrak{B} -model, presented a mean field analysis of the model (valid over any regular graph), and analysed the resulting mean field equation.

In Section 5.3, we described a set of simulation experiments that were conducted to explore the behaviour of the single species \mathfrak{B} -model over a ring of cells. The results of these experiments were visualised as space-time diagrams, displaying the complete evolution of particular simulations, which allowed for a complete qualitative description of possible model behaviours.

In the case of simulations for which $\eta = 0$ (where η is the parameter governing the rate of individual mortality due to overcrowding), the link between model behaviour and the model parameters was found to be extremely clear, with the equilibrium behaviour being very well predicted by the mean field equation. However, for simulations with $\eta \neq 0$, the situation was less straightforward.

Using the space-time diagrams alongside density-time plots, an empirical map of the model parameter space and analyses of the autocorrelation structure of the final microstates of each simulation, treated as periodic binary sequences, we were able to deduce a link between the observed behaviours, the parameter values and corresponding transition-types, the level of correspondence with the predictions of mean field theory and the degree of mixing or clumping of individuals within the system. Specifically, β -transitions (movement), γ -transitions (reproduction) and η -transitions (death due to overcrowding) appear to be consistent with homogeneous individual mixing and with behaviour that is therefore well represented by the mean field equation. However, α -transitions (death of isolated individuals) appear to lead to spatially heterogeneous distributions of individuals, producing systems that exhibit visible clumping and whose behaviour is not well represented by the mean field equations.

In Chapter 6, we look more deeply at the nature of the simple transitions that occur in single species \mathfrak{B} -models, in an attempt to understand the fundamental differences between α -transitions on the one hand and β , γ and η -transitions on the other, which lead to such significant discrepancies in the character of a system's global behaviour.

Chapter 6

Understanding the relationship between local transitions and global dynamics in the one-dimensional, single species \mathfrak{B} -model

6.1 Introduction

In Chapter 5, it was observed that (excluding certain special cases) one-dimensional, single species \mathfrak{B} -models with $\alpha = 0$ tended to exhibit population dynamics in line with the predictions of mean field theory, while models with $\alpha > 0$ did not. In the latter case, mean populations at equilibrium were observed to be either lower than the mean field equilibrium or equal to zero, with the discrepancy between the observed and predicted equilibria increasing as α was increased relative to the other parameters.

It was hypothesised that this effect was somehow due to the fact that the combined effect of β , γ and η -transitions was consistent with good ‘mixing’ of individuals throughout the model, in the sense that the separate cell states at a given iteration could be considered as realisations of a set of independent Bernoulli random variables, while α -transitions instead had a negative effect on this mixing, producing robust local correlations between cell states, which rendered the independence assumption (vital for the validity of the mean field equations) invalid.

This hypothesis was supported by the calculation of autocorrelations between cell states in microstates drawn from experimental simulations (see Section 5.4), which did indeed show strong local correlations in microstates drawn from simulations with positive values of α and no such correlations in simulations with $\alpha = 0$ (once again, excluding certain special cases).

A version of this phenomenon, in which the precise nature of the local transitions that drive a discrete model may interfere with the progress of the model towards a state of equilibrium, is discussed in general terms by Wolfram (2002, pp. 342-351). Wolfram calls into question the value of attempting to explain the long term behaviour of complex systems in terms of progress towards particular invariant or equilibrium states, suggesting that in many cases it is in fact the “effects of explicit evolution rules” that are the most significant factor in determining long term patterns of model behaviour. Although Wolfram’s comments are concerned more with the attainment of static invariant states, rather than the quasi-stable dynamic equilibria that we are investigating, they nonetheless provide an interesting conceptual backdrop for our work.

Of more direct relevance, McKane and Newman (2004, Section IV) noted that certain types of local transition (specifically, those relating to competition between species) had an important effect on the extent to which the long term behaviour of certain ecological patch models – to which, as generalisations of the NANIA model, \mathfrak{B} -models are closely related (see Section 4.4.1) – matched the predictions of mean field theory. However, the authors did not explicitly investigate why these particular transitions had this effect, merely observing that their inclusion or otherwise affected the threshold patch size below which model behaviour diverted from the predictions of mean field theory.

In this chapter, the aim is to go beyond the simple observation of model behaviour, in an attempt to *understand* the causal mechanism behind the difference in the effect of α -transitions relative to β , γ and η -transitions in the one-dimensional, single species \mathfrak{B} -model. To achieve this, we will transform the dynamics of the system into another space and examine the effect of each transition in this new framework. In the new space, we define a measure of the degree of spatial clumping of individuals and then use this measure as the basis for an argument as to why the mean field equilibrium can be considered ‘stable’ when $\alpha = 0$ and ‘unstable’ when $\alpha > 0$.

However, before commencing this work, we examine a much simpler difference between the various transitions, that of whether or not their effects are immediately reversible, which serves to provide an intuitive starting point for the more involved mathematical analysis that follows.

6.2 Reversible and irreversible local transitions

Consider the relationship between the possible transitions of the single species \mathfrak{B} -model, as visualised in Figure 6.1. The figure shows that certain of the transitions may be matched up, such that the effect of the first transition on a pair of neighbouring cells may be precisely reversed by the other (provided that the states of the cells are not altered by other transitions in any intervening iterations), returning the cells to their previous states. Specifically, an η -transition reverses the effect of a γ -transition and vice versa, while the β -transition may be considered to be self-inverse.

However, as seen in the figure, α -transitions differ from the other three kinds in an important respect. Owing to the condition prohibiting the spontaneous generation of individuals, the α -transition has no inverse in the sense described above. An α -transition may therefore be seen as a sort of local catastrophe, since its effect cannot generally be reversed in a single step, but may require a sequence of other transitions to return the system to the microstate previously occupied. Such a sequence may necessitate changes to the states of a large number of other cells, some of which may be far from the original pair. Indeed, the α -transition is the only one whose effects may be absolutely irreversible (assuming that $\alpha, \beta, \gamma, \eta > 0$), since it is the only transition capable of transforming the system to the equilibrium extinction state in which all cells are empty.

Through this consideration of the reversibility of local transitions, we may begin to understand why positive values of the parameters β , γ and η are consistent with good individual mixing while positive values of α are not. Although both α and η -transitions result in the same reduction in population size, and therefore are considered to have an identical effect in simplified representations such as the basic mean field equations of Section 5.2.2, we see that their effects on the future evolution of the system may actually be quite different.

Intuitively, we might imagine that, since α -transitions are capable of *irreversibly* removing isolated individuals from the system, these transitions could create persistent ‘fractures’ in the distribution of individuals, separating them into separate clumps (such as those observed in Figure 5.14) and thus introducing a degree of spatial structure to the system that would invalidate the independence assumptions necessary for the mean field equations to hold.

In some sense, the remainder of this chapter could be considered to be an indirect formalisation of the argument given above, in which these mechanisms of fracturing and clump formation are identified and described in detail.

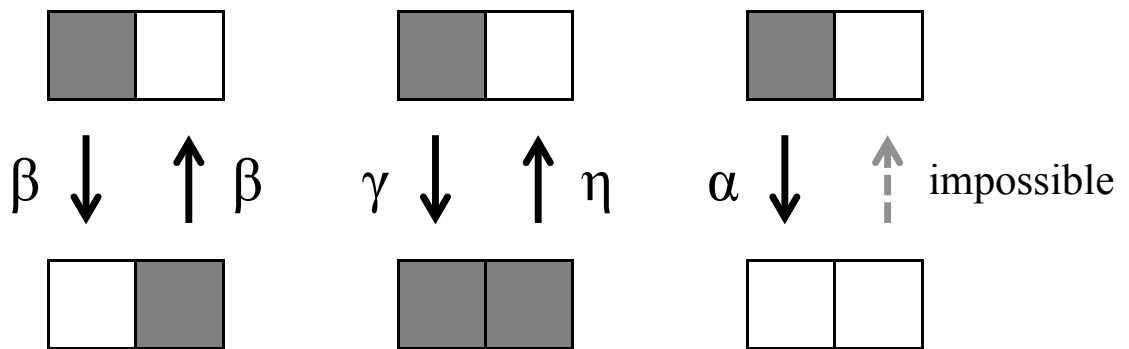


Figure 6.1: In a single species \mathfrak{B} -model, each pair of consecutive cells in the top row can be transformed into the pair immediately below in a single iteration by means of the transformation indicated. Transformations in the opposite sense are also shown. β , γ and η -transitions have an inverse transition which returns the pair to its original state. No such inverse exists for an α -transition.

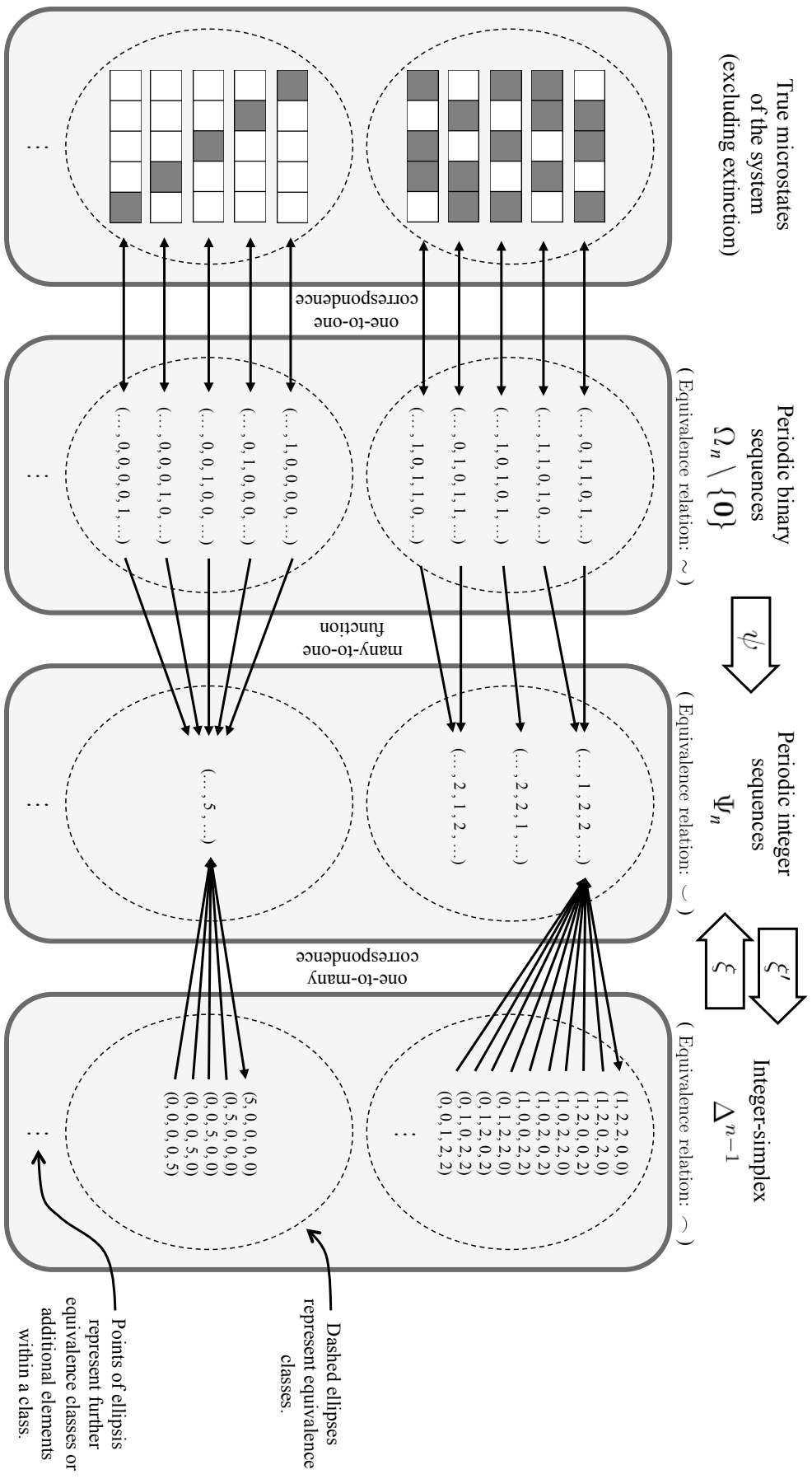


Figure 6.2: Diagrammatic representation of the relationship between the microstates of a single species \mathfrak{B} -model over a ring of n cells and the elements of Ω_n , Ψ_n and Δ^{n-1} and of the relationships between the equivalence classes of \sim , \sim and \sim over these sets. Although not directly visualised here, the bijection χ from the equivalence classes of $\Omega_n \setminus \{0\}$ to the equivalence classes of Δ^{n-1} is implicit from the layout of the equivalence classes (dashed ellipses).

6.3 Transforming the microstates of a \mathfrak{B} -model into a new space

6.3.1 Summary of approach

Up to this point, a particular microstate of the system has been represented by a periodic binary sequence $\mathbf{c} = (c_i)_{i \in \mathbb{Z}} \in \{0, 1\}^{\mathbb{Z}}$, from which any n consecutive terms represent the occupancies of every cell in the system. However, in Section 4.4.4, it was observed that for \mathfrak{A} -models (of which \mathfrak{B} -models form a subfamily), if adjacency-preserving symmetries of the underlying graph of the model are considered to be indistinguishable, then the dynamics of the system do not depend upon the precise microstate occupied at a given iteration but rather on the equivalence class of the microstate with respect to these symmetries.

In this section, we therefore apply a transformation from the state space Ω_n to a space in which the dynamics over the equivalence classes may be more naturally observed. For reasons of practicality, the sequence of zeros $\mathbf{0} \in \Omega_n$ is excluded from this transformation. Note that this exclusion does not present a significant issue, since $\mathbf{0}$ represents the state of extinction of all species and there are therefore no interesting dynamics after this state is reached.

Ultimately, we wish to define a transformation χ from $(\Omega_n \setminus \{\mathbf{0}\})/\sim$, the set of equivalence classes of the microstates (where \sim is the relevant equivalence relation, as defined in Section 4.4.4), to a corresponding set of equivalence classes in a new space. This will be accomplished by combining two separate mappings, the first from $\Omega_n \setminus \{\mathbf{0}\}$ to a new set called Ψ_n , the second from Ψ_n to a third set Δ^{n-1} . The transformation χ will then be derived from these mappings by demonstrating that each respects the equivalence classes of \sim in $\Omega_n \setminus \{\mathbf{0}\}$ and the corresponding equivalence classes in Ψ_n and Δ^{n-1} .

6.3.2 Step one: Ω_n to Ψ_n

We first define a function of the following form:

$$\psi : \Omega_n \setminus \{\mathbf{0}\} \rightarrow \Psi_n$$

$$\mathbf{c} = (c_i)_{i \in \mathbb{Z}} \mapsto \mathbf{d} = (d_i)_{i \in \mathbb{Z}}$$

Here, Ω_n is the set of periodic binary sequences whose period divides n (see Section 4.4.5), and $\Psi_n \subset \mathbb{N}^{\mathbb{Z}}$ is the set of periodic positive integer sequences for

which there exists a positive integer U' such that the sum of any U' consecutive terms is equal to n :

$$\Psi_n = \left\{ (d_i)_{i \in \mathbb{Z}} \in \mathbb{N}^{\mathbb{Z}} : \exists U' \in \mathbb{N} \text{ such that } \sum_{j=k}^{k+U'-1} d_j = n, \forall k \in \mathbb{Z} \right\} \quad (6.1)$$

Note that (6.1) does not explicitly state that the elements of Ψ_n are periodic, since periodicity is implied by the condition that specifies the sum of consecutive terms.

The transformation ψ is defined to operate according to the following rule: ψ transforms \mathbf{c} to \mathbf{d} such that any U' consecutive terms of \mathbf{d} correspond to the distances between the occupied cells of \mathbf{c} in the appropriate order, where distance is defined as the minimum path length in G (the ring of cells). The term d_0 corresponds to the distance between the two occupied cells of \mathbf{c} with the smallest non-negative indices.

A simple example of the application of ψ can be found in the first part of Example 6.3.3.

This rule may be formalised as follows:

Definition 6.3.1. Given $\mathbf{c} = (c_i)_{i \in \mathbb{Z}} \in \Omega_n \setminus \{\mathbf{0}\}$, let $I_{\mathbf{c}} = (I_j)_{j \in \mathbb{Z}}$ be the sequence formed from the elements of the set $\hat{I}_{\mathbf{c}} = \{i \in \mathbb{Z} : c_i = 1\}$, such that:

$$\dots < I_{-2} < I_{-1} < 0 \leq I_0 < I_1 < I_2 < \dots$$

The function $\psi : \Omega_n \setminus \{\mathbf{0}\} \rightarrow \Psi_n$ is defined such that $\psi(\mathbf{c}) = \mathbf{d} = (d_i)_{i \in \mathbb{Z}}$ with:

$$d_i = I_{i+1} - I_i, \quad \forall i \in \mathbb{Z}$$

To see that this definition is equivalent to the preceding informal description of ψ , observe simply that $I_{\mathbf{c}}$ is the sequence of the indices of the non-zero terms of \mathbf{c} , arranged in increasing order, with I_0 set equal to the smallest such non-negative index. As the differences between consecutive indices, the terms of \mathbf{d} then clearly represent the distances between consecutive occupied cells of \mathbf{c} , as required.

Note that ψ is not injective, since, for example, all microstates for which $U = 1$ are mapped to the same sequence $(\dots, n, \dots) \in \Psi_n$. Furthermore, we see that the

sum of any U consecutive terms of \mathbf{d} is equal to n , because:

$$\sum_{i=j}^{j+U-1} d_i = \sum_{i=j}^{j+U-1} (I_{i+1} - I_i) = I_{j+U} - I_j, \quad \forall j \in \mathbb{Z}$$

and $I_{j+U} - I_j = n$ since \mathbf{c} is periodic with period equal to a factor of n and contains precisely U occupied cells in any finite subsequence of length n . This means that, by definition, the value of U' for a particular $\mathbf{d} = \psi(\mathbf{c}) \in \Psi_n$ is equal to U , the total population of a system occupying the microstate \mathbf{c} . From this point forward, we therefore exclusively refer to this quantity as the population, denoted by U .

Now, we define an equivalence relation \smile on Ψ_n that will correspond to the equivalence relation \sim on Ω_n . Since two microstates $\mathbf{c}_1, \mathbf{c}_2$ are considered to be equivalent if the order of their terms is the same, allowing for translations and reflections, it is clear that the sequences of distances between consecutive occupied cells in such microstates, as recorded in $\psi(\mathbf{c}_1)$ and $\psi(\mathbf{c}_2)$, will also be the same. It therefore makes sense to also consider sequences $\mathbf{d}_1, \mathbf{d}_2 \in \Psi_n$ to be equivalent if their terms are the same up to translations and reflections. Specifically, we may adapt (4.7) from Section 4.4.5:

$$\mathbf{d}_1 \smile \mathbf{d}_2 \Leftrightarrow \exists a \in \{-1, 1\}, b \in \mathbb{Z}, \text{ such that } d_{2,i} = d_{1,ai+b}, \forall i \in \mathbb{Z} \quad (6.2)$$

The fact that \smile is an equivalence relation follows for the same reason that \sim is an equivalence relation: it is based on the automorphism group of a ring of n cells, as discussed in Sections 4.4.4 and 4.4.5. As with \sim , given $\mathbf{d} \in \Psi_n$, $[\mathbf{d}]$ denotes the equivalence class of \mathbf{d} with respect to \smile , while Ψ_n/\smile denotes the set of all equivalence classes of \smile .

Observe that ψ respects the equivalence classes of Ω_n and of Ψ_n , in the sense of the following proposition:

Proposition 6.3.2. *If $\mathbf{c}_1, \mathbf{c}_2 \in \Omega_n \setminus \{\mathbf{0}\}$, then:*

$$\mathbf{c}_1 \sim \mathbf{c}_2 \Leftrightarrow \psi(\mathbf{c}_1) \smile \psi(\mathbf{c}_2)$$

Proof. Let $\mathbf{d}_1 = \psi(\mathbf{c}_1)$ and $\mathbf{d}_2 = \psi(\mathbf{c}_2)$.

Proof of (\Rightarrow): By definition:

$$\mathbf{c}_1 \sim \mathbf{c}_2 \Leftrightarrow \exists a \in \{-1, 1\}, b' \in \mathbb{Z}, \text{ such that } c_{2,i} = c_{1,ai+b'}, \forall i \in \mathbb{Z}$$

Let $I_{\mathbf{c}_1} = (I_{1,j})_{j \in \mathbb{Z}}$ and $I_{\mathbf{c}_2} = (I_{2,j})_{j \in \mathbb{Z}}$ be defined as in 6.3.1. Therefore, $I_{\mathbf{c}_2}$ is an ordered sequence formed from the elements of the set:

$$\begin{aligned}\hat{I}_{\mathbf{c}_2} &= \{i \in \mathbb{Z} : c_{2,i} = 1\} \\ &= \{i \in \mathbb{Z} : c_{1,ai+b'} = 1\} \\ &= \{aj - ab' \in \mathbb{Z} : c_{1,j} = 1\} \\ &= \{aj - ab' : j \in \hat{I}_{\mathbf{c}_1}\} \\ &= \{aI_{1,j} - ab'\}_{j \in \mathbb{Z}}\end{aligned}$$

To put these terms in order to create $I_{\mathbf{c}_2}$, we observe that:

$$I_{2,i} = aI_{1,k+ai} - ab' , \quad \forall i \in \mathbb{Z}$$

where $k \in \mathbb{Z}$ is chosen such that:

$$aI_{1,k} - ab' = \min_{j \in \mathbb{Z}} \{aI_{1,j} - ab' : aI_{1,j} - ab' \geq 0\}$$

Now, observe that:

$$\begin{aligned}d_{2,i} &= I_{2,i+1} - I_{2,i} , \quad \forall i \in \mathbb{Z} \\ &= (aI_{1,k+a(i+1)} - ab') - (aI_{1,k+ai} - ab') , \quad \forall i \in \mathbb{Z} \\ &= |I_{1,k+a(i+1)} - I_{1,k+ai}| , \quad \forall i \in \mathbb{Z} \\ &= I_{1,ai+b+1} - I_{1,ai+b} , \quad \forall i \in \mathbb{Z} \\ &= d_{1,ai+b} , \quad \forall i \in \mathbb{Z}\end{aligned}$$

where $b = k + (a - 1)/2$.

Therefore, $\mathbf{d}_1 \smile \mathbf{d}_2$, as required.

Proof of (\Leftarrow): By definition:

$$\mathbf{d}_1 \smile \mathbf{d}_2 \Leftrightarrow \exists a \in \{-1, 1\}, b' \in \mathbb{Z}, \text{ such that } d_{2,i} = d_{1,ai+b'}, \forall i \in \mathbb{Z}$$

Observe that:

$$I_{\nu,j} = I_{\nu,k} + \sum_{i=k}^{j-1} d_{\nu,i} , \quad \forall \nu \in \{1, 2\} , \quad j, k \in \mathbb{Z} \text{ with } k < j$$

Therefore, more specifically, for all $j \in \{0, 1, 2, \dots\}$, we have:

$$\begin{aligned}
I_{2,j} &= I_{2,-1} + \sum_{i=-1}^{j-1} d_{2,i} \\
&= I_{2,-1} + \sum_{i=-1}^{j-1} d_{1,ai+b'} \\
&= I_{2,-1} + \sum_{l=m(j)}^{M(j)} d_{1,l} \\
&= I_{2,-1} + I_{1,M(j)+1} - I_{1,m(j)}
\end{aligned} \tag{6.3}$$

where:

$$\begin{aligned}
M(j) &= \max\{b' - a, b' + a(j - 1)\} = [(a + 1)/2] j + (b' - a) \\
m(j) &= \min\{b' - a, b' + a(j - 1)\} = [(a - 1)/2] j + (b' - a)
\end{aligned}$$

(6.3) can be rewritten such that only one term on the right hand side depends on j :

$$I_{2,j} = I_{2,-1} + aI_{1,[aj+b'+(1-a)/2]} - aI_{1,[b'+(1-3a)/2]}, \quad \forall j \in \{0, 1, 2, \dots\}$$

Now, consider $i \in \{0, \dots, n - 1\}$ and observe that:

$$\begin{aligned}
c_{2,i} &= 1 \\
\Leftrightarrow i &= I_{2,j'}, \quad \text{for some } j' \in \{0, \dots, U - 1\} \\
\Leftrightarrow i &= I_{2,-1} + aI_{1,[aj'+b'+(1-a)/2]} - aI_{1,[b'+(1-3a)/2]}, \quad \text{for some } j' \in \{0, \dots, U - 1\} \\
\Leftrightarrow I_{1,[aj'+b'+(1-a)/2]} &= ai - aI_{2,-1} + I_{1,[b'+(1-3a)/2]}, \quad \text{for some } j' \in \{0, \dots, U - 1\} \\
\Leftrightarrow I_{1,j} &= ai + b, \quad \text{for some } j \in \{h, \dots, h + U - 1\} \\
\Leftrightarrow c_{1,ai+b} &= 1
\end{aligned}$$

where $h = [(a - 1)/2](U - 1) + b' + (1 - a)/2$ and $b = I_{1,[b'+(1-3a)/2]} - aI_{2,-1}$.

It remains only to observe that showing that $c_{2,i} = c_{1,ai+b}$ for all $i \in \{0, \dots, n - 1\}$ is sufficient to demonstrate the equality for all $n \in \mathbb{Z}$, since \mathbf{c}_1 and \mathbf{c}_2 are periodic sequences whose periods do not exceed n . Therefore, $\mathbf{c}_1 \sim \mathbf{c}_2$, as required, which completes the proof. \square

The proposition demonstrates that, despite the fact that the function ψ is not a

bijective map from $\Omega_n \setminus \{\mathbf{0}\}$ to Ψ_n , there nonetheless exists a one-to-one correspondence between the equivalence classes of \sim in $\Omega_n \setminus \{\mathbf{0}\}$ and \smile in Ψ_n that is based on ψ .

The following example is an application of the proposition in a specific case.

Example 6.3.3. Consider a single species \mathfrak{B} -model over a ring of n cells, with state space Ω_n as usual. Let $n = 7$ and consider the following periodic binary sequences (recalling the notation introduced in Definition 4.4.5):

$$\begin{aligned}\mathbf{c}_1 &= (\dots, 0, 0, 1, 0, 1, 1, 0, \dots) \\ \mathbf{c}_2 &= (\dots, 1, 0, 1, 0, 0, 0, 1, \dots)\end{aligned}$$

Using the definition of ψ stated above, we have:

$$\begin{aligned}\mathbf{d}_1 &= \psi(\mathbf{c}_1) = (\dots, 2, 1, 4, \dots) \\ \mathbf{d}_2 &= \psi(\mathbf{c}_2) = (\dots, 2, 4, 1, \dots)\end{aligned}$$

Observe that $d_{1,i} = d_{2,-i}$, $\forall i \in \mathbb{Z}$ (note that the first integer shown in each of the above sequences is indexed by $i = 0$). Therefore, by (6.2), $\mathbf{d}_1 \smile \mathbf{d}_2$ and consequently, by Proposition 6.3.2, we conclude that $\mathbf{c}_1 \sim \mathbf{c}_2$; \mathbf{c}_1 and \mathbf{c}_2 lie in the same equivalence class.

Indeed, this conclusion may be verified directly by observing that $c_{2,i} = c_{1,-i+4}$, $\forall i \in \mathbb{Z}$, so $\mathbf{c}_1 \sim \mathbf{c}_2$ by definition.

6.3.3 Step two: Ψ_n to Δ^{n-1}

We now consider a new space Δ^{n-1} , the set of all points with integer coordinates lying on the regular $(n - 1)$ -simplex embedded in \mathbb{R}^n . In other words, Δ^{n-1} is the set of all length n vectors of non-negative integers $\boldsymbol{\delta}$ whose terms sum to n :

$$\Delta^{n-1} = \left\{ (\delta_0, \dots, \delta_{n-1}) \in \mathbb{Z}^n : \delta_i \geq 0, \forall i \in \{0, \dots, n-1\}, \sum_{i=0}^{n-1} \delta_i = n \right\}$$

For convenience, we describe this set as an “integer-simplex”.

There exists a natural correspondence between the elements of Δ^{n-1} and the elements of Ψ_n :

Definition 6.3.4. Given $\boldsymbol{\delta} = (\delta_0, \dots, \delta_{n-1}) \in \Delta^{n-1}$, let U'' equal the number of non-zero terms of $\boldsymbol{\delta}$ and $J = (J_0, \dots, J_{U''-1})$ be the vector formed from the elements of the set $\hat{J} = \{j \in \{0, \dots, n-1\} : \delta_j \neq 0\}$, such that:

$$J_0 < \dots < J_{U''-1}$$

The function ξ is defined as follows:

$$\begin{aligned}\xi &: \Delta^{n-1} \rightarrow \Psi_n \\ \boldsymbol{\delta} &\mapsto \mathbf{d} = (d_i)_{i \in \mathbb{Z}}\end{aligned}$$

where $d_i = \delta_{J_i}$, $\forall i \in \{0, \dots, U'' - 1\}$ and $d_j = d_{j+U''}$, $\forall j \in \mathbb{Z}$

Observe that, given $\boldsymbol{\delta} \in \Delta^{n-1}$, the sum of any U'' consecutive terms of $\xi(\boldsymbol{\delta})$ is necessarily equal to n , since the terms of $\boldsymbol{\delta}$ lie on the $n-1$ simplex. So U'' plays the same role as U' and therefore also corresponds to the population U of a microstate and will be referred to as such from this point onward.

The function ξ simply removes any zero terms from the vector $\boldsymbol{\delta} \in \Delta^{n-1}$ and produces a sequence $\mathbf{d} \in \Psi_n$ by infinitely repeating the remaining terms. Clearly, ξ is surjective, but not injective; indeed we observe that for each $\mathbf{d} \in \Psi_n$ of population U , there exist precisely $\binom{n}{U}$ distinct vectors $\boldsymbol{\delta} \in \Delta^{n-1}$ for which $\xi(\boldsymbol{\delta}) = \mathbf{d}$, since this is the number of ways in which the U non-zero terms may be placed in a vector of length n without changing their order. A one-to-many correspondence from Ψ_n to Δ^{n-1} is therefore induced by ξ .

Clearly therefore, there does not exist a true inverse of ξ . However, it will be useful to define an inverse-like function ξ' from Ψ_n to Δ^{n-1} with the property $\xi(\xi'(\mathbf{d})) = \mathbf{d}$, $\forall \mathbf{d} \in \Psi_n$, which maps sequences in Ψ_n to representative members of their corresponding equivalence class in Δ^{n-1} :

Definition 6.3.5. Define the function:

$$\begin{aligned}\xi' &: \Psi_n \rightarrow \Delta^{n-1} \\ \mathbf{d} &\mapsto \boldsymbol{\delta}\end{aligned}$$

with $\delta_i = d_i$, $\forall i \in \{0, \dots, U-1\}$ and $\delta_i = 0$, $\forall i \in \{U, \dots, n-1\}$ (unless $U = n$, in which case there are no zero terms), where U is the population of \mathbf{d} .

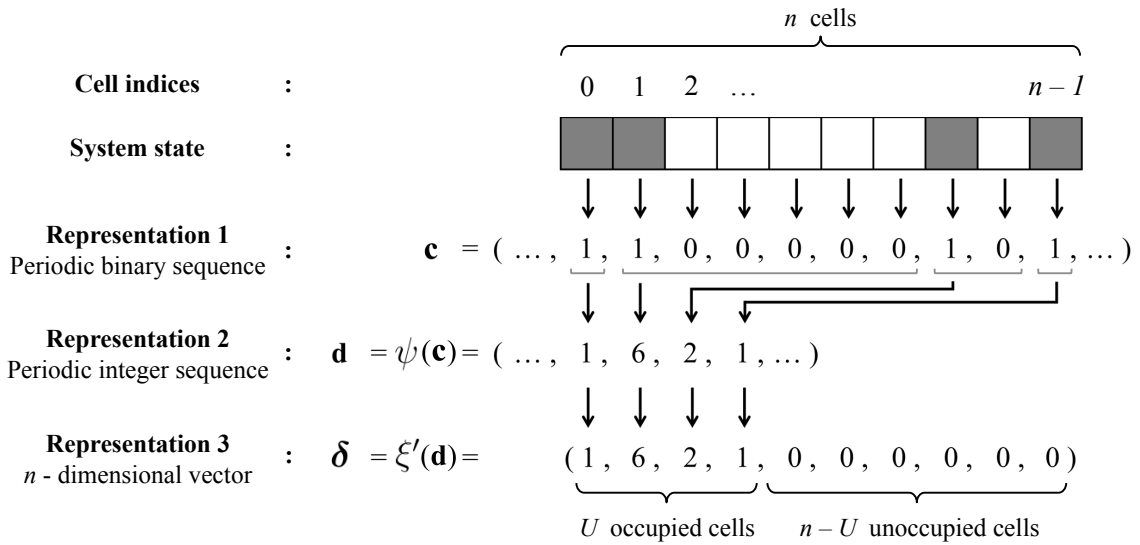


Figure 6.3: Example of a particular state of a one-dimensional, single species \mathfrak{B} -model on a ring of n cells, of which U are occupied, and of corresponding representations as a periodic binary sequence \mathbf{c} as a periodic integer sequence \mathbf{d} and as an n -dimensional vector $\boldsymbol{\delta}$. The non-zero terms of $\boldsymbol{\delta}$ represent the distances between occupied cells of the system, in order. In this example, $n = 10$ and $U = 4$.

Figure 6.3 demonstrates how a particular microstate of the system corresponds to a periodic sequence $\mathbf{c} \in \Omega_n$, to a periodic sequence $\mathbf{d} \in \Psi_n$ via the function ψ and to a vector $\boldsymbol{\delta} \in \Delta^{n-1}$ via the function ξ' .

The function ξ and the equivalence relation \sim may be combined to produce an equivalence relation \sim on Δ^{n-1} , in the following way:

Definition 6.3.6. Consider $\boldsymbol{\delta}_1, \boldsymbol{\delta}_2 \in \Delta^{n-1}$ and let $\mathbf{d}_1 = \xi(\boldsymbol{\delta}_1) \in \Psi_n$ and $\mathbf{d}_2 = \xi(\boldsymbol{\delta}_2) \in \Psi_n$. The binary relation \sim on Δ^{n-1} is defined such that $\boldsymbol{\delta}_1 \sim \boldsymbol{\delta}_2$ if and only if $\mathbf{d}_1 \sim \mathbf{d}_2$.

Definition 6.3.6 has an analogous role to Proposition 6.3.2, in that it guarantees that ξ respects the equivalence classes of \sim in Ψ_n and \sim in Δ^{n-1} in the same way that ψ respects the equivalence classes of \sim in $\Omega_n \setminus \{\mathbf{0}\}$ and \sim in Ψ_n . This means that there exists a one-to-one correspondence between the equivalence classes of Ψ_n and Δ^{n-1} based on ξ , which in turn implies that there is a one-to-one correspondence between the equivalence classes of $\Omega_n \setminus \{\mathbf{0}\}$ and Δ^{n-1} . This allows us to make the following definition.

Definition 6.3.7. *The bijection χ between the equivalence classes of \sim in $\Omega_n \setminus \{\mathbf{0}\}$ and the equivalence classes of \frown in Δ^{n-1} is defined as follows:*

$$\begin{aligned} \chi : (\Omega_n \setminus \{\mathbf{0}\}) / \sim &\rightarrow \Delta^{n-1} / \frown \\ [\mathbf{c}] &\mapsto [\xi'(\psi(\mathbf{c}))] \end{aligned}$$

At this point, we pause to present a summary of what has been achieved.

By Proposition 4.4.4, we know that in a \mathfrak{A} -model (and hence in a \mathfrak{B} -model), the dynamics essentially depend only on the equivalence class of a microstate relative to the automorphisms of the underlying graph and not on the precise microstate occupied by the system at any given time. In this section, we have shown that for a single species \mathfrak{B} -model over a ring of n cells, with state space Ω_n , each microstate of the system (excluding extinction), represented by the periodic sequence \mathbf{c} , corresponds to a particular collection of vectors on the integer simplex Δ^{n-1} (specifically, \mathbf{c} corresponds to the set of all vectors $\boldsymbol{\delta} \in \Delta^{n-1}$ for which $\xi(\boldsymbol{\delta}) = \psi(\mathbf{c})$).

We have further shown that there exists an equivalence relation over this integer simplex such that the equivalence classes in Ω_n defined by the automorphism group correspond exactly with the equivalence classes of this new relation on Δ^{n-1} . Therefore, the dynamics of the system may be seen as a movement between these equivalence classes on the integer simplex. In other words, we may represent the dynamics of the system as a point moving around the integer simplex, whose precise location may be considered to be whichever vector of the appropriate equivalence class that we find to be most convenient.

A diagrammatic representation of the relationship between a system and the sets Ω_n , Ψ_n and Δ^{n-1} is presented in Figure 6.2.

6.3.4 Cardinalities of equivalence classes

In Section 4.4.5, it was observed that the number of microstates in the equivalence class $[\mathbf{c}] \in (\Omega_n \setminus \{\mathbf{0}\}) / \sim$ is equal to $P(\mathbf{c})[1 + R(\mathbf{c})]$, where $P(\mathbf{c})$ is the period of \mathbf{c} and $R(\mathbf{c})$ is the chirality of \mathbf{c} . Observing that a single period of \mathbf{c} contains $UP(\mathbf{c})/n$ occupied cells and that each entry of $\mathbf{d} = \psi(\mathbf{c})$ corresponds to a particular occupied cell, we may conclude that the period of \mathbf{d} is given by:

$$P(\mathbf{d}) = UP(\mathbf{c})/n$$

We may also observe that the chirality of \mathbf{d} (see (4.8)) matches the chirality of \mathbf{c} :

$$R(\mathbf{d}) = R(\mathbf{c})$$

Therefore, following the same logic used to count the number of sequences in the equivalence class $[\mathbf{c}] \in (\Omega_n \setminus \{\mathbf{0}\})/\sim$, the number of sequences in the equivalence class $[\psi(\mathbf{c})] \in \Psi_n/\sim$ is equal to:

$$UP(\mathbf{c})[1 + R(\mathbf{c})]/n$$

As previously observed, each vector \mathbf{d} corresponds to precisely $\binom{n}{U}$ distinct vectors $\boldsymbol{\delta} \in \Delta^{n-1}$ through the function ξ , so the number of vectors in the equivalence class $[\xi'(\psi(\mathbf{c}))] = \chi([\mathbf{c}]) \in \Delta^{n-1}/\sim$ is equal to $\binom{n}{U} UP(\mathbf{c})[1 + R(\mathbf{c})]/n$ or:

$$\binom{n-1}{U-1} P(\mathbf{c})[1 + R(\mathbf{c})]$$

Table 6.1 provides a complete summary of these equivalence classes for the case $n = 6$, whose microstates are visualised in Figure 4.12.

One important consequence of these results, is that, given U and n , the ratio of the number of microstates in the equivalence class of \mathbf{c} to the number of vectors in the corresponding equivalence class of $\xi'(\psi(\mathbf{c}))$ is constant for all possible \mathbf{c} . This may be written as:

$$\frac{|[\xi'(\psi(\mathbf{c}))]|}{|[\mathbf{c}]|} = \binom{n-1}{U-1}, \quad \forall \mathbf{c} \in \left\{ \mathbf{c}' \in \Omega_n : \sum_{i=0}^{n-1} c'_i = U \right\} \quad (6.4)$$

where the notation $|\bullet|$ refers to the cardinality of a given set, as usual.

This result implies that, since all elements of an equivalence class (whether in Ω_n or Δ^{n-1}) are interchangeable, if the population U is fixed then each microstate in Ω_n may be considered to correspond to the ‘same number’ of vectors in Δ^{n-1} .

An important consequence of this fact is that a process that selects microstates \mathbf{c} of a particular population U by means of an appropriate random uniform distribution over Ω_n and a process that selects vectors $\boldsymbol{\delta}$ of population U by means of an appropriate random uniform distribution over Δ^{n-1} will sample their corresponding equivalence classes (of \sim and \sim respectively) with the same relative frequencies. This means that, for example, if the initial conditions for a simulation are selected by means of a uniform distribution over all microstates of a particular population U , an equivalent effect could be achieved by selecting an initial vector $\boldsymbol{\delta} \in \Delta^{n-1}$ by means of a uniform distribution over all such vectors of population U .

Class	U	P	R	Number of microstates \mathbf{c}	Number of sequences \mathbf{d}	Number of vectors $\boldsymbol{\delta}$	Representative microstate	Representative sequence	Representative vector
0	0	1	0	1	0	0	(..., 0, 0, 0, 0, 0, ...)	N/A	N/A
I	1	6	0	6	1	6	(..., 1, 0, 0, 0, 0, ...)	(..., 6, ...)	(6, 0, 0, 0, 0, 0)
II	2	6	0	6	2	30	(..., 1, 1, 0, 0, 0, ...)	(..., 1, 5, ...)	(1, 5, 0, 0, 0, 0)
III	2	6	0	6	2	30	(..., 1, 0, 1, 0, 0, 0, ...)	(..., 2, 4, ...)	(2, 4, 0, 0, 0, 0)
IV	2	3	0	3	1	15	(..., 1, 0, 0, 1, 0, 0, ...)	(..., 3, 3, ...)	(3, 3, 0, 0, 0, 0)
V	3	6	0	6	3	60	(..., 1, 1, 1, 0, 0, 0, ...)	(..., 1, 4, ...)	(1, 1, 4, 0, 0, 0)
VI	3	6	1	12	6	120	(..., 1, 1, 0, 1, 0, 0, ...)	(..., 1, 2, 3, ...)	(1, 2, 3, 0, 0, 0)
VII	3	2	0	2	1	20	(..., 1, 0, 1, 0, 1, 0, ...)	(..., 2, 2, 2, ...)	(2, 2, 2, 0, 0, 0)
VIII	4	6	0	6	4	60	(..., 1, 1, 1, 1, 0, 0, ...)	(..., 1, 1, 1, 3, ...)	(1, 1, 1, 3, 0, 0)
IX	4	6	0	6	4	60	(..., 1, 1, 1, 0, 1, 0, ...)	(..., 1, 1, 2, 2, ...)	(1, 1, 2, 2, 0, 0)
X	4	3	0	3	2	30	(..., 1, 1, 0, 1, 1, 0, ...)	(..., 1, 2, 1, 2, ...)	(1, 2, 1, 2, 0, 0)
XI	5	6	0	6	5	30	(..., 1, 1, 1, 1, 1, 0, ...)	(..., 1, 1, 1, 2, ...)	(1, 1, 1, 1, 2, 0)
XII	6	1	0	1	1	1	(..., 1, 1, 1, 1, 1, 1, ...)	(..., 1, 1, 1, 1, 1, ...)	(1, 1, 1, 1, 1, 1)

Table 6.1: Summary of the correspondences between equivalence classes of \sim , \frown and \frown in Ω_n , Ψ_n and Δ^{n-1} respectively, for the case $n = 6$. The complete set of microstates in Ω_6 is visualised in Figure 4.12.

6.4 The dynamics of the transformed model

6.4.1 Introduction

As we have shown, the microstate occupied by the system at any given time may be represented as an imaginary particle positioned at a point $\boldsymbol{\delta}$ of the integer simplex Δ^{n-1} , although the location of this particle need only be defined up to its particular equivalence class with respect to \sim . The dynamics of the system are represented by the movement of this particle around Δ^{n-1} .

In this section, we focus on understanding the characteristics of the model dynamics in this new space. To do this, we first examine the effect of each of the four transitions α , β , γ and η on a fixed vector $\boldsymbol{\delta} \in \Delta^{n-1}$. We then change our perspective, considering $\boldsymbol{\delta}$ to be a vector random variable, and re-examine the effects of the four transitions, both with and without the mean field assumptions (see Section 3.2). Finally, we present partial visualisations of the model dynamics over Δ^{n-1} and use these to make some geometric observations on the effects of different transitions.

6.4.2 The effect of particular transitions in Δ^{n-1}

Consider a vector $\boldsymbol{\delta} = (\delta_0, \dots, \delta_{n-1}) \in \Delta^{n-1}$, and recall that the number of non-zero terms of $\boldsymbol{\delta}$ is equal to U , the population of any corresponding microstate in Ω_n . The non-zero terms of $\boldsymbol{\delta}$ themselves represent the distances between consecutive occupied cells of such a corresponding microstate, and the order of these distances is invariant (up to translation and reflection) between the two representations. Furthermore, the number of zero terms of $\boldsymbol{\delta}$ is equal to the number of unoccupied cells $n - U$ in such a microstate.

Recall that in a \mathfrak{B} -model, a transition begins with the selection of a cell by means of a discrete uniform distribution across all cells, followed by the selection of a neighbour of this cell by means of a discrete uniform distribution across all such neighbours. However, for the purposes of the forthcoming analysis, it will be useful to limit ourselves exclusively to the case in which the right hand neighbour is chosen. Fortunately, since any microstate $\mathbf{c}_+ \in \Omega_n$ lies in the same equivalence class as its own reflection \mathbf{c}_- and these microstates are therefore interchangeable from the point of view of the dynamics (they may indeed be identical), this limitation may be made without loss of generality by first deciding, with equal probability, whether to consider \mathbf{c}_+ or \mathbf{c}_- , and then selecting a cell at random from the chosen microstate, along with its right hand neighbour.

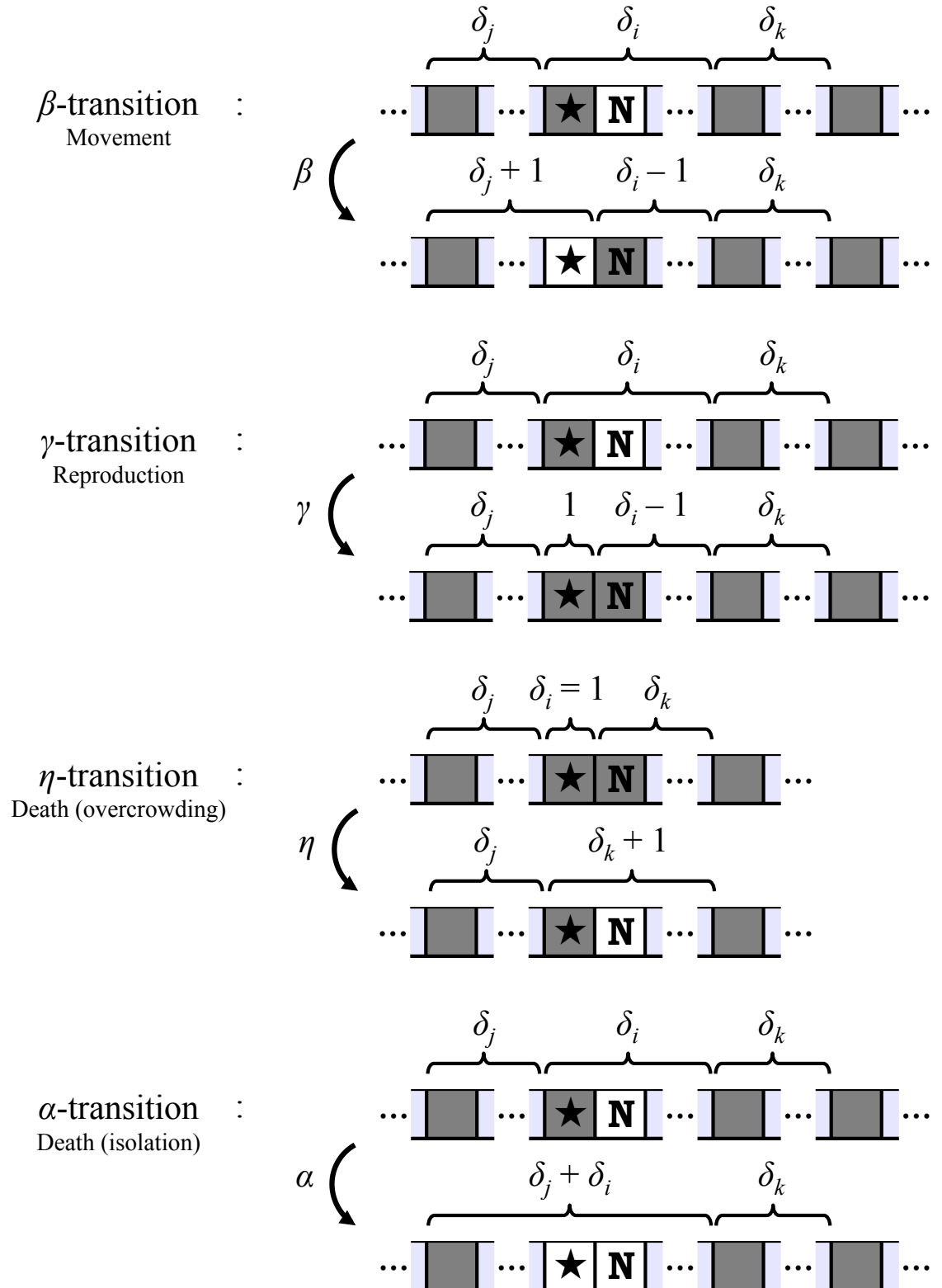


Figure 6.4: The effect of each of the possible transitions in a single species \mathfrak{B} -model over a ring of n cells in terms of the entries of a corresponding vector $\delta \in \Delta^{n-1}$. The initial cell selected by the transition rule is marked with a star; the selected neighbour is marked with the letter “N”. Points of ellipsis represent unknown numbers of empty cells (possibly zero) or the continuation of the microstate beyond the bounds of the diagram.

The same transition represented in Δ^{n-1} may therefore be initiated by choosing between a vector $\boldsymbol{\delta}_+$ representing the current state of the system and its reflection $\boldsymbol{\delta}_-$, with equal probability, and denoting the chosen vector by $\boldsymbol{\delta}$. A term δ_i is then selected by means of a discrete uniform distribution over all terms of $\boldsymbol{\delta}$. If $\delta_i = 0$, this corresponds to the selection of an unoccupied cell, and the rules of a \mathfrak{B} -model dictate that the system remains unchanged. If, however, $\delta_i > 0$, this corresponds to the selection of an occupied cell, along with its right hand neighbour.

To go further, if $\delta_i = 1$, this corresponds to a situation in which the initial chosen cell is both occupied and immediately adjacent to the next occupied cell to its right. Using the notation of Section 5.2, the chosen pair of cells therefore have states ('S', 'S'). If, on the other hand, $\delta_i > 1$, then this corresponds to a situation in which the initial chosen cell is occupied, but is separated from the next occupied cell to its right by at least one unoccupied cell. The chosen pair of cells therefore have states ('S', 'E').

Supposing that $\delta_i > 0$, letting δ_j and δ_k be the previous and the next non-zero terms of δ_i in $\boldsymbol{\delta}$ respectively (with the final non-zero term considered to be “previous” to the first and the first considered to be “next” after the final)¹, we are now in a position to determine the precise effect of each of the transitions α , β , γ and η in this context. Let $\boldsymbol{\delta}'_\alpha$, $\boldsymbol{\delta}'_\beta$, $\boldsymbol{\delta}'_\gamma$ and $\boldsymbol{\delta}'_\eta$ be vectors that represent the state of the system following any particular transition of the corresponding type (assuming, in each case separately, that the configuration of $\boldsymbol{\delta}$ is such that a transition of this type is possible).

First suppose that $\delta_i = 1$ and therefore that the chosen pair of cells have states ('S', 'S'). This implies that only an η -transition is possible. Since, in reality, an η -transition may represent either an ϵ or a ζ -transition (see Section 5.2.1), the final states of the chosen cells may be either ('S', 'E') or ('E', 'S'). However, without loss of generality, we may suppose that an η -transition always has the former effect (the other possibility would effectively occur if the opposite decision had been made when choosing between $\boldsymbol{\delta}_+$ and $\boldsymbol{\delta}_-$).

η -transition : The effect of an η -transition is to change the state of the neighbouring cell from 'S' to 'E', reducing the population U by 1. In terms of a representation of the transition in Δ^{n-1} , this means that the two separate entries δ_i and δ_k in $\boldsymbol{\delta}$ are replaced in a new vector $\boldsymbol{\delta}'_\eta$ by the entries $\delta_k + 1$ (since the distance from the

¹ Note that the special cases in which these three terms are not all distinct are discussed at the end of this section.

selected initial cell to its next occupied neighbour has increased by δ_k) and a zero entry (since the population of the system has decreased by 1). All other entries of $\boldsymbol{\delta}$ are unchanged in $\boldsymbol{\delta}'_\eta$.

This effect, and those of the other transitions discussed below, is visualised in Figure 6.4.

Now suppose that $\delta_i > 1$ and therefore that the chosen pair of cells have states ('S', 'E'). Consider the following possibilities:

β -transition : The effect of a β -transition is to switch the states of these two cells, leaving the population U unchanged. In terms of a representation of the transition in Δ^{n-1} , this means that the two separate entries δ_j and δ_i in $\boldsymbol{\delta}$ are replaced in $\boldsymbol{\delta}'_\beta$ by the entries $\delta_j + 1$ and $\delta_i - 1$, since the selected occupied cell has 'moved to the right', thus increasing its distance to the previous occupied cell and decreasing its distance to the next occupied cell. All other entries of $\boldsymbol{\delta}$ are unchanged in $\boldsymbol{\delta}'_\beta$.

γ -transition : The effect of a γ -transition is to change the state of the neighbouring cell from 'E' to 'S', increasing the population U by 1. In terms of a representation of the transition in Δ^{n-1} , this means that the entry δ_j in $\boldsymbol{\delta}$ along with a zero entry (without loss of generality, we may suppose that these terms are consecutive, since the placement of zero terms does not affect the equivalence class of $\boldsymbol{\delta}$ under \sim) are replaced in $\boldsymbol{\delta}'_\gamma$ by the entries 1 (since the distance from the selected occupied cell to the next occupied cell is now 1) and $\delta_i - 1$ (since the distance from the newly created occupied cell to the next occupied cell is equal to $\delta_i - 1$). All other entries of $\boldsymbol{\delta}$ are unchanged in $\boldsymbol{\delta}'_\gamma$.

α -transition : The effect of an α -transition is to change the state of the initially selected cell from 'S' to 'E', decreasing the population U by 1. In terms of a representation of the transition in Δ^{n-1} , this means that the entries δ_j and δ_i in $\boldsymbol{\delta}$ are replaced in $\boldsymbol{\delta}'_\alpha$ by the entries $\delta_j + \delta_i$ (the distance from the previous to the next occupied cells, the selected occupied cell having been removed) and a zero entry (since the population of the system has decreased by 1). All other entries of $\boldsymbol{\delta}$ are unchanged in $\boldsymbol{\delta}'_\alpha$.

A summary of these results in terms of complete vectors in Δ^{n-1} is presented below. In these expressions, standard points of ellipsis represent (possibly empty) sequences of arbitrary terms, while raised points of ellipsis represent (possibly empty) sequences of zero terms only. As in the discussion above, in each case, we start from the assumption that the i th term has been selected and found to be non-zero. The previous

and next non-zero terms are assumed to occupy positions j and k respectively.

$$\begin{aligned} \beta : \quad \boldsymbol{\delta} &= (\delta_0, \dots, \delta_{j-1}, \delta_j, \dots, \delta_i, \dots, \delta_{i+1}, \dots, \delta_{n-1}) \\ \boldsymbol{\delta}'_\beta &= (\delta_0, \dots, \delta_{j-1}, \delta_j + 1, \dots, \delta_i - 1, \delta_{i+1}, \dots, \delta_{n-1}) \end{aligned} \quad (6.5)$$

$$\begin{aligned} \gamma : \quad \boldsymbol{\delta} &= (\delta_0, \dots, \delta_{i-2}, 0, \dots, \delta_i, \dots, \delta_{i+1}, \dots, \delta_{n-1}) \\ \boldsymbol{\delta}'_\gamma &= (\delta_0, \dots, \delta_{i-2}, 1, \dots, \delta_i - 1, \delta_{i+1}, \dots, \delta_{n-1}) \end{aligned} \quad (6.6)$$

$$\begin{aligned} \eta : \quad \boldsymbol{\delta} &= (\delta_0, \dots, \delta_{i-1}, 1, \dots, \delta_k, \dots, \delta_{k+1}, \dots, \delta_{n-1}) \\ \boldsymbol{\delta}'_\eta &= (\delta_0, \dots, \delta_{i-1}, 0, \dots, \delta_k + 1, \delta_{k+1}, \dots, \delta_{n-1}) \end{aligned} \quad (6.7)$$

$$\begin{aligned} \alpha : \quad \boldsymbol{\delta} &= (\delta_0, \dots, \delta_{j-1}, \delta_j, \dots, \delta_i, \dots, \delta_{i+1}, \dots, \delta_{n-1}) \\ \boldsymbol{\delta}'_\alpha &= (\delta_0, \dots, \delta_{j-1}, \delta_j + \delta_i, \dots, 0, \dots, \delta_{i+1}, \dots, \delta_{n-1}) \end{aligned} \quad (6.8)$$

Each of the above vector descriptions excludes those variables that are not relevant to the corresponding transition. Specifically, δ_k is not relevant in α , β or γ -transitions and δ_j is not relevant in γ or η -transitions. Observe also that the term δ_i does not appear explicitly in the vector description of an η -transition, since this variable is necessarily equal to 1 in this case (otherwise an η -transition cannot occur). Hence, δ_i is represented by the 1 in the first vector of (6.7).

Note that there are certain restrictions on the validity of (6.5)-(6.8), since there exist vectors $\boldsymbol{\delta} \in \Delta^{n-1}$ of population U for which not all transitions are possible or for which the analysis fails for other reasons. Naturally, for the model to function, we require $n > 1$. We also require that $U > 0$, since $\boldsymbol{\delta}$ is otherwise undefined. Furthermore, for the β and α analysis to hold, we must have $U > 1$ (otherwise there is only one non-zero term and $i = j$); for the β , γ and α analysis to hold, we must have $U < n$ (otherwise these transitions are impossible), while for the η analysis to hold, we must have $U > 1$ (otherwise η -transitions are impossible).

However, these conditions clearly represent special cases, in which the number of individuals attains its maximum value or is close to its minimum value. (6.5)-(6.8) are therefore accurate descriptions of the effects of each of the four possible transitions in all cases of practical interest.

6.4.3 Describing transitions in terms of vector random variables

For the purposes of later work, in which we will consider expectations related to model transitions, it will be necessary to understand the status of δ_i , δ_j and δ_k in (6.5), (6.6), (6.7) and (6.8) as random variables.

We note that, given a particular initial vector $\boldsymbol{\delta} \in \Delta^{n-1}$, if $\boldsymbol{\delta}'$ represents the vector that results from a single (non-specific, possibly null) \mathfrak{B} -model transition applied to $\boldsymbol{\delta}$, then $\boldsymbol{\delta}'$ is a vector random variable whose distribution over Δ^{n-1} depends on $\boldsymbol{\delta}$. $\boldsymbol{\delta}'_\alpha$, $\boldsymbol{\delta}'_\beta$, $\boldsymbol{\delta}'_\gamma$ and $\boldsymbol{\delta}'_\eta$ are also vector random variables dependent on $\boldsymbol{\delta}$, each derived from the distribution of $\boldsymbol{\delta}'$ by conditioning on different assumptions (specifically, that an appropriate term and neighbour had been chosen for the corresponding transition to occur and that this transition did indeed occur).

In this context, given a particular $\boldsymbol{\delta} \in \Delta^{n-1}$, we note that the terms labelled δ_i that appear in (6.5), (6.6) and (6.8) are identically distributed random variables. This is because they are all selected from $\boldsymbol{\delta}$ by means of an identical procedure (a discrete uniform random selection across all terms of $\boldsymbol{\delta}$) and are all subject only to the condition that $\delta_i > 1$. The δ_i in these expressions may therefore be considered to be distributed according to a discrete uniform random selection across all terms of $\boldsymbol{\delta}$ of value greater than 1.

Note that, in (6.7), δ_i is instead subject to the condition $\delta_i = 1$, so its value is known, and it therefore need not be treated as a random variable.

We may go further, and observe that, given a particular $\boldsymbol{\delta} \in \Delta^{n-1}$, the joint distribution of the random variables δ_i and δ_j (and hence, given that the δ_i variables are identically distributed, also the distribution of δ_j considered singly) is identical in the two cases in which they both appear explicitly, (6.5) and (6.8). Again, this holds because the variables are selected by means of an identical procedure, with δ_j being equal to the previous non-zero term to δ_i in both cases (recalling that $\boldsymbol{\delta}$ must first be selected from between the two vectors $\boldsymbol{\delta}_+$ and $\boldsymbol{\delta}_-$), subject once again to the condition that $\delta_i > 1$. It is clear, however, that δ_i and δ_j cannot be considered to be independent.

Finally, we may observe that, given a particular $\boldsymbol{\delta} \in \Delta^{n-1}$ as usual, the distribution of the random variable defined by δ_k may also be unambiguously described, since it is always equal to the first non-zero term after the initially selected term, conditional

on the fact that the initial cell is equal to one (again recalling that $\boldsymbol{\delta}$ must first be selected from between the two vectors $\boldsymbol{\delta}_+$ and $\boldsymbol{\delta}_-$).

Given n and U , the maxima and minima of each of these random variables may also be derived from a consideration of the procedures by which they are generated. For example, since (for those cases in which it appears explicitly) δ_i is generated by means of a random uniform selection over all terms of $\boldsymbol{\delta}$ greater than or equal to 2, its minimum possible value is 2 (considered over all possible $\boldsymbol{\delta} \in \Delta^{n-1}$), while its maximum possible value is $n - U + 1$, since the sum of the terms must equal n and there are $U - 1$ other non-zero terms.

The maxima and minima of each of the variables and of two important combinations of variables are given in Table 6.2.

Random variable	Minimum	Maximum
δ_i	2	$n - U + 1$
δ_j	1	$n - U$
δ_k	1	$n - U + 1$
$\delta_j - \delta_i$	$-(n - U)$	$n - U - 2$
$\delta_i \delta_j$	2	$\left\lfloor \frac{n - U + 2}{2} \right\rfloor \left\lceil \frac{n - U + 2}{2} \right\rceil$

Table 6.2: The maximum and minimum values of particular terms of $\boldsymbol{\delta}$ and of certain combinations of these terms, considered as random variables. Note that the variables used here refer specifically to those mentioned explicitly in the vector descriptions (6.5)-(6.8). Hence, the row for δ_k is conditional on the fact that $\delta_i = 1$ (as in (6.7)) while all other rows are conditional on the fact that $\delta_i > 1$ (as in (6.5), (6.6) and (6.8)).

The notation $\lfloor \cdot \rfloor$ and $\lceil \cdot \rceil$, used in Table 6.2, represents the floor function (which returns the greatest integer less than or equal to the argument) and the ceiling function (which returns the smallest integer greater than or equal to the argument) respectively.

Most of these results have a very simple derivation. The exception is the maximum value that may be attained by the product of the random variables δ_i and δ_j . To derive this result, note that $\delta_i + \delta_j \leq n - U + 2$ (since there are $U - 2$ other non-zero terms, and all such terms must sum to n). Clearly, the maximum value of the product is attained when this inequality is, in fact an equality. We then have:

$$\delta_i \delta_j = \delta_i(n - U + 2 - \delta_i)$$

The maximum of this expression is attained when δ_i (which must be an integer) is as close as possible to $(n - U + 2)/2$. This explains the expression given in Table 6.2.

The results of Table 6.2 provide a useful indication of the possible range of certain key quantities and will be used extensively in Section 6.6.3 when investigating the effect of different transitions on the clumping of individuals.

6.4.4 Expectations of the terms of $\boldsymbol{\delta}$ under the mean field assumptions

Although a full description of the distributions of δ_i , δ_j and δ_k is not possible without complete knowledge of the current microstate of the system (up to its equivalence class, as usual) as represented by $\boldsymbol{\delta}$, under the mean field assumptions it is possible to write expressions for their expectations in terms of the density of the system $u = U/n$. These calculations will later prove useful in analysing the ‘stability’ of mean field type behaviour in a one-dimensional single species \mathfrak{B} -model under different transitions, discussed in Section 6.6.4.

The mean field approach employed in this section uses the first of the assumptions presented in our analysis of the NANIA model, in Section 4.3.4. This assumption is reproduced here, in the context of the single species \mathfrak{B} -model:

- For a particular time t , the states of all cells may be treated as realisations of independent identically distributed Bernoulli variables, each with parameter equal to the current overall density of the system u .

Loosely speaking then, the mean field assumption says that the current microstate of the system $\mathbf{c} \in \Omega_n$ (and thus, by the results of Section 6.3.4, also its representation $\boldsymbol{\delta} \in \Delta^{n-1}$) ‘looks like’ it has simply been chosen randomly uniformly across all possible microstates of density u . However, as stated in Section 4.3.4, for the assumption to be at all reasonable, we require that n , U and $n - U$ are all sufficiently large to prevent significant, unavoidable dependencies between cell states over small neighbourhoods.

Note that the second of the mean field assumptions given in Section 4.3.4 is not relevant here, since it relates to the continuing evolution of the system, while we are currently concerned only with the instantaneous expected values of the terms of $\boldsymbol{\delta}$.

As observed in Section 6.4.3, given $\boldsymbol{\delta} \in \Delta^{n-1}$ representing the current microstate of the system $\mathbf{c} \in \Omega_n$, δ_i is a random variable representing a term of $\boldsymbol{\delta}$, randomly

uniformly selected among all those terms of value greater than 1. We can therefore write:

$$E[\delta_i] = E[\delta \mid \delta > 1]$$

where δ represents a random variable corresponding to an unconditional random uniform selection over all terms of $\boldsymbol{\delta}$. Note that these expectations are only defined for $0 < u < 1$, since $u = 1 \Rightarrow \delta = 1$, so the condition $\delta > 1$ cannot be fulfilled, while $\boldsymbol{\delta}$ is not defined when $u = 0$.

Now:

$$\begin{aligned} E[\delta] &= E[\delta \mid \delta > 1] P[\delta > 1] + E[\delta \mid \delta = 1] P[\delta = 1] + E[\delta \mid \delta = 0] P[\delta = 0] \\ \Rightarrow 1 &= E[\delta_i] (1 - P[\delta = 1] - P[\delta = 0]) + P[\delta = 1] \\ \Rightarrow E[\delta_i] &= \frac{1 - P[\delta = 1]}{1 - P[\delta = 1] - P[\delta = 0]} \\ \Rightarrow E[\delta_i] &= \frac{1 - P[\delta = 1]}{u - P[\delta = 1]} \end{aligned} \tag{6.9}$$

Observe that the fact $E[\delta] = 1$, used in the first implication, follows from the fact that $\boldsymbol{\delta}$ has n terms, and that these terms must sum to n .

Up to this point, the mean field assumption has not been used, and equation (6.9) is valid in all circumstances, no matter what process is used to generate $\boldsymbol{\delta}$. However, in order to calculate $P[\delta = 1]$, a particular distribution for $\boldsymbol{\delta}$ must be assumed.

The probability that $\delta = 1$ is the probability that a randomly chosen cell will be both occupied and immediately adjacent to its next occupied neighbour (looking to the right, though the direction is arbitrary). The mean field assumption suggests that the states of the two cells should be considered to be independent, and that $P[\delta = 1]$ should therefore be assumed to be equal to u^2 , the probability u that the first chosen cell is occupied multiplied by the probability u that its chosen neighbour is occupied.

Substituting into (6.9) then gives:

$$\begin{aligned} E[\delta_i] &= \frac{1 - u^2}{u - u^2} \\ &= \frac{1 + u}{u} \end{aligned}$$

So if $\boldsymbol{\delta}$ represents a particular instantaneous state of a model whose behaviour is observed to be consistent with that predicted by the mean field equations, we would expect that the expectation of δ_i (the mean size of an entry of $\boldsymbol{\delta}$ with value greater

than 1) should be approximately equal to $(1 + u)/u$. Conversely, given a model whose instantaneous state, as represented by $\boldsymbol{\delta}$, produces an expectation of δ_i that is significantly different from $(1 + u)/u$, the only possible explanation would be that the proportion of occupied cells in the corresponding microstate \mathbf{c} for which the right hand neighbour is also occupied is not well approximated by u , since this was the only assumption made in the derivation of $E[\delta_i]$. This, in turn would imply that the mean field assumption was invalid and we would not expect the system to behave as predicted by the mean field equations.

The derivation of expectations for δ_j and δ_k is more simple. δ_j is a random variable representing the previous non-zero term to δ_i in $\boldsymbol{\delta}$ while δ_k is a random variable representing the next non-zero term following a randomly uniformly selected unit term of $\boldsymbol{\delta}$. The mean field assumption makes no distinction between these two situations, since the states of cells are locally modelled as independent variables. In each case, δ_j and δ_k represent the expected number of sequential cells that must be checked until an occupied cell is found. Such variables clearly follow a geometric distribution with parameter u . Therefore, the mean field assumptions suggest that:

$$E[\delta_j] = E[\delta_k] = \frac{1}{u}$$

and, moreover, that the variables δ_i , δ_j and δ_k may be considered to be independent.

Clearly, in order for these results to be reasonable, we require that the expected value $1/u$ is significantly smaller than the total number of unoccupied cells $n - U$ and certainly much smaller than the total number of cells n , otherwise the dependencies inherent in considering large numbers of cells simultaneously and the periodicity of the system would render the analysis invalid in terms of the true model. However, the earlier requirement that n , U and $n - U$ are large ensures that these conditions are met.

Again, if $\boldsymbol{\delta}$ represents the instantaneous state of a system whose behaviour is observed to be consistent with that predicted by the mean field equations, we would expect that the true expectations of δ_j and δ_k for this particular vector should be approximately equal to $1/u$.

It is worth recalling that mean field analysis naturally represents a significant simplification of the true situation. Even without consideration of correlations between local cell states that may be generated by the specific dynamics of the model, it is clear that considering δ_i and δ_j to be independent is a bold assumption, since the

condition that the δ_m must sum to n and the knowledge that (in the true model) precisely U of these terms are non-zero clearly means that the larger the particular value of δ_i , the smaller the likely value of δ_j and vice versa. However, the purpose of this section is not a justification of mean field analysis, but an examination of the values that we would expect to see for the expectations of the random variables δ_i , δ_j and δ_k derived from a vector $\boldsymbol{\delta}$ representing the instantaneous state of a \mathfrak{B} -model whose behaviour is observed to conform to that predicted by the mean field equations.

For ease of reference, the expectations of these variables and of those combinations of random variables that were considered in Table 6.2 are summarised in Table 6.3 . Note that, the assumption of independence ensures that the expectations of $\delta_j - \delta_i$ and $\delta_i\delta_j$ may be calculated simply by subtracting and multiplying the separate expectations of the relevant variables.

Random variable	Expectation under the mean field assumptions
δ_i	$\frac{1+u}{u}$
δ_j	$\frac{1}{u}$
δ_k	$\frac{1}{u}$
$\delta_j - \delta_i$	-1
$\delta_i\delta_j$	$\frac{1+u}{u^2}$

Table 6.3: The expectations of particular terms of $\boldsymbol{\delta}$ and of certain combinations of these terms under the mean field assumptions. As in Table 6.2, the variables used here refer specifically to those mentioned explicitly in the vector descriptions (6.5)-(6.8). Hence, the row for δ_k is conditional on the fact that $\delta_i = 1$ (as in (6.7)) while all other rows are conditional on the fact that $\delta_i > 1$ (as in (6.5), (6.6) and (6.8)).

To summarise, in this section, we have calculated the expected values of certain quantities of interest derived from the vector $\boldsymbol{\delta}$, representing the microstate of a one-dimensional single species \mathfrak{B} -model for which the mean field assumptions are supposed to be (at least instantaneously) valid. These results will be used in Section 6.6.4, the final part of this chapter, to draw conclusions linking the different types of transition with the global dynamics of the model.

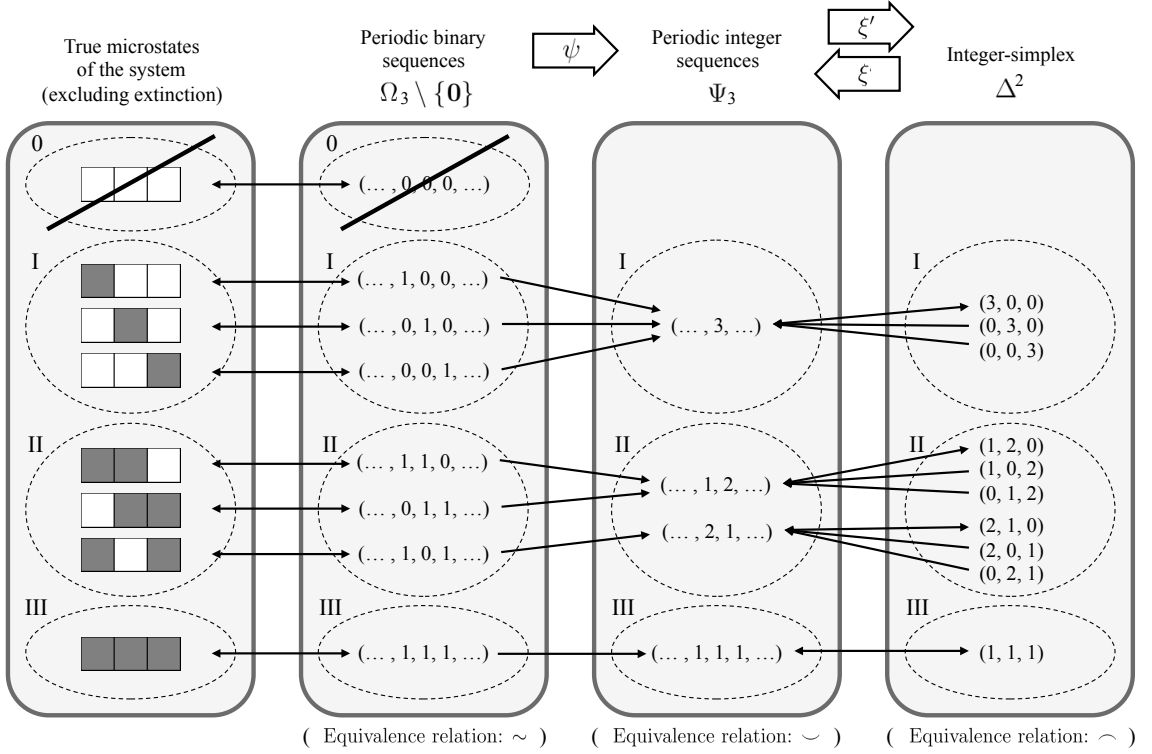


Figure 6.5: The complete set of microstates of a single species \mathfrak{B} -model over a ring of n cells and the corresponding elements of Ω_n , Ψ_n and Δ^{n-1} , for the case $n = 3$. The appropriate equivalence classes in each space are labelled with Roman numerals, such that corresponding classes in different spaces are allocated the same numeral. The class labelled 0 corresponds to the microstate of population 0 (extinction) and has no corresponding class in Ψ_n or Δ^{n-1} .

6.4.5 Visualising and analysing the dynamics in Δ^{n-1}

We now turn our attention to the dynamics of the one-dimensional single species \mathfrak{B} -model, as represented on the integer simplex Δ^{n-1} . Our objective is to gain a qualitative understanding of how α , β , γ and η -transitions affect the movement of δ across Δ^{n-1} through presenting visual representations of these dynamics. These qualitative observations will then inform the subsequent analytical work pursued in the remainder of the chapter, particularly in Section 6.6.3, where we examine the effect of different transitions on individual clumping.

In this section, we will require the following definition, which states that points of the integer simplex Δ^{n-1} are considered to be adjacent when the distance between the points is minimal:

Definition 6.4.1. *The points $\delta_1 = (\delta_{1,i})_{i \in \{0, \dots, n-1\}}$ and $\delta_2 = (\delta_{2,i})_{i \in \{0, \dots, n-1\}}$ of the integer simplex Δ^{n-1} for some $n \in \mathbb{N}$ are defined to be **adjacent** if and only if:*

$$|\delta_2 - \delta_1| = \min\{|\delta^{**} - \delta^*| : \delta^* \neq \delta^{**} \in \Delta^{n-1}\} \quad (6.10)$$

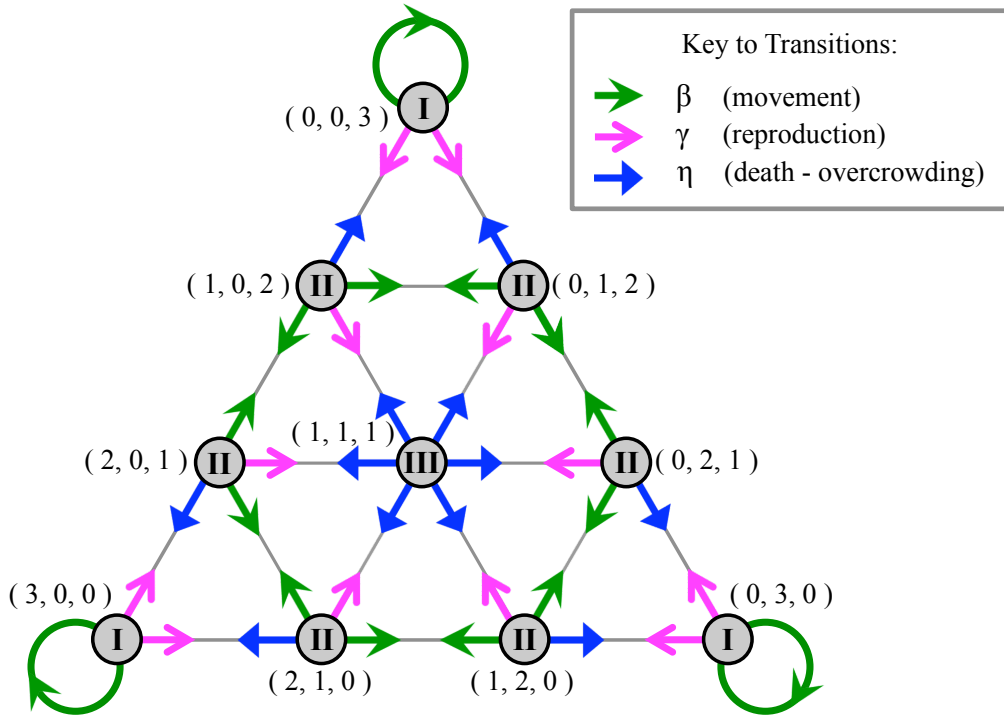


Figure 6.6: The dynamics of a single species \mathfrak{B} -model over a ring of 3 cells under the influence of β , γ and η -transitions, as represented on the integer simplex Δ^2 . Roman numerals denote the equivalence classes of the system, corresponding with those enumerated in Figure 6.5. Class 0 (extinction) is omitted, both since the system cannot move to this class under the influence of β , γ and η -transitions only and since this class does not correspond to any points on the integer simplex.

The following corollary is immediate:

Corollary 6.4.2. *Given $\delta_1, \delta_2 \in \Delta^{n-1}$ as defined in Definition 6.4.1, (6.10) holds if and only if $\exists j, k \in \{0, \dots, n-1\}$ such that:*

$$\delta_{2,i} = \begin{cases} \delta_{1,i} + 1 & , \quad i = j \\ \delta_{1,i} - 1 & , \quad i = k \\ \delta_{1,i} & , \quad \text{otherwise.} \end{cases}$$

To better understand how the dynamics of the system may be represented on the integer simplex Δ^{n-1} , consider the case $n = 3$. This case is sufficiently simple that we can easily list the complete set of true microstates of the system, along with all the elements of Ω_n , Ψ_n and Δ^{n-1} , as seen in Figure 6.5.

Δ^2 is a two-dimensional object - an equilateral triangular lattice embedded in \mathbb{R}^3 - and may therefore be easily visualised. Also, using the results of Section 6.4.2, as part of such a visualisation, we may also indicate the possible effect of the various

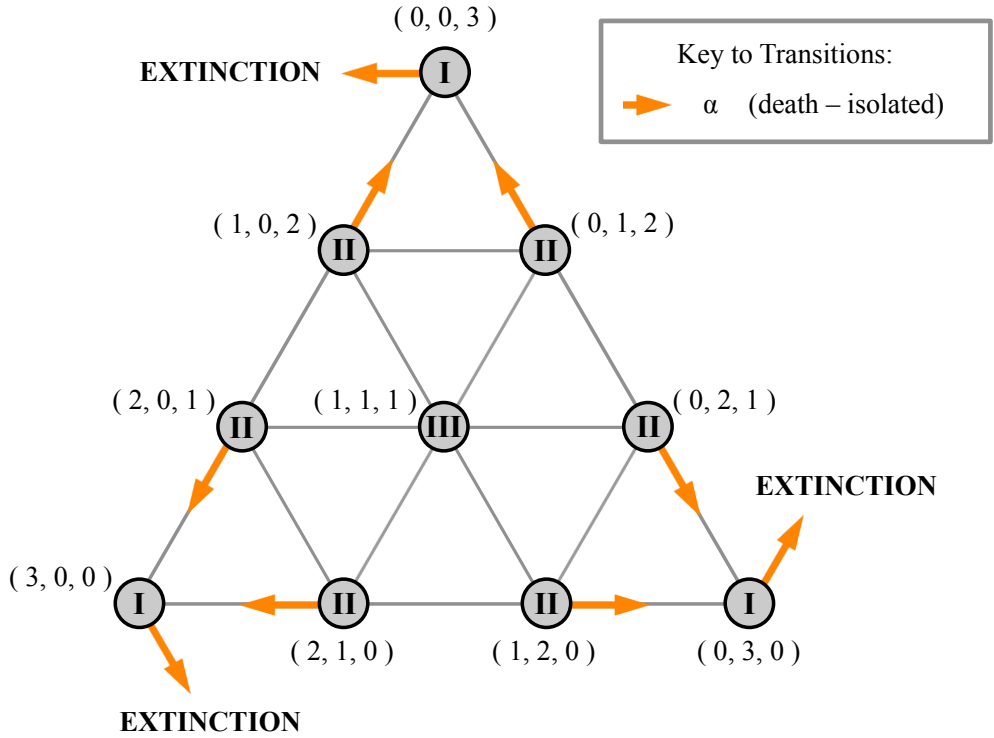


Figure 6.7: The dynamics of a single species \mathfrak{B} -model over a ring of 3 cells under the influence of α -transitions, as represented on the integer simplex Δ^2 . Roman numerals denote the equivalence classes of the system, corresponding with those enumerated in Figure 6.5.

transitions in terms of movements over this lattice. Figure 6.6 presents such a visualisation, with arrows representing the possible effects of β , γ and η -transitions for all microstates of the system. Figure 6.7 presents a similar visualisation, with arrows representing the possible effects of α -transitions.

Note that, in creating these visualisations, since all elements of an equivalence class are interchangeable, we have not been concerned with the precise point of Δ^2 that lies at the head of each arrow. Rather, for each point of the integer-simplex, all equivalence classes to which the system may be transformed from this point under the influence of a single β , γ , η or α -transition have been identified and the appropriate arrows have been drawn to all the closest members of these classes in terms of the Euclidean distance in \mathbb{R}^3 . In this way, all possible movements of the system between equivalence classes under the influence of these transitions are represented in the diagrams.

Note that, for reasons of clarity, situations in which a particular transition may transform between microstates lying in the same equivalence class have only been represented by loops where no transition between adjacent points of the integer simplex could convey the same information. For example, all transitions between points

in Class **II** could instead have been represented by loops on the appropriate vertices.

The first thing to note from Figure 6.6 is that β , γ and η -transitions correspond exclusively to movements between adjacent points (or, exceptionally, identical points) on the integer simplex, in the following sense. If there exists a transition of one of these three types that may transform a microstate in one particular equivalence class of the system to a microstate in another particular equivalence class of the system, then there exist two points, one in each of the corresponding equivalence classes of Δ^2 that are adjacent (or, exceptionally, identical) on the integer simplex. The exception concerns the case where a β -transition leaves the equivalence class of a microstate unchanged and a ‘movement’ from an appropriate point of Δ^2 to itself is permitted. For an example of such a case, see the loops at the corners of the lattice of Figure 6.6.

Indeed, for β , γ and η -transitions, the adjacency property identified above is a general result and not specific to the case $n = 3$, as may be immediately observed by considering the results of Section 6.4.2. In that section it was demonstrated that each of the transitions β , γ and η operating on the vector $\boldsymbol{\delta} \in \Delta^{n-1}$ has the effect of adding 1 to one term of $\boldsymbol{\delta}$, subtracting 1 from another and leaving all other terms unchanged (see (6.5), (6.6), (6.7)). However, according to Corollary 6.4.2, points that are adjacent on the integer simplex are related in precisely this way, so we may conclude that the effect of any one of these transitions is like a single step between adjacent points of Δ^{n-1} .

Note, however, that the analysis of Section 6.4.2 requires that $U > 1$, and hence does not apply to the exceptional cases of points in Class **I**, which have population $U = 1$ and which are associated with β -transitions represented by loops in Figure 6.6.

Figure 6.7 shows that, excluding transitions from points in Class **I** to extinction, α -transitions can also be represented as steps between adjacent points of the lattice. However, this is not a general result. For higher values of n , unlike other transitions, α -transitions may transform the system between equivalence classes that have no adjacent points in Δ^{n-1} . This is because, as seen in Section 6.4.2, an α -transition operating on the vector $\boldsymbol{\delta} \in \Delta^{n-1}$ has the effect of replacing two terms of $\boldsymbol{\delta}$ with a zero term and a term equal to their sum (see (6.8)). Such a transformation will not generally correspond to a single step between adjacent points of Δ^{n-1} .

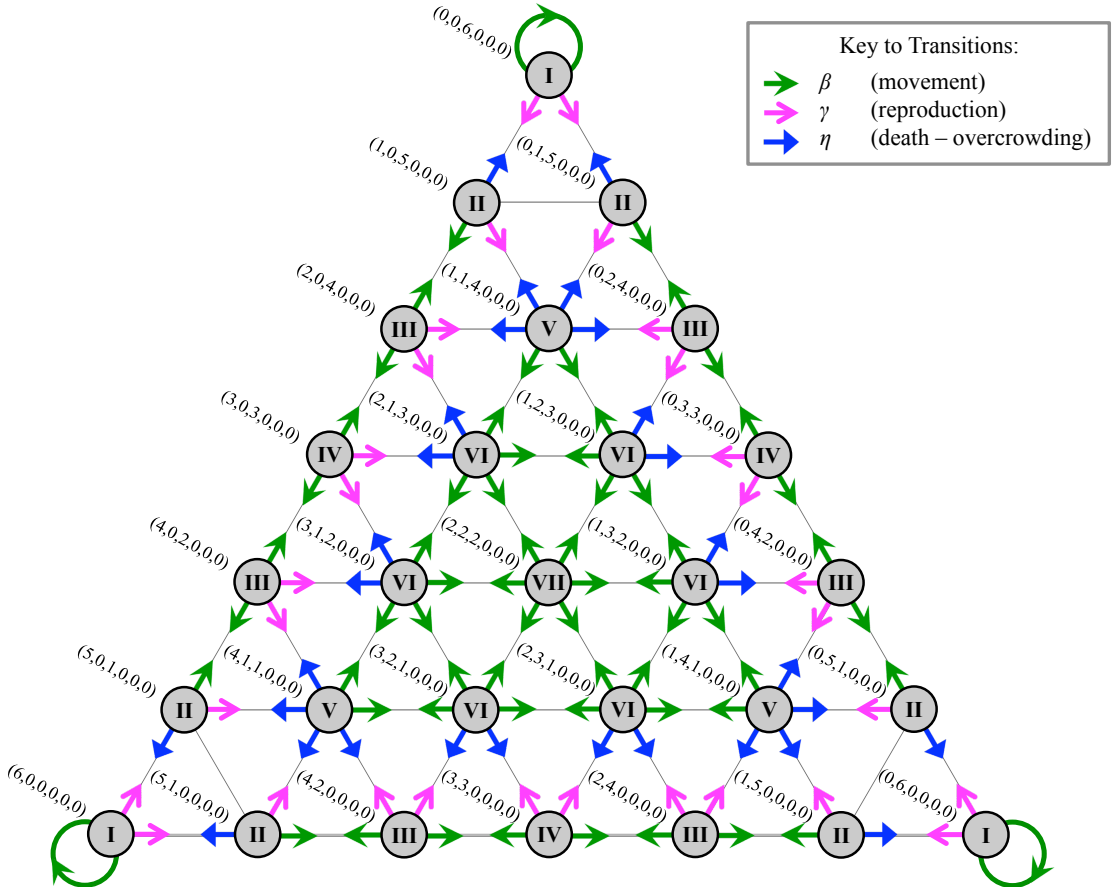


Figure 6.8: The dynamics of a single species \mathfrak{B} -model over a ring of 6 cells under the influence of β , γ and η -transitions, for microstates of population $U \leq 3$, as represented on a section of the integer simplex Δ^5 . Roman numerals denote the equivalence classes of the system, corresponding with those described in Table 6.1. Class 0 (extinction) is omitted, both since the system cannot move to this class under the influence of β , γ and η -transitions only and since this class does not correspond to any points on the integer simplex.

Although the dynamics of models for higher values of n cannot be completely visualised in two dimensions, it is possible to visualise part of the dynamics. Figures 6.8 and 6.9 present visualisations of the dynamics of a \mathfrak{B} -model with $n = 6$ over a section of the integer simplex Δ^5 . Since Δ^5 is a five-dimensional object embedded in \mathbb{R}^6 , containing vectors of the form $\boldsymbol{\delta} = (\delta_0, \delta_1, \delta_2, \delta_3, \delta_4, \delta_5)$, only points for which $\delta_3 = \delta_4 = \delta_5 = 0$ have been considered, producing a two-dimensional slice of the system.

Since the position of the zero terms of $\boldsymbol{\delta}$ is arbitrary and the number of non-zero terms is equal to the population U of the system, this is equivalent to visualising the complete dynamics of the system between microstates with populations of less than or equal to 3. When viewing the figures, it should therefore be remembered that transitions between the points depicted and points representing states of population 4 or more are not represented.

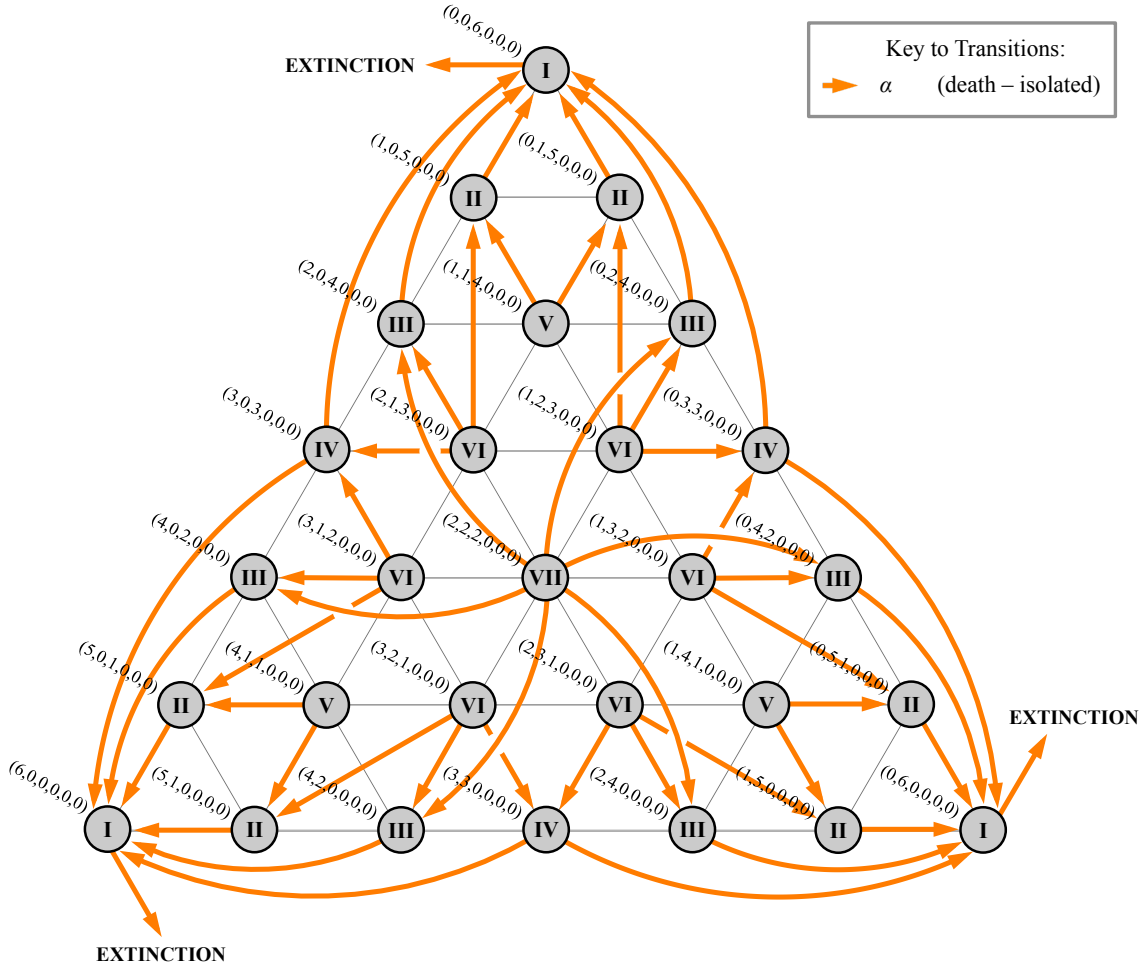


Figure 6.9: The dynamics of a single species \mathfrak{B} -model over a ring of 6 cells under the influence of α -transitions, for microstates of population $U \leq 3$, as represented on a section of the integer simplex Δ^5 . Roman numerals denote the equivalence classes of the system, corresponding with those described in Table 6.1.

Figures 6.8 and 6.9 starkly support the above comments on the different nature of β , γ and η as opposed to α -transitions. All the β , γ and η -transitions depicted appear as movements between adjacent points of Δ^5 , while many of the possible α -transitions correspond to much larger steps across the space, and may also induce extinction.

These informal arguments serve to develop our understanding of the fundamental difference between these different types of transition and go some way toward explaining the different effects that they may have on macroscopic features of the system, as identified in Section 5.3.10. A more quantitative approach to this analysis will be employed in the following sections.

6.5 Taking account of the spatial distribution of individuals in the one-dimensional single species \mathfrak{B} -model

6.5.1 Motivations and discussion

The importance of spatial clumping and its effect on model dynamics has been acknowledged and discussed by a number of authors. For example, in the context of one-dimensional CAs, Wolfram (2002, pp. 359-360) discusses the processes by which separate spatial regions, exhibiting distinct cell states or patterns of behaviour, can grow and merge to produce “nested” patterns; Mirabet et al. (2007) investigate the ways in which local behavioural rules can affect the formation of “subgroups” of individuals in ABMs of flocking; while Fibich and Gibori (2010, pp. 1461-1464) consider the dynamics of an ABM for the adoption of new products in terms of the expansion and merging of different clusters of individuals, in both one-dimensional and multi-dimensional cases.

In this section, we introduce a family of measures of clumping that can be used to analyse the microstates of the one-dimensional single species \mathfrak{B} -model. These measures will ultimately allow for a quantitative analysis of the effects of different transitions on the spatial distribution of individuals in this model, which will be presented in Section 6.6.

In Section 5.4, autocorrelations were used to build up a picture of the degree of clumping of the individuals in a system and it was observed that α -transitions seem to lead to increased individual clumping, invalidating the spatial independence assumptions that are necessary for mean field theory to meaningfully describe the dynamics of the system. However, describing individual clumping in this way requires many separate measures, each representing an autocorrelation of a different lag. If possible, to aid analysis and interpretation, it would be preferable to describe clumping using a single measure.

It should be noted that no such measure could be hoped to completely describe the distribution of individuals throughout the system; this information could not be usefully conveyed by a single number. Instead, any measure will be somewhat heuristic, in that while it may not give a precise description of the state of the system and how it will evolve, it may nonetheless provide a useful indication of individual clumping, suggesting which patterns of behaviour may be considered more likely from a given microstate. Clearly, since we have shown that the dynamics of the model do not

depend on the current microstate but on the equivalence class of that state, for such a measure to be at all meaningful, it must at least be constant over all elements of an equivalence class.

In discussing individual clumping in the one-dimensional case, we are essentially interested in the distribution of the sizes of the gaps between occupied cells of a microstate $\mathbf{c} \in \Omega_n$. If these gaps are all of similar size, then individuals are highly spread out throughout the system and clumping is low. If, on the other hand, the distribution of gap sizes is highly uneven, with some gaps much larger than others, then individual clumping is higher.

It is on this basis that the clumping measures presented in the following section have been constructed.

6.5.2 Definition and discussion of clumping measures

Consider the following definition:

Definition 6.5.1. *Given a vector $\boldsymbol{\delta} \in \Delta^{n-1}$ and a positive integer $U' > 1$, we define the **clumping measure at population U' of $\boldsymbol{\delta}$** , denoted $\text{Cl}_{U'}[\boldsymbol{\delta}]$, as:*

$$\text{Cl}_{U'}[\boldsymbol{\delta}] = \frac{1}{n} \sqrt{\frac{U'^2}{U' - 1}} (\text{Re} - \text{Im}) \left[\sqrt{\frac{1}{U'} \sum_{m=0}^{n-1} \delta_m^2 - \left(\frac{n}{U'}\right)^2} \right] \quad (6.11)$$

where the square root of a real number is taken to refer exclusively to the positive real or ‘positive’ imaginary root, as appropriate, and where we define the function:

$$\begin{aligned} (\text{Re} - \text{Im}) : \mathbb{C} &\rightarrow \mathbb{R} \\ z &\mapsto \text{Re}[z] - \text{Im}[z] \end{aligned}$$

If U is the population of $\boldsymbol{\delta}$, then we call $\text{Cl}_U[\boldsymbol{\delta}]$ the **natural clumping measure of $\boldsymbol{\delta}$** , which will be denoted $\text{Cl}[\boldsymbol{\delta}]$.

The use of the function $(\text{Re} - \text{Im})$ ensures that the clumping measure at population U' is real. Observe also that, since the argument of $(\text{Re} - \text{Im})$ in (6.11) is either purely real or purely imaginary, in this instance, the function is either equal to its real argument (in the former case) or to i times its purely imaginary argument (otherwise). Furthermore, the sign of $\text{Cl}_{U'}[\boldsymbol{\delta}]$ matches that of the argument of the square root in the function $(\text{Re} - \text{Im})$.

A plot of the function $y = (\text{Re} - \text{Im})[\sqrt{x}]$, for $x \in \mathbb{R}$, and a discussion of its derivative is provided in Figure 6.10.

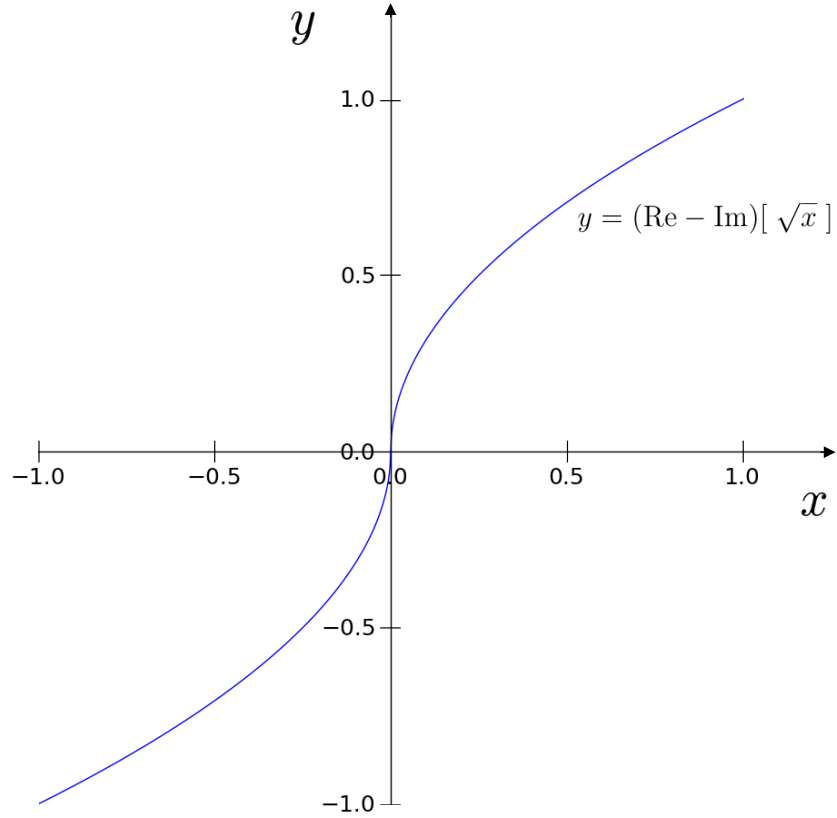


Figure 6.10: The function $y = (\text{Re} - \text{Im})[\sqrt{x}]$ for $x \in [-1, 1]$. Observe that $y = \sqrt{x}$ for all $x \geq 0$ and $y = -\sqrt{|x|}$ for all $x \leq 0$. We therefore have:

$$\frac{d}{dx} ((\text{Re} - \text{Im})[\sqrt{x}]) = \frac{1}{2\sqrt{|x|}}, \quad \forall x \neq 0$$

In the remainder of this section, we investigate this clumping measure and discuss the reasoning behind its definition.

We first consider certain conditions under which the function $(\text{Re} - \text{Im})$ may be disregarded, since it is equal to the identity function. For $\boldsymbol{\delta} \in \Delta^{n-1}$ with population U , we have that:

$$\begin{aligned} \frac{1}{U'} \sum_{m=0}^{n-1} \delta_m^2 &\geq \left(\frac{U}{U'} \right) \left(\frac{n}{U} \right)^2 \\ &= \left(\frac{n}{U} \right) \left(\frac{n}{U'} \right) \end{aligned}$$

Hence, if $U \leq U'$, then the use of the function $(\text{Re} - \text{Im})$ is not necessary to ensure that $\text{Cl}_{U'}[\boldsymbol{\delta}]$ is real, since:

$$\frac{1}{U'} \sum_{m=0}^{n-1} \delta_m^2 - \left(\frac{n}{U'}\right)^2 \geq 0$$

and the argument of $(\text{Re} - \text{Im})$ is therefore purely real.

In particular, this implies that the natural clumping measure $\text{Cl}[\boldsymbol{\delta}]$ is always non-negative and may be written in the simpler form:

$$\text{Cl}[\boldsymbol{\delta}] = \frac{1}{n} \sqrt{\frac{U^2}{U-1}} \sqrt{\frac{1}{U} \sum_{m=0}^{n-1} \delta_m^2 - \left(\frac{n}{U}\right)^2} \quad (6.12)$$

In this case, n/U is equal to the mean of the non-zero terms of $\boldsymbol{\delta}$, since the terms of any vector on the integer-simplex Δ^{n-1} must sum to n . Hence, in the case of the natural clumping measure, the right hand square root of (6.12) is equal to the empirical standard deviation of the non-zero terms of $\boldsymbol{\delta}$. Since these non-zero terms represent the sizes of the gaps between individuals in a corresponding microstate of the system, $\text{Cl}[\boldsymbol{\delta}]$ is indeed related to the distribution of sizes of these gaps, as desired.

Given n and U' , since the function $(\text{Re} - \text{Im})[\sqrt{x}]$ is strictly increasing in x (see Figure 6.10), we observe that $\text{Cl}_{U'}[\boldsymbol{\delta}]$ attains a maximum (over all $\boldsymbol{\delta} \in \Delta^{n-1}$) where $\sum \delta_m^2$ attains a maximum. Since the δ_m must sum to n , this maximum is attained when one term of $\boldsymbol{\delta}$ is equal to n and all other terms are equal to 0. Conversely, $\text{Cl}_{U'}[\boldsymbol{\delta}]$ attains a minimum where $\sum \delta_m^2$ attains a minimum. This minimum is attained when all terms of $\boldsymbol{\delta}$ are equal to 1.

Substituting these maxima and minima into (6.11) and simplifying, we see that:

$$-1 \leq -\sqrt{\frac{1}{U'-1}} \sqrt{1 - \frac{U'}{n}} \leq \text{Cl}_{U'}[\boldsymbol{\delta}] \leq 1, \quad \forall U' \in \{2, \dots, n\}$$

The choice of the multiplier $n^{-1} \sqrt{U'^2/(U'-1)}$ in (6.11) is therefore seen to ensure that $\text{Cl}_{U'}[\boldsymbol{\delta}] \in [-1, 1], \forall U' \in \{2, \dots, n\}$, with values of $\text{Cl}_{U'}[\boldsymbol{\delta}]$ below 0 indicating that the current clumping measure at population U' is below the minimal possible value for a system of population U' .

The fact that $\text{Cl}_{U'}[\boldsymbol{\delta}]$ can only be defined for $U' > 1$ poses no significant problem, since it is meaningless to talk about the degree of ‘clumping’ of a single individual in any case.

It will prove useful to note the following alternative forms of $\text{Cl}_{U'}[\boldsymbol{\delta}]$:

$$\text{Cl}_{U'}[\boldsymbol{\delta}] = \frac{1}{n} \sqrt{\frac{U'}{U' - 1}} (\text{Re} - \text{Im}) \left[\sqrt{\sum_{m=0}^{n-1} \delta_m^2 - U' \left(\frac{n}{U'} \right)^2} \right] \quad (6.13)$$

$$= \sqrt{\frac{U'}{U' - 1}} (\text{Re} - \text{Im}) \left[\sqrt{\sum_{m=0}^{n-1} \left(\frac{\delta_m}{n} \right)^2 - \frac{1}{U'}} \right] \quad (6.14)$$

As with (6.11), in the case of the natural clumping measure (and, indeed, any case in which $U \leq U'$), the function $(\text{Re} - \text{Im})$ in each of these expressions may be replaced with the identity function, since its argument is purely real.

We note in passing that in (6.14), if U' and each of the δ_m/n are held constant, then $\text{Cl}_{U'}$ remains meaningful as $n \rightarrow \infty$, demonstrating that the measure could be extended to a continuous case in which individuals may occupy any point of the interval $[0, 1]$.

Verifying that $\text{Cl}_{U'}$ is constant over equivalence classes is straightforward. This property follows immediately from the observations that any two vectors, $\boldsymbol{\delta}_1, \boldsymbol{\delta}_2$, that are equivalent under \sim may differ only in the arrangement of their terms (see Section 6.3) and that $\text{Cl}_{U'}[\boldsymbol{\delta}]$ is clearly invariant under any permutation of the terms of $\boldsymbol{\delta}$.

Although it is the natural clumping measure $\text{Cl}[\boldsymbol{\delta}]$ that will generally be of most interest, we will also need to consider clumping measures at populations other than that of the argument $\boldsymbol{\delta}$. The reasons for this will become clear in the following sections, but essentially it will prove more straightforward to analyse the model dynamics through tracking changes in all clumping measures $\text{Cl}_{U'}[\boldsymbol{\delta}]$ simultaneously rather than restricting our attention to the natural clumping measure $\text{Cl}[\boldsymbol{\delta}]$.

6.5.3 A geometric interpretation of the clumping measure

In this section, we examine the natural clumping measure $\text{Cl}[\boldsymbol{\delta}]$ from a geometric perspective. This will allow us to understand the relationship between this quantity and the structure of the integer simplex Δ^{n-1} , providing an intuitive link between the measures of clumping and the visualisations of the model dynamics over Δ^{n-1} that were presented in Section 6.4.5.

Returning to (6.12), recall that the natural clumping measure $\text{Cl}[\boldsymbol{\delta}]$ is defined to be equal to the empirical standard deviation of the non-zero terms of $\boldsymbol{\delta}$ multiplied

by the factor $n^{-1}\sqrt{U^2/(U-1)}$. To understand why this factor has been chosen, we demonstrate that $\text{Cl}[\boldsymbol{\delta}]$ has an intuitive geometric interpretation over the integer simplex Δ^{n-1} .

We will require the following definitions:

Definition 6.5.2. Given a vector $\boldsymbol{\delta} = (\delta_m)_{m \in \{0, \dots, n-1\}} \in \Delta^{n-1}$ of population U :

- The **local centre** of $\boldsymbol{\delta}$, denoted $\text{LC}[\boldsymbol{\delta}] = (\text{LC}_m)_{m \in \{0, \dots, n-1\}} \in \mathbb{R}^n$, is defined:

$$\text{LC}_m = \begin{cases} \frac{n}{U}, & \text{if } \delta_m > 0 \\ 0, & \text{if } \delta_m = 0 \end{cases}$$

- The **local extremity** of $\boldsymbol{\delta}$, denoted $\text{LE}[\boldsymbol{\delta}] = (\text{LE}_m)_{m \in \{0, \dots, n-1\}} \in \Delta^{n-1}$, is defined:

$$\text{LE}_m = \begin{cases} n, & \text{if } m = \min\{l \in \{0, \dots, n-1\} : \delta_l = \max\{\delta_0, \dots, \delta_{n-1}\}\} \\ 0, & \text{otherwise.} \end{cases}$$

Observe that, while the local extremity of $\boldsymbol{\delta}$ clearly lies on the integer simplex Δ^{n-1} , the local centre of $\boldsymbol{\delta}$ may not, since n/U is not necessarily an integer. Geometrically, note also that $\text{LC}[\boldsymbol{\delta}]$ is the closest point to $\boldsymbol{\delta}$ in \mathbb{R}^n with precisely U non-zero terms, which sum to n and which are all equal, while $\text{LE}[\boldsymbol{\delta}]$ is the closest point (or one of several closest points) to $\boldsymbol{\delta}$ in \mathbb{R}^n with precisely one non-zero term, which is equal to n . Equivalently, the local extremity is the closest point of Δ^{n-1} with population 1.

Given a particular $\boldsymbol{\delta} \in \Delta^{n-1}$, consider the Euclidean distance from $\boldsymbol{\delta}$ to its local centre:

$$\begin{aligned} |\boldsymbol{\delta} - \text{LC}[\boldsymbol{\delta}]| &= \sqrt{\sum_{m=0}^{n-1} \left(\delta_m - \frac{n}{U}\right)^2 \mathbf{1}_{\mathbb{R}^+}[\delta_m]} \\ &= \sqrt{\sum_{m=0}^{n-1} \delta_m^2 - 2\frac{n}{U} \sum_{m=0}^{n-1} \delta_m + \sum_{m=0}^{n-1} \left(\frac{n}{U}\right)^2 \mathbf{1}_{\mathbb{R}^+}[\delta_m]} \\ &= \sqrt{\sum_{m=0}^{n-1} \delta_m^2 - 2n\frac{n}{U} + U \left(\frac{n}{U}\right)^2} \\ &= \sqrt{\sum_{m=0}^{n-1} \delta_m^2 - \frac{n^2}{U}} \end{aligned}$$

Here, $\mathbf{1}_{\mathbb{R}^+}$ represents the indicator function of \mathbb{R}^+ over \mathbb{R} :

$$\begin{aligned}\mathbf{1}_{\mathbb{R}^+} : \mathbb{R} &\rightarrow \{0, 1\} \\ x &\mapsto \begin{cases} 1, & x \in \mathbb{R}^+ \\ 0, & \text{otherwise} \end{cases}\end{aligned}\tag{6.15}$$

We observe that, for the natural clumping measure $\text{Cl}[\boldsymbol{\delta}]$, the final square root of (6.13) is therefore equal to the Euclidean distance in \mathbb{R}^n from $\boldsymbol{\delta}$ to its local centre (recalling that the function $(\text{Re} - \text{Im})$ may be ignored in this case).

Now consider the Euclidean distance from the local centre to the local extremity of $\boldsymbol{\delta}$, which may be expressed as follows:

$$\begin{aligned}|\text{LE}[\boldsymbol{\delta}] - \text{LC}[\boldsymbol{\delta}]| &= \sqrt{\left(n - \frac{n}{U}\right)^2 + (U-1)\left(0 - \frac{n}{U}\right)^2} \\ &= n \sqrt{\frac{U-1}{U}}\end{aligned}$$

By comparing with (6.13) once again, we may observe that the natural clumping measure $\text{Cl}[\boldsymbol{\delta}]$ is the ratio of the distance from $\boldsymbol{\delta}$ to its local centre over the distance from its local centre to its local extremity:

$$\text{Cl}[\boldsymbol{\delta}] = \frac{|\boldsymbol{\delta} - \text{LC}[\boldsymbol{\delta}]|}{|\text{LE}[\boldsymbol{\delta}] - \text{LC}[\boldsymbol{\delta}]|}\tag{6.16}$$

Figure 6.11 demonstrates this geometric interpretation of the natural clumping measure for some particular simple examples.

This link between the empirical standard deviation of the gaps between individuals for a microstate $\mathbf{c} \in \Omega_n$ and the geometry of Δ^{n-1} illustrates why representing the dynamics of the system over the integer-simplex is appropriate when considering the degree of clumping of the individuals.

The geometric interpretation of the natural clumping measure also offers an intuitive route for understanding the different effects of local transitions on individual clumping that were observed in Section 5.4. In Section 6.4.5, it was noted that β , γ and η -transitions correspond to steps between adjacent points of the integer simplex, while α -transitions may correspond to larger steps. Moreover, in the example visualised in Figure 6.9, we observe that these large steps are directed away from the local centre and towards the local extremities.

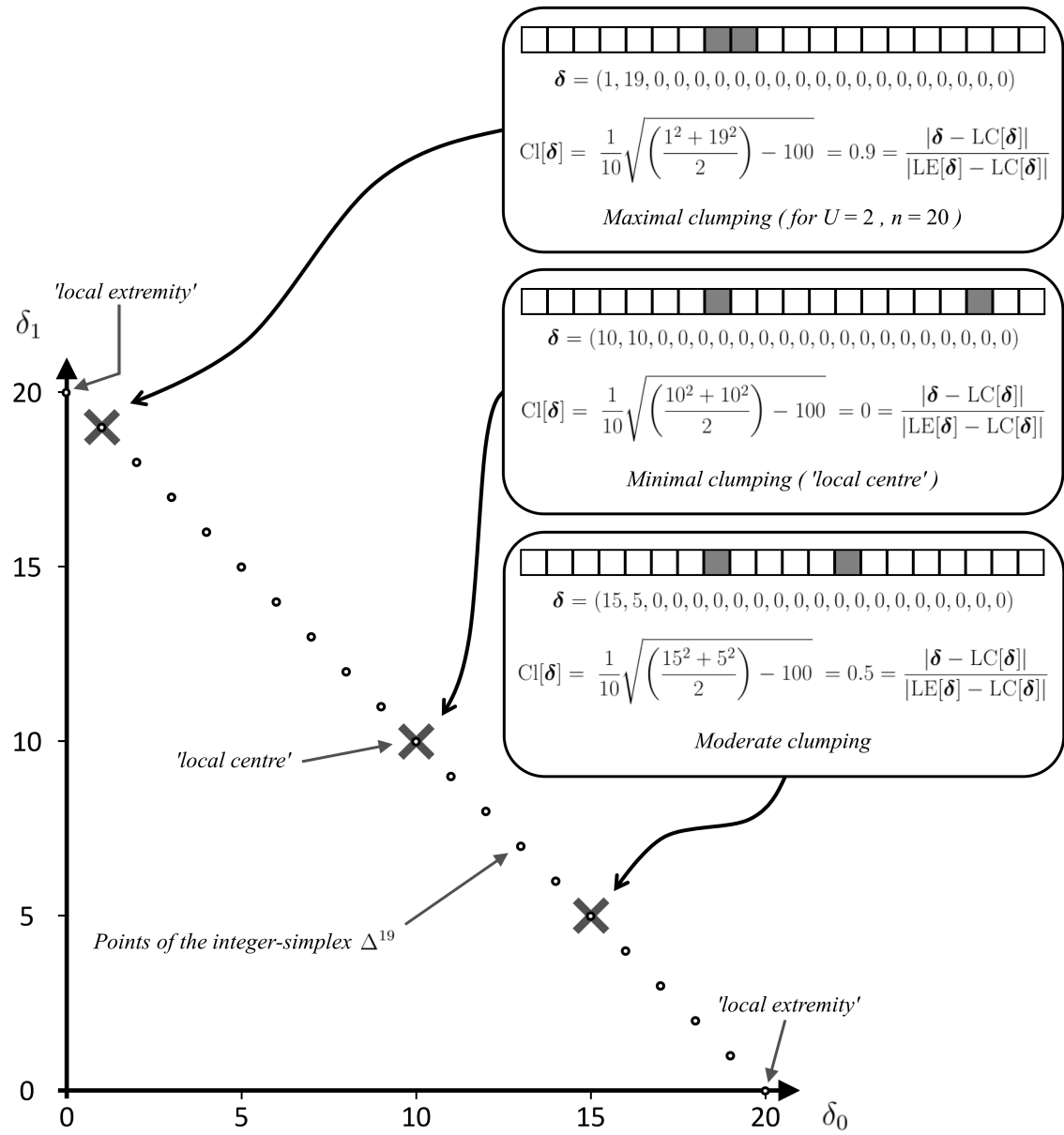


Figure 6.11: A demonstration of how the natural clumping measure $Cl[\boldsymbol{\delta}]$ is related to the geometry of the integer-simplex, for three microstates with $n = 20$ and $U = 2$. The plot depicts a one-dimensional cross section of Δ^{19} , embedded in \mathbb{R}^2 (recall that Δ^{19} is defined as a subset of \mathbb{R}^{20}), for vectors $\boldsymbol{\delta}$ for which $\delta_2 = \dots = \delta_{19} = 0$. Observe that $Cl[\boldsymbol{\delta}]$ (as defined in (6.12)) represents the Euclidean distance of $\boldsymbol{\delta}$ from its ‘local centre’ as a proportion of the distance from the ‘local centre’ to a nearby ‘local extremity’ of the integer simplex.

In the context of (6.16), we might therefore surmise that β , γ and η -transitions would lead to small changes in individual clumping, while α -transitions could instead lead to sudden large increases. A quantitative argument of this nature will be presented in Section 6.6.

6.5.4 Remarks on clumping measures

To better understand why α -transitions appear to cause the clumping of individuals while β , γ and η -transitions do not, we will examine the effect of each transition on the clumping measures $\text{Cl}_{U'}$. However, before beginning this analysis, we make some preliminary observations.

Firstly, it should once again be stressed that, given a particular $\boldsymbol{\delta} \in \Delta^{n-1}$ of population U , although the clumping measure $\text{Cl}_{U'}[\boldsymbol{\delta}]$ is defined for all $U' \in \{2, \dots, n\}$, and while it will prove useful to consider measures for which $U' \neq U$, only the natural clumping measure has a meaningful intuitive interpretation as a scaled version of the empirical standard deviation of the gaps between individuals in a corresponding microstate.

Secondly, it should be noted that the natural clumping measure may only be reasonably used to compare the clumping of individuals between microstates of equal population. Specifically, given two vectors $\boldsymbol{\delta}_1$ and $\boldsymbol{\delta}_2$, with respective populations U_1 and U_2 , if $U_1 = U_2$ and $\text{Cl}[\boldsymbol{\delta}_1] > \text{Cl}[\boldsymbol{\delta}_2]$ then it is meaningful to state that the individuals of a microstate corresponding to $\boldsymbol{\delta}_1$ are more highly clumped than those of a microstate corresponding to $\boldsymbol{\delta}_2$, since we know that the empirical standard deviation of the gaps separating the individuals is higher in the former case than in the latter. However, if $U_1 \neq U_2$, then no such comparison should be made.

Furthermore, comparing vectors with different populations in terms of the empirical standard deviation of their non-zero terms alone would not be reasonable, because this quantity is not of interest to us in isolation. Rather, it is intended as a proxy measure for a concept (individual clumping) which we expect to have a certain influence on the behaviour of the system. It is clearly not sensible to infer that two microstates with equal empirical standard deviations of this kind will exhibit similar behaviour if they do not also have the same population, since we know that the behaviour of a \mathfrak{B} -model is strongly influenced by population density.

Bearing this in mind, we will consider the relationship between the dynamics of the system and the clumping measures $\text{Cl}_{U'}$ from the following perspective. As was

observed in Section 6.3, the dynamics may be represented as an imaginary particle moving around the integer-simplex Δ^{n-1} . Each position $\boldsymbol{\delta}$ occupied by the particle has a set of $n - 1$ associated clumping values at different populations:

$$\text{Cl}_2[\boldsymbol{\delta}] , \dots , \text{Cl}_n[\boldsymbol{\delta}]$$

As discussed above, of these values, only the natural clumping measure $\text{Cl}[\boldsymbol{\delta}] = \text{Cl}_U[\boldsymbol{\delta}]$, where U is the population of $\boldsymbol{\delta}$, represents a meaningful description of individual clumping in corresponding microstates of the system. However, all of the measures are well-defined and may be considered to vary as the system evolves.

Now, to simplify the notation, given $\boldsymbol{\delta} \in \Delta^{n-1}$ of population U , let:

$$\Sigma[\boldsymbol{\delta}] = \frac{1}{n^2} \sum_{m=0}^{n-1} \delta_m^2$$

Since the δ_m must sum to n , we clearly have $0 < \Sigma[\boldsymbol{\delta}] \leq 1$ for all populations $U \in \{1, \dots, n\}$.

Now, by (6.14):

$$\text{Cl}_{U'}[\boldsymbol{\delta}] = \sqrt{\frac{U'}{U' - 1}} (\text{Re} - \text{Im}) \left[\sqrt{\Sigma[\boldsymbol{\delta}] - \frac{1}{U'}} \right] \quad (6.17)$$

Once again, as with (6.11), (6.13) and (6.14), when $U' \geq U$, the function $(\text{Re} - \text{Im})$ in this expression may be replaced with the identity function, since its argument is purely real.

We observe that, for any fixed $U' \in \{2, \dots, n\}$, $\text{Cl}_{U'}[\boldsymbol{\delta}]$ is strictly increasing in $\Sigma[\boldsymbol{\delta}]$. Thus, the degree of clumping of individuals in the system *at a particular population* U' may be studied by examining the changes in $\Sigma[\boldsymbol{\delta}]$ only. As the system evolves, the population will vary accordingly, *but any time that the population is equal to U'* , the degree of clumping of the individuals will be determined by the current value of $\Sigma[\boldsymbol{\delta}]$, with higher values indicating greater clumping. In this sense, the evolution of $\Sigma[\boldsymbol{\delta}]$ over time determines the degree of clumping of the system at all populations $U' \in \{2, \dots, n\}$.

This perspective will be particularly relevant when discussing the behaviour of the system around a prospective equilibrium population, since, under the influence of stochastic noise, we expect the system to repeatedly visit and revisit such equilibria as it evolves.

6.6 Using clumping to understand global behaviour

6.6.1 Aims and approach

In this Section, we combine the results presented throughout the chapter to provide a quantitative answer to the question posed in Section 6.1: why do one-dimensional single species \mathfrak{B} -models with $\alpha = 0$ exhibit population dynamics in line with those predicted by mean field theory, while models with $\alpha > 0$ do not?

To achieve this, we first use the results of Section 6.4 on the effect of different transitions on the vector $\boldsymbol{\delta}$ to determine how the clumping measures $\text{Cl}_{U'}$, defined in Section 6.5, respond to a particular change in $\Sigma[\boldsymbol{\delta}]$. We then establish the possible effects of each of the four transitions on these clumping measures, demonstrating a quantitative difference in the potential effect of α -transitions as compared with β , γ and η -transitions.

Finally, we use the results of Section 6.4.4 on the expected values of the terms of $\boldsymbol{\delta}$ in situations in which the mean field equations are valid to demonstrate that the clumping of the individuals in a model whose microstates are consistent with the mean field assumptions can, in some sense, be considered to be ‘stable’ when $\alpha = 0$ and ‘unstable’ when $\alpha > 0$.

6.6.2 Determining the response of $\text{Cl}_{U'}[\boldsymbol{\delta}]$ to changes in $\boldsymbol{\delta}$

For fixed $U' \in \{2, \dots, n\}$ and $\boldsymbol{\delta} \in \Delta^{n-1}$, let $\Delta\text{Cl}_{U'}$ represent the change in $\text{Cl}_{U'}[\boldsymbol{\delta}]$ resulting from a change $\Delta\Sigma$ in $\Sigma[\boldsymbol{\delta}]$. By (6.17), observing that $(\text{Re} - \text{Im})$ distributes across addition, we have that:

$$\Delta\text{Cl}_{U'} = \sqrt{\frac{U'}{U' - 1}} \left((\text{Re} - \text{Im}) \left[\sqrt{\Sigma[\boldsymbol{\delta}] + \Delta\Sigma - \frac{1}{U'}} - \sqrt{\Sigma[\boldsymbol{\delta}] - \frac{1}{U'}} \right] \right) \quad (6.18)$$

We now derive upper and lower bounds on $|\Delta\text{Cl}_{U'}|$ for a particular $\Delta\Sigma$.

First let:

$$x = \min \left\{ \Sigma[\boldsymbol{\delta}] - \frac{1}{U'}, \Sigma[\boldsymbol{\delta}] + \Delta\Sigma - \frac{1}{U'} \right\}$$

Observe that $x \in (-1, 1 - |\Delta\Sigma|)$, and that:

$$|\Delta\text{Cl}_{U'}| = \sqrt{\frac{U'}{U' - 1}} \left((\text{Re} - \text{Im}) \left[\sqrt{x + |\Delta\Sigma|} - \sqrt{x} \right] \right) \quad (6.19)$$

Considering $\Delta\Sigma$ to be fixed, we seek upper and lower bounds on $|\Delta\text{Cl}_{U'}|$ as a function of x , considering all x in the interval $[-1, 1]$. Any such bounds will then be valid for all possible $\Sigma[\delta]$ and $\Delta\Sigma$.

The gradient of the function $(\text{Re} - \text{Im})[\sqrt{x}]$ is equal to $(2\sqrt{|x|})^{-1}$, $\forall x \neq 0$ (see Figure 6.10). The minimum value of the gradient of this function on the interval $[-1, 1]$ is therefore equal to $1/2$, from which a lower bound on $|\Delta\text{Cl}_{U'}|$ may be simply derived (given the continuity of $|\Delta\text{Cl}_{U'}|$ on $[-1, 1]$, when considered as a function of x only):

$$\begin{aligned} |\Delta\text{Cl}_{U'}| &\geq \frac{1}{2} \sqrt{\frac{U'}{U' - 1}} |\Delta\Sigma| \\ &\geq \frac{1}{2} |\Delta\Sigma| \end{aligned} \quad (6.20)$$

To find an upper bound, we first observe that, for all $x \in [-1, 1] \setminus \{-|\Delta\Sigma|, 0\}$:

$$\frac{d}{dx} |\Delta\text{Cl}_{U'}| = \frac{1}{2} \sqrt{\frac{U'}{U' - 1}} \left(\left(\sqrt{|x + |\Delta\Sigma||} \right)^{-1} - \left(\sqrt{|x|} \right)^{-1} \right) \quad (6.21)$$

Since $|\Delta\text{Cl}_{U'}|$ is continuous on $[-1, 1]$ (as seen from (6.19)), it must attain a maximum for some $x_{\max} \in [-1, 1]$. Furthermore, x_{\max} must fulfil one of the following conditions:

- x_{\max} is one of the bounds of the interval: $x_{\max} = -1$ or $x_{\max} = 1$;
- The derivative of $|\Delta\text{Cl}_{U'}|$ with respect to x is undefined for $x = x_{\max}$: $x_{\max} = 0$ or $x_{\max} = -|\Delta\Sigma|$;
- The derivative of $|\Delta\text{Cl}_{U'}|$ with respect to x is equal to zero for $x = x_{\max}$.

We consider each of these cases in turn, substituting the appropriate values into (6.19), recalling that $\Sigma[\delta] \in (0, 1]$ and therefore that $|\Delta\Sigma| < 1$.

When $x = -1$:

$$\begin{aligned} |\Delta\text{Cl}_{U'}| &= \sqrt{\frac{U'}{U' - 1}} \left(1 - \sqrt{1 - |\Delta\Sigma|} \right) \\ &\leq \sqrt{\frac{U'}{U' - 1}} |\Delta\Sigma| \\ &< \sqrt{\frac{U'}{U' - 1}} \sqrt{|\Delta\Sigma|} \end{aligned} \quad (6.22)$$

When $x = 1$:

$$\begin{aligned} |\Delta \text{Cl}_{U'}| &= \sqrt{\frac{U'}{U'-1}} \left(\sqrt{1+|\Delta\Sigma|} - 1 \right) \\ &\leq \sqrt{\frac{U'}{U'-1}} |\Delta\Sigma| \\ &< \sqrt{\frac{U'}{U'-1}} \sqrt{|\Delta\Sigma|} \end{aligned} \quad (6.23)$$

When $x = 0$ or $x = -|\Delta\Sigma|$:

$$|\Delta \text{Cl}_{U'}| = \sqrt{\frac{U'}{U'-1}} \sqrt{|\Delta\Sigma|} \quad (6.24)$$

From (6.21), we see that the derivative of $|\Delta \text{Cl}_{U'}|$ with respect to x is equal to zero when:

$$\begin{aligned} (\sqrt{|x+|\Delta\Sigma||})^{-1} &= (\sqrt{|x|})^{-1} \\ \Leftrightarrow |x+|\Delta\Sigma|| &= |x| \end{aligned}$$

So the derivative is equal to zero when:

$$x = -\frac{1}{2} |\Delta\Sigma| \quad (6.25)$$

From (6.19), we see that the corresponding value of $|\Delta \text{Cl}_{U'}|$ is:

$$|\Delta \text{Cl}_{U'}| = \sqrt{2} \sqrt{\frac{U'}{U'-1}} \sqrt{|\Delta\Sigma|} \quad (6.26)$$

A comparison of (6.22), (6.23), (6.24) and (6.26) shows that $|\Delta \text{Cl}_{U'}|$ is bounded above, as follows:

$$\begin{aligned} |\Delta \text{Cl}_{U'}| &\leq \sqrt{2} \sqrt{\frac{U'}{U'-1}} \sqrt{|\Delta\Sigma|} \\ &\leq 2 \sqrt{|\Delta\Sigma|} \end{aligned}$$

In summary, we have shown that for all $U' \in \{2, \dots, n\}$ and $\boldsymbol{\delta} \in \Delta^{n-1}$, a change $\Delta\Sigma$ in $\Sigma[\boldsymbol{\delta}]$ (for example, as the result of a transition, transforming $\boldsymbol{\delta}$ to $\boldsymbol{\delta}'$) results in a change $\Delta \text{Cl}_{U'}$ in $\text{Cl}_{U'}[\boldsymbol{\delta}]$, whose absolute value is bounded in the following way:

$$\frac{1}{2} |\Delta\Sigma| \leq |\Delta \text{Cl}_{U'}| \leq 2 \sqrt{|\Delta\Sigma|} \quad (6.27)$$

6.6.3 The effect of different transitions on $\Sigma[\boldsymbol{\delta}]$ and $\text{Cl}_{U'}[\boldsymbol{\delta}]$

We may now determine the potential effect of each type of transition on $\Sigma[\boldsymbol{\delta}]$, employing the results and notation of Sections 6.4.2-6.4.3. Specifically, given a vector $\boldsymbol{\delta} \in \Delta^{n-1}$ representing the current state of the system, we let the following vector random variables represent the new state of the system, given, respectively, that an α , β , γ or η -transition occurs:

$$\begin{aligned}\boldsymbol{\delta}'_\alpha &= (\delta'_{\alpha,0}, \dots, \delta'_{\alpha,n-1}) \\ \boldsymbol{\delta}'_\beta &= (\delta'_{\beta,0}, \dots, \delta'_{\beta,n-1}) \\ \boldsymbol{\delta}'_\gamma &= (\delta'_{\gamma,0}, \dots, \delta'_{\gamma,n-1}) \\ \boldsymbol{\delta}'_\eta &= (\delta'_{\eta,0}, \dots, \delta'_{\eta,n-1})\end{aligned}$$

Component-wise descriptions of these vector random variables and a discussion of the distributions associated with their separate terms were presented in Sections 6.4.2 and 6.4.3.

We also introduce the following scalar random variables, which represent the potential change in $\Sigma[\boldsymbol{\delta}]$ and $\text{Cl}_{U'}[\boldsymbol{\delta}]$ caused by each of the four transitions:

$$\Delta\Sigma_\alpha[\boldsymbol{\delta}] = \Sigma[\boldsymbol{\delta}'_\alpha] - \Sigma[\boldsymbol{\delta}]$$

$$\Delta\Sigma_\beta[\boldsymbol{\delta}] = \Sigma[\boldsymbol{\delta}'_\beta] - \Sigma[\boldsymbol{\delta}]$$

$$\Delta\Sigma_\gamma[\boldsymbol{\delta}] = \Sigma[\boldsymbol{\delta}'_\gamma] - \Sigma[\boldsymbol{\delta}]$$

$$\Delta\Sigma_\eta[\boldsymbol{\delta}] = \Sigma[\boldsymbol{\delta}'_\eta] - \Sigma[\boldsymbol{\delta}]$$

$$\Delta\text{Cl}_{U'\alpha}[\boldsymbol{\delta}] = \text{Cl}_{U'}[\boldsymbol{\delta}'_\alpha] - \text{Cl}_{U'}[\boldsymbol{\delta}]$$

$$\Delta\text{Cl}_{U'\beta}[\boldsymbol{\delta}] = \text{Cl}_{U'}[\boldsymbol{\delta}'_\beta] - \text{Cl}_{U'}[\boldsymbol{\delta}]$$

$$\Delta\text{Cl}_{U'\gamma}[\boldsymbol{\delta}] = \text{Cl}_{U'}[\boldsymbol{\delta}'_\gamma] - \text{Cl}_{U'}[\boldsymbol{\delta}]$$

$$\Delta\text{Cl}_{U'\eta}[\boldsymbol{\delta}] = \text{Cl}_{U'}[\boldsymbol{\delta}'_\eta] - \text{Cl}_{U'}[\boldsymbol{\delta}]$$

The potential effect of each transition on $\Sigma[\boldsymbol{\delta}]$ may thus be calculated as follows. Note that the differing range of values of n and U for which the analysis of each transition is valid are clearly stated in each case (see the end of Section 6.4.2 for further details of these validity conditions):

β -transition If $n \geq 3$ and $2 \leq U \leq n - 1$, we have:

$$\begin{aligned}\Delta\Sigma_\beta[\boldsymbol{\delta}] &= \frac{1}{n^2} \sum_{m=0}^{n-1} (\delta'_{\beta,m})^2 - \frac{1}{n^2} \sum_{m=0}^{n-1} (\delta_m)^2 \\ &= \frac{1}{n^2} [((\delta_j + 1)^2 + (\delta_i - 1)^2) - (\delta_j^2 + \delta_i^2)] \quad [\text{by (6.5)}] \\ &= \frac{2}{n^2} [\delta_j - \delta_i + 1]\end{aligned}\tag{6.28}$$

$$\therefore |\Delta\Sigma_\beta[\boldsymbol{\delta}]| \leq \frac{2}{n^2} [n - U - 1] \quad (*) \quad [\text{Table 6.2}] \tag{6.29}$$

$$< \frac{2}{n}, \quad \forall U \in \{2, \dots, n - 1\} \tag{6.30}$$

γ -transition If $n \geq 2$ and $1 \leq U \leq n - 1$, we have:

$$\begin{aligned}\Delta\Sigma_\gamma[\boldsymbol{\delta}] &= \frac{1}{n^2} \sum_{m=0}^{n-1} (\delta'_{\gamma,m})^2 - \frac{1}{n^2} \sum_{m=0}^{n-1} (\delta_m)^2 \\ &= \frac{1}{n^2} [(1^2 + (\delta_i - 1)^2) - (0^2 + \delta_i^2)] \quad [\text{by (6.6)}] \\ &= \frac{2}{n^2} [1 - \delta_i]\end{aligned}\tag{6.31}$$

$$\therefore |\Delta\Sigma_\gamma[\boldsymbol{\delta}]| \leq \frac{2}{n^2} [n - U] \quad (*) \quad [\text{Table 6.2}] \tag{6.32}$$

$$< \frac{2}{n}, \quad \forall U \in \{1, \dots, n - 1\} \tag{6.33}$$

η -transition If $n \geq 2$ and $2 \leq U \leq n$, we have:

$$\begin{aligned}\Delta\Sigma_\eta[\boldsymbol{\delta}] &= \frac{1}{n^2} \sum_{m=0}^{n-1} (\delta'_{\eta,m})^2 - \frac{1}{n^2} \sum_{m=0}^{n-1} (\delta_m)^2 \\ &= \frac{1}{n^2} [(0^2 + (\delta_k + 1)^2) - (1^2 + \delta_k^2)] \quad [\text{by (6.7)}] \\ &= \frac{2}{n^2} [\delta_k]\end{aligned}\tag{6.34}$$

$$\therefore |\Delta\Sigma_\eta[\boldsymbol{\delta}]| \leq \frac{2}{n^2} [n - U + 1] \quad (*) \quad [\text{Table 6.2}] \tag{6.35}$$

$$< \frac{2}{n}, \quad \forall U \in \{2, \dots, n\} \tag{6.36}$$

α -transition If $n \geq 3$ and $2 \leq U \leq n - 1$, we have:

$$\begin{aligned}\Delta\Sigma_\alpha[\boldsymbol{\delta}] &= \frac{1}{n^2} \sum_{m=0}^{n-1} (\delta'_{\alpha,m})^2 - \frac{1}{n^2} \sum_{m=0}^{n-1} (\delta_m)^2 \\ &= \frac{1}{n^2} [((\delta_j + \delta_i)^2 + 0^2) - (\delta_j^2 + \delta_i^2)] \quad [\text{by (6.8)}] \\ &= \frac{2}{n^2} [\delta_i \delta_j]\end{aligned}\tag{6.37}$$

$$\therefore |\Delta\Sigma_\alpha[\boldsymbol{\delta}]| \leq \frac{2}{n^2} \left\lfloor \frac{n-U+2}{2} \right\rfloor \left\lceil \frac{n-U+2}{2} \right\rceil \quad (*) \quad [\text{Table 6.2}] \tag{6.38}$$

$$\rightarrow \frac{1}{2} \text{ as } n \rightarrow \infty, \quad \forall U \in \{2, \dots, n-1\} \tag{6.39}$$

Note that, for all valid values of n and U , there exists a vector $\boldsymbol{\delta} \in \Delta^{n-1}$ and a particular transition of the appropriate type for which each of the upper bounds marked ‘(*)’ is actually attained (this follows from the derivation of the values in Table 6.2). For large systems (i.e. when $n \gg 1$), this fact is of fundamental importance for the following reason.

For any valid value of U , the least upper bounds of the maxima of the absolute values of the random variables $\Delta\Sigma_\beta[\boldsymbol{\delta}]$, $\Delta\Sigma_\gamma[\boldsymbol{\delta}]$ and $\Delta\Sigma_\eta[\boldsymbol{\delta}]$ (considered over all possible vectors $\boldsymbol{\delta}$ of population U) all go to 0 as $n \rightarrow \infty$ (consider (6.30), (6.33) and (6.36)). However, from (6.39), we see that the least upper bound of the maximum of the absolute value of the random variable $\Delta\Sigma_\alpha[\boldsymbol{\delta}]$ instead goes to $1/2$ as $n \rightarrow \infty$.

By (6.27), this implies that for all $\boldsymbol{\delta} \in \Delta^{n-1}$ of any population $U \in \{2, \dots, n-1\}$, the maxima of the absolute values of the random variables $\Delta\text{Cl}_{U'\beta}[\boldsymbol{\delta}]$, $\Delta\text{Cl}_{U'\gamma}[\boldsymbol{\delta}]$ and $\Delta\text{Cl}_{U'\eta}[\boldsymbol{\delta}]$ go to 0 as $n \rightarrow \infty$, $\forall U' \in \{2, \dots, n\}$. However, by (6.38), (6.39) and (6.27), there exists a $\boldsymbol{\delta} \in \Delta^{n-1}$ of population U , such that the maximum of the absolute value of the random variable $\Delta\text{Cl}_{U'\alpha}[\boldsymbol{\delta}]$ is greater than or equal to $(1/n^2) \lfloor (n-U+2)/2 \rfloor \lceil (n-U+2)/2 \rceil$, a quantity which goes to $1/4$ as $n \rightarrow \infty$.

In other words, as the number of cells in a one-dimensional single species \mathfrak{B} -model is increased, the maximum possible size of the effect of a single β , γ or η -transition on all the clumping measures $\text{Cl}_{U'}$, calculated at any population $U' \geq 2$, goes to zero. However, this is not true of α -transitions, which may produce ‘large’ changes in a clumping measure $\text{Cl}_{U'}$, even for arbitrarily large systems. What is more, we observe from (6.37) that this step is always positive; i.e. α -transitions always result in an increase in individual clumping.

What is more, if an α -transition causing a large positive change $2/n \ll \Delta\Sigma_\alpha < 1/2$ in $\Sigma[\boldsymbol{\delta}]$ were to occur in this system, we see from (6.30) and (6.33) that it would require more than $n(\Delta\Sigma_\alpha/2) \gg 1$ separate β and γ -transitions (η -transitions can only increase clumping, since, by (6.34), $\Delta\Sigma_\eta[\boldsymbol{\delta}] > 0$) to restore $\Sigma[\boldsymbol{\delta}]$ to its previous level (and, consequently, to restore all clumping measures $\text{Cl}_{U'}[\boldsymbol{\delta}]$ to their previous levels), even without the occurrence of further large α -transitions. Clearly, for systems in which n is large, this opens the possibility of a series of catastrophic α -transitions greatly increasing the level of clumping of the system, possibly leading it to a region of the state space in which large α -transitions are extremely rare or pushing it towards extinction.

These results provide a quantitative analogy of the observations of Section 6.4.3, in which it was noted that β , γ and η -transitions correspond to steps between adjacent points of the integer simplex Δ^{n-1} , while α -transitions may correspond to larger steps across the space.

6.6.4 Clumping measures and the mean field equation

In this section, we discuss the relationship between the clumping measures $\text{Cl}_{U'}$ and the mean field equation (see Section 5.2.2) in a bid to explain why a one-dimensional, single species \mathfrak{B} -model with $\alpha = 0$ behaves as the equation would predict, while a model with $\alpha \neq 0$ does not.

Recall that, given a microstate $\mathbf{c} \in \Omega_n$ with population U of a one-dimensional, single species \mathfrak{B} -model over n cells, corresponding to a vector $\boldsymbol{\delta} = \xi'(\psi(\mathbf{c})) \in \Delta^{n-1}$, the natural clumping measure $\text{Cl}[\boldsymbol{\delta}]$ is a positive real number in the interval $[0, 1]$ that describes the degree of clumping of the individuals in \mathbf{c} , given the current population U . This is of interest because we expect the degree of individual clumping to affect the behaviour of the system, since more highly clumped individuals will interact more frequently. Since the only true ‘interaction’ that is possible in a single species \mathfrak{B} -model is the death of an individual due to overcrowding by an adjacent individual (an η -transition), we expect more highly clumped systems to experience higher rates of η -transitions (relative to the other possible transition types), which will lead to a decrease in population density.

The mean field equation for the one-dimensional, single species \mathfrak{B} -model is based on the assumption that the states of each cell in the system may locally, at all times, be treated as independent identically distributed Bernoulli variables with parameter equal to the system density $u = U/n$ (see Section 6.4.4), and therefore that the behaviour of the system depends only on the density u (note that this assumption

directly contradicts the line of argument on the effect of individual clumping given in the previous paragraph). Clearly, for this assumption to be reasonable, n , U and $n - U$ must be large, since otherwise knowing the state of a particular cell could provide significant information about the density of individuals in the remaining cells, by simple counting arguments.

Loosely, we might also state that the mean field assumption requires that the degree of clumping of individuals remains broadly constant over time, maintaining a level at which the states of adjacent cells appear to be independent. If this were not the case, and the system were to become more clumped over time (or indeed less clumped, though this situation will not be relevant to our argument), correlations would be observed between the states of nearby cells and the requirement that cells be considered locally independent would be invalid.

We will demonstrate that a system occupying the apparent equilibrium described by the mean field equation, whose individuals are distributed in such a way that the assumptions necessary for the validity of the equation are consistent with the current microstate, as represented by the vector $\boldsymbol{\delta}$, may be considered stable under the influence of β , γ and η -transitions, in the sense that its degree of clumping is subject only to random drift, but is not stable if α -transitions are also admitted, since the system will then tend to become systematically more clumped over time.

To see this, first consider some scalar variable p which evolves according to the system dynamics (such as, for example, u , U , $\Sigma[\boldsymbol{\delta}]$ or $\text{Cl}_{17}[\boldsymbol{\delta}]$). For the sake of clarity, we will refer to p as a “descriptor”, since we suppose that it describes the current state of the system in some way.

Observe that, given some vector $\boldsymbol{\delta} \in \Delta^{n-1}$ representing the current state of the system, the expected change in p over a single iteration, denoted by Δp , is described by the following equation:

$$\begin{aligned} E[\Delta p] = u [& P[\delta > 1 \mid \delta > 0] (\beta E[\Delta p_\beta] + \gamma E[\Delta p_\gamma] + \alpha E[\Delta p_\alpha]) \\ & + P[\delta = 1 \mid \delta > 0] (\eta E[\Delta p_\eta])] \end{aligned} \quad (6.40)$$

In this equation, Δp is a random variable representing the change in p as a result of a single transition (possibly null), δ is a random variable representing the result of a random uniform selection over all terms of $\boldsymbol{\delta}$ (see Section 6.4.4), Δp_β , Δp_γ , Δp_α and Δp_η are random variables representing the change in p resulting from a particular transition of the given kind, while E refers to the expectation of a random variable, as usual. We reiterate that the distributions of all these variables are dependent on

the current state of the system, as represented by the vector $\boldsymbol{\delta}$. Note also that, in writing (6.40), we have used the fact that $P[\delta > 0] = u$.

Observe that, when $p = u$, (6.40) becomes:

$$E[\Delta u] = \frac{1}{n} u [(\gamma - \alpha) - P[\delta = 1 \mid \delta > 0](\gamma - \alpha + \eta)] \quad (6.41)$$

If we further assume that $P[\delta = 1 \mid \delta > 0] = u$ (equivalent to the mean field assumption that cell states can locally be treated as independent Bernoulli random variables with parameter u), then (6.41) may be used to derive the mean field equation (5.1).

However, (6.40) holds for any descriptor p and does not require any assumptions on $\boldsymbol{\delta}$. In particular, it holds for $p = \Sigma[\boldsymbol{\delta}]$, a quantity that is directly related to individual clumping, as discussed in Section 6.5.4, since all clumping measures $Cl_{U'}$ are strictly increasing in $\Sigma[\boldsymbol{\delta}]$.

So, using the notation of Section 6.6.3, the results (6.28), (6.31), (6.34) and (6.37), and letting $P = P[\delta = 1 \mid \delta > 0]$, we have:

$$\begin{aligned} & E[\Delta \Sigma] \\ &= u [(1 - P)(\beta E[\Delta \Sigma_\beta] + \gamma E[\Delta \Sigma_\gamma] + \alpha E[\Delta \Sigma_\alpha]) + P(\eta E[\Delta \Sigma_\eta])] \\ &= \frac{2}{n^2} u [(1 - P)(\beta E[\delta_j - \delta_i + 1] + \gamma E[1 - \delta_i] + \alpha E[\delta_j \delta_i]) + P(\eta E[\delta_k])] \\ &= \frac{2}{n^2} u [(1 - P)(\beta E[\delta_j - \delta_i] - \gamma E[\delta_i] + \alpha E[\delta_j \delta_i] + \beta + \gamma) + P(\eta E[\delta_k])] \end{aligned} \quad (6.42)$$

Up to this point, no assumptions have been made and (6.42) describes the true expected change in $\Delta \Sigma$ for any $\boldsymbol{\delta} \in \Delta^{n-1}$, provided only that the basic validity conditions of (6.28), (6.31), (6.34) and (6.37) are satisfied, namely that $n \geq 3$ and that $2 \leq U \leq n - 1$. In general, however, the expectations in (6.42) cannot be determined without knowledge of $\boldsymbol{\delta}$ (up to its equivalence class).

We wish to understand how the clumping of the system would be likely to change if the distribution of individuals throughout the system were consistent with the mean field assumptions. As we have discussed, under these assumptions, it is assumed that $P[\delta = 1 \mid \delta > 0] = u$, while the various expectations that feature in (6.42) were discussed in Section 6.4.4, with the appropriate values given in Table 6.3. Substituting this information into (6.42), we therefore have:

$$\begin{aligned} \mathbb{E}[\Delta\Sigma] &= \frac{2}{n^2}u \left[(1-u) \left(-\beta - \gamma \left(\frac{1+u}{u} \right) + \alpha \left(\frac{1+u}{u^2} \right) + \beta + \gamma \right) + u\eta \frac{1}{u} \right] \\ &= \frac{2}{n^2} \left[u(\gamma + \eta - \alpha) - \gamma + \frac{1}{u}\alpha \right] \end{aligned} \quad (6.43)$$

So, (6.43) describes the expected change in $\Delta\Sigma$ for a \mathfrak{B} -model in which the distribution of individuals is, at least instantaneously, consistent with the mean field assumptions. Now, in this scenario, examine the value of $\Delta\Sigma$ at the non-trivial mean field equilibrium given in (5.3):

$$\begin{aligned} \mathbb{E}[\Delta\Sigma] &= \frac{2}{n^2} \left[\left(\frac{\gamma - \alpha}{\gamma - \alpha + \eta} \right) (\gamma + \eta - \alpha) - \gamma + \left(\frac{\gamma - \alpha + \eta}{\gamma - \alpha} \right) \alpha \right] \\ &= \frac{2}{n^2} \left[\frac{\alpha\eta}{\gamma - \alpha} \right] \end{aligned} \quad (6.44)$$

If $\gamma \leq \alpha$, the non-trivial equilibrium of the mean field equation does not exist ($u = 0$ is the only valid fixed point), while if $\eta = 0$ then the non-trivial equilibrium is $u = 1$ and the behaviour of the system is simple (see Section 5.3.4). So, for the cases of interest, with $\eta \neq 0$ and $\gamma > \alpha$, (6.44) shows us that a system whose density is equal to the non-trivial equilibrium density predicted by the mean field equation and whose individuals are distributed in such a way as to be consistent with the mean field assumptions, can only be expected to remain in equilibrium if $\alpha = 0$. Otherwise, we would expect to see an increase in the value of $\Sigma[\delta]$, implying an increase in $\text{Cl}_{U'}[\delta]$ at all populations U' , leading to a likely increase of correlations between the states of nearby cells and a consequent breakdown in the validity of the mean field assumptions, at least at iterations when the population density is close to the predicted mean field ‘equilibrium’.

What, if anything, then can be said about the non-trivial equilibrium density of a single species \mathfrak{B} -model with $\eta \neq 0$ and $\gamma > \alpha > 0$, if it exists? To answer this question, we return to equation (6.41), which describes the expected change in the population density u without invoking the mean field assumptions. From this equation, we see that for a non-trivial equilibrium, in the continuum limit as $n \rightarrow \infty$, we must have:

$$\mathbb{P}[\delta = 1 \mid \delta > 0] = \frac{\gamma - \alpha}{\gamma - \alpha + \eta} \quad (6.45)$$

Note, that the right hand side of this equation is equal to the non-trivial equilibrium density u_1^* predicted by mean field analysis (see (5.3)).

Now, our earlier analysis suggests that the degree of clumping in a system with $\alpha > 0$ will likely increase above a level which is consistent with the mean field assumptions. This means that we would expect to see correlations developing between the states of nearby cells. In particular, we would expect that $P[\delta = 1 | \delta > 0]$, which represents the probability that a given neighbour of an occupied cell will also be occupied, would exceed the overall population density u .

Therefore, for a one-dimensional, single species \mathfrak{B} -model with $\eta \neq 0$ and $\gamma > \alpha > 0$, we would expect that the density u at a non-trivial equilibrium should satisfy the inequality:

$$u < \frac{\gamma - \alpha}{\gamma - \alpha + \eta} \quad (6.46)$$

In other words, we would expect the equilibrium value of u to be less than the value u_1^* predicted by the mean field equation.

This conclusion is supported by the results of the simulation experiments, as presented in Figure 5.23, in which many such systems with $\alpha > 0$ were observed in which the population converged to an equilibrium value below that predicted by mean field analysis.

6.7 Summary and conclusions

In this chapter, we have performed a thorough investigation into the fundamental differences between the effects of the possible transitions in the one-dimensional, single species \mathfrak{B} -model. This work built upon the conclusions of Chapter 5, in which it was observed that, for models with $\eta \neq 0$ (models where $\eta = 0$ display very simple behaviour), those with $\alpha = 0$ exhibited behaviour in line with the predictions of mean field theory, while those with $\alpha \neq 0$ did not. Based on a consideration of space-time plots of the model dynamics and of autocorrelations of the cell states in microstates drawn from model simulations, it was conjectured that this difference was due to a propensity of α -transitions to produce spatial clumping in the distribution of individuals, while β , γ and η -transitions were instead conducive to good mixing of individuals throughout the system. Our aim was to explain the causal mechanisms responsible for this difference in the effects of the different possible transitions.

As a starting point towards achieving this goal, in Section 6.2, we observed that β , γ and η -transitions can be considered ‘reversible’, in the sense that any such transition may be reversed at the next iteration by means of a particular β , γ or η -transition, operating on the same pair of cells. However, we observed that the effect of an α -transition cannot, in general, be reversed by a single transition in this way. Hence, α -transitions can be considered to operate as local catastrophes, whose effects cannot be easily undone.

In Section 6.3, in order to make further progress with our investigation of the effects of different transitions, we transformed the microstates of the one-dimensional, single species \mathfrak{B} -model into a new space, in which key features of the dynamics would be easier to observe and analyse. More specifically, rather than representing microstates as binary vectors (or binary periodic sequences) as would be usual, we instead chose to represent them as points $\boldsymbol{\delta}$ of the integer simplex Δ^{n-1} , whose non-zero terms represented the distances between consecutive occupied cells of the true microstates of the system. It was also observed that, in order to comprehensively represent the dynamics of the system over Δ^{n-1} , it was only necessary to know $\boldsymbol{\delta}$ up to its current equivalence class given translations and reflection of the order of its terms.

Having defined the relationship between the model state space Ω_n and the integer simplex Δ^{n-1} , in Section 6.4 we examined the precise effect of each of the transition types, α , β , γ and η , on the terms of the vector $\boldsymbol{\delta}$, representing the current state of the system. These terms were first considered as fixed quantities and then as random variables, whose distribution was defined by the stochastic cell-selection process common to all \mathfrak{B} -models. The maximum and minimum values of various key terms and combinations of terms were identified and their expectations were determined under the mean field assumptions. The effects of the different transition in Δ^{n-1} were also visualised in some fairly simple cases, allowing for the important observation that β , γ and η -transitions correspond to single steps between adjacent points of the integer simplex, while α -transitions may correspond to much larger steps between non-adjacent points.

In Section 6.5, we introduced a family of clumping measures $\text{Cl}_{U'}[\boldsymbol{\delta}] \in [-1, 1]$ related to the empirical standard deviation of the terms of $\boldsymbol{\delta}$, in order to allow for a quantitative analysis of the effect of different transitions on the spatial distribution of individuals throughout the system. The clumping measure for which U' is equal to the current population U was designated the “natural clumping measure”, $\text{Cl}[\boldsymbol{\delta}]$, and it was observed that this quantity had a geometrical interpretation as a measure

of the position of $\boldsymbol{\delta}$ relative to other key points of the integer simplex Δ^{n-1} . It was thus observed that the possible large steps across Δ^{n-1} induced by α -transitions would correspond to large increases in individual clumping.

Finally, in Section 6.6, the results of the rest of the chapter were combined to provide a quantitative answer to the question of why α -transitions alone are incompatible with the behaviour predicted by the mean field equations. To do this, we determined the magnitude of the effect of each of the four possible transitions on the clumping measures $\text{Cl}_{U'}[\boldsymbol{\delta}]$. It was observed that while β , γ and η -transitions gave rise to changes in $\text{Cl}_{U'}[\boldsymbol{\delta}]$ of order not exceeding $n^{-1/2}$, α -transitions could induce similar changes of absolute value approximately equal to $1/4$, with the latter always leading to increases in clumping. This result demonstrated that, for large n , a single α -transition could cause an increase in clumping that could only be reversed by a large number of separate β and γ -transitions.

Ultimately, we were able to draw a direct link between mean field analysis and the clumping measures $\text{Cl}_{U'}[\boldsymbol{\delta}]$, demonstrating that a model for which $\eta \neq 0$ and $\gamma > \alpha > 0$, whose instantaneous density was equal to the non-trivial equilibrium predicted by mean field theory u_1^* and whose instantaneous microstate was consistent with the mean field assumptions, would be expected to display an increase in individual clumping, leading to a corresponding increase in the correlations of local cell states and a consequent breakdown in the validity of the mean field assumptions. We further demonstrated that the equilibrium density of such a system should be less than u_1^* , a conclusion that is confirmed by the experiments conducted in Chapter 5.

Thinking more broadly about these results and their wider relevance, we suggest that they should essentially be seen as a proof of concept for further work. Clearly, the system under consideration, the one-dimensional, single species \mathfrak{B} -model, is extremely simple and much of the analysis conducted here has used methods developed specifically for use with this model. However, we have demonstrated that considering the dynamics of an individual-based model of this kind from an alternative mathematical perspective (in this case, through transformation to a new space in which individual clumping could be more easily analysed and in which key equivalence classes of the microstates could be tracked geometrically) can be fruitful in terms of determining the mechanisms linking local interactions with global behaviour, a key goal in the field of agent-based and individual-based modelling and of complexity science more generally, as discussed in Section 2.2.8. Moreover, as a special case of the ecological patch models discussed in Section 3.3.3, \mathfrak{B} -models are an important

focus of study in their own right, since any theoretical results derived from these systems could ultimately allow for a deeper understanding of the real world systems that such patch models are used to represent.

In the next part of this thesis, we take on a new perspective, moving from a consideration of individuals as simple automata to an examination of individuals as decision-making agents. Rather than investigating the impact that spatial factors, such as individual clumping, can have on the global behaviour of an IBM, we instead consider the relationship between the structure of a space and the relative strategic value of the points within it, from the point of view of a particular individual. This shift in focus also necessitates a change of modelling paradigm, from individual-based modelling to game theory.

Part III

A general framework for static, spatially explicit games of search and concealment

Chapter 7

Background and motivation

The material in Chapters 7-9 is adapted from the article *Static search games played over graphs and general metric spaces*, published in the *European Journal of Operational Research* (Oléron Evans and Bishop, 2013).

Please note that, beyond the use of standard mathematical symbols, there is no crossover of notation between Parts II and III.

7.1 Introduction to Part III

In Part II, we considered a simple IBM to analyse the ways in which local interactions between individuals influenced the character of the global behaviour of a particular system. The key feature underlying this analysis was spatial structure. In the conclusions to Part II, presented at the end of Chapter 6, it was the crucial influence of different local transitions on the spatial distribution of individuals throughout the system that was seen to determine whether or not the global dynamics would be in line with the predictions of mean field theory.

In Part III, we change our perspective. Rather than seeking to understand how local interactions influence behaviour over a given geography, we consider a scenario in which individual behaviour may be controlled and where the key is to determine how different spatial structures will influence the strategy employed when attempting to optimise this behaviour. While the individuals in the previous model were essentially just parts of an aggregated stochastic automaton, we now examine individuals that possess genuine agency, using game theory to study a connection between local spatial structure and global strategy.

To achieve this, we will define a general search and concealment game that takes full account of the spatial structure of the set over which it is played. The game is

static in the sense that players do not move, but deploy simultaneously at particular spatial points and receive payoffs based on their relative positions. In this way, the Static Spatial Search Game (SSSG) provides a theoretical foundation for the study of the relative strategic value of different positions in a geography. Using the theory of metric spaces, we model situations in which the searching player may simultaneously search multiple locations based on concepts of distance or adjacency relative to the point at which they are deployed.

The SSSG was inspired by the “geometric games” of Ruckle (1983) and particularly by White’s “games of strategy on trees” (1994), of which this work may be seen as a significant generalisation. However, while the SSSG certainly builds upon previous work, its simplicity and generality together with its explicit consideration of spatial structure set it apart from much of the literature (see Section 7.3 for a detailed review of related work) and lend it the versatility to describe games over a huge variety of different spaces. The primary contributions of this work are therefore to both propose a highly general model of spatial search and concealment situations, which unites several other games presented in the literature (see Section 8.2.2), and to present new propositions and approaches for the strategic analysis of such scenarios.

While the approach presented here is theoretical in nature, the SSSG provides a framework for the analysis of a diverse range of operational research questions. Aside from explicit search and concealment scenarios, the game may be used to model situations in which some structure or region must be protected against ‘attacks’ that could arise at any spatial point; for example, the deployment of security personnel to protect cities against terrorist attacks or outbreaks of rioting, security software scanning computer networks to eliminate threats, the defence of shipping lanes against piracy, the protection of a rail network against cable theft or the deployment of stewards at public events to respond to emergency situations.

In this chapter, we provide a brief overview of all necessary game theoretic concepts and a review of the literature on games of search and security. Then, in Chapter 8, we formally define the SSSG, examine its relationship to other games in the literature and present some initial propositions relating to its strategies. We then restrict our attention to the case of the SSSG played on a graph (the “Graph Search Game” or GSG) and identify upper and lower bounds on the value of such games.

Chapter 9 explores several different methods for the analysis and solution of GSGs, starting with an algorithmic approach that employs the iterated elimination of dom-

inated strategies, with a particular focus on games played on trees. Further results include a way to simplify GSGs through consideration of graph automorphisms and an examination of a particular type of strategy for such games, which we describe as an “equal oddments strategy”. The concept of an equal oddments strategy is then used to find analytic solutions for a particular family of GSGs.

Finally, Chapter 10 extends the SSSG to encompass situations in which the points of the underlying geography can be assigned non-uniform values. This extension is used to determine strategies of optimal random patrol for a player attempting to protect a particular space from an infiltrator.

7.2 Game theoretic concepts

The definitions and notation relating to game theory used in this section are adapted from Blackwell and Girshick (1979) and Morris (1994).

When discussing two-player games, we assume the following definition:

Definition 7.2.1. A *two-player game in normal form* between Players A and B, consists of:

- *strategy sets* Σ_A, Σ_B
- *payoff functions* p_A, p_B , with:

$$\begin{aligned} p_A : \Sigma_A \times \Sigma_B &\rightarrow \mathbb{R} \\ p_B : \Sigma_A \times \Sigma_B &\rightarrow \mathbb{R} \end{aligned}$$

If the payoffs are such that for some constant c :

$$p_A(x, y) + p_B(x, y) = c, \quad \forall x \in \Sigma_A, \forall y \in \Sigma_B$$

then the game is described as a *constant-sum game*.

The game is played by Players A and B simultaneously choosing **strategies** (described as **pure strategies** in cases where there may be any ambiguity with mixed strategies, described below) from their respective strategy sets $x \in \Sigma_A, y \in \Sigma_B$ and receiving payoffs $p_A(x, y), p_B(x, y)$. The objective of each player is to maximise their payoff.

If Σ_A and Σ_B are finite, with:

$$\begin{aligned}\Sigma_A &= \{x_1, \dots, x_{\kappa_A}\} \\ \Sigma_B &= \{y_1, \dots, y_{\kappa_B}\}\end{aligned}\tag{7.1}$$

for some positive integers κ_A, κ_B , then it is often convenient to collect the payoffs to each player in **payoff matrices**:

$$\begin{aligned}\mathfrak{P}_A &= (p_A(x_i, y_j))_{i \in \{1, \dots, \kappa_A\}, j \in \{1, \dots, \kappa_B\}} \\ \mathfrak{P}_B &= (p_B(x_j, y_i))_{i \in \{1, \dots, \kappa_B\}, j \in \{1, \dots, \kappa_A\}}\end{aligned}\tag{7.2}$$

Note that, as defined here, the rows of each matrix correspond to the strategies of the player receiving the relevant payoffs, while the columns correspond to the strategies of their opponent.

In certain circumstances, we may allow players to adopt **mixed strategies**, whereby they choose their pure strategy according to a specified probability distribution. If the strategy sets are finite, as given in (7.1), the mixed strategies σ_A, σ_B can simultaneously be regarded as vectors:

$$\begin{aligned}\sigma_A &= (\sigma_A[x_1], \dots, \sigma_A[x_{\kappa_A}]) \in [0, 1]^{\kappa_A} \\ \sigma_B &= (\sigma_B[y_1], \dots, \sigma_B[y_{\kappa_B}]) \in [0, 1]^{\kappa_B}\end{aligned}$$

and as functions, which allocate probabilities to pure strategies:

$$\sigma_A : \Sigma_A \rightarrow [0, 1]$$

$$x \mapsto \sigma_A[x]$$

$$\sigma_B : \Sigma_B \rightarrow [0, 1]$$

$$y \mapsto \sigma_B[y]$$

$$\sum_{x \in \Sigma_A} \sigma_A[x] = \sum_{y \in \Sigma_B} \sigma_B[y] = 1$$

The following definitions relate to the maximum expected payoff that players can guarantee themselves through careful choice of their mixed strategies:

Definition 7.2.2. Given a two-player game, the **values of the game** u_A , u_B to Players A and B respectively, are defined as:

- $u_A = \max_{\tau_A} \min_{\tau_B} E[p_A(\tau_A, \tau_B)]$
- $u_B = \max_{\tau_B} \min_{\tau_A} E[p_B(\tau_A, \tau_B)]$

where τ_A and τ_B range across all possible mixed strategies for Players A and B respectively and

$$\begin{aligned} E[p_A(\tau_A, \tau_B)] \\ E[p_B(\tau_A, \tau_B)] \end{aligned}$$

represent the expected payoffs to each player, given that they respectively adopt mixed (or pure) strategies τ_A and τ_B .

Definition 7.2.3. Given a two-player constant-sum game, where the payoffs sum to $c \in \mathbb{R}$, mixed strategies σ_A , σ_B for Players A and B are described as **optimal mixed strategies** (OMSs) if and only if:

- $\min_{\tau_B} E[p_A(\sigma_A, \tau_B)] = u_A$
- $\min_{\tau_A} E[p_B(\tau_A, \sigma_B)] = u_B$

where τ_A and τ_B range across all possible mixed strategies for Players A and B respectively.¹

For a constant-sum game, where the payoffs sum to $c \in \mathbb{R}$, we have:

$$u_A + u_B = c \quad (7.3)$$

Also, provided that Σ_A and Σ_B are finite, OMSs are guaranteed to exist for both players.

Both of these facts are consequences of the Minimax Theorem (see Morris, 1994, p. 102).

Given a constant-sum two-player game with finite strategy sets, a **solution** of the game comprises OMSs σ_A , σ_B and values u_A , u_B for each player.

The following definition allows for a crude comparison of the efficacy of different strategies.

¹ Note that, under this definition, it is possible for a mixed strategy to be simultaneously optimal and inadmissible (weakly dominated by some other strategy, in the sense of Definition 7.2.4). While some authors restrict the definition of an optimal mixed strategy to prohibit such cases, we follow the example of Morris (1994, p. 44), who does not.

Definition 7.2.4. Consider a two-player game with strategy sets Σ_A , Σ_B and payoff functions p_A , p_B . Given particular pure strategies $x_1, x_2 \in \Sigma_A$ for Player A, we have:

- x_2 **very weakly dominates** x_1 if and only if:

$$p_A(x_2, y) \geq p_A(x_1, y), \quad \forall y \in \Sigma_B$$

- x_2 **weakly dominates** x_1 if and only if:

$$p_A(x_2, y) \geq p_A(x_1, y), \quad \forall y \in \Sigma_B$$

and $\exists y^* \in \Sigma_B$ such that:

$$p_A(x_2, y^*) > p_A(x_1, y^*)$$

- x_2 **strictly dominates** x_1 if and only if:

$$p_A(x_2, y) > p_A(x_1, y), \quad \forall y \in \Sigma_B$$

- x_2 is **equivalent** to x_1 if and only if:

$$p_A(x_2, y) = p_A(x_1, y), \quad \forall y \in \Sigma_B$$

Since the designation of the players as A and B is arbitrary, obtaining corresponding definitions of strategic dominance and equivalence for Player B is simply a matter of relabelling.

Note that weak dominance, strict dominance and equivalence are all special cases of very weak dominance. Also, strict dominance is a special case of weak dominance.

In the work presented in the following chapters, weak dominance is of most relevance. Therefore, for reasons of clarity, the terms “dominance” and “dominated strategies” will be used to refer to weak dominance unless otherwise stated.

Since a player aims to maximise his or her payoff, we would intuitively expect that they should not play any dominated strategies. Indeed, it is known that any strategy that is strictly dominated by some other strategy must be allocated zero probability in an OMS (see, for example, Theorem 2.9 in Morris, 1994, p. 49), though this is not necessarily true of weakly or very weakly dominated strategies.

For a general definition of dominance in game theory, see Leyton-Brown and Shoham (2008, pp. 20-23), from which the above definition was adapted.

7.3 Games of search and security: A review

7.3.1 Simple search games

Games of search and concealment, in which one player attempts to hide themselves or to conceal some substance in a specified space while another player attempts to locate or capture the player or substance, have been widely studied. One of the simplest search games is the well-known high-low number guessing game in which one player chooses an integer in a given range, while the other player makes a sequence of guesses to identify it, each time being informed whether the guess was too high or too low (Gal, 1974). Continuous versions of the game have also been studied (Gal, 1978; Baston and Bostock, 1985; Alpern, 1985).

Another simple search game involves one player attempting to locate an object that the opposing player has hidden at a location chosen from a finite or countably infinite set with no spatial structure (except a possible ordering). Variants of these games include examples where the searching player has some chance of overlooking the object despite searching the correct location (Neuts, 1963; Subelman, 1981) or where the searcher must simultaneously avoid the location of a second hidden object (Ruckle, 1990).

7.3.2 Search games with immobile targets

A more complicated class of search games is that in which the searching player is mobile and their target is immobile, with payoffs to each player typically (though not universally) being dependent on the amount of time that elapses (or the distance travelled) before the target is located. Such games have been examined over many different types of graph (Anderson and Aramendia, 1990; Reijnierse and Potters, 1993; Kikuta and Ruckle, 1994; Buyang, 1995; Pavlović, 1995; Kikuta, 2004; Alpern, 2008, 2010), though in the most general case the space may be a continuous region (Gal, 1979). While the starting position of the searching player is often fixed, games in which the searching player can choose their position have also been studied (Alpern et al., 2008a; Dagan and Gal, 2008), as have games with multiple searchers (Alpern and Reyniers, 1994; Alpern and Howard, 2000).

7.3.3 Accumulation games

Accumulation games are an extension of the above concept in which there may be many hidden objects (Kikuta and Ruckle, 1997) or in which hidden objects are replaced with some continuous material that the hiding player can distribute across a set of discrete locations (Kikuta and Ruckle, 2002; Zoroa et al., 2004) or across a continuous space (Ruckle and Kikuta, 2000). The payoffs in these games are typically dependent on the number of objects or the quantity of material that the searching player is able to locate.

7.3.4 Search games with mobile targets

Adding a further layer of complication, there is the class of search game in which both the searching player and the hiding player are mobile, including so-called “princess and monster” games. Again, the payoffs in such games are typically dependent on the amount of time that elapses before the hiding player is captured and players are typically ‘invisible’ to each other, only becoming aware of the location of their opponent at the moment of capture.

Such games have been considered over continuous one-dimensional spaces such as the circle (Alpern, 1974) and the unit interval (Alpern et al., 2008b), over continuous graphs or networks (Alpern and Asic, 1986; Anderson and Aramendia, 1992; Alpern and Asic, 1985) and over continuous two-dimensional spaces (Foreman, 1977; Garnaev, 1991; Chkhartishvili and Shikin, 1995). In the latter case, it is necessary to introduce the concept of a *detection radius*, with a capture occurring if the distance between the players drops below this value. In some cases, the probability of capture is allowed to vary based on the distance between the players (Garnaev, 1992).

Analyses of search games over discrete spaces in which both searcher and hider are mobile have tended to consider spatial structure in only a very limited way. While this structure may determine the freedom of movement of the players, very little work has been done to introduce an analogous concept to the detection radius to such games. Generally, players move sequentially and may only move to locations that are sufficiently close to their current position (e.g. Eagle and Washburn, 1991), though variants have been considered in which either the searching player (Zoroa et al., 2012) or the hiding player (Thomas and Washburn, 1991) has the freedom to move to any location regardless of adjacency or distance.

Further variations on the search game with mobile searcher and hider include games in which the searching player follows a predetermined path and must decide how

thoroughly to search each location visited (Hohzaki and Iida, 2000), games in which the searching player must intercept an opponent attempting to move from a given start point to a given end point (Alpern, 1992) and games with a variegated environment and the possibility that the hiding player will be betrayed by ‘citizens’ of the space (Owen and McCormick, 2008). Such games have also been used to model predator-prey interactions (Alpern et al., 2011a).

7.3.5 Allocation games

Allocation games are a related concept, in which the searching player does not move around the space individually, but rather distributes ‘search resources’ to locate the mobile hiding player. Such games may include false information (Hohzaki, 2007) and may incorporate spatial structure by allowing the influence of resources to spread across space (“reachability”), an area which has seen “little research” (Hohzaki, 2008).

Variations on this idea include situations in which searching resources are deployed sequentially (Dendris et al., 1997) or in which both players distribute resources to respectively locate or protect a hidden object (Baston and Garnaev, 2000). Cooperative allocation games, in which multiple players combine their searching resources to locate a moving target, have also been considered (Hohzaki, 2009).

7.3.6 Rendez-vous games

Rendez-vous games are a parallel concept to games with mobile searching and hiding players, the difference being that these games are cooperative, with both players wishing to locate the other as soon as possible (see Alpern, 2002, for an overview). Typically, in a rendez-vous game, the structure of the space is known to all, with consideration given to the amount of information available to players regarding their relative positions, and their ability to distinguish between symmetries of the space (whether they have a common understanding of “North”, for example).

Rendez-vous games have been studied over various continuous one-dimensional spaces, such as the line (Alpern and Gal, 1995; Lim and Alpern, 1996; Alpern and Beck, 2000) and the circle (Alpern, 2000), over continuous two-dimensional spaces, such as the plane (Kikuta and Ruckle, 2010) or a general compact metric space (Alpern, 1995) and over discrete spaces, such as lattices (Alpern and Baston, 2005; Ruckle, 2007) and other graphs (Alpern et al., 1999). Costs may also be introduced for movement and examination of particular locations (Kikuta and Ruckle, 2007).

Work has also been done on ‘hybrid’ games of search and rendez-vous, where, for example, two individuals attempt to meet without being located by a third (Alpern and Lim, 1998) or where the searching player does not know whether the other player is attempting to rendez-vous or to evade capture (Alpern and Gal, 2002).

7.3.7 Security games

Security games are used to model situations in which some public resource (e.g. airports, transport infrastructure, power facilities) must be protected from attack with limited defensive resources. A good introduction to the topic is provided by Tambe (2012).

Such situations tend to be modelled as Stackelberg games, where it is assumed that the defensive player first commits to some strategy to protect the vulnerable sites and that this strategy is observed by the attacking player, who then chooses an optimal response (Tambe, 2012, pp. 4-8). Stackelberg-type security games related to the mobile-searcher-immobile-hider games of Section 7.3.2 have also been proposed to examine optimal patrolling strategies (Alpern et al., 2011b; Basilico et al., 2012).

A related concept is that of the much studied Colonel Blotto game, in which two players must simultaneously distribute a fixed quantity of discrete or continuous resources across a number of sites, each site being ‘won’ by the player who distributed the greater quantity of resources to it, with payoffs determined by the number of sites that each player wins (see Roberson, 2006). The many extensions of the Colonel Blotto game have included asymmetric versions (Tofias et al., 2007; Hortala-Vallve and Llorente-Saguer, 2012), examples in which resources are allocated to battlefields sequentially rather than simultaneously (Powell, 2009) and examples in which defensive resources are heterogeneous (Cohen, 1966).

Though the deployment sites in such models are often assumed to be wholly separate, with events at one location having no effect on events at other locations, certain security games and Colonel Blotto-type games with strategically interdependent sites have been considered. For example, Shubik and Weber (1981) introduce the concept of a “characteristic function” for such games, which allocates values to subsets of the sites, thus allowing interdependencies to be captured. Other approaches to modelling such interdependence include an extension of the Colonel Blotto game in which a successful attack on a “radar site” ensures the success of attacks on other sites (Grometstein and Shoham, 1989), while Hausken (2010, 2011) discusses a classification of the underlying infrastructures of security games based on the interdependence of their sites (series, parallel, complex, ...) and Powell (2007) anal-

yses the relative value of defending borders over protecting strategic targets directly.

Though analyses of interdependence in security games and Blotto games may be quite general (that of Shubik and Weber, for example), interdependence that arises explicitly from the spatial structure of the deployment sites has not been considered in a general setting.

7.3.8 Geometric games

One of the most general and theoretical analyses of search and concealment type situations is Ruckle's *Geometric games and their applications* (1983). In this book, the author defines a geometric game as a two-player zero-sum game (with players called "RED" and "BLUE") played over a given set S , where the strategy sets for each player $\Sigma_{\text{RED}}, \Sigma_{\text{BLUE}}$ are subsets of the power set $\mathcal{P}(S)$ (the set of subsets of S). Pure strategies for each player are therefore subsets $R, B \subseteq S$. The payoff to each player is a function of R and B , typically depending directly on the intersection $R \cap B$.

This concept of a geometric game allows Ruckle to model a wide variety of situations of search, ambush and pursuit, as well as a range of abstract games, taking full consideration of the structure of the space S over which the games are played.

Most published work based on Ruckle's ideas (e.g. Baston et al., 1989; Zoroa and Zoroa, 1993; Zoroa et al., 1999a, Zoroa et al., 1999b, 2001, 2003; Alpern et al., 2009, 2010) has focused on specific examples of geometric games, rather than on general results.

7.4 Motivation for the Static Spatial Search Game

Much of the literature on search games and related concepts has focused on analysing specific games, rather than attempting to present general frameworks for such situations and identifying more broadly applicable results. While spatial structure may be considered for games in which players are mobile, the geography of the space over which games are played is often given little or limited consideration, particularly in the literature on security games. The concept of "reachability", as described by Hohzaki (2008), in which a searcher or searching resource deployed at a point has influence over a local neighbourhood, has received very little attention. Games that concentrate purely on the strategic value of a player's chosen position in a space, rather than on strategies for moving through the space for the purposes of search or rendez-vous, have also seen little research, at least since the work of Ruckle (1983).

Chapter 8

Defining and analysing spatial games

8.1 Introduction

In this chapter, taking into account the conclusions discussed in Section 7.4, we focus on the third of our research objectives (see Section 1.5), defining a general game that forms a basis for modelling situations of static search and concealment over regions with spatial structure. We examine the concepts of strategic dominance and equivalence in the context of this game, before focusing on the more specific case of games played over graphs. Methods to simplify the analysis of these games are presented and upper and lower bounds on the value of the game to each player are identified.

8.2 The Static Spatial Search Game (SSSG)

The definitions and notation relating to metric spaces used in this section are from Sutherland (1975), pp. 19-44.

8.2.1 Definition of the SSSG

The Static Spatial Search Game (SSSG) is a two-player game played over a metric space $M = (\Omega, d)$, where Ω is a set of points x and $d : \Omega \times \Omega \rightarrow [0, \infty)$ is the metric or distance, which has the standard properties:

- $$\begin{aligned} (M1) \quad & d(x, y) \geq 0 ; & d(x, y) = 0 \Leftrightarrow x = y \\ (M2) \quad & d(x, y) = d(y, x) , & \forall x, y \in \Omega \\ (M3) \quad & d(x, y) + d(y, z) \geq d(x, z) , & \forall x, y, z \in \Omega \end{aligned}$$

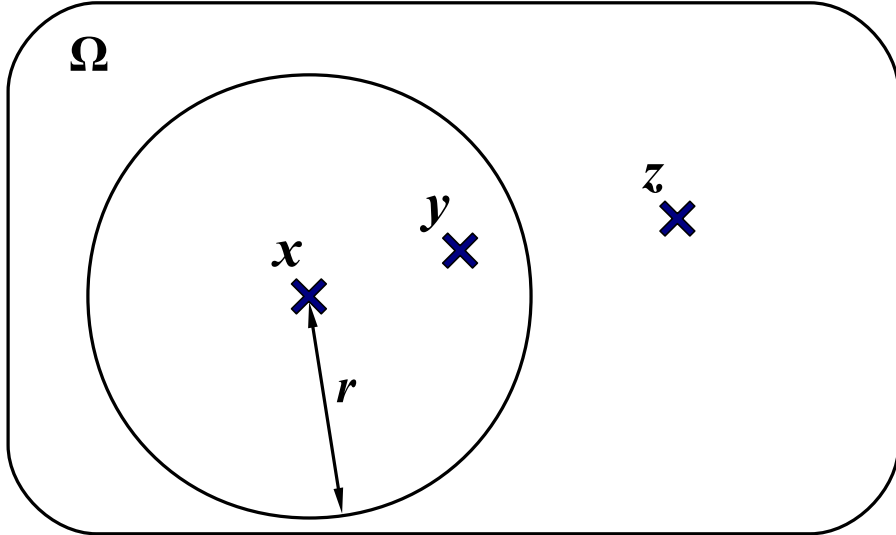


Figure 8.1: The Static Spatial Search Game (SSSG).

Players deploy simultaneously at points in some metric space Ω . Suppose Player A deploys at x and can search all points within a radius r . Player B loses the game if deployed at y , but wins if deployed at z . A win results in a payoff of 1; a loss results in a payoff of 0.

The metric d reflects the spatial structure of Ω . In \mathbb{R}^n , d may be the Euclidean distance, while in a graph d may be the length of the shortest path connecting two points. However, depending on the interpretation of the game, d could also represent an abstract distance, indicating dissimilarity, difficulty of communication or perceived costs.

In specific cases, it may be sensible to relax some of these conditions. For example, in a graph that is not connected, we could allow infinite distances between vertices that are not joined by a path (yielding an extended metric). Alternatively, to represent a directed graph, we may wish to ignore the symmetry condition (M2) (yielding a quasi-metric; see Steen and Seebach Jr., 1970). However, for the sake of simplicity, we do not consider such cases at this time.

We define a non-negative real number r called the detection radius and use the notation $B_r[x]$ to designate the closed ball centred on x :

$$B_r[x] = \{y \in \Omega : d(x, y) \leq r\}$$

The strategies for Player A (the searching player) and Player B (the concealing player) are specific points of Ω at which they may choose to deploy. In a single play of the game, each player simultaneously picks a point x_A, x_B from their own strategy set, $\Sigma_A, \Sigma_B \subseteq \Omega$.

For the sake of clarity, from this point forward, we use masculine pronouns to refer to Player A and feminine pronouns to refer to Player B.

We define the payoff functions for Player A and Player B respectively as:

$$p_A(x_A, x_B) = \begin{cases} 1 & , x_B \in B_r[x_A]; \\ 0 & , \text{otherwise.} \end{cases}$$

$$p_B(x_A, x_B) = 1 - p_A(x_A, x_B)$$

This is a constant-sum game and can be analysed accordingly.

In interpreting the game, we imagine that Player B chooses to hide somewhere in Ω , while Player A attempts to locate his opponent. To do this, Player A selects a point of Ω and searches a neighbourhood of this point. If Player B's hiding place falls within the detection radius of Player A's chosen point, the attempt to hide is unsuccessful and Player B is located. Otherwise, Player B remains undetected.

The game is illustrated in Figure 8.1.

8.2.2 The SSSG and other games

As mentioned in Section 7.1, the main sources of inspiration for the SSSG were *Geometric games and applications* (Ruckle, 1983) and, more particularly, *Games of strategy on trees* (White, 1994). Indeed the SSSG could be seen as occupying a middle-ground between the extremely abstract formulation of Ruckle's "geometric games" and the quite specific family of games studied by White.

It should be noted that the SSSG is not strictly a geometric game by Ruckle's definition (1983, p. 2), since it is not zero-sum. However, it could be transformed into a zero-sum game without altering the subsequent analysis, simply by subtracting $\frac{1}{2}$ from all payoffs. The decision that all payoffs should be 0 or 1 has been taken to ensure the clarity of the payoff matrices considered later.

Given this proviso, certain of Ruckle's geometric games can be formulated as particular cases of the SSSG. For example, if transformed to a zero-sum game as described, game AAGV (Ruckle, 1983 p. 86; adapted from Arnold, 1962) is an example of the SSSG, with $\Omega = [0, 1] \subset \mathbb{R}$, $\Sigma_A = \Sigma_B = \Omega$ and $d(x, y) = |x - y|$.

Similarly, White’s “games of strategy on trees” (1994) may be seen to be examples of the SSSG, where Ω is the set of vertices of a tree, $\Sigma_A = \Sigma_B = \Omega$, $r = 1$ and d is the length of the shortest path between two vertices.

A game that demonstrates the potential complexity that can arise from apparently simple cases of the SSSG is the “Cookie-Cutter” game (or the “Hiding in a Disc” game), in which Player A chooses a point in a disc of unit radius and Player B simultaneously places a circular ‘cookie-cutter’ centred at any point of the disc, winning the game if Player A’s point lies within the ‘cookie-cutter’. Given appropriate payoffs, this game is an example of the SSSG, where Ω is the closed unit disc, $\Sigma_A = \Sigma_B = \Omega$ and $d(\mathbf{x}, \mathbf{y}) = |\mathbf{x} - \mathbf{y}|$.

The particular case of this game with $r = 1/2$ was originally proposed by Gale and Glassey (1974), for which OMSs were presented by Evans (1975). The game was extended to all $r > 0$ by Bordelon (1975), who proposed OMSs for all $r > 1/2$, but these results were disputed by Ruckle (1983, p. 108). Ruckle’s disproof was disputed in turn by Danskin (1990), who showed that Bordelon’s results were correct for some values of $r > 1/2$, though false in general. Despite the apparent simplicity of the problem, Danskin was only able to find OMSs for a small range of values of r around $r = 1/2$ and for all $r \geq \sqrt{2}/2$, thus illustrating the hidden complexity of many games of this form.

A particularly simple example of a game that can be represented as an SSSG is “Matching Pennies” (see Blackwell and Girshick, 1979, p. 13), in which Players A and B simultaneously call “Heads” or “Tails”, with Player A receiving a payoff of 1 if the calls are the same and -1 otherwise, and Player B receiving a payoff of -1 if the calls are the same and 1 otherwise. Taking $\Sigma_A = \Sigma_B = \Omega = \{\text{“Heads”, “Tails”}\}$, $r = 0$, with d as any valid metric, this is an SSSG, again with the proviso that the payoffs must be transformed appropriately.

A more complicated example of a game that can be represented as an SSSG is the graph security game of Mavronicolas et al. (2008) if the number of attackers is restricted to one. This game is played over an undirected graph $G = (V(G), E(G))$ with one defender and (in general) multiple attackers.¹ Simultaneously, the defender chooses an edge and the attackers each choose a vertex. The defender receives a payoff equal to the number of attackers who choose vertices incident to his chosen edge. Each attacker receives a payoff equal to 0 if their chosen vertex is incident to the

¹ Here (and throughout Part III), $V(G)$ and $E(G)$ respectively represent the vertex set and the edge set of G , as defined in Section 4.4.4.

defender's edge and 1 otherwise.

Consider the graph G' obtained by inserting a new vertex at the midpoint of each of the edges of G . Let the set of new vertices created in this way be denoted $V(G')^*$ while the complete vertex set $V(G')$ includes both the new vertices and the original vertices. With the defender as Player A, a single attacker as Player B, $\Omega = V(G')$, $\Sigma_A = V(G')^*$, $\Sigma_B = V(G)$, $r = 1$ and with d as the length of the shortest path between two vertices in G' , this game is also an example of the SSSG.

The SSSG provides a framework that unites all of these games and allows for a general consideration of the relative strategic values of the different points of a space. It implicitly encompasses the concepts of reachability, interdependence based on spatial structure and the detection radius, as discussed in Section 7.3.

8.2.3 The SSSG with finite strategy sets

Consider an example of the SSSG in which the strategy sets Σ_A , Σ_B are finite. One of the simplest possible mixed strategies available to each player in such a case is the mixed strategy that allocates equal probabilities to all points in a player's strategy set. We denote these mixed strategies by ρ_A and ρ_B for Players A and B respectively.

The following proposition establishes a sufficient condition for ρ_A , ρ_B to be OMSs:

Proposition 8.2.1. *Consider the SSSG played over a metric space Ω , with finite strategy sets Σ_A , Σ_B and distance d . If there exists a positive integer χ such that:*

$$\begin{aligned} |B_r[x_A] \cap \Sigma_B| &= \chi, \quad \forall x_A \in \Sigma_A \\ |B_r[x_B] \cap \Sigma_A| &= \chi, \quad \forall x_B \in \Sigma_B \end{aligned} \tag{8.1}$$

then ρ_A , ρ_B are OMSs for Players A and B respectively and $\chi|\Sigma_A|^{-1} = \chi|\Sigma_B|^{-1} = u$ is the value of the game to Player A.

Proof. Suppose that Player A employs the mixed strategy ρ_A which allocates a uniform probability of $|\Sigma_A|^{-1}$ to all points $x_A \in \Sigma_A$. In a particular play of the game, suppose that Player B deploys at point $x_B \in \Sigma_B$.

In this situation, since $|B_r[x_B] \cap \Sigma_A| = \chi$, the expected payoff to Player A is $\chi|\Sigma_A|^{-1}$, the probability that Player A's point x_A lies in $B_r[x_B]$. Therefore, for any mixed strategy σ_B for Player B:

$$E[p_A(\rho_A, \sigma_B)] = \chi|\Sigma_A|^{-1}$$

and thus:

$$u = \max_{\sigma_A} \min_{\sigma_B} E[p_A(\sigma_A, \sigma_B)] \geq \chi |\Sigma_A|^{-1} \quad (8.2)$$

Now suppose that Player B employs the mixed strategy ρ_B which allocates a uniform probability of $|\Sigma_B|^{-1}$ to all points $x_B \in \Sigma_B$. In a particular play of the game, suppose that Player A deploys at point $x_A \in \Sigma_A$.

In this situation, since $|B_r[x_A] \cap \Sigma_B| = \chi$, the expected payoff to Player A is $\chi |\Sigma_B|^{-1}$, the probability that Player B's point x_B lies in $B_r[x_A]$. Therefore, for any mixed strategy σ_A for Player A:

$$E[p_A(\sigma_A, \rho_B)] = \chi |\Sigma_B|^{-1}$$

and thus:

$$u = \max_{\sigma_A} \min_{\sigma_B} E[p_A(\sigma_A, \sigma_B)] \leq \chi |\Sigma_B|^{-1} \quad (8.3)$$

Now, (8.1) together with the symmetric property of the distance (M2) imply that $\chi |\Sigma_A| = \chi |\Sigma_B|$ and thus that $|\Sigma_A| = |\Sigma_B|$. By (8.2) and (8.3), we therefore have:

$$|\Sigma_A|^{-1} \leq u \leq |\Sigma_B|^{-1} \Rightarrow u = |\Sigma_A|^{-1} = |\Sigma_B|^{-1}$$

and ρ_A, ρ_B are OMSs, by Definition 7.2.3. □

8.2.4 Dominance and equivalence in the SSSG

We can now examine strategic dominance and equivalence (see Definition 7.2.4) in the context of the SSSG using the notation established in Section 8.2.

Proposition 8.2.2. *Consider the SSSG played over a metric space Ω , with strategy sets Σ_A, Σ_B and distance d . For strategies $x_1, x_2 \in \Sigma_A$, $x_1 \neq x_2$, for Player A:*

- x_2 **very weakly dominates** x_1 if and only if:

$$(B_r[x_1] \cap \Sigma_B) \subseteq (B_r[x_2] \cap \Sigma_B)$$

- x_2 **weakly dominates** x_1 if and only if:

$$(B_r[x_1] \cap \Sigma_B) \subset (B_r[x_2] \cap \Sigma_B)$$

- x_2 strictly dominates x_1 if and only if:

$$(B_r[x_1] \cap \Sigma_B) = \emptyset$$

$$(B_r[x_2] \cap \Sigma_B) = \Sigma_B$$

- x_2 is equivalent to x_1 if and only if:

$$(B_r[x_1] \cap \Sigma_B) = (B_r[x_2] \cap \Sigma_B)$$

This proposition states that for Player A:

- x_2 very weakly dominates x_1 if and only if, when deployed at x_2 , Player A can search every potential location of Player B that could be searched from x_1 .
- This dominance is weak if there exist potential locations of Player B that can be searched from x_2 but that cannot be searched from x_1 (inclusion is strict).
- Strict dominance only occurs in the trivial case in which no potential locations of Player B can be searched from x_1 while every potential location of Player B can be searched from x_2 .
- x_2 and x_1 are equivalent if and only if precisely the same set of potential locations of Player B can be searched from both points.

Proof. We consider each of the four parts of Definition 7.2.4 and show that, in the context of the SSSG, they are equivalent to the corresponding statements of Proposition 8.2.2. Recall that p_A takes values in $\{0, 1\}$.

- **Very weak dominance**

$$\begin{aligned} p_A(x_2, y) &\geq p_A(x_1, y), \quad \forall y \in \Sigma_B & (*) \\ \Leftrightarrow [p_A(x_1, y) = 1 &\Rightarrow p_A(x_2, y) = 1], \quad \forall y \in \Sigma_B \\ \Leftrightarrow [y \in B_r[x_1] &\Rightarrow y \in B_r[x_2]], \quad \forall y \in \Sigma_B \\ \Leftrightarrow (B_r[x_1] \cap \Sigma_B) &\subseteq (B_r[x_2] \cap \Sigma_B) & (**) \end{aligned}$$

- **Weak dominance**

Since $(*) \Leftrightarrow (**)$, it suffices to observe that, if $(**)$ is assumed to be true:

$$\begin{aligned} \exists y^* \in \Sigma_B : p_A(x_2, y^*) &> p_A(x_1, y^*) \\ \Leftrightarrow \exists y^* \in \Sigma_B : y^* &\in B_r[x_2] \text{ and } y^* \notin B_r[x_1] \\ \Leftrightarrow (B_r[x_1] \cap \Sigma_B) &\subset (B_r[x_2] \cap \Sigma_B) \quad [\text{by } (**)] \end{aligned}$$

- **Strict dominance**

$$\begin{aligned}
 & p_A(x_2, y) > p_A(x_1, y) , \quad \forall y \in \Sigma_B \\
 \Leftrightarrow & \quad y \in B_r[x_2] \text{ and } y \notin B_r[x_1] , \quad \forall y \in \Sigma_B \\
 \Leftrightarrow & \quad \begin{cases} (B_r[x_1] \cap \Sigma_B) = \emptyset , \\ (B_r[x_2] \cap \Sigma_B) = \Sigma_B \end{cases}
 \end{aligned}$$

- **Equivalence**

$$\begin{aligned}
 & p_A(x_2, y) = p_A(x_1, y) , \quad \forall y \in \Sigma_B \\
 \Leftrightarrow & \quad [y \in B_r[x_2] \Leftrightarrow y \in B_r[x_1]] , \quad \forall y \in \Sigma_B \\
 \Leftrightarrow & \quad (B_r[x_2] \cap \Sigma_B) = (B_r[x_1] \cap \Sigma_B) \quad \square
 \end{aligned}$$

We now consider dominance and equivalence for Player B:

Proposition 8.2.3. Consider the SSSG played over a metric space Ω , with strategy sets Σ_A , Σ_B and distance d . For strategies $x_1, x_2 \in \Sigma_B$, $x_1 \neq x_2$, for Player B:

- x_2 **very weakly dominates** x_1 if and only if:

$$[x_2 \in B_r[y] \Rightarrow x_1 \in B_r[y]] , \quad \forall y \in \Sigma_A$$

- x_2 **weakly dominates** x_1 if and only if:

$$[x_2 \in B_r[y] \Rightarrow x_1 \in B_r[y]] , \quad \forall y \in \Sigma_A$$

and $\exists y^* \in \Sigma_A$ such that:

$$x_1 \in B_r[y^*] \text{ and } x_2 \notin B_r[y^*]$$

- x_2 **strictly dominates** x_1 if and only if:

$$x_1 \in B_r[y] \text{ and } x_2 \notin B_r[y] , \quad \forall y \in \Sigma_A$$

- x_2 is **equivalent** to x_1 if and only if:

$$[x_2 \in B_r[y] \Leftrightarrow x_1 \in B_r[y]] , \quad \forall y \in \Sigma_A$$

This proposition states that for Player B:

- x_2 very weakly dominates x_1 if and only if, wherever Player A deploys, if he can search x_2 then he can also search x_1 .
- This dominance is weak if there exists a position for Player A from which he can search x_1 but cannot search x_2 .
- Strict dominance only occurs in the trivial case in which, wherever Player A deploys, he can search x_1 but cannot search x_2 .
- x_2 and x_1 are equivalent if and only if, wherever Player A deploys, he can search x_2 if and only if he can search x_1 .

Proof. We consider each of the four parts of Definition 7.2.4 and show that, in the context of the SSSG, they are equivalent to the corresponding statements of Proposition 8.2.3. Recall that p_B also takes values in $\{0, 1\}$.

- **Very weak dominance**

$$\begin{aligned}
 p_B(y, x_2) &\geq p_B(y, x_1), \quad \forall y \in \Sigma_A & (*) \\
 \Leftrightarrow [p_B(y, x_1) = 1 \Rightarrow p_B(y, x_2) = 1], \quad \forall y \in \Sigma_A \\
 \Leftrightarrow [x_1 \notin B_r[y] \Rightarrow x_2 \notin B_r[y]], \quad \forall y \in \Sigma_A \\
 \Leftrightarrow [x_2 \in B_r[y] \Rightarrow x_1 \in B_r[y]], \quad \forall y \in \Sigma_A & (**)
 \end{aligned}$$

- **Weak dominance**

Since $(*) \Leftrightarrow (**)$, it suffices to observe that:

$$\begin{aligned}
 \exists y^* \in \Sigma_A : p_B(y^*, x_2) &> p_B(y^*, x_1) \\
 \Leftrightarrow \exists y^* \in \Sigma_A : x_1 \in B_r[y^*] \text{ and } x_2 \notin B_r[y^*]
 \end{aligned}$$

- **Strict dominance**

$$\begin{aligned}
 p_B(y, x_2) &> p_B(y, x_1), \quad \forall y \in \Sigma_A \\
 \Leftrightarrow x_1 \in B_r[y] \text{ and } x_2 \notin B_r[y], \quad \forall y \in \Sigma_A
 \end{aligned}$$

- **Equivalence**

$$\begin{aligned}
 p_B(y, x_2) &= p_B(y, x_1), \quad \forall y \in \Sigma_A \\
 \Leftrightarrow [x_2 \in B_r[y] \Leftrightarrow x_1 \in B_r[y]], \quad \forall y \in \Sigma_A & \square
 \end{aligned}$$

The necessary and sufficient conditions for dominance and equivalence for Player B established in Proposition 8.2.3 can be shown to be equivalent to a simpler set of conditions, clearly analogous to those relating to dominance and equivalence for Player A seen in Proposition 8.2.2:

Proposition 8.2.4. *Consider the SSSG played over a metric space Ω , with strategy sets Σ_A , Σ_B and distance d . For strategies $x_1, x_2 \in \Sigma_B$, $x_1 \neq x_2$, for Player B:*

- x_2 **very weakly dominates** x_1 if and only if:

$$(B_r[x_2] \cap \Sigma_A) \subseteq (B_r[x_1] \cap \Sigma_A)$$

- x_2 **weakly dominates** x_1 if and only if:

$$(B_r[x_2] \cap \Sigma_A) \subset (B_r[x_1] \cap \Sigma_A)$$

- x_2 **strictly dominates** x_1 if and only if:

$$\begin{aligned} (B_r[x_1] \cap \Sigma_A) &= \Sigma_A \\ (B_r[x_2] \cap \Sigma_A) &= \emptyset \end{aligned}$$

- x_2 is **equivalent** to x_1 if and only if:

$$(B_r[x_2] \cap \Sigma_A) = (B_r[x_1] \cap \Sigma_A)$$

Proof. We consider each of the four statements of Proposition 8.2.3 (which has already been proven) and show that they are equivalent to the corresponding statements of Proposition 8.2.4.

- **Very weak dominance**

$$\begin{aligned} [x_2 \in B_r[y] \Rightarrow x_1 \in B_r[y]] , \quad &\forall y \in \Sigma_A & (*) \\ \Leftrightarrow [y \in B_r[x_2] \Rightarrow y \in B_r[x_1]] , \quad &\forall y \in \Sigma_A \quad [\text{by (M2)}] \\ \Leftrightarrow (B_r[x_2] \cap \Sigma_A) \subseteq (B_r[x_1] \cap \Sigma_A) & & (**) \end{aligned}$$

- **Weak dominance**

Since $(*) \Leftrightarrow (**)$, it suffices to observe that, if $(**)$ is assumed to be true:

$$\begin{aligned} & \exists z \in \Sigma_A : x_1 \in B_r[z] \text{ and } x_2 \notin B_r[z] \\ \Leftrightarrow & \exists z \in \Sigma_A : z \in B_r[x_1] \text{ and } z \notin B_r[x_2] \quad [\text{by (M2)}] \\ \Leftrightarrow & (B_r[x_2] \cap \Sigma_A) \subset (B_r[x_1] \cap \Sigma_A) \quad [\text{by } (**)] \end{aligned}$$

- **Strict dominance**

$$\begin{aligned} & x_1 \in B_r[y] \text{ and } x_2 \notin B_r[y], \quad \forall y \in \Sigma_A \\ \Leftrightarrow & y \in B_r[x_1] \text{ and } y \notin B_r[x_2], \quad \forall y \in \Sigma_A \quad [\text{by (M2)}] \\ \Leftrightarrow & \begin{cases} (B_r[x_1] \cap \Sigma_A) = \Sigma_A, \\ (B_r[x_2] \cap \Sigma_A) = \emptyset \end{cases} \end{aligned}$$

- **Equivalence**

$$\begin{aligned} & [x_2 \in B_r[y] \Leftrightarrow x_1 \in B_r[y]], \quad \forall y \in \Sigma_A \\ \Leftrightarrow & [y \in B_r[x_2] \Leftrightarrow y \in B_r[x_1]], \quad \forall y \in \Sigma_A \quad [\text{by (M2)}] \\ \Leftrightarrow & (B_r[x_2] \cap \Sigma_A) = (B_r[x_1] \cap \Sigma_A) \quad \square \end{aligned}$$

While Proposition 8.2.4 is apparently simpler than Proposition 8.2.3, note that every part of its proof depends on the symmetric property of the distance (M2). If this condition were to be relaxed, as discussed in Section 8.2.1, Proposition 8.2.4 would not be valid and dominance and equivalence for Player B would have to be analysed on the basis of Proposition 8.2.3.

Definition 8.2.5. Consider the SSSG played over a metric space Ω , with strategy sets Σ_A , Σ_B and distance d . For Player A or Player B, a subset of their strategy set $\hat{\Sigma} \subseteq \Sigma_A$ or $\hat{\Sigma} \subseteq \Sigma_B$ exhibits **pairwise equivalence** if and only if x is equivalent to y , $\forall x, y \in \hat{\Sigma}$.

We conclude that a subset $\hat{\Sigma} \subseteq \Sigma_A$ or $\hat{\Sigma} \subseteq \Sigma_B$ exhibiting pairwise equivalence can be reduced to any singleton $\{\hat{x}\} \subseteq \hat{\Sigma}$ without altering the analysis of the game. Since all points in $\hat{\Sigma}$ are equivalent, a player would neither gain nor lose by playing another point in the set over \hat{x} .

The following proposition states that if x_2 very weakly dominates x_1 for Player A (and x_1 is adjacent to at least one potential location for Player B), then the distance between the two points must be no greater than $2r$.

Proposition 8.2.6. *For the SSSG played over a metric space Ω , with strategy sets Σ_A , Σ_B and distance d , if x_2 very weakly dominates x_1 for Player A and $B_r[x_1] \cap \Sigma_B \neq \emptyset$, then $x_2 \in B_{2r}[x_1] \cap \Sigma_A$.*

Proof. If x_2 very weakly dominates x_1 for Player A and $B_r[x_1] \cap \Sigma_B \neq \emptyset$, then:

$$\begin{aligned} \emptyset \neq (B_r[x_1] \cap \Sigma_B) &\subseteq (B_r[x_2] \cap \Sigma_B) && [\text{by 8.2.2}] \\ \Rightarrow \quad \exists y \in B_r[x_1] \cap B_r[x_2] \\ \Rightarrow \quad d(x_1, y) \leq r \text{ and } d(x_2, y) \leq r \\ \Rightarrow \quad d(x_1, x_2) \leq 2r && [\text{by (M2), (M3)}] \\ \Rightarrow \quad x_2 \in B_{2r}[x_1] \cap \Sigma_A && \square \end{aligned}$$

The condition that $B_r[x_1] \cap \Sigma_B \neq \emptyset$ simply removes trivial strategies that are very weakly dominated by every other strategy.

An analogous result holds for Player B. The proof is similar to that of 8.2.6 and is therefore omitted:

Proposition 8.2.7. *For the SSSG played over a metric space Ω , with strategy sets Σ_A , Σ_B and distance d , if x_2 very weakly dominates x_1 for Player B and $B_r[x_2] \cap \Sigma_A \neq \emptyset$, then $x_2 \in B_{2r}[x_1] \cap \Sigma_B$.*

In this case, the condition that $B_r[x_2] \cap \Sigma_A \neq \emptyset$ removes strategies that very weakly dominate every other strategy.

Note that both of these propositions depend on the symmetric property of the distance (M2) and the triangle inequality (M3) (see Section 8.2.1).

8.2.5 Iterated elimination of dominated strategies

The concepts of dominance and equivalence provide us with a method for reducing the SSSG through an iterative process of removing dominated strategies from Σ_A and Σ_B , reducing pairwise equivalent subsets to singletons and reassessing dominance in the new strategy sets. This is known as the iterated elimination of dominated strategies (IEDS) (see, for example, Berwanger, 2007; Börgers, 1992;

Dufwenberg and Stegeman, 2002). Given any game, the aim of IEDS is to identify a simplified game, whose solutions are also solutions of the complete game. These solutions can then be identified using standard techniques (see, for example, Morris, 1994, pp. 99-114). The application of this method to games played over graphs is discussed in Section 9.2.

It should be noted that because we are considering weak rather than strict dominance, IEDS may not be suitable for identifying all the solutions of a particular game. The results of this form of IEDS are dependent on the order in which dominated strategies are removed (Leyton-Brown and Shoham, 2008, pp. 20-23) and some solutions may be lost. It is also necessary to observe that, while IEDS has been shown to be valid for games with finitely many possible strategies, for games with infinitely many possible strategies the process may fail (Berwanger, 2007). Indeed, such infinite games may not have solutions (Ruckle, 1983, p. 10).

However, although IEDS is not guaranteed to produce OMSs for the SSSG in such cases, given a pair of mixed strategies σ_A , σ_B obtained by this method, it is straightforward to check whether or not they are optimal by verifying that, for some $u \in [0, 1]$, we have:

$$\begin{aligned} \inf_{x \in \Sigma_B} E[p_A(\sigma_A, x)] &= u \\ \inf_{y \in \Sigma_A} E[p_B(y, \sigma_B)] &= 1 - u \end{aligned} \tag{8.4}$$

where u is the value of the game to Player A.

This method is described by Blackwell and Girshick (1979, p. 65) and used extensively by Ruckle (1983, the method is introduced on pp. 8-9) to verify proposed OMSs for geometric games.

8.3 The Graph Search Game (GSG)

The definitions and notation relating to graph theory used in this section are adapted from Bondy and Murty (1976).

8.3.1 Definition of the GSG

Consider a simple graph G , characterised by the symmetric adjacency matrix $\mathfrak{M} = (a_{ij})$, with a set of κ vertices:

$$V(G) = \{v_1, \dots, v_\kappa\}$$

and a set of edges:

$$E(G) = \{\{v_i, v_j\} : v_i, v_j \in V(G) \text{ and } a_{ij} = 1\}$$

We suppose that G is connected, to ensure that the metric space axioms are fulfilled, but this assumption could be relaxed if we allowed for infinite distances between vertices. We also suppose that all edges of G have unit weight.

The Graph Search Game (GSG) $\mathfrak{G} = (G, \Sigma_A, \Sigma_B, r)$ over a finite graph G is defined to be an example of the SSSG, with $\Omega = V(G)$, $\emptyset \neq \Sigma_A, \Sigma_B \subseteq V(G)$, r a positive real number, and the distance function $d_G(v, w)$ for $v, w \in V(G)$, $v \neq w$, defined to be the length of the shortest path from v to w in G . We also define $d_G(v, v) = 0$, $\forall v \in V(G)$. The assumption that G is undirected ensures that the symmetry condition $d_G(v, w) = d_G(w, v)$ holds $\forall v, w \in V(G)$.

Setting $r = 1$, we have that $B_r[v]$, the zone that can be searched by Player A when deployed at v , is the closed neighbourhood $N[v]$ of v , the set of all vertices adjacent to v united with $\{v\}$ itself.

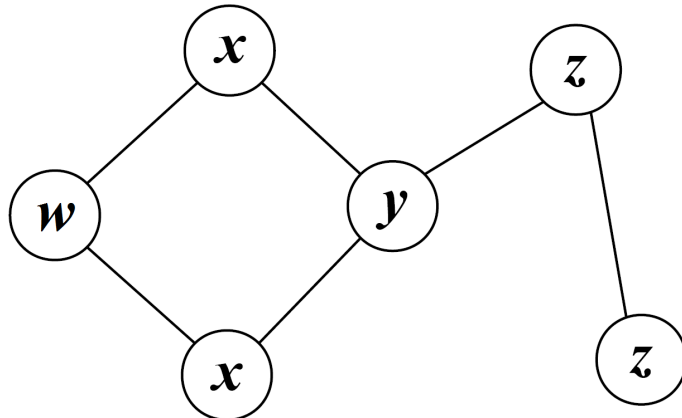


Figure 8.2: The Graph Search Game (GSG).

Players deploy simultaneously at vertices of the graph. Suppose that Player A deploys at the vertex marked w . If $r = 1$, Player B loses the game if she deploys at any of the vertices marked w or x , but wins if she deploys at any of the vertices marked y or z . If $r = 2$, Player B loses the game if she deploys at any of the vertices marked w , x or y , but wins if she deploys at either of the vertices marked z . A win results in a payoff of 1; a loss results in a payoff of 0.

The game proceeds by Player A choosing a vertex $v_A \in \Sigma_A$ and Player B simultaneously choosing a vertex $v_B \in \Sigma_B$. The payoff functions are:

$$p_A(v_A, v_B) = \begin{cases} 1, & \text{if } v_A \text{ and } v_B \text{ are equal or adjacent;} \\ 0, & \text{otherwise.} \end{cases}$$

$$p_B(v_A, v_B) = 1 - p_A(v_A, v_B)$$

In this game, the pure strategies for each player are particular vertices. In the following analysis, we use the words “strategy” and “vertex” interchangeably, depending on the context.

The GSG is illustrated in Figure 8.2:

8.3.2 The GSG with $r \neq 1$

The restriction to $r = 1$ is not a significant constraint, since any GSG can be reduced to this case by means of a minor alteration.

For situations with $r \neq 1$, we can define:

$$G' = (V(G), E(G'))$$

such that:

$$E(G') = \{\{v_i, v_j\} : v_i, v_j \in V(G) \text{ and } 1 \leq d_G(v_i, v_j) \leq r\}$$

and apply our analysis to G' with $r = 1$.

Equivalently, if $r \in \mathbb{N} \setminus \{1\}$, we can replace the adjacency matrix $\mathfrak{M} = (a_{ij})$ of G with $\mathfrak{M}' = (a'_{ij})$, where:

$$a'_{ij} = \begin{cases} 0 & , \text{if } b_{ij} = 0 \text{ or } i = j \\ 1 & , \text{otherwise.} \end{cases}$$

with $(b_{ij}) = \sum_{q=1}^r \mathfrak{M}^q$, the matrix which shows the number of paths in G of length no greater than r connecting v_i to v_j .

It therefore suffices to exclusively study GSGs with $r = 1$, since these methods for redefining G ensure that such analysis will be applicable to games for any $r \in \mathbb{N}$.

8.3.3 Preliminary observations

Analysis of the GSG requires the statement of some preliminary results and definitions. For these results, we use the following notation:

- $N_A[v] = N[v] \cap \Sigma_A$
The set of all potential positions for Player A in $N[v]$.
- $N_B[v] = N[v] \cap \Sigma_B$
The set of all potential positions for Player B in $N[v]$.
- $\alpha[v] = |N_A[v]|$
The number of potential positions for Player A in $N[v]$.
- $\beta[v] = |N_B[v]|$
The number of potential positions for Player B in $N[v]$.
- $\Delta(G) = \max_{w \in V(G)} [\deg(w)]$
The maximum degree of the vertices of G .
- $\delta(G) = \min_{w \in V(G)} [\deg(w)]$
The minimum degree of the vertices of G .

The following proposition states that if Player A can search a globally maximal number of potential positions for Player B from a vertex v , then v is not dominated by any other vertex and is only equivalent to those vertices which have the same closed neighbourhood as v . In a graph in which all vertices have a distinct closed neighbourhood, such as a rectangular grid graph, such a vertex v cannot be very weakly dominated by any other vertex.

Proposition 8.3.1. *For the GSG $\mathfrak{G} = (G, \Sigma_A, \Sigma_B, r)$, with $r = 1$, consider a vertex $v \in \Sigma_A$ and the subset $\Sigma_A^{(v)} = \{z \in \Sigma_A : N[z] = N[v]\}$. We have that if:*

$$\beta[v] = \Delta(G) + 1 \tag{8.5}$$

then:

- (i) $\Sigma_A^{(v)}$ exhibits pairwise equivalence for Player A;
- (ii) v is not very weakly dominated for Player A by any strategy in $\Sigma_A \setminus \Sigma_A^{(v)}$.

Proof. To prove (i), observe that for all $w_1, w_2 \in \Sigma_A^{(v)}$, $N[w_1] = N[w_2]$. Hence, $N_B[w_1] = N_B[w_2]$ and therefore w_1 is equivalent to w_2 for Player A, so $\Sigma_A^{(v)}$ exhibits pairwise equivalence for Player A.

To prove (ii), suppose for a contradiction that v satisfies (8.5) and is very weakly dominated by $\hat{v} \in \Sigma_A \setminus \Sigma_A^{(v)}$.

Observe also that:

$$\begin{aligned} \text{If } \beta[w] &= \Delta(G) + 1, \text{ for some } w \in V(G), \\ \text{then } N_B[w] &= N[w]. \end{aligned} \quad (8.6)$$

and note that $\Delta(G) + 1$ is an upper bound for $\beta[w]$.

Now, we have that:

$$\begin{aligned} N_B[v] &\subseteq N_B[\hat{v}] \quad [\text{by very weak dominance}] \\ \Rightarrow \Delta(G) + 1 &\leq \beta[\hat{v}] \leq |N[\hat{v}]| \quad [\text{by (8.5)}] \\ \Rightarrow \Delta(G) + 1 &\leq \beta[\hat{v}] \leq \Delta(G) + 1 \\ \Rightarrow \Delta(G) + 1 &= \beta[v] = \beta[\hat{v}] \\ \Rightarrow N_B[v] &= N_B[\hat{v}] \quad [\text{since } N_B[v] \subseteq N_B[\hat{v}]] \\ \Rightarrow N[v] &= N[\hat{v}] \quad [\text{by (8.6)}] \\ \Rightarrow \hat{v} &\in \Sigma_A^{(v)} \end{aligned}$$

This is a contradiction, since we supposed that $\hat{v} \in \Sigma_A \setminus \Sigma_A^{(v)}$. \square

The next proposition is a stronger result. It states that, for Player A, given a vertex v that is known not to be very weakly dominated by any vertices outside of a certain subset S , if Player A can search strictly more potential hiding places for Player B when deployed at v than could be searched from any other vertex in S , then v is not very weakly dominated by any other vertex.

Proposition 8.3.2. *For the GSG $\mathfrak{G} = (G, \Sigma_A, \Sigma_B, r)$, with $r = 1$, consider a vertex $v \in \Sigma_A$. Let $S \subseteq \Sigma_A$ be such that $v \in S$ and such that $\Sigma_A \setminus S$ contains no vertices that very weakly dominate v for Player A. We have that if:*

$$\beta[v] > \max_{w \in S \setminus \{v\}} (\beta[w]) \quad (8.7)$$

then v is not very weakly dominated for Player A by any other strategy in Σ_A .

Proof. For a contradiction, suppose that v satisfies (8.7) and is very weakly dominated by $\hat{v} \in \Sigma_A$ for Player A. We must have that $\hat{v} \in S$, since vertices outside S cannot very weakly dominate v .

From the very weak dominance, we have:

$$\begin{aligned} N_B[v] &\subseteq N_B[\hat{v}] \\ \Rightarrow \max_{w \in S \setminus \{v\}} (\beta[w]) &< \beta[v] \leq \beta[\hat{v}] \quad [\text{by (8.7)}] \end{aligned}$$

This is a contradiction, since $\hat{v} \in S \setminus \{v\}$. \square

The following proposition is a restatement of Proposition 8.2.6, reformulated in the context of the GSG. It states that any vertex that very weakly dominates v for Player A can be no more than 2 steps away from v on the graph. Its proof is identical to that of Proposition 8.2.6 and is thus omitted.

Proposition 8.3.3. *For the GSG $\mathfrak{G} = (G, \Sigma_A, \Sigma_B, r)$, with $r = 1$, if w very weakly dominates v for Player A and $N_B[v] \neq \emptyset$, then:*

$$w \in B_2[v] \cap \Sigma_A$$

Corollary 8.3.4. *For the GSG $\mathfrak{G} = (G, \Sigma_A, \Sigma_B, r)$, with $r = 1$, consider a vertex $v \in \Sigma_A$. We have that if:*

$$\beta[v] > \max_{w \in S'} (\beta[w])$$

where:

$$S' = B_2[v] \cap \Sigma_A \setminus \{v\}$$

then v is not very weakly dominated for Player A by any other strategy.

Proof. This follows directly from Propositions 8.3.2 and 8.3.3, where the set S from Proposition 8.3.3 is defined as:

$$S = B_2[v] \cap \Sigma_A$$

\square

The corollary states that any vertex from which Player A can search strictly more potential hiding places for Player B than could be searched from any other valid vertex lying no more than two steps away, cannot be very weakly dominated by any other vertex. These results allow us to considerably narrow down our search for dominated and equivalent vertices.

Analogous results to Propositions 8.3.2 and 8.3.3 and Corollary 8.3.4 hold for very weak dominance for Player B. The proofs of these results are similar to those presented above and are thus omitted.

Proposition 8.3.5. For the GSG $\mathfrak{G} = (G, \Sigma_A, \Sigma_B, r)$, with $r = 1$, consider a vertex $v \in \Sigma_B$. Let $S \subseteq \Sigma_B$ be such that $v \in S$ and such that $\Sigma_B \setminus S$ contains no vertices that very weakly dominate v for Player B. We have that if:

$$\alpha[v] < \min_{w \in S \setminus \{v\}} (\alpha[w])$$

then v is not very weakly dominated for Player B by any other strategy in Σ_B .

Proposition 8.3.6. For the GSG $\mathfrak{G} = (G, \Sigma_A, \Sigma_B, r)$, with $r = 1$, if w very weakly dominates v for Player B and $N_A[w] \neq \emptyset$, then:

$$w \in B_2[v] \cap \Sigma_B$$

Corollary 8.3.7. For the GSG $\mathfrak{G} = (G, \Sigma_A, \Sigma_B, r)$, with $r = 1$, consider a vertex $v \in \Sigma_B$, $\alpha[v] \neq 0$. We have that if:

$$\alpha[v] < \min_{w \in S'} (\alpha[w])$$

where:

$$S' = B_2[v] \cap \Sigma_B \setminus \{v\}$$

then v is not very weakly dominated for Player B by any other strategy.

8.3.4 Bounds on the value of the GSG

A first step in the analysis of a particular GSG is to determine lower and upper bounds on the values of the game (see Definition 7.2.2).

Recall that for a two-player constant-sum game, it makes sense to restrict discussion to the value to Player A, since this also determines the value to Player B through the condition that the sum of the two values is a fixed constant (see (7.3)).

Proposition 8.3.8. For the GSG $\mathfrak{G} = (G, \Sigma_A, \Sigma_B, r)$, with $r = 1$, let u represent the value to Player A. u is bounded as follows:

$$\min_{v \in \Sigma_B} \frac{\alpha[v]}{|\Sigma_A|} \leq u \leq \max_{v \in \Sigma_A} \frac{\beta[v]}{|\Sigma_B|}$$

Note that in the case where $\Sigma_A = \Sigma_B = V(G)$, these inequalities become:

$$\frac{\delta(G) + 1}{|V(G)|} \leq u \leq \frac{\Delta(G) + 1}{|V(G)|} \quad (8.8)$$

The proposition derives from a consideration of ρ_A and ρ_B , defined in Section 8.2.3 as the mixed strategies that allocate equal probabilities to all vertices in a player's strategy set. If Player A employs mixed strategy ρ_A , then Player B can do no better than to deploy at the vertex whose closed neighbourhood contains the fewest possible vertices in Σ_A . The value of the game to Player A cannot therefore be less than the sum of the probabilities that ρ_A assigns to these vertices. This reasoning produces the left hand inequality. The right hand inequality follows in a similar fashion from an analysis of ρ_B as a strategy for Player B. A formal proof follows:

Proof. Suppose that Player A employs the mixed strategy ρ_A which allocates a uniform probability of $|\Sigma_A|^{-1}$ to all vertices $w \in \Sigma_A$. In a particular play of the game, suppose that Player B deploys at vertex $v \in \Sigma_B$.

In this situation, the expected payoff to Player A is $\alpha[v]|\Sigma_A|^{-1}$. Therefore, for any mixed strategy σ_B for Player B:

$$E[p_A(\rho_A, \sigma_B)] \geq \min_{v \in \Sigma_B} \frac{\alpha[v]}{|\Sigma_A|}$$

and thus:

$$u = \max_{\sigma_A} \min_{\sigma_B} E[p_A(\sigma_A, \sigma_B)] \geq \min_{v \in \Sigma_B} \frac{\alpha[v]}{|\Sigma_A|}$$

The proof of the right hand inequality is similar. \square

The following corollary is a consequence of (8.8):

Corollary 8.3.9. *Consider the GSG:*

$$\mathfrak{G} = (G, \Sigma_A, \Sigma_B, r)$$

where $G = (V(G), E(G))$ is a regular graph of degree D , $\Sigma_A = \Sigma_B = V(G)$, $r = 1$ and let u be the value of \mathfrak{G} to Player A. Then:

- $u = (D + 1)/|V(G)|$
- The strategy ρ that allocates a uniform probability of $|V(G)|^{-1}$ to all vertices, is an OMS for both players.

u can also be bounded in a different way:

Proposition 8.3.10. *For the GSG $\mathfrak{G} = (G, \Sigma_A, \Sigma_B, r)$ with $r = 1$, let u represent the value to Player A and:*

$$W = \left\{ W' \subseteq \Sigma_A : \bigcup_{w \in W'} N[w] \supseteq \Sigma_B \right\}$$

$$Z = \{ Z' \subseteq \Sigma_B : d_G(z_1, z_2) > 2, \forall z_1, z_2 \in Z' \}$$

Then u is bounded as follows:

$$\left[\min_{W' \in W} |W'| \right]^{-1} \leq u \leq \left[\max_{Z' \in Z} |Z'| \right]^{-1}$$

The left hand inequality is derived from consideration of the mixed strategy τ_A for Player A that allocates uniform probabilities to a minimal subset of vertices whose closed neighbourhoods cover Σ_B .

The right hand inequality is derived from consideration of the mixed strategy τ_B for Player B that allocates uniform probabilities to a maximal subset of vertices with the property that no two vertices are connected by a path of length less than 3.

Proof. First consider the left hand inequality.

Consider a subset of vertices $W' \in W$ of minimum cardinality. Suppose that Player A employs the mixed strategy τ_A that allocates uniform probability $|W'|^{-1}$ to vertices $w \in W'$ and zero probability to all other vertices.

In a particular play of the game, suppose that Player B deploys at vertex $v \in \Sigma_B$. Since $W' \in W$, we have:

$$\bigcup_{w \in W'} N[w] \supseteq \Sigma_B$$

Therefore $\exists w' \in W'$ such that $v \in N[w']$. Since τ_A allocates a probability of $|W'|^{-1}$ to w' , the expected payoff to Player A is greater than or equal to $|W'|^{-1}$. Therefore, for any mixed strategy σ_B for Player B:

$$E[p_A(\tau_A, \sigma_B)] \geq \left[\min_{W' \in W} |W'| \right]^{-1}$$

and thus:

$$u = \max_{\sigma_A} \min_{\sigma_B} E[p_A(\sigma_A, \sigma_B)] \geq \left[\min_{W' \in W} |W'| \right]^{-1}$$

Now consider the right hand inequality.

Consider a subset of vertices $Z' \in Z$ of maximum cardinality. Suppose that Player B employs the mixed strategy τ_B that allocates uniform probability $|Z'|^{-1}$ to vertices $v \in Z'$ and zero probability to all other vertices.

In a particular play of the game, suppose that Player A deploys at vertex $w \in \Sigma_A$. Since $d_G(z_1, z_2) > 2, \forall z_1, z_2 \in Z'$, we clearly have that:

$$|N[w] \cap Z'| \leq 1$$

So, in this situation, the expected payoff to Player A is less than or equal to $|Z'|^{-1}$. Therefore, for any mixed strategy σ_A for Player A:

$$E[p_A(\sigma_A, \tau_B)] \leq \left[\max_{Z' \in Z} |Z'| \right]^{-1}$$

and thus:

$$u = \max_{\sigma_A} \min_{\sigma_B} E[p_A(\sigma_A, \sigma_B)] \leq \left[\max_{Z' \in Z} |Z'| \right]^{-1}$$

□

Following these results, we label the bounds on u as follows:

- $LB_1 = \min_{v \in \Sigma_B} \frac{\alpha[v]}{|\Sigma_A|}$
- $LB_2 = \left[\min_{W' \in W} |W'| \right]^{-1}$
- $UB_1 = \max_{v \in \Sigma_A} \frac{\beta[v]}{|\Sigma_B|}$
- $UB_2 = \left[\max_{Z' \in Z} |Z'| \right]^{-1}$

For a particular GSG, each of these bounds may or may not be attained. For example, consider the four graphs shown in Figure 8.3. In each case, consider the GSG $\mathfrak{G} = (G, \Sigma_A, \Sigma_B, r)$ with $\Sigma_A = \Sigma_B = V(G)$ and $r = 1$. For such small graphs, OMSs are easy to calculate (for example, using the method described by Morris (1994), pp. 99-114). Table 8.1 summarises the OMSs, the true values of u (the value of \mathfrak{G} to Player A) and the values of the bounds for each of the four games.

It should be noted that while LB_1 and UB_1 will generally be easy to calculate, LB_2 and UB_2 may not be, since the minimal and maximal cardinalities of $W' \in W$ and $Z' \in Z$ respectively may be difficult to determine.

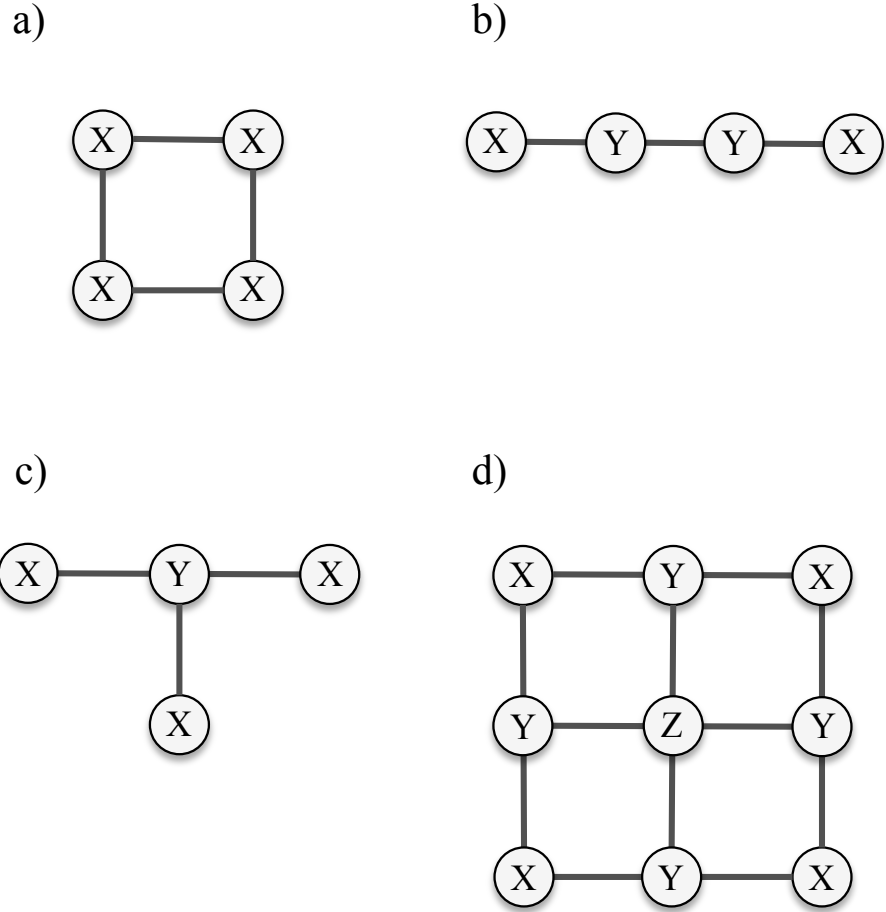


Figure 8.3: Four simple graphs. Solutions of GSGs played over these graphs and the values of the four bounds LB_1 , LB_2 , UB_1 , UB_2 are summarised in Table 8.1.

Graph	u	Bounds				Optimal strategies					
						Player A			Player B		
		LB_1	LB_2	UB_1	UB_2	X	Y	Z	X	Y	Z
a	0.75	0.75	0.50	0.75	1.00	0.25	N/A	N/A	0.25	N/A	N/A
b	0.50	0.50	0.50	0.75	0.50	0.00	0.50	N/A	0.50	0.00	N/A
c	1.00	0.50	1.00	1.00	1.00	0.00	1.00	N/A	0.33	0.00	N/A
d	0.40	0.33	0.33	0.56	0.50	0.00	0.20	0.20	0.15	0.10	0.00

Table 8.1: Summary of the values of bounds LB_1 , LB_2 , UB_1 , UB_2 , the true values u to Player A and examples of OMSs for each player for GSGs played over the four graphs shown in Figure 8.3, with $\Sigma_A = \Sigma_B = V(G)$ and $r = 1$. Shaded cells indicate that the relevant bounds are attained. All figures are rounded to two decimal places.

8.4 Summary and conclusions

In this chapter, we have defined the SSSG, a general, explicitly spatial game for the modelling of search and concealment scenarios. In line with the research objectives set out in Section 1.5, we have demonstrated that the SSSG provides a framework to unite other games presented in the literature and we have derived some initial results on the OMSs of the game and on the values of the game to each player, focusing particularly on games with finite strategy sets and on the special case of the SSSG played over a graph, the Graph Search Game (GSG).

In Chapter 9, we will present a number of additional methods to identify the OMSs of a GSG, including an algorithm based on the iterated elimination of dominated strategies, a technique for exploiting symmetries of the graph over which a game is played and a means of identifying exact solutions for games played over a particular family of graphs.

Chapter 9

Methods for solving GSGs

9.1 Introduction

In Chapters 7 and 8, we first discussed the background and motivations for the SSSG and then defined the game, first in its most general form, over a metric space, then over a graph. Certain initial results were also presented, relating to games with finite strategy sets (which include all games on finite graphs) in Section 8.2.3, concepts of strategic dominance and equivalence in Sections 8.2.4 and 8.3.3, GSGs with non-unit detection radius in Section 8.3.2 and upper and lower bounds on the values of the GSG in Section 8.3.4.

In this chapter, we present some broader methods and concepts for simplifying and analysing GSGs. The first of these concerns the specification of an algorithm that applies the IEDS procedure (see Section 8.2.5) in the context of the GSG; the second involves a method to exploit the automorphisms of a graph to reduce the complexity of a corresponding game; while the third relates to the identification of a specific form of mixed strategy, labelled an “equal oddments strategy”, which, if it exists for a particular graph, must be optimal for both players.

The latter two concepts are combined to present a general method for the solution of a particular family of graphs, which we call “poly-level graphs”.

9.2 Simplifying GSGs algorithmically

9.2.1 An IEDS algorithm for the GSG

The results of Section 8.2.4 and Section 8.3.3 allow for the creation of an IEDS algorithm (see Section 8.2.5) for the GSG $\mathfrak{G} = (G, \Sigma_A, \Sigma_B, r)$. Since the game has finitely many strategies, this approach is always a valid method for finding a solu-

tion of the game (though it may not identify all OMSs), as discussed in Section 8.2.5.

The algorithm identifies vertices that may be very weakly dominated for Player A or Player B and checks for dominance and equivalence over a small subset of their surrounding vertices. Very weakly dominated vertices are eliminated and the strategy sets for the players are iteratively reduced, forming sequences $(\Sigma_{A,K})_{K \in \mathbb{N} \cup \{0\}}$ and $(\Sigma_{B,K})_{K \in \mathbb{N} \cup \{0\}}$ of subsets of Σ_A and Σ_B respectively, until there is no dominance or equivalence in the remaining vertices. The aim is to simplify the game as far as possible, such that OMSs can be more easily identified.

The explicit identification of vertices that cannot be dominated and the subsequent restriction of the set of vertices that should be examined when searching for dominance of a given vertex are intended to facilitate the creation of an efficient computer program to apply IEDS in the GSG. An application of the algorithm in a very simple case is presented in Section 9.2.4.

For the purpose of iteration, our existing notation is extended as follows:

$$\begin{aligned} N_{A,K}[v] &= N[v] \cap \Sigma_{A,K} \\ N_{B,K}[v] &= N[v] \cap \Sigma_{B,K} \\ \alpha_K[v] &= |N_{A,K}[v]| \\ \beta_K[v] &= |N_{B,K}[v]| \end{aligned}$$

Step One: Transformation of G to G'

If $r \neq 1$, we transform G to G' using the method outlined in Section 8.3.2.

We then set the iteration variable $K = 0$ and define:

$$\begin{aligned} \Sigma_{A,0} &= \Sigma_A \\ \Sigma_{B,0} &= \Sigma_B \end{aligned}$$

Step Two: Identify vertices that cannot be very weakly dominated for Player A

By Propositions 8.3.1 and 8.3.3 and Corollary 8.3.4, in a graph in which all vertices have a distinct closed neighbourhood, a vertex v for which:

$$\begin{aligned}
\beta_K[v] &= \Delta(G) + 1 \\
\text{or } N_{B,K}[v] &\neq \emptyset \quad \text{and} \quad B_2[v] \cap \Sigma_{A,K} = \{v\} \\
\text{or} \quad \beta_K[v] &> \max_{w \in S'(v)} (\beta_K[w])
\end{aligned}$$

where:

$$S'(v) = B_2[v] \cap \Sigma_{A,K} \setminus \{v\}$$

cannot be very weakly dominated for Player A by any other vertex. We need not therefore consider such vertices when looking for dominated or equivalent strategies.

Formally, we define a reduced set of strategies for Player A:

$$\Sigma_{A,K}^- = \Sigma_{A,K} \setminus \left[C_{A,K}^{(0)} \cup C_{A,K}^{(1)} \cup C_{A,K}^{(2)} \right]$$

with:

$$\begin{aligned}
C_{A,K}^{(0)} &= \{v \in \Sigma_{A,K} : \beta_K[v] = \Delta(G) + 1\} \\
C_{A,K}^{(1)} &= \{v \in \Sigma_{A,K} : N_{B,K}[v] \neq \emptyset ; B_2[v] \cap \Sigma_{A,K} = \{v\}\} \\
C_{A,K}^{(2)} &= \left\{ v \in \Sigma_{A,K} : \beta_K[v] > \max_{w \in S'(v)} (\beta_K[w]) \right\}
\end{aligned}$$

For a graph in which two vertices may have the same closed neighbourhood, Proposition 8.3.1 is not used, and we instead define:

$$\Sigma_{A,K}^- = \Sigma_{A,K} \setminus \left[C_{A,K}^{(1)} \cup C_{A,K}^{(2)} \right]$$

Step Three: Eliminate very weakly dominated vertices for Player A

Now we must look for very weakly dominated vertices for Player A in $\Sigma_{A,K}^-$.

Vertices $v \in \Sigma_{A,K}$ for which $N_{B,K}[v] = \emptyset$ are dominated automatically by any vertex $w \in \Sigma_{A,K}$ for which $N_{B,K}[w] \neq \emptyset$, while Proposition 8.3.3 states that for each $v \in \Sigma_{A,K}^-$ with $N_{B,K}[v] \neq \emptyset$ we need only look for vertices that very weakly dominate v in $B_2[v] \cap \Sigma_{A,K}$.

Vertices are checked sequentially according to some predetermined ordering and very weakly dominated vertices are removed and are not considered when searching for dominance and equivalence of any remaining vertices. Sequential checking and the immediate removal of identified vertices ensure that pairwise equivalent subsets are

not eliminated from $\Sigma_{A,K}$ in their entirety, but rather reduced to singletons as required.

Let the set of very weakly dominated vertices identified in this way be denoted as $\Psi_{A,K}$.

Formally, we define a new strategy set for Player A:

$$\Sigma_{A,K+1} = \Sigma_{A,K} \setminus \Psi_{A,K}$$

Note that in the trivial case where $N_{B,K}[v] = \emptyset, \forall v \in \Sigma_{A,K}$, all vertices under consideration are equivalent for Player A, so we choose any vertex $\bar{v} \in \Sigma_{A,K}$, define $\Sigma_{A,K+1} = \{\bar{v}\}$, $\Psi_{A,K} = \Sigma_{A,K} \setminus \{\bar{v}\}$ and continue to *Step Four*. This ensures that $\Sigma_{A,K+1}$ is not empty.

Step Four: Identify vertices that cannot be very weakly dominated for Player B

In a similar fashion to *Step Two*, we use Proposition 8.3.6 and Corollary 8.3.7 to define a reduced set of strategies for Player B, removing those strategies that cannot be very weakly dominated:

$$\Sigma_{B,K}^- = \Sigma_{B,K} \setminus \left[C_{B,K}^{(1)} \cup C_{B,K}^{(2)} \right]$$

with:

$$C_{B,K}^{(1)} = \{v \in \Sigma_{B,K} : N_{A,K+1}[v] \neq \emptyset ; B_2[v] \cap \Sigma_{B,K} = \{v\}\}$$

$$C_{B,K}^{(2)} = \left\{ v \in \Sigma_{B,K} : \alpha_{K+1}[v] < \min_{w \in S''(v)} (\alpha_{K+1}[w]) \right\}$$

where:

$$S''(v) = B_2[v] \cap \Sigma_{B,K} \setminus \{v\}$$

However, in the trivial case where $\exists v^* \in \Sigma_{B,K}$ with $N_{A,K+1}[v^*] = \emptyset$, observe that v^* (which need not be unique) very weakly dominates every other vertex for Player B, so we define $\Sigma_{B,K}^- = \Sigma_{B,K}$ and continue to *Step Five*.

Note the use of $N_{A,K+1}[v]$ and $\alpha_{K+1}[v]$ rather than $N_{A,K}[v]$ and $\alpha_K[v]$ at this step.

Step Five: Eliminate very weakly dominated vertices for Player B

Now we must look for very weakly dominated vertices for Player B in $\Sigma_{B,K}^-$.

If $\exists v^* \in \Sigma_{B,K}^-$ with $N_{A,K+1}[v^*] = \emptyset$ then v^* very weakly dominates every other vertex for Player B, as discussed, so we define $\Sigma_{B,K+1} = \{v^*\}$, $\Psi_{B,K} = \Sigma_{B,K} \setminus \{v^*\}$ and continue to *Step Six*.

Otherwise, Proposition 8.3.6 states that for each $v \in \Sigma_{B,K}^-$ we need only look for vertices that very weakly dominate v in $B_2[v] \cap \Sigma_{B,K}$.

Vertices are checked sequentially and very weakly dominated vertices are removed and are not considered when searching for dominance and equivalence of any remaining vertices.

Let the set of very weakly dominated vertices identified in this way be denoted as $\Psi_{B,K}$.

Formally, we define a new strategy set for Player B:

$$\Sigma_{B,K+1} = \Sigma_{B,K} \setminus \Psi_{B,K}$$

Step Six: Condition for continued iteration

If no very weakly dominated vertices were identified at *Step Three* and *Step Five* ($\Psi_{A,K} = \Psi_{B,K} = \emptyset$), then no further pure strategy dominance or equivalence exists. In this case, proceed to *Step Seven*. Otherwise, increase the iteration variable K by one and return to *Step Two*.

Step Seven: Find OMSs for the simplified game

Construct the payoff matrix for the simplified game defined by the strategy sets $\Sigma_{A,K}$, $\Sigma_{B,K}$. If OMSs for this game can be found (for example, using the method described by Morris (1994), pp. 99-114), they are OMSs for the complete GSG (see Morris (1994), pp. 48-49; Berwanger (2007), p. 2).

9.2.2 Termination and efficiency of the algorithm

Note that this algorithm must terminate for some $K \in \mathbb{N} \cup \{0\}$. The condition for continued iteration (*Step Six*) is only fulfilled if new pure strategy dominance or equivalence is identified and this necessarily results in the elimination of strategies from one player's strategy set. Also, the GSG has been defined on graphs with a finite set of κ vertices, which implies that $\Sigma_{A,0}$ and $\Sigma_{B,0}$ are finite sets. Therefore the integer sequence:

$$(|\Sigma_{A,K}| + |\Sigma_{B,K}|)_{K \in \mathbb{N} \cup \{0\}} \quad (9.1)$$

is strictly decreasing and positive, and so must terminate for some $K = K' \in \mathbb{N} \cup \{0\}$.

Though a thorough investigation of the computational complexity of the algorithm is beyond the scope of this current work (and would depend to some extent on its precise implementation), a crude measure of the algorithm's efficiency can be determined by considering the number of pairs of vertices that must be tested for very weak dominance before the algorithm terminates. Given a GSG $\mathfrak{G} = (G, \Sigma_A, \Sigma_B, r)$ with $|V(G)| = \kappa$, an (extremely conservative) upper bound for this number can be determined as follows.

At each of *Steps Three* and *Five*, a particular vertex can be tested against no more than $\kappa - 1$ other vertices. Therefore, the number of vertex pairs tested for very weak dominance at a single iteration certainly does not exceed $2\kappa^2$. Also, since (9.1) is a strictly decreasing positive sequence and $|\Sigma_{A,0}|, |\Sigma_{B,0}| \leq \kappa$, the number of iterations clearly cannot exceed 2κ . Therefore, for any GSG, the total number of vertex pairs that must be tested for very weak dominance before the algorithm terminates will not exceed a cubic function of the number of vertices κ .

Alternatively, since the algorithm only tests vertex pairs for very weak dominance if the distance between them is less than 3, at each of *Steps Three* and *Five*, a particular vertex will be tested against no more than $\Delta(G')^2$ other vertices (where $\Delta(G')$ is the maximum degree of the vertices of the graph after the completion of *Step One*). Therefore, the number of vertex pairs tested in a single iteration certainly does not exceed $2\Delta(G')^2\kappa$. Again using the fact that the number of iterations cannot exceed 2κ , we may conclude that, for any GSG, the total number of vertex pairs tested before termination will not exceed a quadratic function of $\Delta(G')\kappa$.

Which of these bounds is more useful will depend on the structure of the graphs under consideration.

9.2.3 The algorithm applied to games on trees

In this section and the next, we demonstrate that the algorithm of Section 9.2.1 offers a distinct advantage over the method proposed by White (1994) for solving games played on trees (with $r = 1$).¹ Proposition 9.2.2 establishes that the algorithm always succeeds in reducing games of this type to cases that are trivially simple to solve, while Section 9.2.4 presents a simple example which shows that the algorithm can also be applied to games on graphs that are not trees. Also note that White exclusively considers situations where $\Sigma_A = \Sigma_B = V(G)$, while the algorithm presented here is not restricted to such cases.

As in Section 8.2.3, let ρ_A and ρ_B represent the mixed strategies for each player that allocate equal probabilities to all vertices in their strategy set. The following proposition is a restatement of Proposition 8.2.1 in the context of the GSG, with $\chi = 1$.

Proposition 9.2.1. *Consider the GSG:*

$$\mathfrak{G} = (G, \Sigma_A, \Sigma_B, r)$$

with $r = 1$. If we have:

$$\begin{aligned}\alpha[v] &= 1, \quad \forall v \in \Sigma_B \\ \beta[w] &= 1, \quad \forall w \in \Sigma_A\end{aligned}$$

then ρ_A and ρ_B are OMSs for Players A and B respectively and $|\Sigma_A|^{-1} = |\Sigma_B|^{-1} = u$ is the value of the game to Player A.

The following proposition states that, for GSGs on trees with $r = 1$, either the value of the game to Player A is zero and analysis of the game is trivial or the algorithm of Section 9.2.1 reduces the game to the form given in Proposition 9.2.1, for which ρ_A and ρ_B have been shown to be OMSs.

¹ Recall that a tree is a graph in which there is a unique path between any pair of vertices.

Proposition 9.2.2. Consider the GSG:

$$\mathfrak{G} = (G, \Sigma_A, \Sigma_B, r)$$

where G is a tree and $r = 1$. When applied to \mathfrak{G} , the algorithm of Section 9.2.1 terminates for some $K = K' \in \mathbb{N} \cup \{0\}$, such that:

- Either:

$$\begin{aligned}\Sigma_{A,K'} &= \{w\}, \quad \beta_{K'}[w] = 0 \\ \Sigma_{B,K'} &= \{v\}, \quad \alpha_{K'}[v] = 0\end{aligned}$$

and u , the value of the game to Player A, is 0;

- Or:

$$\begin{aligned}\alpha_{K'}[v] &= 1, \quad \forall v \in \Sigma_{B,K'} \\ \beta_{K'}[w] &= 1, \quad \forall w \in \Sigma_{A,K'}\end{aligned}$$

and thus, by Proposition 9.2.1, the mixed strategies $\rho_{A,K'}$ and $\rho_{B,K'}$, which allocate equal probabilities to all vertices in the players' respective strategy sets $\Sigma_{A,K'}$ and $\Sigma_{B,K'}$, are OMSs and the value of the game to Player A is:

$$u = |\Sigma_{A,K'}|^{-1} = |\Sigma_{B,K'}|^{-1}$$

Owing to its length and complexity, the proof of this proposition is presented separately in Section 9.2.5.

9.2.4 An application of the algorithm

A computer program was written in Python (Python Software Foundation, 2012) using NumPy (NumPy Developers, 2012) to implement the algorithm described in Section 9.2.1.

The single example presented here is clearly very simple and is included purely to demonstrate that the algorithm can be applied to games on graphs other than trees, though the extent to which it is able to simplify such games varies greatly. Note particularly that this example has $r \neq 1$ and $\Sigma_A \neq \Sigma_B$.

Consider the GSG $\mathfrak{G}^* = (G^*, \Sigma_A, \Sigma_B, r)$, where $r = 2$ and G^* is the graph over 14 vertices v_0 to v_{13} defined by the adjacency matrix:

$$\mathfrak{M} = \begin{pmatrix} 0 & 0 & 0 & 0 & 0 & 0 & 0 & 0 & 0 & 1 & 0 & 0 & 0 & 0 \\ 0 & 0 & 1 & 0 & 0 & 1 & 0 & 0 & 0 & 0 & 0 & 1 & 0 & 0 \\ 0 & 1 & 0 & 1 & 0 & 0 & 1 & 0 & 0 & 0 & 0 & 0 & 0 & 1 \\ 0 & 0 & 1 & 0 & 0 & 0 & 0 & 0 & 0 & 1 & 0 & 0 & 0 & 0 \\ 0 & 0 & 0 & 0 & 0 & 1 & 0 & 0 & 0 & 0 & 0 & 0 & 1 & 1 \\ 0 & 1 & 0 & 0 & 1 & 0 & 1 & 0 & 0 & 0 & 0 & 0 & 0 & 1 \\ 0 & 0 & 1 & 0 & 0 & 1 & 0 & 0 & 0 & 0 & 1 & 0 & 0 & 0 \\ 0 & 0 & 0 & 0 & 0 & 0 & 0 & 0 & 0 & 0 & 1 & 1 & 1 & 0 \\ 0 & 0 & 0 & 1 & 0 & 0 & 0 & 0 & 0 & 0 & 1 & 0 & 1 & 1 \\ 1 & 0 & 0 & 0 & 0 & 0 & 0 & 1 & 1 & 0 & 0 & 0 & 0 & 1 \\ 0 & 0 & 0 & 0 & 0 & 0 & 1 & 1 & 0 & 0 & 0 & 1 & 1 & 0 \\ 0 & 1 & 0 & 0 & 1 & 0 & 0 & 1 & 1 & 0 & 1 & 0 & 0 & 0 \\ 0 & 0 & 0 & 0 & 1 & 1 & 0 & 1 & 1 & 0 & 0 & 1 & 0 & 0 \\ 0 & 0 & 1 & 0 & 0 & 0 & 0 & 0 & 0 & 1 & 0 & 0 & 0 & 0 \end{pmatrix}$$

and where:

$$\Sigma_A = V(G^*)$$

$$\Sigma_B = \{v_0, v_1, v_2, v_5, v_6, v_8, v_{10}, v_{11}, v_{12}, v_{13}\}$$

The graph G^* is shown in Figure 9.1.

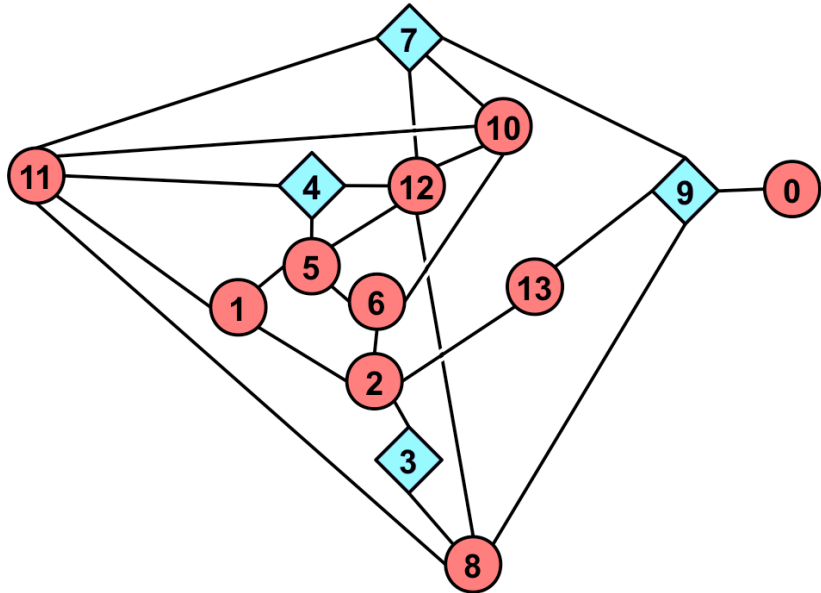


Figure 9.1: The graph G^* . Square vertices lie in Σ_A only, while circular vertices lie in $\Sigma_A \cap \Sigma_B$.

At *Step One*, using the method of Section 8.3.2, the adjacency matrix \mathfrak{M} is replaced with an alternative adjacency matrix \mathfrak{M}' , which represents a graph $G^{*\prime}$ in which all vertices separated by no more than $r = 2$ steps in G^* are connected by an edge:

$$\mathfrak{M}' = \begin{pmatrix} 0 & 0 & 0 & 0 & 0 & 0 & 0 & 1 & 1 & 1 & 0 & 0 & 0 & 1 \\ 0 & 0 & 1 & 1 & 1 & 1 & 1 & 1 & 1 & 1 & 0 & 1 & 1 & 1 \\ 0 & 1 & 0 & 1 & 0 & 1 & 1 & 0 & 1 & 1 & 1 & 1 & 0 & 1 \\ 0 & 1 & 1 & 0 & 0 & 0 & 1 & 0 & 1 & 1 & 0 & 1 & 1 & 1 \\ 0 & 1 & 0 & 0 & 0 & 1 & 1 & 1 & 1 & 0 & 1 & 1 & 1 & 0 \\ 0 & 1 & 0 & 0 & 0 & 1 & 1 & 1 & 1 & 1 & 0 & 1 & 1 & 1 \\ 0 & 1 & 1 & 0 & 1 & 0 & 1 & 1 & 1 & 0 & 1 & 1 & 1 & 0 \\ 0 & 1 & 1 & 1 & 1 & 1 & 1 & 0 & 1 & 0 & 0 & 1 & 1 & 1 \\ 1 & 1 & 0 & 0 & 1 & 1 & 1 & 0 & 1 & 1 & 1 & 1 & 1 & 1 \\ 1 & 1 & 1 & 1 & 1 & 1 & 1 & 0 & 1 & 0 & 1 & 1 & 1 & 1 \\ 1 & 0 & 1 & 1 & 0 & 0 & 0 & 1 & 1 & 1 & 0 & 1 & 1 & 1 \\ 0 & 1 & 1 & 0 & 1 & 1 & 1 & 1 & 1 & 1 & 0 & 1 & 1 & 0 \\ 0 & 1 & 1 & 1 & 1 & 1 & 1 & 1 & 1 & 1 & 1 & 1 & 0 & 0 \\ 0 & 1 & 0 & 1 & 1 & 1 & 1 & 1 & 1 & 1 & 1 & 1 & 1 & 0 \\ 1 & 1 & 1 & 1 & 1 & 0 & 0 & 1 & 1 & 1 & 1 & 0 & 0 & 0 \end{pmatrix}$$

At the first iteration of *Steps Two to Five*, v_0 (very weakly dominated by v_7), v_2, v_3, v_4, v_5, v_6 (by v_1), v_9 (by v_8), v_{10}, v_{11} and v_{12} (by v_1) are eliminated for Player A, and v_1 (very weakly dominated by v_0), v_5 (by v_{10}), v_8 (by v_0), v_{10} (by v_{11}), v_{11} (by v_{12}) and v_{13} (by v_0) are eliminated for Player B, in that order.

At the second iteration, no further dominance is identified, so the algorithm proceeds to *Step Seven*. By this stage, the game has been reduced to the following case:

- Remaining strategies for Player A: v_1, v_7, v_8, v_{13}
- Remaining strategies for Player B: v_0, v_2, v_6, v_{12}
- Payoff matrix (for Player A):

$$\begin{array}{c}
 & \text{Player B} \\
 & v_0 \ v_2 \ v_6 \ v_{12} \\
 \text{Player A} & \begin{array}{c} v_1 \\ v_7 \\ v_8 \\ v_{13} \end{array} \left(\begin{array}{cccc} 0 & 1 & 1 & 1 \\ 1 & 0 & 1 & 1 \\ 1 & 1 & 0 & 1 \\ 1 & 1 & 1 & 0 \end{array} \right)
 \end{array}$$

Calculating the OMSs from this matrix is simple, for example, using the method described by Morris (1994, pp. 99-114). Alternatively, observe that we may apply Proposition 8.2.1 to this reduced game, setting $\chi = 3$.

An OMS for Player A is to play vertices v_1, v_7, v_8, v_{13} , each with probability 0.25; an OMS for Player B is to play vertices v_0, v_2, v_6, v_{12} , each with probability 0.25. The value of the game to Player A is 0.75.

9.2.5 Proof of Proposition 9.2.2

We reproduce the proposition here for ease of reference:

Proposition 9.2.2. *Consider the GSG:*

$$\mathfrak{G} = (G, \Sigma_A, \Sigma_B, r)$$

where G is a tree and $r = 1$. When applied to \mathfrak{G} , the algorithm of Section 9.2.1 terminates for some $K = K' \in \mathbb{N} \cup \{0\}$, such that:

- Either:

$$\begin{aligned}
 \Sigma_{A,K'} &= \{w\}, \quad \beta_{K'}[w] = 0 \\
 \Sigma_{B,K'} &= \{v\}, \quad \alpha_{K'}[v] = 0
 \end{aligned}$$

and u , the value of the game to Player A, is 0;

- Or:

$$\begin{aligned}\alpha_{K'}[v] &= 1, \quad \forall v \in \Sigma_{B,K'} \\ \beta_{K'}[w] &= 1, \quad \forall w \in \Sigma_{A,K'}\end{aligned}$$

and thus, by Proposition 9.2.1, the mixed strategies $\rho_{A,K'}$ and $\rho_{B,K'}$, which allocate equal probabilities to all vertices in the players' respective strategy sets $\Sigma_{A,K'}$ and $\Sigma_{B,K'}$, are OMSs and the value of the game to Player A is:

$$u = |\Sigma_{A,K'}|^{-1} = |\Sigma_{B,K'}|^{-1}$$

The proof of this proposition will require some additional terminology.

As we know, a tree is a graph in which there is a unique path between any pair of vertices. Therefore, if G is a tree, we may designate a vertex $t \in V(G)$ as the “root” of G , such that any vertex $v \neq t$ has precisely one neighbour v_p (the “parent” of v) for which:

$$d_G(t, v_p) = d_G(t, v) - 1$$

For any other neighbour v_c of v (a “child” of v) we have:

$$d_G(t, v_c) = d_G(t, v) + 1$$

We now prove Proposition 9.2.2.

Proof. To derive a contradiction, assume that, when applied to \mathfrak{G} , the algorithm of Section 9.2.1 terminates for some $K = K' \in \mathbb{N} \cup \{0\}$ for which at least one of the following two conditions holds:

- $\exists v' \in \Sigma_{B,K'}$ such that $\alpha_{K'}[v'] > 1$
- $\exists w' \in \Sigma_{A,K'}$ such that $\beta_{K'}[w'] > 1$

We will demonstrate that this assumption is false by identifying two vertices in $\Sigma_{A,K'}$ or $\Sigma_{B,K'}$, one of which very weakly dominates the other for the appropriate player. This will be a contradiction, since the algorithm only terminates when no dominance or equivalence can be found in the reduced strategy sets.

Define the following subsets of $V(G)$:

$$\begin{aligned} S_1 &= \{s \in \Sigma_{B,K'} : \alpha_{K'}[s] > 1\} \\ S_2 &= \{s \in \Sigma_{A,K'} : \beta_{K'}[s] > 1\} \\ S &= S_1 \cup S_2 \end{aligned}$$

Now choose a vertex $t \in V(G)$ to designate as the root of G and let $s' \in S$ be such that:

$$d_G(t, s') = \max_{s \in S} [d_G(t, s)] \quad (9.2)$$

Since $S = S_1 \cup S_2$ there are two possible (non-mutually exclusive) cases: $s' \in S_1$ or $s' \in S_2$.

If $s' \in S_1$ then $s' \in \Sigma_{B,K'}$ and at least two vertices in $N_{K'}[s']$ lie in $\Sigma_{A,K'}$. We consider two possible scenarios.

- First, suppose that at least one of the children of s' lies in $\Sigma_{A,K'}$. So, since $s' \in S_1$, there exist distinct $s_1, s_2 \in N_{A,K'}[s']$ such that:

$$d_G(t, s_1) \leq d_G(t, s_2) = d_G(t, s') + 1 \quad (9.3)$$

Observe that neither s_2 nor any of its children lies in $\Sigma_{B,K'}$, since this would imply that $s_2 \in S_2 \in S$, which is a contradiction by (9.2) and (9.3). Therefore:

$$N_{B,K'}[s_2] = \{s'\} \subseteq N_{B,K'}[s_1]$$

which means that s_1 very weakly dominates s_2 for Player A, by Proposition 8.2.2.

- Now suppose that none of the children of s' lies in $\Sigma_{A,K'}$. Since $s' \in S_1$, this means that s' and its parent both lie in $\Sigma_{A,K'}$. i.e. there exist $s_1, s_2 \in N_{A,K'}[s']$ (where $s_2 = s'$) such that:

$$d_G(t, s_1) < d_G(t, s_2) = d_G(t, s')$$

If none of the children of s_2 lies in $\Sigma_{B,K'}$, then:

$$N_{B,K'}[s_2] \subseteq N_{B,K'}[s_1]$$

which means that s_1 very weakly dominates s_2 for Player A, by Proposition 8.2.2.

Otherwise, at least one child of s_2 lies in $\Sigma_{B,K'}$. Call this child s'' and note that:

$$d_G(t, s'') = d_G(t, s') + 1 \quad (9.4)$$

Observe that neither s'' nor any of its children lies in $\Sigma_{A,K'}$, since this would imply that $s'' \in S_1 \in S$, which is a contradiction by (9.2) and (9.4). Therefore:

$$N_{A,K'}[s''] = \{s'\} \subseteq N_{A,K'}[s']$$

which means that s'' very weakly dominates s' for Player B, by Proposition 8.2.4.

So if $s' \in S_1$, in both possible scenarios, we have identified very weak dominance in one of the strategy sets $\Sigma_{A,K'}$ or $\Sigma_{B,K'}$. In the case where $s' \in S_2$, very weak dominance can also be identified by following very similar logic (the complete proof is omitted). As previously discussed, this is a contradiction and thus our initial assumption was false. Therefore:

$$\begin{aligned} \alpha_{K'}[v] &\leq 1, \quad \forall v \in \Sigma_{B,K'} \\ \beta_{K'}[w] &\leq 1, \quad \forall w \in \Sigma_{A,K'} \end{aligned} \quad (9.5)$$

To complete the proof, note that:

- Any vertex $w \in \Sigma_{A,K'}$ for Player A such that $\beta_{K'}[w] = 0$ is clearly very weakly dominated by any other vertex for Player A.
- Any vertex $v \in \Sigma_{B,K'}$ for Player B such that $\alpha_{K'}[v] = 0$ clearly very weakly dominates any other vertex for Player B.
- Statements $(*)$ and $(**)$ are equivalent:

$$[\alpha_{K'}[v] = 0 ; \quad \forall v \in \Sigma_{B,K'}] \quad (*)$$

$$[\beta_{K'}[w] = 0 ; \quad \forall w \in \Sigma_{A,K'}] \quad (**)$$

- Since the algorithm has terminated, no very weak dominance exists in $\Sigma_{A,K'}$ or $\Sigma_{B,K'}$.

These facts, combined with (9.5) imply that:

- Either:

$$\begin{aligned}\Sigma_{A,K'} &= \{w\}, \quad \beta_{K'}[w] = 0 \\ \Sigma_{B,K'} &= \{v\}, \quad \alpha_{K'}[v] = 0\end{aligned}$$

and u , the value of the game to Player A, is clearly 0;

- Or:

$$\begin{aligned}\alpha_{K'}[v] &= 1, \quad \forall v \in \Sigma_{B,K'} \\ \beta_{K'}[w] &= 1, \quad \forall w \in \Sigma_{A,K'}\end{aligned}$$

and, by Proposition 9.2.1, $\rho_{A,K'}$ and $\rho_{B,K'}$ are OMSs for each player and the value of the game to Player A is:

$$u = |\Sigma_{A,K'}|^{-1} = |\Sigma_{B,K'}|^{-1}$$

This proves the proposition. \square

9.3 Further methods for analysing GSGs

9.3.1 Exploiting the automorphisms of the GSG

The definitions and notation relating to group theory used in this section are from Neumann et al. (1994).

An automorphism of a graph $G = (V(G), E(G))$ is a mapping of the graph to itself, which preserves adjacencies. The following definition is adapted from Bondy and Murty (1976), pp. 5-7:

Definition 9.3.1. Consider a simple graph $G = (V(G), E(G))$.

- An **automorphism** ϕ of G is a permutation of the vertices:

$$\begin{aligned}\phi &: V(G) \rightarrow V(G) \\ v &\mapsto \phi(v)\end{aligned}$$

such that:

$$\{v, w\} \in E(G) \Leftrightarrow \{\phi(v), \phi(w)\} \in E(G)$$

- The **automorphism group** $\Gamma(G)$ is the permutation group formed by the set of all automorphisms of G , with the operation of composition.
- The **orbit** $\mathcal{O}_H[v]$ of a vertex $v \in V(G)$ under a subgroup $H \leq \Gamma(G)$ is the set:

$$\mathcal{O}_H[v] = \{w \in V(G) : \exists \phi \in H \text{ with } \phi(v) = w\}$$

The orbits of the vertices of G under H form a partition of $V(G)$.

Note that this definition is valid for simple graphs. For more general graphs, which may include directed edges, loops, or multiple edges connecting the same vertices, a permutation of the edges also needs to be specified.

We extend the concept of a graph automorphism to that of a graph game automorphism, an automorphism of the graph that also preserves the strategic status of the vertices:

Definition 9.3.2. Consider a GSG:

$$\mathfrak{G} = (G, \Sigma_A, \Sigma_B, r)$$

with $r = 1$. A **graph game automorphism** ϕ of \mathfrak{G} is an automorphism of G , such that:

- $v \in \Sigma_A \Leftrightarrow \phi(v) \in \Sigma_A , \forall v \in V(G)$
- $v \in \Sigma_B \Leftrightarrow \phi(v) \in \Sigma_B , \forall v \in V(G)$

We can also define automorphism groups and vertex orbits in terms of graph game automorphisms:

Proposition 9.3.3. Consider a GSG:

$$\mathfrak{G} = (G, \Sigma_A, \Sigma_B, r)$$

with $r = 1$.

- The set of all graph game automorphisms of \mathfrak{G} , with the operation of composition, forms a subgroup $\Gamma(\mathfrak{G})$ (the **graph game automorphism group**) of $\Gamma(G)$.
- The orbits of the vertices of G under any subgroup $H \leq \Gamma(\mathfrak{G})$ form a partition of $V(G)$.

For $\Gamma(\mathfrak{G})$ to be a subgroup of $\Gamma(G)$, we require that $\Gamma(\mathfrak{G})$ is closed under composition, contains the identity and contains an inverse for every element. Since the only restriction on $\Gamma(\mathfrak{G})$ is that Σ_A, Σ_B are invariant under its elements, these conditions are clearly satisfied. The second part of the proposition is true of any permutation group.

The following proposition describes a relationship between certain OMSs of \mathfrak{G} and the graph game automorphism group $\Gamma(\mathfrak{G})$.

Proposition 9.3.4. *Consider a GSG:*

$$\mathfrak{G} = (G, \Sigma_A, \Sigma_B, r)$$

with $V(G) = \{v_1, \dots, v_\kappa\}$ and $r = 1$. Let $\mathcal{O}[v]$ denote the orbit of v under some subgroup H of the graph game automorphism group $\Gamma(\mathfrak{G})$.

There exists a pair of OMSs:

$$\begin{aligned}\boldsymbol{\sigma}_A &= (\sigma_A[v_1], \dots, \sigma_A[v_\kappa]) \\ \boldsymbol{\sigma}_B &= (\sigma_B[v_1], \dots, \sigma_B[v_\kappa])\end{aligned}$$

where $\boldsymbol{\sigma}_A$ and $\boldsymbol{\sigma}_B$ respectively allocate probabilities $\sigma_A[v_i]$ and $\sigma_B[v_i]$ to vertex v_i , such that $\forall i, j \in \{1, \dots, \kappa\}$:

$$\mathcal{O}[v_i] = \mathcal{O}[v_j] \Rightarrow \begin{cases} \sigma_A[v_i] = \sigma_A[v_j] \\ \sigma_B[v_i] = \sigma_B[v_j] \end{cases} \quad (9.6)$$

Note that in particular the proposition is true for $H = \Gamma(\mathfrak{G})$.

In order to avoid interrupting the thread of this section, the lengthy proof of Proposition 9.3.4 is presented separately in Section 9.3.4.

Proposition 9.3.4 implies that, when looking for OMSs for a GSG \mathfrak{G} , it suffices to consider those strategies that allocate equal probability to all vertices lying in the same orbit under graph game automorphisms. For graphs with high numbers of symmetries, this can significantly simplify the analysis of the game.

Furthermore, the fact that the proposition is valid for any subgroup $H \leq \Gamma(\mathfrak{G})$ ensures that even if not all graph game automorphisms of \mathfrak{G} are known, to find a pair of OMSs, it is sufficient to restrict consideration to those strategies that allocate equal

probability to all vertices lying in the same orbit under the subgroup generated by those graph game automorphisms that can be identified.

Note that, though stated and proved in a different setting, this proposition is strongly related to Zoroa and Zoroa's Theorem 2.1 (1993, pp. 526-528), which relates to games played over sets that admit certain transformations. However, Zoroa and Zoroa require that the transformations considered be commutative, which is not necessarily true of the automorphisms of a graph.

9.3.2 Example: Using automorphisms to find solutions of \mathfrak{G}

Consider the GSG $\mathfrak{G} = (G_{5,5}, \Sigma_A, \Sigma_B, r)$, where $G_{5,5}$ is the 5×5 rectangular grid graph depicted in Figure 9.2, $\Sigma_A = \Sigma_B = V(G_{5,5})$ and $r = 1$. Each player has 25 possible pure strategies: $V(G_{5,5}) = \{v_1, \dots, v_{25}\}$.

Note that since both Players may deploy at any vertex, $\Gamma(\mathfrak{G}) = \Gamma(G_{5,5})$, so we consider all automorphisms of $G_{5,5}$. These automorphisms are rotations through multiples of $\pi/2$, reflection about a vertical axis and compositions of these transformations. The vertices can be partitioned into six orbits, which we denote as $\mathcal{O}^{(i)}$, $i \in \{1, \dots, 6\}$. The vertices belonging to each orbit are indicated in Figure 9.2.

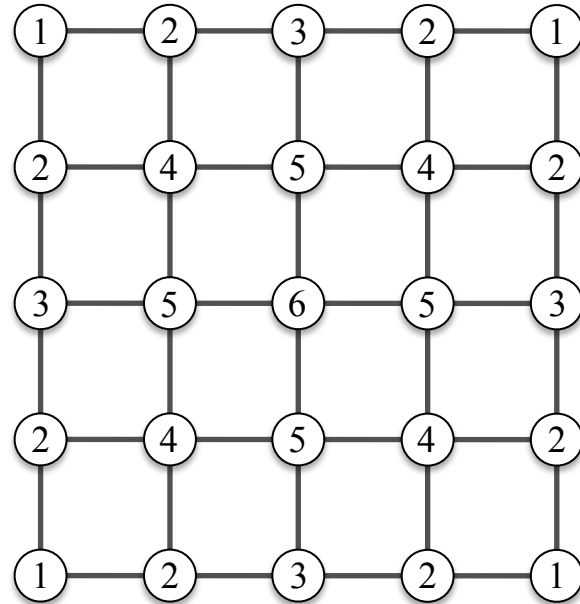


Figure 9.2: The 5×5 rectangular grid graph $G_{5,5}$. Vertices marked i belong to orbit $\mathcal{O}^{(i)}$ under $\Gamma(G_{5,5})$.

By Proposition 9.3.4, there exist OMSs σ_A , σ_B for Players A and B, which allocate the same probability to all vertices lying in the same orbit. Let $\omega_A^{(i)}$ and $\omega_B^{(i)}$ be the respective probabilities that σ_A and σ_B allocate to individual vertices in orbit $\mathcal{O}^{(i)}$, and define:

$$A_i = |\mathcal{O}^{(i)}| \omega_A^{(i)}, \quad B_i = |\mathcal{O}^{(i)}| \omega_B^{(i)}, \quad \forall i \in \{1, \dots, 6\} \quad (9.7)$$

Observe that:

$$\sum_{i=1}^6 A_i = \sum_{i=1}^6 B_i = 1$$

A_i and B_i represent the total probability that σ_A and σ_B respectively allocate to all vertices in orbit $\mathcal{O}^{(i)}$.

Let $\sigma^{(1)}, \dots, \sigma^{(6)}$ be the mixed strategies (for either player), which allocate uniform probability to all vertices in the corresponding orbit and zero probability to other vertices:

$$\sigma^{(i)} = (\sigma^{(i)}[v_1], \dots, \sigma^{(i)}[v_{25}])$$

with:

$$\sigma^{(i)}[v_j] = \begin{cases} |\mathcal{O}^{(i)}|^{-1}, & v_j \in \mathcal{O}^{(i)} \\ 0, & \text{otherwise.} \end{cases}$$

We see that σ_A and σ_B are linear combinations of the $\sigma^{(i)}$, weighted by the orbit probabilities A_i and B_i :

$$\sigma_A = \sum_{i=1}^6 A_i \sigma^{(i)}, \quad \sigma_B = \sum_{i=1}^6 B_i \sigma^{(i)}$$

This observation allows us to take a different perspective on the problem. Suppose that we treat the $\sigma^{(i)}$ as if they were pure strategies. The following strategies would be optimal strategies of such a game:

$$\begin{aligned} \tau_A &= (\tau_A[\sigma^{(1)}], \dots, \tau_A[\sigma^{(6)}]) \\ \tau_B &= (\tau_B[\sigma^{(1)}], \dots, \tau_B[\sigma^{(6)}]) \end{aligned}$$

with:

$$\begin{aligned} \tau_A[\sigma^{(i)}] &= A_i, \quad \forall i \in \{1, \dots, 6\} \\ \tau_B[\sigma^{(i)}] &= B_i, \quad \forall i \in \{1, \dots, 6\} \end{aligned}$$

To find these OMSs, we analyse the matrix of expected payoffs to Player A for each of these six strategies against one another:

		Player B					
		$\sigma^{(1)}$	$\sigma^{(2)}$	$\sigma^{(3)}$	$\sigma^{(4)}$	$\sigma^{(5)}$	$\sigma^{(6)}$
Player A		$\sigma^{(1)}$	1/4	1/4	0	0	0
		$\sigma^{(2)}$	1/4	1/8	1/4	1/4	0
		$\sigma^{(3)}$	0	1/4	1/4	0	1/4
		$\sigma^{(4)}$	0	1/4	0	1/4	1/2
		$\sigma^{(5)}$	0	0	1/4	1/2	1/4
		$\sigma^{(6)}$	0	0	0	0	1
							1

The OMSs τ_A and τ_B can be computed from this payoff matrix using standard methods (see, for example, Morris (1994), pp. 99-114), giving:

$$(A_1, \dots, A_6) = 69^{-1}(16, 28, 10, 4, 6, 5)$$

$$(B_1, \dots, B_6) = 69^{-1}(16, 28, 10, 4, 6, 5)$$

Using (9.7) we then find:

$$\left(\omega_A^{(1)}, \dots, \omega_A^{(6)}\right) = 138^{-1}(8, 7, 5, 2, 3, 10)$$

$$\left(\omega_B^{(1)}, \dots, \omega_B^{(6)}\right) = 138^{-1}(8, 7, 5, 2, 3, 10)$$

This fully determines the OMSs σ_A and σ_B for \mathfrak{G} . These OMSs are illustrated in Figure 9.3.

Note that by identifying the six orbits of $V(G)$ under graph game automorphisms of \mathfrak{G} , rather than solving a game with a 25×25 payoff matrix, we needed only to solve a game with a 6×6 payoff matrix. A similar method could be applied to any GSG $\mathfrak{G} = (G, \Sigma_A, \Sigma_B, r)$ with $r = 1$, for which non-trivial graph game automorphisms can be found.

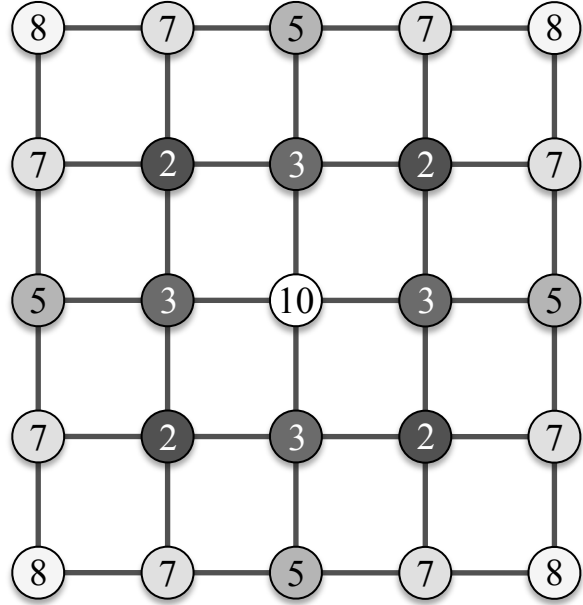


Figure 9.3: Probability oddments (integer values proportional to the probabilities) allocated to each vertex of $G_{5,5}$ by the (identical) OMSs σ_A and σ_B for the GSG $\mathfrak{G} = (G_{5,5}, \Sigma_A, \Sigma_B, r)$, with $r = 1$ and $\Sigma_A = \Sigma_B = V(G_{5,5})$. Darker shading indicates lower probability oddments.

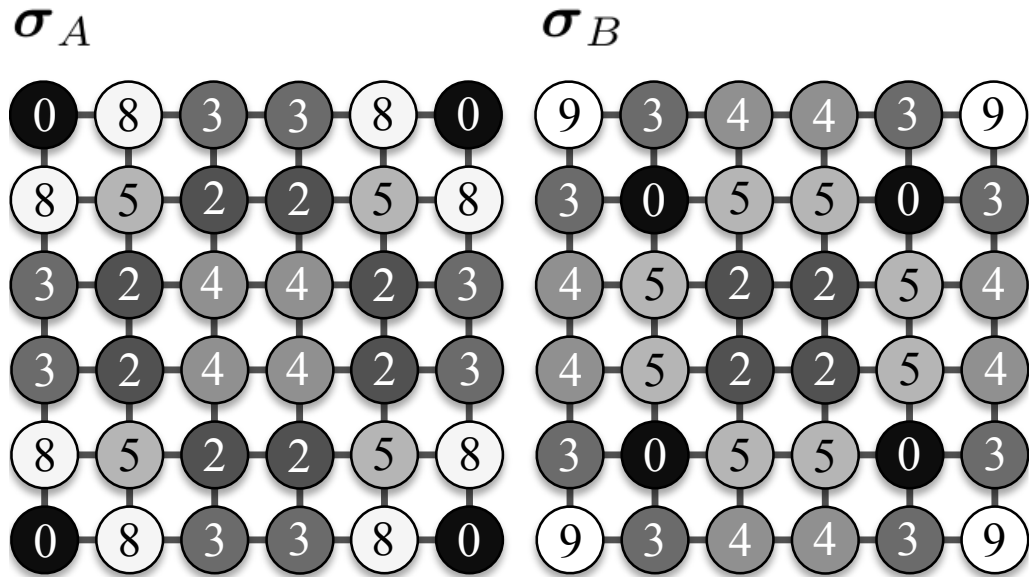


Figure 9.4: Probability oddments allocated to each vertex of $G_{6,6}$ by the OMSs σ_A and σ_B for the GSG $\mathfrak{G} = (G_{6,6}, \Sigma_A, \Sigma_B, r)$, with $r = 1$ and $\Sigma_A = \Sigma_B = V(G_{6,6})$. Darker shading indicates lower probability oddments.

9.3.3 Equal oddments strategies

The example of the GSG \mathfrak{G} played over the 5×5 rectangular grid $G_{5,5}$ exhibits two curious and related properties.

Firstly, and most obviously, the OMSs that were calculated for each player are identical $\sigma_A = \sigma_B = \sigma$. This means that the OMS for Player A allocates identical probabilities to the vertices of $G_{5,5}$ as does the OMS for Player B (though these OMSs need not be unique). Given the interpretation of the game, this is a surprising result. Player B is attempting to hide from Player A, so we might have expected that her best mixed strategy would involve avoiding vertices at which Player A was more likely to deploy.

Note that the method of Section 9.3.1 does not produce identical OMSs for all graphs, nor for all grid graphs. For example, when applied to the 6×6 grid graph $G_{6,6}$, the method produces distinct OMSs σ_A, σ_B (see Figure 9.4) that appear to be more consistent with our intuition, in that vertices to which σ_A allocates fairly high probability seem to be allocated fairly low probability by σ_B and vice-versa.

Secondly, in Figure 9.3, observe that for all vertices $v \in V(G_{5,5})$, the sum of the probability oddments allocated by σ to the vertices in the closed neighbourhood $N[v]$ is equal to 22. Formally, we make the following definition:

Definition 9.3.5. *Given a GSG, $\mathfrak{G} = (G, \Sigma_A, \Sigma_B, r)$, for which $r = 1$ and $\Sigma_A = \Sigma_B = V(G) = \{v_1, \dots, v_\kappa\}$, an **equal oddments strategy** σ is a vector:*

$$\sigma = (\sigma[v_1], \dots, \sigma[v_\kappa])$$

with:

$$0 \leq \sigma[v_i] \leq 1, \quad \forall i \in \{1, \dots, \kappa\} \quad (9.8)$$

$$\sum_{i=1}^{\kappa} \sigma[v_i] = 1 \quad (9.9)$$

such that:

$$\sum_{w \in N[v_j]} \sigma[w] = u, \quad \forall j \in \{1, \dots, \kappa\} \quad (9.10)$$

For some $u \in \mathbb{R}$. We call u the **neighbourhood sum** of σ .

The following proposition links those situations in which Players A and B have identical OMSs with the existence of equal oddments strategies.

Proposition 9.3.6. *Given a GSG, $\mathfrak{G} = (G, \Sigma_A, \Sigma_B, r)$, for which $r = 1$ and $\Sigma_A = \Sigma_B = V(G)$, then the following statements are equivalent:*

- σ is an equal oddments strategy of \mathfrak{G} with neighbourhood sum $u \in \mathbb{R}$.
- σ is an OMS of \mathfrak{G} for both players and $u \in \mathbb{R}$ is the value of the game to Player A.

Proof. Suppose that σ is an equal oddments strategy of \mathfrak{G} with neighbourhood sum $u \in \mathbb{R}$. Observe that for all pure strategies $v \in V(G)$ for either player, we have:

$$\begin{aligned} E[p_A(v, \sigma)] &= u \\ E[p_B(\sigma, v)] &= 1 - u \end{aligned}$$

Therefore, by (8.4), σ is an OMS of \mathfrak{G} for both players and u is the value of the game to Player A.

To prove the opposite implication, suppose that σ is an OMS of \mathfrak{G} for both players and that u is the value of the game to Player A. Let:

$$\begin{aligned} V(G) &= \{v_1, \dots, v_\kappa\} \\ \sigma &= (\sigma[v_1], \dots, \sigma[v_\kappa]) \end{aligned}$$

Also let:

$$\begin{aligned} m_- &= \min_{v \in V(G)} \left[\sum_{w \in N[v]} \sigma[w] \right] \\ m_+ &= \max_{v \in V(G)} \left[\sum_{w \in N[v]} \sigma[w] \right] \end{aligned}$$

and let v_- , v_+ be vertices for which this minimum and maximum are respectively attained.

Assume (to derive a contradiction) that σ is not an equal oddments strategy. Then:

$$m_- < m_+ \tag{9.11}$$

Therefore:

$$\begin{aligned} m_+ &= \text{E}[p_A(v_+, \sigma)] \geq \text{E}[p_A(\sigma, \sigma)] = u \\ 1 - m_- &= \text{E}[p_B(\sigma, v_-)] \geq \text{E}[p_B(\sigma, \sigma)] = 1 - u \end{aligned}$$

Since σ is an OMS, the above inequalities must be equalities. Specifically:

$$m_- = m_+ = u$$

This contradicts (9.11). Therefore σ is an equal oddments strategy. \square

Proposition 9.3.6 means that, given a GSG $\mathfrak{G} = (G, \Sigma_A, \Sigma_B, r)$, with $r = 1$ and $\Sigma_A = \Sigma_B = V(G)$, if we can find a distribution of positive real numbers across the vertices such that the sum of these numbers in any closed neighbourhood is equal to a constant, and we scale these numbers to produce a valid probability distribution across the vertices, this distribution defines a mixed strategy that is optimal for both players. This offers an alternative approach to proving Corollary 8.3.9 on OMSs for GSGs played over regular graphs, since the mixed strategy ρ , as defined in the corollary, is clearly an equal oddments strategy.

9.3.4 Proof of Proposition 9.3.4

The definitions and notation relating to group theory used in this section are from Neumann et al. (1994). The proof requires the orbit-stabilizer theorem (adapted from Neumann et al., 1994, p. 62):

Theorem 9.3.7. *Orbit-Stabilizer Theorem*

Given a group Γ , which acts on a finite set X :

$$|\text{Stab}_\Gamma(x)| = \frac{|\Gamma|}{|\mathcal{O}_\Gamma[x]|}, \quad \forall x \in X$$

*where $\mathcal{O}_\Gamma[x]$ is the orbit of x under the action of Γ , and $\text{Stab}_\Gamma(x)$ is the **stabilizer** of x under Γ :*

$$\text{Stab}_\Gamma(x) = \{g \in \Gamma : gx = x\}$$

To prove Proposition 9.3.4, we will use the following corollary of the theorem. It states that if two vertices v, w of a GSG lie in the same orbit with respect to graph game automorphisms, then the number of graph game automorphisms that map v to some other vertex z is the same as the number that map w to z .

Corollary 9.3.8. Consider a subgroup H of the graph game automorphism group $\Gamma(\mathfrak{G})$ for the GSG $\mathfrak{G} = (G, \Sigma_A, \Sigma_B, r)$, with $r = 1$ and let $\mathcal{O}[v]$ be the orbit of $v \in V(G)$ under H .

Then, for all $v, w, z \in V(G)$, we have:

$$\begin{aligned} \mathcal{O}[v] &= \mathcal{O}[w] \\ \Rightarrow |H[v, z]| &= |H[w, z]| = \begin{cases} \frac{|H|}{|\mathcal{O}[v]|}, & z \in \mathcal{O}[v] \\ 0, & z \notin \mathcal{O}[v] \end{cases} \end{aligned}$$

where we define:

$$H[v, z] = \{\phi \in H : \phi(v) = z\}$$

Proof. Clearly, if $\mathcal{O}[v] = \mathcal{O}[w]$ and $z \notin \mathcal{O}[v]$ then by the definition of an orbit under H , we have that:

$$|H[v, z]| = |H[w, z]| = 0$$

We claim that in the case where $z \in \mathcal{O}[v]$, we have:

$$H[v, z] = \psi_{v,z} \text{Stab}_H(v) \quad (9.12)$$

where $\psi_{v,z} \in H$ is any graph game automorphism in H such that $\psi_{v,z}(v) = z$ and $\psi_{v,z} \text{Stab}_H(v)$ is the left coset of $\text{Stab}_H(v)$ in H containing $\psi_{v,z}$:

$$\psi_{v,z} \text{Stab}_H(v) = \{\psi_{v,z} \circ \phi \in H : \phi \in \text{Stab}_H(v)\}$$

where \circ represents the operation of composition.

To justify the claim, we first observe that:

$$\psi \in \psi_{v,z} \text{Stab}_H(v) \Rightarrow \psi \in H[v, z]$$

because:

$$\begin{aligned} \psi &\in \psi_{v,z} \text{Stab}_H(v) \\ \Rightarrow \psi(v) &= \psi_{v,z}(\phi(v)), \quad \phi(v) \in \text{Stab}_H(v) \\ &= \psi_{v,z}(v) \\ &= z \\ \Rightarrow \psi &\in H[v, z] \end{aligned}$$

We also observe that:

$$\psi \in H[v, z] \Rightarrow \psi \in \psi_{v,z} \text{Stab}_H(v)$$

because:

$$\begin{aligned} \psi &\in H[v, z] \\ \Rightarrow \psi &= \psi_{v,z} \circ (\psi_{v,z}^{-1} \circ \psi) \end{aligned}$$

and:

$$\psi_{v,z}^{-1}(\psi(v)) = \psi_{v,z}^{-1}(z) = v$$

so:

$$\psi_{v,z}^{-1} \circ \psi \in \text{Stab}_H(v)$$

and therefore:

$$\psi \in \psi_{v,z} \text{Stab}_H(v)$$

This demonstrates the claim (9.12).

Now, combining this result with a standard result about cosets (Neumann et al., 1994, p. 3) gives us that:

$$|H[v, z]| = |\psi_{v,z} \text{Stab}_H(v)| = |\text{Stab}_H(v)|$$

So by the orbit-stabilizer theorem:

$$|H[v, z]| = \frac{|H|}{|\mathcal{O}[v]|}$$

Clearly, bearing in mind that $|\mathcal{O}[v]| = |\mathcal{O}[w]|$, identical logic could be employed to demonstrate that:

$$|H[w, z]| = \frac{|H|}{|\mathcal{O}[v]|}$$

This proves the corollary. \square

We now prove Proposition 9.3.4, reproduced here for ease of reference:

Proposition 9.3.4. *Consider a GSG:*

$$\mathfrak{G} = (G, \Sigma_A, \Sigma_B, r)$$

with $V(G) = \{v_1, \dots, v_\kappa\}$ and $r = 1$. Let $\mathcal{O}[v]$ denote the orbit of v under some subgroup H of the graph game automorphism group $\Gamma(\mathfrak{G})$.

There exists a pair of OMSs:

$$\begin{aligned}\boldsymbol{\sigma}_A &= (\sigma_A[v_1], \dots, \sigma_A[v_\kappa]) \\ \boldsymbol{\sigma}_B &= (\sigma_B[v_1], \dots, \sigma_B[v_\kappa])\end{aligned}$$

where $\boldsymbol{\sigma}_A$ and $\boldsymbol{\sigma}_B$ respectively allocate probabilities $\sigma_A[v_i]$ and $\sigma_B[v_i]$ to vertex v_i , such that $\forall i, j \in \{1, \dots, \kappa\}$:

$$\mathcal{O}[v_i] = \mathcal{O}[v_j] \Rightarrow \begin{cases} \sigma_A[v_i] = \sigma_A[v_j] \\ \sigma_B[v_i] = \sigma_B[v_j] \end{cases} \quad (9.6)$$

Proof. Let $\boldsymbol{\tau}_A, \boldsymbol{\tau}_B$ be any OMSs for Players A and B:

$$\begin{aligned}\boldsymbol{\tau}_A &= (\tau_A[v_1], \dots, \tau_A[v_\kappa]) \\ \boldsymbol{\tau}_B &= (\tau_B[v_1], \dots, \tau_B[v_\kappa])\end{aligned}$$

Given $\phi \in H$, let:

$$\begin{aligned}\boldsymbol{\tau}_{A,\phi} &= (\tau_A[\phi(v_1)], \dots, \tau_A[\phi(v_\kappa)]) \\ \boldsymbol{\tau}_{B,\phi} &= (\tau_B[\phi(v_1)], \dots, \tau_B[\phi(v_\kappa)])\end{aligned}$$

So $\boldsymbol{\tau}_{A,\phi}, \boldsymbol{\tau}_{B,\phi}$ are the mixed strategies that respectively allocate probabilities $\tau_A[\phi(v_i)]$ and $\tau_B[\phi(v_i)]$ to vertex v_i , for all $i \in \{1, \dots, \kappa\}$.

We first show that if $\boldsymbol{\tau}_A$ is an OMS for Player A, then $\boldsymbol{\tau}_{A,\phi}$ is also an OMS for Player A, for all $\phi \in H$.

For a particular $\phi \in H$, consider the graph $G' = (V(G'), E(G'))$ and the sets Σ'_A, Σ'_B constructed by relabelling the vertices of G such that:

$$v_i \mapsto \phi^{-1}(v_i), \quad \forall i \in \{1, \dots, \kappa\}$$

$\boldsymbol{\tau}_{A,\phi}$ and $\boldsymbol{\tau}_{B,\phi}$ are clearly OMSs for the resulting game $\mathfrak{G}' = (G', \Sigma'_A, \Sigma'_B, r)$.

However, since $\phi \in H \leq \Gamma(\mathfrak{G})$, Σ_A, Σ_B are invariant under ϕ (see Definition 9.3.2) and thus:

$$\Sigma'_A = \Sigma_A, \quad \Sigma'_B = \Sigma_B$$

Also, because ϕ is an automorphism, we have:

$$V(G') = V(G) \quad , \quad E(G') = E(G)$$

Therefore $\mathfrak{G}' = \mathfrak{G}$ and so $\tau_{A,\phi}$ and $\tau_{B,\phi}$ are OMSs of \mathfrak{G} for Players A and B respectively, as required.

Now, let:

$$\begin{aligned} \sigma_A &= \frac{1}{|H|} \sum_{\phi \in H} \tau_{A,\phi} \\ \sigma_B &= \frac{1}{|H|} \sum_{\phi \in H} \tau_{B,\phi} \end{aligned}$$

These mixed strategies are OMSs for \mathfrak{G} , because any weighted average of OMSs is itself an OMS.

It remains to prove that σ_A and σ_B satisfy Property (9.6). Observe that, for all $i \in \{1, \dots, \kappa\}$:

$$\begin{aligned} \sigma_A[v_i] &= \frac{1}{|H|} \sum_{j=1}^{\kappa} |H[v_i, v_j]| \tau_A[v_j] \\ \sigma_B[v_i] &= \frac{1}{|H|} \sum_{j=1}^{\kappa} |H[v_i, v_j]| \tau_B[v_j] \end{aligned} \tag{9.13}$$

where $H[v_i, v_j]$ is defined as in Corollary 9.3.8.

Using the corollary, (9.13) can be rewritten as follows, $\forall v \in V(G)$:

$$\begin{aligned} \sigma_A[v] &= \frac{1}{|\mathcal{O}[v]|} \sum_{w \in \mathcal{O}[v]} \tau_A[w] \\ \sigma_B[v] &= \frac{1}{|\mathcal{O}[v]|} \sum_{w \in \mathcal{O}[v]} \tau_B[w] \end{aligned}$$

This demonstrates that σ_A and σ_B satisfy Property (9.6) and thus proves Proposition 9.3.4. \square

9.4 Games on poly-level graphs

9.4.1 Poly-level graphs

The concepts discussed in Section 9.3 suggest a potential approach for finding general expressions for the OMSs of GSGs played over certain families of graphs. To demonstrate this approach, we consider GSGs played over a specific family of graphs, which we describe as **poly-level graphs**. The vertices in such graphs are arranged in levels and each vertex exhibits a local structural similarity in the way that it is connected to other vertices in its own level and to those in the levels above and below.

Definition 9.4.1. A graph $G = (V(G), E(G))$ is called a **poly-level graph** if and only if the vertices can be partitioned into h subsets $L_1, L_2, \dots, L_h \subseteq V(G)$ called **levels**, with $|L_i| = c_i$, such that each vertex in L_i is adjacent to precisely:

- j other vertices in L_i (the **intradegree**) ;
- k vertices in L_{i+1} (the **superdegree**), for $i \neq h$;
- l vertices in L_{i-1} (the **subdegree**), for $i \neq 1$;
- 0 vertices in any other level.

where j is a non-negative integer and h, k, l, c_1, \dots, c_h are positive integers.

Figure 9.5 provides a visual representation of a general poly-level graph, while Figures 9.6-9.10 show specific examples of such graphs. In each example, vertices in L_1 are coloured black, with higher levels being indicated by progressively lighter shades.

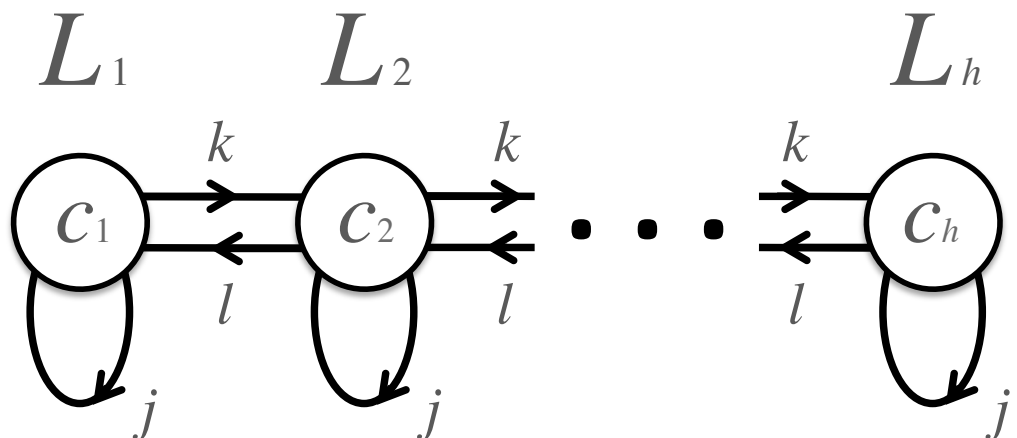


Figure 9.5: Visual representation of a poly-level graph. c_i represents the number of vertices in level L_i ; j, k and l represent the number of edges connecting a single vertex in the level at the tail of the arrow to vertices in the level at the head of the arrow.

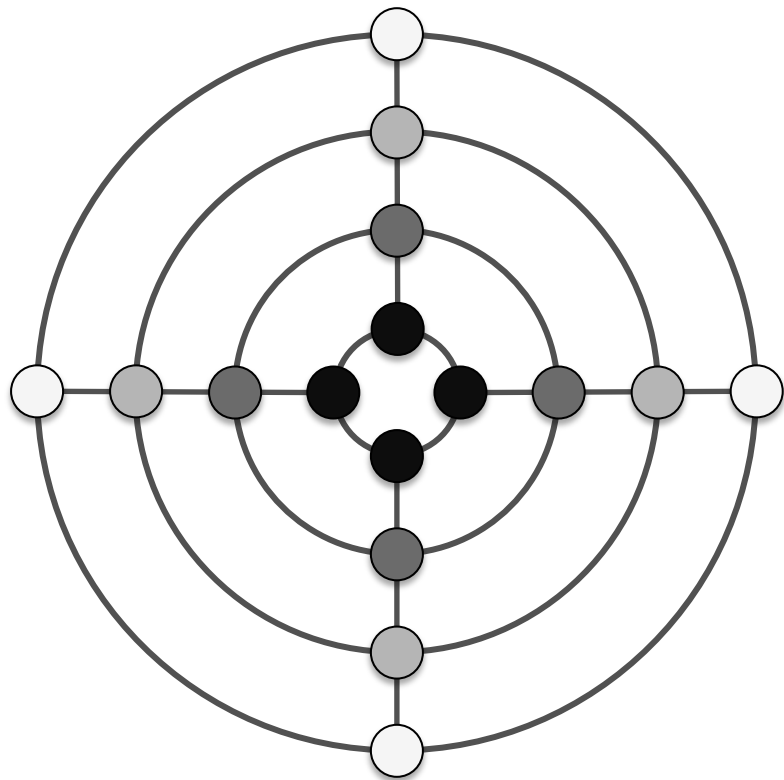


Figure 9.6: Poly-level graph with $h = 4, j = 2, k = 1, l = 1, c_1 = 4$.

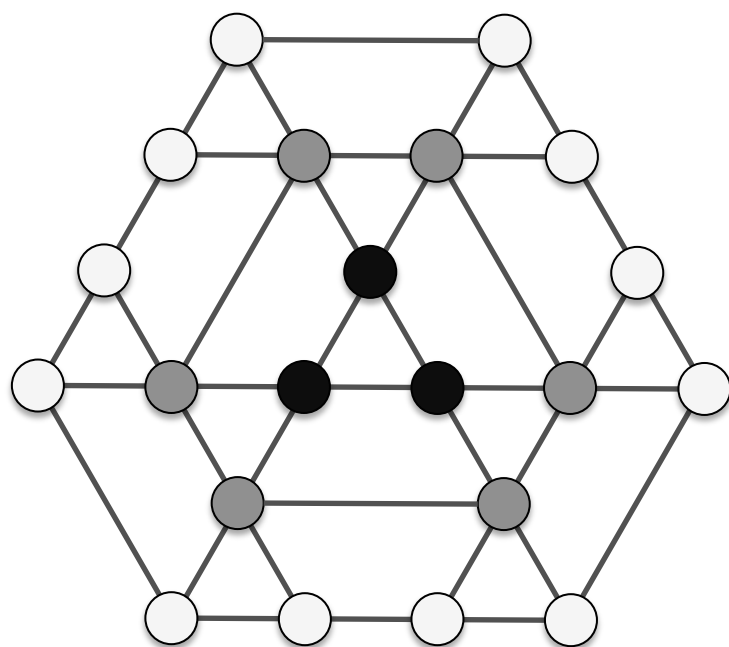


Figure 9.7: Poly-level graph with $h = 3, j = 2, k = 2, l = 1, c_1 = 3$.

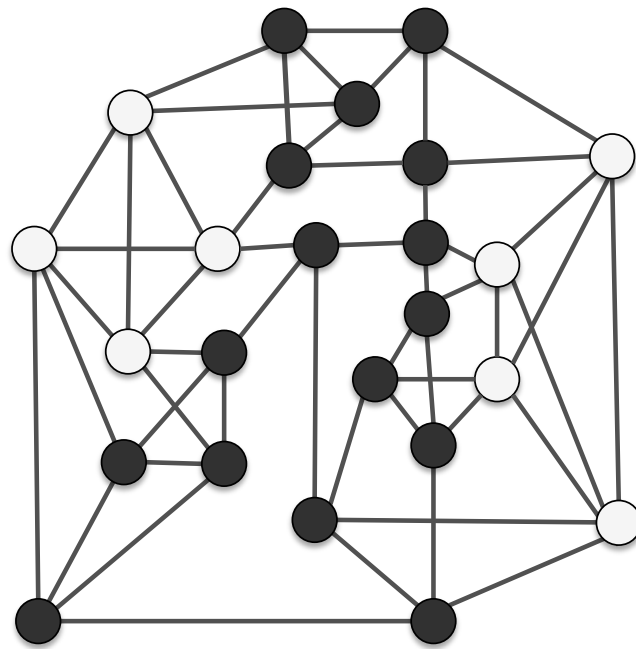


Figure 9.8: Poly-level graph with $h = 2, j = 3, k = 1, l = 2, c_1 = 16$.

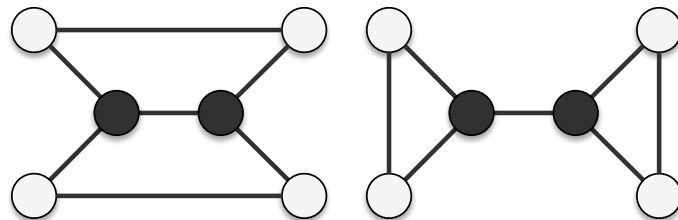


Figure 9.9: Two topologically different poly-level graphs with identical parameters $h = 2, j = 1, k = 2, l = 1, c_1 = 2$.

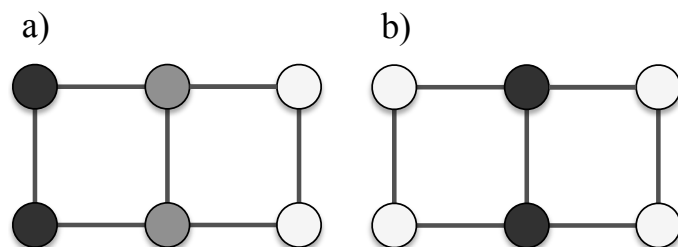


Figure 9.10: A poly-level graph that admits two different sets of parameters:

- a) $h = 3, j = 1, k = 1, l = 1, c_1 = 2$
- b) $h = 2, j = 1, k = 2, l = 1, c_1 = 2$

The appearance of a poly-level graph may be highly symmetric (Figures 9.6 and 9.7) or quite irregular (Figure 9.8). Also, two poly-level graphs with the same parameters may be topologically quite different (Figure 9.9), while the parameters used to describe a particular poly-level graph are generally not unique (Figure 9.10).

Note that it suffices to specify the number of vertices c_1 in L_1 to determine the number of vertices c_i in any level L_i , as established in the following simple proposition:

Proposition 9.4.2. *Given a poly-level graph G , with levels L_1, \dots, L_h , superdegree k , subdegree l and $|L_i| = c_i$, we have:*

$$c_i = (kl^{-1})^{i-1}c_1, \quad \forall i \in \{1, \dots, h\}$$

Proof. The number of edges linking vertices in L_i to vertices in L_{i+1} can be expressed in two forms, which must be equal:

$$lc_i = kc_{i-1}, \quad \forall i \in \{2, 3, \dots, h\}$$

Thus, the c_i form a geometric progression with common ratio kl^{-1} and the proposition follows immediately. \square

The following proposition establishes two intuitively obvious constraints on the parameters of a poly-level graph.

Proposition 9.4.3. *Given a poly-level graph G , with levels L_1, \dots, L_h , intradegree j , superdegree k , subdegree l and $|L_i| = c_i$, we have that $\forall i \in \{1, \dots, h\}$:*

- (a) $(kl^{-1})^{i-1}c_1 \in \mathbb{Z}$
- (b) $(kl^{-1})^{i-1}c_1 \geq j + 1$

These constraints arise immediately from the fact that the number of vertices c_i in any level L_i (replaced in Proposition 9.4.3 by the expression from Proposition 9.4.2) must (a) be an integer and (b) exceed the intradegree j .

9.4.2 Equal oddments solutions on poly-level graphs

Given a poly-level graph G , from Section 9.3.3, we know that if there exists a probability distribution across the vertices of the graph such that the sum of the probabilities in any closed neighbourhood is equal to some constant $u \in (0, 1]$, then this probability distribution defines an OMS for both players for the game $\mathfrak{G} = (G, \Sigma_A, \Sigma_B, r)$, with $r = 1$, $\Sigma_A = \Sigma_B = V(G)$, and the value of the game to Player A is u .

Suppose that such a distribution exists, and suppose that this distribution allocates an equal probability ω_i to each vertex in level L_i . Through consideration of the structure of the graph, we can write the following equations, which must hold for all $i \in \{2, 3, \dots, h-1\}$:

$$\left. \begin{aligned} (j+1)\omega_1 + k\omega_2 &= u \\ l\omega_{h-1} + (j+1)\omega_h &= u \\ l\omega_{i-1} + (j+1)\omega_i + k\omega_{i+1} &= u \end{aligned} \right\} \quad (9.14)$$

We also have the following constraints, to ensure that the ω_i define a valid probability distribution:

$$\sum_{i=1}^h \omega_i c_i = 1 \quad (9.15)$$

$$\omega_i \geq 0, \quad \forall i \in \{1, 2, \dots, h\} \quad (9.16)$$

Note that it is not necessary to explicitly include the constraint $\omega_i \leq 1$, since this is implied by (9.15) and (9.16).

We now perform the change of variables:

$$w_i = u^{-1}(j+k+l+1)\omega_i, \quad \forall i \in \{1, \dots, h\} \quad (9.17)$$

and introduce additional unknowns $w_i, \forall i \in \mathbb{Z}$.

The question of finding a function ω_i of i that satisfies (9.14), (9.15) and (9.16) can be reformulated as follows:

- Given a non-negative integer j and positive integers h, k, l, c_1 satisfying the conditions of Proposition 9.4.3, find a function w_i of i , such that, $\forall i \in \mathbb{Z}$:

$$lw_{i-1} + (j+1)w_i + kw_{i+1} = j+k+l+1 \quad (9.18)$$

- Subject to the boundary conditions:

$$w_0 = w_{h+1} = 0 \quad (9.19)$$

- With the constraint:

$$w_i \geq 0, \quad \forall i \in \{1, 2, \dots, h\} \quad (9.20)$$

If suitable w_i can be found, an equal oddments solution is then given by:

$$u = c_1^{-1}(j+k+l+1) \left[\sum_{i=1}^h (kl^{-1})^{i-1} w_i \right]^{-1} \quad (9.21)$$

$$\omega_i = w_i u(j+k+l+1)^{-1}, \quad \forall i \in \{1, \dots, h\} \quad (9.22)$$

Applying the change of variables (9.17): (9.18) and (9.19) are derived from (9.14); (9.20) is derived from (9.16); (9.21) is derived from (9.15) and Proposition 9.4.2, while (9.22) is immediate.

9.4.3 Exact solutions

To find a solution to the problem, let:

$$w_i = w_i^{\text{GS}} + w_i^{\text{PS}}$$

where w_i^{PS} is any particular solution of (9.18), and w_i^{GS} is the most general solution of the homogeneous difference equation:

$$lw_{i-1} + (j+1)w_i + kw_{i+1} = 0, \quad \forall i \in \mathbb{Z} \quad (9.23)$$

An obvious candidate for the particular solution is:

$$w_i^{\text{PS}} = 1$$

For w_i^{GS} , there are three cases to consider:

Case 1: $(j+1)^2 > 4kl$

Look for a solution of the form:

$$w_i^{\text{GS}} = A_+ \nu_+^i + A_- \nu_-^i$$

where A_+, A_- are arbitrary constants and ν_+, ν_- are unknown constants to be determined. Substituting into (9.23), we find:

$$\nu_{\pm} = \frac{-(j+1) \pm \sqrt{(j+1)^2 - 4kl}}{2k}$$

So:

$$w_i = A_+ \nu_+^i + A_- \nu_-^i + 1$$

Applying the boundary conditions gives:

$$A_+ + A_- = -1$$

$$A_+ \nu_+^{h+1} + A_- \nu_-^{h+1} = -1$$

which can be solved to give:

$$A_+ = \frac{1 - \nu_-^{h+1}}{\nu_-^{h+1} - \nu_+^{h+1}}$$

$$A_- = \frac{1 - \nu_+^{h+1}}{\nu_+^{h+1} - \nu_-^{h+1}}$$

Note that in this case, $\nu_+ \neq \nu_-$, and therefore A_+ and A_- both exist.

Case 2: $(j+1)^2 = 4kl$

Look for a solution of the form:

$$w_i^{\text{GS}} = (A + iB)\nu^i$$

where A, B are arbitrary constants and ν is an unknown constant to be determined. Substituting into (9.23), we find:

$$\nu = -\frac{j+1}{2k}$$

So:

$$w_i = (A + iB)\nu^i + 1$$

Applying the boundary conditions gives:

$$A = -1$$

$$B = \frac{1 - \nu^{-[h+1]}}{h+1}$$

Again, A and B exist for all values of the parameters.

Case 3: $(j+1)^2 < 4kl$

Look for a solution of the form:

$$w_i^{\text{GS}} = \nu^i [P \cos(\theta i) + Q \sin(\theta i)]$$

where P, Q are arbitrary constants and ν, θ are unknown constants to be determined.

Substituting into (9.23), we find:

$$\nu = \sqrt{l/k} \quad (9.24)$$

$$\theta = \arg \left[-(j+1) + i\sqrt{4kl - (j+1)^2} \right] \quad (9.25)$$

So:

$$w_i = \nu^i [P \cos(\theta i) + Q \sin(\theta i)] + 1$$

Provided that $\theta[h+1]$ is not an integer multiple of π , applying the boundary conditions gives:

$$P = -1$$

$$Q = \frac{\cos(\theta[h+1]) - \nu^{-[h+1]}}{\sin(\theta[h+1])}$$

If $\theta[h+1]$ is an integer multiple of π then no values of P and Q can be found to satisfy the boundary conditions (9.19) and no solution w_i exists, except in the particular case where $\theta[h+1]$ is an even multiple of π and $k = l$. In the latter instance, the boundary conditions are satisfied for all values of Q , with $P = -1$, identifying an infinite family of possible solutions.

9.4.4 Review of key results

To summarise the results of this section, given any poly-level graph G with suitable parameters h, j, k, l, c_1 , we have found w_i satisfying (9.18) and (9.19) in all cases except where $(j+1)^2 < 4kl$ and $\theta[h+1]$ is an integer multiple of π (barring the special case where $\theta[h+1]$ is an even multiple of π and $k = l$), where θ is defined as in (9.25).

Note that the non-existence of such a w_i in the specific cases mentioned does not necessarily imply that no equal oddments strategy exists for the corresponding GSG, simply that any such strategy cannot be expressed as the solution to a difference equation of the form discussed.

Where such a w_i does exist, it remains to check whether constraint (9.20) is satisfied. If so, then there exists an equal oddments solution to the GSG $\mathfrak{G} = (G, \Sigma_A, \Sigma_B, r)$, with $r = 1$ and $\Sigma_A = \Sigma_B = V(G)$, defined by (9.21) and (9.22), which allocates a probability of ω_i to each vertex in level L_i . By Proposition 9.3.6, this equal oddments solution is an OMS of \mathfrak{G} for both players.

Table 9.1 summarises the equal oddments strategies for the graphs shown in Figures 9.6-9.8.

Figure	Poly-level graph parameters					Equal oddments solution				Game values	
	h	j	k	l	c_1	ω_1	ω_2	ω_3	ω_4	u_A	u_B
9.6	4	2	1	1	4	3/40	1/20	1/20	3/40	11/40	29/40
9.7	3	2	2	1	3	1/15	0	1/15	N/A	1/5	4/5
9.8	2	3	1	2	16	3/64	1/32	N/A	N/A	7/32	25/32

Table 9.1: Table detailing the equal oddments solutions of the poly-level graphs shown in Figures 9.6-9.8. ω_i is the probability that the equal oddments strategy (an OMS for both players) allocates to each vertex in level L_i .

In this section, we have demonstrated that the concepts outlined in Section 9.3 may be used to find general expressions for OMSs of GSGs played over a particular family of graphs. It may therefore be possible to use or adapt this approach to seek OMSs for GSGs played over other families of graphs, thus suggesting a potentially valuable focus for future work.

9.5 Summary and conclusions

In this chapter, we have presented a number of methods to facilitate the identification of OMSs in the GSG. These have included the presentation of an IEDS algorithm, which was demonstrated to be particularly effective when applied to games played on trees; a method for exploiting the symmetries of the underlying graph of a GSG; the identification of a particular family of strategies, known as “equal oddments strategies”, and a proof that such strategies are always OMSs for both players; and the derivation of exact solutions for games played over a particular family of graphs, known as “poly-level graphs”.

In Chapter 10, we will present two major extensions to the SSSG, with the aim of increasing its flexibility and relevance to real world problems. The first involves the consideration of situations in which not all points of the game geography are of equal value to the players, while the second relaxes the constraint that players must deploy at a fixed location, instead allowing Player A to move around the space according to a predetermined stochastic patrol strategy.

Chapter 10

Extensions and adaptations of the SSSG

10.1 Introduction

A key limitation of the SSSG, as described in the preceding chapters, is that it assumes that all points of the game geography Ω are of equal importance. However, in real life applications, this will not necessarily be the case.

For example, if Ω were intended to model the commercial centre of a city, with Player A representing a police unit attempting to protect the area from a group of looters, represented by Player B, it would be reasonable to assume that the value of property at different points of Ω may vary. A jeweller's would have a higher value to looters, and consequently to police, than an abandoned building.

Additionally, in many situations, the assumption that Players A and B deploy simultaneously at particular points and remain there is not appropriate.

For example, suppose that Ω represents the physical space in which a large public event is being held, such as the route of a parade and the surrounding streets, with Player A representing a security unit tasked with protecting the event from a terrorist, represented by Player B. In this instance, while it may indeed be reasonable to model Player B as deploying directly and instantaneously at a particular point, as in the SSSG, for Player A, the situation is quite different. Since Player A does not know exactly when Player B will deploy, the strategy of choosing a particular point and remaining there indefinitely would potentially be unwise. If Player B were able to observe Player A's location before her deployment, she could simply select a point outside Player A's detection radius, guaranteeing herself the maximum possible payoff.

In this scenario, it may be more appropriate to allow Player A to choose a particular strategy of *patrol* through the space. Player B could then be allowed to observe this strategy before deciding on a point at which to deploy. This interpretation transforms the SSSG into something akin to a Stackelberg security game, as discussed in Section 7.3.7, and examined in a wide variety of scenarios by Tambe (2012). However, the extended SSSG that we will discuss in Section 10.4 is distinct from the vast majority of games of this kind in that it maintains its spatially explicit nature, with Player A’s ability to intercept Player B being dependent on the spatial structure of Ω , rather than simply on whether the two players occupy the same precise location.

The twin aims of this chapter are therefore to extend the SSSG for use over spaces of non-uniform value and, in the case of games played over graphs, to use the extended model to analyse situations in which Player A does not deploy at a particular vertex, but rather must patrol through the space in an unpredictable manner, in an attempt to intercept Player B, who may deploy at any time and at any vertex in her strategy set. One important outcome of this work will be the development of a method to derive strategies of optimal random patrol through consideration of the OMSs (for Player A) of an appropriate static game, by carefully specifying the probabilities of moving between vertices and the dwell times at each vertex.

10.2 Games over spaces of non-uniform value

10.2.1 The Extended SSSG (ESSSG)

We begin by extending the SSSG to incorporate information about the different values of the points of Ω , as discussed in Section 10.1.

The Extended SSSG (ESSSG) for spaces of non-uniform value is a two-player game played over a metric space $M = (\Omega, d)$, as before. However, this new form of the game includes a value function γ , which assigns a non-negative real number to each point of Ω :

$$\begin{aligned} \gamma: \Omega &\rightarrow \mathbb{R}^+ \cup \{0\} \\ x &\mapsto \gamma(x) \end{aligned} \tag{10.1}$$

Once again, each player chooses a point x_A, x_B from their own strategy set, $\Sigma_A, \Sigma_B \in \Omega$. The detection radius r and the closed ball $B_r[x]$ are defined as in

the standard SSSG, but the payoff functions are different:

$$p_A(x_A, x_B) = \begin{cases} 0 & , x_B \in B_r[x_A]; \\ -\gamma(x_B) & , \text{otherwise.} \end{cases} \quad (10.2)$$

$$p_B(x_A, x_B) = \begin{cases} 0 & , x_B \in B_r[x_A]; \\ \gamma(x_B) & , \text{otherwise.} \end{cases} \quad (10.3)$$

In other words, if the distance $d(x_A, x_B)$ between the positions at which the players deploy is less than or equal to the detection radius r , Player A catches Player B and both players receive a payoff of 0. Otherwise, if the distance is greater than the detection radius, Player B successfully evades Player A and receives a payoff equal to the value $\gamma(x_B)$ of the point at which she has deployed, while Player A receives a negative payoff of the same absolute value.

Note that, unlike the original SSSG, the extended version is a true zero-sum game, since the total of the players' payoffs is always zero. Note also that these payoff functions implicitly assume that Player A gains nothing from capturing Player B, and that there is no cost to Player B of being captured. While this assumption is potentially unrealistic, provided that the sum of the payoffs remains constant, it could effectively be relaxed without affecting the essential structure of the game by means of a simple alteration to γ ; for example, by adding a constant to the zero payoff of Player A and subtracting the same constant from the zero payoff of Player B.

In this version of the game, rather than attempting to maximise his chance of catching Player B, we may imagine that Player A is attempting to minimise the damage $\gamma(x_B)$ that Player B is able to cause, while Player B simultaneously attempts to maximise the value of this damage. This interpretation would correspond, for example, to a scenario of counter-terrorism, in which Player A represented a security unit attempting to protect some area, represented by Ω , from an attack by a terrorist unit, represented by Player B.

10.2.2 The Extended GSG (EGSG)

Consider a simple graph G , with the symmetric adjacency matrix $\mathfrak{M} = (a_{ij})$, a finite set of κ vertices:

$$V(G) = \{v_1, \dots, v_\kappa\} \quad (10.4)$$

and a set of edges:

$$E(G) = \{\{v_i, v_j\} : v_i, v_j \in V(G) \text{ and } a_{ij} = 1\}$$

with an associated value function:

$$\begin{aligned}\gamma : V(G) &\rightarrow \mathbb{R}^+ \cup \{0\} \\ v &\mapsto \gamma(v)\end{aligned}$$

The Extended Graph Search Game (EGSG) $\mathfrak{G} = (G, \Sigma_A, \Sigma_B, r, \gamma)$ is defined to be an example of the ESSSG with $\Omega = V(G)$, $\emptyset \neq \Sigma_A, \Sigma_B \subseteq V(G)$, r a positive real number, value function γ , and the distance function $d_G(v, w)$ for $v, w \in V(G)$, $v \neq w$, defined to be the length of the shortest path from v to w in G .

For convenience, we also let $\boldsymbol{\gamma}$ be a column vector of the values assigned by γ to the vertices of G :

$$\boldsymbol{\gamma} = [\gamma(v_1), \dots, \gamma(v_\kappa)]^\top$$

and we let $m[\boldsymbol{\gamma}]$ designate the maximum of the value function across $V(G)$:

$$m[\boldsymbol{\gamma}] = \max_{v \in V(G)} [\gamma(v)]$$

Without loss of generality, it suffices to consider games with $r = 1$, since all other games can be reduced to this case. This result was demonstrated in Section 8.3.2, in the case of the basic GSG, and is unaffected by the introduction of the value function γ .

10.3 Optimal mixed strategies of games over spaces of non-uniform value

10.3.1 Initial discussion

Having defined the EGSG, we now consider how we might go about identifying good strategies for this game for each player. We begin by constructing explicit expressions for the expected payoffs of the game in terms of the value function γ and other known objects, before going on to consider the structure of the payoff matrix in Section 10.3.2, in order to facilitate the identification of OMSs. In Section 10.3.3, we discuss how the value of a general mixed strategy can be assessed in cases where

OMSs cannot be identified, and, in Section 10.3.4, we present a proposition that allows for the simplification of an EGSG through consideration of its vertex values.

Here, and in all that follows, the notation $\mathbf{1}_S$ will be used to refer to the indicator function¹ of some subset $S \subseteq V(G)$:

$$\begin{aligned} \mathbf{1}_S : V(G) &\rightarrow \{0, 1\} \\ v &\mapsto \begin{cases} 1, & v \in S \\ 0, & \text{otherwise} \end{cases} \end{aligned} \tag{10.5}$$

Consider the expected payoff to Player A if he uses the mixed strategy τ_A and Player B deploys at vertex v_B . In the following expression, the point v_A at which Player A deploys is temporarily considered to be a discrete random variable, which takes values in Σ_A according to the distribution defined by τ_A :

$$\begin{aligned} E[p_A(\tau_A, v_B)] &= - \sum_{w \in \Sigma_A} \gamma(v_B) \mathbf{1}_{V(G) \setminus N[w]}[v_B] P[v_A = w] \\ &= - \gamma(v_B) \sum_{w \in \Sigma_A \setminus N[v_B]} \tau_A[w] \end{aligned} \tag{10.6}$$

Therefore, the expected payoff to Player A if he uses the mixed strategy τ_A and Player B uses the mixed strategy τ_B is:

$$E[p_A(\tau_A, \tau_B)] = - \sum_{v \in \Sigma_B} \sum_{w \in \Sigma_A \setminus N[v]} \gamma(v) \tau_A[w] \tau_B[v] \tag{10.7}$$

Now consider the expected payoff to Player B if she uses the mixed strategy τ_B and Player A deploys at vertex v_A (no longer considered to be a random variable). In this expression, the point v_B at which Player B deploys is considered to be a discrete random variable, which takes values in Σ_B according to the distribution defined by τ_B .

$$\begin{aligned} E[p_B(v_A, \tau_B)] &= \sum_{w \in \Sigma_B} \gamma(w) \mathbf{1}_{V(G) \setminus N[v_A]}[w] P[v_B = w] \\ &= \sum_{w \in \Sigma_B \setminus N[v_A]} \gamma(w) \tau_B[w] \end{aligned} \tag{10.8}$$

Therefore, the expected payoff to Player B if she uses the mixed strategy τ_B and

¹ Compare with (6.15), in Part II, where indicator functions were defined over \mathbb{R} .

Player A uses the mixed strategy τ_A is:

$$E[p_B(\tau_A, \tau_B)] = \sum_{v \in \Sigma_A} \sum_{w \in \Sigma_B \setminus N[v]} \gamma(w) \tau_A[v] \tau_B[w] \quad (10.9)$$

Note that, since the game is zero-sum, the absolute values of (10.7) and (10.9) are equal.

As discussed in Section 7.2, the concept of an OMS for Player A is that he attempts to choose τ_A to maximise the minimum of (10.7) over all possible τ_B . Similarly, the concept of an OMS for Player B is that she attempts to choose τ_B to maximise the minimum of (10.9) over all possible τ_A . In this way, each player chooses a mixed strategy so as to optimise their own personal worst case scenario (in terms of payoff).

However, as mentioned in Section 8.2.5, it actually suffices to consider these minima over all possible pure strategies of the opponent, rather than across all possible mixed strategies (Morris 1994, pp. 46-47). Finding OMSs of the game for each player is therefore equivalent to solving two optimisation problems: finding τ_A to maximise the minimum of (10.6) across all $v_B \in \Sigma_B$ and finding τ_B to maximise the minimum of (10.8) across all $v_A \in \Sigma_A$.

Alternatively, if mixed strategies σ_A, σ_B for Players A and B can be found for which these minima sum to zero:

- $\min_{v_B \in \Sigma_B} E[p_A(\sigma_A, v_B)] = -u$
- $\min_{v_A \in \Sigma_A} E[p_B(v_A, \sigma_B)] = u$

then σ_A and σ_B are OMSs for each player (Blackwell and Girshick 1979, p. 65) and u is known as the value of the game to Player B (and $-u$ is the value of the game to Player A).

Recall also that if the strategy sets Σ_A and Σ_B are finite, OMSs are guaranteed to exist for both players (a consequence of the Minimax Theorem, Morris 1994, p102). The EGSG \mathfrak{G} clearly satisfies this condition, so OMSs for \mathfrak{G} must exist for Players A and B.

10.3.2 Identifying payoff matrices for the EGSG

In the previous section, we explicitly described the expressions that must be minimised in order to identify the OMSs of a particular EGSG, \mathfrak{G} . We now seek to establish the form of the payoff matrix of this game for Player A (as the row player)

in terms of the known objects \mathfrak{M} (the adjacency matrix of G), Σ_A , Σ_B and γ . If the form of this matrix were known, standard game theoretic methods could be employed (see, for example, Morris, 1994, pp. 99-114), thus offering an alternative route to identify the OMSs.

To determine the form of the matrix, we first consider the simpler game $\mathfrak{G}^* = (G, V(G), V(G), r, \gamma)$, derived from \mathfrak{G} by setting $\Sigma_A = \Sigma_B = V(G)$. In this restricted case, defining the payoff matrix, which we designate as \mathfrak{P}^* , is straightforward:

$$\mathfrak{P}^* = -[J_\kappa - (\mathfrak{M} + I_\kappa)] \text{diag}(\gamma) \quad (10.10)$$

Here, I_κ is the $\kappa \times \kappa$ identity matrix, J_κ is a $\kappa \times \kappa$ matrix of ones and $\text{diag}(\gamma)$ is a diagonal matrix formed from the terms of γ :

$$\text{diag}(\gamma) = (\delta_{ij} \gamma(v_i))_{i,j \in \{1, \dots, \kappa\}}$$

where δ_{ij} is the Kronecker delta:

$$\delta_{ij} = \begin{cases} 1 & \text{if } i = j ; \\ 0 & \text{otherwise.} \end{cases} \quad (10.11)$$

To see that (10.10) is true, observe that $[J_\kappa - (\mathfrak{M} + I_\kappa)]$ is effectively an “anti-adjacency matrix” of G (derived from the adjacency matrix by switching the zeros and ones, but still with zeros on the leading diagonal), which corresponds to the fact that non-zero payoffs are only awarded when players deploy at non-adjacent (and non-identical) vertices. Post-multiplying by $\text{diag}(\gamma)$ ensures that positive entries are equal to the value of the vertex at which Player B (the column player) deploys, while the negation is due to the fact that payoffs to Player A are always non-positive.

Observe also that, since the game is zero-sum, the payoff matrix for Player B is equal to $-\mathfrak{P}^{*\top}$ (now with Player B as the row player).

For the more general situation in which Σ_A and Σ_B are not both equal to $V(G)$, a suitable expression for the payoff matrix is a little more difficult to write explicitly. The apparently straightforward approach of deleting those rows and columns of \mathfrak{M} and of γ that relate to vertices that do not feature in the strategy set of a particular player is undesirable, since, under this approach, the simple correspondence between rows and vertices would be lost. This would make it both more inconvenient to work

further with the resulting mixed strategies and more difficult to relate them to the geography of the space.

For these reasons, we prefer not to reduce the size of the payoff matrix, but rather to replace those rows and columns that relate to invalid strategies for the appropriate player with alternative rows and columns, such that the OMSs of the game are unchanged. To do this, we make use of the fact that a pure strategy that is strictly dominated by some other pure strategy must be allocated zero probability in an OMS (see Section 7.2). Therefore, by replacing those rows of \mathfrak{P}^* that relate to vertices that are not in Σ_A with rows that are strictly dominated by all remaining rows, the OMSs for Player A of the game defined by the resulting payoff matrix must be identical to those of the EGSG \mathfrak{G} . Performing an equivalent procedure for the columns of \mathfrak{P}^* yields the payoff matrix \mathfrak{P} (for Player A) of a game whose OMSs match those of the EGSG for both players.

More specifically, we adopt the following procedure. Given an EGSG \mathfrak{G} , with strategy sets $\emptyset \neq \Sigma_A, \Sigma_B \subseteq V(G) = \{v_1, \dots, v_\kappa\}$ and fixing an arbitrary $\epsilon > 0$, those rows of \mathfrak{P}^* (defined in (10.10)) that correspond to vertices that do not appear in Σ_A are replaced with rows containing the value $-m[\gamma] - \epsilon$, which is less than the minimum possible payoff to Player A. Similarly, those columns of \mathfrak{P}^* that correspond to vertices that do not appear in Σ_B are replaced with columns containing the value ϵ , whose negative is less than the minimum possible payoff to Player B. The intersections of such rows and columns are allocated the value $-m[\gamma]/2$.

The entry-wise relationship between $\mathfrak{P}^* = (p_{ij}^*)_{i,j \in \{1, \dots, \kappa\}}$ and $\mathfrak{P} = (p_{ij})_{i,j \in \{1, \dots, \kappa\}}$ is summarised below:

$$p_{ij} = \begin{cases} p_{ij}^* , & \text{if } v_i \in \Sigma_A \text{ and } v_j \in \Sigma_B ; \\ -m[\gamma] - \epsilon , & \text{if } v_i \notin \Sigma_A \text{ and } v_j \in \Sigma_B ; \\ \epsilon , & \text{if } v_i \in \Sigma_A \text{ and } v_j \notin \Sigma_B ; \\ -m[\gamma]/2 , & \text{if } v_i \notin \Sigma_A \text{ and } v_j \notin \Sigma_B . \end{cases} \quad (10.12)$$

Given (10.12), we now prove the assertion that the rows and columns of \mathfrak{P} that correspond respectively to invalid strategies for Players A and B are strictly dominated by all rows and columns that correspond to valid strategies.

Proposition 10.3.1. Consider an EGSG $\mathfrak{G} = (G, \Sigma_A, \Sigma_B, r, \gamma)$ with $r = 1$ and let $\mathfrak{P}^* = (p_{ij}^*)_{i,j \in \{1, \dots, \kappa\}}$ and $\mathfrak{P} = (p_{ij})_{i,j \in \{1, \dots, \kappa\}}$ be defined as in (10.10) and (10.12). If \mathfrak{P} is taken to be the payoff matrix of a zero-sum game (whose entries represent payoffs to the row player), then, identifying rows and columns with pure strategies for each player as usual, we have:

1. $v_i \in \Sigma_A, v_j \notin \Sigma_A \Rightarrow$ Row i strictly dominates row j .
2. $v_i \in \Sigma_B, v_j \notin \Sigma_B \Rightarrow$ Column i strictly dominates column j .

Proof. Let \mathfrak{G}^* designate the EGSG derived from \mathfrak{G} by replacing the strategy sets Σ_A and Σ_B with $V(G)$: $\mathfrak{G}^* = (G, V(G), V(G), r, \gamma)$. By construction, \mathfrak{P}^* is the payoff matrix of \mathfrak{G}^* , with Player A as the row player.

Proof of statement 1: Suppose that $v_i \in \Sigma_A$ and $v_j \notin \Sigma_A$. To prove statement 1, we require that:

$$p_{ik} > p_{jk}, \quad \forall k \in \{1, \dots, \kappa\}$$

There are two cases to consider. Firstly, suppose that $v_k \in \Sigma_B$. Then by (10.12), $p_{ik} = p_{ik}^*$ and $p_{jk} = -m[\gamma] - \epsilon$. Since $p_{ik}^* = p_A(v_i, v_k)$ in the EGSG \mathfrak{G}^* , where p_A is the payoff function for Player A, as defined in (10.2), we have that $p_{ik}^* = 0$ or $p_{ik}^* = -\gamma(v_k)$. Therefore:

$$p_{ik} = p_{ik}^* \geq -\gamma(v_k) \geq -\max_{v \in V(G)} [\gamma(v)] > -m[\gamma] - \epsilon = p_{jk}$$

So, $p_{ik} > p_{jk}$, as required.

Secondly, suppose that $v_k \notin \Sigma_B$. Then by (10.12), $p_{ik} = \epsilon$ and $p_{jk} = -m[\gamma]/2$. Therefore, it is clear that $p_{ik} > p_{jk}$, as required.

Proof of statement 2: Suppose that $v_i \in \Sigma_B$ and $v_j \notin \Sigma_B$. To prove statement 2, we require that:

$$p_{ki} < p_{kj}, \quad \forall k \in \{1, \dots, \kappa\}$$

Again, there are two cases to consider. Firstly, suppose that $v_k \in \Sigma_A$. Then by (10.12), $p_{ki} = p_{ki}^*$ and $p_{kj} = \epsilon$. Since $p_{ki}^* = p_A(v_k, v_i)$ in \mathfrak{G}^* , we have that $p_{ki}^* = 0$ or $p_{ki}^* = -\gamma(v_i)$. Therefore:

$$p_{ki} = p_{ki}^* \leq 0 < \epsilon = p_{kj}$$

So, $p_{ki} < p_{kj}$, as required.

Secondly, suppose that $v_k \notin \Sigma_A$. Then by (10.12), $p_{ki} = -m[\gamma] - \epsilon$ and $p_{kj} = -m[\gamma]/2$. Therefore, it is clear that $p_{ki} < p_{kj}$, as required.

This completes the proof of the proposition. \square

In fact, the relationship represented by (10.12) can be written as a single matrix equation.

If we define the following binary (column) vectors, which store information about whether or not a given vertex is in a player's strategy set:

$$\begin{aligned}\mathbf{s}_A &= (\mathbf{1}_{\Sigma_A}[v_i])_{i \in \{1, \dots, \kappa\}} \\ \mathbf{s}_B &= (\mathbf{1}_{\Sigma_B}[v_i])_{i \in \{1, \dots, \kappa\}}\end{aligned}\tag{10.13}$$

then the transformation from \mathfrak{P}^* to \mathfrak{P} can also be expressed as:

$$\mathfrak{P} = P_1(\mathfrak{P}^*, \mathbf{s}_A, \mathbf{s}_B) - P_2(\gamma, \mathbf{s}_A) + P_3(\mathbf{s}_B) + P_4(\gamma, \mathbf{s}_A, \mathbf{s}_B)\tag{10.14}$$

where:

$$\begin{aligned}P_1(\mathfrak{P}^*, \mathbf{s}_A, \mathbf{s}_B) &= \text{diag}(\mathbf{s}_A) \mathfrak{P}^* \text{diag}(\mathbf{s}_B) \\ P_2(\gamma, \mathbf{s}_A) &= (m[\gamma] + \epsilon) (I_\kappa - \text{diag}(\mathbf{s}_A)) J_\kappa \\ P_3(\mathbf{s}_B) &= \epsilon J_\kappa (I_\kappa - \text{diag}(\mathbf{s}_B)) \\ P_4(\gamma, \mathbf{s}_A, \mathbf{s}_B) &= \frac{m[\gamma]}{2} (J_{\kappa,1} - \mathbf{s}_A) (J_{\kappa,1} - \mathbf{s}_B)^\top\end{aligned}$$

and where $J_{\kappa,1}$ is a κ -dimensional column vector of ones.

Since the OMSs of the ESGG, \mathfrak{G} , are the same as those of the game defined by the payoff matrix \mathfrak{P} , equations (10.10) and (10.14) allow for the application of the standard techniques of matrix games to compute these OMSs (see, for example, Morris, 1994, pp. 99-114).

\mathfrak{P} also offers an alternative to the formulae (10.7) and (10.9) for calculating the expected payoffs of different mixed strategies.

Specifically, suppose that the vectors

$$\begin{aligned}\boldsymbol{\tau}_A &= (\tau_A[v_1], \dots, \tau_A[v_\kappa])^\top \in [0, 1]^\kappa \\ \boldsymbol{\tau}_B &= (\tau_B[v_1], \dots, \tau_B[v_\kappa])^\top \in [0, 1]^\kappa\end{aligned}$$

allocate probabilities to the vertices of G such that each constitutes a valid mixed strategy for Players A and B respectively. That is, we suppose that $\sum_{i=1}^{\kappa} \tau_A[v_i] = 1$, $\sum_{i=1}^{\kappa} \tau_B[v_i] = 1$ and that $v_i \notin \Sigma_A \Rightarrow \tau_A[v_i] = 0$ and $v_i \notin \Sigma_B \Rightarrow \tau_B[v_i] = 0$. We have:

$$E[p_A(\boldsymbol{\tau}_A, \boldsymbol{\tau}_B)] = -E[p_B(\boldsymbol{\tau}_A, \boldsymbol{\tau}_B)] = \boldsymbol{\tau}_A^\top \mathfrak{P} \boldsymbol{\tau}_B \quad (10.15)$$

To summarise, we have defined the payoff matrix \mathfrak{P} of a game whose OMSs are identical to the OMSs of a given ESGG, \mathfrak{G} , and whose rows and columns correspond directly to the vertices of the graph G over which \mathfrak{G} is played. The definition of this matrix will serve to facilitate both the calculation of OMSs and expected payoffs for \mathfrak{G} , as discussed above, and the work on patrol games presented in Section 10.4.

10.3.3 Measuring the value of a general mixed strategy for the ESGG

In certain cases, computing the true OMSs of an ESGG may be impossible or impractical, perhaps owing to the size or complexity of the space over which the game is played. In such situations, it would be useful to have some measure of the quality of a general mixed strategy, to allow different options to be compared or to serve as an objective function for some form of iterative optimisation.

One very simple measure of the quality of a mixed strategy is given by the minimum possible expected payoff that can be obtained when the strategy is employed, considered across all possible pure strategy responses from the opponent. The payoff matrix \mathfrak{P} , defined in Section 10.3.2, can be used to facilitate the calculation of these values.

Given a particular ESGG, \mathfrak{G} , consider the following vector functions of the mixed strategies $\boldsymbol{\tau}_A$ for Player A and $\boldsymbol{\tau}_B$ for Player B:

$$\mathbf{z}_A(\boldsymbol{\tau}_A) = \mathfrak{P}^\top \boldsymbol{\tau}_A = [z_A(\boldsymbol{\tau}_A, v_1), \dots, z_A(\boldsymbol{\tau}_A, v_\kappa)]^\top$$

$$\mathbf{z}_B(\boldsymbol{\tau}_B) = -\mathfrak{P} \boldsymbol{\tau}_B = [z_B(\boldsymbol{\tau}_B, v_1), \dots, z_B(\boldsymbol{\tau}_B, v_\kappa)]^\top$$

Observe that the terms of $\mathbf{z}_A(\boldsymbol{\tau}_A)$ and $\mathbf{z}_B(\boldsymbol{\tau}_B)$ are the expected payoffs to the corresponding players when using the mixed strategies $\boldsymbol{\tau}_A$ and $\boldsymbol{\tau}_B$ when the opponent deploys at each vertex of G , except where a vertex does not lie in the relevant opponent's strategy set, in which case the term is replaced with an upper bound on

the player's possible payoffs from the game (note that $m[\gamma]$, which appears in the definition of \mathfrak{P} (see (10.14)), is greater than or equal to Player B's maximum payoff by definition):

$$z_A(\tau_A, v_B) = \begin{cases} E[p_A(\tau_A, v_B)] & , v_B \in \Sigma_B; \\ \epsilon & , \text{otherwise.} \end{cases} \quad (10.16)$$

$$z_B(\tau_B, v_A) = \begin{cases} E[p_B(v_A, \tau_B)] & , v_A \in \Sigma_A; \\ m[\gamma] + \epsilon & , \text{otherwise.} \end{cases} \quad (10.17)$$

Finding OMSs σ_A and σ_B is thus equivalent to choosing τ_A and τ_B to maximise the minimum term of each of the vectors $\mathfrak{P}^\top \tau_A$ and $-\mathfrak{P} \tau_B$.

Therefore, if the true OMSs of an EGSG cannot be calculated, a measure of the quality of any given mixed strategy, τ_A for Player A or τ_B for Player B, may nonetheless be calculated on the basis of the values of the following objective functions:

$$\begin{aligned} Z_A(\tau_A) &= \min_{v_B \in V(G)} z_A(\tau_A, v_B) = \min [\mathfrak{P}^\top \tau_A] \\ Z_B(\tau_B) &= \min_{v_A \in V(G)} z_B(\tau_B, v_A) = \min [-\mathfrak{P} \tau_B] \end{aligned} \quad (10.18)$$

Note that, by definition, σ_A and σ_B are OMSs for each player if and only if $Z_A(\sigma_A) \geq Z_A(\tau_A)$ for all valid mixed strategies τ_A for Player A and $Z_B(\sigma_B) \geq Z_B(\tau_B)$ for all valid mixed strategies τ_B for Player B, respectively.

The notation that has been introduced in this section will prove helpful in Section 10.3.4, where we will prove a useful result on the OMSs of the EGSG for Player B.

10.3.4 A proposition on the optimal mixed strategies of the EGSG for Player B

In this section, we present a proposition that provides a useful indication of whether a given vertex should be considered by Player B as part of a good mixed strategy for a given EGSG. The proposition is based on a consideration of the value function γ , and allows for vertices whose value is too low to be part of an OMS for Player B to be removed from consideration, thus simplifying the analysis of the game.

Proposition 10.3.2. Consider an EGSG $\mathfrak{G} = (G, \Sigma_A, \Sigma_B, r, \gamma)$ with $r = 1$ and suppose that σ_B is an OMS of the game for Player B. Consider also a subset of Player B's strategy set $S_B \subseteq \Sigma_B$ for which $|N[v_A] \cap S_B| \leq 1, \forall v_A \in \Sigma_A$.

Suppose that there exists $y \in \Sigma_B$ such that:

$$\gamma(y) < \left(\frac{|S_B| - 1}{|S_B|} \right) \min_{x \in S_B} \gamma(x) \quad (10.19)$$

Then $\sigma_B(y) = 0$.

Essentially, this proposition states that if a set of vertices can be found for Player B such that the closed neighbourhoods of these vertices do not intersect (or, more precisely, such that any such pairwise intersection of these neighbourhoods contains no vertices in Σ_A), then Player B should not play any vertex that has a lower value than $Z_B(\tau_{S_B})$, where τ_{S_B} is the mixed strategy which chooses a vertex by means of a discrete uniform distribution over S_B . In fact, the proposition as stated is a slightly weaker result than this, since the right hand side of (10.19) is actually a lower bound on $Z_B(\tau_{S_B})$.

The proof of the proposition requires the following lemma:

Lemma 10.3.3. In the EGSG $\mathfrak{G} = (G, \Sigma_A, \Sigma_B, r, \gamma)$ with $r = 1$, if $S_B \subseteq \Sigma_B$ is such that $|N[v_A] \cap S_B| \leq 1, \forall v_A \in \Sigma_A$ and τ_{S_B} is the mixed strategy defined by:

$$\tau_{S_B}(v_B) = \begin{cases} |S_B|^{-1}, & v_B \in S_B; \\ 0, & \text{otherwise.} \end{cases}$$

then:

$$Z_B(\tau_{S_B}) \geq \min_{x \in S_B} \gamma(x) \left(\frac{|S_B| - 1}{|S_B|} \right)$$

Proof. Observe that:

$$\begin{aligned} Z_B(\tau_{S_B}) &= \min_{v_A \in V(G)} z_B(\tau_{S_B}, v_A) \\ &= \min_{v_A \in \Sigma_A} E[p_B(v_A, \tau_{S_B})] \\ &= \min_{v_A \in \Sigma_A} \sum_{w \in S_B \setminus N[v_A]} \gamma(w) |S_B|^{-1} \\ &\geq \min_{v_A \in \Sigma_A} \left[|S_B \setminus N[v_A]| |S_B|^{-1} \min_{x \in S_B} \gamma(x) \right] \end{aligned}$$

The required result follows by observing that, since $|N[v_A] \cap S_B| \leq 1$ by definition, we have that:

$$\min_{v_A \in \Sigma_A} |S_B \setminus N[v_A]| \geq |S_B| - 1$$

□

We now prove Proposition 10.3.2 .

Proof. Given an EGSG, \mathfrak{G} , with $r = 1$, let σ_B be an OMS for Player B and let the set S_B and the vertex y be as defined in the proposition. Assume (for a contradiction) that $\sigma_B(y) = \zeta > 0$ and let the vector $\hat{\sigma}_B = (\hat{\sigma}_B(v_1), \dots, \hat{\sigma}_B(v_\kappa))$ be defined by:

$$\hat{\sigma}_B(v_B) = \begin{cases} 0, & v_B = y; \\ \sigma_B(v_B), & \text{otherwise.} \end{cases}$$

Note that $\hat{\sigma}_B$ is not a valid mixed strategy, because its terms do not sum to 1, but rather to $1 - \zeta$. However, the following vector clearly is a valid mixed strategy for Player B:

$$\rho_B = \hat{\sigma}_B + \zeta \tau_{S_B}$$

where τ_{S_B} is as defined in Lemma 10.3.3.

Now, observe that:

$$\begin{aligned} & Z_B(\rho_B) \\ &= \min_{v_A \in V(G)} z_B(\rho_B, v_A) \\ &= \min_{v_A \in \Sigma_A} E[p_B(v_A, \rho_B)] \\ &= \min_{v_A \in \Sigma_A} \sum_{w \in \Sigma_B \setminus N[v_A]} \gamma(w) (\hat{\sigma}_B(w) + \zeta \tau_{S_B}(w)) \\ &= \min_{v_A \in \Sigma_A} \left[\sum_{w \in \Sigma_B \setminus N[v_A]} \gamma(w) \sigma_B(w) + \zeta \sum_{w \in \Sigma_B \setminus N[v_A]} \gamma(w) \tau_{S_B}(w) - \gamma(y) \sigma_B(y) \mathbf{1}_{\Sigma_B \setminus N[v_A]}[y] \right] \\ &= \min_{v_A \in \Sigma_A} [E[p_B(v_A, \sigma_B)] + \zeta E[p_B(v_A, \tau_{S_B})] - \zeta \gamma(y) \mathbf{1}_{\Sigma_B \setminus N[v_A]}[y]] \\ &\geq Z_B(\sigma_B) + \zeta Z_B(\tau_{S_B}) - \zeta \gamma(y) \\ &\geq Z_B(\sigma_B) + \zeta \left[\min_{x \in S_B} \gamma(x) \left(\frac{|S_B| - 1}{|S_B|} \right) - \gamma(y) \right] \quad (\text{By Lemma 10.3.3}) \\ &> Z_B(\sigma_B) \quad (\text{By (10.19)}) \end{aligned}$$

So $Z_B(\rho_B) > Z_B(\sigma_B)$, but this is a contradiction, since σ_B is an OMS. Therefore the assumption was invalid and $\sigma_B(y) = 0$, as required. □

As mentioned earlier, Proposition 10.3.2 provides a method for the simplification of EGSGs through consideration of their vertex values. Specifically, if a set S_B can be identified which satisfies the conditions specified in the proposition, then the right hand side of (10.19) represents a lower bound on the value of any vertex that must be considered for the allocation of a positive probability in an OMS for Player B. All vertices with values below this value may effectively be removed from Σ_B , though they may naturally still represent valuable strategies for Player A.

In this section, we have extended the concept of the SSSG through the consideration of situations in which the value of the underlying space is non-uniform. In Section 10.4 we will further extend the game by allowing Player A to move through the space according to a flexible stochastic patrol strategy.

10.4 The Graph Patrol Game (GPG)

10.4.1 Preliminary definitions

For the remainder of this chapter, we turn our attention to the scenario discussed in Section 10.1, in which, rather than requiring Players A and B to simultaneously pick points of a space at which to deploy, we instead suppose that Player A must choose a certain strategy of patrol around the space to best protect it against the deployment of Player B, which will occur at an unknown moment in the future.

This concept will be formalised through the definition of the Graph Patrol Game (GPG). We begin by setting out the key components of the GPG here, with a more detailed explanation of how the game is played and how payoffs are calculated presented in Section 10.4.3. A discussion of the optimal strategies of the game is provided in later sections.

Note that, throughout the course of this section, we extensively employ the terminology and results presented in Section 2.4, relating to time homogeneous Markov chains.

As with the EGSG, we consider a simple graph G , with the symmetric adjacency matrix $\mathfrak{M} = (a_{ij})$, a finite set of κ vertices:

$$V(G) = \{v_1, \dots, v_\kappa\} \quad (10.20)$$

a set of edges:

$$E(G) = \{\{v_i, v_j\} : v_i, v_j \in V(G) \text{ and } a_{ij} = 1\}$$

an associated value function:

$$\gamma : V(G) \rightarrow \mathbb{R}^+ \cup \{0\}$$

$$v \mapsto \gamma(v)$$

two non-empty subsets $\emptyset \neq \Sigma_A, \Sigma_B \subseteq V(G)$ and a positive real number r , referred to as the detection radius.

For the work presented in this section, we require that G is a connected graph. Therefore:

$$d_G(v_i, v_j) < \infty , \quad \forall i, j \in \{1, \dots, \kappa\} \quad (10.21)$$

$$\deg(v_i) > 0 , \quad \forall i \in \{1, \dots, \kappa\} \quad (10.22)$$

where $d_G(v_i, v_j)$ represents the length of the shortest path connecting v_i to v_j in G and $\deg(v_i)$ represents the degree of v_i in G , as usual. We also fix a positive real number λ , which is bounded above by the reciprocal of the maximum degree of G :

$$0 < \lambda \leq \Delta(G)^{-1} \quad (10.23)$$

The role of λ will be discussed later.

The Graph Patrol Game (GPG), $\mathfrak{G}_{\text{patrol}} = (G, \Sigma_A, \Sigma_B, r, \gamma, \lambda)$, is a two-player game played over G . In this game, Player B chooses a vertex v_B from his strategy set Σ_B , as in the EGSG. However, rather than choosing a point $v_A \in \Sigma_A$, Player A instead chooses a $\kappa \times \kappa$ **transition matrix**, $T_A = (t_{A,ij})_{i,j \in \{1, \dots, \kappa\}}$, and a column vector of non-negative real numbers of length κ , $\mathbf{d}_A = (d_{A,1}, \dots, d_{A,\kappa})^\top$, whose components will be referred to as **dwell times**.

The matrix T_A is chosen so as to define a time homogeneous Markov chain over $V(G)$, with $t_{A,ij}$ representing the probability of a transition to v_i from v_j . This matrix is further constrained such that only transitions between adjacent vertices of G are permissible, with all other transitions being allocated zero probability.

The dwell time vector \mathbf{d}_A alters the dynamics of the Markov chain by establishing the amounts of time that the process waits at each vertex before undergoing a change of state in line with the relevant transition probabilities. The dwell times at vertices that do not belong to Σ_A are constrained to be equal to zero.

Together, the random sequence of vertices generated by the Markov chain defined by T_A and the dwell times contained in \mathbf{d}_A describe the patrol strategy employed by Player A. This concept will be discussed in greater depth in Section 10.4.3.

The complete sets \mathfrak{T}_A and \mathfrak{D}_A from which T_A and \mathbf{d}_A are respectively chosen, may be written as follows:

$$\mathfrak{T}_A = \{ T_A \in \mathbb{R}^{\kappa \times \kappa} : T_A^\top J_{\kappa,1} = J_{\kappa,1}, \lambda \mathfrak{M} \preccurlyeq T_A \preccurlyeq \mathfrak{M} \} \quad (10.24)$$

$$\mathfrak{D}_A = \{ \mathbf{d}_A \in \mathbb{R}^\kappa : \mathbf{d}_A \succcurlyeq \mathbf{0}_{\kappa,1}, \text{diag}(\mathbf{s}_A) \mathbf{d}_A = \mathbf{d}_A \} \quad (10.25)$$

Here, $\mathbb{R}^{\kappa \times \kappa}$ is the set of all $\kappa \times \kappa$ real-valued matrices, $J_{\kappa,1}$ and $\mathbf{0}_{\kappa,1}$ are column vectors of length κ containing ones and zeros respectively, \preccurlyeq and \succcurlyeq represent the inequalities \leq and \geq applied component-wise, while \mathbf{s}_A is a representation of Σ_A as a binary vector, as defined in (10.13).

Considering (10.24) more closely, the condition $T_A^\top J_{\kappa,1} = J_{\kappa,1}$ states that the columns of T_A each sum to 1. Also, the condition $\lambda \mathfrak{M} \preccurlyeq T_A \preccurlyeq \mathfrak{M}$ is equivalent to the statements:

$$\left. \begin{array}{l} a_{ij} = 0 \Rightarrow t_{A,ij} = 0 \\ \text{and } a_{ij} = 1 \Rightarrow t_{A,ij} \in [\lambda, 1] \end{array} \right\} \forall i, j \in \{1, \dots, \kappa\} \quad (10.26)$$

In other words, this condition ensures that T_A allocates a probability of 0 to transitions between non-adjacent vertices of G and a probability of at least λ to transitions between adjacent vertices. This explains why λ was constrained not to exceed $\Delta(G)^{-1}$ in (10.23), since columns of T_A representing vertices of maximum degree might otherwise be forced to sum to some value greater than 1, which would contradict the condition $T_A^\top J_{\kappa,1} = J_{\kappa,1}$.

Taken together, the conditions imposed on T_A ensure that it is a valid transition matrix for a Markov chain.

Turning to (10.25), observe that the conditions $\mathbf{d}_A \succcurlyeq \mathbf{0}_{\kappa,1}$ and $\text{diag}(\mathbf{s}_A) \mathbf{d}_A = \mathbf{d}_A$ are respectively equivalent to the statements:

$$d_{A,i} \geq 0, \forall i, j \in \{1, \dots, \kappa\} \quad (10.27)$$

$$\text{and } v_i \notin \Sigma_A \Rightarrow d_{A,i} = 0, \forall i \in \{1, \dots, \kappa\} \quad (10.28)$$

Given \mathfrak{T}_A and \mathfrak{D}_A , we may precisely specify the strategy sets of the GPG for each player.

Clearly, Σ_B is the strategy set of the GPG for Player B, just as it was in the EGSG. However, while Σ_A clearly affects the range of strategies available to Player A through its influence on the dwell times, it is no longer his true strategy set. Instead, the strategy sets for the GPG are defined as:

$$\begin{aligned}\Sigma_{A,\text{patrol}} &= \mathfrak{T}_A \times \mathcal{D}_A \\ \Sigma_{B,\text{patrol}} &= \Sigma_B\end{aligned}\tag{10.29}$$

10.4.2 Properties of a GPG Markov chain

In Section 10.4.3, we will discuss the GPG and its interpretations in detail. First, however, we will prove a result (Corollary 10.4.2) on the properties of the Markov chain defined by T_A , which is of fundamental importance for the rest of the work presented in this chapter. Note that the following arguments rely on concepts defined in Definitions 2.4.3, 2.4.4 and 2.4.5.

Since we have specified that G is a connected, undirected graph with a finite number of vertices, the fact that the probabilities corresponding to transitions between adjacent vertices of G are constrained to equal or exceed λ allows us to make the following statement:

Proposition 10.4.1. *The time homogeneous Markov chain defined over the finite state space $V(G)$ by any transition matrix $T_A \in \mathfrak{T}_A$ is irreducible.*

Proof. To demonstrate that the Markov chain defined by T_A is irreducible, it suffices to show that any two vertices $v_i, v_j \in V(G)$ communicate (in the sense $v_i \rightarrow v_j$), when considered as states of the Markov chain. In other words, for all $i, j \in \{1, \dots, \kappa\}$, we must show that there exists some positive integer K , such that the K -step transition probability $p_{ij}^{(K)}$ is strictly positive.

There are two cases to consider. Firstly, if $i \neq j$, then by (10.21), there exists a path of finite length $d_G(v_i, v_j)$ connecting v_i to v_j in G , so in this case we set $K = d_G(v_i, v_j)$. Secondly, if $i = j$, then since G is an undirected graph and $\deg(v_i) > 0$ (by (10.22)), there is clearly a closed path of length 2 in G (if we allow the repetition of an edge), which begins and ends at v_i , so in this case we set $K = 2$.

In both cases, by (10.26), the transition probability associated with each step between adjacent vertices along the path that has been identified between v_i and v_j is greater than or equal to the strictly positive value λ . Therefore, in both cases, $p_{ij}^{(K)} \geq \lambda^K > 0$, which proves the proposition. \square

The key result of this section is a corollary of the above proposition:

Corollary 10.4.2. *The time homogeneous Markov chain defined over the finite state space $V(G)$ by any transition matrix $T_A \in \mathfrak{T}_A$ has a unique stationary distribution $\pi[T_A] = (\pi_1[T_A], \dots, \pi_\kappa[T_A])^\top \in [0, 1]^\kappa$, satisfying:*

$$T_A \pi[T_A] = \pi[T_A] \quad (10.30)$$

$$\pi[T_A]^\top J_{\kappa,1} = 1 \quad (10.31)$$

$$\pi[T_A] \succ \mathbf{0}_{\kappa,1} \quad (10.32)$$

where \succ represents the inequality $>$ applied component-wise.

Proof. This result follows from Propositions 2.4.6, 2.4.7 and 10.4.1. \square

As discussed in Section 2.4, while $\pi[T_A]$ is not necessarily a limiting distribution of the Markov chain, from any starting point, the stochastic process defined by T_A will nevertheless visit every state infinitely many times (since the chain is positive recurrent), with the terms of $\pi[T_A]$ representing the proportion of time spent at each vertex in the long term. Note that this would not necessarily have been the case if transitions between adjacent vertices had been permitted to equal zero, rather than being bounded below by λ , since, under these conditions, some vertices could be completely inaccessible from certain starting points.

As will be explained in the following sections, Corollary 10.4.2 is highly important in relating optimal strategies of the GPG to those of the corresponding EGSG.

10.4.3 A detailed description of the GPG and its payoffs

Before defining the payoff functions for the GPG, we pause to provide a more detailed explanation of the concept of the game and of how it relates to the objects defined in Section 10.4.1.

The GPG proceeds as follows. Player A attempts to protect some space, represented by G , by patrolling randomly according to a Markov chain over the vertices, based on a matrix of transition probabilities T_A , which he chooses. Beyond those requirements that are necessary to define a valid Markov chain, Player A's choice of transition probabilities is further constrained in two ways. Firstly, it is constrained such that he will only ever move between vertices that are adjacent in G , thus respecting the geography of the space. Secondly, it is constrained such that the Markov chain has a unique stationary distribution $\pi[T_A]$ (by Corollary 10.4.2) and such that, no matter at which vertex he begins his patrol, Player A will visit every

vertex of G infinitely many times, a desirable property for a viable patrol strategy.

Unlike a standard Markov chain, Player A does not spend the same amount of time at each vertex, but rather chooses a set of dwell times \mathbf{d}_A to determine the time that he waits at each vertex before continuing his patrol. Each dwell time corresponds to a single vertex, such that Player A passes the same amount of time at a particular vertex every time he arrives there. Vertices that do not appear in the set Σ_A must be allocated a dwell time of zero, indicating that these vertices are effectively passed through instantaneously. Transitions themselves are also assumed to be instantaneous. In this way, letting ξ represent the time elapsed since the start of the patrol, given an initial deployment vertex for Player A $v_A[0]$, the Markov chain and the dwell times define a stochastic process that generates a current vertex $v_A[\xi]$ for Player A for any positive real time $\xi > 0$.

Player A's initial deployment location is chosen according to the probabilities given in $\boldsymbol{\pi}[T_A]$. This ensures that the probability distribution of his location at any particular iteration (without consideration of dwell times), is also equal to $\boldsymbol{\pi}[T_A]$. In many cases, this specification would not be necessary, since $\boldsymbol{\pi}[T_A]$ will often be a limiting distribution for the Markov chain, with any initial distribution $\boldsymbol{\mu}$ converging to $\boldsymbol{\pi}[T_A]$ for future iterations. However, if the Markov chain exhibits periodic behaviour, convergence of this sort will not occur (although, in such cases, the proportions of visits to each state across the complete history of the process will nonetheless converge to the components of $\boldsymbol{\pi}[T_A]$, as discussed in Section 10.4.2), leading to an undesirable potential source of long term predictability in the patrol strategy (see Ross, 1996, p. 177). Taking $\boldsymbol{\pi}[T_A]$ as the initial distribution is intended to avoid this issue.

For her part, Player B chooses a point v_B at which to deploy, exactly as she would in the EGSG. This deployment happens at some unknown but fixed future time ξ_B , which is supposed to occur long after the start of the patrol. Intuitively, we might express this statement in terms of the largest dwell time, through the relationship $\xi_B \gg \max \mathbf{d}_A$, but, as we will see later in this section, knowledge of the precise moment at which Player B deploys is not relevant to our subsequent analysis. Player B's deployment ends the game and payoffs are determined as in the EGSG, with Player A considered to have deployed at his final location $v_A[\xi_B]$.

Unlike with previous games discussed in this chapter, we treat the GPG as a Stackelberg game (see Section 7.3.7), in which Player B is able to observe the strategy of Player A and is assumed to employ the optimal response. Crucially however, while

Player B knows the strategy (T_A, \mathbf{d}_A) , since she has no information on when Player A commenced his patrol, or of his location at any time prior to her deployment, she is effectively playing against the long term average behaviour of the random process defined by T_A and \mathbf{d}_A .

Based on the above, we know that the payoff functions for the GPG are given by:

$$\begin{aligned} p_{A,\text{patrol}}((T_A, \mathbf{d}_A), v_B) &= p_A(v_A[\xi_B], v_B) \\ p_{B,\text{patrol}}((T_A, \mathbf{d}_A), v_B) &= p_B(v_A[\xi_B], v_B) \end{aligned} \quad (10.33)$$

where, p_A and p_B are the payoff functions of the EGSG, $\mathfrak{G} = (G, \Sigma_A, \Sigma_B, r, \gamma)$, as defined in (10.2) and (10.3), and where $v_A[\xi_B]$ is a random variable whose distribution depends on T_A and \mathbf{d}_A , as discussed. Owing to the simple relationship between their payoffs given in (10.33), the fact that the GPG is a zero-sum game clearly follows immediately from the fact that the ESSSG is a zero-sum game.

We observe that, given strategies (T_A, \mathbf{d}_A) and v_B , the expected values of these payoff functions could be written explicitly if the distribution of $v_A[\xi_B]$ over $V(G)$ were known. In fact, given our assumptions, this distribution is easy to determine. Disregarding the dwell times for a moment, we see that since the distribution of $v_A[0]$ is equal to $\boldsymbol{\pi}[T_A]$ and since $\boldsymbol{\pi}[T_A]$ is the unique stationary distribution of the Markov chain defined by T_A , over any sequence of states generated by the chain, the expected proportion of iterations that Player A will spend at vertex v_i is equal to $\pi_i[T_A]$, for all $i \in \{1, \dots, \kappa\}$. Reintroducing the dwell times, we see that in the limit as $\xi \rightarrow \infty$, the expected proportion of the time interval $[0, \xi]$ spent at vertex v_i is equal to:

$$\frac{\pi_i[T_A] d_{A,i}}{\boldsymbol{\pi}[T_A]^\top \mathbf{d}_A} \quad (10.34)$$

Therefore, since neither player knows the duration of the time interval $[0, \xi_B]$ between the start of Player A's patrol and Player B's deployment, except to the extent that this duration is large in comparison to the time that Player A passes at any vertex, from the perspectives of both players, the term given in (10.34) may effectively be considered to be equal to the probability that Player A will be found at vertex v_i when Player B deploys:

$$P[v_A[\xi_B] = v_i] = \frac{\pi_i[T_A] d_{A,i}}{\boldsymbol{\pi}[T_A]^\top \mathbf{d}_A} \quad (10.35)$$

This means that, given strategies (T_A, \mathbf{d}_A) and v_B , the expected payoffs of the GPG for each player may be written:

$$\begin{aligned} E[p_{A,\text{patrol}}((T_A, \mathbf{d}_A), v_B)] &= \sum_{i=1}^{\kappa} \frac{\pi_i[T_A] d_{A,i}}{\boldsymbol{\pi}[T_A]^\top \mathbf{d}_A} p_A(v_i, v_B) \\ E[p_{B,\text{patrol}}((T_A, \mathbf{d}_A), v_B)] &= \sum_{i=1}^{\kappa} \frac{\pi_i[T_A] d_{A,i}}{\boldsymbol{\pi}[T_A]^\top \mathbf{d}_A} p_B(v_i, v_B) \end{aligned} \quad (10.36)$$

The GPG is therefore effectively reduced to a Stackelberg version of the EGSG in which Player A plays the mixed strategy $\rho[T_A, \mathbf{d}_A]$, defined by:

$$\rho[T_A, \mathbf{d}_A] = (\rho_1[T_A, \mathbf{d}_A], \dots, \rho_\kappa[T_A, \mathbf{d}_A])^\top = \frac{\text{diag}(\boldsymbol{\pi}[T_A]) \mathbf{d}_A}{\boldsymbol{\pi}[T_A]^\top \mathbf{d}_A} \quad (10.37)$$

and we may write:

$$\begin{aligned} E[p_{A,\text{patrol}}((T_A, \mathbf{d}_A), v_B)] &= p_A(\rho[T_A, \mathbf{d}_A], v_B) \\ E[p_{B,\text{patrol}}((T_A, \mathbf{d}_A), v_B)] &= p_B(\rho[T_A, \mathbf{d}_A], v_B) \end{aligned} \quad (10.38)$$

Note that in (10.36) and (10.38) and in all that follows, the notation $E[\cdot]$ is used to refer exclusively to the expectation with respect to variation in the vertex $v_A[\xi_B]$ at which Player A deploys. For the sake of clarity, the calculation of expectations relating to the particular choice of pure strategy made when using a mixed strategy, is here assumed to be included in the payoff functions $p_{A,\text{patrol}}$, $p_{B,\text{patrol}}$, p_A and p_B . Henceforward, therefore, these functions are taken to refer to the *expected* payoff to the corresponding player, given any mixed strategies employed.

(10.38) highlights an important relationship between the payoffs of the GPG and those of the corresponding EGSG. In Section 10.4.4, we will show that there is also a relationship between the optimal strategies of these two games.

10.4.4 Optimal strategies of the GPG

We now investigate the optimal strategies of the GPG and their relationship to the OMSs of the EGSG. As we will see, for the GPG, there is no need to consider mixed strategies, since the conditions for optimality can be satisfied in pure strategies only. This is an intuitively sensible result, since, as we have seen in Section 10.4.3, a pure strategy of the GPG for Player A, $(T_A, \mathbf{d}_A) \in \Sigma_{A,\text{patrol}}$, corresponds to a mixed strategy $\rho[T_A, \mathbf{d}_A]$ of the corresponding EGSG, while Player B has no need of a mixed strategy, since she is able to observe the strategy of Player A and to employ an optimal pure strategy response.

A justification of the above assertions will require the following proposition:

Proposition 10.4.3. Consider a GPG, $\mathfrak{G}_{\text{patrol}} = (G, \Sigma_A, \Sigma_B, r, \gamma, \lambda)$ with $r = 1$, and the corresponding EGSG, $\mathfrak{G} = (G, \Sigma_A, \Sigma_B, r, \gamma)$. Given a valid mixed strategy ς_A of the GPG for Player A and a vertex $v_B \in \Sigma_B$, there exists a valid mixed strategy $\hat{\varsigma}_A$ of the EGSG for Player A such that:

$$E[p_{A,\text{patrol}}(\varsigma_A, v_B)] = p_A(\hat{\varsigma}_A, v_B) \quad (10.39)$$

$$E[p_{B,\text{patrol}}(\varsigma_A, v_B)] = p_B(\hat{\varsigma}_A, v_B) \quad (10.40)$$

where $p_{A,\text{patrol}}$, $p_{B,\text{patrol}}$ and p_A , p_B are the payoff functions to each player for the games $\mathfrak{G}_{\text{patrol}}$ and \mathfrak{G} respectively.

Proof. We prove (10.39), which relates to the payoffs for Player A. The proof of (10.40) would be identical.

By definition, a valid mixed strategy ς_A of the GPG for Player A defines a probability measure P_{ς_A} over the strategy set $\Sigma_{A,\text{patrol}}$. Recalling that $p_{A,\text{patrol}}$ is itself a stochastic function of its arguments, even when considering pure strategies only (see (10.33) and (10.35)), the expected payoff in (10.39) may thus be written explicitly, in terms of the general Lebesgue integral (see Craven, 1982, pp. 90-93), as²:

$$E[p_{A,\text{patrol}}(\varsigma_A, v_B)] = \int_{\Sigma_{A,\text{patrol}}} E[p_{A,\text{patrol}}(x, v_B)] dP_{\varsigma_A} \quad (10.41)$$

Note that, for reasons of clarity, a change of notation has been made, with x replacing (T_A, \mathbf{d}_A) as a general point of $\Sigma_{A,\text{patrol}}$.

By (10.38), and using the linearity of the Lebesgue integral (Craven, 1982, pp. 95-96), we therefore have:

$$\begin{aligned} E[p_{A,\text{patrol}}(\varsigma_A, v_B)] &= \int_{\Sigma_{A,\text{patrol}}} p_A(\rho[x], v_B) dP_{\varsigma_A} \\ &= \int_{\Sigma_{A,\text{patrol}}} \sum_{i=1}^{\kappa} \rho_i[x] p_A(v_i, v_B) dP_{\varsigma_A} \\ &= \sum_{i=1}^{\kappa} \left[\int_{\Sigma_{A,\text{patrol}}} \rho_i[x] dP_{\varsigma_A} \right] p_A(v_i, v_B) \end{aligned} \quad (10.42)$$

² The right hand side of (10.41) is an explicit representation of the expectation related to variation in Player A's particular choice of pure strategy when he employs the mixed strategy ς_A . Variation related to uncertainty in the vertex $v_A[\xi_B]$ at which Player A actually deploys, given that a particular pure strategy has been chosen, is not accounted for in this integral representation, hence the continued presence of the expectation function $E[\cdot]$ in the integrand. This is in line with our explanation of the usage of this notation, provided at the end of Section 10.4.3.

Now, let:

$$\hat{\varsigma}_{A,i} = \int_{\Sigma_{A,\text{patrol}}} \rho_i[x] \, dP_{\varsigma_A}, \quad \text{for } i \in \{1, \dots, \kappa\}$$

and, using the linearity of the Lebesgue integral once again, observe that:

$$\begin{aligned} \sum_{i=1}^{\kappa} \hat{\varsigma}_{A,i} &= \sum_{i=1}^{\kappa} \left[\int_{\Sigma_{A,\text{patrol}}} \rho_i[x] \, dP_{\varsigma_A} \right] \\ &= \int_{\Sigma_{A,\text{patrol}}} \left[\sum_{i=1}^{\kappa} \rho_i[x] \right] \, dP_{\varsigma_A} \\ &= \int_{\Sigma_{A,\text{patrol}}} \, dP_{\varsigma_A} \\ &= 1 \end{aligned}$$

Furthermore, by the definition of $\boldsymbol{\rho}$, given in (10.37), and the relationship between \mathbf{d}_A and Σ_A , defined in (10.28), we have:

$$\begin{aligned} \hat{\varsigma}_{A,i} &\geq 0, \quad \forall i \in \{1, \dots, \kappa\} \\ \text{and } v_i \notin \Sigma_A \Rightarrow \hat{\varsigma}_{A,i} &= 0 \end{aligned}$$

The vector $\hat{\boldsymbol{\varsigma}}_A = (\hat{\varsigma}_{A,1}, \dots, \hat{\varsigma}_{A,\kappa})^\top$ is therefore a valid mixed strategy of \mathfrak{G} for Player A and, by (10.42), we can write:

$$\begin{aligned} E[p_{A,\text{patrol}}(\boldsymbol{\varsigma}_A, v_B)] &= \sum_{i=1}^{\kappa} \hat{\varsigma}_{A,i} p_A(v_i, v_B) \\ &= p_A(\hat{\boldsymbol{\varsigma}}_A, v_B) \end{aligned}$$

This proves the proposition. □

Focusing on Player A only, Proposition 10.4.3 states that mixed strategies of the GPG correspond to mixed strategies of the EGSG. Since we have seen that pure strategies of the GPG also correspond to mixed strategies of the EGSG (see (10.38)), this result demonstrates that both pure and mixed strategies of the GPG can be said to operate in a similar way, in some sense.

At this stage, we pause to consider the optimal strategy of the GPG for Player B. Without loss of generality, we may suppose that Player A employs a mixed strategy $\boldsymbol{\varsigma}_A$, since pure strategies are a special case of mixed strategies.³ Since the GPG is a

³ In fact, the assumption that Player A employs a mixed strategy is made purely for the sake of the clarity of our argument. We will see (by Proposition 10.4.4, Proposition 10.4.5 and Lemma 10.4.6) that Player A has a pure strategy that satisfies the conditions for optimality.

Stackelberg game, Player B observes ς_A and employs her optimal response.

By Proposition 10.4.3, Player B knows that if she plays $v_B \in \Sigma_B$, her expected payoff from the game will be $p_B(\hat{\varsigma}_A, v_B)$, where $\hat{\varsigma}_A$ is the mixed strategy defined in the proof of the proposition. By the results of Section 10.3.2, we see that the expected payoffs $p_B(\hat{\varsigma}_A, v_i)$ for $i \in \{1, \dots, \kappa\}$ are given by the components of the vector $-\mathfrak{P}^\top \hat{\varsigma}_A$, where \mathfrak{P} is defined as in (10.14). Player B's optimal response to $\hat{\varsigma}_A$ in \mathfrak{G} is therefore v_ι , where ι is the index of the maximal entry of $-\mathfrak{P}^\top \hat{\varsigma}_A$, and her expected payoff in this case is:

$$E[p_{B,\text{patrol}}(\varsigma_A, v_\iota)] = \max[-\mathfrak{P}^\top \hat{\varsigma}_A]$$

Note that, by (10.15), if Player B were instead to employ a mixed strategy $\tau_B = (\tau_{B,1}, \dots, \tau_{B,\kappa})^\top$, her expected payoff would be:

$$\begin{aligned} E[p_{B,\text{patrol}}(\varsigma_A, \tau_B)] &= \sum_{i=1}^{\kappa} \tau_{B,i} E[p_{B,\text{patrol}}(\varsigma_A, v_i)] \\ &= -\tau_B^\top \mathfrak{P}^\top \hat{\varsigma}_A \end{aligned}$$

Bearing in mind that the entries of \mathfrak{P} are non-positive, this clearly does not exceed $\max[-\mathfrak{P}^\top \hat{\varsigma}_A]$, and therefore:

$$\max_{v_B \in \Sigma_{B,\text{patrol}}} E[p_{B,\text{patrol}}(\varsigma_A, v_B)] \geq E[p_{B,\text{patrol}}(\varsigma_A, \tau_B)]$$

for all mixed strategies ς_A over $\Sigma_{A,\text{patrol}}$ for Player A and τ_B over $\Sigma_{B,\text{patrol}}$ for Player B in $\mathfrak{G}_{\text{patrol}}$. This confirms the assertion that, in determining her optimal response, Player B need not consider mixed strategies. Henceforth, we therefore consider only pure strategies for Player B.

The next proposition uses Proposition 10.4.3 to identify a potential route for finding a pure strategy of the GPG that fulfils the optimality conditions.

Proposition 10.4.4. *Consider a GPG, $\mathfrak{G}_{\text{patrol}} = (G, \Sigma_A, \Sigma_B, r, \gamma, \lambda)$, with $r = 1$ and let σ_A be an OMS of the corresponding EGSG, $\mathfrak{G} = (G, \Sigma_A, \Sigma_B, r, \gamma)$, for Player A. Suppose that there exists $(T_A^*, \mathbf{d}_A^*) \in \Sigma_{A,\text{patrol}}$ such that $\rho[T_A^*, \mathbf{d}_A^*] = \sigma_A$. Then the pure strategy (T_A^*, \mathbf{d}_A^*) is an OMS of $\mathfrak{G}_{\text{patrol}}$ for Player A.*

Proof. We must prove that:

$$\min_{v_B \in \Sigma_B} E[p_{A,\text{patrol}}((T_A^*, \mathbf{d}_A^*), v_B)] \geq \min_{v_B \in \Sigma_B} E[p_{A,\text{patrol}}(\varsigma_A, v_B)] \quad (10.43)$$

for all valid mixed strategies ς_A over $\Sigma_{A,\text{patrol}}$ of $\mathfrak{G}_{\text{patrol}}$ for Player A.

Using (10.38), Proposition 10.4.3, and the fact that $\rho[T_A^*, \mathbf{d}_A^*] = \sigma_A$, (10.43) may be written:

$$\min_{v_B \in \Sigma_B} p_A(\sigma_A, v_B) \geq \min_{v_B \in \Sigma_B} p_A(\hat{\sigma}_A, v_B)$$

We complete the proof by observing that this inequality holds by definition, since we have assumed that σ_A is an OMS of \mathfrak{G} for Player A. \square

Proposition 10.4.4 tells us that if we know an OMS σ_A of the EGSG for Player A, then finding a pure strategy of $\mathfrak{G}_{\text{patrol}}$ for Player A that satisfies the conditions for optimality requires only that we identify some $(T_A^*, \mathbf{d}_A^*) \in \Sigma_{A,\text{patrol}}$ such that $\rho[T_A^*, \mathbf{d}_A^*] = \sigma_A$. Constructing such a strategy is the objective of the next proposition.

Before stating the proposition, we must define the following additional notation:

$$\deg[V(G)] = [\deg(v_1), \dots, \deg(v_\kappa)]^\top$$

We also recall that, given a valid transition matrix $T_A \in \mathfrak{T}_A$, $\pi[T_A]$ is the unique stationary distribution of the time homogeneous Markov chain over $V(G)$ that is defined by T_A (see Section 10.4.2), while $\mathfrak{M} = (a_{ij})_{i,j \in \{1, \dots, \kappa\}}$ is the adjacency matrix of the graph G over which the GPG is played.

We now state the following proposition.

Proposition 10.4.5. *Consider a GPG, $\mathfrak{G}_{\text{patrol}} = (G, \Sigma_A, \Sigma_B, r, \gamma, \lambda)$, with $r = 1$ and let σ_A be an OMS of the corresponding EGSG, $\mathfrak{G} = (G, \Sigma_A, \Sigma_B, r, \gamma)$, for Player A. Letting $\mathfrak{X} = \text{diag}(\deg[V(G)])^{-1}$, if we set:*

$$\begin{aligned} T_A^* &= \mathfrak{M}\mathfrak{X} \\ \mathbf{d}_A^* &= \text{diag}(\pi[T_A])^{-1}\sigma_A \end{aligned} \tag{10.44}$$

then the strategy $(T_A^, \mathbf{d}_A^*) \in \Sigma_{A,\text{patrol}}$ satisfies:*

$$\rho[T_A^*, \mathbf{d}_A^*] = \sigma_A$$

Note that the two inverse diagonal matrices mentioned in the proposition both exist, since, by (10.22) and (10.32), the vectors from which they are constructed have strictly positive components.

Before proving Proposition 10.4.5 itself, we must demonstrate that (T_A^*, \mathbf{d}_A^*) is indeed a valid strategy for the GPG for Player A. This is the purpose of the following lemma:

Lemma 10.4.6. Given T_A^* and \mathbf{d}_A^* , defined as in Proposition 10.4.5:

$$(T_A^*, \mathbf{d}_A^*) \in \Sigma_{A, \text{patrol}}$$

Proof. We must prove:

1. $T_A^* \in \mathfrak{T}_A$;
2. $\mathbf{d}_A^* \in \mathfrak{D}_A$.

where \mathfrak{T}_A and \mathfrak{D}_A are defined in (10.24) and (10.25) respectively.

Proof of 1. By (10.24), we must show that $T_A^* \in \mathbb{R}^{\kappa \times \kappa}$, $T_A^{*\top} J_{\kappa,1} = J_{\kappa,1}$ and $\lambda \mathfrak{M} \preceq T_A^* \preceq \mathfrak{M}$, where $J_{\kappa,1}$ is a length κ column vector of ones. Each of these statements is easily proved in a component-wise fashion. First observe that:

$$\mathfrak{X} = \left(\frac{\delta_{ij}}{\deg(v_i)} \right)_{i,j \in \{1, \dots, \kappa\}}$$

where δ_{ij} is the Kronecker delta, defined in (10.11). This implies that:

$$T_A^* = \mathfrak{M} \mathfrak{X} = \left(\frac{a_{ij}}{\deg(v_j)} \right)_{i,j \in \{1, \dots, \kappa\}} \in \mathbb{R}^{\kappa \times \kappa} \quad (10.45)$$

since $\deg(v_i) > 0$, $\forall i, j \in \{1, \dots, \kappa\}$. We can also prove that $T_A^{*\top} J_{\kappa,1} = J_{\kappa,1}$ as follows:

$$\begin{aligned} T_A^{*\top} J_{\kappa,1} &= \left(\sum_{j=1}^{\kappa} \frac{a_{ji}}{\deg(v_i)} \right)_{i \in \{1, \dots, \kappa\}} \\ &= \left(\frac{\deg(v_i)}{\deg(v_i)} \right)_{i \in \{1, \dots, \kappa\}} \\ &= J_{\kappa,1} \end{aligned}$$

Next, observe that, in component-wise form, $\lambda \mathfrak{M} \preceq T_A^* \preceq \mathfrak{M}$ is equivalent to the statement:

$$\lambda a_{ij} \leq \frac{a_{ij}}{\deg(v_j)} \leq a_{ij}, \quad \forall i, j \in \{1, \dots, \kappa\}$$

The right hand inequality follows from the fact that $\deg(v_j)$ is a positive integer. We prove the left hand inequality by contradiction. Suppose that there exists some

$i, j \in \{1, \dots, \kappa\}$ such that $\lambda a_{ij} > a_{ij} \deg(v_j)^{-1}$. We would then have:

$$\begin{aligned} a_{ij} (\lambda - \deg(v_j)^{-1}) &> 0 \\ \Rightarrow a_{ij} = 1 \text{ and } \lambda &> \deg(v_j)^{-1} \\ \Rightarrow a_{ij} = 1 \text{ and } \lambda^{-1} &< \deg(v_j) \end{aligned}$$

However, by (10.23):

$$\lambda^{-1} \geq \max_{j \in \{1, \dots, \kappa\}} \deg(v_j)$$

This is a contradiction, and therefore $\lambda a_{ij} \leq a_{ij} \deg(v_j)^{-1}$ for all $i, j \in \{1, \dots, \kappa\}$, as required. This completes the proof that $T_A^* \in \mathfrak{T}_A$.

Proof of 2. By (10.25), we must show that $\mathbf{d}_A^* \in \mathbb{R}^\kappa$, $\mathbf{d}_A^* \succcurlyeq \mathbf{0}_{\kappa,1}$ and $\text{diag}(\mathbf{s}_A) \mathbf{d}_A^* = \mathbf{d}_A^*$, where $\mathbf{0}_{\kappa,1}$ is a length κ column vector of zeros.

As in the proof of 1, we take a component-wise approach. We have that:

$$\mathbf{d}_A^* = \text{diag}(\boldsymbol{\pi}[T_A^*])^{-1} \boldsymbol{\sigma}_A = \left(\frac{\sigma_{A,i}}{\pi_i[T_A^*]} \right)_{i \in \{1, \dots, \kappa\}} \in \mathbb{R}^\kappa$$

since $\pi_i[T_A^*] > 0$, $\forall i \in \{1, \dots, \kappa\}$. Since $\boldsymbol{\sigma}_A$ is a valid mixed strategy of \mathfrak{G} for Player A, we also have that $\sigma_{A,i} \geq 0$, $\forall i \in \{1, \dots, \kappa\}$, which guarantees that $\mathbf{d}_A^* \succcurlyeq \mathbf{0}_{\kappa,1}$, as required.

Now, using the definition of \mathbf{s}_A , given in (10.13), the statement $\text{diag}(\mathbf{s}_A) \mathbf{d}_A^* = \mathbf{d}_A^*$ may be rewritten as:

$$\frac{\mathbf{1}_{\Sigma_A}[v_i] \sigma_{A,i}}{\pi_i[T_A^*]} = \frac{\sigma_{A,i}}{\pi_i[T_A^*]}, \quad \forall i \in \{1, \dots, \kappa\}$$

where $\mathbf{1}_{\Sigma_A}$ is the indicator function of the set Σ_A , as defined in (10.5).

We prove this by contraction. Suppose that there exists $i \in \{1, \dots, \kappa\}$, such that:

$$\frac{\mathbf{1}_{\Sigma_A}[v_i] \sigma_{A,i}}{\pi_i[T_A^*]} \neq \frac{\sigma_{A,i}}{\pi_i[T_A^*]}$$

Then we must have:

$$v_i \notin \Sigma_A \text{ and } \sigma_{A,i} > 0$$

However, since σ_A is a valid mixed strategy for Player A in \mathfrak{G} , this is a contradiction, and $\text{diag}(\mathbf{s}_A) \mathbf{d}_A^* = \mathbf{d}_A^*$, as required. This completes the proof that $\mathbf{d}_A^* \in \mathfrak{D}_A$ and hence proves the lemma. \square

We now prove Proposition 10.4.5.

Proof. We wish to prove that, for the T_A^* and \mathbf{d}_A^* given in (10.44):

$$\rho[T_A^*, \mathbf{d}_A^*] = \sigma_A$$

Observe that, by (10.37):

$$\begin{aligned}\rho[T_A^*, \mathbf{d}_A^*] &= \frac{\text{diag}(\pi[T_A^*]) \mathbf{d}_A^*}{\pi[T_A^*]^\top \mathbf{d}_A^*} \\ &= \frac{\text{diag}(\pi[T_A^*]) \text{diag}(\pi[T_A^*])^{-1} \sigma_A}{\pi[T_A^*]^\top \text{diag}(\pi[T_A^*])^{-1} \sigma_A} \\ &= \frac{\sigma_A}{J_{1,\kappa} \sigma_A} \\ &= \sigma_A\end{aligned}$$

where $J_{1,\kappa}$ is a length κ row vector of ones.

This proves the proposition. \square

In summary then, we have demonstrated that an optimal strategy of the GPG for Player A may be constructed from a known OMS of the corresponding EGSG for Player A. We have also identified Player B's optimal response. These are the key results of this section, which we state concisely in this final proposition:

Proposition 10.4.7. *Consider a GPG, $\mathfrak{G}_{\text{patrol}} = (G, \Sigma_A, \Sigma_B, r, \gamma, \lambda)$, with $r = 1$ and let σ_A be an OMS of the corresponding EGSG, $\mathfrak{G} = (G, \Sigma_A, \Sigma_B, r, \gamma)$, for Player A.*

- The pure strategy $(T_A^*, \mathbf{d}_A^*) \in \Sigma_{A,\text{patrol}}$, as defined in Proposition 10.4.5, is an optimal strategy of $\mathfrak{G}_{\text{patrol}}$ for Player A.
- The pure strategy $v_\iota \in \Sigma_{B,\text{patrol}}$, where ι is the index of a maximal entry of $-\mathfrak{P}^\top \sigma_A$, is an optimal strategy of $\mathfrak{G}_{\text{patrol}}$ for Player B (where \mathfrak{P} is defined as in (10.14)).
- The value of $\mathfrak{G}_{\text{patrol}}$ (to Player A) is $\min [\mathfrak{P}^\top \sigma_A]$, which is equal to the value of \mathfrak{G} (to Player A).

Proof. The first part follows from Propositions 10.4.4 and 10.4.5. The second part follows from Proposition 10.38, 10.4.5 and the definition of \mathfrak{P} in Section 10.3.2. The third part follows from the other two, recalling that the GPG is a zero-sum game, and from the definition of the value of a game. \square

10.4.5 The GPG as an optimisation problem

Through Proposition 10.4.7, we have a method for constructing an optimal strategy of the GPG for Player A using an OMS of the corresponding EGSG. As we have seen, the latter may be calculated through the application of standard techniques to the payoff matrix \mathfrak{P} , which was defined in Section 10.3.2. We have also seen that the optimal strategy for Player B is to observe the strategy (T_A, \mathbf{d}_A) of Player A and to respond by deploying at the vertex v_B that corresponds to the maximum entry of the vector $-\mathfrak{P} \boldsymbol{\rho}[T_A, \mathbf{d}_A]$ (where $\boldsymbol{\rho}[T_A, \mathbf{d}_A]$ is defined in (10.37)).

We now conclude this chapter by asking whether the optimal strategy (T_A^*, \mathbf{d}_A^*) of the GPG for Player A, as defined in Proposition 10.4.5, is the unique pure strategy in $\Sigma_{A,\text{patrol}}$ satisfying the equation $\boldsymbol{\rho}[T_A, \mathbf{d}_A] = \boldsymbol{\sigma}_A$, given a particular OMS $\boldsymbol{\sigma}_A$ of the corresponding EGSG.

To address this question, first observe that the proof that $\mathbf{d}_A^* \in \mathfrak{D}_A$, which forms part of the proof of Lemma 10.4.6, and the proof of Proposition 10.4.5 are unaffected by the multiplication of \mathbf{d}_A^* by a positive real scalar $\eta > 0$. Therefore, if (T_A^*, \mathbf{d}_A^*) is an optimal strategy of the GPG for Player A, then so is $(T_A^*, \eta \mathbf{d}_A^*)$.

Next, consider the entry-wise description of the transition matrix T_A^* , given in (10.45). This expression shows that, from a given vertex $v_j \in V(G)$, T_A^* allocates a probability of 0 to transitions to vertices that are not adjacent to v_j and equal probabilities of $\deg(v_j)^{-1}$ to all other transitions. In other words, T_A^* describes an unbiased random walk over the vertices of G .

However, note that the proof that $\mathbf{d}_A^* \in \mathfrak{D}_A$ and the proof of Proposition 10.4.5, require only that T_A^* corresponds to a unique, positive-valued stationary distribution $\boldsymbol{\pi}[T_A^*]$ over $V(G)$, a requirement that holds for all valid $T_A \in \mathfrak{T}_A$ (by Corollary 10.4.2). We may then observe that *every* $T_A \in \mathfrak{T}_A$ corresponds to an optimal strategy $(T_A, \mathbf{d}_A) \in \Sigma_{A,\text{patrol}}$ of the GPG for Player A, where \mathbf{d}_A is considered to be a function of T_A , given by $\mathbf{d}_A = \text{diag}(\boldsymbol{\pi}[T_A])^{-1} \boldsymbol{\sigma}_A$. We therefore see that the specification of Proposition 10.4.5 that T_A^* should define an unbiased random walk was made purely for the sake of simplicity, this representing, in some sense, the ‘most natural’ set of transitions to choose.

Combining the above observations, we have that, given an OMS $\boldsymbol{\sigma}_A$ of the appropriate EGSG, each $T_A^\dagger \in \mathfrak{T}_A$ defines a one-parameter family of optimal strategies of

the GPG for Player A:

$$(T_A^\dagger, \mathbf{d}_A^\dagger) = (T_A^\dagger, \eta \operatorname{diag}(\boldsymbol{\pi}[T_A^\dagger])^{-1} \boldsymbol{\sigma}_A) \in \Sigma_{A,\text{patrol}} \quad (10.46)$$

Since there may also be many possible choices for $\boldsymbol{\sigma}_A$, we observe that, in general, there will be a wide range of possible optimal strategies of the GPG for Player A.

This raises the possibility that, rather than simply playing the optimal strategy defined in Proposition 10.4.5, Player A might instead choose an optimal strategy of the form given in (10.46) on the grounds that it exhibits a particular desirable property. For example, it may be helpful to specify the mean of the dwell times \hat{d} , to ensure that the rate of progression of a patrol is appropriate for the particular scenario under consideration:

$$\kappa^{-1} \mathbf{d}_A^\top J_{\kappa,1} = \hat{d}$$

This may be achieved by choosing the appropriate value of η . Substituting from (10.46), we have:

$$\eta = \frac{\kappa \hat{d}}{\boldsymbol{\sigma}_A^\top \operatorname{diag}(\boldsymbol{\pi}[T_A^\dagger])^{-1} J_{\kappa,1}} \quad (10.47)$$

It may also be desirable that the dwell times should be roughly equal (excepting those corresponding to vertices that are not in Σ_A , which are constrained to equal zero), since this would make the corresponding patrol strategy simpler to implement. This suggests that we should attempt to minimise the empirical variance of the components of \mathbf{d}_A , given by:

$$\frac{1}{\kappa} \mathbf{d}_A^\top \mathbf{d}_A - \hat{d}^2 \quad (10.48)$$

Since \hat{d} and κ are specified constants, this is equivalent to minimising:

$$\mathbf{d}_A^\top \mathbf{d}_A \quad (10.49)$$

Now, using (10.46) and (10.47), (10.49) may be rewritten as:

$$\kappa^2 \hat{d}^2 \frac{\boldsymbol{\sigma}_A^\top \left[\operatorname{diag}(\boldsymbol{\pi}[T_A^\dagger])^{-1} \right]^2 \boldsymbol{\sigma}_A}{\left[\boldsymbol{\sigma}_A^\top \operatorname{diag}(\boldsymbol{\pi}[T_A^\dagger])^{-1} J_{\kappa,1} \right]^2} \quad (10.50)$$

Finally, since this is a function to be minimised, the positive constant multiplier $\kappa^2 \hat{d}^2$ may clearly be disregarded, resulting in the following objective function to be

minimised over \mathfrak{T}_A :

$$\mathcal{Z}[T_A] = \frac{\boldsymbol{\sigma}_A^\top [\text{diag}(\boldsymbol{\pi}[T_A])^{-1}]^2 \boldsymbol{\sigma}_A}{[\boldsymbol{\sigma}_A^\top \text{diag}(\boldsymbol{\pi}[T_A])^{-1} J_{\kappa,1}]^2}$$

Taken together, these desires and constraints may be stated as the following continuous optimisation problem:

The GPG as an optimisation problem for Player A:

- Given:

- A GPG, $\mathfrak{G}_{\text{patrol}} = (G, \Sigma_A, \Sigma_B, r, \gamma, \lambda)$, with $r = 1$ and $|V(G)| = \kappa$;
- An OMS $\boldsymbol{\sigma}_A$ of the corresponding ESGG, $\mathfrak{G} = (G, \Sigma_A, \Sigma_B, r, \gamma)$, for Player A ;
- A positive real number $\hat{d} > 0$.

- Minimise:

$$\mathcal{Z}[T_A] = \frac{\boldsymbol{\sigma}_A^\top [\text{diag}(\boldsymbol{\pi}[T_A])^{-1}]^2 \boldsymbol{\sigma}_A}{[\boldsymbol{\sigma}_A^\top \text{diag}(\boldsymbol{\pi}[T_A])^{-1} J_{\kappa,1}]^2}$$

- Over:

$$T_A \in \mathbb{R}^{\kappa \times \kappa}$$

- Subject to the constraints:

$$\begin{aligned} T_A^\top J_{\kappa,1} &= J_{\kappa,1} \\ \lambda \mathfrak{M} &\preccurlyeq T_A \\ T_A &\preccurlyeq \mathfrak{M} \end{aligned}$$

- Where $\boldsymbol{\pi}[T_A] \in \mathbb{R}^\kappa$ is the unique vector satisfying:

$$\begin{aligned} T_A \boldsymbol{\pi}[T_A] &= \boldsymbol{\pi}[T_A] \\ \boldsymbol{\pi}[T_A]^\top J_{\kappa,1} &= 1 \\ \boldsymbol{\pi}[T_A] &\succ \mathbf{0}_{\kappa,1} \end{aligned}$$

Despite the linearity of the constraints, the complicated structure of the objective function and its relationship to the optimisation variables (the entries of T_A) means that finding an optimal solution to the problem may not be

straightforward.⁴ Therefore, while a detailed investigation of the problem would provide an interesting avenue for future research, it is beyond the scope of this thesis. However, observing that the objective function may be written as:

$$\mathcal{Z}[T_A] = \frac{\sum_{i=1}^{\kappa} [\sigma_{A,i} \pi_i[T_A]^{-1}]^2}{\left[\sum_{i=1}^{\kappa} \sigma_{A,i} \pi_i[T_A] \right]^2}$$

and since the terms of $\pi[T_A]$ and σ_A are all non-negative, by the triangle inequality (see Sutherland, 2009, p. 39), we see that $\mathcal{Z}[T_A] \in [0, 1]$. Furthermore, since the feasible region is closed and bounded (if considered as a subset of \mathbb{R}^{κ^2}) and non-empty (since T_A^* , as defined in Proposition 10.4.5, is a feasible solution), we would suggest that some form of systematic search of this region would represent a plausible initial approach to the problem.

10.5 Summary and conclusions

In Part III, in line with the research objectives set out in Section 1.5, we have defined a search and concealment game, the SSSG, which differs from the majority of games considered in literature both in its generality and in its explicit consideration of the strategic interdependence of positions based on spatial structure. We believe that formulating the game in terms of metric spaces may allow new tools and results from this area of mathematics to be applied to search and concealment problems, facilitating the identification of OMSs in a variety of different cases.

We have examined the way in which the game theoretic concepts of dominance and equivalence of strategies are manifested in the context of the SSSG and have presented various methods for analysing the SSSG played over a graph (the “Graph Search Game” or GSG), including:

- The reduction of GSGs with detection radius $r \neq 1$ to games with $r = 1$.
- The formulation of lower and upper bounds on the value of the GSG.
- An algorithm that applies the concept of IEDS in the explicit context of the GSG and which has been demonstrated to reduce games played on trees to cases in which OMSs can be immediately determined.

⁴ Indeed, it is known that optimisation problems of this nature can prove extremely challenging to solve. For example, Galli and Letchford (2015) describe non-convex, quadratically constrained, quadratic programs (a specific variety of optimisation problem whose objective function and constraints are quadratic in the optimisation variables) as being “not only NP-hard in the strong sense, but also very difficult in practice.”

- A method for simplifying the analysis of GSGs using automorphisms of the graph.
- The introduction of the concept of an “equal oddments strategy”, and a demonstration that such mixed strategies are optimal for both players.
- The presentation of explicit OMSs for a particular family of GSGs; those played over “poly-level graphs” .

In this chapter, we have extended the SSSG to consider spaces in which the points of the space over which the game is played may differ in value to the two players. We have considered the OMSs of this extended game (the ESSSG), with particular reference to the case in which the game is played over a graph (the EGSG), and derived a proposition that could simplify the task of identifying these strategies (in Section 10.3.4).

Finally, we adapted the EGSG to consider scenarios in which, rather than remaining stationary, the searching player was able to patrol the space, drawing on methods from the theory of Markov chains and demonstrating key connections between the optimal strategies of the patrol game and the static game.

It should be noted that the GPG defined in this chapter differs from the majority of patrol games considered in the literature (such as those proposed by Alpern et al., 2011b and Basilico et al., 2012), both in the stochastic nature of its patrol strategies and in the fact that the patrolling player controls a *neighbourhood* around his current location, rather than simply the location itself. These differences allow the GPG to take full consideration of the geography of the space over which it is played and of the impact of this spatial structure on the interaction between the players, rather than simply using space to determine the set of valid patrol routes.

In the final part of this thesis, we will reflect on the work that has been presented, assessing our results against the research objectives, considering the relevance and limitations of our conclusions and discussing how the work might be built on and extended. We will also present some brief ideas on how the work of Parts II and III could be brought together before drawing our arguments to a close.

Part IV

Conclusions

Chapter 11

Conclusions, synthesis and further work

Some material in Section 11.3.3 is adapted from the article *Static search games played over graphs and general metric spaces*, published in the *European Journal of Operational Research* (Oléron Evans and Bishop, 2013).

11.1 Research outcomes

11.1.1 General comments

In this thesis, we have considered two broad perspectives on the relationship between local interactions, global outcomes and spatial structure in models of systems of interacting individuals. The first may be described as a ‘wide-angle’ perspective, in which individuals are treated as simple stochastic automata, with no explicit decision making capability. The second may be described as a ‘close-up’ perspective, in which individuals are treated as sophisticated decision-making agents.

We have explored each of these perspectives through the use of a different modelling paradigm: individual-based modelling in the first case, where we focused on the collective dynamics that emerge from local interactions between individuals, and game theoretic modelling in the second, where we examined the relationship between the geography of a space and the strategic behaviour of its inhabitants.

A detailed list of the original contributions to knowledge presented in the thesis is provided in Section 1.7. Rather than reproducing that list here, we will instead discuss the outcomes of the research in broader terms, with specific reference to the objectives presented in Section 1.5.

11.1.2 Perspective one: Individuals as automata

The first perspective was examined in Part II, whose major focus was a particular family of stochastic cellular IBMs, described as one-dimensional, single species \mathfrak{B} -models (defined in Section 4.4), which were derived from the NANIA predator-prey model (defined in Section 4.2). This family of models was used as a basis for an examination of our first two research objectives:

- To improve understanding of the relationship between the long term population dynamics of spatially explicit IBMs and the dynamics predicted by corresponding non-spatial models, derived using mean field theory.
- To develop methods to understand and explain the causal link between local spatial interactions and global population dynamics in such models.

The objectives were addressed in two phases. First, in Chapter 5, a large number of computer simulations of one-dimensional, single species \mathfrak{B} -models were performed, systematically varying the model parameters so as to thoroughly explore the parameter space. Through visualisation of the resulting population dynamics, it was possible to create a taxonomy of possible model behaviours, and to broadly define the region of parameter space in which each behaviour was prevalent. A comparison of the observed long term mean population densities in these simulations with the stable equilibria predicted by mean field theory, alongside an analysis of spatial correlations between cell states, allowed us to understand, in an empirical sense, how varying the parameters impacted on the relationship between the IBM and a corresponding mean field model.

Since the \mathfrak{B} -model parameters, $\alpha, \beta, \gamma, \epsilon, \zeta$, are each explicitly related to the frequency with which a particular local transition (individual behaviour) occurs, it was possible to ascertain that α -transitions, representing the mortality of isolated individuals, are associated with poor ‘mixing’ of individuals throughout the system (in the sense that such transitions induce substantial correlations in the states of nearby cells), while all other transition types are associated with good mixing. This explained why higher values of the parameter α were observed to produce simulations with increasingly poor correspondence to mean field models, since local spatial correlations between cell states invalidate the necessary independence assumptions of mean field theory.

While the simulation experiments had identified a connection between α -transitions and local spatial correlations, they did not explain the causal nature of this relationship. Therefore, in order to address this issue and thus to more fully achieve the

second of the above objectives, in Chapter 6, a more theoretical approach was taken. The new approach involved the translation of the dynamics of the one-dimensional, single species \mathfrak{B} -models into a new space and the analysis of the possible effects of each type of transition in this new context. A measure of clumping was introduced to describe the spatial distribution of individuals throughout the system, and this measure was used to explain the unique effect of α -transitions on the spatial distribution of individuals. Using the new representation of the model and the clumping measure, an argument was presented to explain why the mean field equilibrium could be considered, in a certain sense, ‘unstable’ under α -transitions, but ‘stable’ under all other transitions.

11.1.3 Perspective two: Individuals as decision-making agents

The second perspective was examined in Part III, in which we created, analysed and extended a general game theoretic model, the Static Spatial Search Game (SSSG), with the aim of addressing our remaining research objectives:

- To create a general, explicitly spatial, search and concealment game, in order to unite many similar games presented in the literature under a single theoretical framework.
- To develop general results on the optimal mixed strategies of this game and on how these strategies may be determined.

As originally defined in Chapter 8, the SSSG is a two-player game, in which a searching player and a hiding player simultaneously choose points of a known metric space at which to deploy. In this framework, an ‘interaction’ between individuals consists exclusively of whether or not the searching player locates the hiding player. This occurs when the distance between the two deployment locations (in terms of the metric) is smaller than a pre-specified “detection radius”, with a fixed payoff awarded to the searching player if the hiding player is located, or to the hiding player otherwise. To fully address the first of the two objectives listed above, in Section 8.2.2, we discussed several other games from the literature that could be formulated as special cases of the SSSG.

Over the course of Chapters 8-10, a number of special cases and extensions to the SSSG were presented and analysed, most notably the case in which the metric space over which the game is played is a graph (the “Graph Search Game” or GSG), an extension of the model to consider spaces of non-uniform value and the development of a model to represent situations of patrol and infiltration, in which the searching

player moves randomly through the space according to a set of probabilities that he has chosen. The consideration of these cases served two main purposes: firstly, to make the game more amenable to analysis, allowing for the derivation of general results in line with the second objective stated above, and secondly, to broaden the potential applicability and relevance of the game.

In terms of the second objective, results presented in relation to these games can be divided into two categories. Firstly, there are results that serve to simplify the analysis of a game or that seek to approximate important quantities. These include the derivation of bounds on the value of the GSG to each player, a method to reduce all GSGs to games with unit detection radius, a reformulation of the iterated elimination of dominated strategies (IEDS) algorithm to simplify the task of identifying optimal mixed strategies (OMSs), and methods to simplify GSGs by exploiting graph automorphisms. Secondly, there are results which allow for the calculation of precise OMSs in particular cases; for example, in GSGs played over trees or “poly-level” graphs (defined in Section 9.4.1), in GSGs admitting “equal oddments” strategies (defined in Section 9.3.3), and in patrol games over graphs for which the optimal strategies of the corresponding SSSG are known.

11.2 Discussion

11.2.1 The choice of models studied in Part II

We now present a critical discussion of our research outcomes. Our purpose is to highlight the extent and significance of the work and to justify some of the decisions that were made with regard to direction, content and focus.

First, we consider Part II, discussing our choice of models and the scope of the research presented. A natural question that arises is why the NANIA model was chosen as a starting point for our investigation and why, subsequently, the focus was shifted to the family of one-dimensional, single species \mathfrak{B} -models. This question was addressed in Section 4.4.1, and we now expand on and reiterate the arguments given there.

We note that, as discussed in Section 4.2.1, the NANIA model is of relevance in and of itself, both since it is often invoked as an archetypical example of an IBM for the purposes of teaching and visualisation and because it is related to the more widely applied ecological patch models, discussed in Section 3.3.3. We would further contend that the discrete space-time stochastic models of class \mathfrak{B} , of which the

NANIA model is a special case, represent a potentially important and fundamental family of IBMs, whose study could provide important insights for the wider field of agent-based and individual-based modelling as a whole. These models are conceptually simple and have been shown to be related to certain IBMs in the literature, yet although parallels can be drawn between these models and previous objects of study (certain of the “simple programs” examined by Wolfram (2002), for example), general results and analysis of such models are largely absent from the literature.

For these reasons, alongside their simplicity and their compatibility with mean field analysis, \mathfrak{B} -models represented an ideal framework in which to address the first two of our stated research objectives. One-dimensional, single species \mathfrak{B} -models may be considered to represent a minimally complex setting in which the issues raised by these objectives – comparing the population dynamics of spatial IBMs with those of non-spatial mean field models and understanding the causal links between local and global features – may be observed and investigated.

While it could be argued that one-dimensional, single species \mathfrak{B} -models constitute too narrow a category of IBMs to successfully address our objectives, the fact that such models have seen little study in their most general form necessitates a simple initial approach, to form a firm foundation for future work. The approaches that have been employed for the analysis of these simple models may inform the study of more complex systems going forward. Furthermore, the restriction to one-dimensional, single species models served to sufficiently reduce the range of possible dynamics such that a thorough exploration of the parameter space could be conducted through experimental simulation, something that would not have been possible if a more detailed family of models had been considered.

The high level of abstraction of \mathfrak{B} -models is also worthy of comment. It is clear that, in reference to Gilbert’s (2008, pp. 41-44) categorisation of models (see Section 2.2.2), these systems fall firmly into the class of “abstract models”. While it is true that \mathfrak{B} -models would not be suitable for modelling of any particular real world system or class of systems without significant extension and development, they are suitable for the purposes for which we employ them; namely, to investigate more general theoretical questions about the behaviour of IBMs, their relationship to non-spatial mean field models and the causal relationships connecting local and global dynamics.

In support of these arguments, we would once again invoke the words of San Miguel et al. (2012, p.250), previously quoted in Section 4.4.1, who stated that:

“Simple models are essential to uncover the basic mechanisms [of complex systems] and provide insight into fundamental questions.”

It is precisely in this spirit that \mathfrak{B} -models have been employed in this thesis.

11.2.2 The use of mean field theory

Turning to more specific questions on our methodology, there are a number of ways in which mean field theory could be adapted to provide a better match to the behaviour of IBMs. For example, we could have employed a spatial rather than a non-spatial approach, producing a representation of the model as a system of PDEs, rather than a system of ODEs (see Section 3.2.4). However, PDE representations such as these cannot truly be considered to provide *simplified* representations of model dynamics, since they require complete knowledge of the initial microstate of a model to predict its future behaviour, rather than knowledge of the population density only, as in the non-spatial case. If our goal is to reduce the number of variables needed to usefully describe the state of a system, then PDEs are not necessarily an appropriate tool.

Alternatively, rather than describing the state of the system with a single variable, u , representing the population density, further variables could be introduced to account for some limited spatial correlations. For example, we could consider the simultaneous dynamics of a second variable, v , representing the proportion of the neighbours of occupied cells that are themselves occupied (but assuming no other statistical dependencies between cell states). A mean field type approach could then be applied to produce dynamical equations of the form:

$$\begin{aligned}\dot{u} &= f_1(u, v) \\ \dot{v} &= f_2(u, v)\end{aligned}$$

More spatial information could be accounted for by introducing more and more variables of this nature (i.e. w to represent the proportion of the neighbours of pairs of consecutive occupied cells that are themselves occupied, and so on).

While exploratory work in this direction (which is not presented in this thesis) did produce ODEs that provided a better match for the dynamics of our IBMs than had the basic mean field models, there were still discrepancies between the observed and the predicted equilibria. Given a sufficiently large number of variables, it would be possible to account for all spatial correlations in this way and to produce a system of ODEs that precisely represented the behaviour of a particular one-dimensional, single species \mathfrak{B} -model (at least up to effects due to time discretisation). However,

the number of variables would necessarily be large and the approach would not correspond to the way that mean field techniques are used in practice. Nevertheless, it may be possible to use autocorrelation plots such as those presented in Section 5.4.1 to determine the amount of spatial information that a system of ODEs would need to represent in order to provide accurate dynamical predictions for a given model and thus the number of variables that should be used. This approach is, however, beyond the scope of this thesis.

11.2.3 The methods and conclusions of Chapter 6

Moving on to the methods presented in Chapter 6, it could be argued that the technique employed for translating the model into a new space, is so specific to the one-dimensional, single species \mathfrak{B} -model, that it could not be profitably adapted to other contexts. While it is true that the method is quite specialised, there are two reasons why we believe that it may nonetheless have broader relevance across the field of individual-based modelling.

Firstly, the approach can be seen as a simple proof of concept. The problem of explaining the causal relationship between local individual interactions and global emergent behaviours in IBMs is often considered to be largely intractable, and is therefore often not attempted. However, in identifying those local transitions that are conducive to mean field type behaviour and those that are not, and in explaining these differences in terms of the effect of different transitions on the spatial distribution of individuals, we have demonstrated that finding explicit causal relationships between events at the local and the global scales in IBMs is not always a futile pursuit.

Secondly, although the translation procedure – in which a microstate is represented in terms of the distances between consecutive occupied cells in the underlying one-dimensional ring of cells – is clearly not immediately transferable to \mathfrak{B} -models over higher dimensional grids or over more general graphs, nor to situations of multiple species, it is possible to imagine ways in which the procedure could be adapted to these broader contexts. For example, it may be possible to represent a system through the distances between each occupied cell and a certain number of its nearest occupied neighbours. Different species could either be considered equivalent, or there could be multiple different such representations corresponding to each species, or to each ordered pair of species. In this way, many different sets of nearest neighbour distances would be considered, with the combination of these representations providing an overall picture of a current microstate.

Naturally, unlike in the case of the one-dimensional, single species model, such representations may not unambiguously represent the precise microstate of the system. However, they may still be sufficient for the derivation of analogous quantities to the clumping measure defined in Section 6.5, and could conceivably allow for a similar investigation of the link between local interactions and global dynamics. Further research would be necessary to assess the validity of such an approach.

As a final comment on the work presented in Part II, although the different effects of each of the possible single species \mathfrak{B} -model transitions on individual clumping were demonstrated in Section 6.6.3, it should be remarked that a fully rigorous argument on the relationship between local transitions, individual clumping and equilibrium population density proved elusive. While the case presented in Section 6.6.4 went some way towards achieving this goal, providing a causal explanation for the fact that observed equilibrium densities in models with $\alpha > 0$ lie below the predicted mean field equilibrium, the argument relies upon intuitive reasoning on how changes to the clumping of individuals (as measured by our clumping measures) should affect the correspondence between model behaviour and mean field dynamics. Further work in this area, to make this argument more rigorous, would be desirable.

11.2.4 Limitations of the SSSG

Turning to consider our work on the SSSG and its derivatives, the most obvious limitation of the game as a modelling tool is its restriction to situations with only two players. Clearly, some scenarios that we may wish to model would necessitate multiple searching and hiding players or would otherwise require that multiple units are available for each player to deploy at different locations. For example, if we wanted to model the policing of outbreaks of rioting across an urban street network, we might represent the police (the “searching” player, in terms of the SSSG) as a single player with many units to deploy, while groups of rioters (“hiding” players) would be modelled as many independent players.

This limitation represents one reason for which the SSSG should be seen primarily as a basis for further development, rather than as a complete modelling tool. In common with the \mathfrak{B} -models discussed above, the SSSG is certainly an abstract model in terms of Gilbert’s (2008, pp. 41-44) categorisation, and would require significant further enhancement to serve as a valuable representation of a real world system. Indeed, given its intended role as a framework to unite other models, this high level of abstraction is inevitable.

The fact that the model is limited to two-player scenarios does not necessarily mean

that it has nothing to contribute in situations in which there are a greater number of interacting individuals. It may be valuable to investigate to what extent the OMSs of the basic two-player game could form a basis for good strategies of multi-player versions. For example, in a GSG in which the searching player were allocated two units, the first could be deployed according to the OMS for the basic game, while the second could be deployed according to an altered version of the same probability distribution, in which the point at which the first unit is deployed is allocated zero probability, with all other probabilities scaled accordingly. Alternatively, the probability distribution for the deployment of the second unit could be determined by removing all the vertices that lie in the neighbourhood of the point at which the first unit is deployed from the strategy set of the hiding player, and recalculating an OMS for the searching player in this new context.

While neither of these methods would generally give a true OMS of a multi-player or multi-unit game, they may nevertheless provide good benchmark strategies for searching or hiding players, particularly where the underlying graph is large and the effect of removing any one vertex is therefore small. In situations where searching or hiding units act without coordination (for example, in the case of independent groups of rioters), we might also expect the OMS of the two-player game to provide a good strategy for the multi-player extension, since each such player would effectively be playing as if they were alone. Further research would be necessary to determine the true relationship between OMSs of the basic two-player game and good strategies of more general multi-player and multi-unit games.

11.2.5 Results on identifying optimal mixed strategies

It would be true to say that several of the results relating to the OMSs of the SSSG and its derivatives that are presented in this thesis relate only to rather specific cases. For example, while we were successful in determining precise OMSs for poly-level graphs (see Section 9.4), if the game were to be adapted to model real life scenarios, it would be more useful to have results relating to less structured graphs. Some suggestions as to the most valuable developments that could be made in this direction are outlined in Section 11.3.

The IEDS algorithm presented in Section 9.2 could potentially form the basis of an approach to determining good strategies for games over irregular geographies. However, to be considered a valuable tool, the algorithm would have to be strengthened considerably, perhaps through the inclusion and exploitation of results such as Proposition 10.3.2, for spaces of non-uniform value. As it stands, although the algorithm has been demonstrated to be particularly powerful for GSGs played over

trees, for more highly connected graphs it is often unable to simplify them to any great extent, owing to the rarity of pure strategy dominance in such settings. If the algorithm were adapted to detect mixed strategy dominance (in which a weighted average of pure strategies dominates another pure strategy in terms of expected payoff), then it may be able to simplify the analysis of a much wider range of GSGs. An investigation of how effective the algorithm is over specific families of graphs may also be of interest (e.g. complete graphs, bipartite graphs, planar graphs, scale-free graphs, etc.).

11.2.6 Limitations of the GPG

In allowing the searching player to move around the space, the Graph Patrol Game (GPG) of Section 10.4 addresses one of the key weaknesses of the original SSSG. However, certain of the simplifying assumptions made when defining the GPG may limit the immediate applicability of the game to real world scenarios.

For example, it was assumed that the time lapse between the start of Player A's patrol and the moment at which Player B deploys is sufficiently great that the Markov chain governing Player A's movement around the space could be considered to have converged to its equilibrium distribution. However, this assumption probably does not correspond to many of the real world scenarios that we may wish to model. A genuine patrol (for example, of security officers protecting an airport from potential terrorist activity) may need to start afresh each day or to allow for the rotation of personnel. While it would in theory be possible to restart a patrol from the point at which it was halted after such a disruption, or to randomise the starting point in line with the probabilities of the equilibrium distribution, in many cases this may not be practical. To model such situations effectively, alterations would need to be made to the ways in which the GPG is defined and analysed.

The assumption that Player B only has access to information about the patrol strategy, rather than about the precise location of Player A at any particular time prior to Player B's deployment, is also problematic. In cases in which the expected time required to get from one point of the patrol (vertex v_1 , say) to another (vertex v_2) is large, observing that Player A is at v_1 at time t_1 might allow Player B to deploy safely at v_2 at some later time t_2 . Concerns of this nature could potentially be addressed through careful tuning of the optimisation procedure discussed in Section 10.4.5. Including terms relating to the maximum expected travel-time between pairs of vertices in the objective function could allow vulnerabilities of this nature to be mitigated.

11.3 Directions for further research

11.3.1 Research scope

Some potential directions for future research were suggested in Section 11.2, with the goal of addressing specific limitations of our results and methodology. In this section, we present further suggestions to develop, extend and build on the work presented in this thesis.

One potential starting point for further work would be to extend the scope of our investigation to consider more detailed and sophisticated models. As we have remarked, both the IBMs of Part II and the game theoretic models of Part III were specifically chosen to be very simple, owing to the theoretical nature of the research objectives we have sought to study (see Section 1.5). However, most models used to represent real world systems involve significantly more detail than those considered here. Therefore, to accurately gauge the scope and relevance of our conclusions, and to fully understand the extent to which we have successfully addressed our objectives, it would be useful to consider a broader range of models.

In the case of the IBMs studied in Part II, increasing model detail could simply mean considering \mathfrak{B} -models with more species or over higher dimensional grids. Alternatively, more fundamental enhancements could be made, based around the introduction of some of the agent-based modelling concepts discussed in Section 2.2, such as allowing individuals to choose their actions based on sophisticated goal-oriented decision making procedures or to adapt their behaviour based on past experience. On the other hand, rather than augmenting models that we have already considered, we could expand our investigation to include other ABMs and IBMs from the literature, such as the Schelling model (Schelling, 1971) or some of the many flocking models that have been proposed (see, for example, Mirabet et al., 2007; Chen et al., 2008; Sun, 2013).

Similarly, for the game theoretic models, detail could be enhanced in simple ways, such as by introducing additional players or by allocating multiple units for each player to deploy, as discussed in Section 11.2, or in more complex ways, such as by allowing both players to be mobile or by considering more sophisticated patterns of movement in the patrol game. It may also be of interest to attempt to derive results for games over specific families of graphs, such as regular graphs or scale-free graphs.

In more general terms, for any new model that were to be considered, there are two key questions that should be addressed in relation to the work presented in this

thesis. Firstly, can the methods used to investigate and analyse the simple models treated here be successfully adapted for use with the new model? Secondly, how do the results derived for these simple models relate to the new model and under what conditions (if any) do they hold?

Thinking more broadly, a third question also presents itself: do any of our current results represent general principles, which may have broader implications across a wider range of complex models? A general investigation of these questions, in the context of a more extensive selection of models, would be of vital importance to fully understand the scope and relevance of our work.

Going beyond these considerations, although our IBMs and game theoretic models are quite abstract, as has been discussed, it may nonetheless be of interest to use them to model real systems and to compare the model outputs with reality. For example, a multi-species \mathfrak{B} -model could be used to represent a particular ecosystem, with the values of model parameters calibrated against empirical observations. However, given the level of abstraction of this family of IBMs, such an approach should necessarily be seen strictly as an exploratory investigation of the model itself, rather than as a genuinely informative representation of the system in question. A valid aim would be to determine which aspects of reality the \mathfrak{B} -model is able to replicate and which it is not, in order to inform the development of more realistic models.

Despite its simplicity, in its current form, the SSSG is perhaps better suited to direct application than the \mathfrak{B} -model IBMs. For example, following the riots in England in the summer of 2011, the game could be used to examine possible deployment strategies for the police. To take a specific case, Manchester city centre, where a number of incidents occurred over a relatively compact area (Rogers et al., 2011), could be represented as a graph and OMSs could be sought to determine the best location for a police unit (the searching player) to protect retail centres from a band of rioters (the concealing player). Potential adaptations to the SSSG, which could allow for the consideration of multiple police or rioter units were discussed briefly in Section 11.2.4.

11.3.2 Extensions to the work on individual-based modelling

Moving on to some more specific suggestions for further research, given its role as an exemplar for the communication and visualisation of ABMs (see Section 4.2.1), a more detailed study of the basic NANIA predator-prey model would be of interest. Although a theoretical correspondence between this model and the Lotka-Volterra equations was demonstrated in Section 4.3.4, it would be instructive to know under

what conditions and to what extent the behaviour of the NANIA model is well represented by both these equations and by its corresponding, spatially explicit, mean field PDE model (see Section 3.2.4).

An interesting research question relating both to the NANIA model and to \mathfrak{B} -models more generally would be to investigate the possibility of using time series observations of the models to identify situations in which one or more species in a system is at risk of becoming extinct. From informal experimentation, we have observed that, for certain choices of the model parameters, the underlying graph and the initial conditions, the NANIA model can display Lotka-Volterra-like coupled population oscillations that appear to be stable over many thousands of iterations (see, for example, Figure 4.5), but which are nonetheless subject to rare stochastic extinctions. Reliable methods for predicting such extinctions through examination of current and past system states, both in the NANIA model and in other \mathfrak{B} -models, would represent a step forward in the understanding and control of such systems, with potential implications for mathematical modelling in the field of conservation. It would be particularly useful if methods were also sought to suggest interventions (the introduction of a group of individuals at a particular location, for example) that could “nudge” a system containing a species at risk of extinction back to a more secure region of its phase space.

Some exploratory work on this question, which has not been included in this thesis, used image recognition techniques and machine learning (specifically, linear principal component analysis (see Sahani, 2013) and support vector machines (see Yang et al., 2007; Steinwart and Christmann, 2008)), achieving some limited success in predicting extinctions in the NANIA model through consideration of the densities of the prey and predator prey species only. Further work would be required to determine whether additional spatial information might be incorporated to improve prediction performance.

The main focus of Part II was on understanding the relationship between the behaviour of one-dimensional single species \mathfrak{B} -models and that of corresponding mean field ODE models, in line with the first of the research objectives stated in Section 1.5. However, this issue was examined exclusively through a comparison of the predicted mean field equilibrium population density with the observed noisy equilibrium of the \mathfrak{B} -model. To address the objective in greater depth, it would also be necessary to investigate the manner in which these equilibria were attained. For example, if, for some set of parameters, the equilibrium density predicted by the mean field equation and the observed noisy equilibrium of the corresponding

\mathfrak{B} -model were equal, but one of the two models approached this equilibrium directly, while the other exhibited oscillations that decayed to the equilibrium, this might indicate a fundamental difference between the two representations that would not be identified by our current analysis. A more detailed consideration of this issue would complement the conclusions presented in Part II.

As a final note on our work on IBMs, we would reiterate the contention that \mathfrak{B} -models (and the broader class of \mathfrak{A} -models) could be considered to represent a fundamental family of discrete space-time stochastic IBMs, which has seen relatively little theoretical study. It is our belief that further work on the foundations and features of such models could have implications for many more complicated systems with which these models share key characteristics. The simplicity of these models and their discrete nature combine to make them potentially significantly more tractable than many more widely studied IBMs, meaning that they could form an ideal “sandpit of complexity”, in which to examine key concepts such as emergence and self-organisation.

11.3.3 Extensions to the work on game theoretic modelling

Regarding future research directions for the SSSG, it would be desirable to develop more results for the most general version of the game, played over a metric space. The majority of the work presented in Part III relates to the simpler case of the GSG, where the game is played over a graph. However, results on the optimal strategies of a metric space version of the game would potentially be of more value, since they would allow for the modelling of a wider variety of real world environments. A particular area of interest is the analysis of games in which Ω is a region of \mathbb{R}^2 , where the searching player can search a disc of radius r . An understanding of such cases would make the game more applicable in real operational research scenarios, such as the deployment of patrol ships to locate pirates over areas of the ocean or searching archaeological sites for features of historical interest.

A possible starting point for research on metric space games would be the reformulation of some of our graph specific results to apply in the more general case. It may be possible to formulate analogues of many of these results for games over metric spaces through the careful application of topology and measure theory. This would be an important first step in increasing the applicability and relevance of the SSSG.

However, since general results for games over metric spaces may prove elusive, it would be useful to derive results for the OMSs of games played over rectangular grids (or indeed over graphs based on other regular tessellations in the plane), or of

graphs formed from multiple connected grid-like components. Lattices such as these could potentially be overlaid on maps of geographical regions, thus enhancing the potential applicability of games played over such graphs and the consequent importance of any general strategic results derived for them.

In the case of regular lattices, it may be possible to produce analytic expressions for their OMSs by extending the ideas used to analyse games played over poly-level graphs. However, for large, irregularly shaped graphs or graphs formed from connected segments of lattices, it seems likely that developing improved algorithms for the approximation of OMSs, rather than searching for exact solutions, may be the only realistic way forward.

One possibility would be to seek algorithmic methods for the identification of equal oddments strategies. Even where equal oddments strategies do not exist, it may nonetheless be possible to find an equal oddments ‘distribution’: a distribution of real numbers over the vertices of a graph, which satisfies condition (9.10) of Definition 9.3.5 (the “neighbourhood sum” condition), but which does not necessarily define a valid probability distribution. An investigation into the connection between the true OMSs and these invalid equal oddments distributions may be instructive.

With regard to the algorithm of Section 9.2, it would be useful to have explicit results on its computational efficiency and on how the structure of a graph affects the extent to which a corresponding GSG can be simplified using IEDS. It may be possible, for example, to identify other families of GSGs (aside from those played on trees) for which the method is particularly effective.

With regard to the representation of geographical spaces, it would also be interesting to know to what extent (if at all) the OMSs of games played over continuous metric spaces matched the OMSs of games played over discretised versions of these spaces, such as grid graphs. Such results would indicate whether or not the discretisation of a continuous geographical region may be a valid approach for determining good strategies for a search and concealment game played over that space.

A simpler method for extending the scope of the SSSG would be to relax certain of the metric space axioms (as discussed in Section 8.2.1), to consider spaces in which distance is not symmetric (i.e. where the distance from x to y is not necessarily the same as the distance from y to x), as in directed graphs, or spaces in which the distance between two points may be infinite, as in disconnected graphs. However, it

is not clear to what extent such versions of the game would be relevant to any real scenarios that we may wish to model.

Moving on to the GPG of Chapter 10, observe that none of the methods or analyses presented there necessarily require that the adjacency matrix \mathfrak{M} of the corresponding EGSG and the adjacency matrix used to determine permissible patrol strategies in the GPG should be the same. In other words, it would be possible to consider a game in which the adjacencies used to determine whether or not Player A successfully intercepts Player B and the adjacencies used to determine how Player A was able to move around the space were defined differently. Consideration of such situations would add an additional degree of flexibility to the GPG, which may be worthy of further attention.

Clearly though, one of the most pressing unresolved questions of the thesis is how to find solutions to the optimisation problem outlined in Section 10.4.5, which aims to identify particular optimal strategies of the GPG. For this game to be of value as a modelling tool, it would be necessary to identify some approaches by which solutions to this problem might be identified. However, the nonlinear nature of the objective function $\mathcal{Z}[T_A]$ and particularly of the constraint $T_A\pi[T_A] = \pi[T_A]$, suggest that these optimisations may be extremely difficult to solve (see footnote 4, p. 328). A deeper investigation of this problem would therefore be a valuable focus for future work.

Finally, in relation to all the work in Part III, it must be remembered that when games are used to model real world scenarios, employing a mathematically optimal strategy is not necessarily the best course of action. This is because the assumption that other players will themselves employ optimal strategies may well not be appropriate. Human beings often do not use mathematically optimal strategies, whether because they fail to identify them, because they do not have complete knowledge of their situation, because they are incapable of the randomness required to effectively implement a mixed strategy, or because they expect their fellow players to act in a particular (suboptimal) way.

In game theoretic scenarios, when an opponent is using a suboptimal strategy, employing an OMS will not generally guarantee the largest possible expected payoff. For this reason, with all of the games that we have proposed, it may be valuable to undertake experiments to determine common characteristics of strategies that human players might employ if they were actually required to play the game. This process would involve enlisting human subjects to play selected spatial games, ei-

ther once or many times (possibly via a website), and recording and comparing the results. This would allow for the calculation of “super-optimal” mixed strategies, or algorithms for creating such strategies, which could then be tested against further human subjects.

11.3.4 Synthesis of the two modelling perspectives

Throughout this thesis, the two perspectives that we have considered – treating individuals in spatially explicit multi-agent systems as simple automata or treating them as decision-making entities – have largely been examined separately. We now present a brief discussion of how the two approaches might be brought together.

Firstly, as we observed in the introduction (see, in particular, Figure 1.1), for the majority of the work in this thesis, both in Part II, based around individual-based modelling, and Part III, based on game theory, space is modelled as a graph, with individuals occupying particular vertices. In both \mathfrak{B} -models and GSGs, the structure of this graph is of critical importance, because whether or not two individuals may interact is determined purely on the basis of whether their vertices are adjacent.

Consider the basic NANIA predator-prey model, which was defined in Section 4.2. In this \mathfrak{B} -model, there are two species: prey, which may reproduce if they are adjacent to an empty cell, and predators, which may reproduce if they are adjacent to a cell containing a prey individual (the prey individual is consumed).

Now, under our first perspective, individuals are treated as stochastic automata. They do not choose their actions to advance towards any particular goal, but merely act according to predetermined probabilities. However, if we were to enhance the model to incorporate goal-oriented decision making, as discussed in Section 11.3, it would be reasonable to specify that these individuals should act so as to attempt to maximise their chances of survival and reproduction.

Given these goals, predators would like to be positioned such that their local neighbourhood contains a prey individual, while prey would like to be positioned such that their local neighbourhood does not contain any predator individuals (and such that it contains a large number of empty cells, into which they might reproduce). If predator and prey individuals were to be given control over their direction of movement, they would be free to make strategic decisions about how to move so as to achieve such positions.

Note that the positional aims of the predators and the prey correspond closely to those of the searching and hiding players respectively in the GSG. We might therefore conjecture that the OMSs for each player of a GSG played over the underlying graph of this NANIA model may provide valuable information about how the predators and prey should move through the space to maximise their reproductive success, in this goal-oriented version of the NANIA model. More specifically, a good strategy for the predators may be to move according to an optimal strategy (for Player A) of the corresponding patrol game over this graph.

Such a correspondence between our two modelling perspectives could have broader implications for the way in which goal-oriented agents should behave in spatially explicit systems driven by local interactions. If a link of this nature were identified between these modelling approaches, then the OMSs of the GSG could potentially be thought of as strategic maps of the space, indicating the most tactically advantageous points for each player. However, a deeper investigation would be necessary to determine whether it would be valuable to combine our two perspectives in this way.

11.4 Concluding remarks

In this thesis, we have examined two different perspectives on the relationship between local interactions and global outcomes in systems of interacting individuals. Our first perspective involved considering individuals as simple stochastic automata, using individual-based modelling to examine and identify the causal mechanisms linking local events and global dynamics in a particular family of models. Our second perspective involved considering individuals as sophisticated decision-making agents, using game theory to model situations of search and concealment and deriving results on the OMSs of the resulting games in a variety of contexts.

Through these investigations, we have gone some way towards addressing the research objectives set out in Section 1.5, building understanding of the links between the local and global dynamical scales in IBMs and formulating a general game for the analysis of spatial search and concealment scenarios. However, as discussed in Sections 11.2-11.3, there is a good deal more work to be done in these areas, both in terms of broadening the scope of work on the dynamics of IBMs and producing further theoretical results on the OMSs of spatial games, but also on the far larger question of developing a unified mathematical theory of agent-based and individual-based modelling, an issue that was discussed in detail in Section 2.2.8.

It is to be hoped that the work presented in this thesis may provide a basis for further research in these directions, along the lines set out in the preceding sections. In any case, we conclude by reiterating our belief that, given their widespread use as research tools across the social sciences and beyond, the goal of constructing a solid theoretical foundation for models of systems of interacting individuals is of vital importance to ensure that future researchers can have complete confidence in the results and conclusions drawn from such models.

Acknowledgements

I would like to thank the following people for their help, information, support, guidance and inspiration (in various combinations):

Prof. Graeme Ackland	Dr. Elsa Arcaute	Dennis Barnett
Dr. Peter Baudains	Janina Beiser	Prof. Steven Bishop
Prof. Immanuel Bomze	Prof. Mark Broom	Clare Crabb
Russell T. Davies	Dr. Toby Davies	Dr. Adam Dennett
Dr. Rob Downes	Catherine Evans	Emily Evans
Gareth Evans	Sydney Evans	Thelma Evans
Dr. Hannah Fry	Steven Gray	Helen Griffiths
William Hawkins	Winifred Hawkins	Dr. Peter Kent
Dr. Anthony Korte	Verity Lambert	Rob Levy
Dr. Emilie Oléron Evans	Prof. Frank Smith	Elizabeth Swan
Dr. John Talbot	Joss Whedon	Dr. Lynda White
Prof. Sir Alan Wilson	Julie Woodhouse	Dr. Martin Zaltz Austwick

I would also like to thank the anonymous reviewers of Oléron Evans and Bishop (2013) and Oléron Evans and Bishop (2014), the Centre for Advanced Spatial Analysis (CASA) and the Department of Mathematics at University College London and the UK Engineering and Physical Sciences Research Council (EPSRC), for its financial support under the grant ENFOLD-ing - Explaining, Modelling, and Forecasting Global Dynamics (reference EP/H02185X/1).

Bibliography

- Ackland, G. J., Jul 2008. “Lotka-Volterra: the classic predator-prey model” (Course notes), *Mathematical and Spatial Modelling of Ecology*, School of Physics, University of Edinburgh. Available at: http://www2.ph.ed.ac.uk/~gja/MEID_NANIA.pdf [Accessed: 10 Feb 2015].
- Ackland, G. J. (uncredited), 2009. “Lotka-Volterra dynamics”, NANIA Project. Available at: <https://web.archive.org/web/20120722125154/http://www2.ph.ed.ac.uk/nania/lv/lv.html> [Accessed: 06 Feb 2015].
- Alonso, D., McKane, A., Sep 2002. Extinction dynamics in mainland-island metapopulations: An N-patch stochastic model. *Bulletin of Mathematical Biology* 64 (5), 913–958.
- Alpern, S., 1974. The search game with mobile hider on the circle. *Proceedings of the Conference on Differential Games and Control Theory, 1973*. In: Roxin, E. O., Liu, T. P., Sternberg, R. L. (Eds.), *Differential Games and Control Theory*. Dekker, New York, USA, 181–200.
- Alpern, S., Nov 1985. Search for point in interval, with high-low feedback. *Mathematical Proceedings of the Cambridge Philosophical Society* 98 (3), 569–578.
- Alpern, S., Jan 1992. Infiltration games on arbitrary graphs. *Journal of Mathematical Analysis and Applications* 163 (1), 286–288.
- Alpern, S., May 1995. The rendezvous search problem. *SIAM Journal on Control and Optimization* 33 (3), 673–683.
- Alpern, S., Jan 2000. Asymmetric rendezvous search on the circle. *Dynamics and Control* 10 (1), 33–45.
- Alpern, S., Sep 2002. Rendezvous search: A personal perspective. *Operations Research* 50 (5), 772–795.
- Alpern, S., Oct 2008. Hide-and-seek games on a tree to which Eulerian networks are attached. *Networks* 52 (3), 162–166.

- Alpern, S., Sep 2010. Search games on trees with asymmetric travel times. SIAM Journal on Control and Optimization 48 (8), 5547–5563.
- Alpern, S., Asic, M., Jun 1985. The search value of a network. Networks 15 (2), 229–238.
- Alpern, S., Asic, M., Jan 1986. Ambush strategies in search games on graphs. SIAM Journal on Control and Optimization 24 (1), 66–75.
- Alpern, S., Baston, V., Gal, S., Jun 2008a. Network search games with immobile hider, without a designated searcher starting point. International Journal of Game Theory 37 (2), 281–302.
- Alpern, S., Baston, V. J., Nov 2005. Rendezvous on a planar lattice. Operations Research 53 (6), 996–1006.
- Alpern, S., Baston, V. J., Essegaeir, S., Mar 1999. Rendezvous search on a graph. Journal of Applied Probability 36 (1), 223–231.
- Alpern, S., Baston, V. J., Gal, S., Jul 2009. Searching symmetric networks with utilitarian-postman paths. Networks 53 (4), 392–402.
- Alpern, S., Beck, A., May 2000. Pure strategy asymmetric rendezvous on the line with an unknown initial distance. Operations Research 48 (3), 498–501.
- Alpern, S., Fokkink, R., Kikuta, K., 2010. On Ruckle’s conjecture on accumulation games. SIAM Journal on Control and Optimization 48 (8), 5073–5083.
- Alpern, S., Fokkink, R., Lindelauf, R., Olsder, G.-J., Jan 2008b. The “Princess and Monster” game on an interval. SIAM Journal on Control and Optimization 47 (3), 1178–1190.
- Alpern, S., Fokkink, R., Timmer, M., Casas, J., Nov 2011a. Ambush frequency should increase over time during optimal predator search for prey. Journal of the Royal Society Interface 8 (64), 1665–1672.
- Alpern, S., Gal, S., Jul 1995. Rendezvous search on the line with distinguishable players. SIAM Journal on Control and Optimization 33 (4), 1270–1276.
- Alpern, S., Gal, S., Mar 2002. Searching for an agent who may or may not want to be found. Operations Research 50 (2), 311–323.
- Alpern, S., Howard, J. V., Dec 2000. Alternating search at two locations. Dynamics and Control 10 (4), 319–339.

- Alpern, S., Lim, W. S., May 1998. The symmetric rendezvous-evasion game. SIAM Journal on Control and Optimization 36 (3), 948–959.
- Alpern, S., Morton, A., Papadaki, K., Sep 2011b. Patrolling games. Operations Research 59 (5), 1246–1257.
- Alpern, S., Reyniers, D. J., Dec 1994. The rendezvous and coordinated search problems. In: Peshkin, M. (Ed.), Proceedings of the 33rd IEEE Conference on Decision and Control. Vol. 1. IEEE Control Systems Society, Lake Buena Vista, USA, 513–517.
- Amouroux, E., Desvaux, S., Drogoul, A., 2008. Towards virtual epidemiology: An agent-based approach to the modelling of H5N1 propagation and persistence in North-Vietnam. In: Bui, T. D., Ho, T. V., Ha, Q. T. (Eds.), Intelligent Agents and Multi-Agent Systems. No. 5357 in Lecture Notes in Artificial Intelligence. Pacific Rim International Conference on Multi-Agents, Springer, Berlin, Germany, 26–33.
- Anderson, E. J., Aramendia, M. A., Dec 1990. The search game on a network with immobile hider. Networks 20 (7), 817–844.
- Anderson, E. J., Aramendia, M. A., May 1992. A linear programming approach to the search game on a network with mobile hider. SIAM Journal on Control and Optimization 30 (3), 675–694.
- Argonne National Laboratory, 2013. The Repast Suite. Available at: <http://repast.sourceforge.net>.
- Arnold, R. D., Jan 1962. Avoidance in one dimension: a continuous-matrix game. Interim Research Memorandum - 10 277843, Operations Evaluation Group, Washington D. C., USA.
- Bak, P., Tang, C., Wiesenfeld, K., Jul 1987. Self-organized criticality: An explanation of $1/f$ noise. Physical Review Letters 59 (4), 381–384.
- Basilico, N., Gatti, N., Amigoni, F., Jun 2012. Patrolling security games: Definition and algorithms for solving large instances with single patroller and single intruder. Artificial Intelligence 184, 78–123.
- Baston, V. J., Bostock, F. A., Mar 1985. A high-low search game on the unit interval. Mathematical Proceedings of the Cambridge Philosophical Society 97 (2), 345–348.
- Baston, V. J., Bostock, F. A., Ferguson, T. S., Oct 1989. The number hides game. Proceedings of the American Mathematical Society 107 (2), 437–447.

- Baston, V. J., Garnaev, A. Y., Mar 2000. A search game with a protector. *Naval Research Logistics* 47 (2), 85–96.
- Bellomo, N., Bianca, C., Delitala, M., Sep 2009. Complexity analysis and mathematical tools towards the modelling of living systems. *Physics of Life Reviews* 6 (3), 144–175.
- Bellomo, N., Bianca, C., Mongiovì, M. S., Nov 2010. On the modeling of nonlinear interactions in large complex systems. *Applied Mathematics Letters* 23 (11), 1372–1377.
- Berwanger, D., 2007. Admissibility in infinite games. In: Thomas, W., Weil, P. (Eds.), STACS 2007. Vol. 4393 of Lecture Notes in Computer Science. Springer, Berlin, Germany, 188–199.
- Blackwell, D., Girshick, M. A., 1979. Theory of Games and Statistical Decisions [Reprint of 1954 original]. Dover Publications, New York, USA.
- Bondy, J. A., Murty, U. S. R., 1976. Graph Theory with Applications. Macmillan Press, London, UK.
- Bordelon, D. J., May 1975. Solutions of elementary problems - E 2469 - Editor's comment. *The American Mathematical Monthly* 82 (5), 522.
- Börgers, T., Jan 1992. Iterated elimination of dominated strategies in a Bertrand-Edgeworth model. *Review of Economic Studies* 59 (1), 163–176.
- Buhr, R. J. A., Oct 1996. Understanding large-scale behaviour patterns in complex systems. In: Proceedings: Second IEEE International Conference on Engineering of Complex Computer Systems. Institute of Electrical and Electronics Engineers, 143–146.
- Buyang, C., Jan 1995. Search-hide games on trees. *European Journal of Operational Research* 80 (1), 175–183.
- Cannas, S. A., Marco, D. E., Páez, S. A., May 2003. Modelling biological invasions: species traits, species interactions, and habitat heterogeneity. *Mathematical Biosciences* 183 (1), 93–110.
- Caron-Lormier, G., Humphry, R. W., Bohan, D. A., Hawes, C., Thorbek, P., Apr 2008. Asynchronous and synchronous updating in individual-based models. *Eco-logical Modelling* 212 (3-4), 522–527.
- Cartwright, J. H. E., May 2010. Agent-based social simulation: A dynamical systems viewpoint. *Cybernetics and Systems* 41 (4), 281–286.

- CASA, 2015. Centre for Advanced Spacial Analysis. The Bartlett, University College London. London, UK. Website. <http://www.bartlett.ucl.ac.uk/casa> [Accessed: 09 Mar 2015].
- Chen, S., Zhao, L., Han, Y., Feb 2008. Multi-agent aggregation behavior analysis: the dynamic communication topology. *Journal of Systems Science and Complexity* 21 (2), 209–216.
- Chkhartishvili, A. G., Shikin, E. V., Nov 1995. Simple search games on an infinite circular cylinder. *Mathematical Notes* 58 (5), 1216–1222.
- Clauset, A., Shalizi, C. R., Newman, M. E. J., Dec 2009. Power-law distributions in empirical data. *SIAM Review* 51 (4), 661–703.
- Cohen, N. D., Aug 1966. An attack-defense game with matrix strategies. *Naval Research Logistics Quarterly* 13 (4), 391–402.
- Cosner, C., Lazer, A. C., Dec 1984. Stable coexistence states in the Volterra-Lotka competition model with diffusion. *SIAM Journal on Applied Mathematics* 44 (6), 1112–1132.
- Cotar, C., Nov-Dec 2012. “Stochastic Processes” (Lecture course), London Taught Course Centre (LTCC); www.ltcc.ac.uk.
- Craven, B. D., 1982. Lebesgue Measure and Integral, 1st Edition. Pitman, Marshfield, USA.
- Dagan, A., Gal, S., Oct 2008. Network search games, with arbitrary searcher starting point. *Networks* 52 (3), 156–161.
- Danskin, J. M., Nov 1990. On the cookie-cutter game - search and evasion on a disk. *Mathematics of Operational Research* 15 (4), 573–596.
- De Angelis, E., Delitala, M., Jun 2006. Modelling complex systems in applied sciences; methods and tools of the mathematical kinetic theory for active particles. *Mathematical and Computer Modelling* 43 (11-12), 1310–1328.
- Deffuant, G., Gilbert, N., 2011. Preface. In: Deffuant, G., Gilbert, N. (Eds.), *Viability and Resilience of Complex Systems: Concepts, Methods and Case Studies from Ecology and Society. Understanding Complex Systems*. Springer, Berlin, Germany, v–viii.
- Dendris, N. D., Kirousis, L. M., Thilikos, D. M., Feb 1997. Fugitive-search games on graphs and related parameters. *Theoretical Computer Science* 172 (1), 233–254.

Department of Mathematics, 2015. Faculty of Mathematical and Physical Sciences, University College London. London, UK. Website. <http://www.ucl.ac.uk/math> [Accessed: 09 Mar 2015].

Drogoul, A., 2008. Keynote speech: A review of the ontological status, computational foundations and methodological processes of agent-based modeling and simulation approaches: Open challenges and research perspectives. In: Bui, T. D., Ho, T. V., Ha, Q. T. (Eds.), Intelligent Agents and Multi-Agent Systems. No. 5357 in Lecture Notes in Artificial Intelligence. Pacific Rim International Conference on Multi-Agents, Springer, Berlin, Germany, 1.

Drossel, B., Schwabl, F., Sep 1992. Self-organized critical forest-fire model. *Physical Review Letters* 69 (1), 1629–1632.

Dufwenberg, M., Stegeman, M., Sep 2002. Existence and uniqueness of maximal reductions under iterated strict dominance. *Econometrica* 70 (5), 2007–2023.

Dunstan, P. K., Johnson, C. R., Aug 2005. Predicting global dynamics from local interactions: individual-based models predict complex features of marine epibenthic communities. *Ecological Modelling* 186 (2), 221–233.

Eagle, J. N., Washburn, A. R., Aug 1991. Cumulative search-evasion games. *Naval Research Logistics* 38 (4), 495–510.

Eisinger, D., Thulke, H., Apr 2008. Spatial pattern formation facilitates eradication of infectious diseases. *Journal of Applied Ecology* 45 (2), 415–423.

Eisinger, D., Thulke, H., Selhorst, T., Müller, T., Mar 2005. Emergency vaccination of rabies under limited resources - combating or containing? *BMC Infectious Diseases* 5 (10).

ENFOLD-ing, 2010. Explaining, Modelling, and Forecasting Global Dynamics (EPSRC Grant EP/H02185X/1): Project website. <http://enfolding.blogs.casa.ucl.ac.uk> [Accessed: 03 Mar 2015].

EPSRC, 2015. Engineering and Physical Sciences Research Council. Website. <http://www.epsrc.ac.uk> [Accessed: 04 Mar 2015].

Evans, R., May 1975. Solutions of elementary problems - E 2469: Hide and Seek in the Unit Disk. *The American Mathematical Monthly* 82 (5), 521–522.

Fenichel, E. P., Castillo-Chavez, C., Cuddia, M. G., Chowell, G., Gonzalez Parra, P. A., Hickling, G. J., Holloway, G., Horan, R., Morin, B., Perrings, C., Springborn, M., Velazquez, L., Villalobos, C., Apr 2011. Adaptive human behavior in

- epidemiological models. *Proceedings of the National Academy of Sciences* 108 (15), 6306–6311.
- Fibich, G., Gibori, R., Sep-Oct 2010. Aggregate diffusion dynamics in agent-based models with a spatial structure. *Operations Research* 58 (5), 1450–1468.
- Foote, R., Oct 2007. Mathematics and complex systems. *Science* 318 (5849), 410–412.
- Foreman, J. G., Aug 1977. Differential search games with mobile hider. *SIAM Journal on Control and Optimization* 15 (5), 841–856.
- Forrest, S., 2014. “Predator-Prey Models” (Course notes), *Introduction to Scientific Modeling*, Department of Computer Science, University of New Mexico. Available at: <https://www.cs.unm.edu/~forrest/classes/cs365/lectures/Lotka-Volterra.pdf> [Accessed: 10 Feb 2015].
- Funk, S., Salathé, M., Jansen, A. A., Sep 2010. Modelling the influence of human behaviour on the spread of infectious diseases: a review. *Journal of the Royal Society Interface* 7 (50), 1247–1256.
- Gal, S., Dec 1974. A discrete search game. *SIAM Journal on Applied Mathematics* 27 (4), 641–648.
- Gal, S., Jan 1978. A stochastic search game. *SIAM Journal on Applied Mathematics* 34 (1), 205–210.
- Gal, S., Jan 1979. Search games with mobile and immobile hider. *SIAM Journal on Control and Optimization* 17 (1), 99–122.
- Gale, D., Glassey, C. R., Apr 1974. Problems and solutions - E 2469. *The American Mathematical Monthly* 81 (4), 405.
- Galli, L., Letchford, A. N., Feb 2015. A binarisation approach to non-convex quadratically constrained quadratic programs [Unpublished]. Submitted to the *Journal of Global Optimization*. Available at: <http://www.lancaster.ac.uk/staff/letchfoa/publications.htm> [Accessed: 09 Mar 2015].
- García-Morales, V., Oct 2013. Origin of complexity and conditional predictability in cellular automata. *Physical Review E* 88 (4), 042814.
- Gardner, M., Oct 1970. Mathematical Games : The fantastic combinations of John Conway’s new solitaire game “life”. *Scientific American* 223 (4), 120–123.

Gardner, M., Feb 1971. Mathematical Games : On cellular automata, self-reproduction, the Garden of Eden and the game “life”. *Scientific American* 224 (2), 112–117.

Garnaev, A. Y., Jun 1991. Search game in a rectangle. *Journal of Optimization Theory and Applications* 69 (3), 531–542.

Garnaev, A. Y., Sep 1992. A remark on the princess and monster search game. *International Journal of Game Theory* 20 (3), 269–276.

Gilbert, N., 2008. Agent-Based Models. No. 153 in Quantitative Applications in the Social Sciences. SAGE Publications, Thousand Oaks, USA.

Gómez-Mourela, P., Oct 2005. From individual-based models to partial differential equations: An application to the upstream movement of elvers. *Ecological Modelling* 188 (1), 93–111.

Grimm, V., Berger, U., Bastiansen, F., Eliassen, S., Ginot, V., Giske, J., Goss-Custard, J., Grand, T., Heinz, S. K., Huse, G., Huth, A., Jepsen, J. U., Jørgensen, C., Mooij, W. M., Müller, B., Pe'er, G., Piou, C., Railsback, S. F., Robbins, A. M., Robbins, M. M., Rossmanith, E., Rüger, N., Strand, E., Souissi, S., Stillman, R. A., Vabø, R., Visser, U., DeAngelis, D. L., Sep 2006. A standard protocol for describing individual-based and agent-based models. *Ecological Modelling* 198 (1-2), 115–126.

Grimm, V., Berger, U., DeAngelis, D. L., Polhill, G., Giske, J., Railsback, S. F., Nov 2010. The ODD protocol: A review and first update. *Ecological Modelling* 221 (23), 2760–2768.

Grimmet, G., Stirzaker, D., 2001. Probability and Random Processes, 3rd Edition. Oxford University Press, Oxford, UK.

Grometstein, A. A., Shoham, D., Jul 1989. Colonel Richard’s game. *The Lincoln Laboratory Journal* 2 (2), 235–246.

Hare, M., Deadman, P., Jan 2004. Further towards a taxonomy of agent-based simulation models in environmental management. *Mathematics and Computers in Simulation* 64 (1), 25–40.

Hartman, C., Heule, M. J. H., Kwekkeboom, K., Noels, A., Aug 2013. Symmetry in Gardens of Eden. *The Electronic Journal of Combinatorics* 20 (3), P16.

Hatzikirou, H., Brusch, L., Schaller, C., Simon, M., Deutsch, A., Apr 2010. Prediction of traveling front behavior in a lattice-gas cellular automaton model for tumor invasion. *Computers and Mathematics with Applications* 59 (7), 2326–2339.

- Hausken, K., Jan 2010. Defense and attack of complex and dependent systems. *Reliability Engineering & System Safety* 95 (1), 29–42.
- Hausken, K., Jan 2011. Protecting complex infrastructures against multiple strategic attackers. *International Journal of Systems Science* 42 (1), 11–29.
- He, M., Ruan, H., Yu, C., Nov 2003. A predator-prey model based on the fully parallel cellular automata. *International Journal of Modern Physics C* 14 (9), 1237–1249.
- He, S., 2013. “Modelling with cellular automata” (Course notes), *Computational Modelling with MATLAB*, School for Computational Science, University of Birmingham. Available at: http://www.cs.bham.ac.uk/~szh/teaching/2013backup/matlabmodeling/Lecture12_body_CellularAutomata.pdf [Accessed: 10 Feb 2015].
- Hinkelmann, F., Murrugarra, D., Salam Jarrah, A., Laubenbacher, R., Jul 2011. A mathematical framework for agent based models of complex biological networks. *Bulletin of Mathematical Biology* 73 (7), 1583–1602.
- Hogeweg, P., Jul 1988. Cellular automata as a paradigm for ecological modeling. *Bioinformatics* 27 (1), 81–100.
- Hohzaki, R., Feb 2007. Discrete search allocation game with false contacts. *Naval Research Logistics* 54 (1), 46–58.
- Hohzaki, R., Feb 2008. A search game taking account of attributes of searching resources. *Naval Research Logistics* 55 (1), 76–90.
- Hohzaki, R., Feb 2009. A cooperative game in search theory. *Naval Research Logistics* 56 (3), 264–278.
- Hohzaki, R., Iida, K., Jul 2000. A search game when a search path is given. *European Journal of Operational Research* 124 (1), 114–124.
- Holland, J. H., Jul 1992. Genetic algorithms. *Scientific American* 267 (1), 66–72.
- Hortala-Vallve, R., Llorente-Saguer, A., May 2012. Pure strategy Nash equilibria in non-zero sum Colonel Blotto games. *International Journal of Game Theory* 41 (2), 331–343.
- Hübler, A. W., Jan-Feb 2005. Predicting complex systems with a holistic approach. *Complexity* 10 (3), 11–16.
- Hübler, A. W., May 2007. Understanding complex systems. *Complexity* 12 (5), 9–11.

- Huet, S., Deffuant, G., Mar 2008. Differential equation models derived from an individual-based model can help to understand emergent effects. *Journal of Artificial Societies and Social Simulation* 11 (2).
- Idkowiak, L., Komosinski, M., 2014. “Predators and Prey: the Lotka-Volterra model”. Life Modeling Simulation. Available at: <http://en.alife.pl/predators-and-prey-the-Lotka-Volterra-model> [Accessed: 06 Feb 2015].
- Internet Archive, 1996. <https://archive.org> [Accessed: 06 Feb 2015].
- Itakura, J., Kurosaki, M., Itakura, Y., Maekawa, S., Asahina, Y., Izumi, N., Enomoto, N., Jan 2010. Reproducibility and usability of chronic virus infection model using agent-based simulation; comparing with a mathematical model. *Biosystems* 99 (1), 70–78.
- Itami, R. M., Oct 1994. Simulating spatial dynamics: cellular automata theory. *Landscape and Urban Planning* 30 (1-2), 27–47.
- Janssen, M. A., Walker, B. H., Langridge, J., Abel, N., Jul 2000. An adaptive agent model for analysing co-evolution of management and policies in a complex rangeland system. *Ecological Modelling* 131 (2-3), 249–268.
- Jeltsch, R., Müller, M. S., Grimm, V., Wissel, C., Brandl, R., Apr 1997. Pattern formation triggered by rare events: Lessons from the spread of rabies. *Proceedings: Biological Sciences* 264 (1381), 495–503.
- Kikuta, K., Oct 2004. A search game on a cyclic graph. *Naval Research Logistics* 51 (7), 977–993.
- Kikuta, K., Ruckle, W. H., Oct 1994. Initial point search on weighted trees. *Naval Research Logistics* 41 (6), 821–831.
- Kikuta, K., Ruckle, W. H., Aug 1997. Accumulation games, part 1: Noisy search. *Journal of Optimization Theory and Applications* 94 (2), 395–408.
- Kikuta, K., Ruckle, W. H., Feb 2002. Continuous accumulation games on discrete locations. *Naval Research Logistics* 49 (1), 60–77.
- Kikuta, K., Ruckle, W. H., Aug 2007. Rendezvous search on a star graph with examination costs. *European Journal of Operational Research* 181 (1), 298–304.
- Kikuta, K., Ruckle, W. H., Nov 2010. Two point one sided rendezvous. *European Journal of Operational Research* 207 (1), 78–82.

- Lam, Y. H., Alhashmi, S. M., 2008. Simulation of halal food supply chain with certification system: A multi-agent system approach. In: Bui, T. D., Ho, T. V., Ha, Q. T. (Eds.), Intelligent Agents and Multi-Agent Systems. No. 5357 in Lecture Notes in Artificial Intelligence. Pacific Rim International Conference on Multi-Agents, Springer, Berlin, Germany, 259–266.
- Lewis, R. J., Sep 2007. Modeling complex systems: Gaining valid insights and avoiding mathematical delusions. *Academic Emergency Medicine* 14 (9), 795–798.
- Leyton-Brown, K., Shoham, Y., 2008. Essentials of game theory: A concise, multidisciplinary introduction. Synthesis Lectures on Artificial Intelligence and Machine Learning. Morgan & Claypool, San Rafael, USA.
- Lim, W. S., Alpern, S., Sep 1996. Minimax rendezvous on the line. *SIAM Journal on Control and Optimization* 34 (5), 1650–1665.
- Lipsitz, L. A., Jul 2012. Understanding health care as a complex system: The foundation for unintended consequences. *Journal of the American Medical Association* 308 (3), 243–244.
- Lotka, A. J., Aug 1920. Undamped oscillations derived from the law of mass action. *Journal of the American Chemical Society* 42 (8), 1595–1599.
- Luck, M., d'Inverno, M., Fisher, M., FOMAS'97 Contributors, Sep 1998. Foundations of multi-agent systems: Techniques, tools and theory. *The Knowledge Engineering Review* 13 (3), 297–302.
- Macal, C. M., Dec 2010. To agent-based simulation from system dynamics. In: Johansson, B., Jain, S., Montoya-Torres, J., Hugan, J., Yücesan, E. (Eds.), Proceedings of the 2010 Winter Simulation Conference. Institute of Electrical and Electronics Engineers, New York, USA, 371–382.
- Marion, G. (Principal Investigator), 2004. Novel Approaches to Networks of Interacting Autonomes (EPSRC Grant GR/T11777/01): Application summary. Available at: <http://gow.epsrc.ac.uk/NGBOViewGrant.aspx?GrantRef=GR/T11777/01> [Accessed: 08 Sep 2014].
- Mavronikolas, M., Papadopoulou, V., Philippou, A., Spirakis, P., Jul 2008. A network game with attackers and a defender. *Algorithmica* 51 (3), 315–341.
- McBurney, P., Omicini, A., May 2008. Editorial: Special issue on foundations, advanced topics and industrial perspectives of multi-agent systems. *Autonomous Agents and Multi-Agent Systems* 17 (3), 367–371.

- McKane, A. J., Newman, T. J., Oct 2004. Stochastic models in population biology and their deterministic analogs. *Physical Review E* 70 (4), 041902.
- McLaughlin, J. F., Roughgarden, J., Oct 1991. Pattern and stability in predator-prey communities: How diffusion in spatially variable environments affects the Lotka-Volterra model. *Theoretical Population Biology* 40 (2), 148–172.
- Meloni, S., Perra, N., Arenas, A., Gómez, S., Moreno, Y., Vespignani, A., Aug 2011. Modeling human mobility responses to the large-scale spreading of infectious diseases. *Scientific Reports* 1, 00062.
- Mirabet, V., Auger, P., Lett, C., Mar 2007. Spatial structures in simulations of animal grouping. *Ecological Modelling* 201 (3-4), 468–476.
- Mock, K. J., Ward Testa, J., Taylor, C., Koyuk, H., Coyle, J., Waggoner, R., Newman, K., May 2007. Final report: An agent-based model of predator-prey relationships between transient killer whales and other marine mammals. National Marine Mammal Laboratory [online]. Available at: <http://www.math.uaa.alaska.edu/~orca/> [Accessed: 03 Mar 2015].
- Morris, P., 1994. Introduction to Game Theory. Universitext. Springer, New York, USA.
- Murray, J. D., 1993. Mathematical Biology, 2nd Edition. Vol. 19 of Biomathematics Texts. Springer, Berlin, Germany.
- NANIA, 2009. Novel Approaches to Networks of Interacting Autonomes (EPSRC Grant GR/T11777/01): Project website. www2.ph.ed.ac.uk/nania [Accessed: 12 Apr 2013].
- Neumann, P. M., Stoy, G. A., Thompson, E. C., 1994. Groups and Geometry. Oxford Science Publications. Oxford University Press, Oxford, UK.
- Neuts, M. F., Jun 1963. A multistage search game. *Journal of the Society for Industrial and Applied Mathematics* 2 (2), 502–507.
- Newman, M. E. J., Aug 2011. Resource Letter CS-1: Complex Systems. *American Journal of Physics* 79 (8), 800–810.
- Nguyen, N. D., Drogoul, A., Auger, P., 2008. Methodological steps and issues when deriving individual based-models from equation-based models: A case study in population dynamics. In: Bui, T. D., Ho, T. V., Ha, Q. T. (Eds.), Intelligent Agents and Multi-Agent Systems. No. 5357 in Lecture Notes in Artificial Intelligence. Pacific Rim International Conference on Multi-Agents, Springer, Berlin, Germany, 295–306.

- Nguyen, N. T., 2008. Keynote speech: Computational collective intelligence and knowledge inconsistency in multi-agent environments. In: Bui, T. D., Ho, T. V., Ha, Q. T. (Eds.), Intelligent Agents and Multi-Agent Systems. No. 5357 in Lecture Notes in Artificial Intelligence. Pacific Rim International Conference on Multi-Agents, Springer, Berlin, Germany, 2–3.
- Numpy Developers, 2012. NumPy. <http://numpy.scipy.org> [Accessed: 06 Jun 2012].
- Oakes, J. M., May 2008. Invited commentary: Rescuing robinson crusoe. American Journal of Epidemiology 168 (1), 9–12.
- Oléron Evans, T. P., Bishop, S. R., Dec 2013. Static search games played over graphs and general metric spaces. European Journal of Operational Research 231 (3), 667–689.
- Oléron Evans, T. P., Bishop, S. R., Aug 2014. A spatial model with pulsed releases to compare strategies for the sterile insect technique applied to the mosquito *Aedes aegypti*. Mathematical Biosciences 254, 6–27.
- Owen, G., McCormick, G. H., Jun 2008. Finding a moving fugitive. A game theoretic representation of search. Computers & Operations Research 35 (6), 1944–1962.
- Patlolla, P., Gunupudi, V., Mikler, A. R., Jacob, R. T., Jun 2006. Agent-based simulation tools in computational epidemiology. In: Böhme, T., Larios Rosillo, V. M., Unger, H., Unger, H. (Eds.), Innovative Internet Community Systems. Vol. 3473 of Lecture Notes in Computer Science. Springer, Berlin, Germany, 212–223.
- Pavlović, L., Dec 1995. A search game on the union of graphs with immobile hider. Naval Research Logistics 42 (8), 1177–1189.
- Pineda-Krch, M., Blok, H. J., Dieckmann, U., Doebeli, M., Jan 2007. A tale of two cycles - distinguishing quasi-cycles and limit cycles in finite predator-prey populations. Oikos 116 (1), 53–64.
- Powell, R., Aug 2007. Defending against terrorist attacks with limited resources. American Political Science Review 101 (3), 527–541.
- Powell, R., Nov 2009. Sequential, nonzero-sum “Blotto”: Allocating defensive resources prior to attack. Games and Economic Behavior 67 (2), 611–615.
- Python Software Foundation, 2012. Python Programming Language – Official Website. www.python.org [Accessed: 06 Jun 2012].

- Rahman, A., Mahmood, A. K., Schneider, E., 2008. Using agent-based simulation of human behavior to reduce evacuation time. In: Bui, T. D., Ho, T. V., Ha, Q. T. (Eds.), Intelligent Agents and Multi-Agent Systems. No. 5357 in Lecture Notes in Artificial Intelligence. Pacific Rim International Conference on Multi-Agents, Springer, Berlin, Germany, 357–369.
- Railsback, S. F., Grimm, V., 2012. Agent-Based and Individual-Based Modeling: A Practical Introduction. Princeton University Press, Princeton, USA.
- Rausch, R. E., 2001. The relationship between one-dimensional continuous cellular automata and one-dimensional nonlinear dynamical systems. *Complex Systems* 13 (2), 131–142.
- Ray, A., Jul 2004. Symbolic dynamic analysis of complex systems for anomaly detection. *Signal Processing* 84 (7), 1115–1130.
- Reijnierse, J. H., Potters, J. A. M., Dec 1993. Search games with immobile hider. *International Journal of Game Theory* 21 (4), 385–394.
- Roberson, B., Sep 2006. The Colonel Blotto game. *Economic Theory* 29 (1), 1–24.
- Rogers, S., Sedghi, A., Evans, L., Aug 2011. UK riots: Every verified incident - Interactive map. The Guardian [online], 11 Aug. Available at: www.guardian.co.uk/news/datablog [Accessed: 20 Apr 2012].
- Ross, S. M., 1996. Stochastic Processes, 2nd Edition. Wiley Series in Probability and Mathematical Statistics. John Wiley & Sons, New York, USA.
- Ruckle, W. H., 1983. Geometric games and their applications. No. 82 in Research Notes in Mathematics. Pitman, Boston, USA.
- Ruckle, W. H., Mar 1990. The gold-mine game. *Journal of Optimization Theory and Applications* 64 (3), 641–650.
- Ruckle, W. H., Aug 2007. Rendez-vous search on a rectangular lattice. *Naval Research Logistics* 54 (5), 492–496.
- Ruckle, W. H., Kikuta, K., Sep 2000. Continuous accumulation games in continuous regions. *Journal of Optimization Theory and Applications* 106 (3), 581–601.
- Sahani, M., Mar 2013. “Dimensionality Reduction” (Course notes), *Adaptive Modelling of Complex Data*, Gatsby Computational Neuroscience Unit, University College London. Available at: <http://www.gatsby.ucl.ac.uk/~maneesh/dimred/> [Accessed: 10 Feb 2015].

- San Miguel, M., Johnson, J. H., Kertesz, K., Díaz-Guilera, A., MacKay, R. S., Loreto, V., Érdi, P., Hebing, D., Dec 2012. Challenges in complex systems science. European Physical Journal Special Topics 214 (1), 245–271.
- Sayama, H., 2015. “Predator-Prey Ecosystem: A Real-Time Agent-Based Simulation”, Wolfram Demonstrations Project. Available at: <http://demonstrations.wolfram.com/PredatorPreyEcosystemARealTimeAgentBasedSimulation/> [Accessed: 06 Jan 2015].
- Schelling, T. C., 1971. Dynamic models of segregation. Journal of Mathematical Sociology 1 (2), 143–186.
- Seck-Tuoh-Mora, J. C., Medina-Marin, J., Martínez, G. J., Hernández-Romero, N., Apr 2014. Emergence of density dynamics by surface interpolation in elementary cellular automata. Communications in Nonlinear Science and Numerical Simulation 19 (4), 941–966.
- Shoham, Y., Leyton-Brown, K., 2009. Multiagent Systems: Algorithmic, Game-Theoretic, and Logical Foundations. Cambridge University Press, Cambridge, UK.
- Shubik, M., Weber, R. J., Jun 1981. Systems defense games - Colonel-Blotto, command and control. Naval Research Logistics 28 (2), 281–287.
- Siettos, C. I., Sep 2011. Equation-free multiscale computational analysis of individual-based epidemic dynamics on networks. Applied Mathematics and Computation 218 (2), 324–336.
- Smith, A., 1776. The Wealth of Nations. Available at: www.bibliomania.com [Accessed: 10 Feb 2015].
- Steen, L. A., Seebach Jr., J. A., 1970. Counterexamples in topology. Springer, New York, USA.
- Steinwart, I., Christmann, A., 2008. Support Vector Machines. Information Science and Statistics. Springer, New York, USA.
- Stirzaker, D., 2005. Stochastic Processes & Models. Oxford University Press, Oxford, UK.
- Strauss, W. A., 2008. Partial Differential Equations: An Introduction, 2nd Edition. John Wiley & Sons, Ltd, Hoboken, USA.
- Strogatz, S. H., 1994. Nonlinear Dynamics and Chaos. Studies in Nonlinearity. Westview, Cambridge, USA.

- Stroock, D. W., 2014. An Introduction to Markov Processes, 2nd Edition. No. 230 in Graduate Texts in Mathematics. Springer, Berlin, Germany.
- Subelman, E. J., Sep 1981. A hide-search game. *Journal of Applied Probability* 18 (3), 628–640.
- Sun, Y., Apr 2013. Stability analysis of flocking for multi-agent dynamic systems. *Nonlinear Analysis: Real World Applications* 14 (2), 1075–1081.
- Sutherland, W. A., 1975. Introduction to metric and topological spaces, 1st Edition. Oxford University Press, Oxford, UK.
- Sutherland, W. A., 2009. Introduction to metric and topological spaces, 2nd Edition. Oxford University Press, Oxford, UK.
- Svirezhev, Y. M., Dec 1999. Simplest dynamic models of the global vegetation pattern. *Ecological Modelling* 124 (2-3), 131–144.
- Tambe, M., 2012. Security and game theory: Algorithms, deployed systems, lessons learned, 1st Edition. Cambridge University Press, New York, USA.
- Thomas, L. C., Washburn, A. R., May 1991. Dynamic search games. *Operations Research* 39 (3), 415–422.
- Thomson Reuters, 2014. Web of Science. <http://apps.webofknowledge.com> [Accessed: 05 Aug 2014].
- Thulke, H., Eisinger, D., 2008. The strength of 70%: Revision of a standard threshold of rabies control. In: Dodet, B., Fooks, A. R., Müller, T., Tordo, N. (Eds.), Towards the Elimination of Rabies in Eurasia. No. 131 in Developments in Biologicals. World Organisation for Animal Health, Paris, France, 291–298.
- Tian, R., Jul 2009. The mathematical solution of a cellular automaton model which simulates traffic flow with a slow-to-start effect. *Discrete Applied Mathematics* 157 (13), 2904–2917.
- Tofias, M., Merolla, J., Munger, M., Apr 2007. Of colonels and generals: Understanding asymmetry in the Colonel Blotto game [Unpublished]. Prepared for MPSA 2007 Panel 34-6 “Computational Models”. Available at www.uwm.edu/~tofias [Accessed: 10 Feb 2015].
- Tyl, T. Y. (uncredited), Dec 2009. “Lotka Algorithmic Simulation”, JSeed Project. Available at: <http://jseed.sourceforge.net/lotka/> [Accessed: 06 Feb 2015].
- Upton, G., Cook, I., 2011. Dictionary of Statistics, 2nd Edition. Oxford Paperback References. Oxford University Press, Oxford, UK.

- Valdés, M., Cubillos, C., 2008. Design of a multiagent system over mobile devices for the planning of touristic travels. In: Bui, T. D., Ho, T. V., Ha, Q. T. (Eds.), Intelligent Agents and Multi-Agent Systems. No. 5357 in Lecture Notes in Artificial Intelligence. Pacific Rim International Conference on Multi-Agents, Springer, Berlin, Germany, 397–404.
- Vanag, V. K., May 1999. Study of spatially distributed dynamical systems using probabilistic cellular automata. *Uspekhi Fizicheskikh Nauk* 169 (5), 481–505.
- Volterra, V., 1926. Variazioni e fluttuazioni del numero d'individui in specie animali conviventi [in Italian]. *Atti della Reale Accademia Nazionale dei Lincei* 2 (3), 31–112. [See also the English translation: Volterra, 1931].
- Volterra, V., 1931. Variations and fluctuations of the number of individuals in animal species living together. In: Chapman, R. N. (Ed.), Animal Ecology, 1st Edition. Publications in the Zoological Sciences. McGraw-Hill, New York, USA, Appendix, 409–448. [English translation of Volterra, 1926. Translated by Wells, M. E.].
- Von Bertalanffy, L., 1969. General System Theory: Foundations, Development, Applications, revised Edition. George Braziller, New York, USA.
- Wang, Q. A., Dec 2011. Editorial. *Chinese Science Bulletin* 56 (34), 3615–3616.
- Wessel, L., Hua, Y., Wu, J., Moghadas, S. M., Feb 2011. Public health interventions for epidemics: implications for multiple infection waves. *BMC Public Health* 11 (Suppl 1), S2.
- White, L. V., Oct 1994. Games of strategy on trees [Unpublished], Technical Report Series, Imperial College London, TR-94-24.
- Wilensky, U., 2015. NetLogo Home Page. <https://ccl.northwestern.edu/netlogo/> [Accessed: 10 Feb 2015].
- Wilson, A. G., 2011. Catastrophe Theory and Bifurcation [Reprint of 1981 original]. Routledge Revivals. Routledge, New York, USA.
- Wilson, A. G. (Principal Investigator), 2010. ENFOLD-ing - Explaining, Modelling, and Forecasting Global Dynamics (EPSRC Grant EP/H02185X/1): Details of grant. Available at: <http://gow.epsrc.ac.uk/NGBOViewGrant.aspx?GrantRef=EP/H02185X/1> [Accessed: 03 Mar 2015].
- Wolfram, S., Jul 1983. Statistical mechanics of cellular automata. *Reviews of Modern Physics* 55 (3), 601–644.
- Wolfram, S., 2002. A new kind of science. Wolfram Media Inc., Champaign, USA.

- Wooldridge, M., Jennings, N. R., Jun 1995. Intelligent agents: theory and practice. *The Knowledge Engineering Review* 10 (2), 115–152.
- Xiang, K. T. Z., Bishop, S. R., Sep 2010. Cellular automata model for free Aeolian sand dunes [Unpublished], MSc dissertation - University College London.
- Yang, X., Song, Q., Wang, Y., 2007. A weighted support vector machine for data classification. *International Journal of Pattern Recognition* 21 (5), 961–976.
- Zoroa, N., Fernández-Sáez, M. J., Zoroa, P., Nov 1999a. A game related to the number of hides game. *Journal of Optimization Theory and Applications* 103 (2), 457–473.
- Zoroa, N., Fernández-Sáez, M. J., Zoroa, P., Nov 2004. Search and ambush games with capacities. *Journal of Optimization Theory and Applications* 123 (2), 431–450.
- Zoroa, N., Fernández-Sáez, M. J., Zoroa, P., Nov 2012. Patrolling a perimeter. *European Journal of Operational Research* 222 (3), 571–582.
- Zoroa, N., Zoroa, P., Jun 1993. Some games of search on a lattice. *Naval Research Logistics* 40 (4), 525–541.
- Zoroa, N., Zoroa, P., Fernández-Sáez, M. J., Dec 1999b. A generalization of Ruckle's results for an ambush game. *European Journal of Operational Research* 119 (2), 353–364.
- Zoroa, N., Zoroa, P., Fernández-Sáez, M. J., Feb 2001. New results on a Ruckle problem in discrete games of ambush. *Naval Research Logistics* 48 (1), 98–106.
- Zoroa, N., Zoroa, P., Fernández-Sáez, M. J., Mar 2003. Raid games across a set with cyclic order. *European Journal of Operational Research* 145 (3), 684–692.